

UNCLASSIFIED



AD NUMBER

AD-506 837

CLASSIFICATION CHANGES

TO UNCLASSIFIED

FROM CONFIDENTIAL

AUTHORITY

AFAL Ltr; Apr 11, 1978

19990805009

THIS PAGE IS UNCLASSIFIED

UNCLASSIFIED



AD NUMBER

AD-506 837

NEW LIMITATION CHANGE

TO

DISTRIBUTION STATEMENT: A

Approved for public release; Distribution is unlimited.

LIMITATION CODE: 1

FROM

No Prior DoD Distr Scty Cntrl St'mt Assgn'd

AUTHORITY

AFAL Ltr; Apr 11, 1978

THIS PAGE IS UNCLASSIFIED

AFAPL-TR-69-92
VOLUME I

UNCLASSIFIED

(UNCLASSIFIED TITLE)
INVESTIGATION OF
A HIGHLY LOADED
TWO-STAGE FAN-DRIVE TURBINE

VOLUME I. Phase I. Preliminary Design Evaluation

H. Welna, D. E. Dahlberg and W. H. Heiser
Pratt & Whitney Aircraft
Division of United Aircraft Corporation

Technical Report
AFAPL-TR-69-92 Volume I
December 1969

Downgraded at 3 Year Intervals;
Declassified after 12 Years,
DOD DIR. 5200.10

SPECIAL HANDLING REQUIRED
NOT RELEASABLE TO FOREIGN NATIONALS
The information contained in this document will not be
disclosed to foreign nationals or their representatives.

This document contains information affecting the national defense of the United States
within the meaning of the Espionage Laws. Its transmission or the revelation of its con-
tents in any manner to an unauthorized person is prohibited by law.

AIR FORCE AERO PROPULSION LABORATORY
AIR FORCE SYSTEMS COMMAND
WRIGHT-PATTERSON AIR FORCE BASE, OHIO

att: HP TC

Reproduced From
Best Available Copy

AFLC-WPAFB-JAN 70 33

UNCLASSIFIED

~~CONFIDENTIAL~~

SECURITY

MARKING

The classified or limited status of this report applies to each page, unless otherwise marked.

Separate page printouts MUST be marked accordingly.

THIS DOCUMENT CONTAINS INFORMATION AFFECTING THE NATIONAL DEFENSE OF THE UNITED STATES WITHIN THE MEANING OF THE ESPIONAGE LAWS, TITLE 18, U.S.C., SECTIONS 793 AND 794. THE TRANSMISSION OR THE REVELATION OF ITS CONTENTS IN ANY MANNER TO AN UNAUTHORIZED PERSON IS PROHIBITED BY LAW.

NOTICE: When government or other drawings, specifications or other data are used for any purpose other than in connection with a definitely related government procurement operation, the U.S. Government thereby incurs no responsibility, nor any obligation whatsoever; and the fact that the Government may have formulated, furnished, or in any way supplied the said drawings, specifications, or other data is not to be regarded by implication or otherwise as in any manner licensing the holder or any other person or corporation, or conveying any rights or permission to manufacture, use or sell any patented invention that may in any way be related thereto.

~~CONFIDENTIAL~~

~~CONFIDENTIAL~~
UNCLASSIFIED

NOTICE

When Government drawings, specifications, or other data are used for any purpose other than in connection with a definitely related Government procurement operation, the United States Government thereby incurs no responsibility nor any obligation whatsoever; and the fact that the Government may have formulated, furnished, or in any way supplied the said drawings, specifications, or other data, is not to be regarded by implication or otherwise as in any manner licensing the holder or any other person or corporation, or conveying any rights or permission to manufacture, use, or sell any patented invention that may in any way be related thereto.

Copies of this report should not be returned unless return is required by security considerations, contractual obligations, or notice on a specific document.

~~CONFIDENTIAL~~
UNCLASSIFIED


UNCLASSIFIED

(UNCLASSIFIED TITLE)
INVESTIGATION OF
A HIGHLY LOADED
TWO-STAGE FAN-DRIVE TURBINE

VOLUME I. Phase I, Preliminary Design Evaluation

H. Welna, D. E. Dahlberg and W. H. Heiser

Downgraded at 3 Year Intervals;
Declassified after 12 Years,
DOD DIR. 5200.10

SPECIAL HANDLING REQUIRED
NOT RELEASABLE TO FOREIGN NATIONALS
The information contained in this document will not be
disclosed to foreign nationals or their representatives.

This document contains information affecting the national defense of the United States within the meaning of the Espionage Laws. Its transmission or the revelation of its contents in any manner to an unauthorized person is prohibited by law.

UNCLASSIFIED


UNCLASSIFIED

FOREWORD

(U) This Interim Technical Status Report (Contractors Reference No. PWA-3456) was prepared by Pratt & Whitney Aircraft, Division of United Aircraft Corporation, East Hartford, Connecticut, as the first Semiannual Report under United States Air Force Contract F33615-68-C-1208, Project No. 3066, Task No. 306606. This report was submitted by the Contractor on 28 June 1968, and covers the Report period from 1 January 1968 to 28 June 1968.

(U) The findings and conclusions of this report are not deemed as final by the Contractor. They are subject to verification or revision in the Final Report to be published upon the completion of this Contract.

(U) The Air Force Program Monitor is Mr. Wayne Tall, APTC, Air Force Aero Propulsion Laboratory, Wright-Patterson Air Force Base, Ohio, 45433.

(U) This report contains no classified information extracted from other classified documents.

(U) Publication of this report does not constitute Air Force approval of the report's findings or conclusions. It is published only for the exchange and stimulation of ideas.

Wayne Tall
Project Engineer
Air Force Aero Propulsion Laboratory

PAGE NO. ii

(This page is Unclassified)

UNCLASSIFIED

UNCLASSIFIED

UNCLASSIFIED ABSTRACT

(U) A three-year program was initiated to provide a direct attack on the problem of attaining high efficiency in highly loaded turbine stages. The goals of this program are to develop turbine aerodynamic techniques and design procedures for efficient, high work, low pressure turbines by means of analytical studies and cascade testing, and to demonstrate the effectiveness of the techniques and procedures by designing and testing a two stage turbine that meets or exceeds the contract stage work and efficiency goals. The first phase effort described in this report was directed toward defining a turbine design with the highest inherent resistance to boundary layer separation and to select boundary layer control techniques that are best suited for extending the loading limits of the basic turbine design.

Distribution of this abstract is unlimited.

(The reverse of this page is blank)

PAGE NO. iii

UNCLASSIFIED

UNCLASSIFIED

TABLE OF CONTENTS

<u>Section</u>	<u>Title</u>	<u>Page</u>
	LIST OF ILLUSTRATIONS	vii
	LIST OF TABLES	xxvii
	LIST OF SYMBOLS	xxviii
I	INTRODUCTION	1
II	PRELIMINARY DESIGN EVALUATION (Task 1a)	3
	1. RFP OBJECTIVE	3
	2. TASK OBJECTIVE	3
	3. FLOWPATH ANALYSIS	5
	4. STAGE-WORK SPLIT	9
	5. REACTION	10
	6. SOLIDITY	20
III	AIRFOIL CONTOUR ANALYSIS (Task 1b)	23
	1. RFP OBJECTIVE	23
	2. TASK OBJECTIVE	23
	3. PRELIMINARY AIRFOIL ANALYSIS	23
	4. PRELIMINARY BOUNDARY LAYER ANALYSIS	26
	5. SELECTION OF AIRFOILS FOR CONTOUR REFINEMENT	41
	6. FINAL AIRFOIL CONTOUR REFINEMENT	41
	7. FINAL AIRFOIL CONTOUR BOUNDARY LAYER CALCULATIONS	44
IV	BOUNDARY LAYER CONTROL SURVEY (Task 1c)	49
	1. RFP OBJECTIVE	49
	2. TASK OBJECTIVE	49
	3. LITERATURE SOURCES	49
	4. SECONDARY LOSSES	50
	5. BOUNDARY LAYER CONTROL	52
	6. SELECTION OF BOUNDARY LAYER CONTROL METHODS	62
V	PRELIMINARY BOUNDARY LAYER CONTROL ANALYSIS (Task 1d)	65
	1. RFP OBJECTIVE	65
	2. TASK OBJECTIVE	65

UNCLASSIFIED

UNCLASSIFIED

TABLE OF CONTENTS (Cont'd)

<u>Section</u>	<u>Title</u>	<u>Page</u>
	3. END WALL CONTOURING	65
	4. VORTEX GENERATORS	65
	5. CORNER SLOTS	72
	6. CORNER FILLETS	75
	7. TENTATIVE RANKING OF BOUNDARY LAYER CONTROL METHODS	81
VI	SELECTION OF BASELINE TURBINE (Task 1e)	83
APPENDIX I	PRELIMINARY AIRFOIL SECTIONS	85
APPENDIX II	FINAL AIRFOIL SECTIONS	245
REFERENCES		313

UNCLASSIFIED

LIST OF ILLUSTRATIONS

<u>Figure</u>	<u>Title</u>	<u>Page</u>
1	Flow Chart - Phase I, Task 1a	4
2	Flowpaths for Turbine Study	6
3	Turbine Parametric Study	7
4	Variation of Turbine Exit Axial Mach Number With Exit Area at Various Reaction Levels	8
5	Variation of Turbine Exit Swirl Angle With Exit Area at Various Reaction Levels	9
6	Effect of Second-Stage Work Distribution on Turbine Exit Conditions	10
7	Variation of Stage Reaction With Span for Various Reaction Levels	11
8	Variation of Exit Guide Vane Inlet Mach Number With Span	12
9	Variation of Exit Guide Vane Turning Angle With Span	13
10	Variation of Choking Margin With Span	13
11	Variation of Inlet Mach Number With Span at Various Reaction Levels	16
12	Variation of Exit Mach Number With Span at Various Reaction Levels	17
13	Variation of Second Stage Work With Span for Various Reaction Levels	18
14	Variation of Exit Guide Vane Turning Angle and Inlet Mach Number With Span at Various Reaction Levels	18
15	Medium Reaction, First Stage Vane Root, Medium Solidity	29

UNCLASSIFIED

UNCLASSIFIED

LIST OF ILLUSTRATIONS (Cont'd)

<u>Figure</u>	<u>Title</u>	<u>Page</u>
16	Medium Reaction, First Stage Vane Root, Low Solidity	30
17	Medium Reaction, First Stage Blade Root, Medium Solidity	31
18	Medium Reaction, First Stage Blade Root, Low Solidity	32
19	Medium Reaction, Second Stage Vane Root, Medium Solidity	33
20	Medium Reaction, Second Stage Vane Root, Low Solidity	34
21	Medium Reaction, Second Stage Blade Root, Medium Solidity	35
22	Medium Reaction, Second Stage Blade Root, Low Solidity	36
23	Medium Reaction, Second Blade Root Section Pressure Distribution	37
24	Medium Reaction, Second Blade, Root Section, Drag Coefficient	38
25	Drag Coefficient vs. Solidity for Vane Root Sections	39
26	Drag Coefficient vs. Solidity for Blade Root Sections	40
27	Medium Reaction, First Blade, Root Section, Low Solidity	42
28	Medium Reaction, First Blade, Root Section, Low Solidity	43
29	Medium Reaction, First Stage Vane Root, Low Solidity	45
30	Medium Reaction, First Stage Blade Root, Low Solidity	46

UNCLASSIFIED

UNCLASSIFIED

LIST OF ILLUSTRATIONS (Cont'd)

<u>Figure</u>	<u>Title</u>	<u>Page</u>
31	Medium Reaction, Second Stage Vane Root, Low Solidity	47
32	Medium Reaction, Second Stage Blade Root, Medium Solidity	48
33	Turbine Cascade Secondary Flows	51
34	Pressure Distribution	54
35	Local Uncambered Airfoil	55
36	Forward Leaning Blade Tip	56
37	Vane Flowpath With Contoured End Wall	66
38	Effect of End Wall Contouring on Vane Root Pressure Distribution	67
39	Vortex Generator Placement	70
40	Medium Reaction - Low Solidity Root Section Hydrodynamic Thickness	71
41	Typical Slotted Airfoil	
42	Medium Reaction, Second Stage Blade, Root Section, Low Solidity	74
43	Effect of Length and Pressure Gradient on Laminar Boundary Layer Formation	75
44	Effect of Momentum Thickness at Gage Point on Momentum Thickness and Friction Coefficient at 92 Percent Chord Point	76
45	Typical Corner Slot Applications	77
46	Simplified Corner Boundary Layer Model	78
47	Root Sections With Fillet Radius Equal to 10δ	80

UNCLASSIFIED

UNCLASSIFIED

LIST OF ILLUSTRATIONS (Cont'd)

<u>Figure</u>	<u>Title</u>	<u>Page</u>
48	Suction Side Root Fillet-Axial View of Passage From Rear	81
49	Low Reaction, High Solidity, First Stage Vane Root, Airfoil Cross Section	86
50	Low Reaction, High Solidity, First Stage Vane Root	87
51	Low Reaction, Normal Solidity, First Stage Vane Root, Airfoil Cross Section	88
52	Low Reaction, Normal Solidity, First Stage Vane Root	89
53	Low Reaction, Medium Solidity, First Stage Vane Root, Airfoil Cross Section	90
54	Low Reaction, Medium Solidity, First Stage Vane Root	91
55	Low Reaction, Low Solidity, First Stage Vane Root, Airfoil Cross Section	92
56	Low Reaction, Low Solidity, First Stage Vane Root	93
57	Low Reaction, Normal Solidity, First Stage Vane Mean, Airfoil Cross Section	94
58	Low Reaction, Normal Solidity, First Stage, Vane Mean	95
59	Low Reaction, Medium Solidity, First Stage Vane Mean, Airfoil Cross Section	96
60	Low Reaction, Medium Solidity, First Stage Vane Mean	97
61	Low Reaction, Low Solidity, First Stage Vane Mean, Airfoil Cross Section	98

UNCLASSIFIED

UNCLASSIFIED

LIST OF ILLUSTRATIONS (Cont'd)

<u>Figure</u>	<u>Title</u>	<u>Page</u>
62	Low Reaction, Low Solidity, First Stage Vane Mean	99
63	Low Reaction, High Solidity, First Stage Vane Tip, Airfoil Cross Section	100
64	Low Reaction, High Solidity, First Stage Vane Tip	101
65	Low Reaction, Normal Solidity, First Stage Vane Tip, Airfoil Cross Section	102
66	Low Reaction, Normal Solidity, First Stage Vane Tip	103
67	Low Reaction, Medium Solidity, First Stage Vane Tip, Airfoil Cross Section	104
68	Low Reaction, Medium Solidity, First Stage Vane Tip	105
69	Low Reaction, Low Solidity, First Stage Vane Tip, Airfoil Cross Section	106
70	Low Reaction, Low Solidity, First Stage Vane Tip	107
71	Low Reaction, High Solidity, First Stage Blade Root, Airfoil Cross Section	108
72	Low Reaction, High Solidity, First Stage Blade Root	109
73	Low Reaction, Normal Solidity, First Stage Blade Root, Airfoil Cross Section	110
74	Low Reaction, Normal Solidity, First Stage Blade Root	111
75	Low Reaction, Medium Solidity, First Stage Blade Root, Airfoil Cross Section	112

UNCLASSIFIED

UNCLASSIFIED

LIST OF ILLUSTRATIONS (Cont'd)

<u>Figure</u>	<u>Title</u>	<u>Page</u>
76	Low Reaction, Medium Solidity, First Stage Blade Root	113
77	Low Reaction, Low Solidity, First Stage Blade Root, Airfoil Cross Section	114
78	Low Reaction, Low Solidity, First Stage Blade Root	115
79	Low Reaction, Normal Solidity, First Stage Blade Mean, Airfoil Cross Section	116
80	Low Reaction, Normal Solidity, First Stage Blade Mean	117
81	Low Reaction, Medium Solidity, First Stage Blade Mean, Airfoil Cross Section	118
82	Low Reaction, Medium Solidity, First Stage Blade Mean	119
83	Low Reaction, Low Solidity, First Stage Blade Mean Airfoil Cross Section	120
84	Low Reaction, Low Solidity, First Stage Blade Mean	121
85	Low Reaction, High Solidity, First Stage Blade Tip, Airfoil Cross Section	122
86	Low Reaction, High Solidity, First Stage Blade Tip	123
87	Low Reaction, Normal Solidity, First Stage Blade Tip, Airfoil Cross Section	124
88	Low Reaction, Normal Solidity, First Stage Blade Tip	125
89	Low Reaction, Medium Solidity, First Stage Blade Tip, Airfoil Cross Section	126
90	Low Reaction, Medium Solidity, First Stage Blade Tip	127

UNCLASSIFIED

UNCLASSIFIED

LIST OF ILLUSTRATIONS (Cont'd)

<u>Figure</u>	<u>Title</u>	<u>Page</u>
91	Low Reaction, Low Solidity, First Stage Blade Tip, Airfoil Cross Section	128
92	Low Reaction, Low Solidity, First Stage Blade Tip	129
93	Low Reaction, High Solidity, Second Stage Vane Root, Airfoil Cross Section	130
94	Low Reaction, High Solidity, Second Stage Vane Root	131
95	Low Reaction, Normal Solidity, Second Stage Vane Root, Airfoil Cross Section	132
96	Low Reaction, Normal Solidity, Second Stage Vane Root	133
97	Low Reaction, Medium Solidity, Second Stage Vane Root, Airfoil Cross Section	134
98	Low Reaction, Medium Solidity, Second Stage Vane Root	135
99	Low Reaction, Low Solidity, Second Stage Vane Root, Airfoil Cross Section	136
100	Low Reaction, Low Solidity, Second Stage Vane Root	137
101	Low Reaction, Normal Solidity, Second Stage Vane Mean, Airfoil Cross Section	138
102	Low Reaction, Normal Solidity, Second Stage Vane Mean	139
103	Low Reaction, Medium Solidity, Second Stage Vane Mean, Airfoil Cross Section	140
104	Low Reaction, Medium Solidity, Second Stage Vane Mean	141

UNCLASSIFIED

UNCLASSIFIED

LIST OF ILLUSTRATIONS (Cont'd)

<u>Figure</u>	<u>Title</u>	<u>Page</u>
105	Low Reaction, Low Solidity, Second Stage Vane Mean, Airfoil Cross Section	142
106	Low Reaction, Low Solidity, Second Stage Vane Mean	143
107	Low Reaction, High Solidity, Second Stage Vane Tip, Airfoil Cross Section	144
108	Low Reaction, High Solidity, Second Stage Vane Tip	145
109	Low Reaction, Normal Solidity, Second Stage Vane Tip, Airfoil Cross Section	146
110	Low Reaction, Normal Solidity, Second Stage Vane Tip	147
111	Low Reaction, Medium Solidity, Second Stage Vane Tip, Airfoil Cross Section	148
112	Low Reaction, Medium Solidity, Second Stage Vane Tip	149
113	Low Reaction, Low Solidity, Second Stage Vane Tip, Airfoil Cross Section	150
114	Low Reaction, Low Solidity, Second Stage Vane Tip	151
115	Low Reaction, High Solidity, Second Stage Blade Root, Airfoil Cross Section	152
116	Low Reaction, High Solidity, Second Stage Blade Root	153
117	Low Reaction, Normal Solidity, Second Stage Blade Root, Airfoil Cross Section	154
118	Low Reaction, Normal Solidity, Second Stage Blade Root	155

UNCLASSIFIED

UNCLASSIFIED

LIST OF ILLUSTRATIONS (Cont'd)

<u>Figure</u>	<u>Title</u>	<u>Page</u>
119	Low Reaction, Medium Solidity (Increased Chord), Second Stage Blade Root, Airfoil Cross Section	156
120	Low Reaction, Medium Solidity (Increased Chord), Second Stage Blade Root	157
121	Low Reaction, Low Solidity, Second Stage Blade Root, Airfoil Cross Section	158
122	Low Reaction, Low Solidity, Second Stage Blade Root	159
123	Low Reaction, Normal Solidity, Second Stage Blade Mean, Airfoil Cross Section	160
124	Low Reaction, Normal Solidity, Second Stage Blade Mean	161
125	Low Reaction, Medium Solidity, Second Stage Blade Mean, Airfoil Cross Section	162
126	Low Reaction, Medium Solidity, Second Stage Blade Mean	163
127	Low Reaction, Low Solidity, Second Stage Blade Mean, Airfoil Cross Section	164
128	Low Reaction, Low Solidity, Second Stage Blade Mean	165
129	Low Reaction, High Solidity, Second Stage Blade Tip, Airfoil Cross Section	166
130	Low Reaction, High Solidity, Second Stage Blade Tip	167
131	Low Reaction, Normal Solidity, Second Stage Blade Tip, Airfoil Cross Section	168
132	Low Reaction, Normal Solidity, Second Stage Blade Tip	169

UNCLASSIFIED

UNCLASSIFIED

LIST OF ILLUSTRATIONS (Cont'd)

<u>Figure</u>	<u>Title</u>	<u>Page</u>
133	Low Reaction, Low Solidity, Second Stage Blade Tip, Airfoil Cross Section	170
134	Low Reaction, Low Solidity, Second Stage Blade Tip	171
135	Medium Reaction, Normal Solidity, First Stage Vane Root, Airfoil Cross Section	172
136	Medium Reaction, Normal Solidity, First Stage Vane Root	173
137	Medium Reaction, Medium Solidity, First Stage Vane Root, Airfoil Cross Section	174
138	Medium Reaction, Medium Solidity, First Stage Vane Root	175
139	Medium Reaction, Low Solidity, First Stage Vane Root, Airfoil Cross Section	176
140	Medium Reaction, Low Solidity, First Stage Vane Root	177
141	Medium Reaction, Normal Solidity, First Stage Vane Mean, Airfoil Cross Section	178
142	Medium Reaction, Normal Solidity, First Stage Vane Mean	179
143	Medium Reaction, Medium Solidity, First Stage Vane Mean, Airfoil Cross Section	180
144	Medium Reaction, Medium Solidity, First Stage Vane Mean	181
145	Medium Reaction, Low Solidity, First Stage Vane Mean, Airfoil Cross Section	182
146	Medium Reaction, Low Solidity, First Stage Vane Mean	183

UNCLASSIFIED

LIST OF ILLUSTRATIONS (Cont'd)

<u>Figure</u>	<u>Title</u>	<u>Page</u>
147	Medium Reaction, Normal Solidity, First Stage Vane Tip, Airfoil Cross Section	184
148	Medium Reaction, Normal Solidity, First Stage Vane Tip	185
149	Medium Reaction, Medium Solidity, First Stage Vane Tip, Airfoil Cross Section	186
150	Medium Reaction, Medium Solidity, First Stage Vane Tip	187
151	Medium Reaction, Low Solidity, First Stage Vane Tip, Airfoil Cross Section	188
152	Medium Reaction, Low Solidity, First Stage Vane Tip	189
153	Medium Reaction, Normal Solidity, First Stage Blade Root, Airfoil Cross Section	190
154	Medium Reaction, Normal Solidity, First Stage Blade Root	191
155	Medium Reaction, Medium Solidity, First Stage Blade Root, Airfoil Cross Section	192
156	Medium Reaction, Medium Solidity, First Stage Blade Root	193
157	Medium Reaction, Low Solidity, First Stage Blade Root, Airfoil Cross Section	194
158	Medium Reaction, Low Solidity, First Stage Blade Root	195
159	Medium Reaction Normal Solidity, First Stage Blade Mean, Airfoil Cross Section	196
160	Medium Reaction, Normal Solidity, First Stage Blade Mean	197

UNCLASSIFIED

UNCLASSIFIED

LIST OF ILLUSTRATIONS (Cont'd)

<u>Figure</u>	<u>Title</u>	<u>Page</u>
161	Medium Reaction, Medium Solidity, First Stage Blade Mean, Airfoil Cross Section	198
162	Medium Reaction, Medium Solidity, First Stage Blade Mean	199
163	Medium Reaction, Low Solidity, First Stage Blade Mean, Airfoil Cross Section	200
164	Medium Reaction, Low Solidity, First Stage Blade Mean	201
165	Medium Reaction, Normal Solidity, First Stage Blade Tip, Airfoil Cross Section	202
166	Medium Reaction, Normal Solidity, First Stage Blade Tip	203
167	Medium Reaction, Medium Solidity, First Stage Blade Tip, Airfoil Cross Section	204
168	Medium Reaction, Medium Solidity, First Stage Blade Tip	205
169	Medium Reaction, Low Solidity, First Stage Blade Tip, Airfoil Cross Section	206
170	Medium Reaction, Low Solidity, First Stage Blade Tip	207
171	Medium Reaction, Normal Solidity, Second Stage Vane Root, Airfoil Cross section	208
172	Medium Reaction, Normal Solidity, Second Stage Vane Root	209
173	Medium Reaction, Medium Solidity, Second Stage Vane Root, Airfoil Cross Section	210
174	Medium Reaction, Medium Solidity, Second Stage Vane Root	211

UNCLASSIFIED

UNCLASSIFIED

LIST OF ILLUSTRATIONS (Cont'd)

<u>Figure</u>	<u>Title</u>	<u>Page</u>
175	Medium Reaction, Low Solidity, Second Stage Vane Root, Airfoil Cross Section	212
176	Medium Reaction, Low Solidity, Second Stage Vane Root	213
177	Medium Reaction, Normal Solidity, Second Stage Vane Mean, Airfoil Cross Section	214
178	Medium Reaction, Normal Solidity, Second Stage Vane Mean	215
179	Medium Reaction, Medium Solidity, Second Stage Vane Mean, Airfoil Cross Section	216
180	Medium Reaction, Medium Solidity, Second Stage Vane Mean	217
181	Medium Reaction, Low Solidity, Second Stage Vane Mean, Airfoil Cross Section	218
182	Medium Reaction, Low Solidity, Second Stage Vane Mean	219
183	Medium Reaction, Normal Solidity, Second Stage Vane Tip, Airfoil Cross Section	220
184	Medium Reaction, Normal Solidity, Second Stage Vane Tip	221
185	Medium Reaction, Medium Solidity, Second Stage Vane Tip, Airfoil Cross Section	222
186	Medium Reaction, Medium Solidity, Second Stage Vane Tip	223
187	Medium Reaction, Low Solidity, Second Stage Vane Tip, Airfoil Cross Section	224

UNCLASSIFIED

UNCLASSIFIED

LIST OF ILLUSTRATIONS (Cont'd)

<u>Figure</u>	<u>Title</u>	<u>Page</u>
188	Medium Reaction, Low Solidity, Second Stage Vane Tip	225
189	Medium Reaction, Normal Solidity, Second Stage Blade Root, Airfoil Cross Section	226
190	Medium Reaction, Normal Solidity, Second Stage Blade Root	227
191	Medium Reaction, Medium Solidity, Second Stage Blade Root, Airfoil Cross Section	228
192	Medium Reaction, Medium Solidity, Second Stage Blade Root	229
193	Medium Reaction, Low Solidity, Second Stage Blade Root, Airfoil Cross Section	230
194	Medium Reaction, Low Solidity, Second Stage Blade Root	231
195	Medium Reaction, Normal Solidity, Second Stage Blade Mean, Airfoil Cross Section	232
196	Medium Reaction, Normal Solidity, Second Stage Blade Mean	233
197	Medium Reaction, Medium Solidity, Second Stage Blade Mean, Airfoil Cross Section	234
198	Medium Reaction, Medium Solidity, Second Stage Blade Mean	235
199	Medium Reaction, Low Solidity, Second Stage Blade Mean, Airfoil Cross Section	236
200	Medium Reaction, Low Solidity, Second Stage Blade Mean	237
201	Medium Reaction, Normal Solidity, Second Stage Blade Tip, Airfoil Cross Section	238

PAGE NO. XX

UNCLASSIFIED

UNCLASSIFIED

LIST OF ILLUSTRATIONS (Cont'd)

<u>Figure</u>	<u>Title</u>	<u>Page</u>
202	Medium Reaction, Normal Solidity, Second Stage Blade Tip	239
203	Medium Reaction, Medium Solidity, Second Stage Blade Tip, Airfoil Cross Section	240
204	Medium Reaction, Medium Solidity, Second Stage Blade Tip	241
205	Medium Reaction, Low Solidity, Second Stage Blade Tip, Airfoil Cross Section	242
206	Medium Reaction, Low Solidity, Second Stage Blade Tip	243
207	Medium Reaction, Low Solidity, First Stage Vane Root, Airfoil Cross Section	246
208	Medium Reaction, Low Solidity, First Stage Vane Root	247
209	Medium Reaction, Low Solidity, First Stage Vane Mean, Airfoil Cross Section	248
210	Medium Reaction, Low Solidity, First Stage Vane Mean	249
211	Medium Reaction, Low Solidity, First Stage Vane Tip, Airfoil Cross Section	250
212	Medium Reaction, Low Solidity, First Stage Vane Tip	251
213	Medium Reaction, Low Solidity, First Stage Blade Root, Airfoil Cross Section	252
214	Medium Reaction, Low Solidity, First Stage Blade Root	253

UNCLASSIFIED

UNCLASSIFIED

LIST OF ILLUSTRATIONS (Cont'd)

<u>Figure</u>	<u>Title</u>	<u>Page</u>
215	Medium Reaction Low Solidity, First Stage Blade Mean, Airfoil Cross Section	254
216	Medium Reaction, Low Solidity, First Stage Blade Mean	255
217	Medium Reaction, Low Solidity, First Stage Blade Tip, Airfoil Cross Section	256
218	Medium Reaction, Low Solidity, First Stage Blade Tip	257
219	Medium Reaction, Low Solidity, Second Stage Vane Root, Airfoil Cross Section	258
220	Medium Reaction, Low Solidity, Second Stage Vane Root	259
221	Medium Reaction, Low Solidity, Second Stage Vane Mean, Airfoil Cross Section	260
222	Medium Reaction, Low Solidity, Second Stage Vane Mean	261
223	Medium Reaction, Low Solidity, Second Stage Vane Tip, Airfoil Cross Section	262
224	Medium Reaction, Low Solidity, Second Stage Vane Tip	263
225	Medium Reaction, Medium Solidity, First Stage Vane Root, Airfoil Cross Section	264
226	Medium Reaction, Medium Solidity, First Stage Vane Root	265
227	Medium Reaction, Medium Solidity, First Stage Vane Mean, Airfoil Cross Section	266

UNCLASSIFIED

UNCLASSIFIED

LIST OF ILLUSTRATIONS (Cont'd)

<u>Figure</u>	<u>Title</u>	<u>Page</u>
228	Medium Reaction, Medium Solidity, First Stage Vane Mean	267
229	Medium Reaction, Medium Solidity, First Stage Vane Tip, Airfoil Cross Section	268
230	Medium Reaction, Medium Solidity, First Stage Vane Tip	269
231	Medium Reaction, Medium Solidity, First Stage Blade Root, Airfoil Cross Section	270
232	Medium Reaction, Medium Solidity, First Stage Blade Root	271
233	Medium Reaction, Medium Solidity, First Stage Blade Mean, Airfoil Cross Section	272
234	Medium Reaction, Medium Solidity, First Stage Blade Mean	273
235	Medium Reaction, Medium Solidity, First Stage Blade Tip, Airfoil Cross Section	274
236	Medium Reaction, Medium Solidity, First Stage Blade Tip	275
237	Medium Reaction, Medium Solidity, Second Stage Vane Root, Airfoil Cross Section	276
238	Medium Reaction, Medium Solidity, Second Stage Vane Root	277
239	Medium Reaction, Medium Solidity, Second Stage Vane Mean, Airfoil Cross Section	278
240	Medium Reaction, Medium Solidity, Second Stage Vane Mean	279

UNCLASSIFIED

UNCLASSIFIED

LIST OF ILLUSTRATIONS (Cont'd)

<u>Figure</u>	<u>Title</u>	<u>Page</u>
267	Medium Reaction, Final Second Stage Blade Root, Normal Solidity	306
268	Medium Reaction, Second Stage Blade Root, Normal Solidity	307
269	Medium Reaction, Normal Solidity, Final Second Stage Blade Mean	308
270	Medium Reaction, Second Stage Blade Mean, Normal Solidity	309
271	Medium Reaction, Normal Solidity, Final Second Stage Blade Tip	310
272	Medium Reaction, Second Stage Blade Tip, Normal Solidity	311

UNCLASSIFIED

LIST OF ILLUSTRATIONS (Cont'd)

<u>Figure</u>	<u>Title</u>	<u>Page</u>
254	Medium Reaction, First Stage Vane Tip, Normal Solidity	293
255	Medium Reaction, Normal Solidity, Final First Stage Blade Root	294
256	Medium Reaction, First Stage Blade Root, Normal Solidity	295
257	Medium Reaction, Normal Solidity, Final First Stage Blade Mean	296
258	Medium Reaction, First Stage Blade Mean, Normal Solidity	297
259	Medium Reaction, Normal Solidity, Final First Stage Blade Tip	298
260	Medium Reaction, First Stage Blade Tip, Normal Solidity	299
261	Medium Reaction, Normal Solidity, Final Second Stage Vane Root	300
262	Medium Reaction, Second Stage Vane Root, Normal Solidity	301
263	Medium Reaction, Normal Solidity, Final Second Stage Vane Mean	302
264	Medium Reaction, Second Stage Vane Mean, Normal Solidity	303
265	Medium Reaction, Normal Solidity, Final Second Stage Vane Tip	304
266	Medium Reaction, Second Stage Vane Tip, Normal Solidity	305

UNCLASSIFIED

UNCLASSIFIED

LIST OF ILLUSTRATIONS (Cont'd)

<u>Figure</u>	<u>Title</u>	<u>Page</u>
241	Medium Reaction, Medium Solidity, Second Stage Vane Tip, Airfoil Cross Section	280
242	Medium Reaction, Medium Solidity, Second Stage Vane Tip	281
243	Medium Reaction, Medium Solidity, Second Stage Blade Root, Airfoil Cross Section	282
244	Medium Reaction, Medium Solidity, Second Stage Blade Root	283
245	Medium Reaction, Medium Solidity, Second Stage Blade Mean, Airfoil Cross Section	284
246	Medium Reaction, Medium Solidity, Second Stage Blade Mean	285
247	Medium Reaction, Medium Solidity, Second Stage Blade Tip, Airfoil Cross Section	286
248	Medium Reaction, Medium Solidity, First Stage Blade Tip	287
249	Medium Reaction, Normal Solidity, Final First Stage Vane Root	288
250	Medium Reaction, First Stage Vane Root, Normal Solidity	289
251	Medium Reaction, Normal Solidity, Final First Stage Vane Mean	290
252	Medium Reaction, First Stage Vane Mean, Normal Solidity	291
253	Medium Reaction, Normal Solidity, Final First Stage Vane Tip	292

UNCLASSIFIED

UNCLASSIFIED

LIST OF TABLES

<u>Table No.</u>	<u>Title</u>	<u>Page</u>
I	TURBINE DESIGN PARAMETERS	3
II	PRELIMINARY AIRFOILS - LOW REACTION	14
III	FIRST STAGE TURBINE DATA - MEDIUM REACTION	19
IV	SECOND STAGE TURBINE DATA - MEDIUM REACTION	20
V	MEDIUM REACTION - MEDIUM SOLIDITY (+15% LOAD COEFFICIENT)	21
VI	MEDIUM REACTION PRELIMINARY AIRFOIL SUMMARY	24
VII	LAMINAR SEPARATION AT ROOT	26
VIII	TURBULENT BOUNDARY LAYER - ROOT SECTION	27
IX	EFFECT OF MOVING TRANSITION POINT, FIRST VANE ROOT SECTION	28
X	EFFECT OF ROOT CONTOUR REFINEMENT ON DRAG COEFFICIENT	44
XI	VORTEX GENERATOR DIMENSIONS (INCH)	69
XII	FILLET RADIUS (INCH)	79

UNCLASSIFIED

UNCLASSIFIED

LIST OF SYMBOLS

A	- area, square inches
B	- axial chord, inches
C	- absolute gas velocity, feet per second
C _F	- drag coefficient
C _L	- Zweifel load coefficient
C _L [*]	- load coefficient, $\Delta C_u/U$
E	- diffusion parameter
H	- boundary layer shape factor
ΔH	- work, Btu per pound
M	- Mach number
P	- pressure, psia
ΔP	- pressure rise from minimum to exit value on suction surface
Q	- exit dynamic head
R	- fillet radius, inches
R _C	- radius of curvature, inches
Re _{θ}	- Reynolds number based on boundary layer momentum thickness
S	- distance along airfoil surface, inches
T	- temperature, °R
u	- tangential velocity, feet per second
W	- relative gas velocity, feet per second
W _g	- gas flow, pounds per second
X	- axial distance, inches
Y	- tangential distance, inches
Z	- number of airfoils
α	- absolute gas angle, degrees
β	- relative gas angle degrees
δ	- boundary layer thickness, inches
δ^*	- boundary layer displacement thickness
θ	- boundary layer momentum thickness, inches
θ_b	- blade camber, degrees
θ_v	- vane camber, degrees
τ	- gap, inches
η	- efficiency, percent

Subscripts

0	inlet to first vane
1	inlet to first blade
2	exit from stage or airfoil section

UNCLASSIFIED

UNCLASSIFIED

G	gage point
ws	wetted surface
ms	mainstream surface
S	static
T	total

(The reverse of this page is blank)

PAGE NO XXIX

UNCLASSIFIED

UNCLASSIFIED

SECTION I INTRODUCTION

(U) The design analysis and optimization of aircraft jet engines have always involved a trade between increasing turbine efficiency and reducing its size and weight. The bypass turbofan engine has become an attractive propulsion system for future multi-mission aircraft. The specific fuel consumption of bypass engines generally decreases with increasing bypass ratio, and it is, therefore, essential to achieve advances in bypass flow. Increased bypass ratios, however, require increased fan power supplied by the low pressure turbine. The objective, then, is to increase fan-drive turbine power, or loading, while maintaining or improving the turbine aerodynamic efficiency.

(U) The turbine designer is constrained by certain unique requirements when designing fan drive turbines. The rotational speed of the low pressure turbine must be limited in order that the fan tip Mach number does not exceed the limit for reasonable losses. This problem becomes more critical as the bypass ratio and fan diameter increase. Applying conventional aerodynamics, when faced with a limiting rotational speed, the designer usually increases the diameter of the low pressure turbine stages or increases the number of stages in order to obtain more work and still maintain turbine efficiency. Conversely, the reduction of turbine diameter or solidity results in a lighter turbine, but with a sacrifice in efficiency due to losses associated with increased loading. Considerable gains can be realized by an engine if the size and weight reduction can be made with no loss in efficiency. Furthermore, because of the time required between the evolution of new concepts and engine production, turbine technology must be improved now, so that the desired level of turbo-fan engine performance can be achieved for aircraft which will be operational in the 1975-1980 time period.

(U) The objective of the work done under this contract is to analyze and test concepts which will increase the low pressure turbine loading and maintain or increase current turbine efficiency levels. The goals of this program are to develop turbine aerodynamic techniques and design procedures for efficient, high work, low pressure turbines by means of analytical studies and cascade testing, and to demonstrate the effectiveness of the techniques, by designing and testing a two-stage turbine that meets or exceeds the contract stage work and efficiency goals.

(U) The program has been planned in four phases over a period of three years. Phase I will define the basic turbine design and analyze promising increased loading concepts. Phases II and III consist of experimental testing to verify and extend the turbine aerodynamic techniques and design procedures for high loading levels. Phase IV will subject the aerodynamic techniques and design procedures to a two-stage rotating rig test.

(U) The results of the Phase I effort are presented in this report.

(The reverse of this page is blank)

PAGE NO 1

UNCLASSIFIED

CONFIDENTIAL

SECTION II

PRELIMINARY DESIGN EVALUATION (Task 1a)

1. RFP OBJECTIVE

(U) Select turbine designs that indicate an inherent high resistance to flow separation at high loading levels.

2. TASK OBJECTIVE

(U) The objective of the initial task of Phase I was to select a turbine design which would satisfy the RFP design parameters as listed in Table I. Based on these parameters, good turbine design practice and current engine cycles, and by considering reasonable variations in work distribution, levels of reaction and solidity, a range of turbine designs was evaluated toward the realization of a satisfactory turbine design. From the resulting velocity triangles, preliminary airfoil contours which provided the lowest profile loss and greatest potential for performance improvement with boundary layer control were defined. In order to achieve a practical and realistic design, structural problems and interface requirements at the turbine inlet and exit were considered.

(U) The path followed in the design analysis is shown in Figure 1. The goal of this analysis was to determine optimum flowpath, stage work split, reaction level and solidity. The description that follows corresponds directly to the path of Figure 1.

TABLE I

TURBINE DESIGN PARAMETERS

Number of Stages	2
Average Load Coefficient, C_L^*	2.2
First Blade Tip Wheel Speed	1000 fps
First Blade Inlet Hub-Tip Diameter Ratio	≤ 0.8
Exit Swirl Angle - Without Exit Guide Vane	20°
- With Exit Guide Vane	0°
Turbine Inlet Temperature	1450°F
Airflow	$\geq 50 \text{ lb/sec}$
Average Stage Efficiency	91%
Life	10,000 hr.

CONFIDENTIAL

PAGE NO 3

DECLASSIFIED AT 5 YEAR INTERVALS
DECLASSIFIED AFTER 12 YEARS
DND DIRM 5 J00 10

THIS DOCUMENT CONTAINS INFORMATION OF A CONFIDENTIAL NATURE
AND IS NOT TO BE RELEASED TO THE PUBLIC OR TO ANY OTHER
PERSON OR ORGANIZATION WITHOUT THE WRITTEN AUTHORIZATION OF THE
OFFICE OF THE SECRETARY OF DEFENSE

CONFIDENTIAL

CONFIDENTIAL

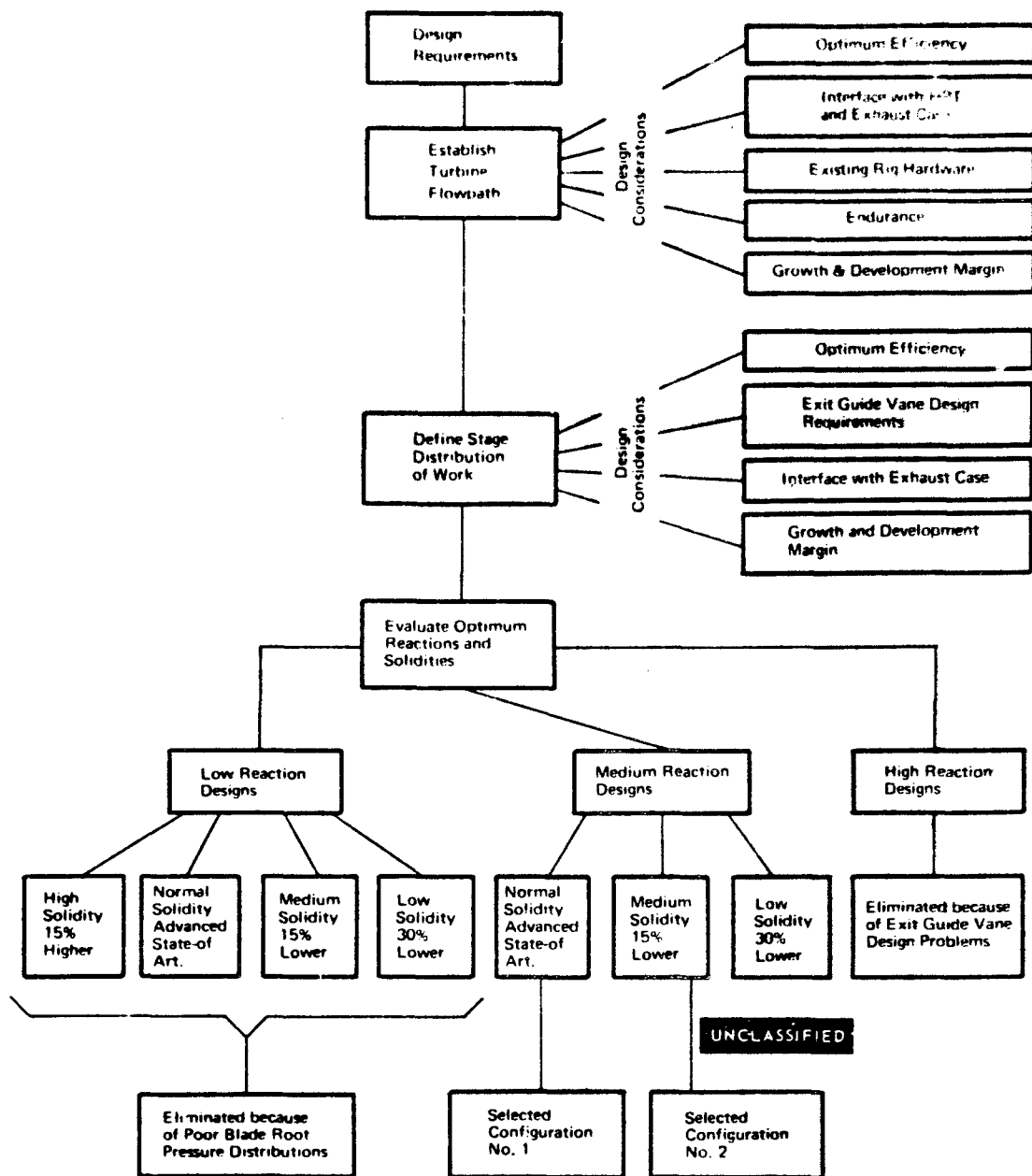


Figure 1 Flow Chart - Phase I, Task 1a

PAGE NO 4

(This page is unclassified)

CONFIDENTIAL

CONFIDENTIAL

3. FLOWPATH ANALYSIS

(U) The turbine configurations are constrained by the contract design parameters which were shown in Table I, namely: load coefficient, first blade tip speed, maximum first blade inlet hub/tip ratio, exit swirl angle, number of stages, turbine inlet temperature, stage efficiency, minimum airflow, and life. In addition to these parameters, values of inlet total pressure and mean inlet swirl angle representative of typical advanced high pressure turbine exit conditions were chosen as 105 psia and 20.4 degrees. An inlet axial Mach number of 0.3 was taken as representative, based on applicable current engine designs. A rotational speed of 10,650 rpm was selected as the greatest possible for the existing turbine test rig, commensurate with the required tip speed and hub/tip ratio. The resulting airflow was 67.7 lb/sec, which will maintain airfoil stress levels within the specified life requirements. Trailing edge radii for all airfoils will be 0.020 inch and shroud clearances will be set at 0.020 inch. These values are representative of advanced turbofan uncooled low pressure turbine designs.

(U) When the above design parameters were established, work on the optimization of the turbine flowpath and flow velocity diagrams proceeded. The existing turbine loss system was used to predict resulting aerodynamic performance.

(U) The flowpaths considered in the study are shown in Figure 2. The inlet area was held constant, since the high pressure turbine flowpath requirements define the inlet vane length for the low pressure turbine. The airfoil lengths were then varied from the minimum inlet value to a maximum at the exit. The inside diameter was held constant in order to provide the largest possible blade velocities.

(C) The results of the flowpath parametric study are shown in Figure 3. In this study, the turbine efficiency was evaluated for a series of turbines, generated by the variation of exit area, reaction level and stage work split. The mean diameter static pressure reaction was varied from 25 to 55 percent, and the work split was varied so that 50, 55 or 60 percent of the total work was extracted from the first stage. The predicted average stage efficiency was above the required 91 percent for almost all of the turbines, with a total variation of only 1 percent (approximate) over the entire study. It should be noted that this variation is of the same order of magnitude as the uncertainty contained in any single prediction; therefore the apparent differences should not be taken too literally.

CONFIDENTIAL

(U) It can be seen that the efficiency was relatively insensitive to exit area variation. The design area of 264 square inches was therefore chosen on the basis of additional considerations: namely, the turbine exit axial Mach number and exit swirl angle. The values of exit swirl are such that an exit guide vane is required to meet the contract specifications of zero exit swirl angle. High-work low pressure turbine optimization studies indicate that these values of exit swirl are required to maintain high efficiencies. Furthermore, practical engine designs require exit guide vanes to provide rear bearing support. It was decided, therefore, to include exit guide vanes to attain a realistic design, and to suffer the associated loss penalty.

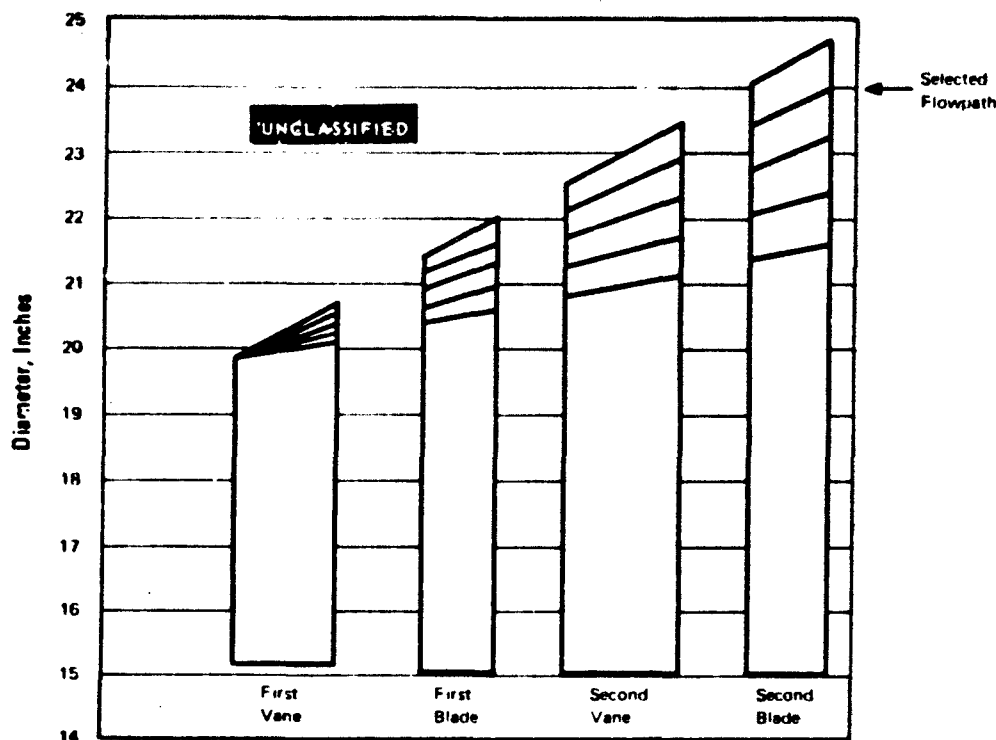


Figure 2 Flowpaths for Turbine Study

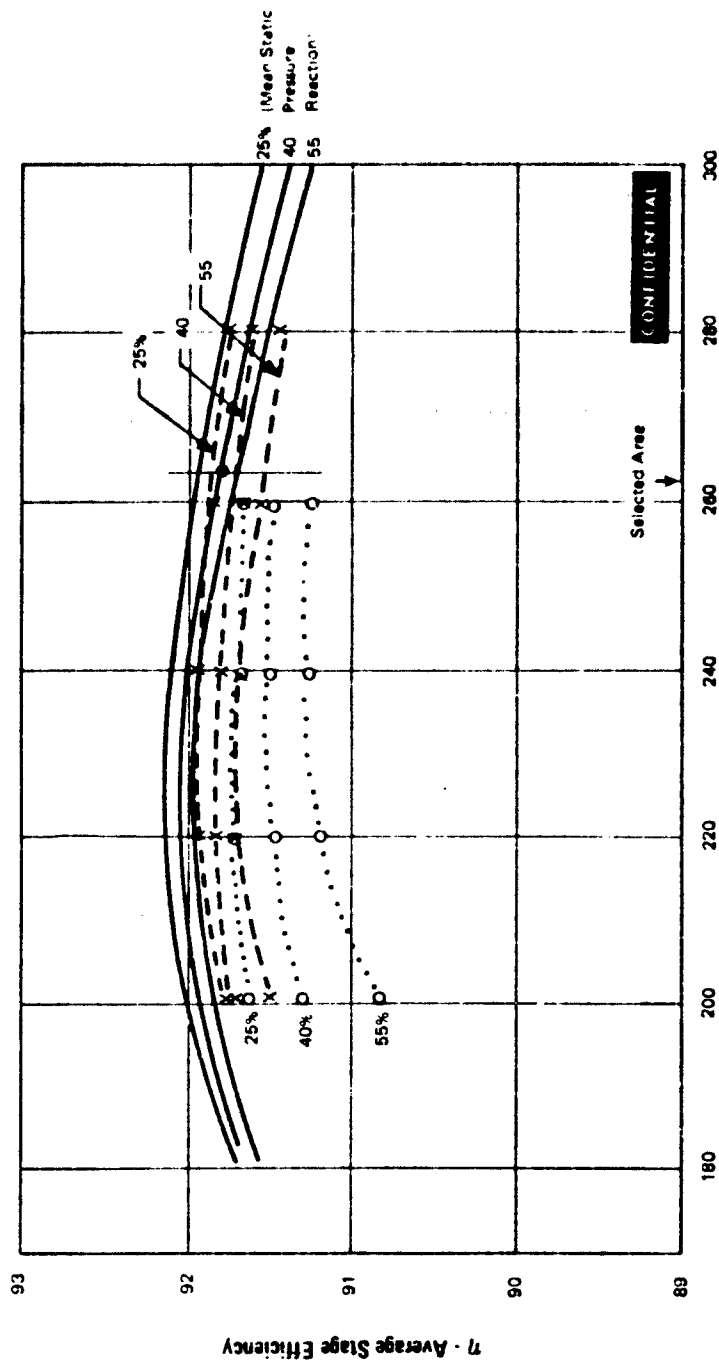
PAGE NO 6

(This page is unclassified)

CONFIDENTIAL

CONFIDENTIAL

Work Split: First Stage
Second Stage
— 50:50
O-O-O 60:40
X-X-X 55:45



Second Stage Exit Annulus Area = in²

Figure 3 Turbine Parametric Study

CONFIDENTIAL

DOWNLOADED AT 1 YEAR INTERVALS
DECLASSIFIED AFTER 12 YEARS
DND ORN 2 200 13

CONFIDENTIAL

(U) Variation of the exit Mach number and exit swirl angle with exit area are shown in Figures 4 and 5, respectively. The reason for choosing a slightly larger exit area than the apparent optimum value was to achieve a much lower exit Mach number. A low Mach number is required for stable combustion in an afterburning engine. A lower turbine exit Mach number allows the use of a shorter and lighter diffuser between the turbine and afterburner. Furthermore, the maximum work potential of the turbine is limited by the choking of the exit guide vanes. Lower turbine exit Mach numbers, therefore, have the additional benefit of increased work potential. A large range of work potential is required for an engine with a variable area jet nozzle. The greater work potential is also beneficial for growth capability and development margin. An exit axial Mach number of 0.43 resulted from the selected exit annulus area. This compares favorably with values of currently applicable Pratt & Whitney Aircraft engines, which range, in exit axial Mach number, from 0.36 to 0.46.

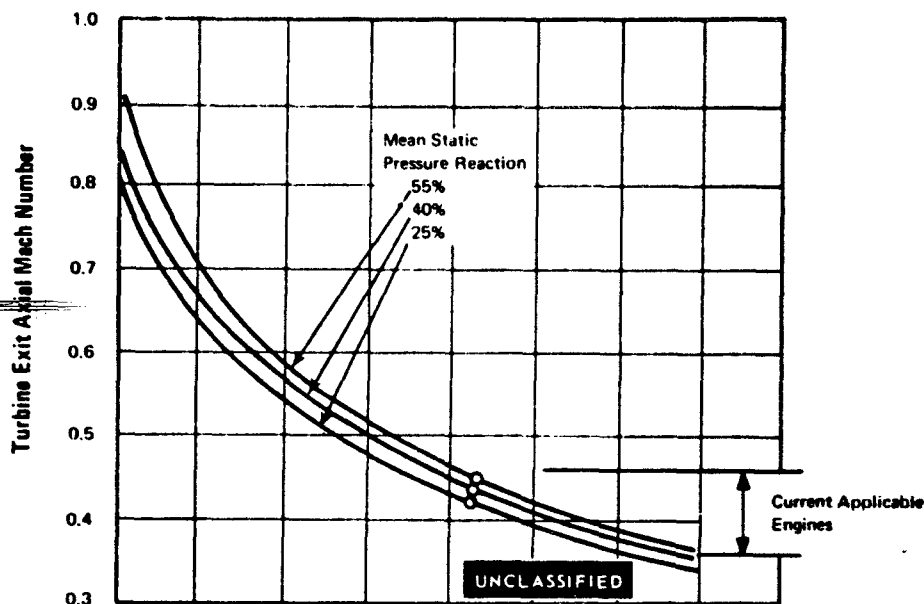


Figure 4 Variation of Turbine Exit Axial Mach Number With Exit Area at Various Reaction Levels

UNCLASSIFIED

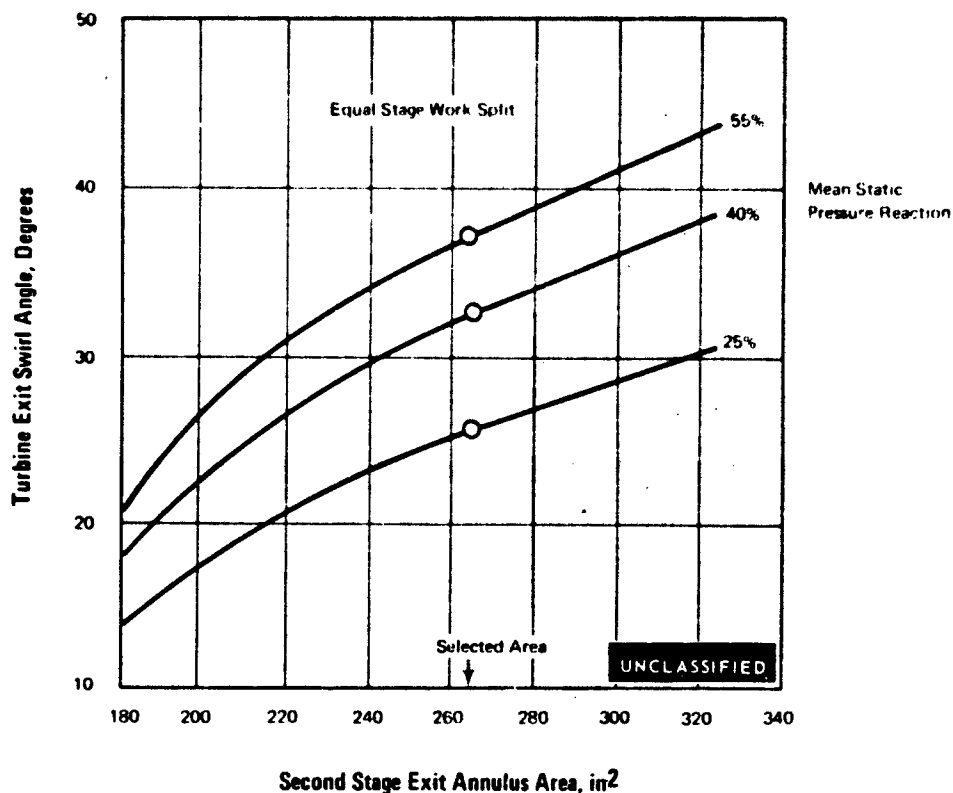


Figure 5 Variation of Turbine Exit Swirl Angle With Exit Area at Various Reaction Levels

4. STAGE-WORK SPLIT

(U) The parametric study (as was shown in Figure 3), which includes the exit guide vane loss, indicates that the optimum stage-work split is 50 percent to each stage at any given reaction level. The exit swirl angle and second blade exit relative Mach number increase rapidly with second-stage work (see Figure 6), which indicates large exit guide vane turning requirements and therefore high exit guide vane losses. Therefore, an equal stage-work split was chosen for the design, and is used throughout the remainder of this study.

UNCLASSIFIED

UNCLASSIFIED

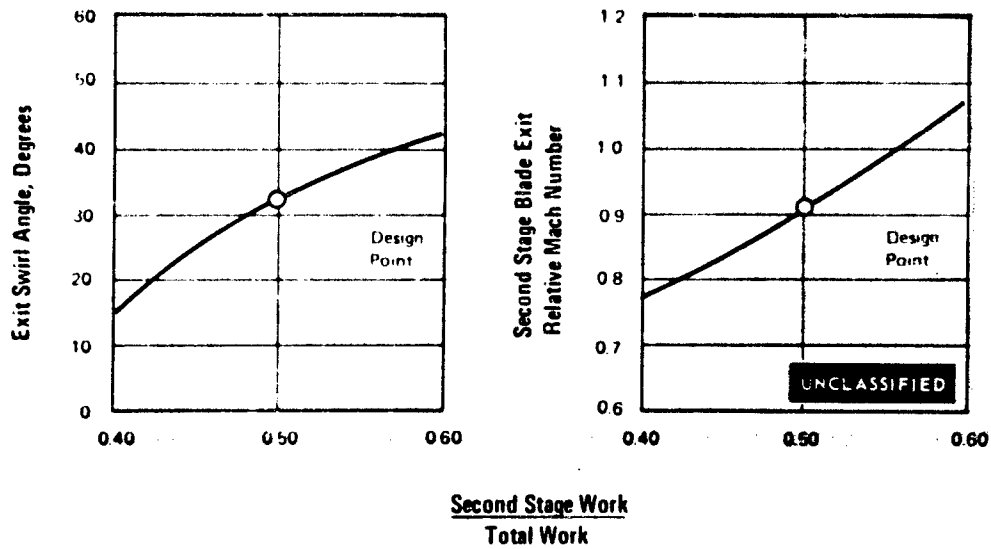


Figure 6 Effect of Second-Stage Work Distribution on Turbine Exit Conditions

5. REACTION

(U) A total of three nominal reaction levels were chosen for the parametric study. A mean second-stage reaction of 55, 40 and 25 percent was used. An additional study indicated that the first-stage reactions should be lower than the corresponding second-stage reactions for optimum turbine efficiency and these were chosen as 45, 30 and 25 percent, respectively. A detailed streamline analysis employing controlled-vortex technique was carried out and a summary is shown in Figure 7, (a) through (c). The solid line indicates the streamline controlled-vortex results while the dashed line indicates the comparable free-vortex distribution. In every case the controlled-vortex designs indicate a much greater root reaction than their free-vortex counterparts, which should reduce corner boundary layer losses.

UNCLASSIFIED

UNCLASSIFIED

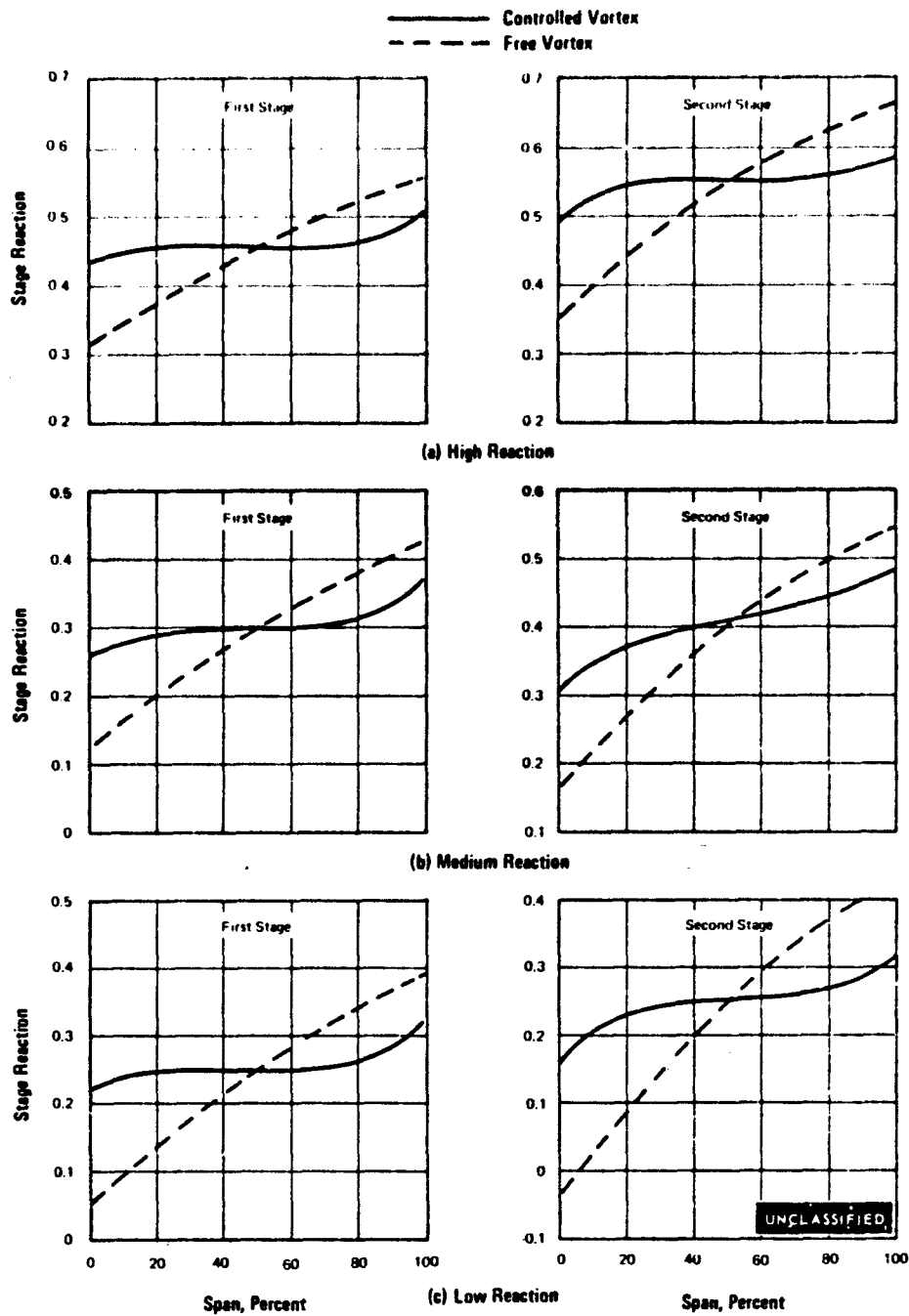


Figure 7 Variation of Stage Reaction With Span for Various Reaction Levels

UNCLASSIFIED

UNCLASSIFIED

(U) Analysis of the exit guide vane performance indicated that an acceptable design could not be achieved for the excessive swirl and Mach numbers which resulted from the combination of high stage loading and high reaction. The exit guide vane inlet Mach number and swirl distribution is shown in Figure 8 and 9, respectively. The swirl angle level was about 38 degrees throughout the span with the Mach number as high as 0.7 even after the blading angles and work distribution had been modified to improve the exit guide vane design. The problem is that a high solidity vane cascade is required to remove the large swirl. Thus the high blockage, resulting from the high solidity and the high inlet Mach number results in a choking condition at the root. Figure 10 shows the exit guide vane choking margin for the high reaction turbine, and indicates that the vane will not pass the required flow at the root. Therefore, the high reaction turbine design was not pursued further in this program.

(U) Airfoils having three solidity levels for the medium reaction and four solidity levels for the low reaction were analyzed. For the preliminary evaluation, the following items were considered to be of significance in making a solidity selection:

- Zweifel Load Coefficient
- Airfoil Pressure Distribution
- Pressure Rise Coefficient ($\Delta P/Q$)
- Maximum Local Surface Mach Number

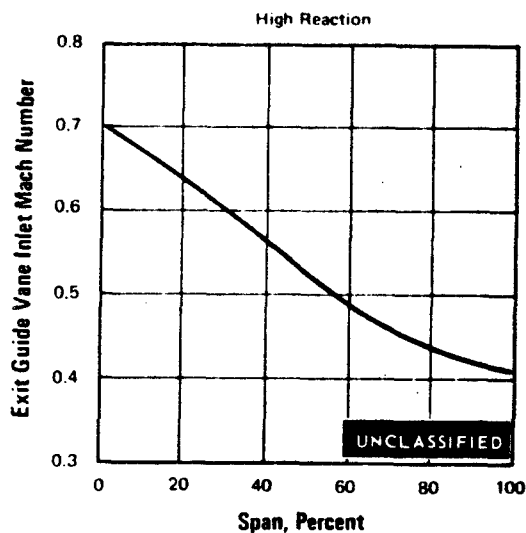


Figure 8 Variation of Exit Guide Vane Inlet Mach Number With Span

UNCLASSIFIED

UNCLASSIFIED

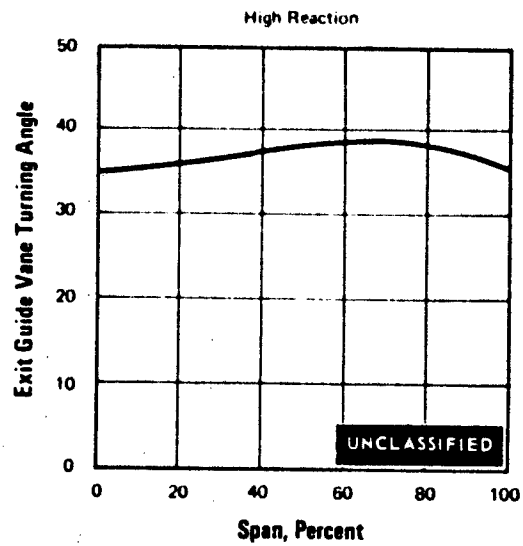


Figure 9 Variation of Exit Guide Vane Turning Angle With Span

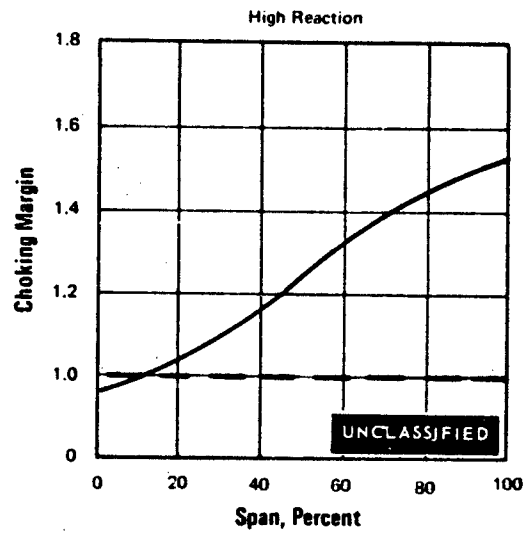


Figure 10 Variation of Choking Margin With Span

UNCLASSIFIED

UNCLASSIFIED

(U) The airfoils designed in this Task required approximately six contour refinements each before adequate pressure distributions resulted, and they are referred to as preliminary airfoils in what follows. The solidity levels were taken in 15% increments about the advanced level referred to as normal in this study. The resulting pressure distributions, convergence ratios, radii of curvature and airfoil sections for all solidities and reactions are found in Appendix I.

(U) Due to the high-stage loading, the turbine blading has higher than normal Mach numbers, and lower than normal airfoil convergence. This is particularly true at the root, since the available wheel speed is lowest at this point. Consequently, the blade root region is potentially a high loss region, especially for a low reaction design. The difficulty is apparent in the low reaction airfoil pressure distribution shown for the preliminary airfoils in Appendix I. The pressure distributions for the low reaction blade roots of the first and second stages indicate that for both blades the lack of convergence has resulted in very low suction surface pressures near the leading edge. Consequently, the gas must decelerate over nearly the entire length of the surface, resulting in an unstable flow condition. The high Mach numbers also introduced the danger of large shock losses. A comparison of the significant design parameters for the low and medium reaction designs of normal solidity is tabulated in Table II. Normal solidity is defined by what are considered advanced state-of-the art Zweifel load coefficients shown in the table.

TABLE II
PRELIMINARY AIRFOILS
LOW REACTION
NORMAL SOLIDITY

UNCLASSIFIED

<u>Section</u>	<u>Pitch Chord</u>	<u>Load Coefficient</u>	<u>Uncovered Turning</u>	<u>$\Delta P/Q$</u>	<u>Maximum Mach Number</u>
First Stage Vane Root	0.942	0.910	14.68	0.363	1.230
First Stage Vane Tip	0.952	0.694	13.18	0.109	0.840
First Stage Blade Root	0.635	0.810	16.00	0.368	1.108
First Stage Blade Tip	0.925	1.095	14.38	0.200	0.800
Second Stage Vane Root	0.760	0.955	13.43	0.378	1.265
Second Stage Vane Tip	0.945	0.769	12.16	0.084	0.918
Second Stage Blade Root	0.555	0.878	17.60	0.598	1.410
Second Stage Blade Tip	0.920	1.106	16.00	0.293	0.931

UNCLASSIFIED

CONFIDENTIAL

TABLE II (Cont'd)

MEDIUM REACTION

NORMAL SOLIDITY

UNCLASSIFIED

<u>Section</u>	<u>Pitch Chord</u>	<u>Load Coefficient</u>	<u>Uncovered Turning</u>	<u>$\Delta P/Q$</u>	<u>Maximum Mach Number</u>
First Stage Vane Root	1.003	0.950	13.8	0.259	1.112
First Stage Vane Tip	1.147	0.799	13.0	0.126	0.820
First Stage Blade Root	0.683	0.840	17.4	0.337	1.108
First Stage Blade Tip	1.088	1.100	13.8	0.210	0.830
Second Stage Vane Root	0.708	0.958	13.3	0.308	1.200
Second Stage Vane Tip	0.967	0.810	12.9	0.179	0.853
Second Stage Blade Root	0.566	0.900	14.8	0.488	1.305
Second Stage Blade Tip	1.193	0.941	12.8	0.250	1.043

The surface Mach numbers and pressure rise coefficients tend to be highest for both the vanes and blades at the low reaction levels. It was, therefore, concluded that the medium reaction turbine design has the greatest potential to attain high turbine efficiencies. The remainder of the study, then, is concerned only with 50/50 work-split medium-reaction turbine designs.

(U) The medium reaction turbine design was selected based on the airfoil surface pressure distribution analysis. The selection of medium reaction was further substantiated by the existing turbine rig test data. Test results from various single stage rotating rigs indicate that the optimum turbine efficiency is achieved at blade root reaction levels of 40 to 60 percent.

(U) It should be noted that the predicted turbine efficiency for the turbines at various reaction levels indicates (refer to Figure 3) that a higher efficiency can be attained at the lowest mean reaction, for all stage-work splits. This is basically due to the fact that the current loss system does not include the effects of corner boundary layer separation and Mach number. A fall-off in efficiency should occur at low reaction because the airfoil pressure distributions indicate that separation would take place in the root region. On the other hand, the efficiency would fall off for very high reaction turbines because of the associated high exit Mach numbers from the blades and additional camber in the second-stage vane and exit guide vane. A comparison of some of the significant vector diagram parameters is presented in Figures 11 and 12 for turbines having the three reactions mentioned above.

(This page is unclassified)

CONFIDENTIAL

CONFIDENTIAL

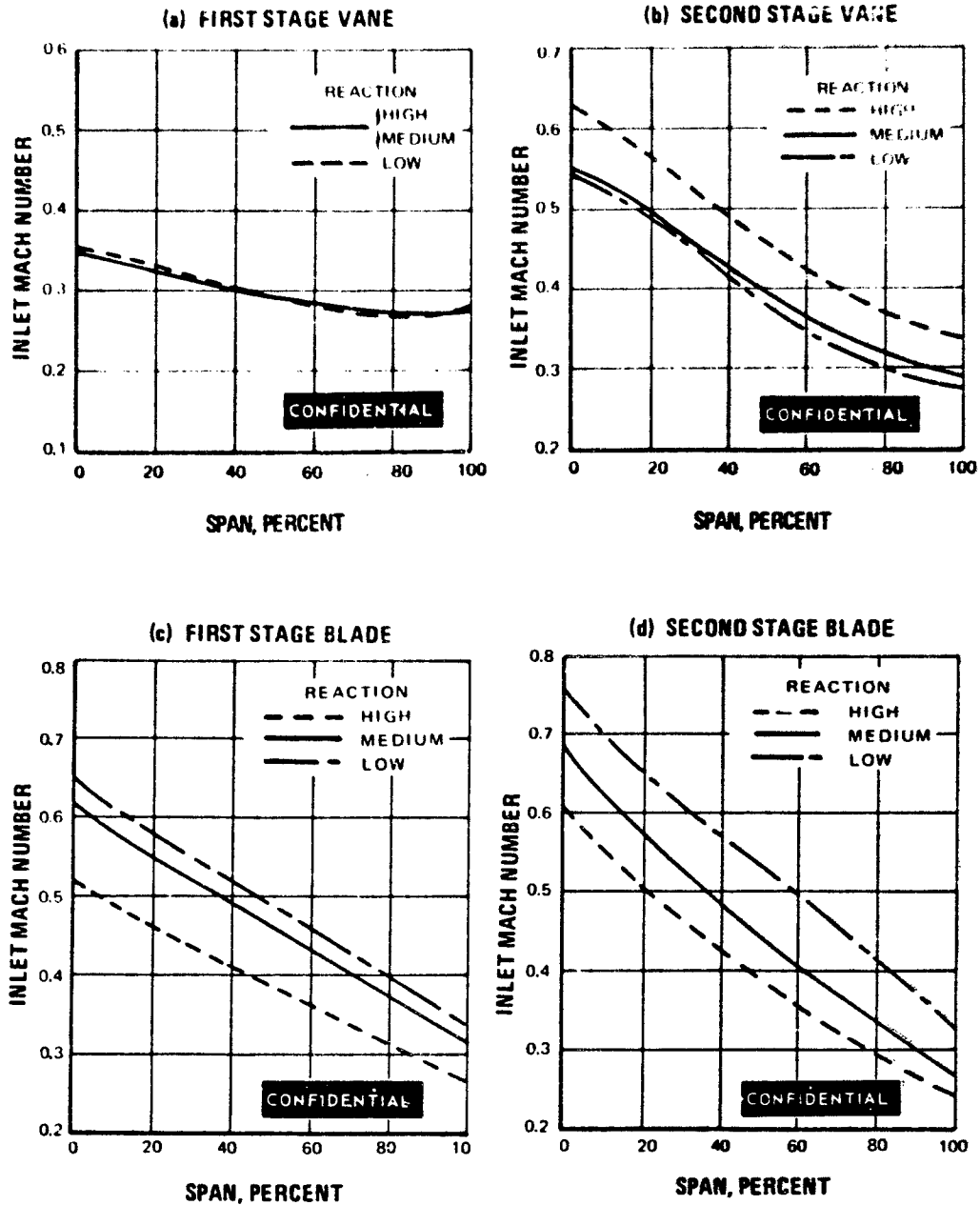


Figure 11 Variation of Inlet Mach Number With Span at Various Reaction Levels

CONFIDENTIAL

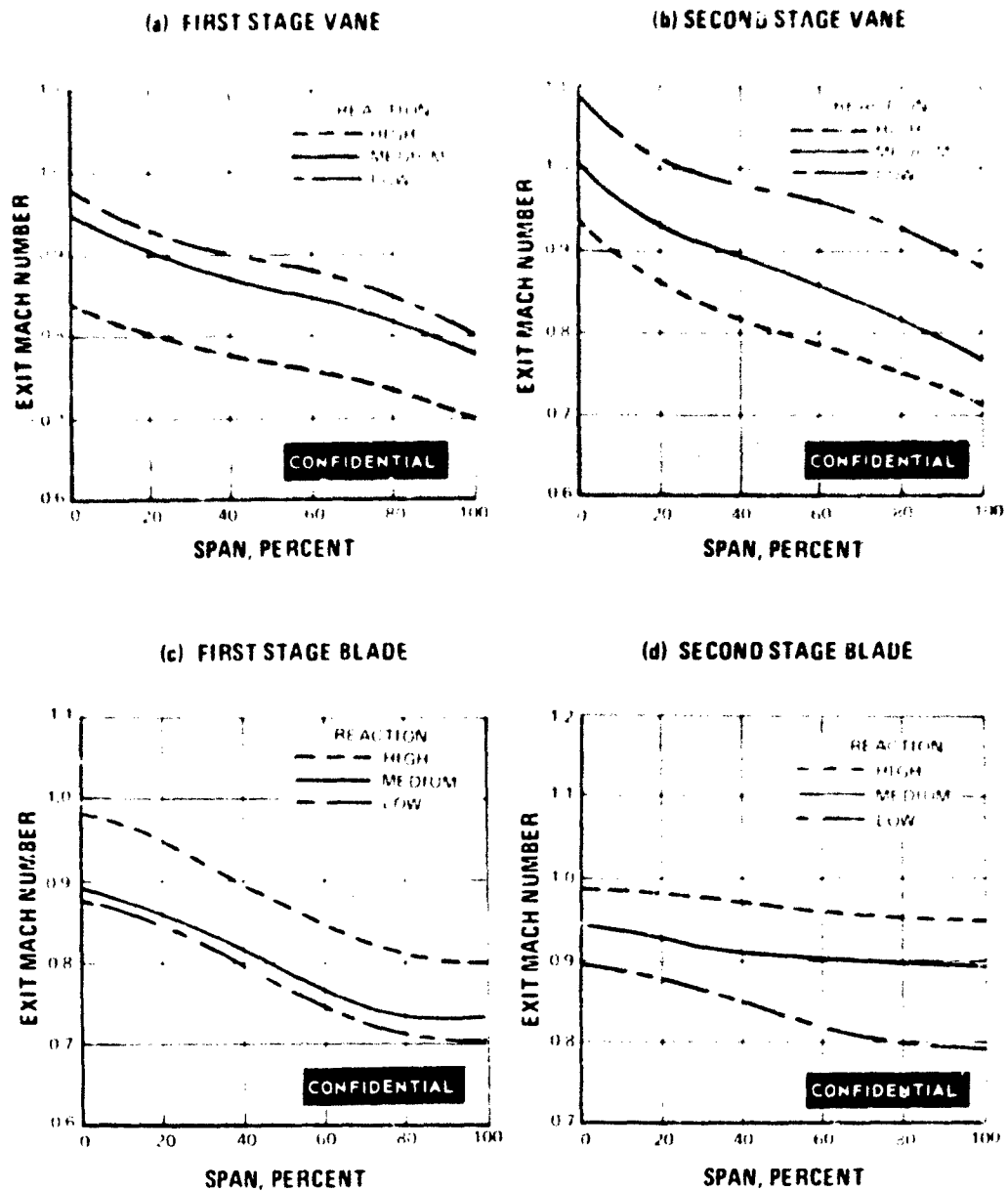


Figure 12 Variation of Exit Mach Number With Span at Various Reaction Levels

CONFIDENTIAL

(C) The radial work distribution for the second-stage is shown in Figure 13. The exit guide vane turning angle and inlet Mach number are shown in Figure 14 for the three reaction levels. Although the general level of exit guide vane turning increased with higher reaction, the increase in root swirl was minimized by the reduction in second-stage root work output. The exit guide vane inlet Mach number increases with increasing reaction. It was this combination of higher Mach number and turning that made the exit guide vane design impractical for the high reaction configuration.

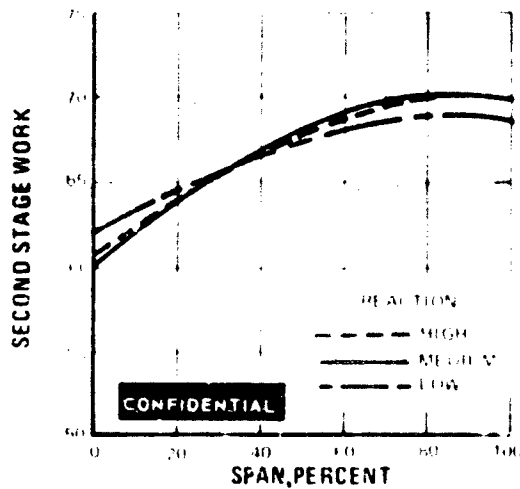


Figure 13 Variation of Second Stage Work With Span for Various Reaction Levels

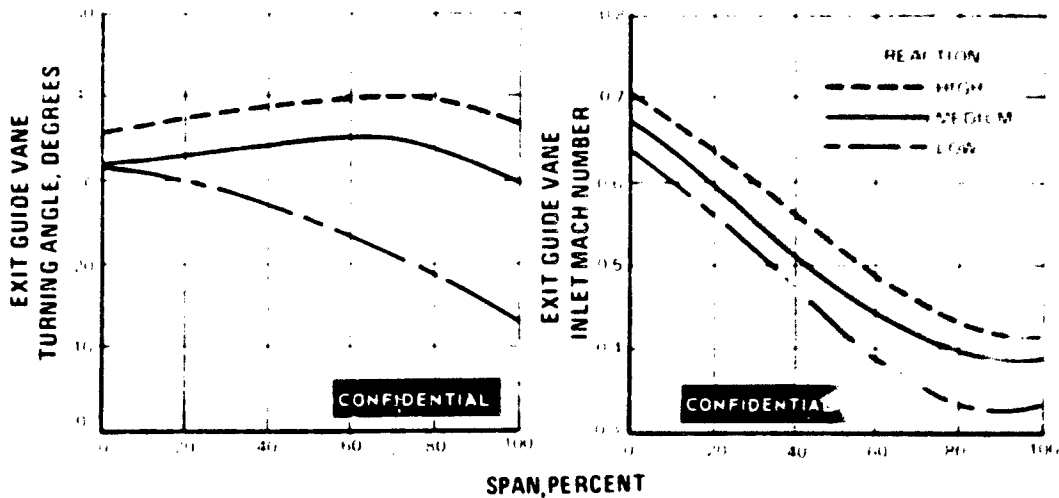


Figure 14 Variation of Exit Guide Vane Turning Angle and Inlet Mach Number With Span at Various Reaction Levels

CONFIDENTIAL

CONFIDENTIAL

(U) In summary, based on the fact that the high reaction configuration had an impractical exit guide vane design, and that the low reaction configuration had potentially high loss blade root airfoil sections, the final configurations resulting from this initial task were for the medium reaction level. The medium reaction velocity diagram data is presented for the first stage in Table III and for the second stage in Table IV.

TABLE III
FIRST STAGE TURBINE DATA - MEDIUM REACTION

Inlet Total Pressure (Pto) psia	-	105.0
Inlet Total Temperature (Tto) (°R)	-	1910.0
Gas Flow (Wg) (lbs/sec)	-	67.7
Total/total Efficiency (Ntt)	-	90.5
Turbine Work (ΔH) (Btu/lb.)	-	67.3

CONFIDENTIAL	Root	Mean	Tip
Stage Total Pressure Ratio (P_{t0}/P_{t2})	1.88	1.85	1.80
Vane Static Pressure Ratio (P_{s0}/P_{s1})	1.66	1.54	1.42
Blade Static Pressure Ratio (P_{s1}/P_{s2})	1.32	1.30	1.34
Vane Inlet Gas Angle (α_0)	64.1	59.6	61.6
Vane Exit Gas Angle (α_1)	26.5	22.7	18.3
Vane Camber (θ_v)	89.4	97.7	100.1
Blade Inlet Gas Angle (β_1)	37.6	39.0	45.4
Blade Exit Gas Angle (β_2)	24.7	24.7	24.7
Blade Camber (θ_b)	117.7	116.3	109.9
Stage Exit Swirl Angle	40.2	52.1	66.4
Blade Inlet Absolute Gas Velocity (C_1)	1820.0	1654.0	1481.0
Blade Exit Absolute Gas Velocity (C_2)	1092.0	822.0	695.0
Blade Inlet Relative Gas Velocity (W_1)	1214.0	928.0	634.0
Blade Exit Relative Gas Velocity (W_2)	1689.0	1499.0	1414.0
Blade Inlet Tangential Velocity (U_1)	701.0	835.0	981.0
Blade Exit Tangential Velocity (U_2)	701.0	862.0	1005.0
Blade Reaction ($P_{s1}-P_{s2}/P_{s0}-P_{s2}$)	25.9	30.1	37.3
Vane Inlet Absolute Mach Number (M_{0ab})	0.345	0.290	0.279
Vane Exit Absolute Mach Number (M_{1ab})	0.949	0.854	0.770
Blade Inlet Relative Mach Number (M_{1rel})	0.622	0.469	0.317
Blade Exit Relative Mach Number (M_{2rel})	0.890	0.780	0.730
Interstage Axial Mach Number	0.371	0.320	0.298

CONFIDENTIAL

TABLE IV

SECOND STAGE TURBINE DATA - MEDIUM REACTION

Inlet Total Pressure (P_{t0}) (psia)	-	56.8
Inlet Total Temperature (T_{t0}) (°R)	-	1663.1
Gas Flow (W_g) (lbs/sec)	-	67.7
Total/Total Efficiency (η_{tt})	-	91.5
Turbine Work (ΔH) (Btu/lb)	-	67.2

CONFIDENTIAL	Root	Mean	Tip
Stage Total Pressure Ratio (P_{t0}/P_{t2})	1.88	2.05	2.09
Vane Static Pressure Ratio (P_{s0}/P_{s1})	1.57	1.50	1.4
Blade Static Pressure Ratio (P_{s1}/P_{s2})	1.32	1.51	1.61
Vane Inlet Gas Angle (α_0)	37.3	50.0	61.9
Vane Exit Gas Angle (α_1)	30.6	24.5	22.6
Vane Camber (θ_v)	112.1	105.5	95.5
Blade Inlet Gas Angle (β_1)	45.4	47.1	67.0
Blade Exit Gas Angle (β_2)	37.0	28.9	22.3
Blade Camber (θ_b)	97.6	104.0	90.7
Stage Exit Swirl Angle (α_2)	57.7	57.9	59.8
Blade Inlet Absolute Gas Velocity (C_1)	1798.0	1570.0	1355.0
Blade Exit Absolute Gas Velocity (C_2)	1178.0	917.0	711.0
Blade Inlet Relative Gas Velocity (W_1)	1242.0	824.0	506.0
Blade Exit Relative Gas Velocity (W_2)	1655.0	1591.0	1586.0
Blade Inlet Tangential Velocity (U_1)	693.0	891.0	1090.0
Blade Exit Tangential Velocity (U_2)	693.0	906.0	1112.0
Blade Reaction ($P_{s1}-P_{s2}/P_{s0}-P_{s2}$)	30.3	40.8	48.5
Vane Inlet Absolute Mach Number (M_{oab})	0.554	0.385	0.292
Vane Exit Absolute Mach Number (M_{lab})	1.003	0.869	0.765
Blade Inlet Relative Mach Number (M_{1rel})	0.698	0.446	0.269
Blade Exit Relative Mach Number (M_{2rel})	0.944	0.904	0.892
Interstage Axial Mach Number	0.568	0.435	0.337

6. SOLIDITY

(U) Once the reaction level was chosen for the design, the solidity had to be determined. The important preliminary airfoil parameters were tabulated for normal solidity levels in Table II and are shown for the medium and low solidity in Table V.

UNCLASSIFIED

TABLE V

MEDIUM REACTION - MEDIUM SOLIDITY (+15% LOAD COEFFICIENT)

Section	<u>Pitch Chord</u>	<u>Load Coefficient</u>	<u>Uncovered Turning</u>	<u>$\Delta P/Q$</u>	<u>Maximum Mach No.</u>
First Stage Vane Root	1.152	1.090	14.7	0.337	1.170
First Stage Vane Tip	1.317	0.920	15.4	0.236	0.884
First Stage Blade Root	0.792	0.966	17.7	0.413	1.160
First Stage Blade Tip	1.262	1.275	14.8	0.309	0.884
Second Stage Vane Root	0.809	1.100	14.4	0.391	1.280
Second Stage Vane Tip	1.105	0.930	14.2	0.248	0.892
Second Stage Blade Root	0.648	1.035	16.4	0.548	1.361
Second Stage Blade Tip	1.366	1.078	13.4	0.317	1.092

MEDIUM REACTION - LOW SOLIDITY (+30% LOAD COEFFICIENT)

First Stage Vane Root	1.296	1.235	16.0	0.444	1.270
First Stage Vane Tip	1.482	1.038	18.5	0.369	0.970
First Stage Blade Root	0.880	1.092	18.5	0.495	1.230
First Stage Blade Tip	1.403	1.419	16.8	0.421	0.955
Second Stage Vane Root	0.913	1.245	16.0	0.511	1.390
Second Stage Vane Tip	1.247	1.052	15.2	0.282	0.907
Second Stage Blade Root	0.743	1.170	18.4	0.656	1.464
Second Stage Blade Tip	1.565	1.236	14.7	0.387	1.148

The lowest solidity possible for which a separation free flow can be predicted was to be selected in order to ensure the required turbine performance. As part of Task 1a, two preliminary turbine designs (ref. Figure 1) had to be chosen, after which a boundary layer analysis was to be applied to determine each design's inherent resistance to flow separation.

(U) Since all of the three loading parameters increase toward flow separation with reduced solidity, one turbine configuration was selected which met all of the present turbine design criteria, that is, the medium reaction normal solidity configuration which was shown in Table II. This configuration would ensure no separation, and minimize the risk of falling below the target efficiency. The second configuration chosen would have solidity levels below present experience. Depending on the results of the airfoil refinement study, the solidity would be selected as low as possible in accordance with our ability to design separation free airfoil sections.

(The reverse of this page is blank)

UNCLASSIFIED

UNCLASSIFIED

SECTION III

AIRFOIL CONTOUR ANALYSIS (Task 1b)

1. REF OBJECTIVE

(U) Design airfoil contours having the highest resistance to flow separation.

2. TASK OBJECTIVE

(U) The turbine flowpath and vector diagram study described in Section II resulted in an optimum turbine with medium reaction level, equal stage-work split and with an elevation such that the exit annulus area is 264 square inches. Three levels of solidity for each airfoil were considered and as part of the Task 1a effort, preliminary airfoil sections were designed but were found to be too crude to make a logical choice of those airfoils which needed further refinement. Therefore, the necessary detailed airfoil contour analysis was conducted during this Task.

3. PRELIMINARY AIRFOIL ANALYSIS

(U) The preliminary airfoils for the medium reaction at three solidities and at three spanwise sections are shown in Appendix I. For convenience the pertinent aerodynamic parameters are tabulated in Table VI. An average of six calculations had to be made to arrive at the airfoils shown in these figures. These root, mean and tip airfoil sections for both vanes and blades ~~were evaluated~~ according to the following considerations:

- Suction and Pressure Surface Pressure Distributions
- Suction Surface Radius of Curvature
- Passage Convergence
- Airfoil Cross Section.

(U) The pressure distribution is the most important preliminary indicator used in the evaluation. Values of suction surface pressure coefficient ($\Delta P/Q$) and diffusion parameter (E), based on the minimum and exit pressures, are the determining factors in the preliminary evaluation. Values of ($\Delta P/Q$) above 0.5 are taken to indicate separating airfoils. At the same time, convergence is examined to insure a uniformly converging channel. The suction surface radius of curvature is also important since the airfoil surface pressure distribution is highly sensitive to this parameter, and therefore it is the most basic design parameter to be varied when

UNCLASSIFIED

modifying the pressure distribution. This is particularly true when some supersonic flow regions exist which is true for most of the resulting airfoils. The design of the airfoil cross section must be examined from a structural standpoint. A radial area distribution or taper must be selected such that the stress levels are acceptable from the standpoint of endurance.

TABLE VI
MEDIUM REACTION PRELIMINARY AIRFOIL SUMMARY

	<u>No. of Foils, Z</u>	<u>Exit Mach Number, M_2</u>	<u>$\Delta P/Q$</u>	<u>E</u>	<u>Max. Surface Mach Number</u>
First Stage Vane Root					
Normal Solidity	62	0.949	0.259	0.235	1.112
Medium Solidity	54	0.949	0.337	0.296	1.170
Low Solidity	48	0.942	0.443	0.384	1.270
First Stage Vane Mean					
Normal Solidity	62	0.852	0.213	0.208	0.966
Medium Solidity	54	0.852	0.348	0.311	1.058
Low Solidity	48	0.852	0.456	0.396	1.144
First Stage Vane Tip					
Normal Solidity	62	0.770	0.126	0.034	0.820
Medium Solidity	54	0.770	0.235	0.225	0.884
Low Solidity	48	0.770	0.369	0.331	0.970
First Stage Blade Root					
Normal Solidity	116	0.890	0.337	0.169	1.108
Medium Solidity	100	0.890	0.413	0.365	1.160
Low Solidity	90	0.890	0.495	0.423	1.230
First Stage Blade Mean					
Normal Solidity	116	0.788	0.331	0.305	0.968
Medium Solidity	100	0.788	0.418	0.376	1.031
Low Solidity	90	0.788	0.527	0.456	1.119
First Stage Blade Tip					
Normal Solidity	116	0.730	0.210	0.243	0.830
Medium Solidity	100	0.730	0.303	0.289	0.884
Low Solidity	90	0.730	0.416	0.382	0.955

UNCLASSIFIED

UNCLASSIFIED

UNCLASSIFIED

TABLE VI (Cont'd)

MEDIUM REACTION PRELIMINARY AIRFOIL SUMMARY

	<u>No. of Foils, Z</u>	<u>Exit Mach Number, M_2</u>	<u>$\Delta P/Q$</u>	<u>E</u>	<u>Max Surface Mach Number</u>
Second Stage Vane Root					
Normal Solidity	80	0.990	0.308	0.275	1.200
Medium Solidity	70	0.990	0.391	0.336	1.280
Low Solidity	62	1.000	0.511	0.415	1.390
Second Stage Vane Mean					
Normal Solidity	80	0.870	0.227	0.214	0.999
Medium Solidity	70	0.870	0.314	0.289	1.060
Low Solidity	62	0.870	0.362	0.328	1.097
Second Stage Vane Tip					
Normal Solidity	80	0.765	0.179	0.185	0.853
Medium Solidity	70	0.765	0.248	0.252	0.892
Low Solidity	62	0.765	0.282	0.271	0.907
Second Stage Blade Root					
Normal Solidity	126	0.944	0.488	0.412	1.305
Medium Solidity	110	0.944	0.548	0.449	1.361
Low Solidity	96	0.944	0.656	0.503	1.464
Second Stage Blade Mean					
Normal Solidity	126	0.904	0.263	0.244	1.067
Medium Solidity	110	0.904	0.378	0.304	1.156
Low Solidity	96	0.904	0.495	0.423	1.256
Second Stage Blade Tip					
Normal Solidity	126	0.892	0.260	0.236	1.051
Medium Solidity	110	0.892	0.321	0.290	1.092
Low Solidity	96	0.892	0.387	0.346	1.148

UNCLASSIFIED

(U) Having established satisfactory preliminary turbine airfoils, the next step in the airfoil contour design was a preliminary two-dimensional boundary layer calculation intended to evaluate the boundary layer characteristics of each airfoil root section at the three solidities. The root sections tend to be most prone to separation and should receive the most attention. The results of these analyses and available correlations of cascade diffusion parameter data determined the selection of airfoils for refinement and final boundary layer calculations.

UNCLASSIFIED

UNCLASSIFIED

4. PRELIMINARY BOUNDARY LAYER ANALYSIS

(U) Two dimensional boundary layer calculations were generated for the preliminary suction surface root sections at normal, medium and low solidity. The purpose of these calculations was to assist in the selection of practical lower solidity limits prior to airfoil contour refinement.

(U) Two boundary layer calculations were made for each root section and these are shown in Tables VII and VIII. The first assumed no transition and continued either until laminar separation was indicated, or the end of the airfoil was reached. Table VII gives the boundary layer parameters at the last calculation point prior to separation. The two-dimensional criteria used to determine if an airfoil section is at the verge of separation was a drag coefficient of 0.001 or less. Values of Reynold's Number based on momentum thickness at the point of transition are also shown. This value was not used as an indicator of transition but is presented for reference only. When compared to the Tetervin's incompressible flat plate, zero turbulence, zero pressure gradient value of approximately 187, it is noted that the airfoil values were always above this number.

TABLE VII
LAMINAR SEPARATION AT ROOT

Solidity	Distance on Surface to Separation, Inches	Separation Reynolds Number, Re θ	P_s/P_T	Shape Factor H	Drag Coefficient C_f
First Vane					
Medium	0.768	406	0.442	3.523	0.00083
Low	0.675	391	0.400	3.851	0.00062
First Blade					
Medium	0.427	292	0.458	3.840	0.00064
Low	0.544	335	0.423	3.836	0.00070
Second Vane					
Medium	0.440	228	0.390	3.572	0.00172
Low	0.737	311	0.330	3.779	0.00126
Second Blade					
Medium	0.601	272	0.368	3.713	0.00138
Low	0.535	260	0.318	4.198	0.00092

UNCLASSIFIED

UNCLASSIFIED

UNCLASSIFIED

TABLE VIII
TURBULENT BOUNDARY LAYER - ROOT SECTION

Solidity	Distance on Surface to Transition, Inches	Transition Reynolds Numbers Re_{θ}	Data Point, C_{smax}	P_s/P_t	Shape Factor H	Drag Coefficient C_f
First Vane						
Medium	0.650	350	87.6	0.545	2.05	0.00261
Low	0.550	320	88.5	0.560	2.03	0.00233
First Blade						
Normal	0.225	185	87.0	0.547	2.02	0.00308
Medium	0.252	197	86.9	0.569	2.07	0.00239
Low	0.351	239	87.0	0.581	2.14	0.00193
Second Vane						
Medium	0.440	228	88.5	0.465	2.23	0.00260
Low	0.487	251	88.4	0.488	2.27	0.00228
Second Blade						
Normal*	0.170	125	89.0	0.463	2.30	0.00282
Medium*	0.200	139	89.0	0.466	2.38	0.00212
Low*	0.228	147	89.0	0.478	2.56	0.00105

*Separation Apparently at About 94 percent of S_{max} .

UNCLASSIFIED

(U) The second boundary layer calculation assumed transition to turbulent flow at the first minimum on the suction side pressure profile. No turbulent boundary layer separation was indicated except near the trailing edge of the second blade root. Table VIII presents a summary of these turbulent boundary layer calculations at approximately 90 percent of the total suction surface length, prior to the predicted sharp recompression near the trailing edge. Cascade test data indicates, however, that the actual measured recompression is much softer than that indicated by the calculation. The validity of the pressure distribution calculation used is questionable for the last 8 percent of the airfoil surface. Therefore, within the limitations of the analysis, none of the airfoil root sections indicate turbulent separation.

UNCLASSIFIED

UNCLASSIFIED

(U) The effect of transition point location was evaluated for the first vane and tabulated in Table IX. Moving the transition point fore or aft of the first minimum pressure point did not have a significant effect on the turbulent boundary layer behavior.

TABLE IX
EFFECT OF MOVING TRANSITION POINT
FIRST VANE ROOT SECTION

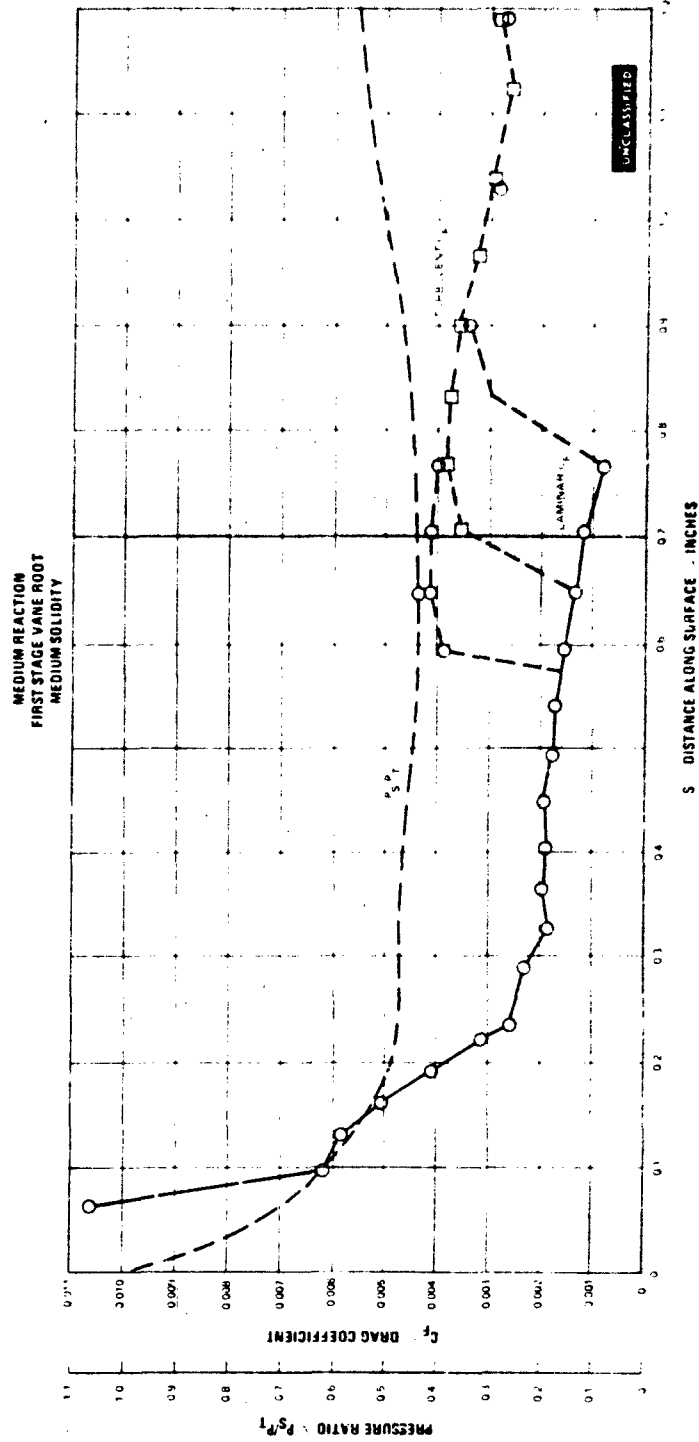
Low Solidity						
Distance to Transition, Inches	$\% S_{max}$	Drag Coefficient C_F	UNCLASSIFIED			
			δ^*	θ	H	δ
0.475	88.5	0.00225	0.00602	0.00294	2.044	0.0295
0.550	88.5	0.00233	0.00567	0.00278	2.039	0.0283
0.675	88.5	0.00246	0.00516	0.00253	2.035	0.0258
Medium Solidity						
0.575	87.5	0.00249	0.00491	0.00240	2.047	0.0250
0.650	87.5	0.00261	0.00447	0.00218	2.051	0.0228
0.768	87.5	0.00271	0.00404	0.00196	2.059	0.0210

(U) Selected plots of static-to-total pressure ratio and drag coefficient as functions of airfoil suction surface distance are shown in Figures 15 through 22. The medium and low solidity root sections of the preliminary turbine airfoils are shown, since these solidities are more critical than the normal solidity. Furthermore, a comparison of the pressure ratio and drag coefficients of all three solidities for the second-stage blade root, the most critical airfoil section in the turbine, are shown in Figure 23 and 24. The early laminar separation indicated for normal solidity is probably caused by lack of contour refinement relative to the more highly loaded airfoils.

(U) The drag coefficient is a significant parameter which indicates turbulent boundary layer behavior. Some trends on the variation of the drag coefficient (at the 90 percent point) with solidity is shown for vane roots in Figure 25, and for blade roots in Figure 26. For two-dimensional turbulent boundary layers, it is doubtful that separation can be avoided with drag coefficients 0.001 or less. Therefore, on a two-dimensional basis, the low solidity second blade root appears to be on the verge of separation, whereas the root section boundary layers of the other foils exhibit some residual strength at low solidity.

UNCLASSIFIED

UNCLASSIFIED



UNCLASSIFIED

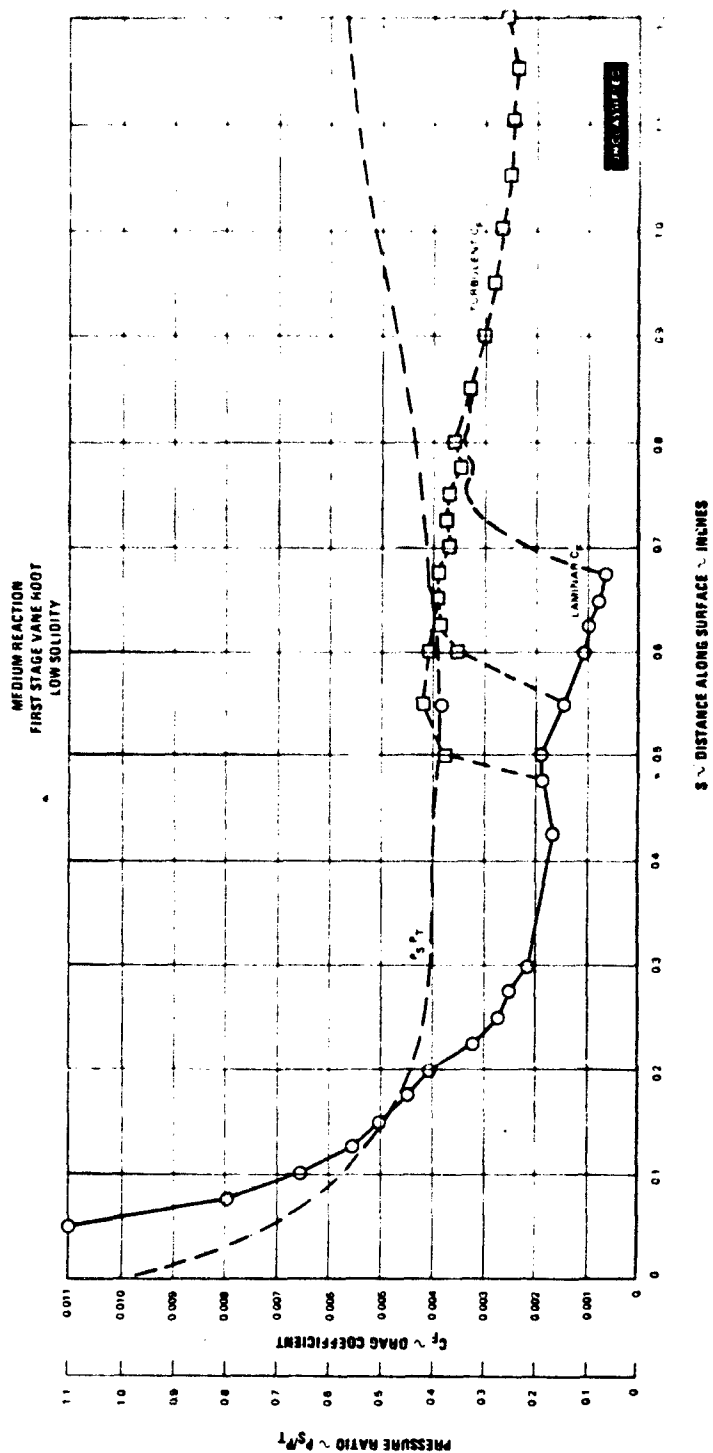


Figure 16

UNCLASSIFIED

UNCLASSIFIED

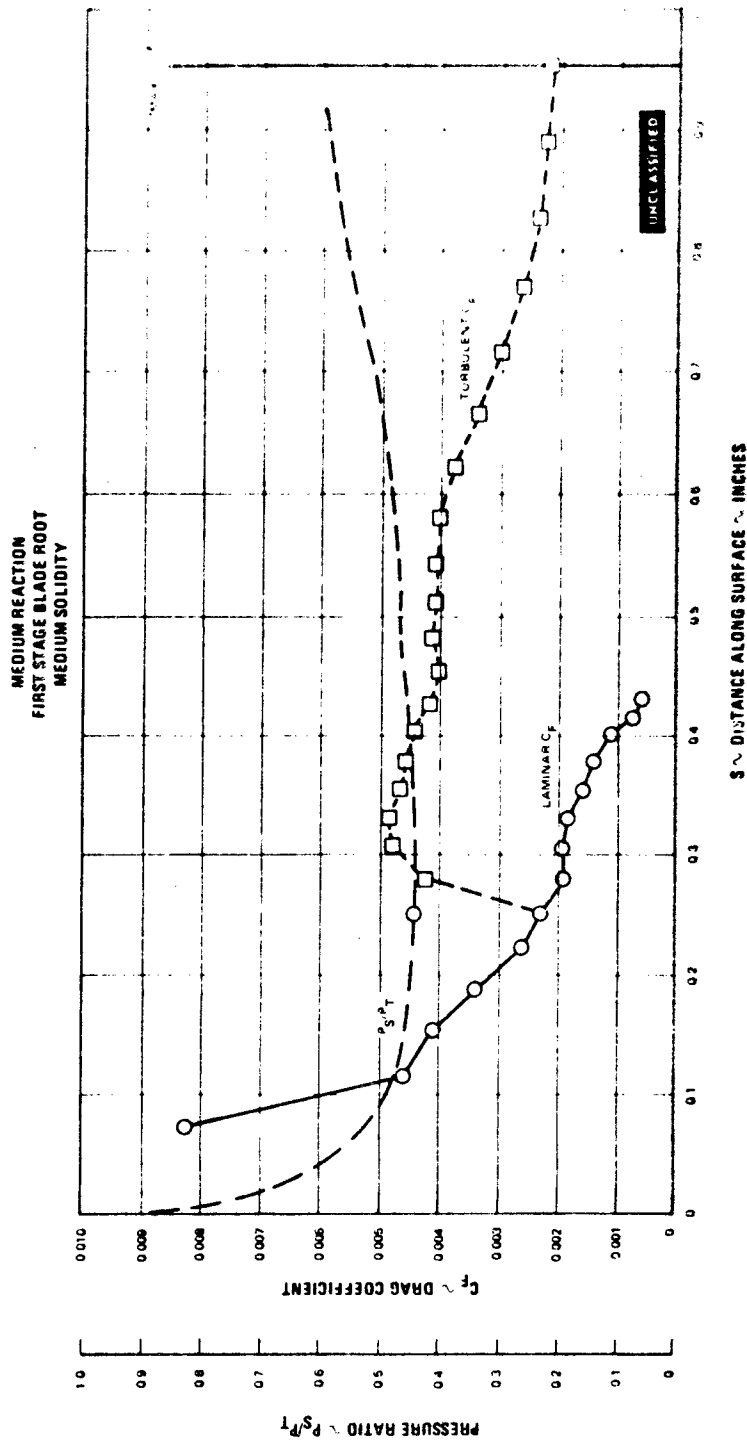


Figure 17

UNCLASSIFIED

UNCLASSIFIED

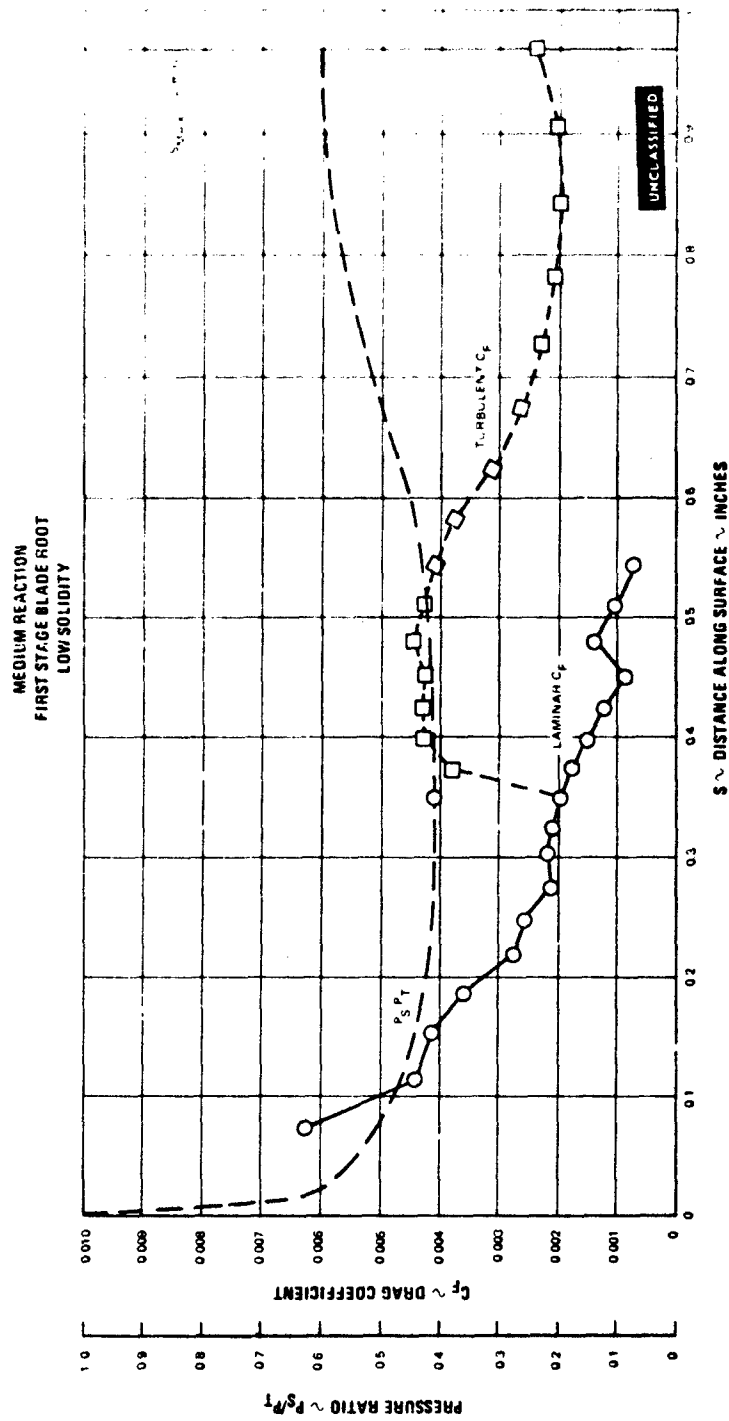


Figure 18

UNCLASSIFIED

UNCLASSIFIED

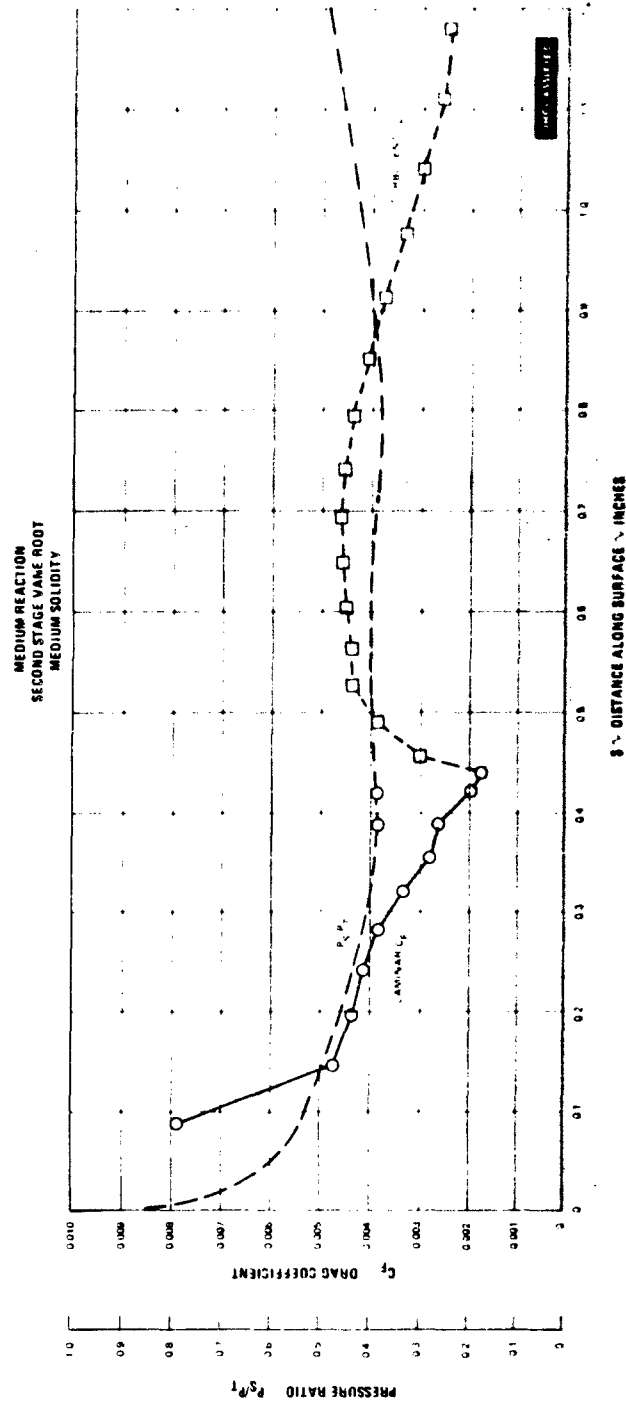


Figure 19

UNCLASSIFIED

UNCLASSIFIED

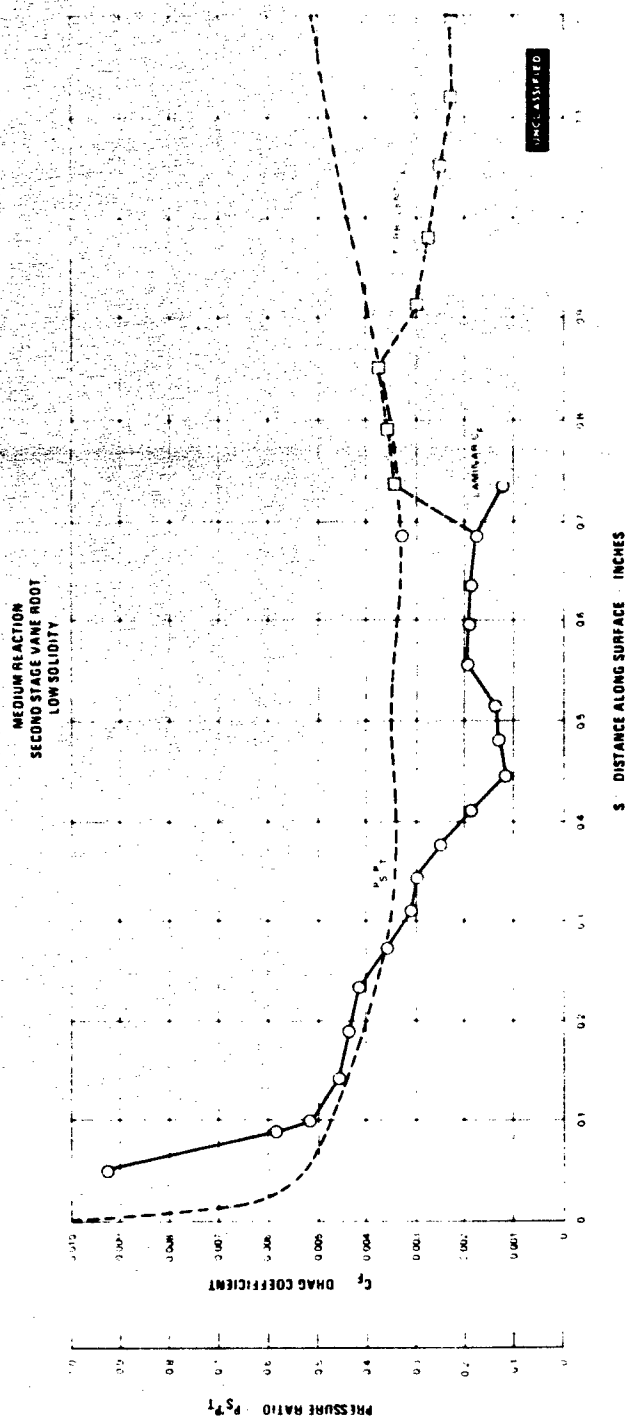


Figure 20

UNCLASSIFIED

UNCLASSIFIED

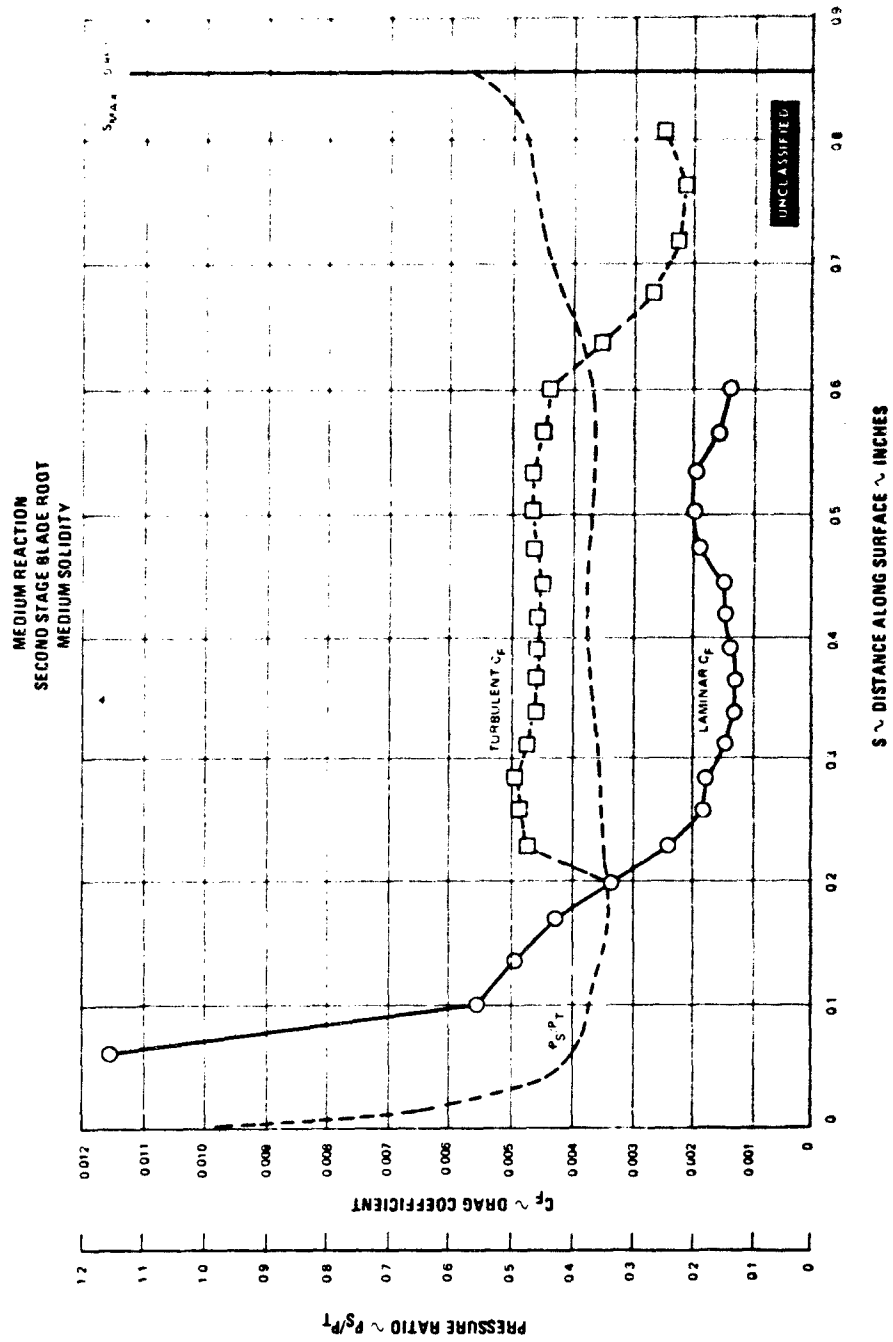


Figure 21

UNCLASSIFIED

UNCLASSIFIED

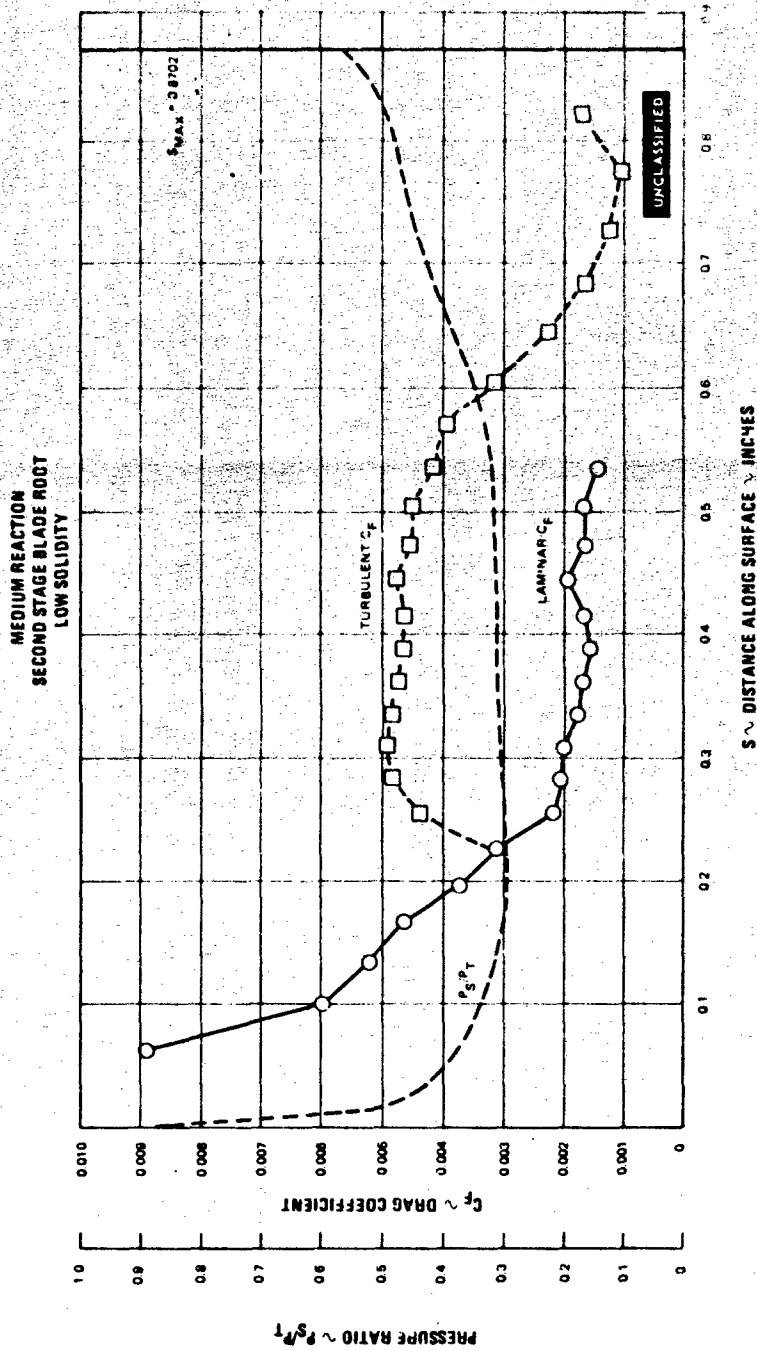


Figure 22

UNCLASSIFIED

UNCLASSIFIED

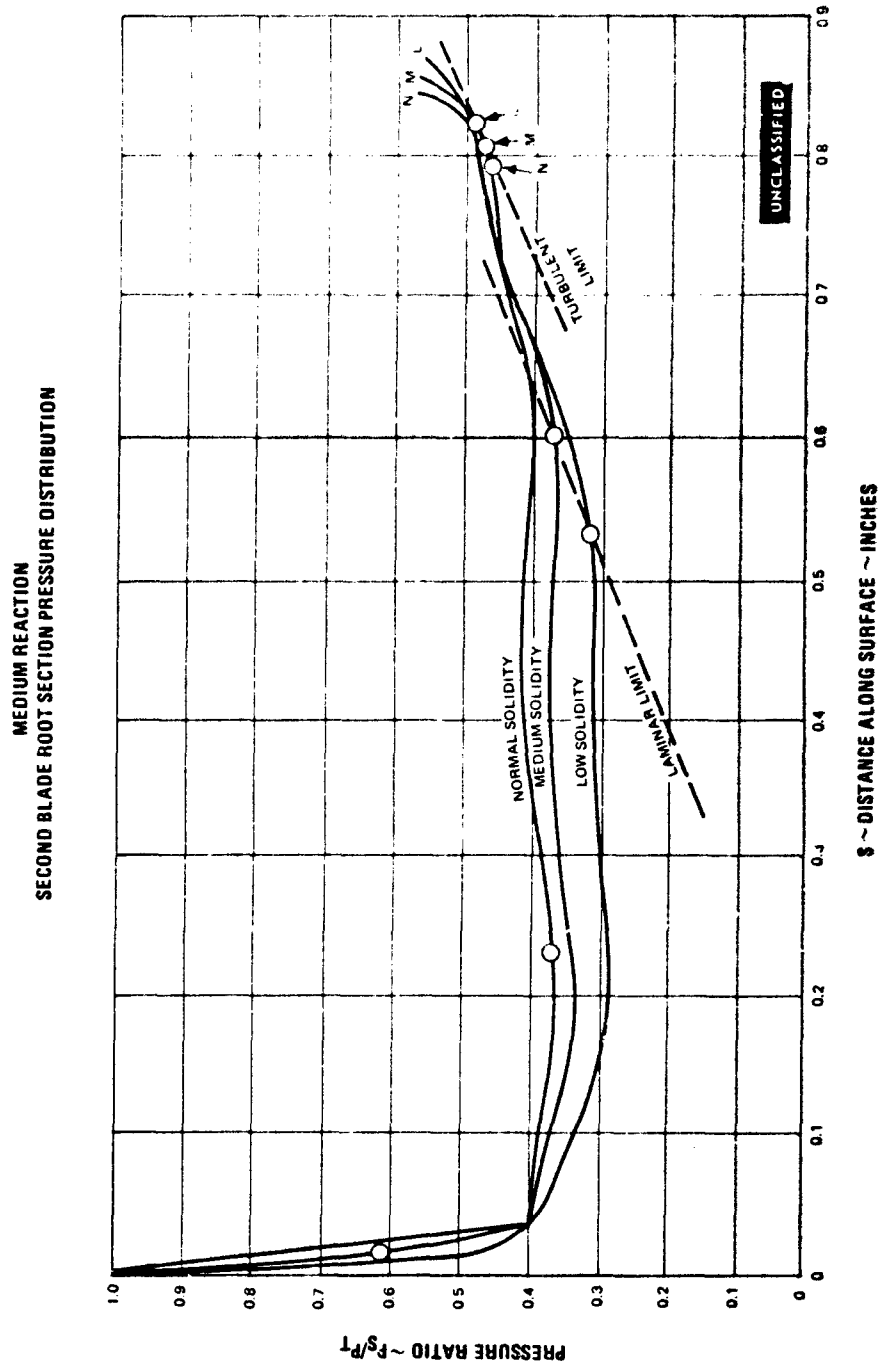


Figure 23

UNCLASSIFIED

UNCLASSIFIED

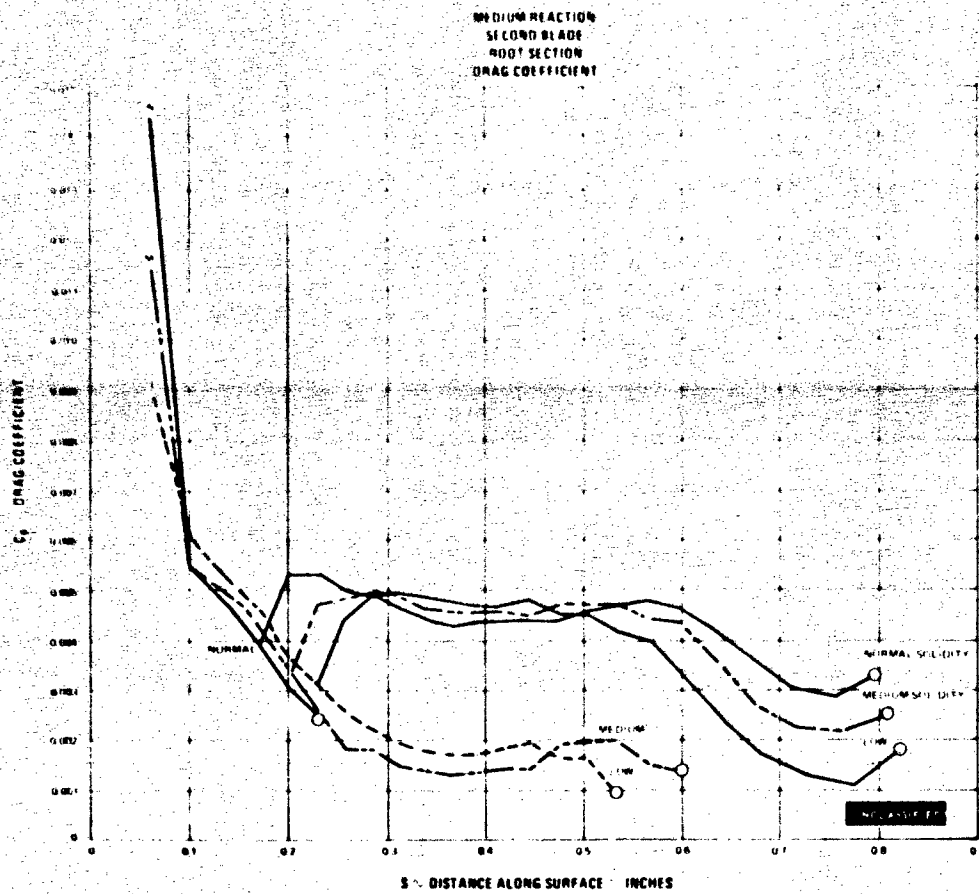


Figure 24

UNCLASSIFIED

UNCLASSIFIED

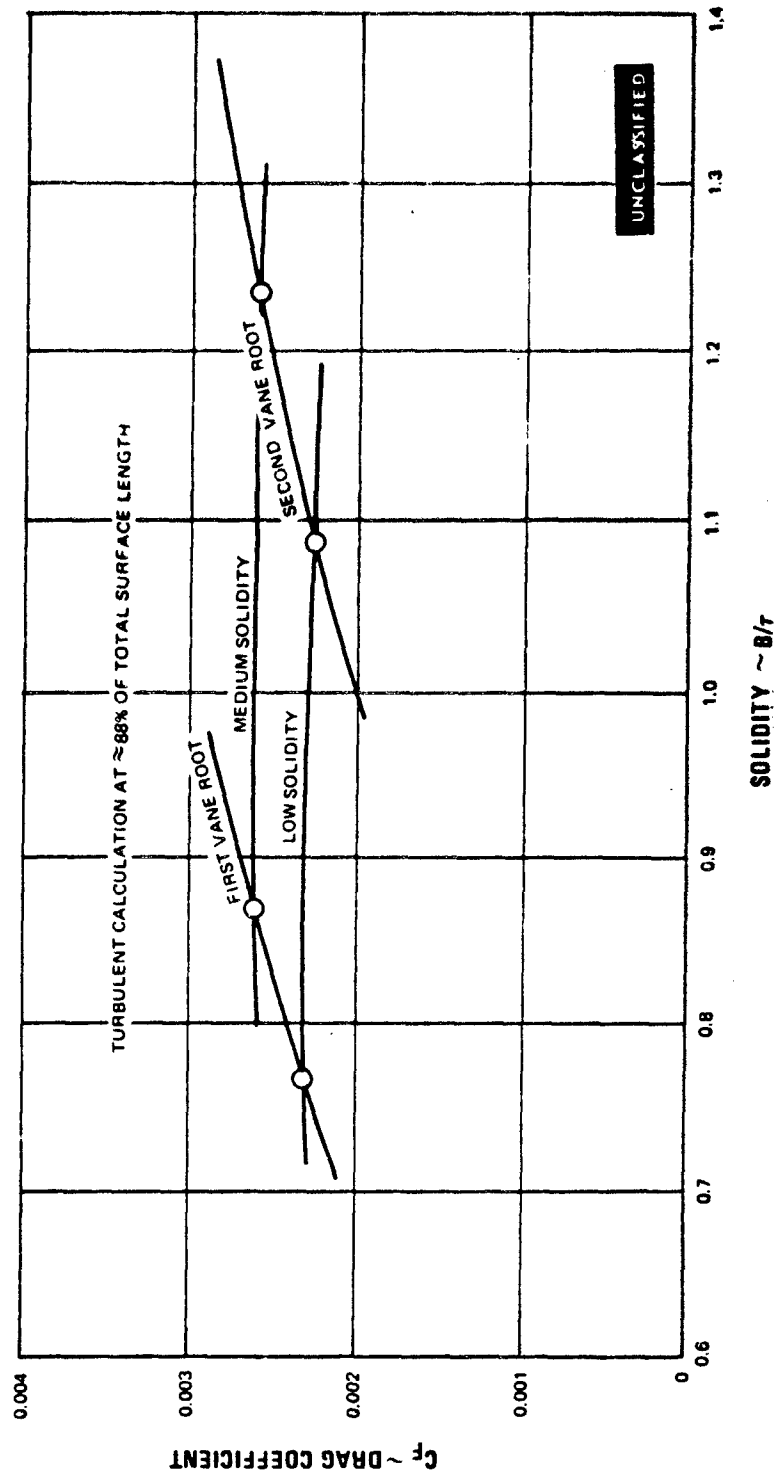
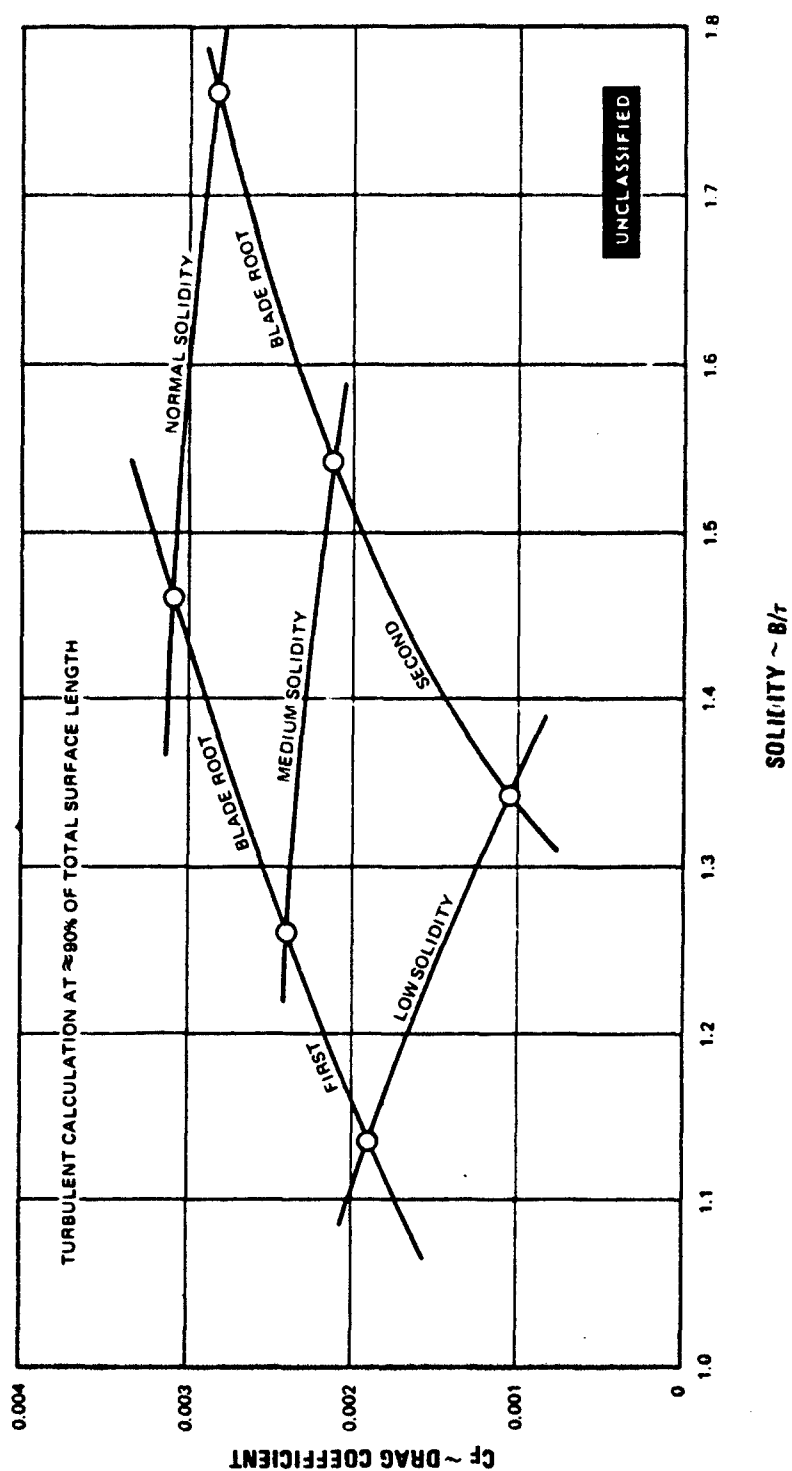


Figure 25 Drag Coefficient vs. Solidity for Vane Root Sections

UNCLASSIFIED

UNCLASSIFIED



PAGE NO. 40

UNCLASSIFIED

Figure 26 Drag Coefficient vs. Solidity for Blade Root Sections

UNCLASSIFIED

5. SELECTION OF AIRFOILS FOR CONTOUR REFINEMENT

(U) Since the two-dimensional boundary layer calculations previously discussed do not account for three-dimensional flow phenomena which cause separation in the suction surface corners prior to two dimensional separation on the airfoil surface, the two-dimensional practical drag coefficient of 0.001 is insufficient to account for the three-dimensional characteristics. There are insufficient data and inadequate analytical tools available at this time to quantitatively define the three-dimensional boundary layer. Local shock losses due to local transonic flow for the foils under consideration may trigger even an earlier separation. Referring to Figures 25 and 26, a drag coefficient of 0.002 corresponds closely to the medium solidity for the second blade and the low solidity for the first three airfoils. Therefore, these solidities are considered to be the reasonable lower limits for the low solidity turbine designs. Based on this boundary layer analysis, then, and in order to provide the necessary range of selection to be considered for the Phase II design, the following preliminary airfoils were selected for contour refinement: first vane, first blade and second vane - normal, medium and low solidity; second blade - normal and medium solidity.

6. FINAL AIRFOIL CONTOUR REFINEMENT

(U) The selected preliminary airfoil contours were refined to further improve pressure distribution and increase resistance to flow separation. Modifications of the contours required several iterations on each section to arrive at the desired pressure distribution. For each solidity, the airfoil radius of curvature, cross section and passage convergence were varied to minimize suction surface pressure coefficient ($\Delta P/Q$) and the rate of recompression in the trailing edge region. The contour which was considered best suited to attain the goal, results in a suction surface pressure distribution that drops rapidly from the leading edge to a relatively flat minimum static pressure, and gradually slopes up to the exit pressure at the trailing edge.

(U) To show the steps taken for each airfoil would result in a voluminous collection of airfoils and their related parameters. As an illustration, however, the refinement of the first blade root section at low solidity is presented in Figure 27. The initial airfoil was the one which was referred to as preliminary, but, as previously noted, it has already undergone several calculations. The refinement steps were as follows:

- Step 1. Lowered airfoil leading edge to shift loading from front portion back toward the minimum radius of curvature region.
- Step 2. Increased trailing edge wedge angle to decrease radius of curvature and reduce pressure gradient at trailing edge.

UNCLASSIFIED

UNCLASSIFIED

- Step 3. Lowered peak of the suction surface (minimum radius of curvature point) to reduce loading in that area.
- Step 4. Repeated Step 3 until suction surface pressure profile was flat as possible.

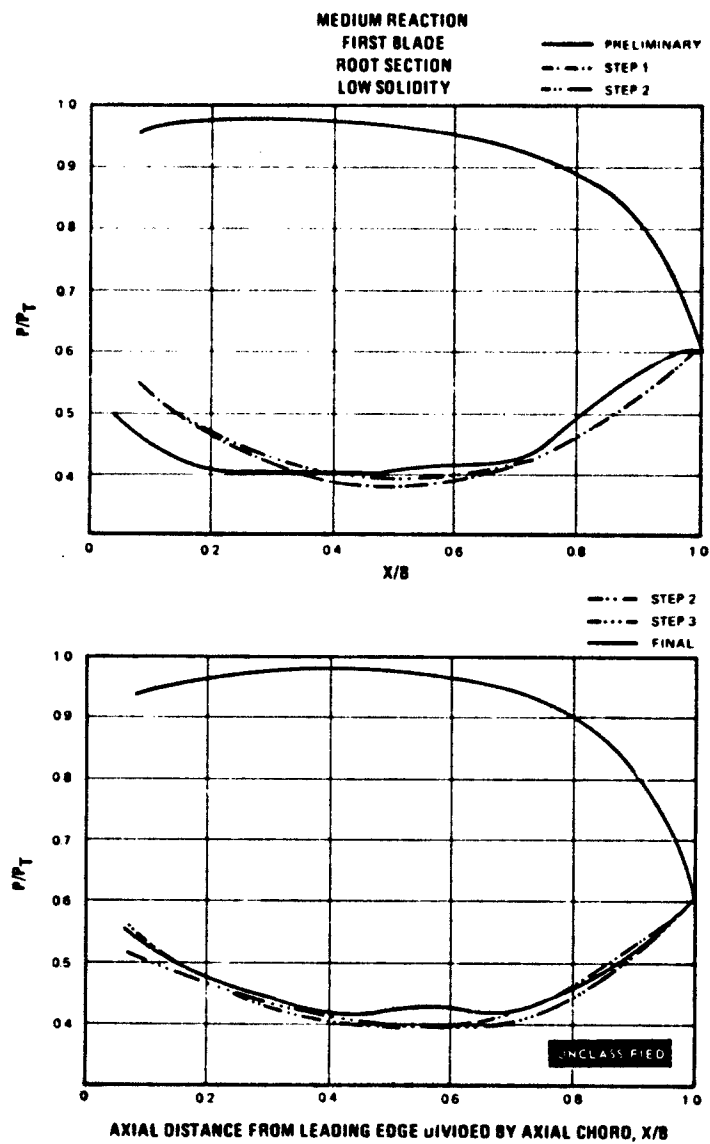


Figure 27

UNCLASSIFIED

UNCLASSIFIED

The change in the airfoil shape from preliminary to final configuration is shown in Figure 28.

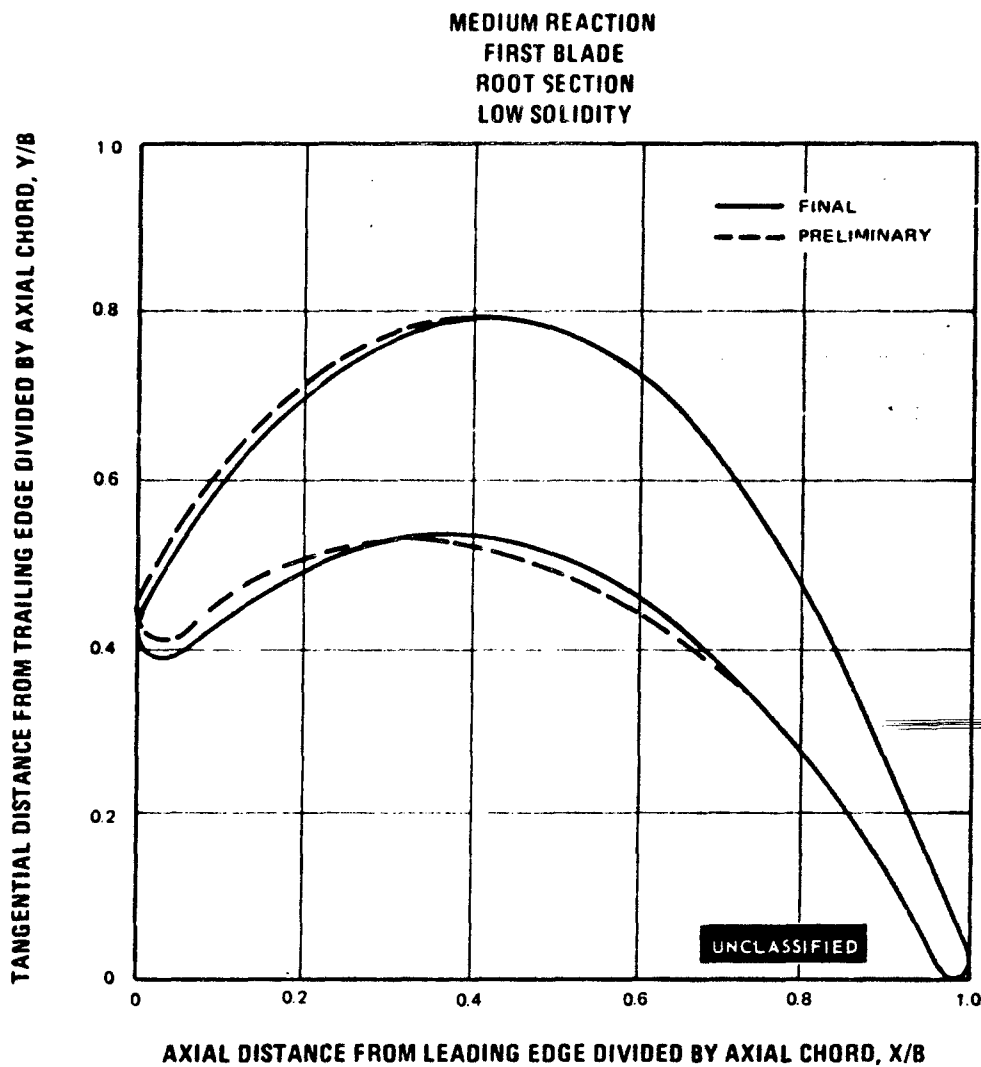


Figure 28

(U) The final airfoil contours for the root, mean and tip sections for the selected airfoils are shown in Appendix II. In addition, for each airfoil the surface pressure distributions and suction surface radius of curvature distributions are shown. When

UNCLASSIFIED

UNCLASSIFIED

the preliminary and final values of the airfoil pressure rise coefficients are compared, the values for the final contours are not in all cases lower than the preliminary values. The discrepancy is due to the fact that the computational procedure was changed between the time that the preliminary calculations and final calculations were made. The change was in the method by which the effect of streamline divergence was evaluated in the airfoil pressure distribution deck. The final method of calculation is felt to be more reliable than the original.

(U) Some general observations concerning these airfoils are that: pressure distributions of the second stage airfoils were more difficult to refine than the first stage; it was more difficult to attain flat suction surface pressure distributions for low solidity airfoils, especially at the root sections; the contour refinement problems become more difficult as the surface maximum Mach number increases, with the result that the hump in the suction surface pressure distribution becomes difficult to eliminate.

7. FINAL AIRFOIL CONTOUR BOUNDARY LAYER CALCULATIONS

(U) Two-dimensional boundary layer calculations were made for the final refined contours of the lowest solidity designs. These included the airfoils of the first three rows with load coefficients 30 percent above normal (low solidity) and the second blade with a load coefficient of 15 percent above normal (medium solidity). It was possible to effect some additional improvement by the refinement procedure over the preliminary airfoils as noted in the results tabulated in Table X. In this table the drag coefficients are compared for the preliminary and final airfoils. In addition, the drag coefficients for the root sections of these airfoils are shown in Figures 29 through 32.

TABLE X

EFFECT OF ROOT CONTOUR REFINEMENT ON DRAG COEFFICIENT

Airfoil	Solidity	% Smax	Preliminary	Final
			Drag Coefficient, C_F	Drag Coefficient, C_F
First Stage Vane	Low	88.5	0.0023	0.0030
First Stage Blade	Low	87.0	0.0019	0.0029
Second Stage Vane	Low	88.4	0.0023	0.0018
Second Stage Blade	Medium	89.0	0.0021	0.0023

UNCLASSIFIED

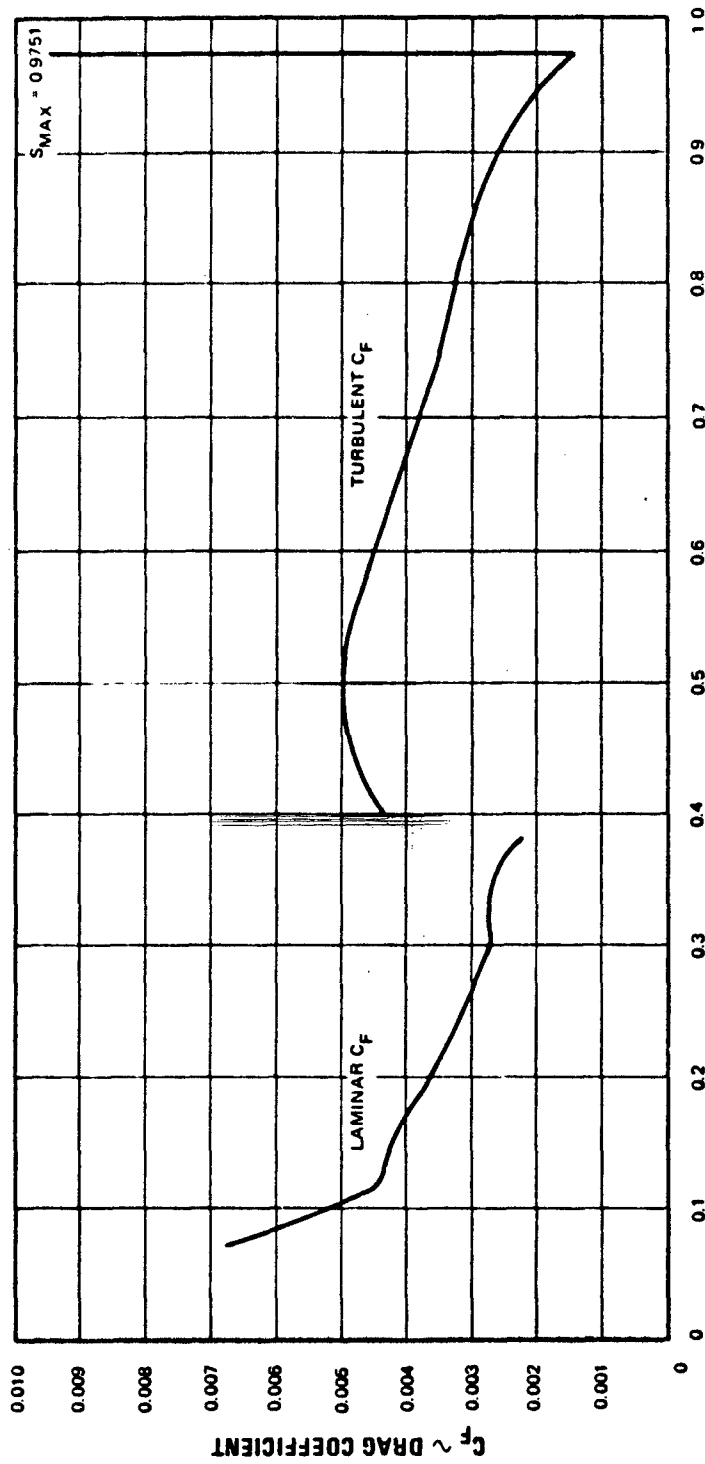
UNCLASSIFIED

UNCLASSIFIED



UNCLASSIFIED

MEDIUM REACTION
FIRST STAGE BLADE ROOT
LOW SOLIDITY



S ~ DISTANCE ALONG SURFACE ~ INCHES

Figure 30

UNCLASSIFIED

UNCLASSIFIED

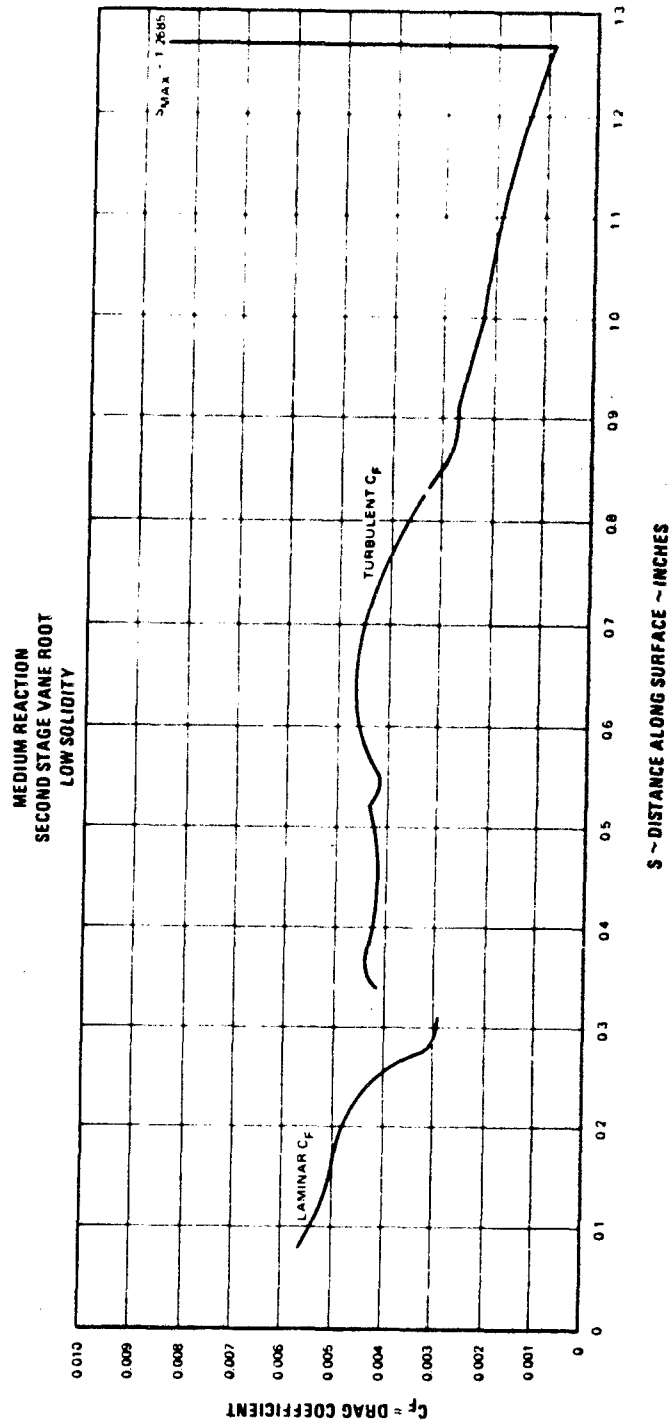


Figure 31

UNCLASSIFIED

UNCLASSIFIED

MEDIUM REACTION
SECOND STAGE BLADE ROOT
MEDIUM SOLIDITY

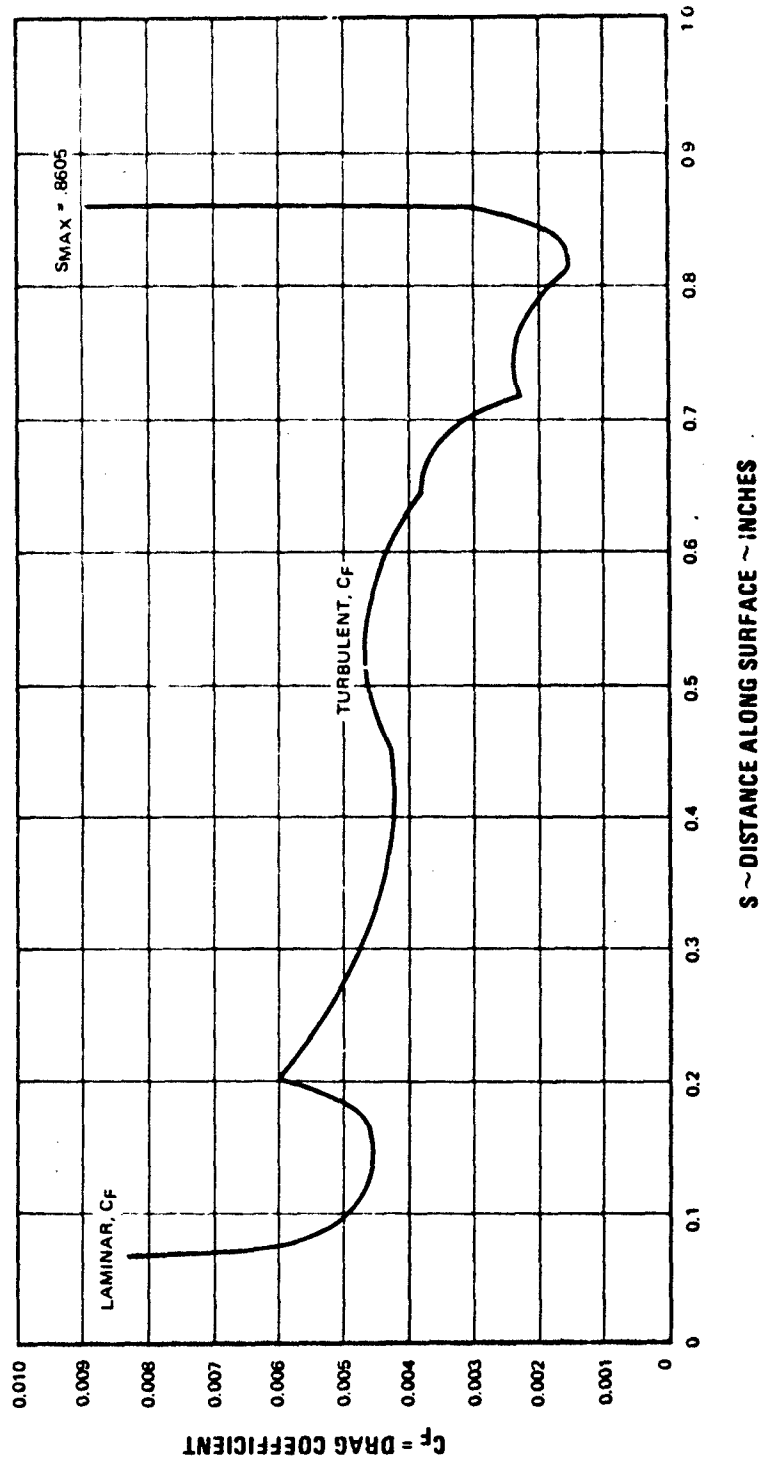


Figure 32

UNCLASSIFIED

UNCLASSIFIED

SECTION IV

BOUNDARY LAYER CONTROL SURVEY (Task 1c)

1. RFP OBJECTIVE

(U) Make a preliminary selection of boundary layer control techniques suitable for reducing corner separation.

2. TASK OBJECTIVE

(U) A comprehensive review of the literature on losses in turbomachinery was conducted to provide the background for a preliminary selection of boundary layer control methods applicable to this program. Particular emphasis was directed toward three-dimensional boundary layer characteristics and control methods related to turbine cascades. The literature was reviewed for information on control methods conforming to the following design criteria:

- applicability to high aspect ratio, uncooled turbines with no external fluid source or sink available, i.e., no blowing or sucking;
- effectiveness in reducing secondary flow or corner boundary layer separation;
- manufacturing feasibility;
- acceptable structural integrity of turbine.

3. LITERATURE SOURCES

(U) The literature sources listed below were searched, including bibliographies in the three listed books. Literature received was reviewed and classified into three categories: (1) relevant and significant information about boundary layers and their control in uncooled turbines (Ref. 1 through 23); (2) background and supporting information pertaining to secondary losses in turbomachinery (Bibliography, 1. Secondary Flow in Turbomachinery); and (3) relevant but inconsequential information related to losses in turbomachinery (Bibliography, 2. Losses in Turbomachinery-General). References in the first category are included in the List of References and reviewed in the following paragraphs. Reports and articles in the second and third categories are listed in the Bibliography.

UNCLASSIFIED

UNCLASSIFIED

Aeronautical Engineering Index	1947-1958
AGARD	1966
Applied Mechanics Reviews	1949-1967
Applied Science & Technology	1958-1966
ASTLA - DDC	1963-1967
DDC Search (Jan. 17, 1968)	1957-1967
Engineering Index	1945-1967
Intl. Aerospace Abstracts	1961-1966
NACA-NASA-Star	1915-1967
Nuclear Science Abstracts	1949-1967
Physics Abstracts	1950-1966
Zeitschrift Fur Flugwissenschaften	1964-1967
UAC Card Catalog	
FRDC Card Catalog	

Schlichting, Dr. Hermann, Boundary Layer Theory, McGraw-Hill, New York, 1960

Lachmann, G. V., Boundary Layer & Flow Control: Its Principles & Applications, Vol. I & II, Pergamon Press, New York, 1961

Horlock, J. H., Axial Flow Turbines; Fluid Mechanics and Thermodynamics, Butterworths, London, 1966

4. SECONDARY LOSSES

(U) Secondary losses in cascade flow are defined as all losses not accounted for by the skin-friction losses on the airfoils and annulus walls. These losses can be either direct or indirect. The direct losses include losses from trailing edge wakes and blockage, tip clearance, increased skin-friction in corners and separation of corners, annulus walls and airfoils. The main forms of indirect losses are passage blockage, and deviations from design flow angles.

(U) The recent literature indicates that the predominate secondary loss occurring in cascade flow is due to the separated boundary layers in the suction surface corners (8, 15, 19)*. The corner boundary layers separate mainly due to the presence of the annulus wall, and the accumulation of low energy fluid in the corners. The low energy fluid which accumulates in the suction surface corners from elsewhere in the cascade, Figure 33, causes additional flow-area blockage and mainstream deflections (7, 15). The main cause of this accumulation is the migration of the annulus boundary layers due to the cross-channel pressure gradient (6, 15, 20). The mainstream rotation caused by turning through the cascade contributes to the accumulation in both suction surface corners whereas the radial pressure gradient causes some slight migration to the inner annulus corners (6, 15).

* Number in parentheses designates References at end of report.

UNCLASSIFIED

UNCLASSIFIED

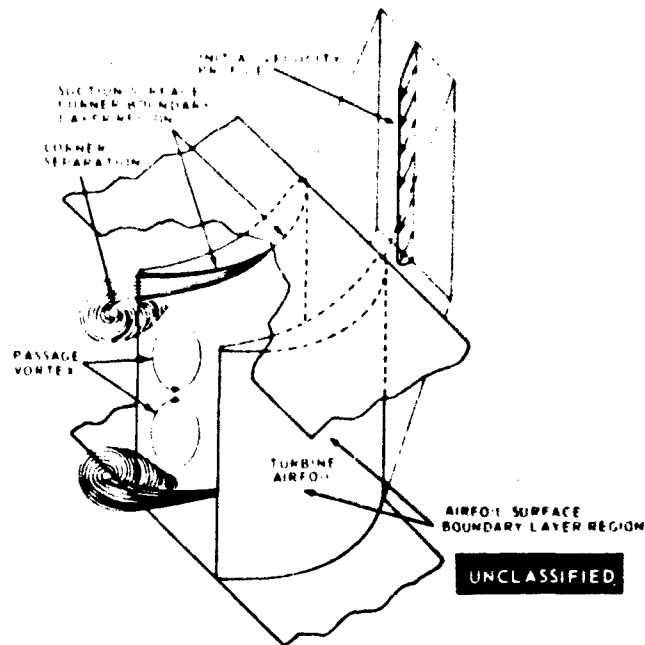


Figure 33 Turbine Cascade Secondary Flows

(U) Some general characteristics of corner boundary layer flow are included in the works of Gersten and Schlichting (4, 16, 17, 19). Transition from laminar to turbulent flow and the start of separation occur earlier in the corner than on the adjoining walls. The skin friction drag of turbulent corner flow is greater than for plates and separation occurs when the kinetic energy in the boundary layer cannot overcome the pressure increase in the direction of flow. Gersten (4) states that the Euler number is the characteristic parameter for flow with a constant adverse pressure gradient, but does not adequately explain its significance with regard to determining the point of separation for turbine airfoils. Further investigation of this parameter should be useful since the Euler number is a ratio of the local pressure gradient to the local freestream kinetic energy.

(U) The corner separation phenomena was observed in cascade flow (11). It was found that boundary layer separation began in the intersection formed by the convex surface of the blade and the adjacent side wall. The complete wall boundary layer did not separate. Instead, during the initial backflow, the wall loss was confined to the annulus and airfoil intersection and gradually spread inward over the blade convex surface, manifesting itself as a blade tip stall condition. On the basis of these observations, it was recommended that corrective measures be applied at the corner rather than at some distance from the wall.

UNCLASSIFIED

UNCLASSIFIED

(U) Several general conclusions regarding secondary losses which were reported in the literature are:

- The inlet boundary layer does not appreciably affect the corner secondary losses (8, 17, 20)
- The corner secondary loss is independent of Reynolds number (17)
- The corner secondary loss is independent of the blade length for aspect ratios greater than 2.0 (19)
- Secondary losses increase with Mach number for subsonic flow (19).

5. BOUNDARY LAYER CONTROL

(U) Boundary layer control is not a recent innovation (18), but relatively little has been accomplished towards controlling the boundary layers in turbomachinery. Boundary layer control is the term applied to various methods of favorably influencing the boundary layer and its resulting effect on the free-stream. The most common means of boundary layer control is by either blowing or sucking (9); however, for this study these methods have been excluded since the control techniques are to be applied to an uncooled turbine without the complexity of externally routing gas into, or out of, the main flow passages. The most promising boundary layer control techniques should be those that improve conditions in the end wall region since the good turbine design procedures will insure high efficiency on the mainstream portion of the airfoil, i. e., controlled vortexing will optimize the radial work distribution, and careful airfoil contouring will provide gradual suction surface pressure recovery. The statement by Carter (1) that "no amount of attention to secondary effects can undo the consequences of a mediocre mean section design" is especially valid for this program due to the relatively large aspect ratios, 3.3 to 7.7 of some of these airfoils.

(U) For purposes of discussion, information on boundary layer control found in the literature survey is divided into two classifications: aerodynamic contouring and local momentum alteration. The former category includes modification of the cascade pressure distribution through airfoil profile changes or end wall contouring. The latter includes control methods that produce a direct local effect on the boundary layer.

a. Aerodynamic Control Methods

(1) Controlled Vortex Design

(U) Experimental evaluation of the controlled vortex concept (3) indicates that this technique can be successfully applied to reduce turbine end wall losses.

UNCLASSIFIED

UNCLASSIFIED

(U) Controlled vortexing entails precise control of the blade row spanwise vortex distribution to prevent excessive corner losses. Evaluation of turbine performance data indicated that high root losses were closely associated with the performance of low-velocity-ratio, highly loaded stages, and that the local reaction level could be increased to solve the problem of poor root performance. Testing results from a variable area turbine provided additional information relating to the problem of low root efficiency associated with low reaction. With the turbine nozzle in a closed position, stage reaction was less than zero and the spanwise efficiency profile for this condition revealed extremely poor root performance. As the nozzle was moved to its design position, the reaction became slightly positive and a very substantial increase in root efficiency resulted. Opening the nozzle still further increased the root reaction to about 30 percent and resulted in an additional increase in efficiency at the root, in spite of the fact that the blade relative Mach number had increased appreciably.

(U) Application of controlled vortexing to turbines has been accomplished through streamline design analysis. With reaction at the blade mean section fixed, the camber is gradually reduced toward the root and gradually increased toward the tip sections, resulting in increased root reaction and decreased tip reaction when compared to a free vortex design. The higher root reaction reduces the adverse pressure gradient imposed on the root suction surface corners. The decreased tip reaction results in a lower Mach number, and hence lower loss at the tip suction surface corner. The results of the present study reveal in detail why this should be the case.

(2) End Wall Contouring

(U) The effect on aerodynamic performance of contouring the vane tip end wall was investigated in an experimental turbine (2). These experiments indicated that the efficiency of stages with low aspect ratio can be substantially increased by contouring the end wall. The end losses in the guide vane cascade were reduced by decreasing the velocity in the passage section where maximum turning occurs. This condition reduces the pressure difference between the suction and pressure surfaces, and consequently the intensity of the secondary flows. This reduced pressure difference in the forward passage section is indicated in figure 34. Also, the end wall contouring formed a convergent flow passage at the exit which reduces the magnitude and length of the adverse pressure gradient on the suction surface corners and produces a favorable effect on the boundary layers on the end walls of the channel. The performance data indicated that, for the low aspect ratio airfoils tested, end wall contouring effectiveness increased as aspect ratio was reduced. With an aspect ratio of unity, the losses were reduced 0.5 to 1 percent and with an aspect ratio of 1/3, 2.0 to 2.5 percent. The effectiveness of end wall contouring was also a function

UNCLASSIFIED

UNCLASSIFIED

of the amount of constriction. The loss measurements also indicated that the effects of the outside diameter wall contouring were most noticeable near the inside diameter wall, a probable consequence of the low airfoil heights tested.

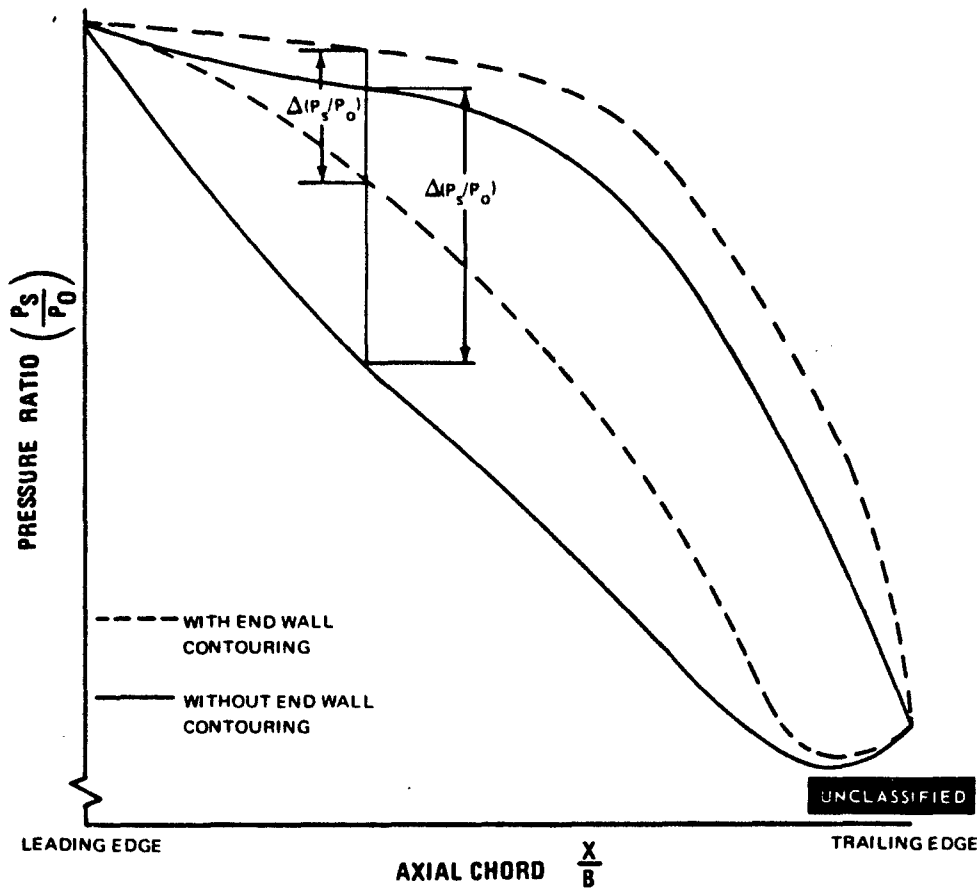


Figure 34 Pressure Distribution

(3) Local Uncambering

(U) It has been suggested (10) that by varying the blade camber in accordance with the inlet velocity distribution, correction can be made for the phenomenon of overturning near the walls. It was anticipated that the reduction of camber at the blade tips which this method necessitates will also favorably affect the position of the separation point on the blade surface in the corners. The approach taken in this report directs attention towards the reduction of span-wise variations in outlet angles. This technique should directly reduce the

UNCLASSIFIED

UNCLASSIFIED

secondary flow velocities and end loss within each airfoil row, and the greater uniformity in the inlet conditions at the succeeding airfoil row should give considerable improvement there. Further, there is the possibility of reducing the tendency for separation from the blade surfaces, this being the primary aim in secondary flow control.

(U) Blades were evaluated with a constant camber angle over the center three-quarters of the span (figure 35). The camber angle at each end decreased linearly to zero. The evaluation indicated the total pressure losses were reduced with this camber arrangement and the tendency to delay corner separation was supported. Reducing the camber to zero at the wall appears to have more than corrected the overturning effect. It was suggested that a camber angle at the wall greater than zero might have led to a greater uniformity of discharge angle over the whole span.

(U) This method of boundary layer control is essentially local controlled vortexing in the root and tip regions. Further work is required to determine if this technique is structurally feasible for blade airfoils with higher camber angles than the 10 and 20 degree used in this reference.

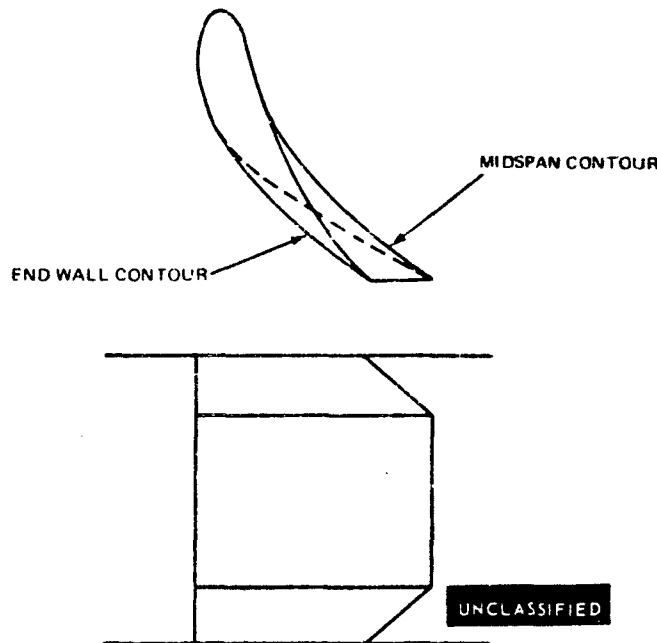


Figure 35 Local Uncambered Airfoil

UNCLASSIFIED

(4) Forward-Leaning Blade Tip

(U) An attempt to control the migration of the low energy boundary layer fluid to the suction surface corner was investigated by leaning the blade tip forward in the direction of mainstream flow while maintaining the leading edge axial position (22). This is shown in figure 36 .

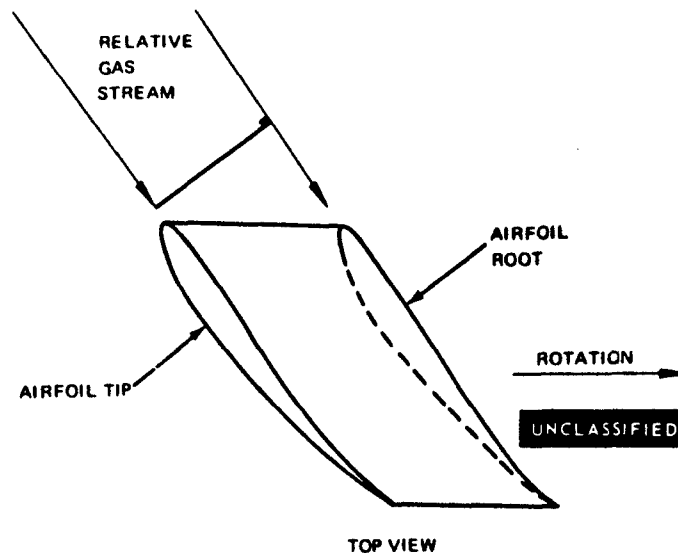


Figure 36 Forward Leaning Blade Tip

(U) Detailed measurements of the inlet and outlet flow patterns showed a marked leakage of fluid around the trailing edge of the forward leaning blade tip from the pressure side of one passage to the suction side of the adjacent passage. The trailing edge cross-flow apparently leads to vigorous mixing of high-energy fluid with the wall-boundary-layer fluid accumulating toward the suction side of the passage. Previous measurements demonstrated that such a mixing pattern did not occur at the trailing edge of straight blades. Carbon-black traces of boundary layer flow on blades and wall showed that suction surface stall had been eliminated almost completely with the forward-leaning tip.

(U) The overall loss evaluation of the forward-leaning tip was rather inconclusive. Passage losses were reported to be less with the forward-leaning tip than with straight blades; however, additional losses occurred due to the fluid mixing at the trailing edge. It was concluded that the total losses for the forward-leaning tip airfoil were slightly lower than a straight tip airfoil, but not significantly different.

UNCLASSIFIED

b. Local Momentum Alteration Methods

(1) Vortex Generators

(U) The value of the mixing device known as the vortex generator has been well established at subsonic speeds through many successful applications (13). The generator is simply an energy converter in the form of a low aspect ratio, semi-span wing mounted with an angle of attack on a surface. The generator accomplishes a conversion of translational energy to rotational energy in the form of a trailing tip vortex. The induced velocities associated with the trailing vortices promote re-energization of the boundary layer by an exchange of kinetic energy from the main stream to the boundary layer, thus making it more resistant to separation in an adverse pressure gradient.

(U) The mixing energy contained in the trailing vortex released by a vortex generator is directly chargeable as induced drag. This induced drag is larger than the profile drag associated with the generator when operating at high lift coefficients and therefore represents a large proportion of the drag introduced by the generator.

(U) Theoretical and experimental work was undertaken by the United Aircraft Research Laboratories to evaluate the relative mixing characteristics of various types of vortex generators. The experimental work (5) was carried out in the UAC Pilot Wind Tunnel diffuser by evaluating the effects of the various generators on the boundary layer velocity profiles and momentum losses at a station approximately 70 boundary layer heights downstream of the generators. These tests indicated that boundary layers, which varied only a small amount, could best be handled with the rectangular shape, whereas the triangular generator adjusted more easily to a changing boundary layer condition. The vortex shed by the triangular shape shifted with the boundary layer and maintained a position close to the boundary layer edge. This vortex location was found to be the most favorable for efficient mixing.

(U) The boundary layer re-energization which may be accomplished through the use of vortex generators has encouraged the extension of generator applications to transonic speeds where shock induced separation has given rise to a wealth of special aerodynamic problems. Among these are such phenomena as buffeting, stability and trim changes, and loss in control effectiveness, which are inherent by-products of separation. The effects of vortex generators on the aerodynamic characteristics of a typical upswept model wing were determined at transonic Mach numbers in the UAC eight-foot wind tunnel to verify the results of the model tunnel study (13).

UNCLASSIFIED

UNCLASSIFIED

(U) The performance characteristics and design requirements for transonic vortex generators parallel those established for low speed application except for differences in generator location and generator geometry. The best location for generators to suppress shock induced separation was found to be 25 boundary layer thicknesses upstream of the shock. The effectiveness of the rectangular generators in the transonic application is sensitive to thickness ratio and is reduced significantly at low ratios (2 percent).

(U) Vortex generators intended to delay shock-induced separation on conventional compressor airfoils were found to be detrimental to cascade performance (21). Tests were made without the vortex generators fitted, and with a single spanwise row of vortex generators at 15 percent chord from the leading edge. It was thought that the 0.005 inch high base of the vortex generator was promoting boundary layer separation and increasing losses. The test was repeated with the base fitted into a recess milled in the blade surface. With the base flush with the blade surface the vortex generator drag was reduced by about one-third; however, they were still detrimental to the cascade performance. The cascade was also tested with the vortex generators fitted to the blades at 6.2 percent chord. The losses were greater with the vortex generator at this position than at the 15 percent chord position. It was concluded that, for the configurations tested, shock induced boundary layer separation was delayed but the overall effect of vortex generators was detrimental to performance.

(2) Slots

(U) The incorporation of slots in airfoils can be utilized to produce two methods of boundary layer control. The existing boundary layer can be energized by introducing high energy fluid from the pressure side of the airfoil (14, 23), or the existing boundary layer can be replaced by another boundary layer originating within the slot (12).

(U) Blade tip slotting to prevent wall stall has been investigated (14). The major conclusion was that blade loading in tip regions may be increased by removing low energy fluid and reducing separated areas on the blade surface, i. e., improving pressure gradients along the profile. However, accuracy of the static pressure measurements in the region of interest were not accurate enough to provide detailed data.

(U) It was evident that unless the slot entrance extended well into the region of high-energy fluid, the mass flow through the slot was insufficient to affect the suction surface conditions. It was also shown that with the slots tested, a highly convergent slot passage was necessary to obtain high exit velocities. This resulted in a very small slot exit area. When this exit area was reduced

UNCLASSIFIED

UNCLASSIFIED

the mass flow was also reduced. The resulting small amount of high-energy fluid had insufficient effect on flow conditions. A minimum slot size of 3/16 inch was recommended for an airfoil with a 2.8 inch chord.

(U) The use of partial span blade slots in the proximity of the end walls intended to control separation was one of several control techniques reported in Reference 23. The first blade tested had a slot confined to the blade extremity from the pressure side to the suction side. The slot intersected the suction surface in the region where flow reversal started. The investigation of the slot effect on flow conditions indicated that the reverse flow opposing the jet was of such strength that it reversed the jet direction shortly after it issued from the slot. The result of the interaction was that the flow disturbances over the blade were intensified. Increasing the slot depth to 12 percent span and changing the slot contour did not appear to reduce this condition.

(U) A second test blade had a slot located approximately three-quarter chord lengths from the leading edge. This test blade was ineffective since the slot was located within a stalled area even for moderate values of stagger angle. The same characteristics of jet flow reversal and increased separation were observed as with the first test blade.

(U) A compressor annular cascade investigation conducted to provide criteria for the design of slotted rotors and stators also indicated the importance of slot location (12). Initial tests of the unslotted stator disclosed that the minimum pressure and separation points occurred at 12 and 85 percent of the chord, respectively. Based on these data, two axial slot locations were selected. The forward location was at 55 percent of the chord on the suction surface, which was approximately half-way between the minimum pressure point and the flow separation point. The rearward point was selected at 75 percent of the chord, which was slightly ahead of the flow separation point for the unslotted configuration. In addition to slot location, several variations of slot geometry were tested at each slot location.

(U) For the forward slot location, the stator wake loss coefficient varied between 17 and 43 percent of the unslotted loss coefficient, depending on the slot geometry utilized. For the rearward location, the loss coefficient ranged between 76 and 137 percent of the unslotted loss coefficient, depending on the slot geometry employed. This result is attributed to two factors:

- The available pressure drop across the stator vane (pressure-to-suction surface) at the 75 percent chord slot location was less than the pressure drop across the vane at the 55 percent chord slot location.
- The suction surface boundary layer at 75 percent chord is thicker than at 55 percent chord.

UNCLASSIFIED

UNCLASSIFIED

(U) The first of the above factors results in a relatively low slot flow velocity and thus reduces the Coanda effect. The thicker boundary layer requires a larger pressure gradient normal to the suction surface to induce freestream flow toward the surface. These factors tend to support the result that the rear slot wake was shifted toward higher turning but not reduced in size.

(U) Data for both slot locations indicated about the same increases in lift coefficient and air turning angle. The slot configuration with the lowest wake loss coefficient showed increases in lift coefficient and turning angle of about 10 percent and 2 degrees, respectively.

(U) The effect of slot geometry on performance was less pronounced than the effect of slot location. The geometry parameter that produced the most significant reduction in wake size for a forward slot configuration was the rear section leading edge radius. When this radius was increased from 0.028 to 0.056 in., the wake loss coefficient decreased from 0.031 to 0.012.

(U) The Coanda radius was the most significant geometry parameter that was varied for the rear slot configuration. A slight increase in Coanda radius produced a slight decrease in wake loss (0.063 to 0.053). Subsequent increase in Coanda radius resulted in a large increase in wake loss coefficient (up to 0.130). This change in wake loss suggests the probability of an optimum Coanda radius. Insufficient data were obtained to evaluate the optimum Coanda radius for the forward slot location.

(3) Flow Inhibitors

(U) A boundary layer control device that appears particularly applicable to cascade flow is the so-called dam, or flow fence. Essentially it is a fin mounted perpendicular to the convex surface of the blade near the sidewall, or on the end wall, and lying parallel to the mainstream flow direction. Its primary purpose is to mechanically hinder the mainstream rotation, boundary layer migration, and corner vortex flow that force the separating sidewall boundary layer inward over the suction surface of the blade.

(U) An attempt (23) was made to reduce the radially inward spread of flow separation over the convex surface of a blade by placing a normal dam, or fin, on this surface near each extremity, the length being parallel to the flow direction. These acted as constraining boundaries, confining any spanwise flow to narrow regions between the dams and sidewalls.

(U) The first test blade had thin wooden dams extending along approximately three-quarters of the chord length from a point ahead of the most forward extent of the stalled region on the blade to the trailing edge, and the maximum

UNCLASSIFIED

UNCLASSIFIED

height was approximately 40 percent of the gap between blades. A test was run in which a single blade with these dams was placed in cascade with the standard assembly in order to compare flow patterns. An improvement of the flow over the blade surface between the dams was apparent from flow pattern comparisons. Further tests were run with variations in length, shape, thickness, maximum height, displacement from the blade extremities, and alignment relative to the sidewalls. Better flow patterns were obtained from a length extending from just ahead of the separated region to the trailing edge than from either full chord length or partial chord length dams starting behind the forward extent of the separated region. Low dams (10 percent gap) were found to be ineffective in halting the inward spread of separation, while those of height equal to 50 percent gap vibrated so badly that they blew off before tests could be completed. The best flow pattern was obtained from a blade having dams close to the sidewalls with the trailing edge slightly convergent toward midspan. A curious effect was observed when dams cut from metal shim-stock were substituted for the wooden models. These seemed to have no effect on the secondary flows, and the flow pattern appeared unchanged. One test was run with a thick dam having a curved surface facing the sidewall and a flat surface facing midspan in an attempt to induce a local flow acceleration in the boundary layer at the blade-wall juncture by means of a constricted passage, but the flow patterns gave an indication that the anticipated results did not materialize. To measure the effect on the cascade pressure-rise, a cascade of blades with the dams installed was assembled and run for a full range of stagger angles at approximately 0.34 Mach number. The results of these tests show that the addition of dams reduced the pressure recovery for all stagger angles tested. At a stagger angle of 24.8 degrees the pressure-rise coefficient was reduced 15 percent and the deflection angle was increased 1 degree.

(U) Another investigation with flow fences (15) showed that sheetmetal fences on the blades were not always effective in blocking the radial flows to reduce the accumulation of low-momentum fluid at the inner wall. The fences increased the wetted surface area in the flow passages which introduces some additional viscous losses. Separation of the modification-induced losses from the original low-momentum fluid losses was not readily feasible. Accordingly, the changes in size of the inner wall loss core were used as criteria for evaluating the effectiveness of the modifications, and as a basis for interpretation of the results.

(U) As expected, none of the modifications used affected the losses near the outer wall under any condition, since the flow-fence was downstream of the outer wall radial flows. The flow-fence modification was tested at a hub Mach number of 0.94. Comparison showed that the flow fence apparently had no noticeable effect on the inner wall loss core. The flow evaluated at a Mach number of 1.46 indicated a sharp reduction in size of the inner wall loss core

UNCLASSIFIED

UNCLASSIFIED

as a result of the flow fence. The circumferentially averaged loss, plotted radially over one-half the blade height indicated a change in the loss distribution; however, an overall integrated blade loss comparing the performance with, and without, the flow fence was not presented.

(U) Flow fences are currently being investigated by Pratt & Whitney Aircraft. Tests are being conducted on a single stage compressor rig with flow fences attached to the end wall platforms. At this time, testing and evaluation has not been completed.

(4) Fillets

(U) A secondary flow visualization study in cascades was reported (7) in which one of the configurations tested had fillets at the intersections of the airfoil and the end wall. It was observed that the fillets apparently had little effect on the formation of the passage vortices and that similar results were obtained with larger fillets. However, no performance data was presented to indicate the effect of fillets on the pressure loss through the cascade.

(U) The topic of fillets was discussed with Professor H. Schlichting. He was of the opinion that corner fillets should have the effect of shifting the corner flow condition from the three-dimensional condition described by Gersten (4), toward the one which is predicted by two-dimensional boundary layer theory. This would delay the corner separation to a point downstream.

6. SELECTION OF BOUNDARY LAYER CONTROL METHODS

a. Characterization of Corner Problem

(U) There appear to be two related mechanisms that contribute to large aerodynamic losses in the end wall regions of turbine cascades. The first involves a thickening of the boundary layer in the suction surface corners as a result of both the boundary layer growth in the mainstream flow direction, and the migration of low momentum fluid along the annular walls to the suction surface corner region. The second is separation of the boundary layer in the suction surface corners (long before airfoil boundary layer separation) due to abnormal thickening resulting from the end wall and the adverse suction surface pressure gradient. Although the literature contains several recent references to corner separation as the predominant effect, there is also evidence indicating that high end wall losses without corner separation may be possible. Therefore, the selection of boundary layer control methods for this program was influenced by the need to consider the two possible situations, one having high end wall loss without separation, and the other with large separated regions in the

UNCLASSIFIED

UNCLASSIFIED

corner. Without separation, the only apparent loss mechanism to attack is the end wall boundary layer migration toward the suction surface corners. If substantial separation does occur, the use of local momentum alteration methods should be effective.

b. Preliminary Selection of Control Methods

(U) All of the airfoils considered for this program were designed using controlled vortexing techniques which are now standard practice at Pratt & Whitney Aircraft. Other methods of boundary layer control which can be applied to reduce secondary flow effects are end wall contouring, local uncambering of the airfoil root and tip sections, and flow fences. End wall contouring and local uncambering provide the additional benefits of locally reducing the adverse pressure gradient in the suction surface corners and thus also contribute to the prevention of corner separation.

(U) Methods that appear to be suitable for preventing suction corner separation by local momentum alteration include vortex generators, corner slots and corner fillets. These techniques have little or no direct effect on the secondary flow problem.

(U) The literature survey revealed little design information that could be used to apply these boundary layer control methods. Design procedures required for controlled vortexing are well established. However, except for vortex generators, no systematic experiments to establish empirical design criteria for the remaining methods have been reported. Preliminary analyses for end wall contouring, vortex generators, corner slots, and fillets are discussed under Task 1d. (Section V).

(The reverse of this page is blank)

UNCLASSIFIED

UNCLASSIFIED

SECTION V

PRELIMINARY BOUNDARY LAYER CONTROL ANALYSIS (Task 1d)

1. RFP OBJECTIVE

(U) Provide initial guide lines for the application of corner boundary layer control technique.

2. TASK OBJECTIVE

(U) Preliminary analyses were conducted to provide initial guidelines for the application of four corner boundary layer control methods to the turbine airfoils designed in Section III, Task 1b. Due to the limitations of available analytical techniques and the lack of data in the literature, it was not possible to absolutely rank the boundary layer control techniques in terms of effectiveness for each selected airfoil design as originally intended. It was, however, possible to gain considerable insight into the probable usefulness of each promising technique. Since the airfoil pressure distributions are all very similar, such a ranking would be of doubtful value. The preliminary analyses conducted for end wall contouring, vortex generators, corner slots, and fillets are discussed in the following paragraphs.

3. END WALL CONTOURING

(U) The proper application of end wall contouring offers potential benefits in reducing both end wall boundary layer migration and corner boundary layer separation. Cascade tests reported in the literature for low aspect ratio vanes indicated a substantial effect of end wall contouring on the opposite wall. However, for the higher aspect ratio airfoils of this contract, the effects of end wall contouring are expected to be confined to a region near the wall. A quasi-three-dimensional numerical analysis of the effects of end wall contouring on cascade static pressure distributions was attempted. This approach involved superimposing a turbine streamline analysis on a two-dimensional cascade pressure distribution calculation. This procedure was developed by the company in order to analyze the effects on pressure distribution of contouring both root and tip end walls of a first-stage turbine vane (Figure 37). The results of this prior analysis, shown in Figure 38, illustrate the dual benefits of wall contouring on the root section: (1) the lower pressure difference between pressure and suction sides in the forward part of the channel, which reduces boundary layer migration to the suction surface corners, and (2) the reduced adverse pressure gradient on the suction surface in the trailing edge region, which tends to delay the onset of separation to a point closer to the trailing edge. A convenient way to interpret the effects of end wall contouring is that the local increase of blade area results in local unloading of the airfoil, which is highly desirable.

UNCLASSIFIED

UNCLASSIFIED

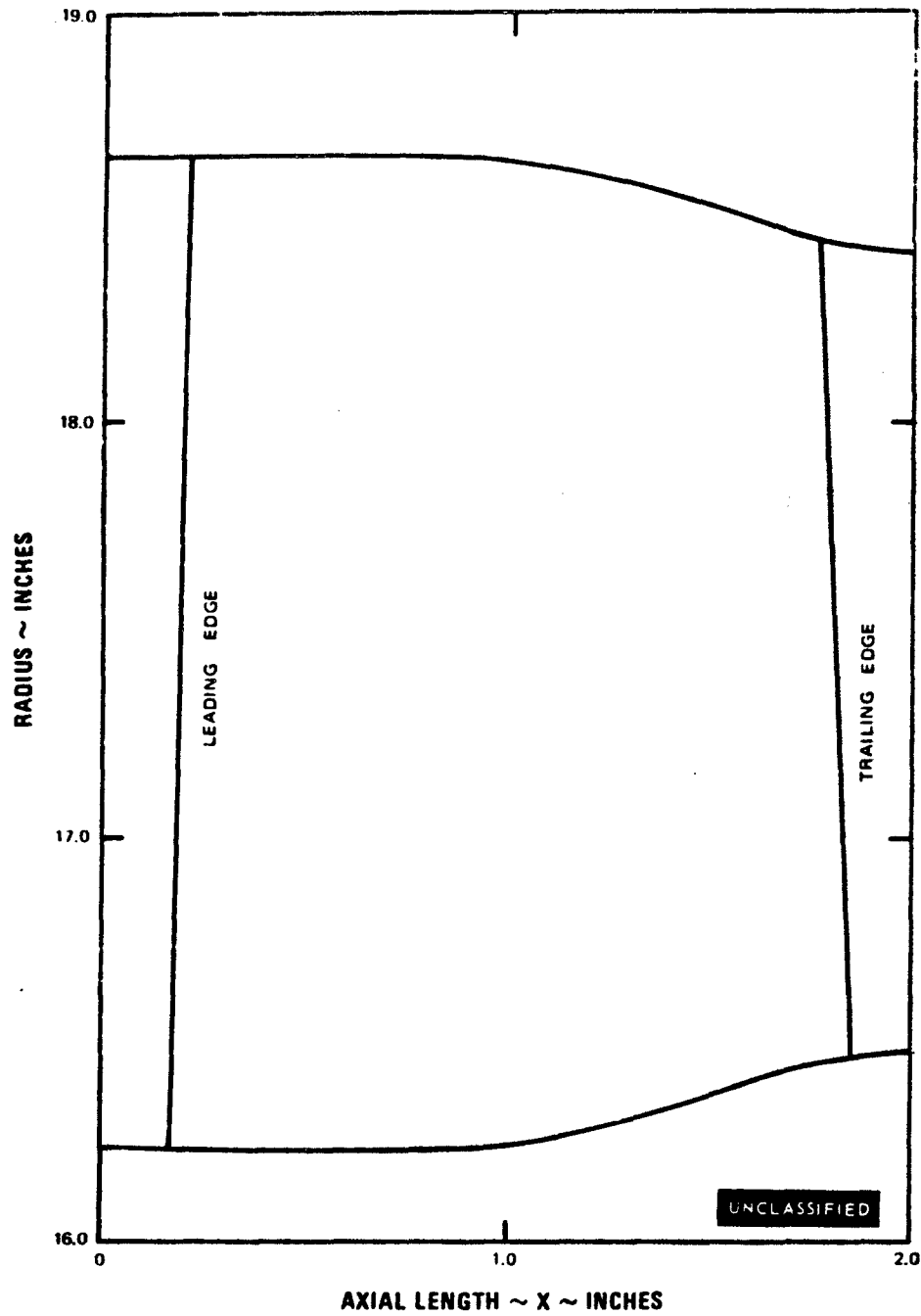


Figure 37 Vane Flowpath With Contoured End Wall

UNCLASSIFIED

UNCLASSIFIED

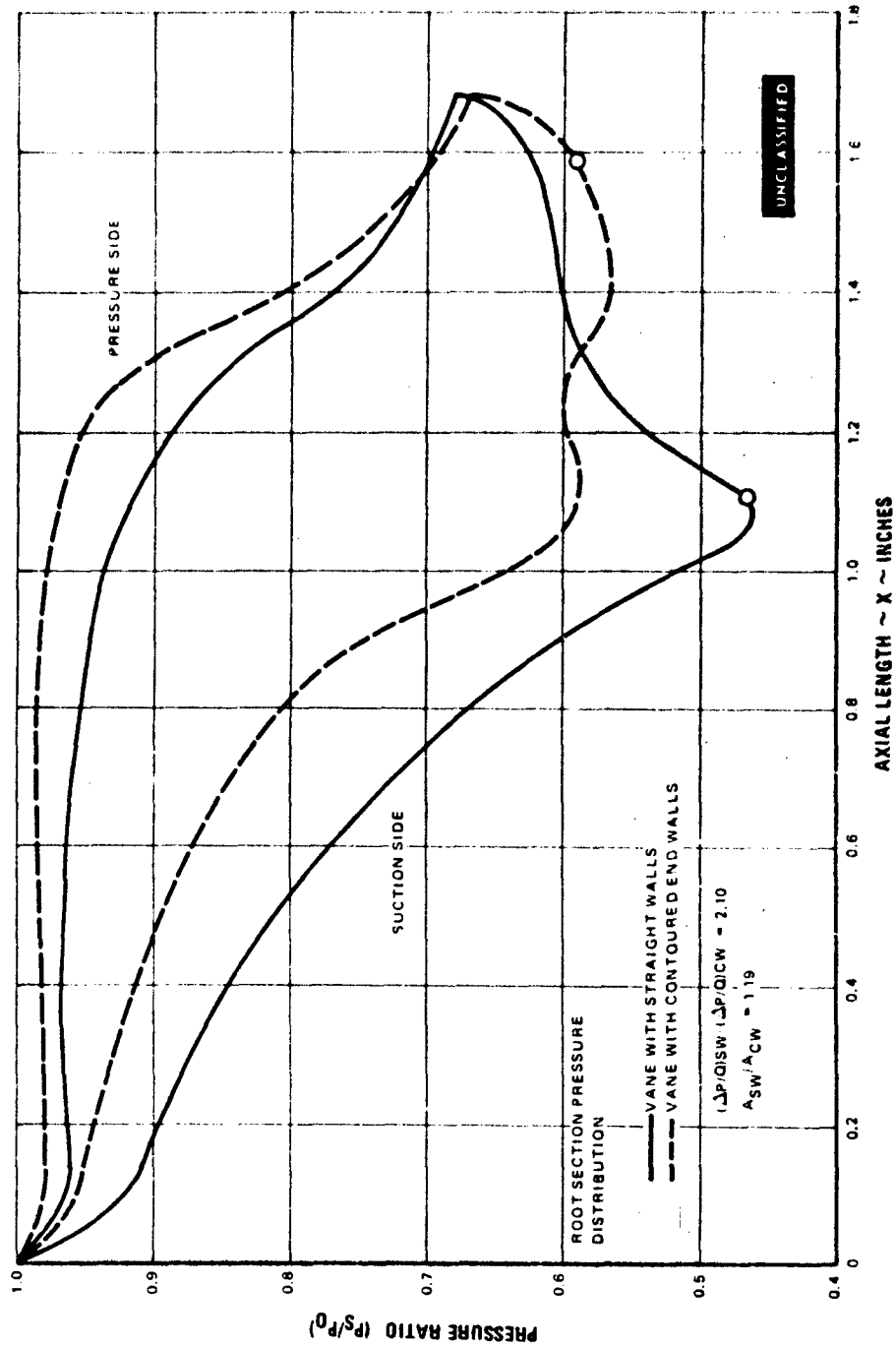


Figure 39 Effect of End Wall Contouring on Vane Root Pressure Distribution

UNCLASSIFIED

UNCLASSIFIED

(U) Two obstacles were encountered in attempting to apply these existing computer programs to the analysis of the contract turbine airfoils. The first is that the existing procedures cannot handle supersonic meridional velocities. Local regions of supersonic flow exist on most of the highly loaded airfoils being considered in the current program. The second problem concerns the convergence of the existing computer programs. For flow paths with relatively small radii of curvature (e.g., contouring of walls for high aspect ratio airfoils), the current numerical techniques allow the streamlines to shift too much between successive iterations and a convergent solution is not obtained.

(U) A good deal of company sponsored work is now being undertaken on this problem. One alternative procedure uses the matrix through-flow method of calculation (H. Marsh, R&M No. 3509, Brit. Aero. Res. Council). Although calculations by this method were not available for inclusion in this report, work will be continued in this area to assist the design of contoured walls for the remainder of this contract study.

(U) At this point, it can only be concluded that end wall contouring is a promising boundary layer control technique.

4. VORTEX GENERATORS

(U) Vortex generators have proved to be useful devices for the prevention of boundary layer separation in inlets and diffusers, and on aircraft wings where relatively thick boundary layers are encountered. The vortex generator is essentially a mixing device which strengthens the boundary layer by an exchange of energy with the mainstream. Pairs of vortex generators that produce counter-rotating vortices are generally more efficient (higher lift/drag ratio) than co-rotating arrays. The vortex generators must be located upstream of the separation point to allow sufficient time for mixing to take place.

(U) Experimental investigations of vortex generators to develop effective boundary layer control have resulted in the following design criteria:

- Rectangular or triangular shaped vortex generators are the most efficient.
- The triangular shaped geometry is more tolerant to variation of the boundary layer thickness δ from the design condition.
- Rectangular vortex generators should have a chord and span dimension of 1.1δ . Triangular vortex generators should have a chord of 2.5δ and a span of 1.25δ .

UNCLASSIFIED

UNCLASSIFIED

- The vortex generators should have a thickness-to-chord ratio of 6 to 8 percent, an incidence angle of 18 degrees, and a lateral spacing of 3.5δ . They should be located 12 to 15δ upstream of the separation point. If the separation is shock induced, the distance upstream should be increased to 25δ .

(U) Boundary layer separation in turbine cascades could begin in the suction surface corners. Therefore, placement of vortex generators for this application should be in the vicinity of the corner as shown in Figure 39. For the high work, low pressure turbine of this contract, the root section, suction side contours all have a favorable pressure gradient for the leading 20 percent of x/B which will prevent separation until after this point. The root section boundary layer thickness distribution calculated for the four low solidity airfoils is indicated in Figure 40. Based on this thickness and the design information presented above, the vortex generator span and chord dimensions are indicated in Table XI for the first vane and second blade of the low solidity turbine. These dimensions are typical for all four airfoils.

TABLE XI
VORTEX GENERATOR DIMENSIONS (INCH)

UNCLASSIFIED

Airfoil x/B	First Stage Vane		Second Stage Blade	
	Span	Chord	Span	Chord
0.2	0.0037	0.0075	0.0081	0.0162
0.4	0.0062	0.012	0.0137	0.0275
0.6	0.0119	0.023	0.0194	0.0388
0.8	0.0232	0.046	0.0281	0.0562

(U) The vortex generator should have a sharp leading edge and a thickness of 6 to 8 percent of the chord length. For the largest generator listed above the thickness would be 0.0045 inch. The fabrication and attachment of conventional vortex generators of this small size is not feasible. The possibility exists that some other type of device would induce mixing of high energy fluid in the boundary layer and produce an effect similar to the vortex generator. However, the design and development of such a device is beyond the scope of this study. Therefore, based on the fabrication and attachment problems, vortex generators are not recommended for boundary layer control on the turbine airfoils of this contract.

UNCLASSIFIED

UNCLASSIFIED

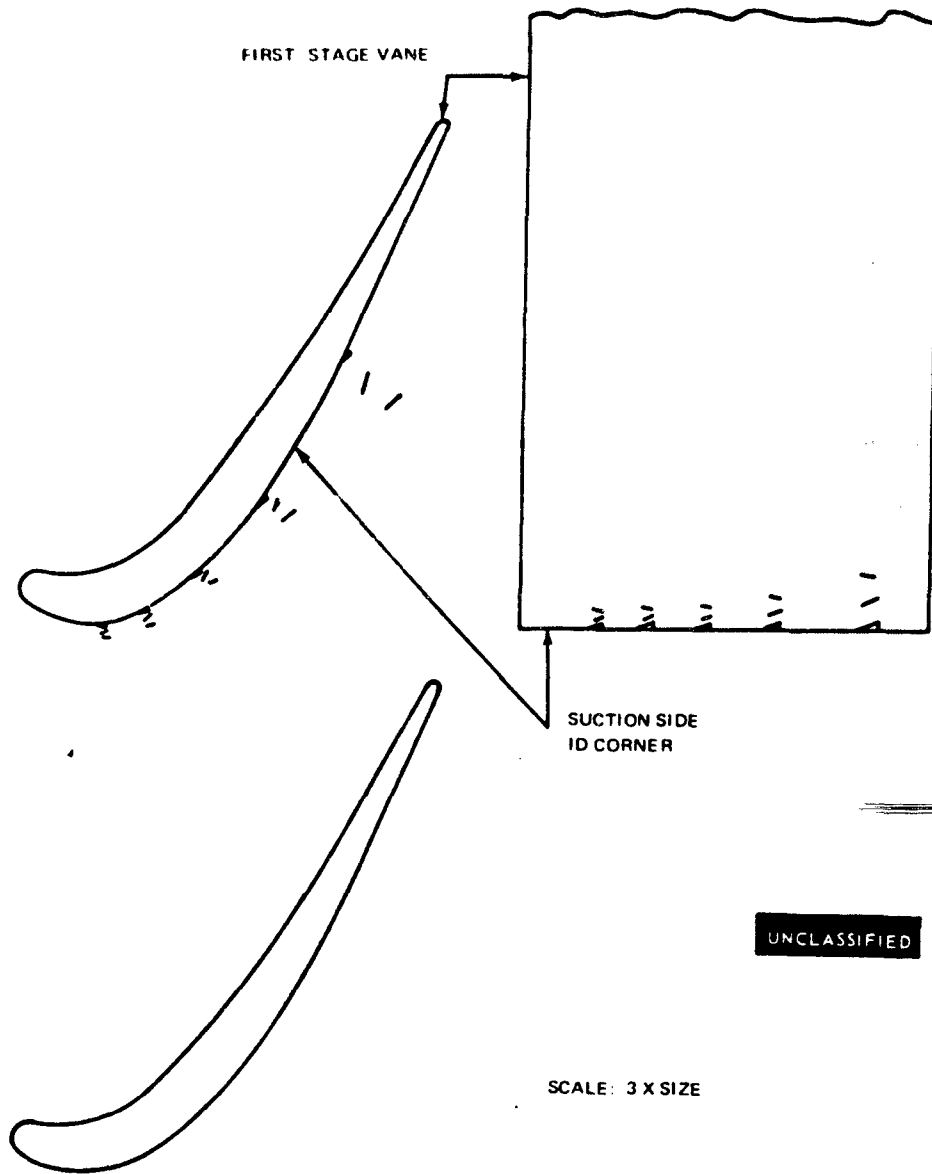


Figure 39 Vortex Generator Placement

UNCLASSIFIED

UNCLASSIFIED

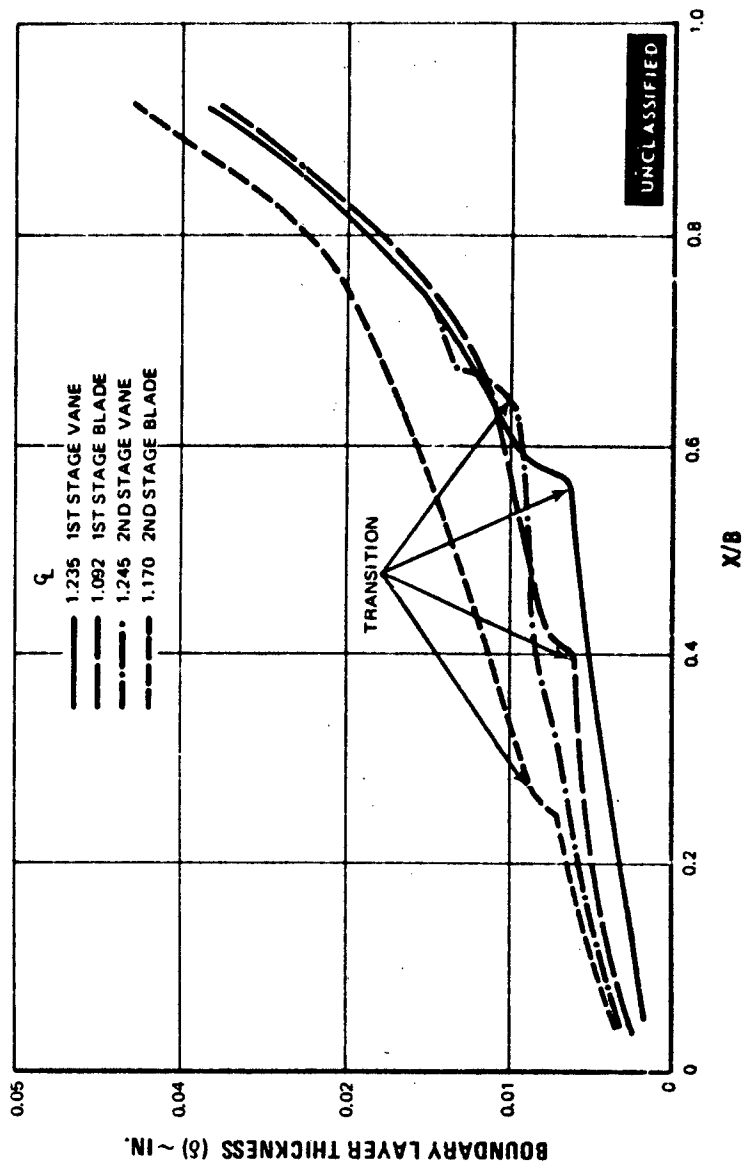


Figure 40 Medium Reaction - Low Solidity Root Section Hydrodynamic Thick-
ness

UNCLASSIFIED

UNCLASSIFIED

5. CORNER SLOTS

(U) Boundary layer re-energization has been applied successfully to diffusers where an external source of high pressure air could be used. However, the use of external air is not allowed under the ground rules established for the contract turbine. Slot flow only channels air from the pressure side of the airfoil to the suction side. Since the total pressure is essentially the same on both sides, there is insufficient power available for re-energization of the suction surface boundary layer. However, an alternative mechanism considered practical is the displacement of the old boundary layer by a new one initiating at the slot as illustrated in Figure 41. The slot boundary layer will be thinner and therefore more resistant to separation than the original boundary layer due to the shorter surface distance available for growth.

(U) Boundary layer calculations were made for a corner slot at the root section of the second stage, low solidity blade (Figure 42) to evaluate the potential of this control method for reducing corner separation. The tendency for corner separation increases after the gage point on the suction surface due to the increased rate of recompression starting at that location, and to the resulting rapid growth in boundary layer thickness. Therefore, the slot opening on the suction surface was located upstream of the gage point. Two basic assumptions in the analysis were that the slot flow does not substantially alter the original pressure distribution around the airfoil, and that the slot boundary layer grows just as though it were immersed in the undisturbed inviscid flow. It was further assumed that reasonable slot widths would be sufficient to prevent merging of the slot boundary layers prior to discharging on the suction surface. Merging of the boundary layers within the slot would result in a thick boundary layer reaching the suction surface, thus reducing the effectiveness of the intended boundary layer replacement.

(U) Figure 43 (a) shows the growth in momentum thickness for the two different assumed pressure distributions of Figure 43(b). The growth of the laminar boundary layer within the slot can be seen to be mainly dependent on surface distance rather than the pressure gradient within the slot. This fortunate result implies that the slot shape is not critical and relieves the need for tight manufacturing tolerances which would be difficult to achieve in the small slots being considered. The momentum thickness of the new boundary layer at the gage point is approximately 0.0004 inch compared to 0.0014 inch for the original unslotted airfoil.

UNCLASSIFIED

UNCLASSIFIED

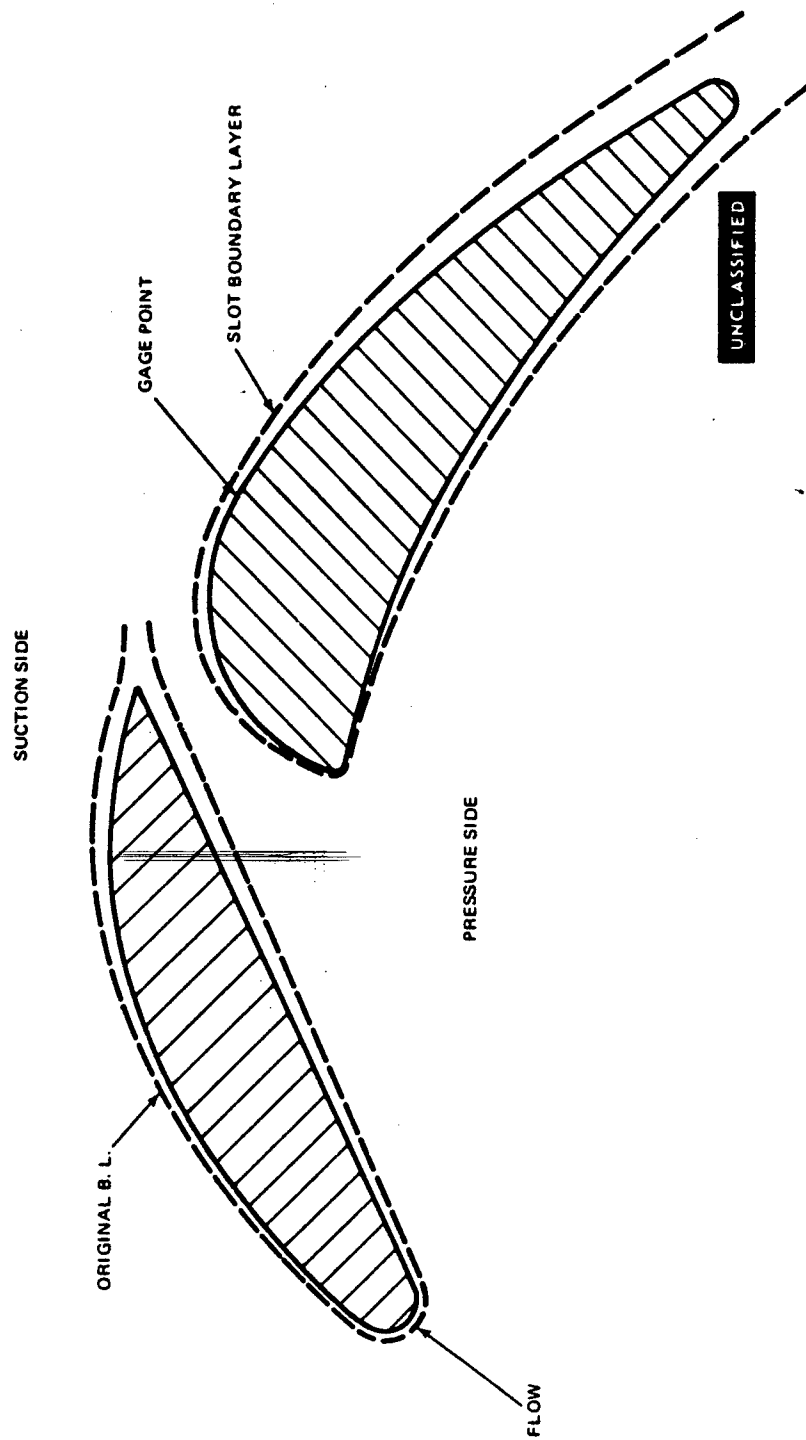


Figure 41 Typical Slotted Airfoil

UNCLASSIFIED

UNCLASSIFIED

MEDIUM REACTION
SECOND STAGE BLADE
ROOT SECTION
LOW SOLIDITY

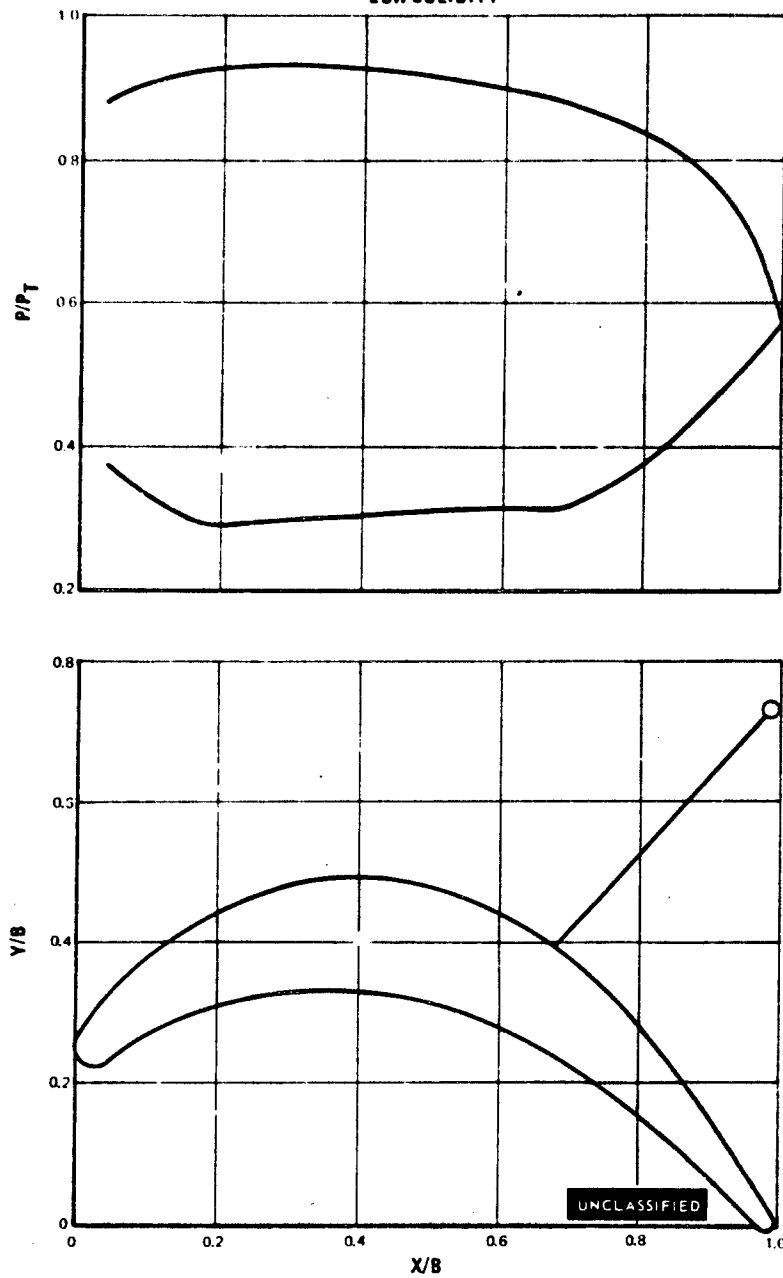


Figure 42

UNCLASSIFIED

UNCLASSIFIED

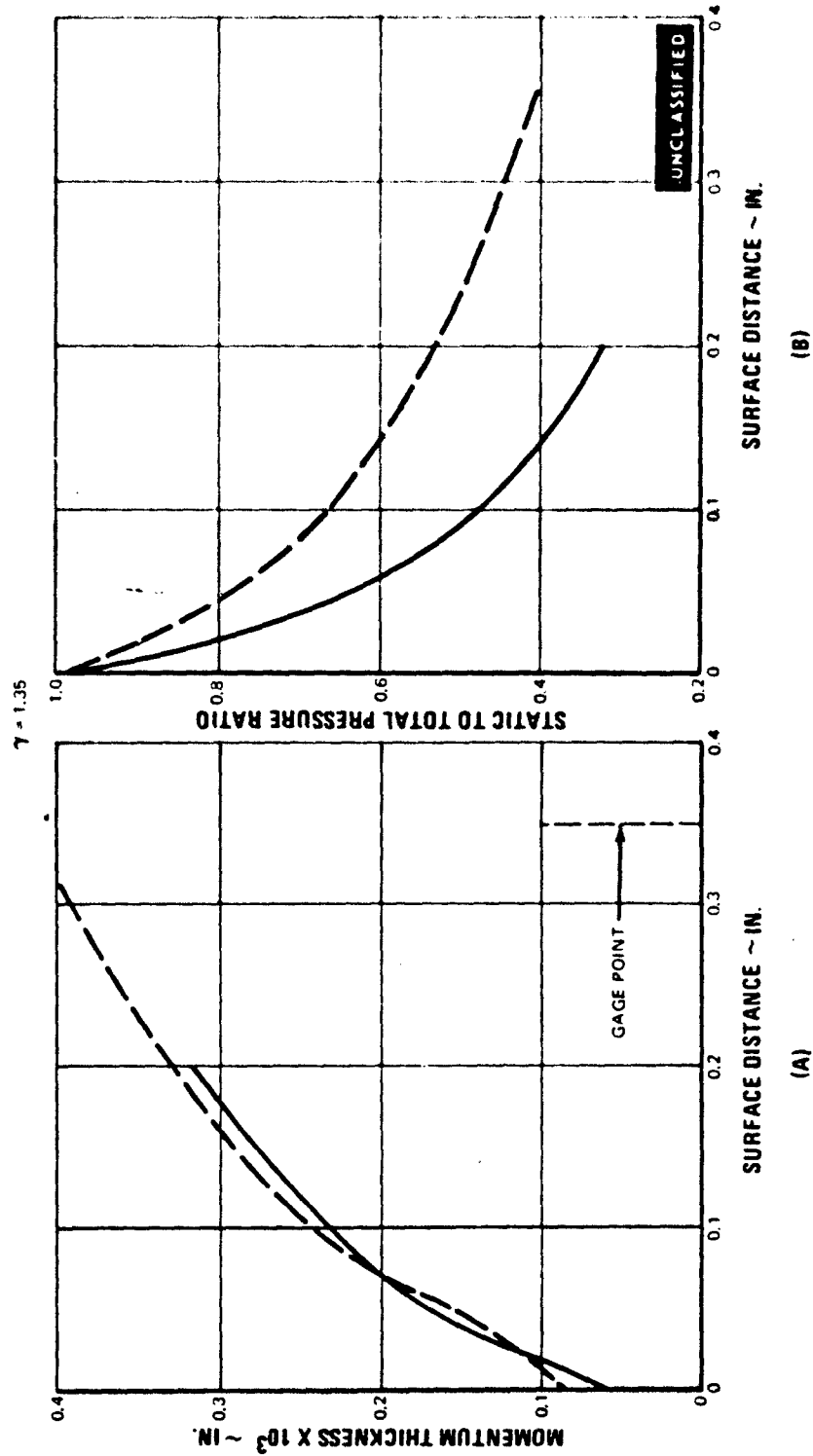


Figure 43 Effect of Length and Pressure Gradient on Laminar Boundary Layer Formation

UNCLASSIFIED

UNCLASSIFIED

(U) Since the suction surface velocities are predominantly supersonic, the slots will usually be choked, which provides better control over the slot flow and simplifies associated calculations. As a result of the above reduction in gage point momentum thickness, the momentum thickness at the trailing edge was reduced from 0.003 to 0.001 (Figure 44) and the drag coefficient was increased from 0.0012 to 0.0022 at 92 percent x/B . These results indicate a substantial strengthening of the trailing edge boundary layer through the use of slots.

(U) Typical corner slot applications are shown in Figure 45 for the low solidity first-stage vane and second-stage blade root sections. The combined thickness of the slot boundary layers is approximately 0.020 inch. Therefore, a slot width of 0.030 inch was selected to ensure that the slot boundary layers do not merge. The aft side of the slot is faired into the suction surface at the gage point to provide a smooth entrance for the new boundary layer formed in the slot. The slots should be located as close as possible to the end wall. A spanwise slot height of 0.20 inch is considered adequate for the low pressure turbine airfoils under consideration. This height is about 10 times the two-dimensional boundary layer thickness on the airfoil surface which would insure sufficient coverage of the corner flow region, without substantially affecting the original pressure distribution or the main foil boundary layer.

(U) Corner slots appear to be both practical and effective devices for the control of corner boundary layer separation.

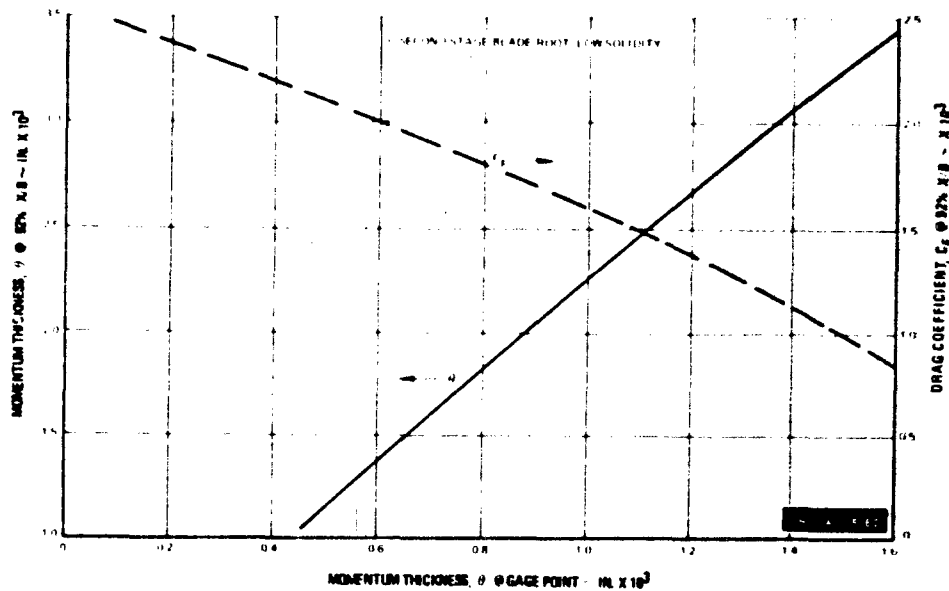


Figure 44 Effect of Momentum Thickness at Gage Point on Momentum Thickness and Friction Coefficient at 92 Percent Chord Point

UNCLASSIFIED

UNCLASSIFIED

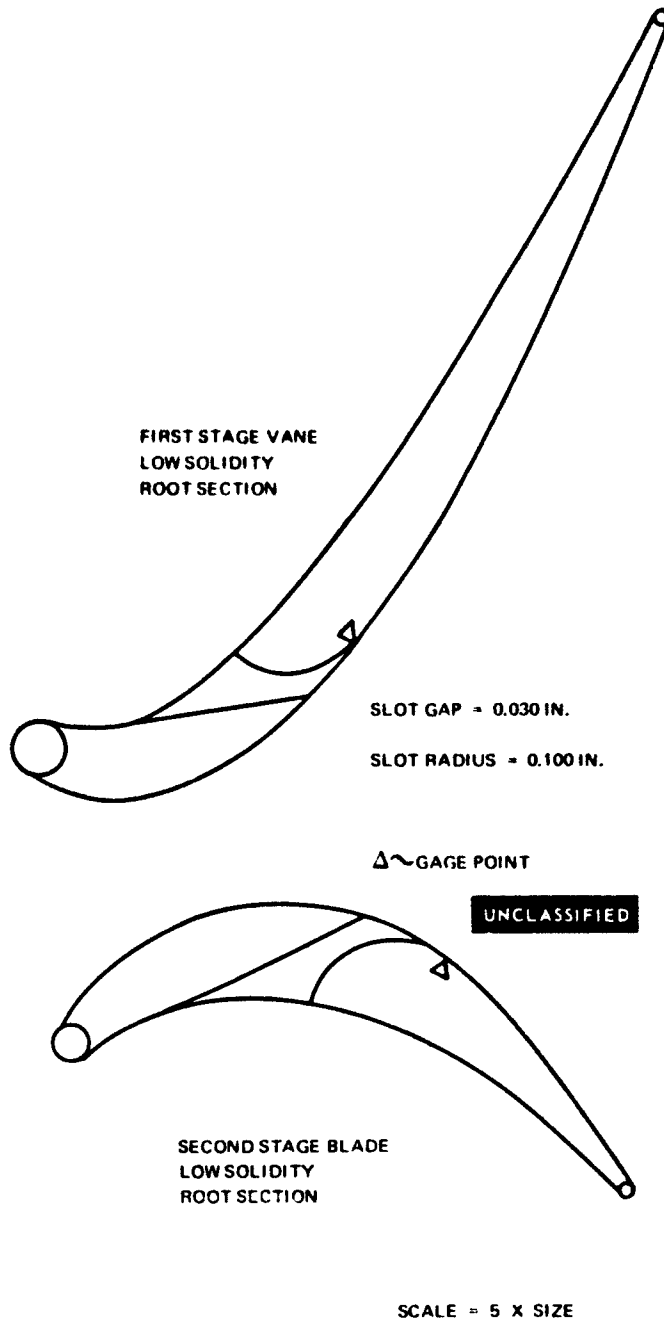


Figure 45 Typical Corner Slot Applications

UNCLASSIFIED

6. CORNER FILLETS

(U) The flow along a corner of two relatively flat surfaces intersecting at a right angle, such as the turbine airfoil and the end wall, has a boundary layer quite different from that of the two-dimensional boundary layer on the adjacent surfaces. At the intersection of the two surfaces, a mixing of the two boundary layers occurs with a strong mutual interference and excessive skin friction. The transition from laminar to turbulent flow occurs further upstream near the corner, rather than on the adjacent surfaces. The boundary layer in the corner is also exposed to a severe adverse pressure gradient which causes it to thicken and separate rapidly. The corner flow phenomena was discussed with Professor H. Schlichting and his opinion was that corner fillets should have the effect of shifting the corner flow condition toward the two-dimensional boundary layer condition present on the adjacent surfaces.

(U) A suitable analytical technique has not been developed for the complex three-dimensional corner flow. Therefore, a simple model of the corner boundary layer was constructed to guide the initial sizing of fillets (Figure 46). The basic hypothesis is that boundary layer behavior in the corner can be made to approach that of a two-dimensional boundary layer by reducing the area of wetted surface in the corner.

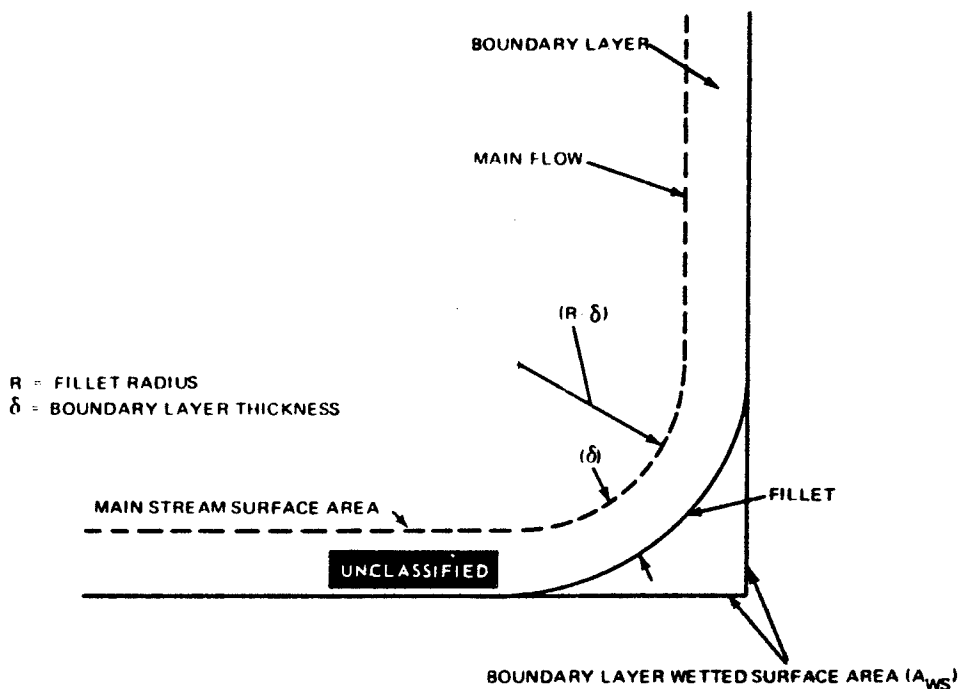


Figure 46 Simplified Corner Boundary Layer Model

UNCLASSIFIED

(U) The difference between the corner boundary layer wetted surface area (A_{ws}) and the main stream surface area (A_{ms}) is a function of fillet radius (R_F) and boundary layer thickness (δ) as expressed in the following equation:

$$\frac{A_{ws} - A_{ms}}{A_{ws}} = \frac{\delta}{R_F}$$

This area difference is reduced to 10 percent with a fillet radius equal to 10δ . Using this criterion, the fillet radius as a function of axial location is indicated in Table XII for the suction side roots of the first vane and second blade.

TABLE XII

<u>x/B</u>	FILLET RADIUS (INCH)	
	<u>First Stage Vane</u>	<u>Second Stage Blade</u>
0.2	0.030	0.065
0.4	0.050	0.110
0.6	0.095	0.155
0.8	0.185	0.225

UNCLASSIFIED

The point of tangency of the fillet with the root platform is indicated in Figure 47. The fillets are faired back into the airfoil leading and trailing edges to avoid abrupt wall geometry changes in these locations. The reduction in flow area (blockage) for the fillet of this type is only 0.46 and 0.55 percent for the first vane and second blade, respectively, as illustrated in Figure 48. Consequently, there should be little disturbance of the original potential flow pressure distribution due to their presence. Although the literature offers little encouragement for their effectiveness, corner fillets appear useful at least in the event of corner boundary layer separation.

UNCLASSIFIED

UNCLASSIFIED

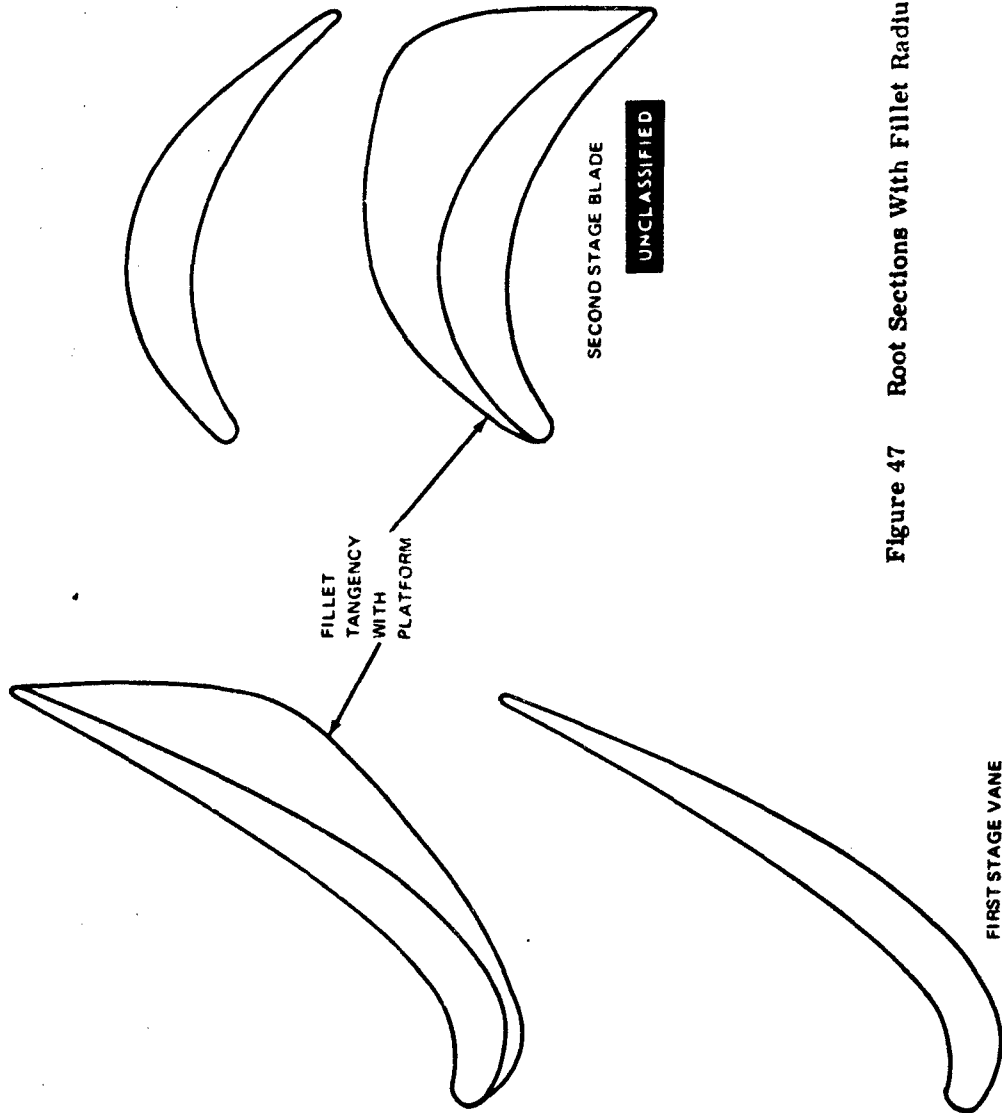


Figure 47 Root Sections With Fillet Radius Equal to 10δ

UNCLASSIFIED

UNCLASSIFIED

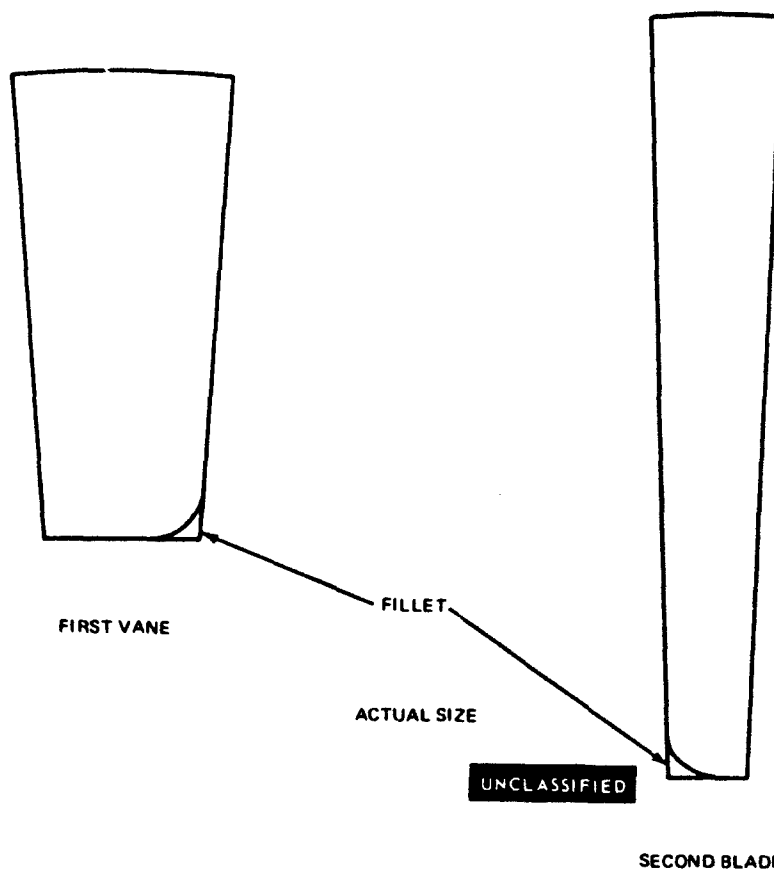


Figure 48 Suction Side Root Fillet-Axial View of Passage From Rear

7. TENTATIVE RANKING OF BOUNDARY LAYER CONTROL METHODS

(U) It has already been noted that the corner boundary layer loss can manifest itself as either an unseparated or a separated flow, and that techniques exist which should control either phenomenon. As the solidity of any row of turbine airfoils is creased, the corner boundary layers will move towards separation. However, contour refinement at any given solidity reduces the possibility of separation in the suction surface corners. Due to the fact that no analytical techniques for predicting the complex behavior of the corner boundary layers exist, the net effect of the contour refinement at the high loadings of this study cannot be determined in advance.

UNCLASSIFIED

UNCLASSIFIED

(U) The application of boundary layer control methods to the Phase II cascade testing will depend directly on the nature of the end loss observed in the baseline airfoil tests. If the baseline tests indicate high corner losses without any significant boundary layer separation, the control methods should be essentially limited to those that tend to reduce boundary layer migration on the end wall, e.g., end wall contouring and local uncambering. In the event that significant corner separation is observed, end wall contouring and local uncambering should still be beneficial since these methods have the potential of reducing both the cross-flow pressure gradient causing boundary layer migration and the adverse streamwise pressure gradient causing separation. The local momentum alteration methods of corner slots and fillets should also be applied to reduce or eliminate the separated region.

(U) As previously mentioned, it was not necessary to rank the various boundary layer control methods according to their effectiveness for individual airfoils. However, a tentative ranking is presented below, for any airfoil, based on the two end loss situations considered possible.

a. Unseparated Corner Boundary Layer:

- End wall contouring at root and tip
- Local uncambering at root and tip

b. Separated Corner Boundary Layer:

- End wall contouring
- Local uncambering
- Corner slots
- Fillets.

UNCLASSIFIED

SECTION VI

SELECTION OF BASELINE TURBINE (Task 1e)

RFP OBJECTIVE

(U) To Fix The Two-Stage Turbine Baseline Design.

(U) The final choice of turbine configuration, including highly refined airfoil contours, rests upon judgments formed from all the information assembled and generated up to this point.

(U) The design system has indicated that a number of turbine configurations are capable of meeting the performance requirements of this contract. In particular, the medium reaction, normal solidity turbine promises to meet the required goals in a configuration that would be practical and realistic. This normal solidity is itself beyond the present state-of-the-art. Furthermore, the medium reaction, lower solidity studies have shown that further improvement may be possible. It should be reiterated, however, that the turbine design systems have deliberately been pushed beyond their presently-established limits during this study, and cannot yet be assumed to be entirely reliable.

(U) It has also been pointed out that the similarity of the resulting airfoil pressure distributions makes differentiation between the various medium reaction turbines, on the basis of boundary layer control, almost impossible. The most important conclusion reached in the boundary layer control portion of this study was that the physical manifestation of the end wall losses cannot be established in advance of experiments. Since the control of unseparated corner boundary layers makes use of different techniques than the control of separated corner boundary layers, the choice of applicable techniques must await the testing of the baseline airfoils.

(U) As a result of such considerations, it is recommended that:

- (1) The baseline turbine be the medium reaction, normal solidity design. This choice is entirely consistent with the goals of the study and with reasonably prudent application of existing analytical techniques.
- (2) The baseline airfoils be carefully tested to determine the nature and extent of the end loss mechanism before choosing and designing appropriate boundary layer control techniques.

UNCLASSIFIED

(3) The rank order of control techniques for unseparated corner boundary layers should be:

- End wall contouring at root and tip
- Local uncambering at root and tip

while for separating corner layers it should be:

- End wall contouring at root and tip
- Local uncambering at root and tip
- Corner slots
- Fillets in suction surface corners

UNCLASSIFIED

UNCLASSIFIED

APPENDIX I
PRELIMINARY AIRFOIL SECTIONS

PAGE NO. 85

UNCLASSIFIED

UNCLASSIFIED

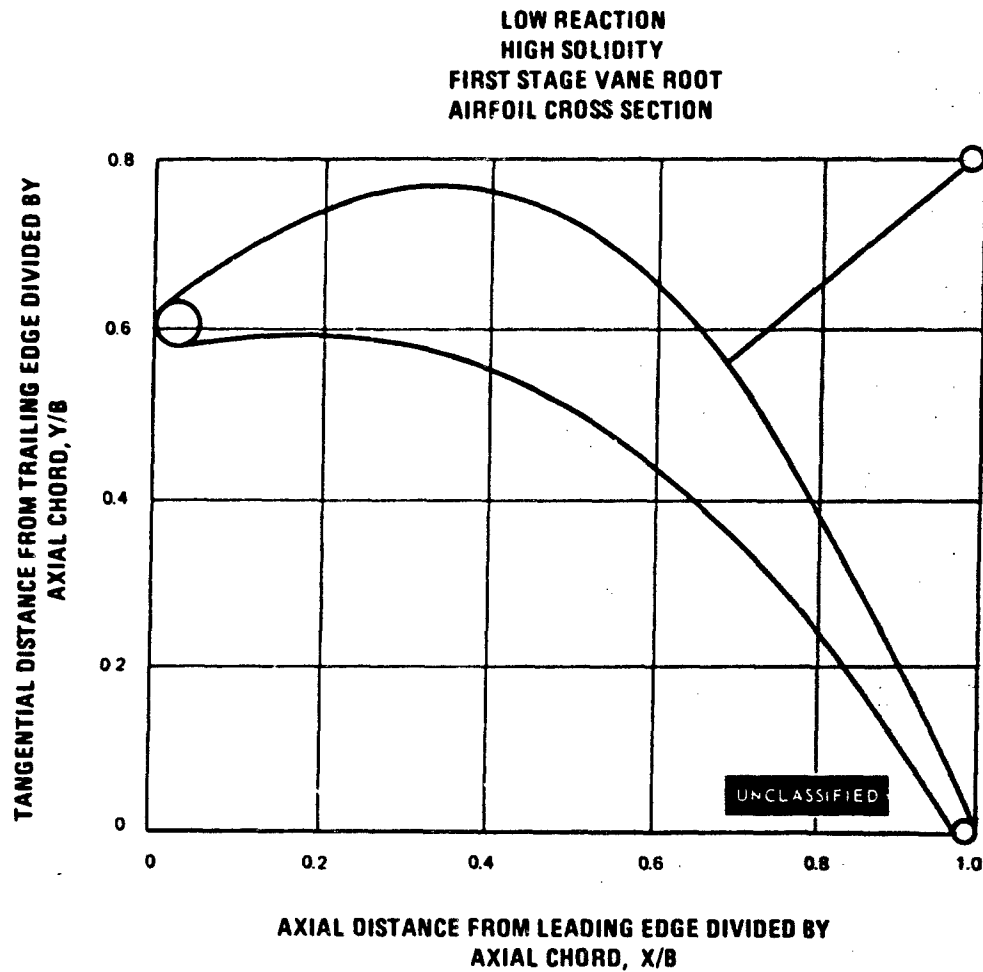


Figure 49

UNCLASSIFIED

UNCLASSIFIED

LOW REACTION
HIGH SOLIDITY
FIRST STAGE VANE ROOT

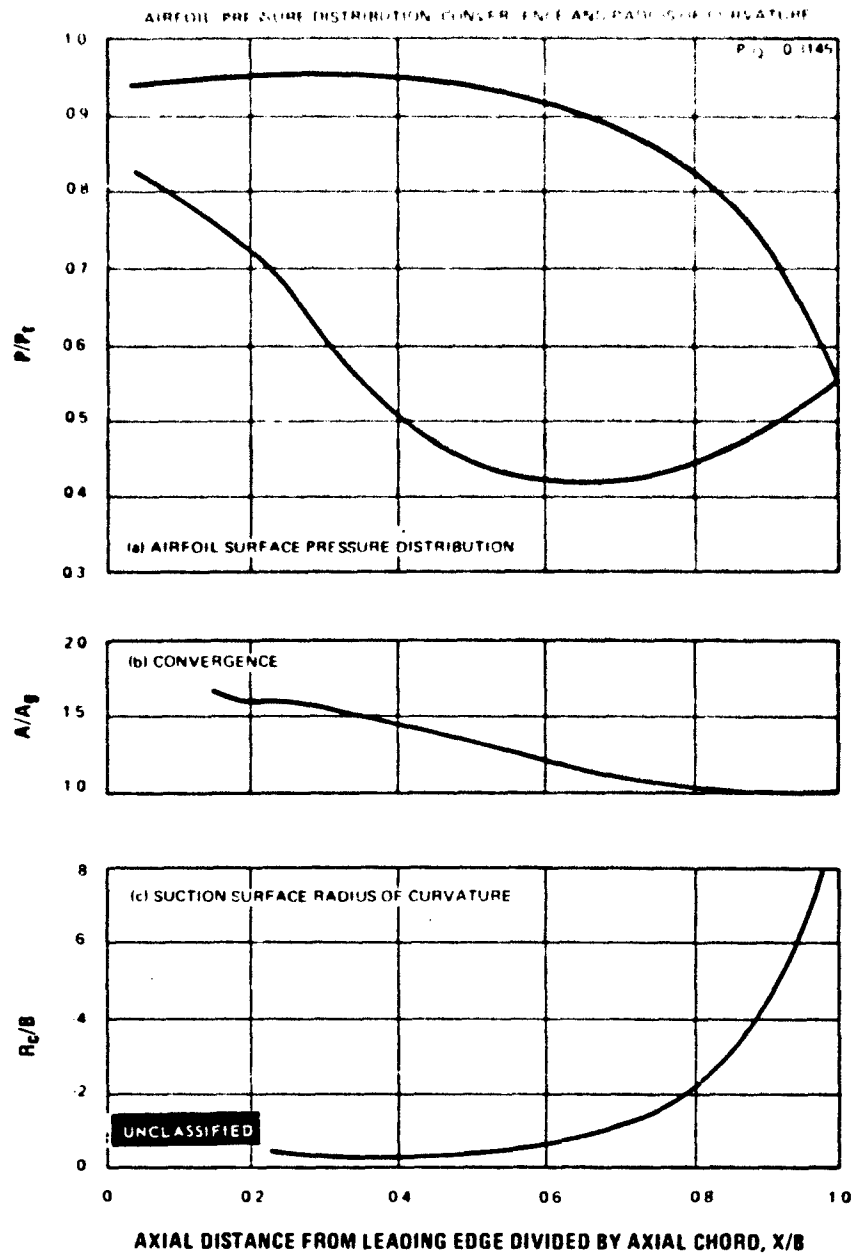


Figure 50

PAGE NO 87

UNCLASSIFIED

UNCLASSIFIED

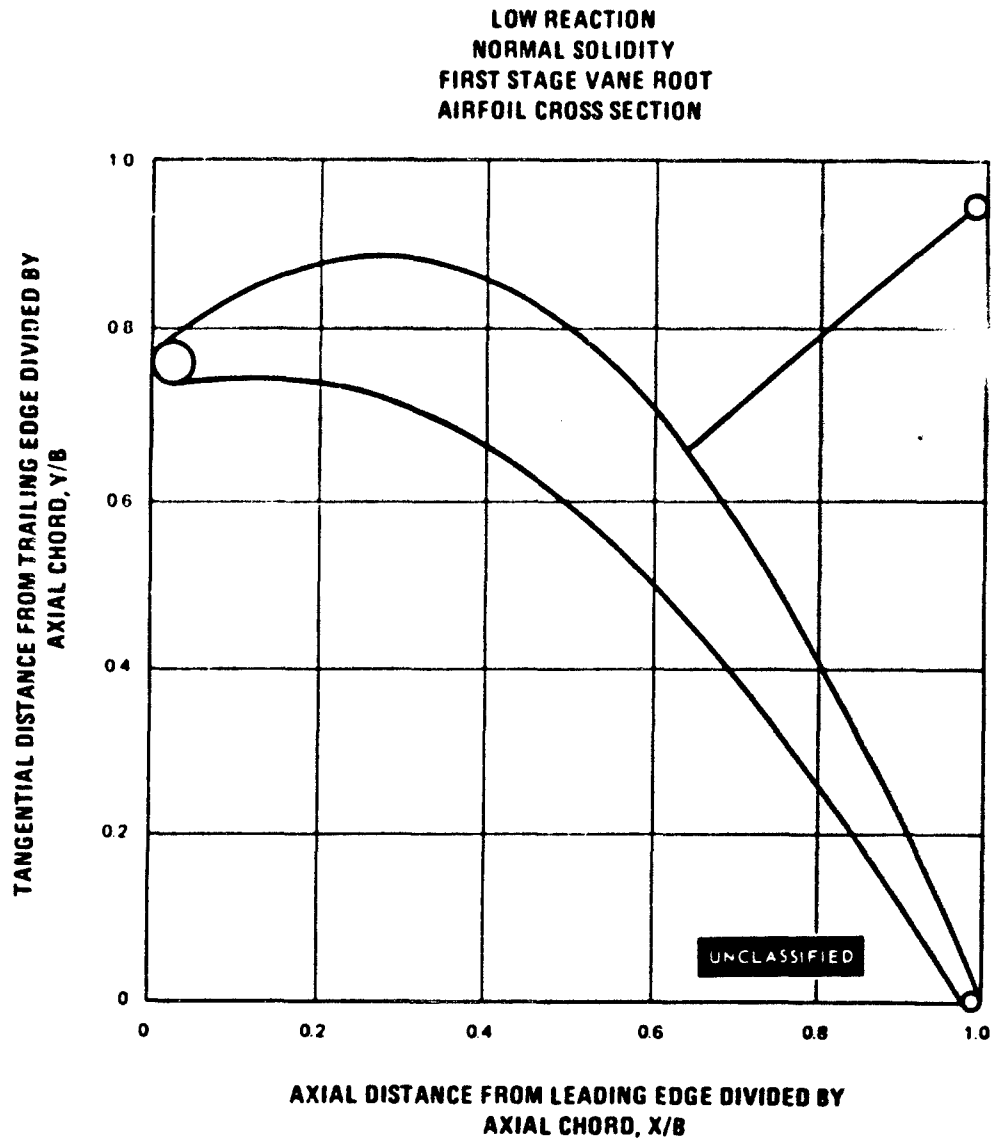


Figure 51

UNCLASSIFIED

UNCLASSIFIED

LOW REACTION
NORMAL SOLIDITY
FIRST STAGE VANE ROOT

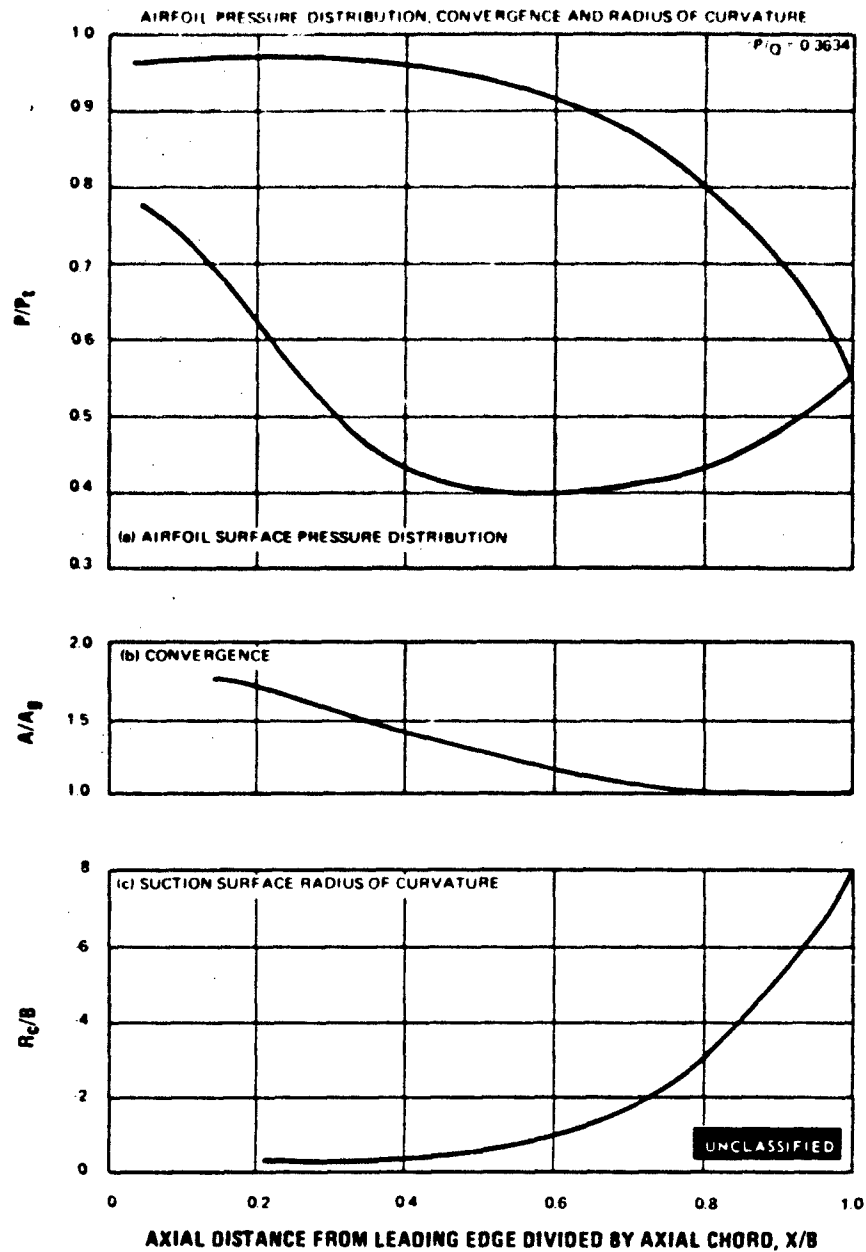


Figure 52

UNCLASSIFIED

UNCLASSIFIED

LOW REACTION
MEDIUM SOLIDITY
FIRST STAGE VANE ROOT
AIRFOIL CROSS SECTION

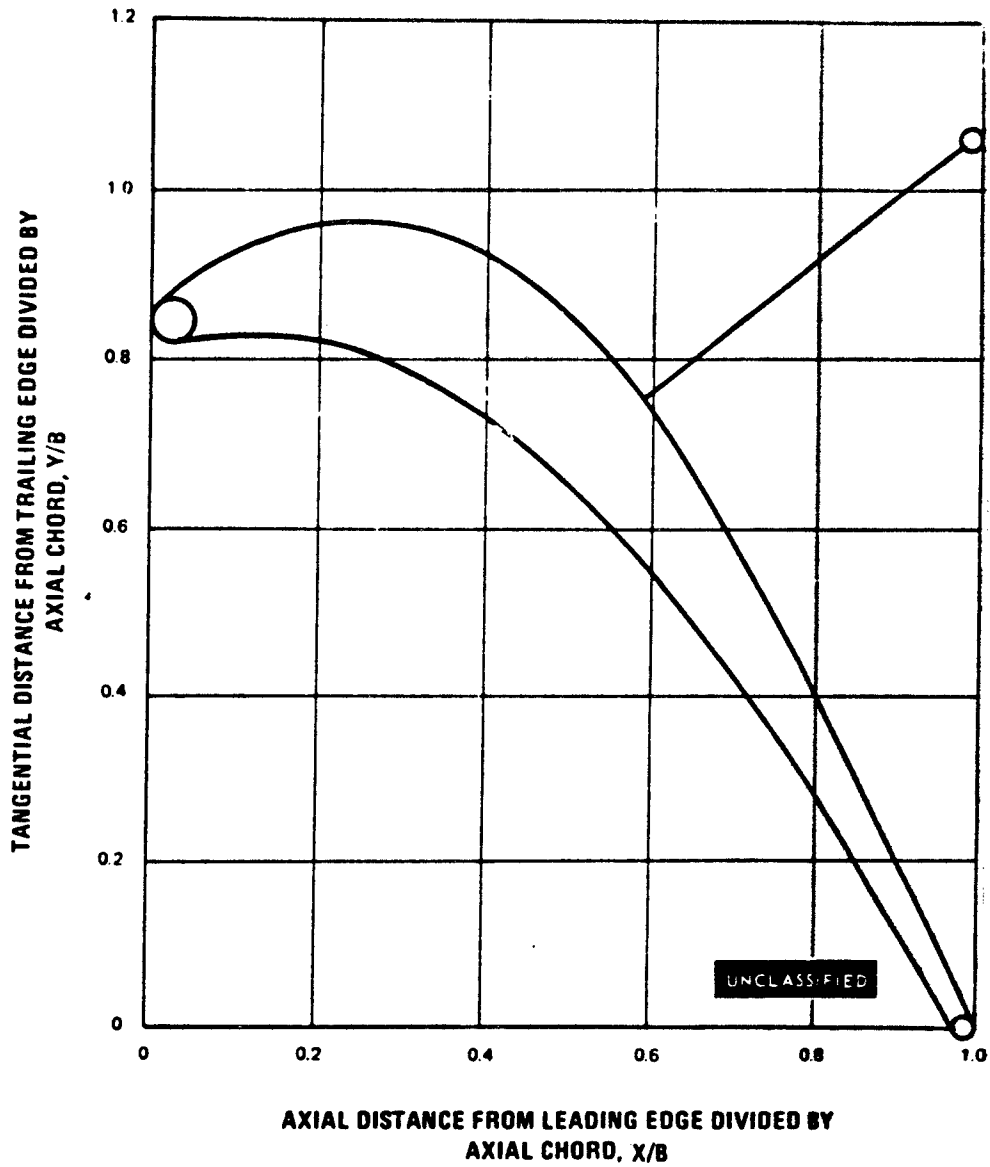


Figure 53

UNCLASSIFIED

UNCLASSIFIED

LOW REACTION
MEDIUM SOLIDITY
FIRST STAGE VANE ROOT

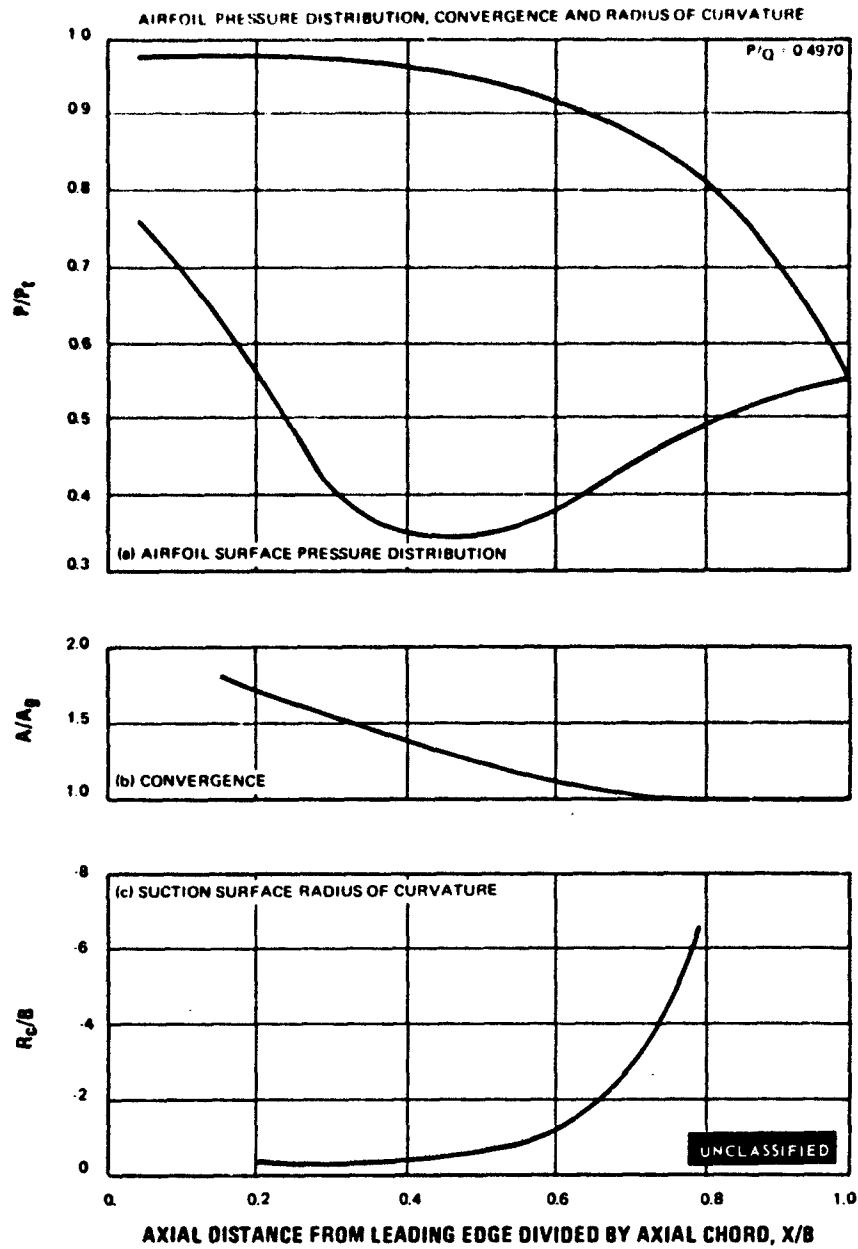


Figure 54

UNCLASSIFIED

UNCLASSIFIED

LOW REACTION
LOW SOLIDITY
FIRST STAGE VANE ROOT
AIRFOIL CROSS SECTION

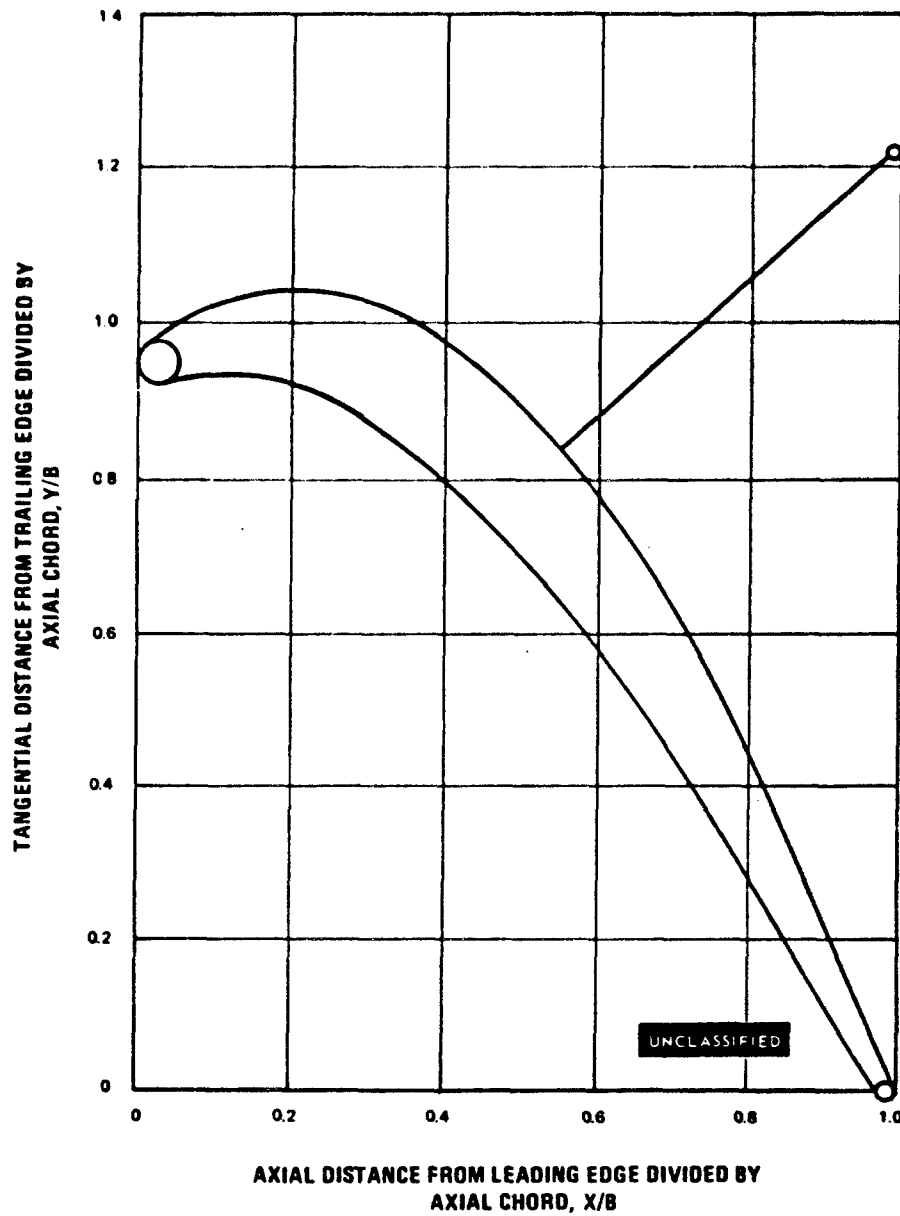


Figure 55

UNCLASSIFIED

UNCLASSIFIED

LOW REACTION
LOW SOLIDITY
FIRST STAGE VANE ROOT

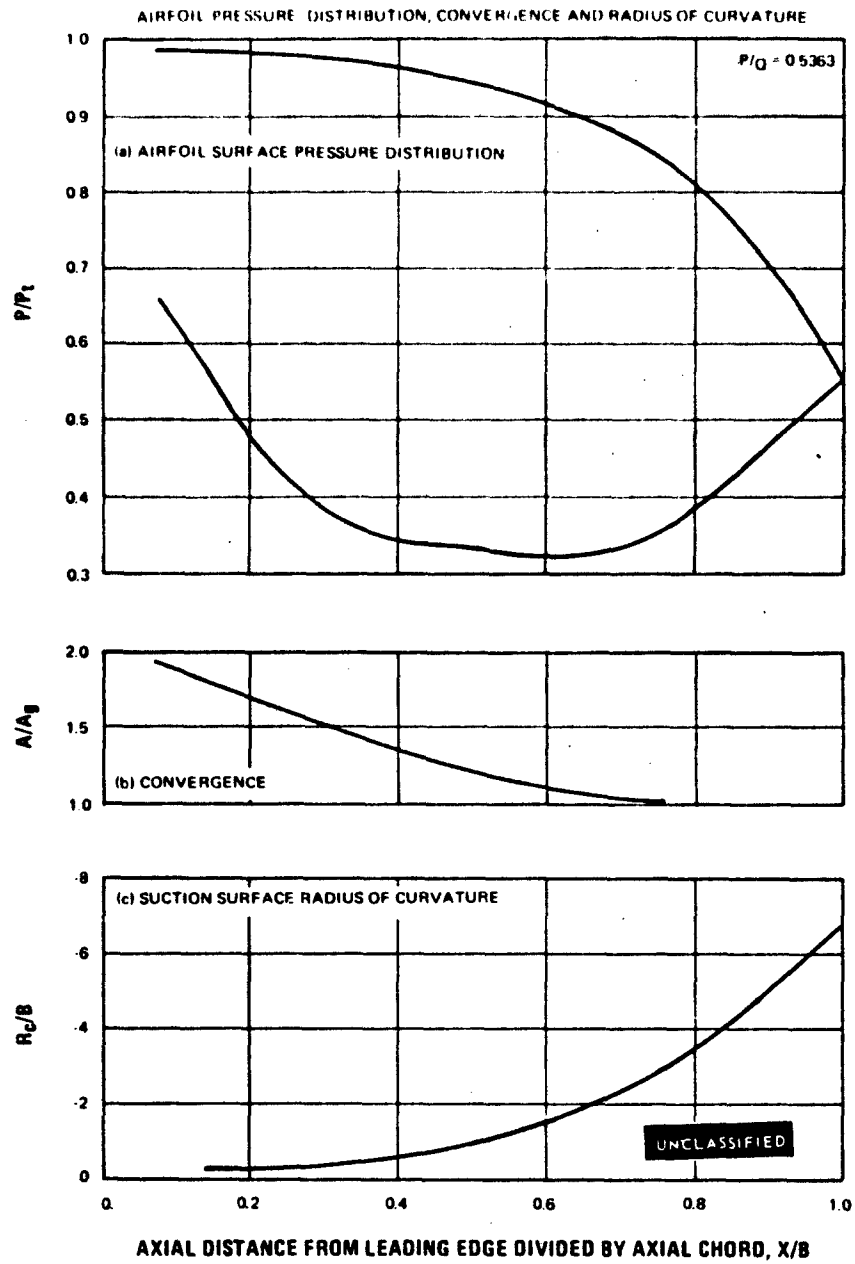


Figure 56

UNCLASSIFIED

UNCLASSIFIED

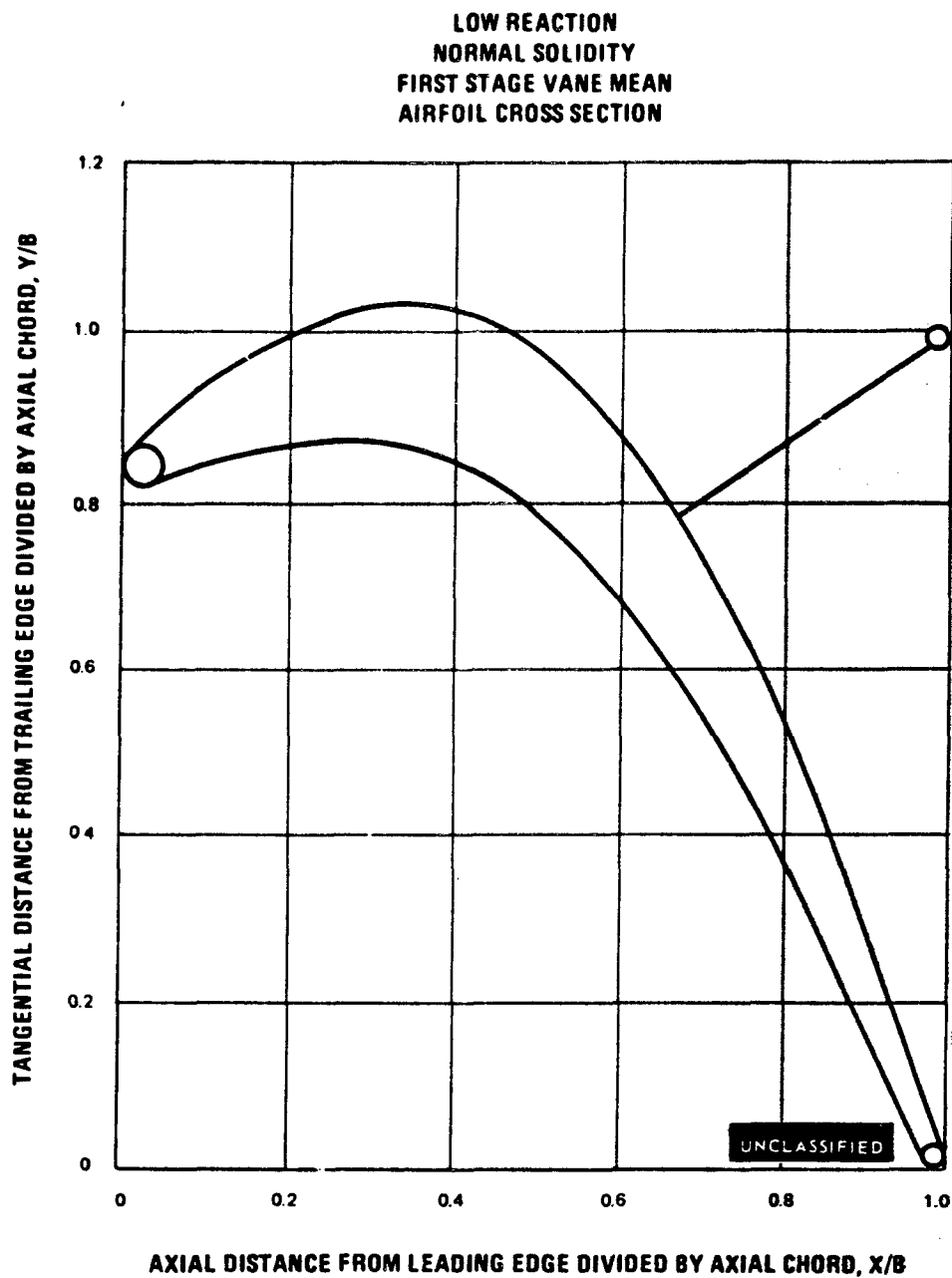


Figure 57

UNCLASSIFIED

UNCLASSIFIED

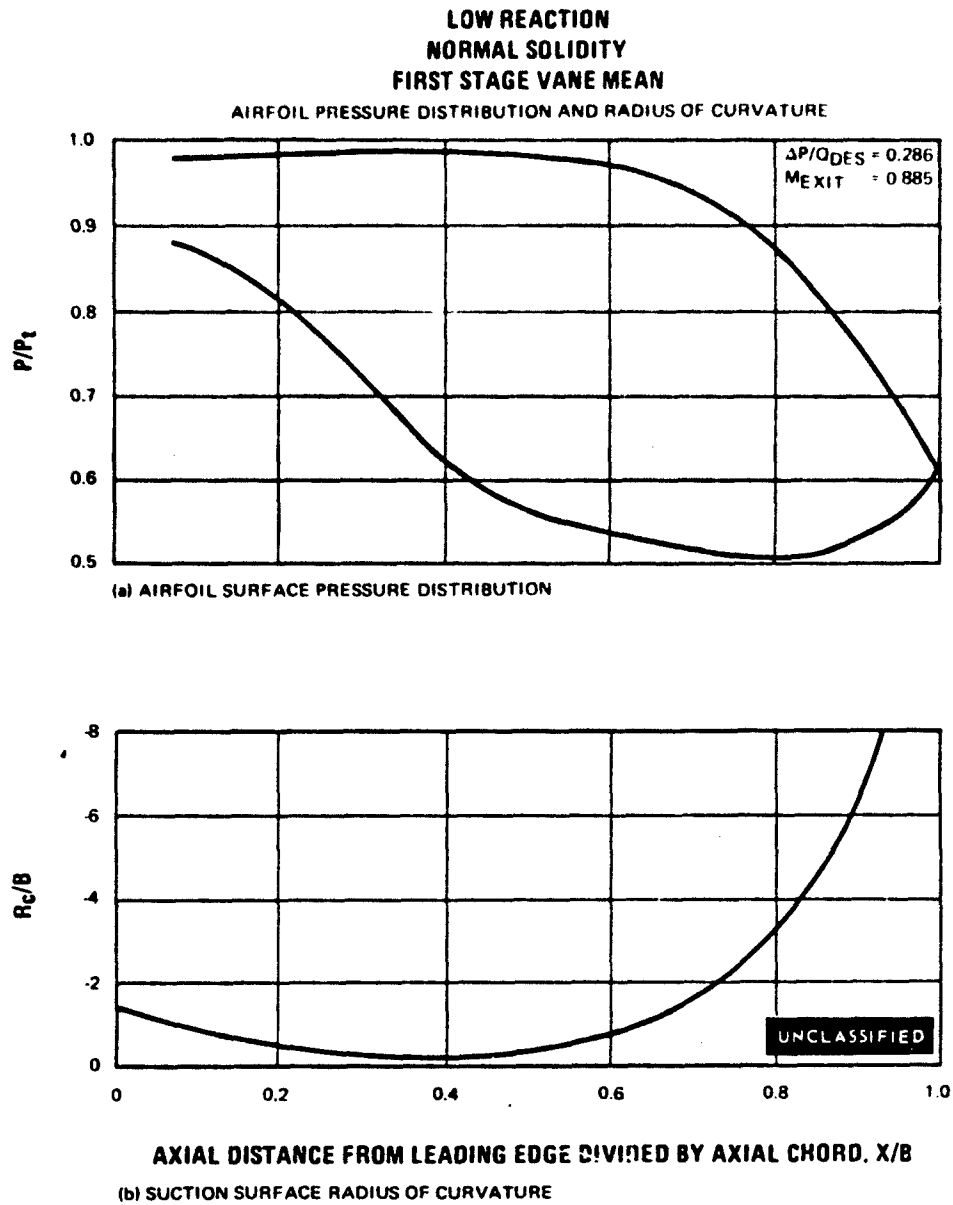


Figure 58

UNCLASSIFIED

UNCLASSIFIED

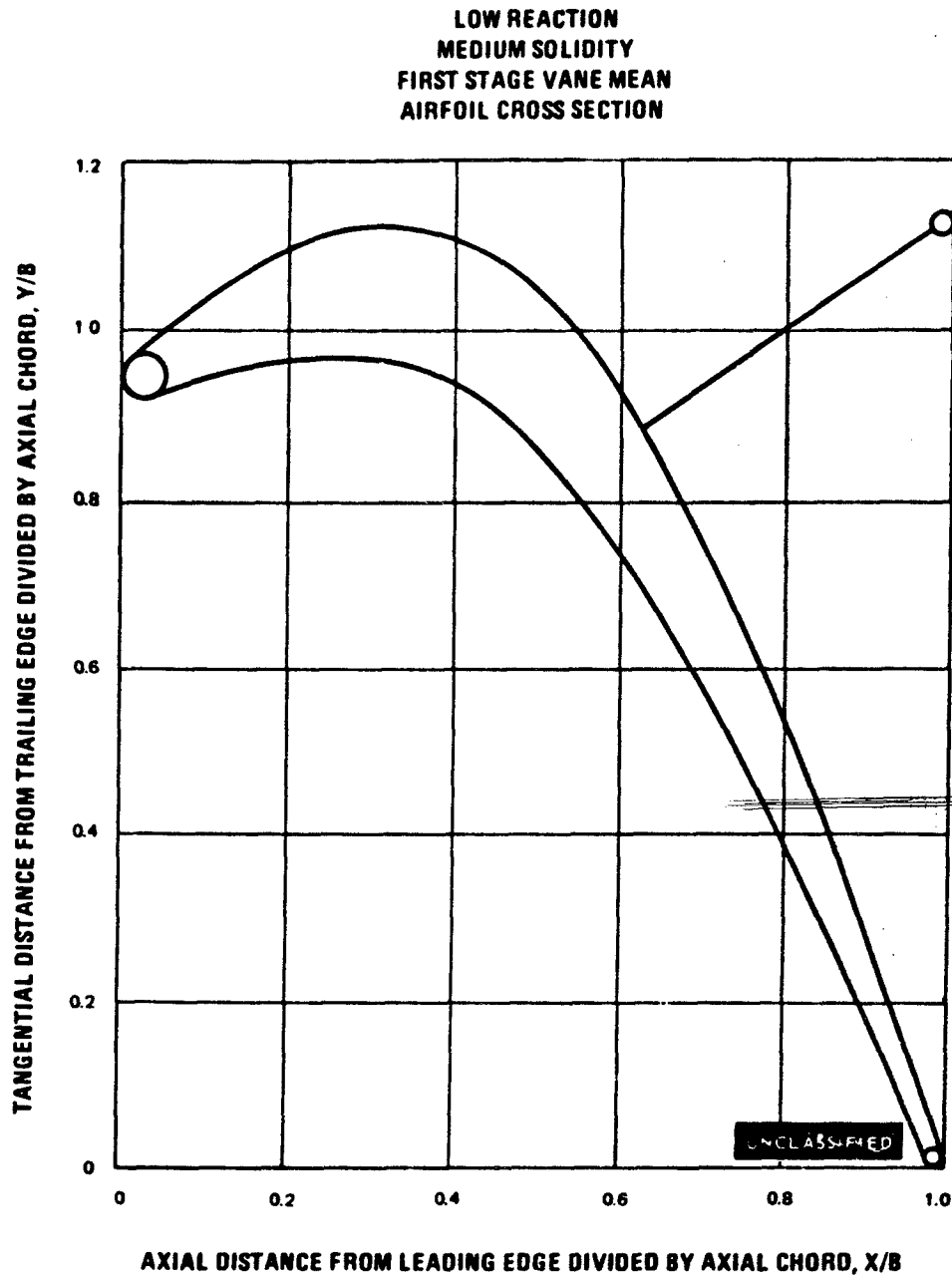


Figure 59

UNCLASSIFIED

UNCLASSIFIED

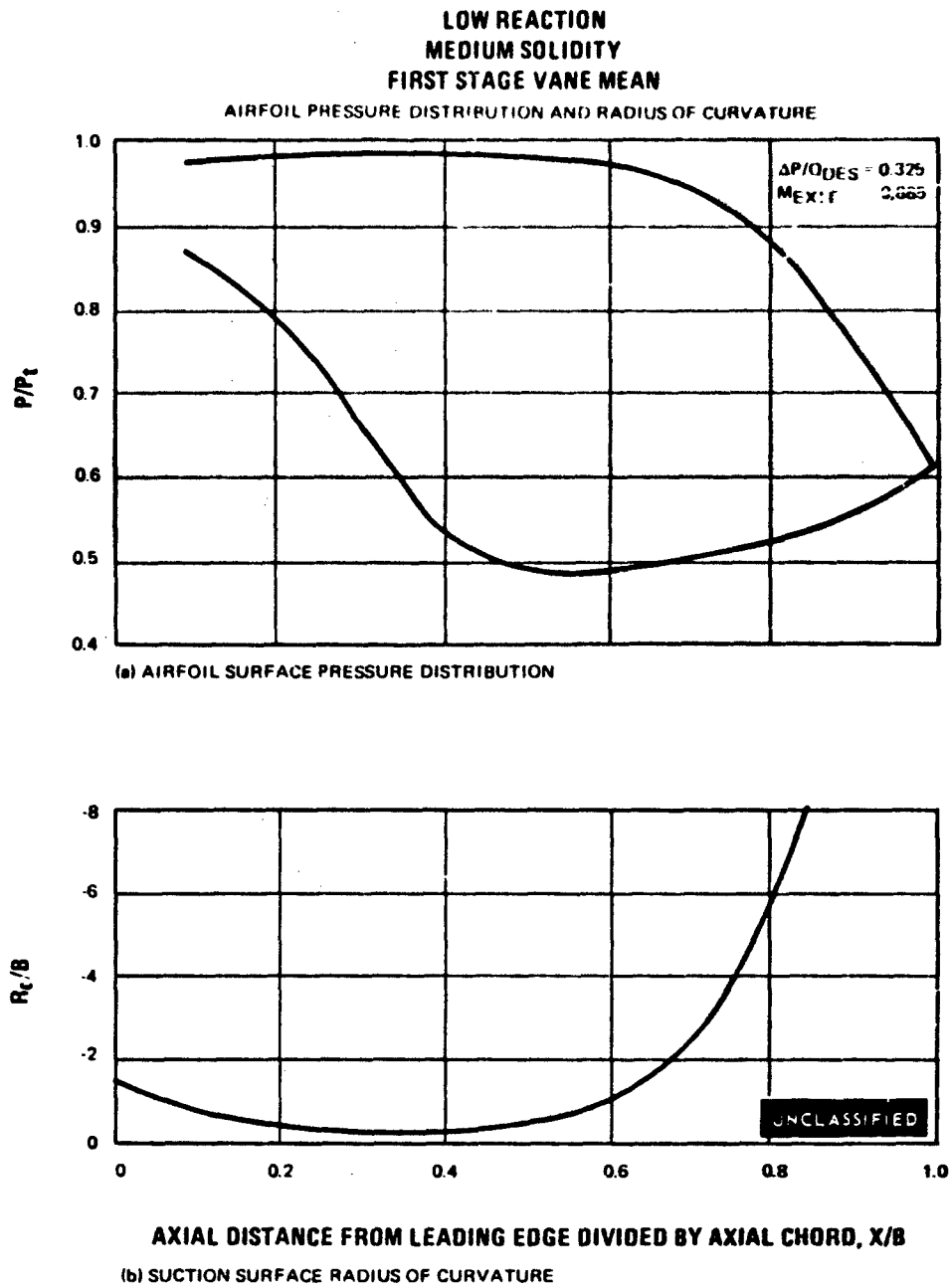


Figure 60

UNCLASSIFIED

UNCLASSIFIED

LOW REACTION
LOW SOLIDITY
FIRST STAGE VANE MEAN
AIRFOIL CROSS SECTION

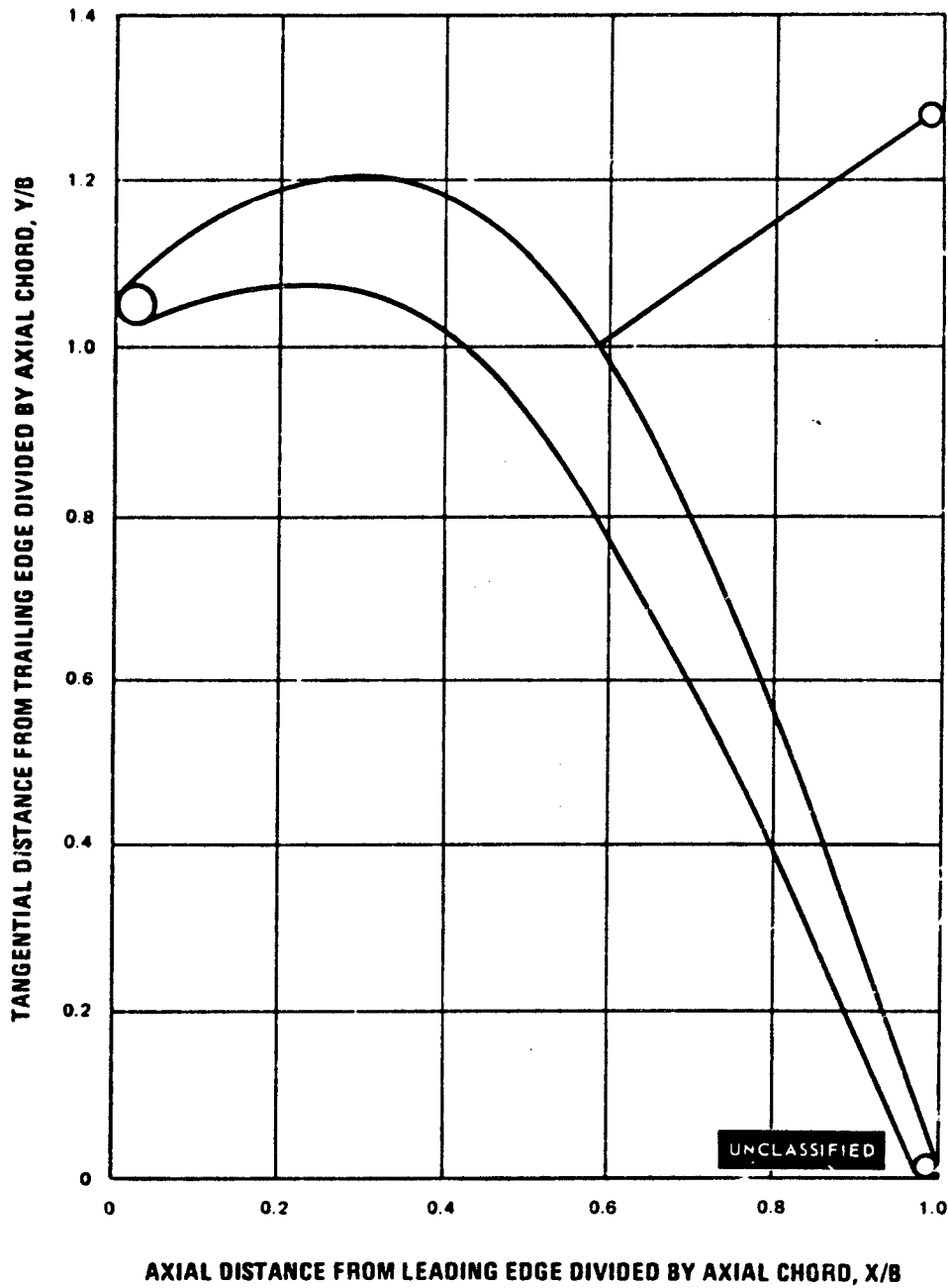


Figure 61

PAGE NO. 98

UNCLASSIFIED

UNCLASSIFIED

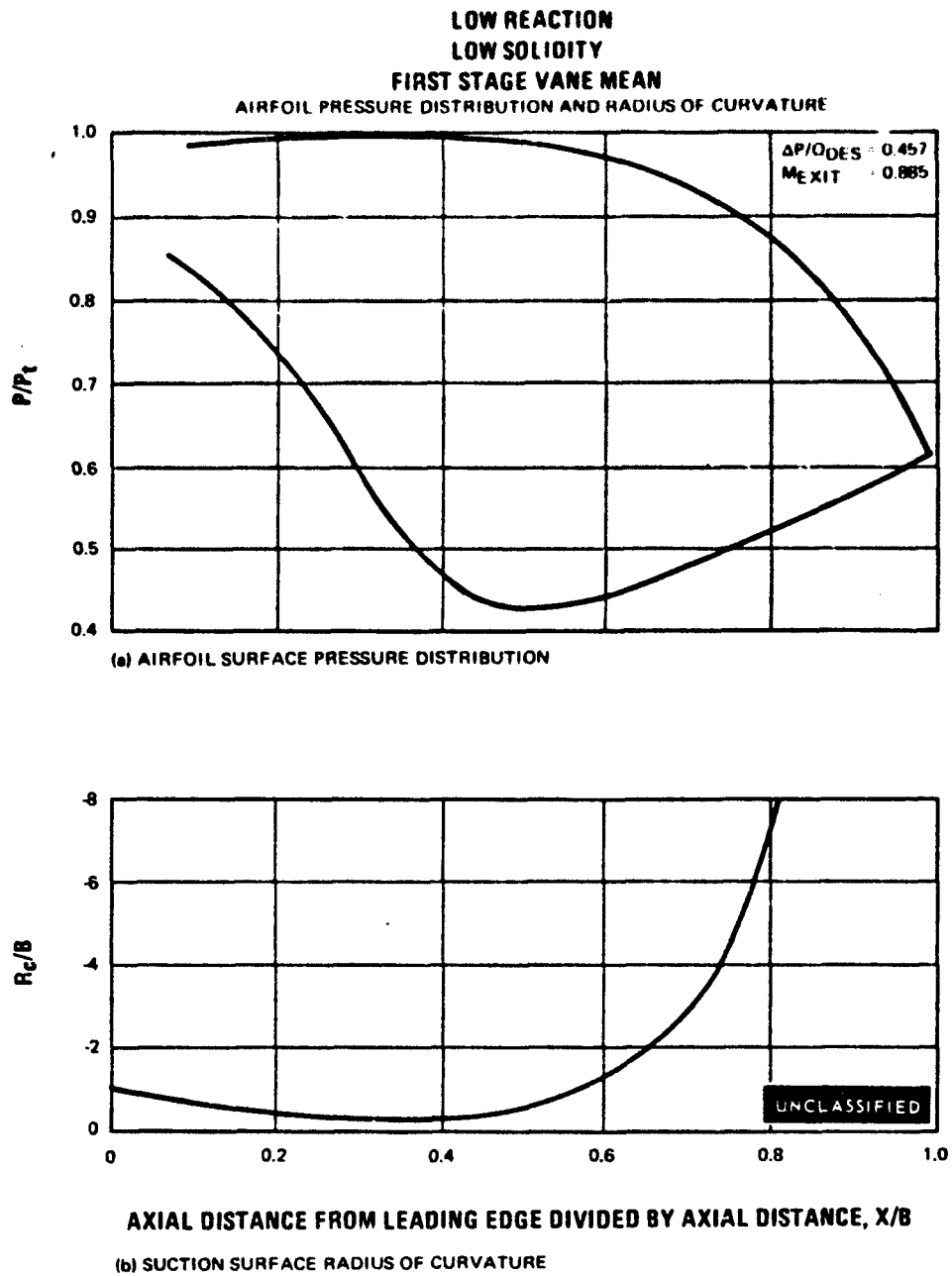


Figure 62

UNCLASSIFIED

UNCLASSIFIED

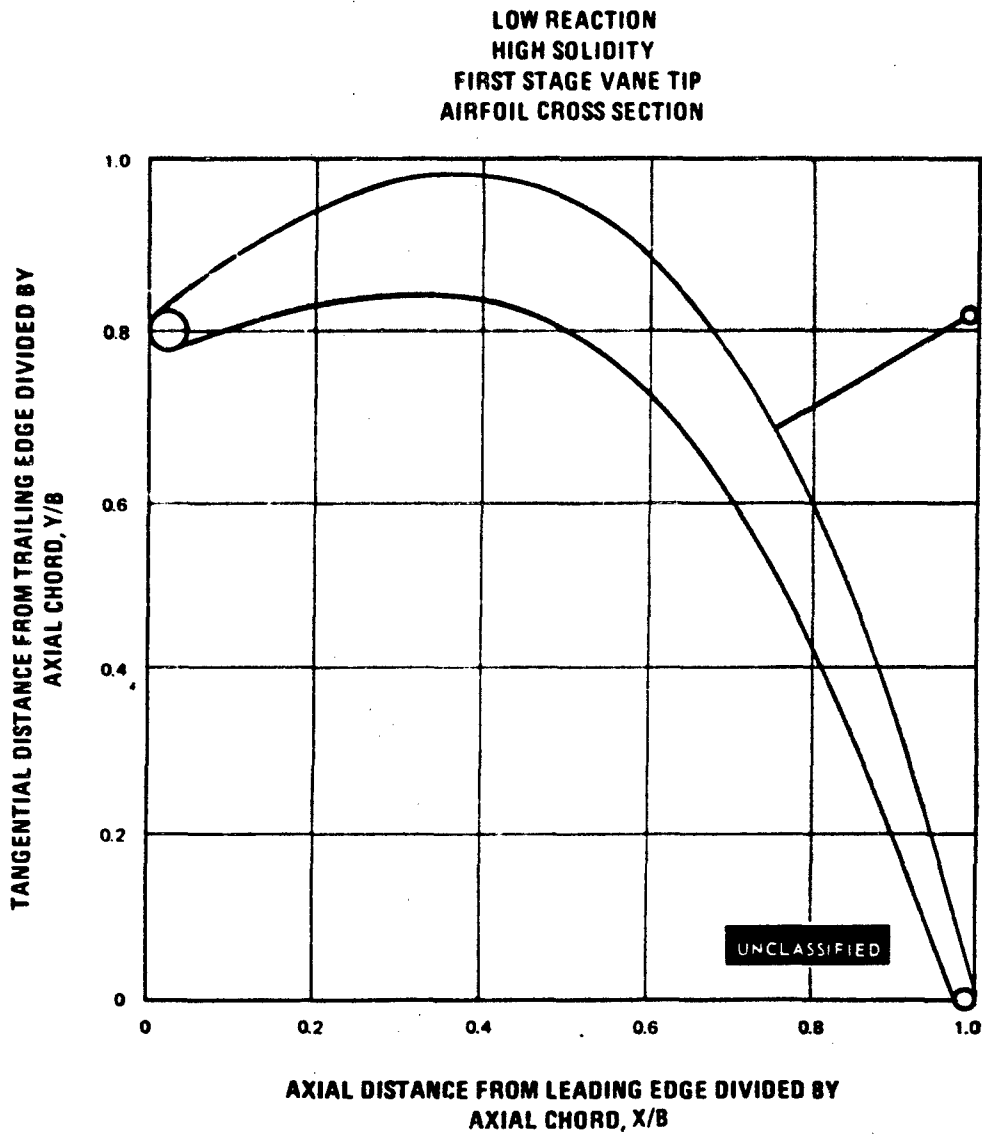


Figure 63

UNCLASSIFIED

UNCLASSIFIED

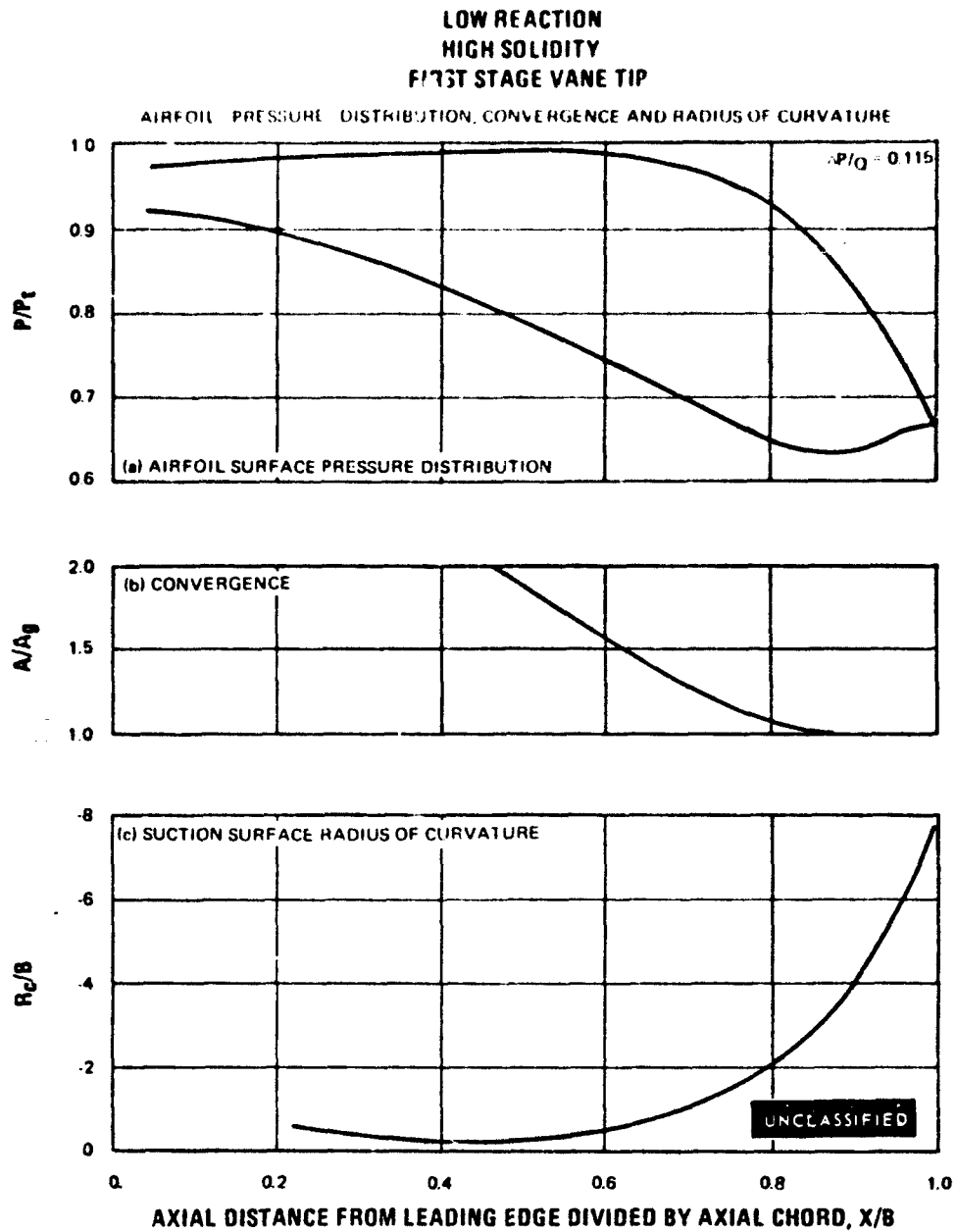


Figure 64

UNCLASSIFIED

UNCLASSIFIED

LOW REACTION
NORMAL SOLIDITY
FIRST STAGE VANE TIP
AIRFOIL CROSS SECTION

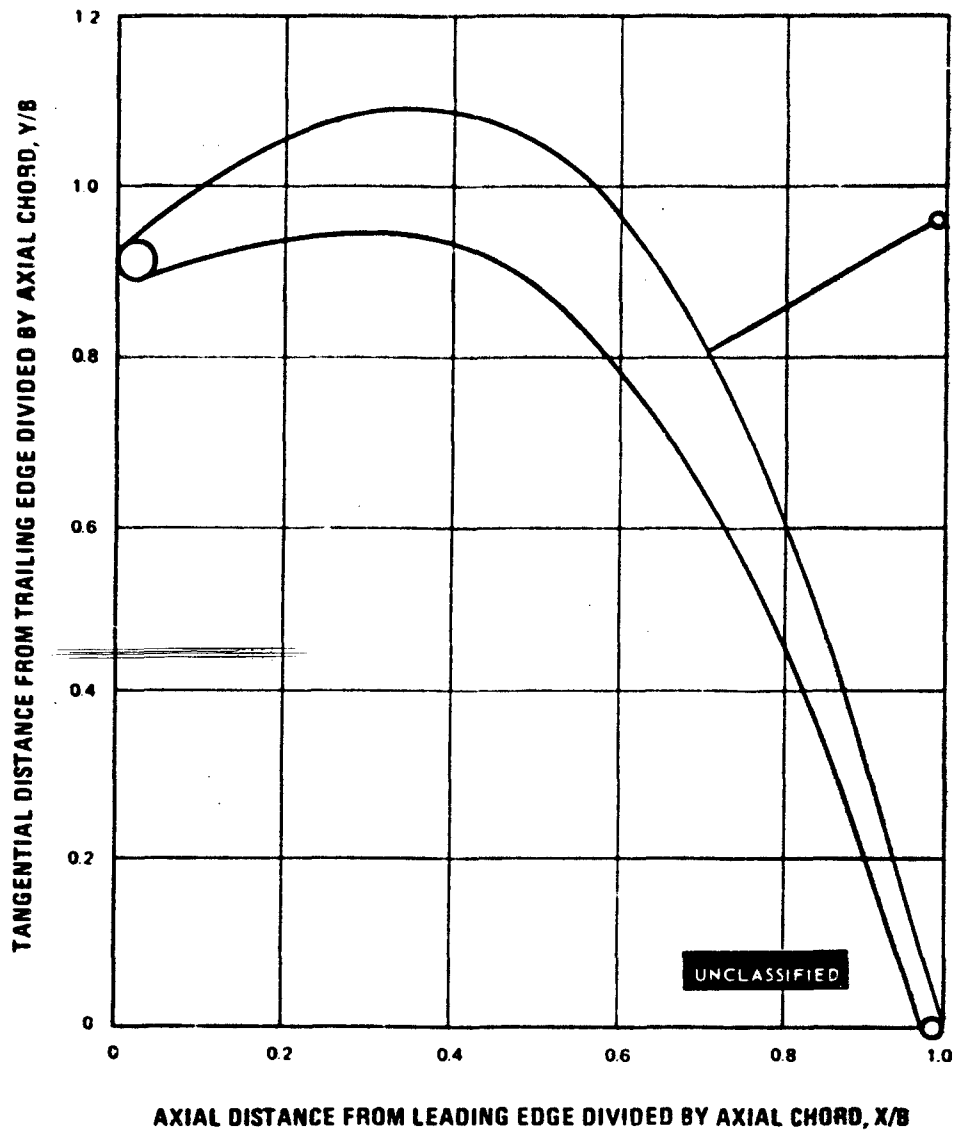


Figure 65

UNCLASSIFIED

UNCLASSIFIED

LOW REACTION
NORMAL SOLIDITY
FIRST STAGE VANE TIP

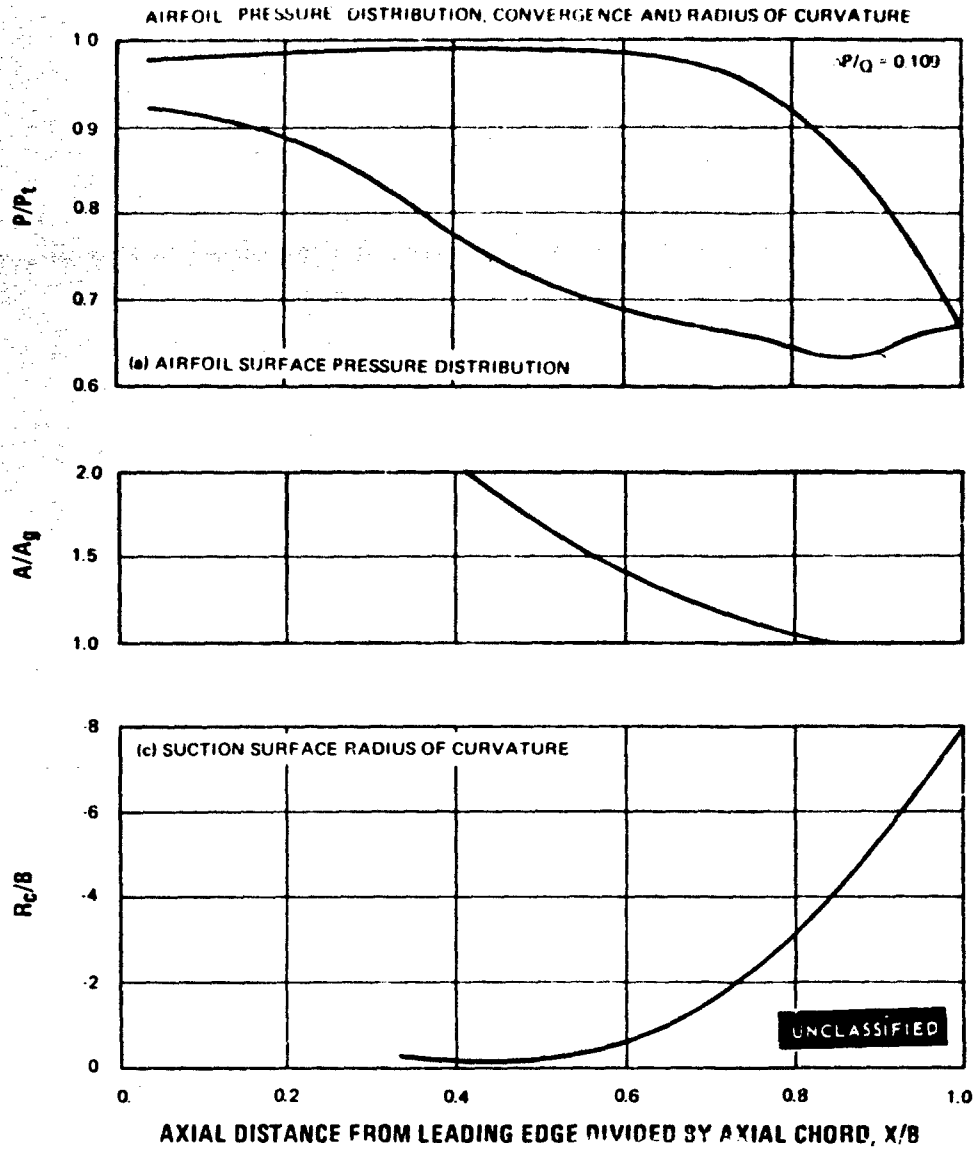


Figure 66

UNCLASSIFIED

UNCLASSIFIED

LOW REACTION
MEDIUM SOLIDITY
FIRST STAGE VANE TIP
AIRFOIL CROSS SECTION

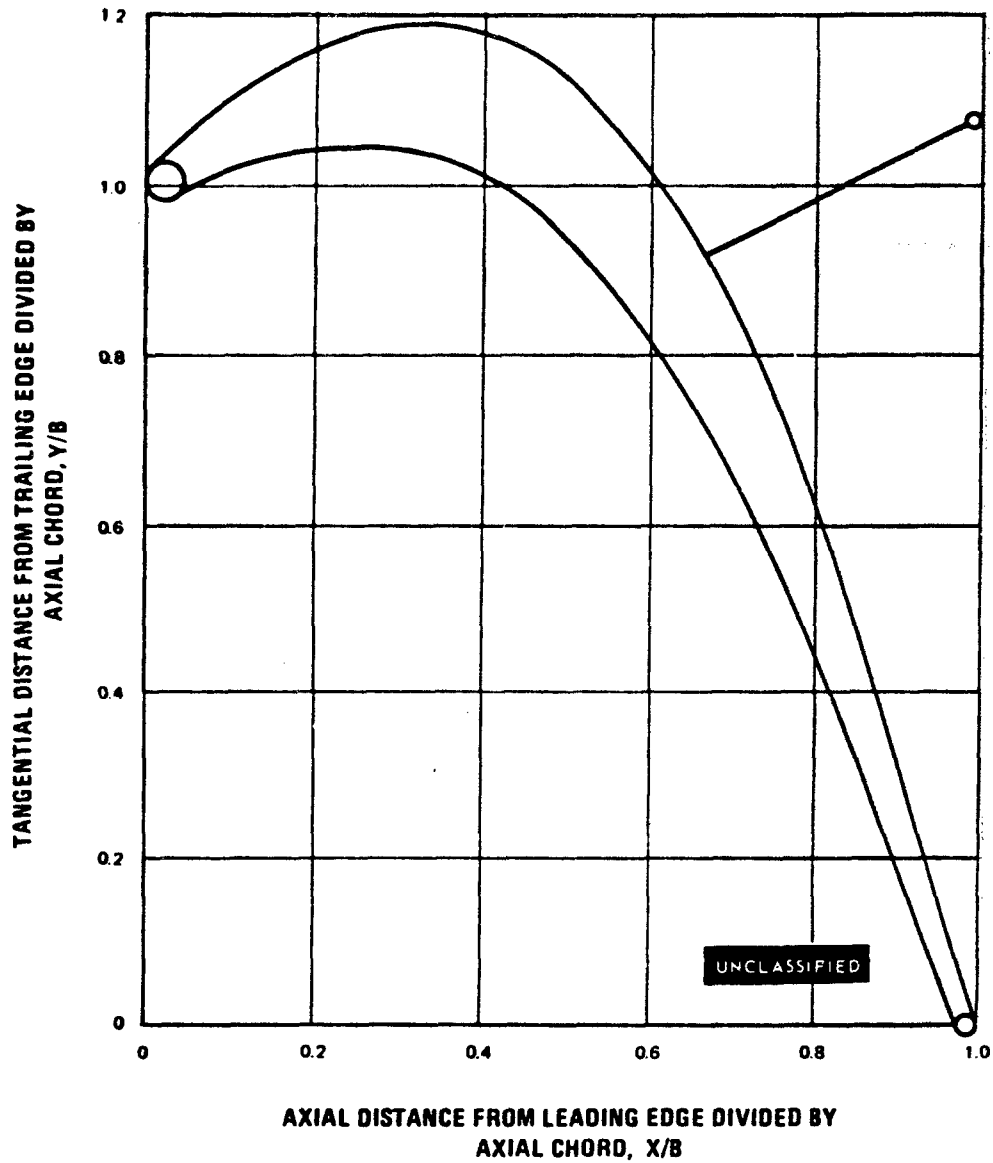


Figure 67

UNCLASSIFIED

UNCLASSIFIED

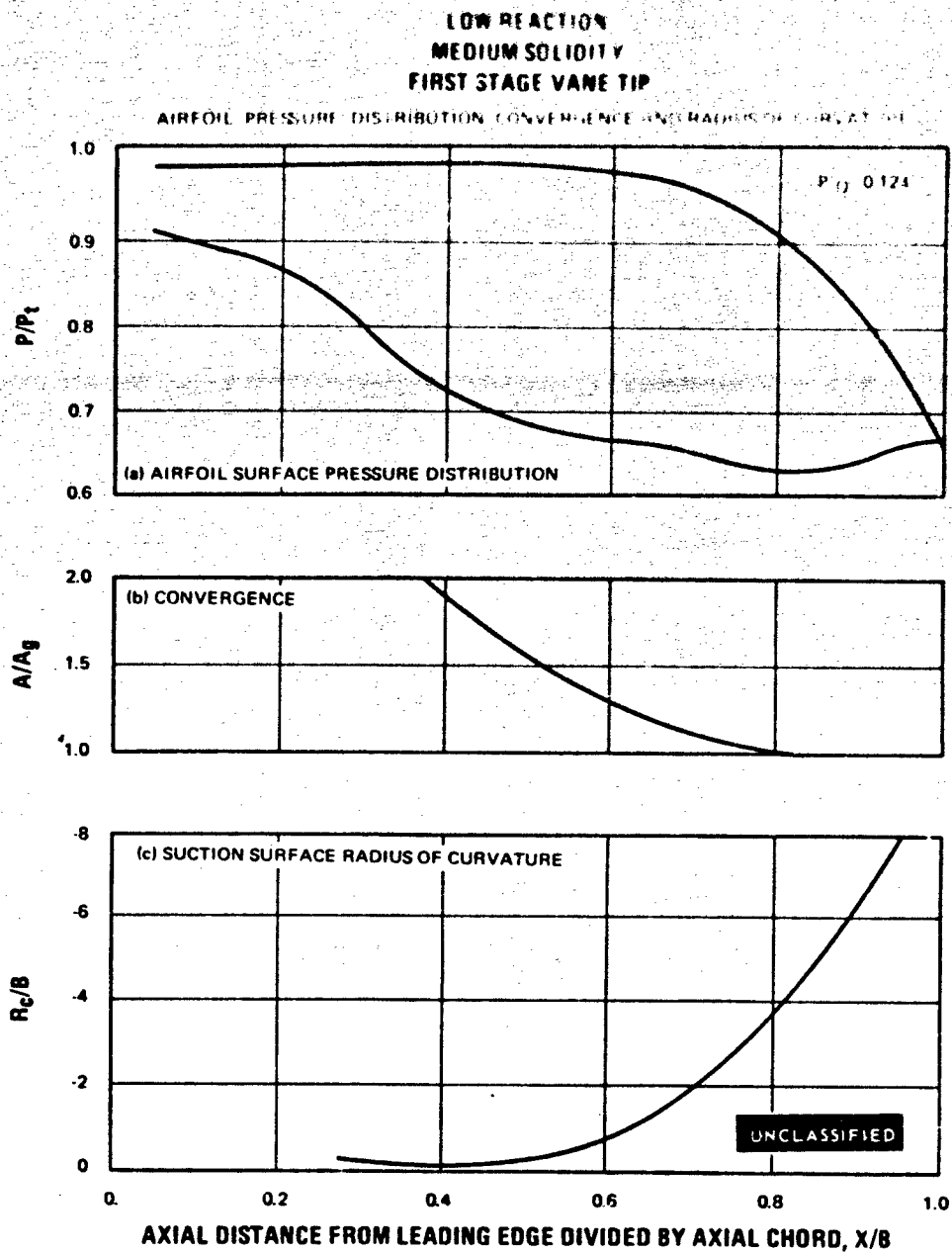


Figure 68

UNCLASSIFIED

UNCLASSIFIED

LOW REACTION
LOW SOLIDITY
FIRST STAGE VANE TIP
AIRFOIL CROSS SECTION

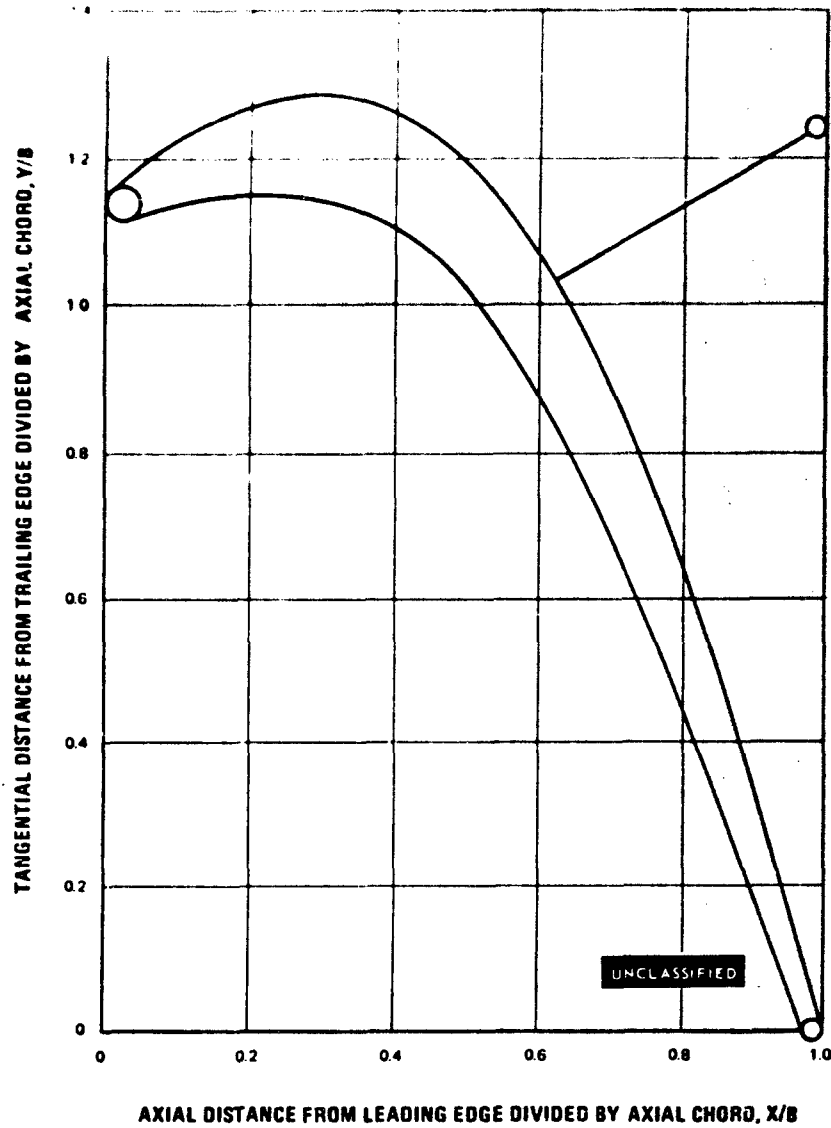


Figure 69

UNCLASSIFIED

UNCLASSIFIED

LOW REACTION
LOW SOLIDITY
FIRST STAGE VANE TIP

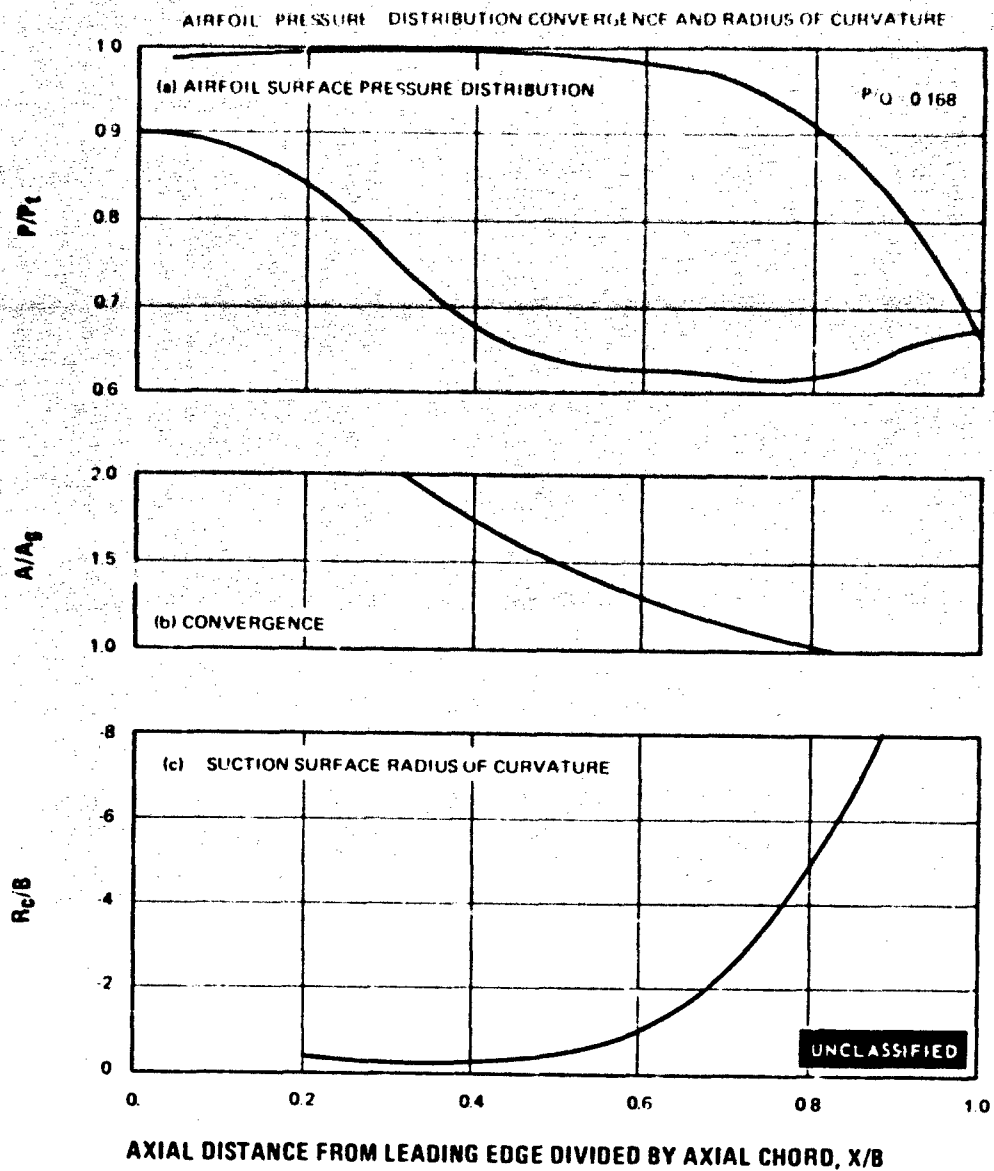


Figure 70

UNCLASSIFIED

UNCLASSIFIED

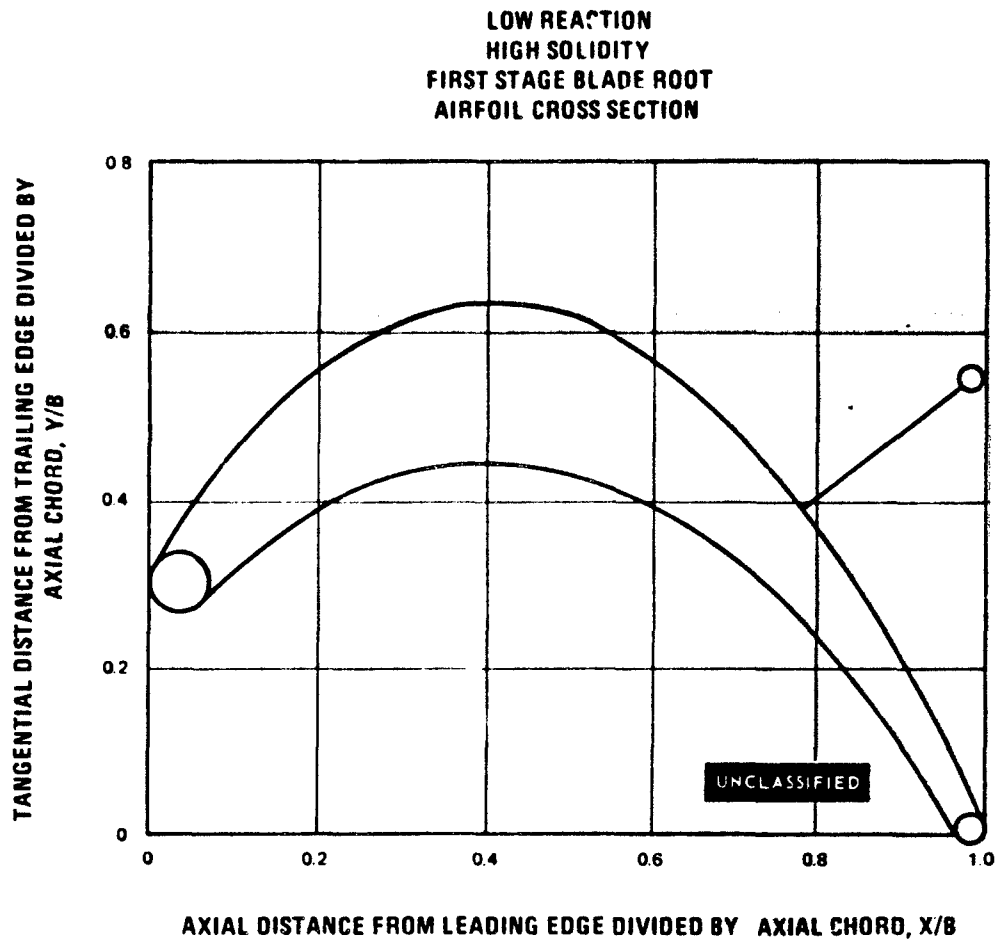


Figure 71

UNCLASSIFIED

UNCLASSIFIED

LOW REACTION
HIGH SOLIDITY
FIRST STAGE BLADE ROOT

AIRFOIL PRESSURE DISTRIBUTION, CONVERGENCE AND RADIUS OF CURVATURE

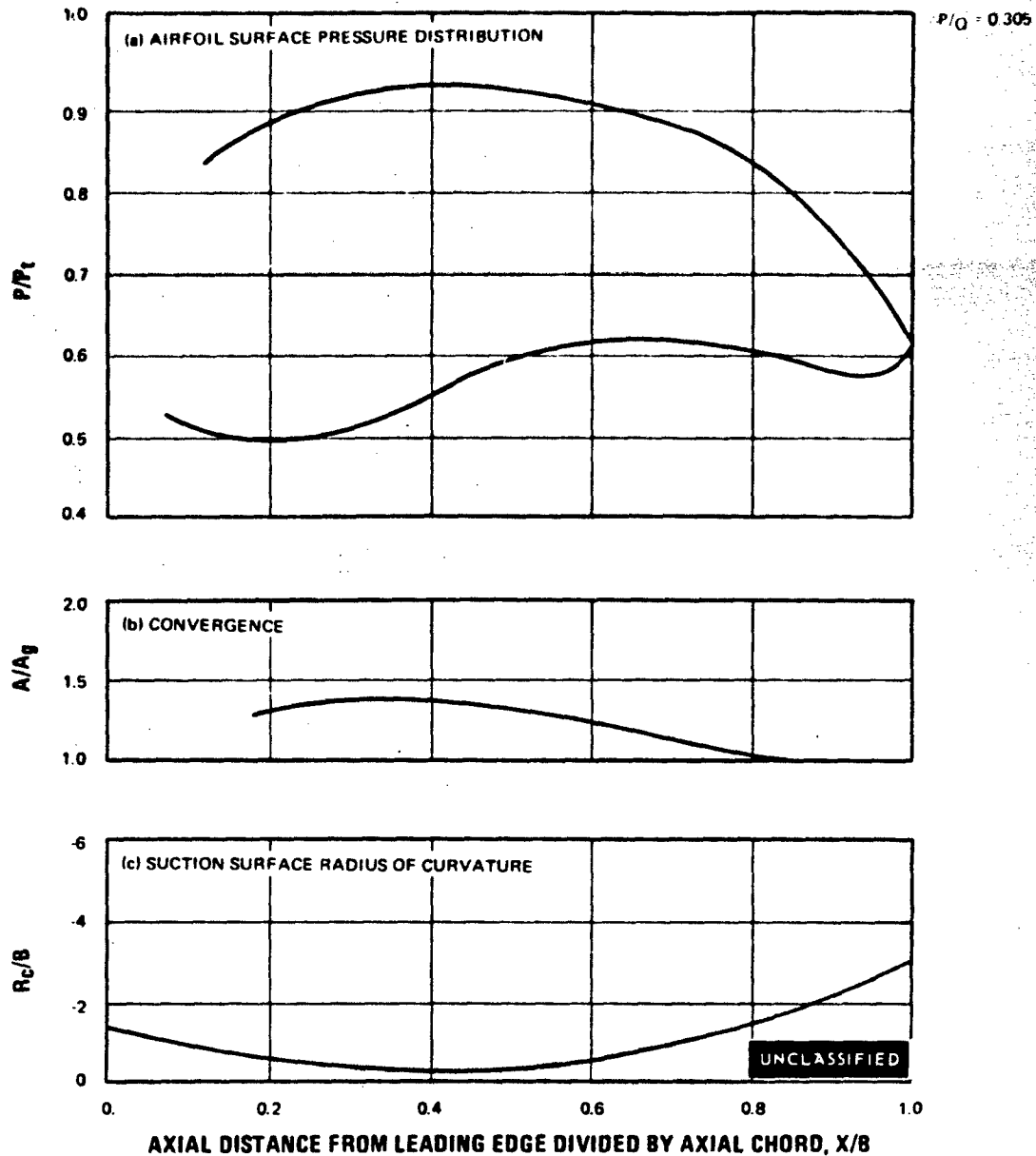


Figure 72

UNCLASSIFIED

UNCLASSIFIED

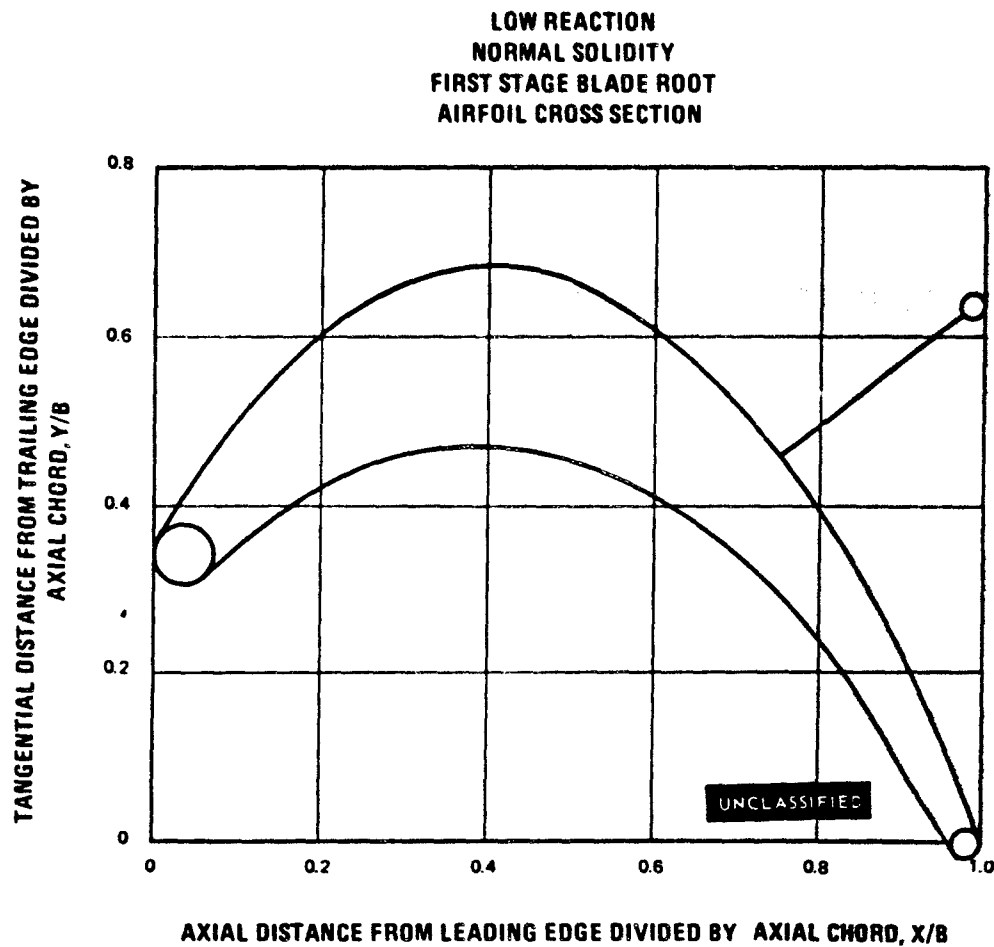


Figure 73

UNCLASSIFIED

UNCLASSIFIED

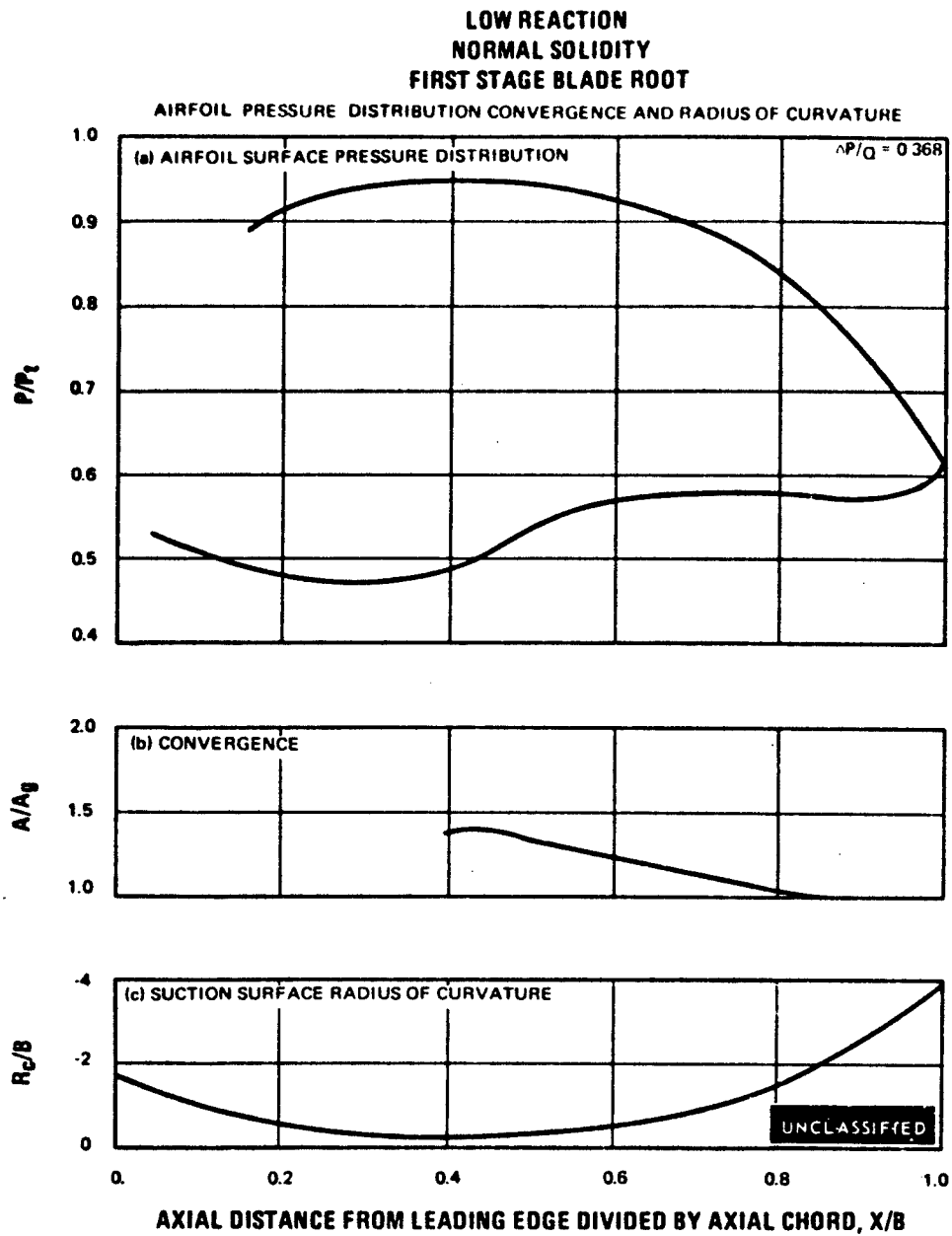


Figure 74

UNCLASSIFIED

UNCLASSIFIED

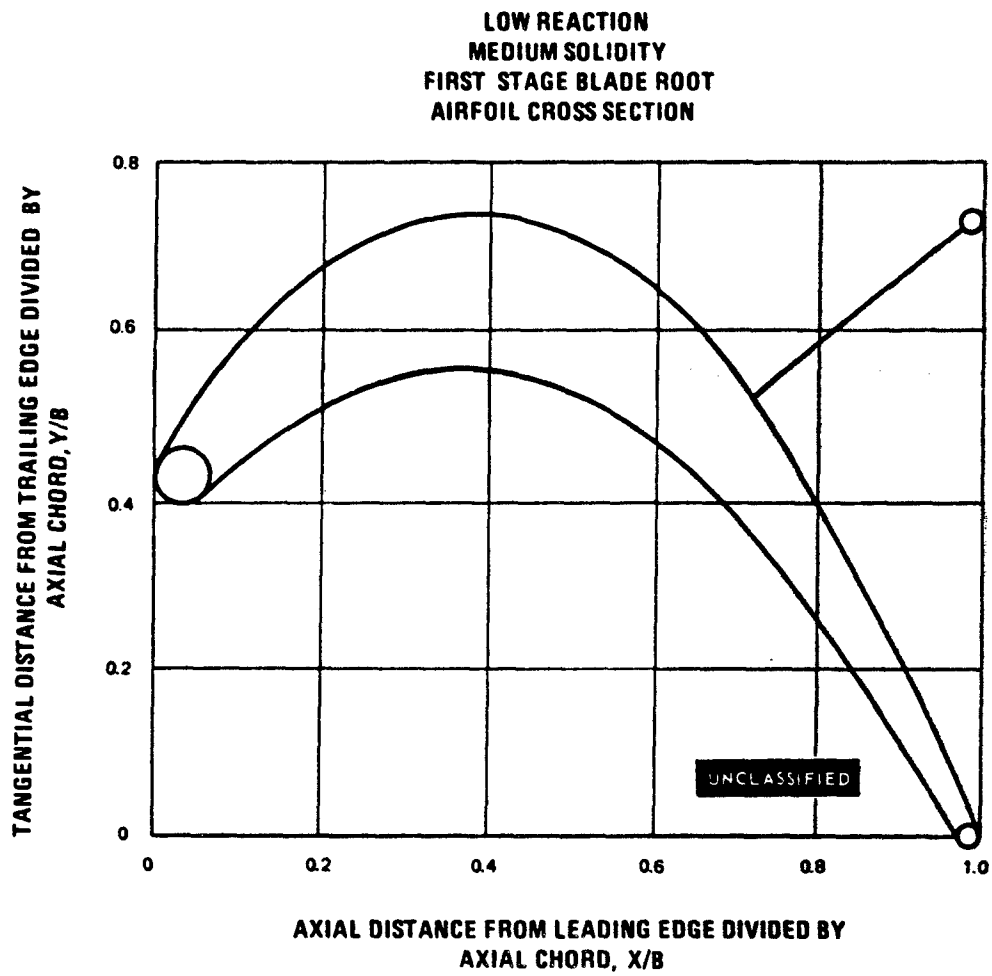


Figure 75

UNCLASSIFIED

UNCLASSIFIED

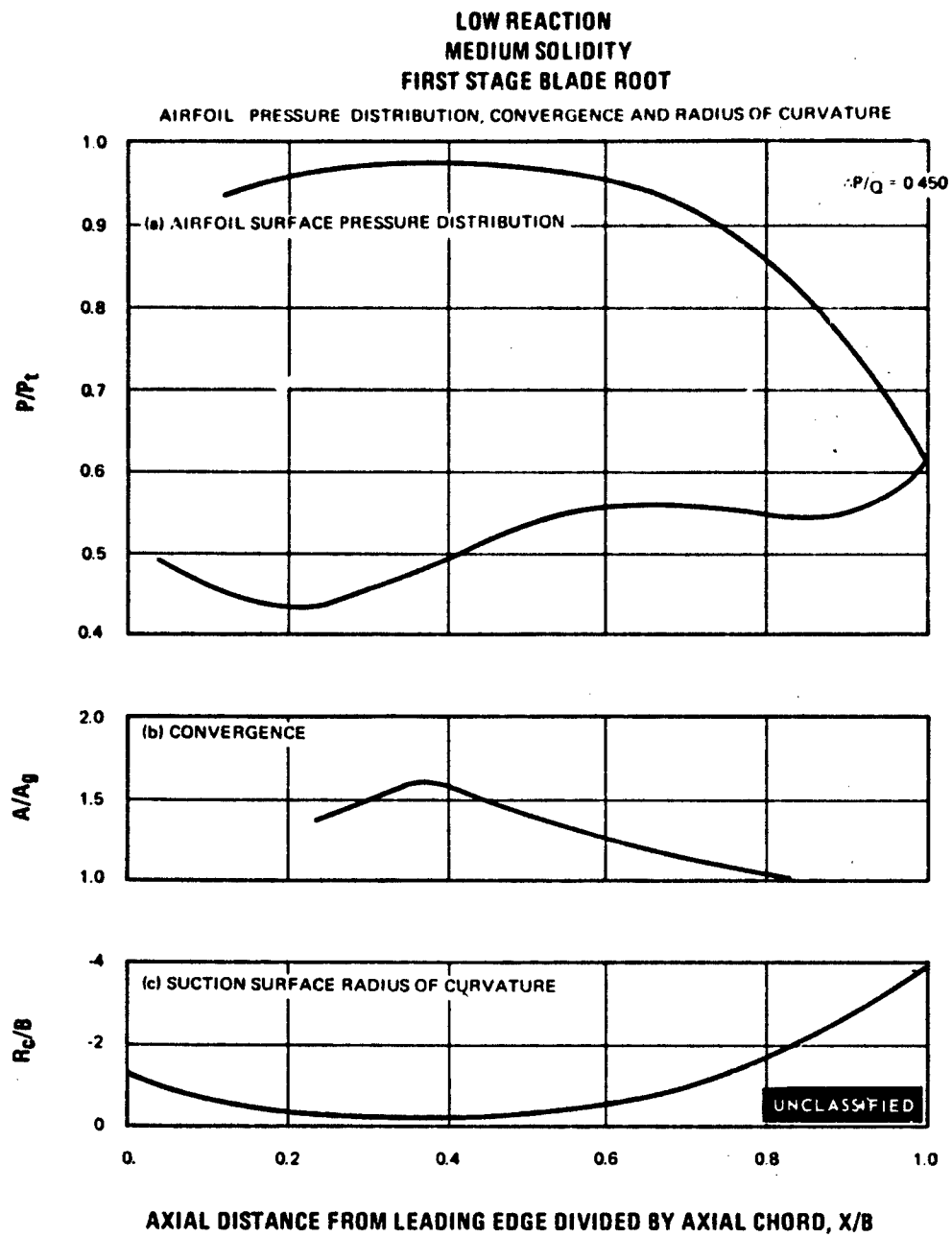


Figure 76

UNCLASSIFIED

UNCLASSIFIED

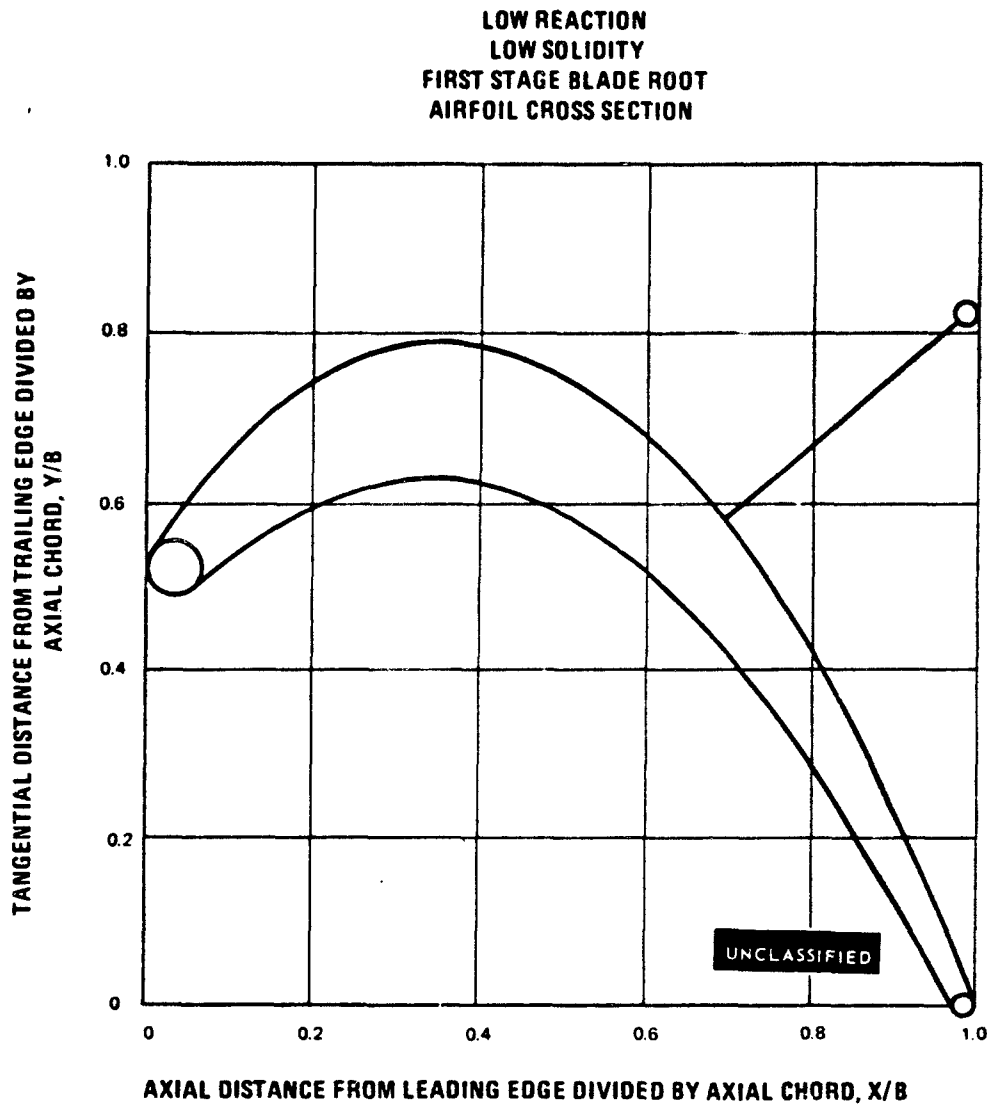


Figure 77

UNCLASSIFIED

UNCLASSIFIED

LOW REACTION
LOW SOLIDITY
FIRST STAGE BLADE ROOT

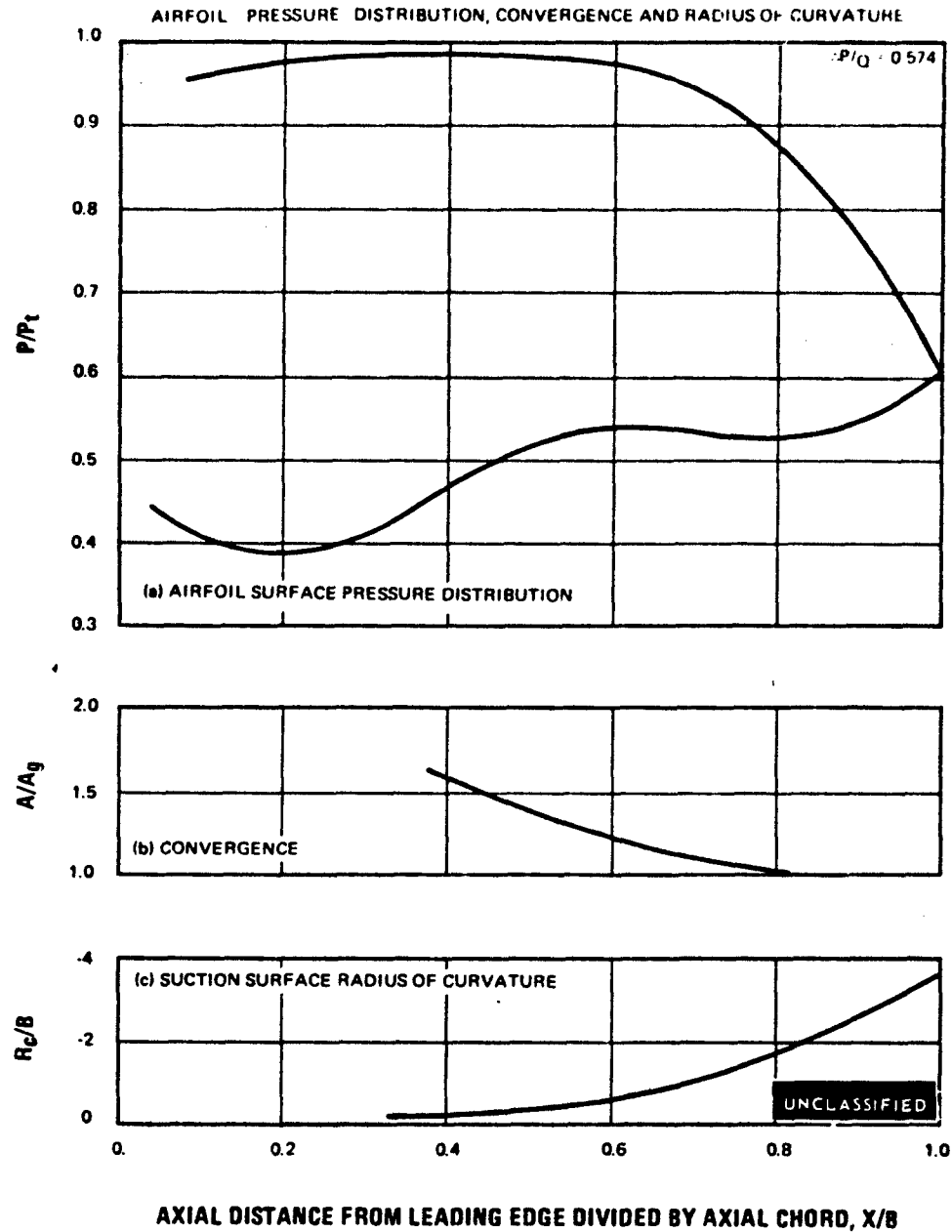


Figure 78

UNCLASSIFIED

UNCLASSIFIED

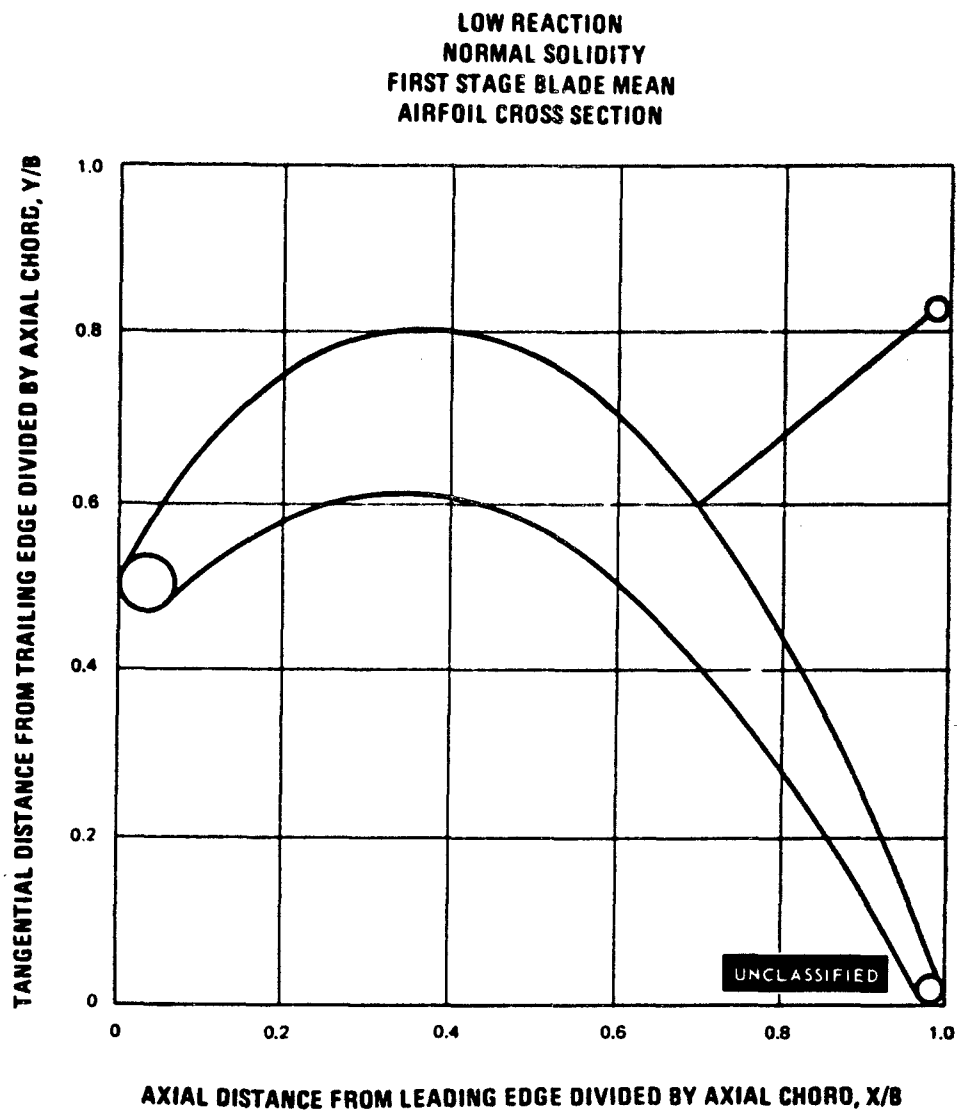


Figure 79

UNCLASSIFIED

UNCLASSIFIED

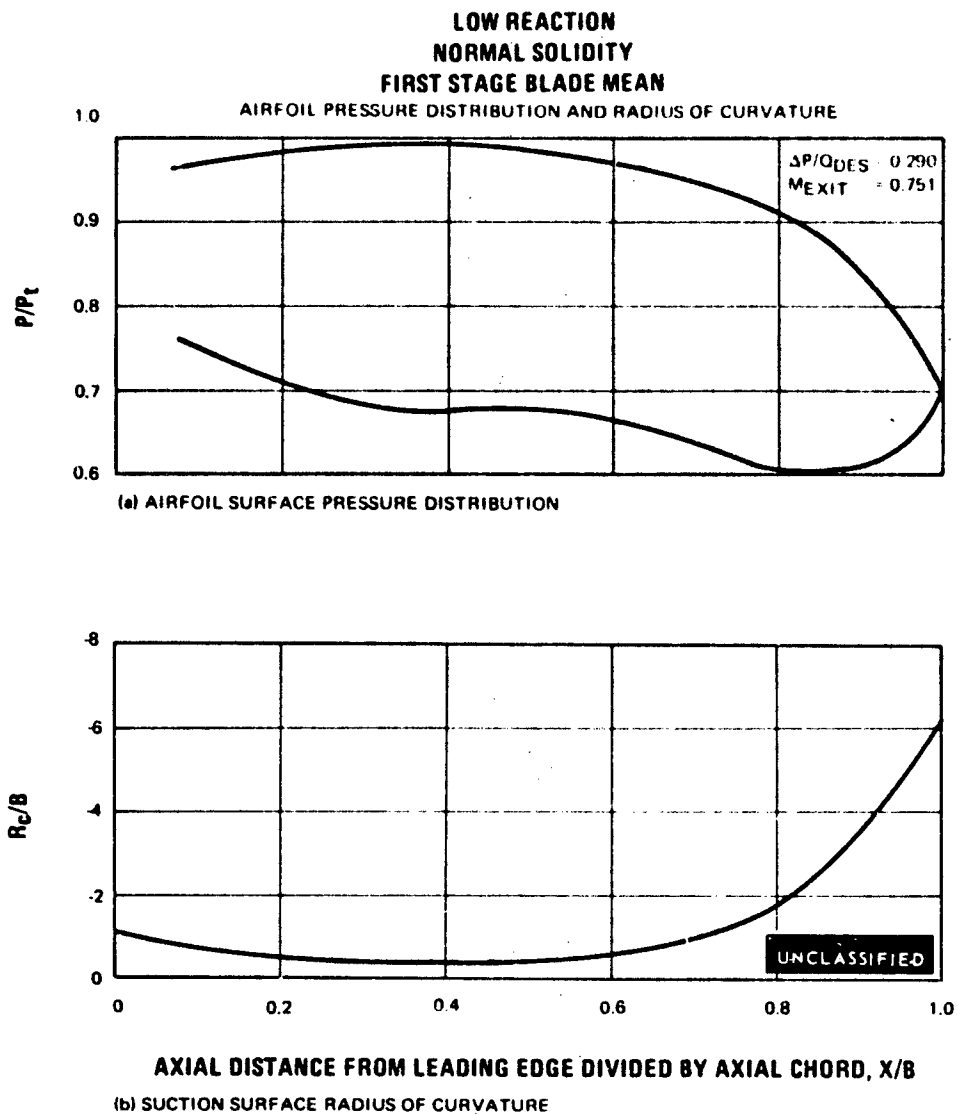


Figure 80

UNCLASSIFIED

UNCLASSIFIED

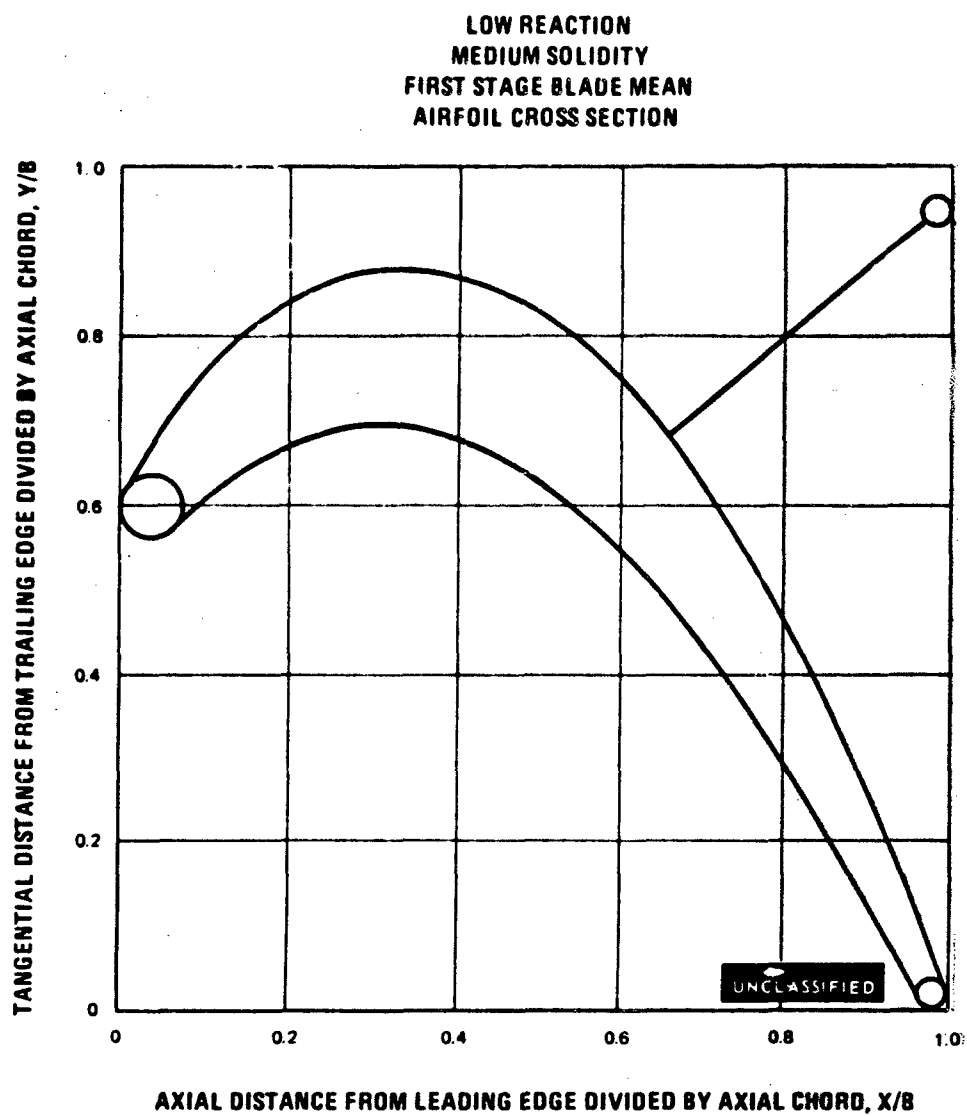


Figure 81

UNCLASSIFIED

UNCLASSIFIED

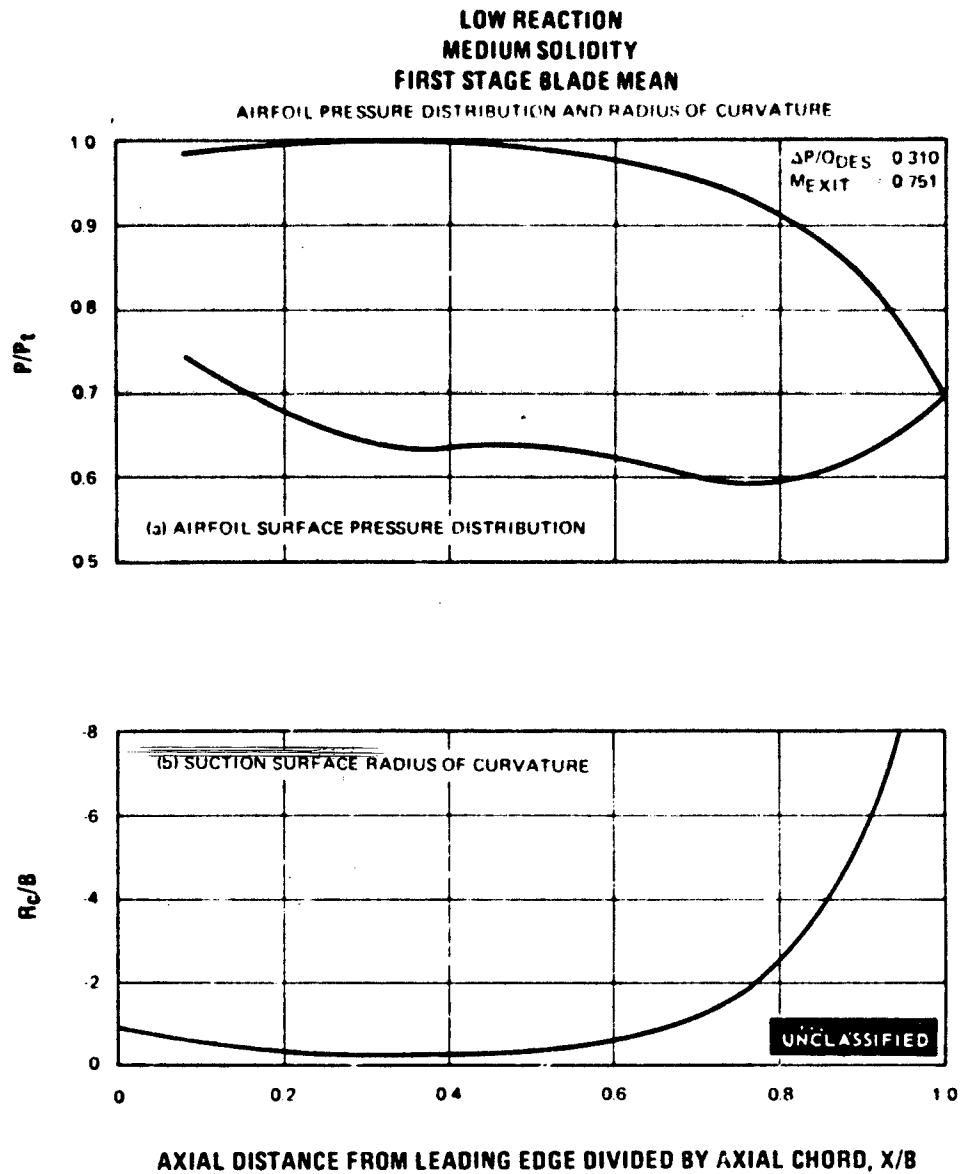


Figure 82

UNCLASSIFIED

UNCLASSIFIED

LOW REACTION
LOW SOLIDITY
FIRST STAGE BLADE MEAN
AIRFOIL CROSS SECTION

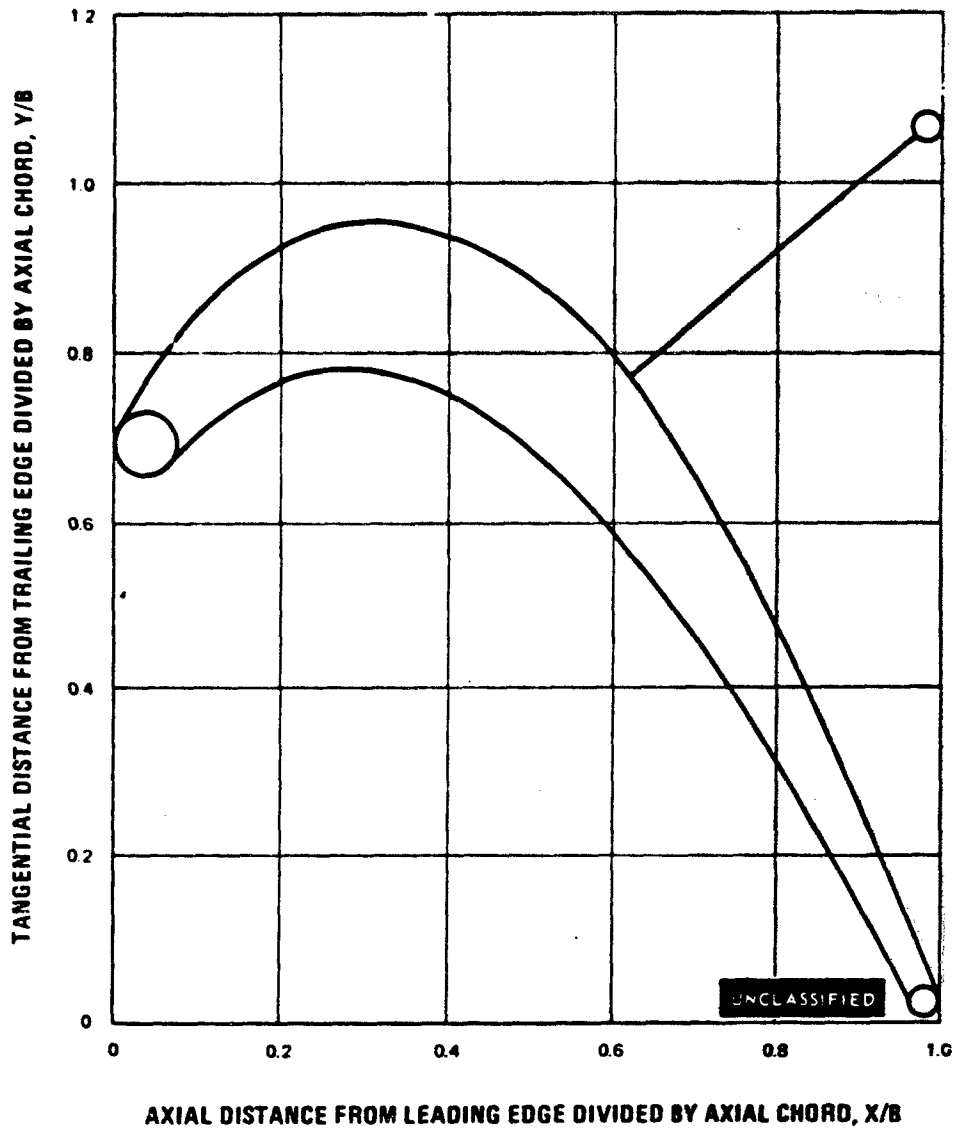


Figure 83

UNCLASSIFIED

UNCLASSIFIED

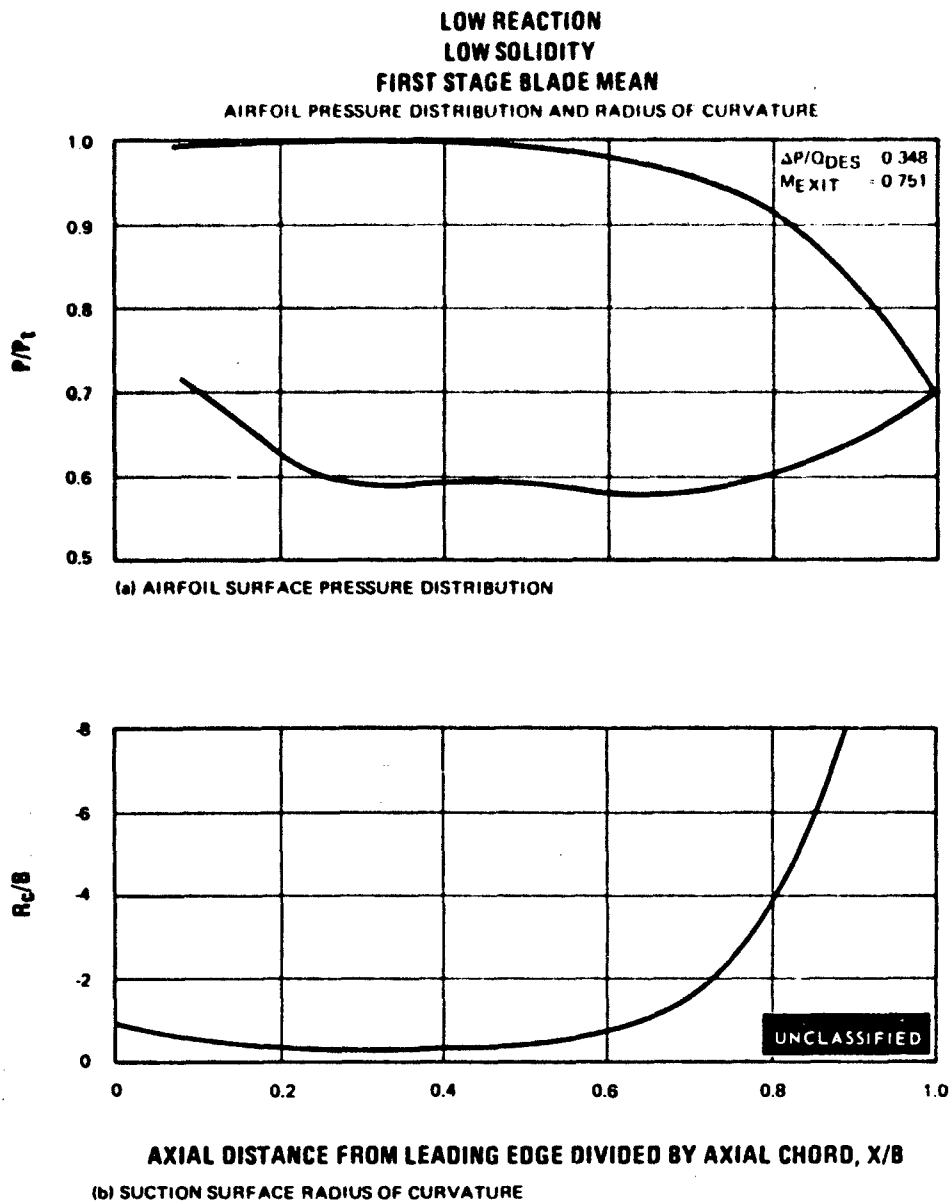


Figure 84

UNCLASSIFIED

UNCLASSIFIED

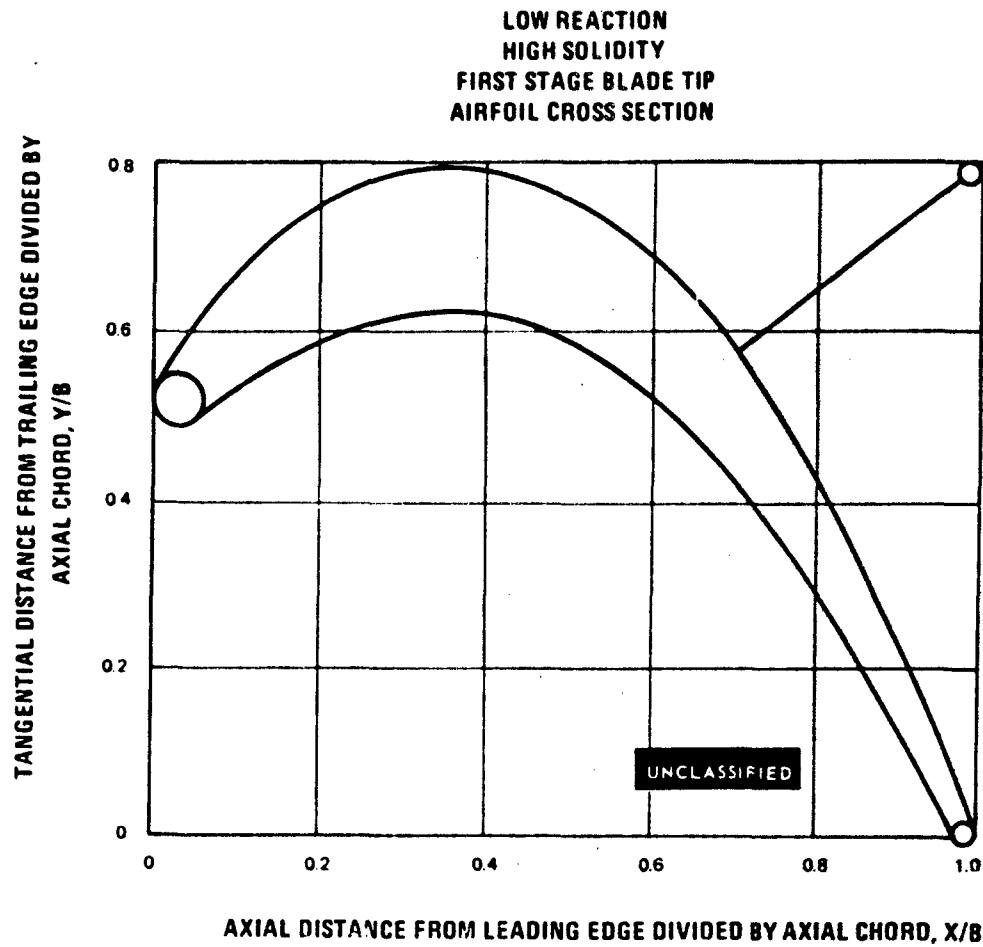


Figure 85

UNCLASSIFIED

UNCLASSIFIED

LOW REACTION
HIGH SOLIDITY
FIRST STAGE BLADE TIP

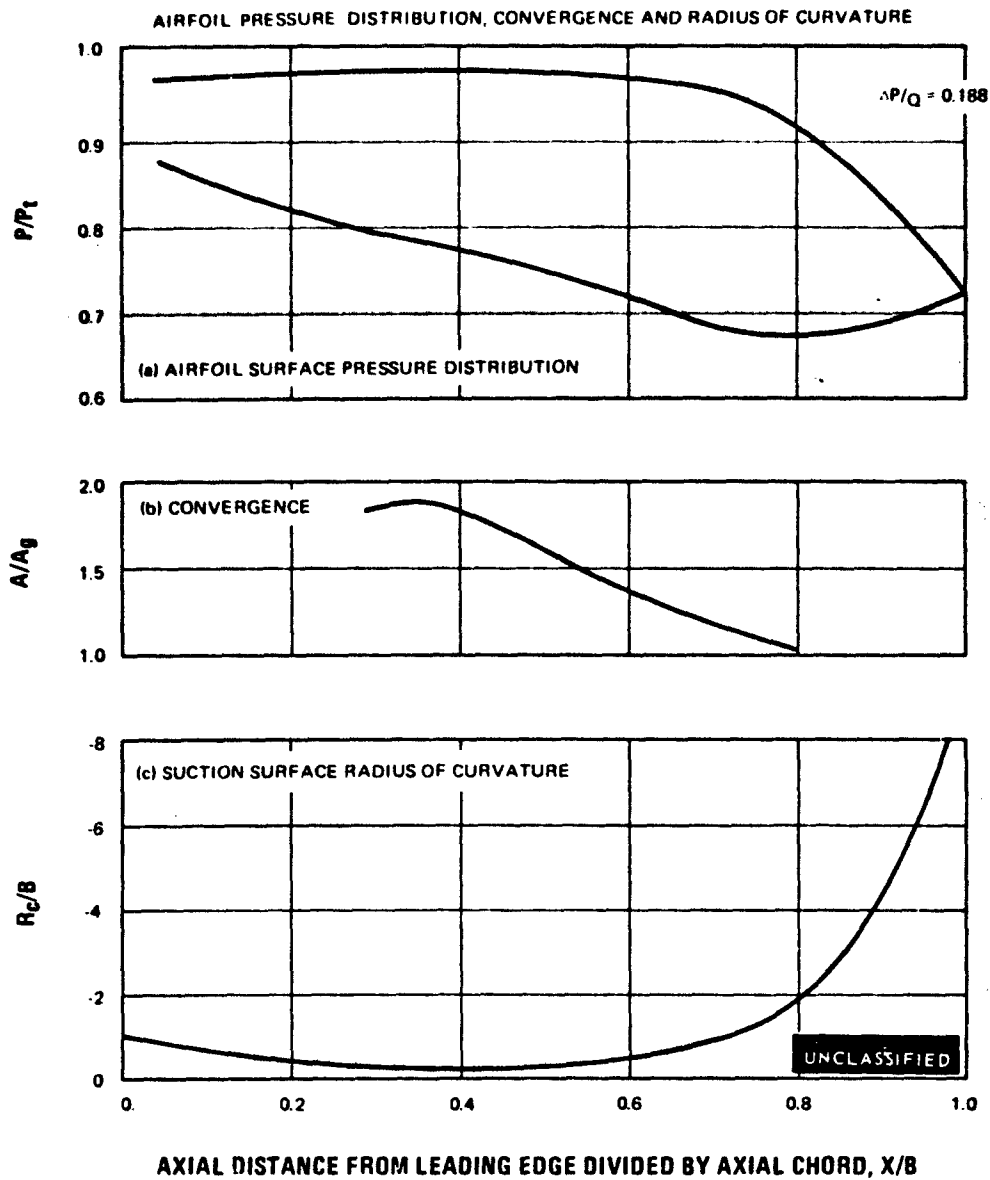


Figure 86

UNCLASSIFIED

UNCLASSIFIED

LOW REACTION
NORMAL SOLIDITY
FIRST STAGE BLADE TIP
AIRFOIL CROSS SECTION

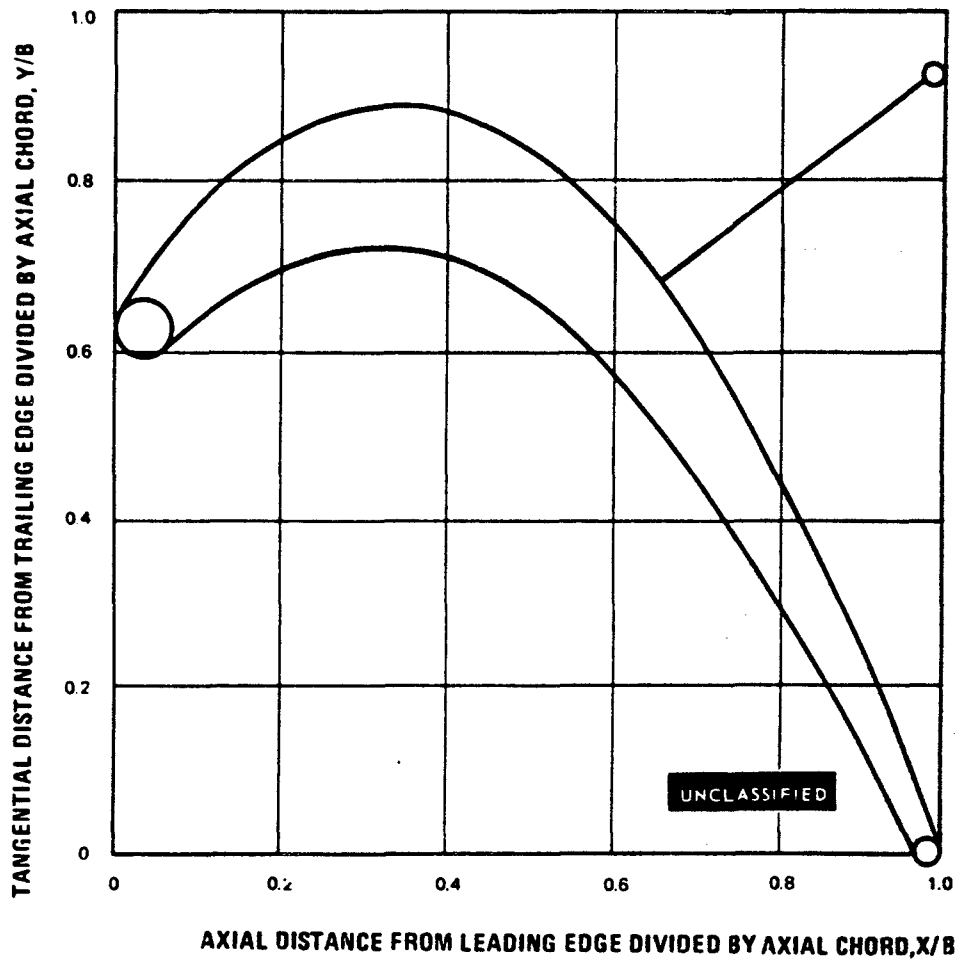


Figure 87

UNCLASSIFIED

UNCLASSIFIED

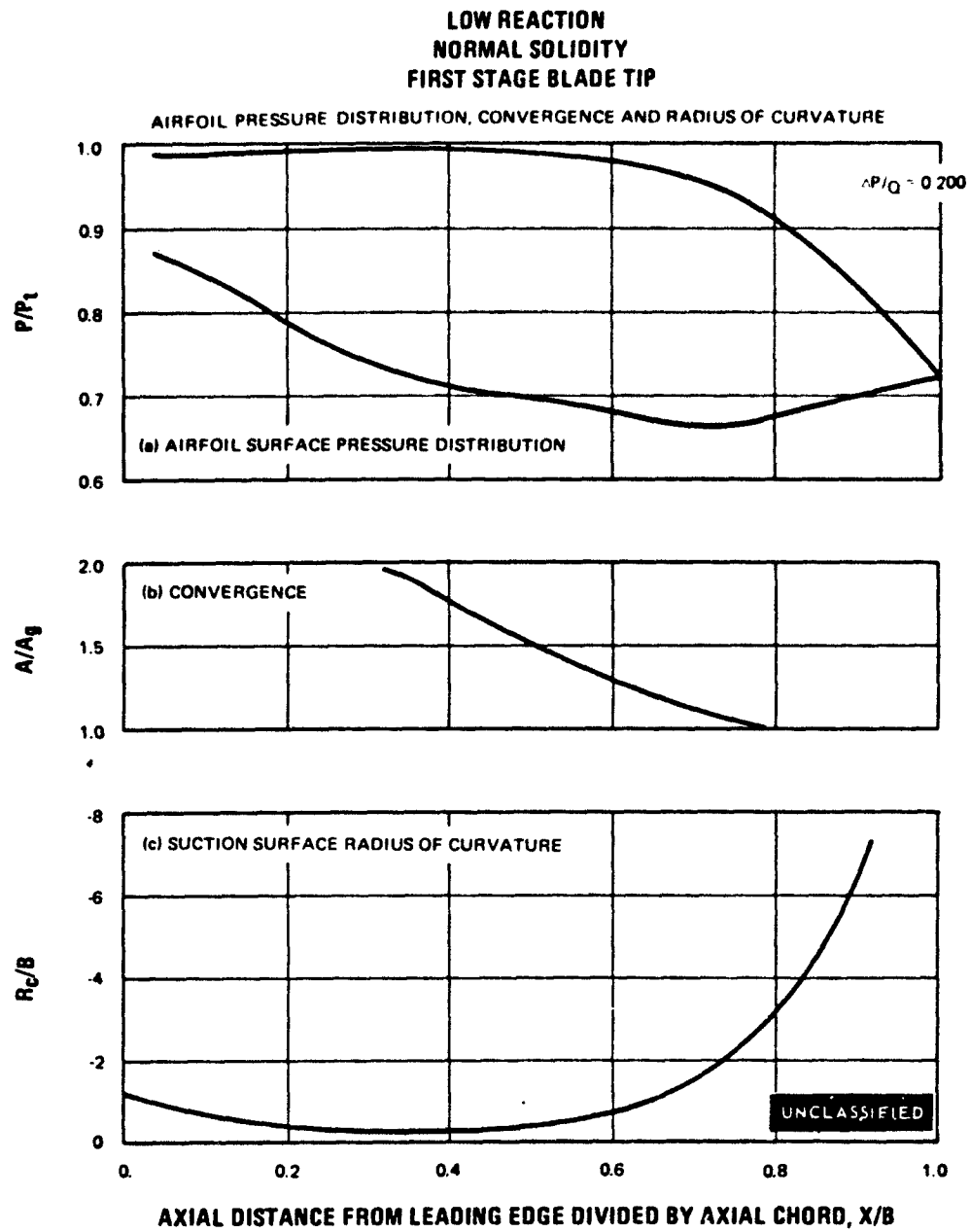


Figure 88

UNCLASSIFIED

UNCLASSIFIED

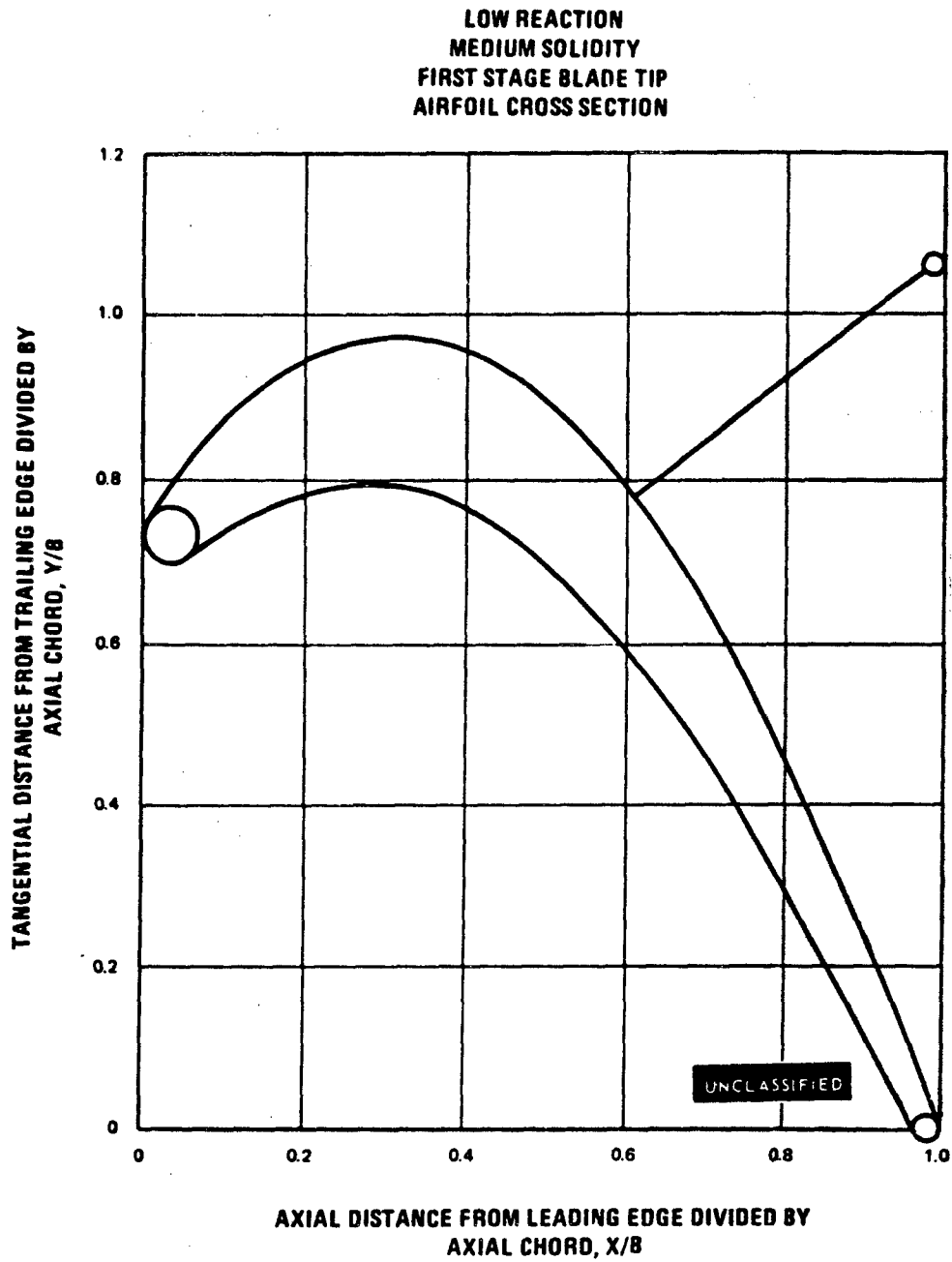


Figure 89

UNCLASSIFIED

UNCLASSIFIED

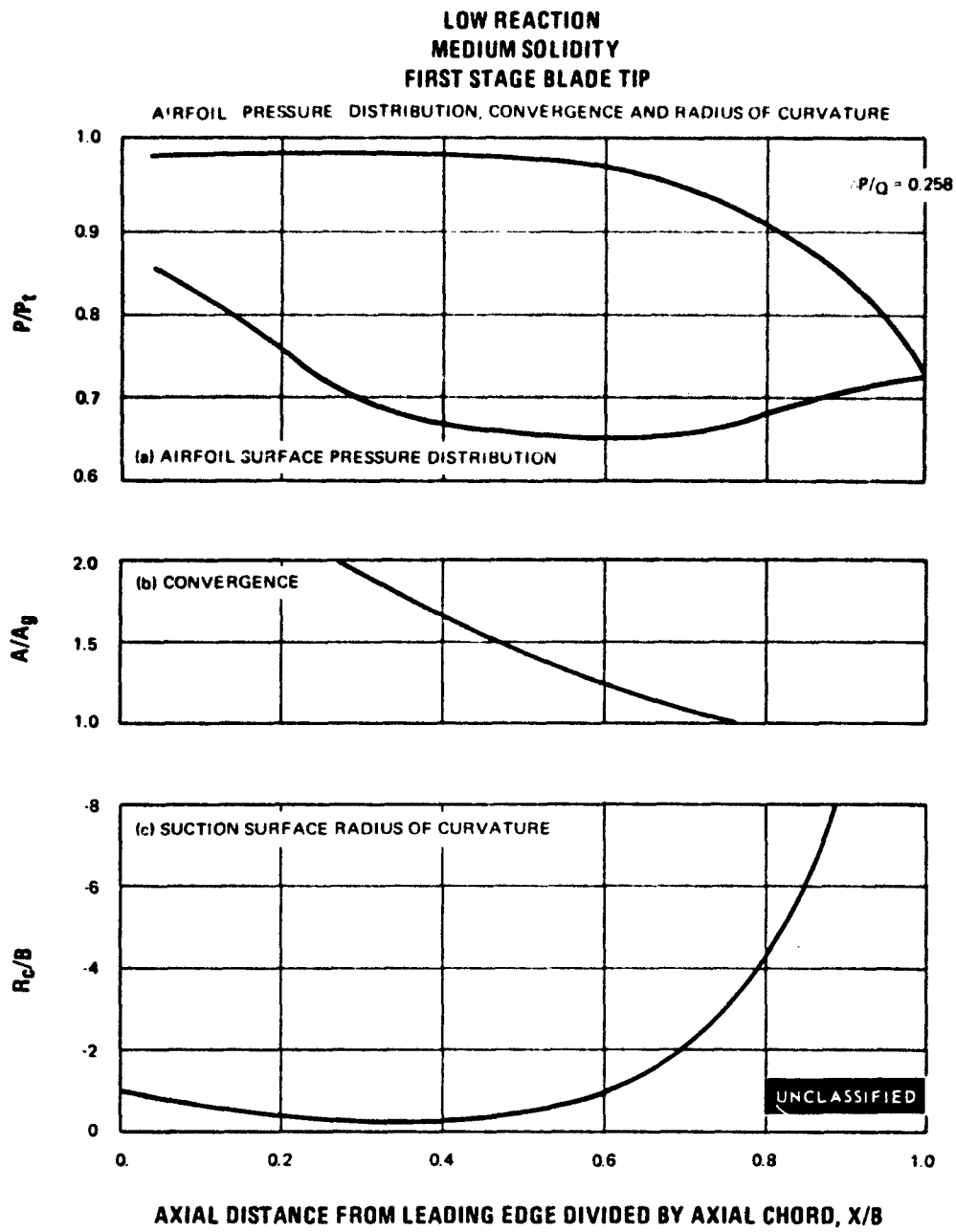


Figure 90

UNCLASSIFIED

UNCLASSIFIED

LOW REACTION
LOW SOLIDITY
FIRST STAGE BLADE TIP
AIRFOIL CROSS SECTION

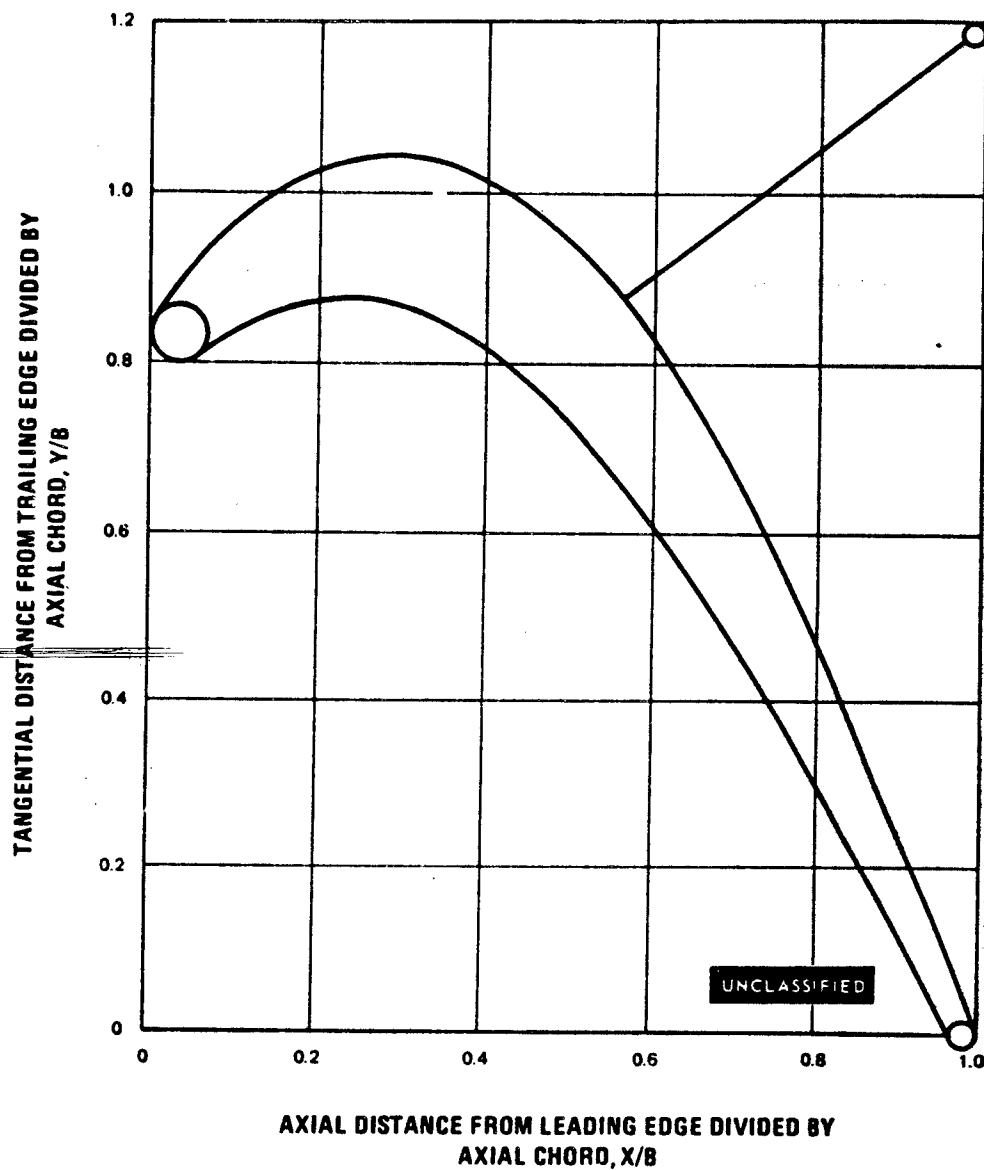


Figure 91

UNCLASSIFIED

UNCLASSIFIED

LOW REACTION
LOW SOLIDITY
FIRST STAGE BLADE TIP

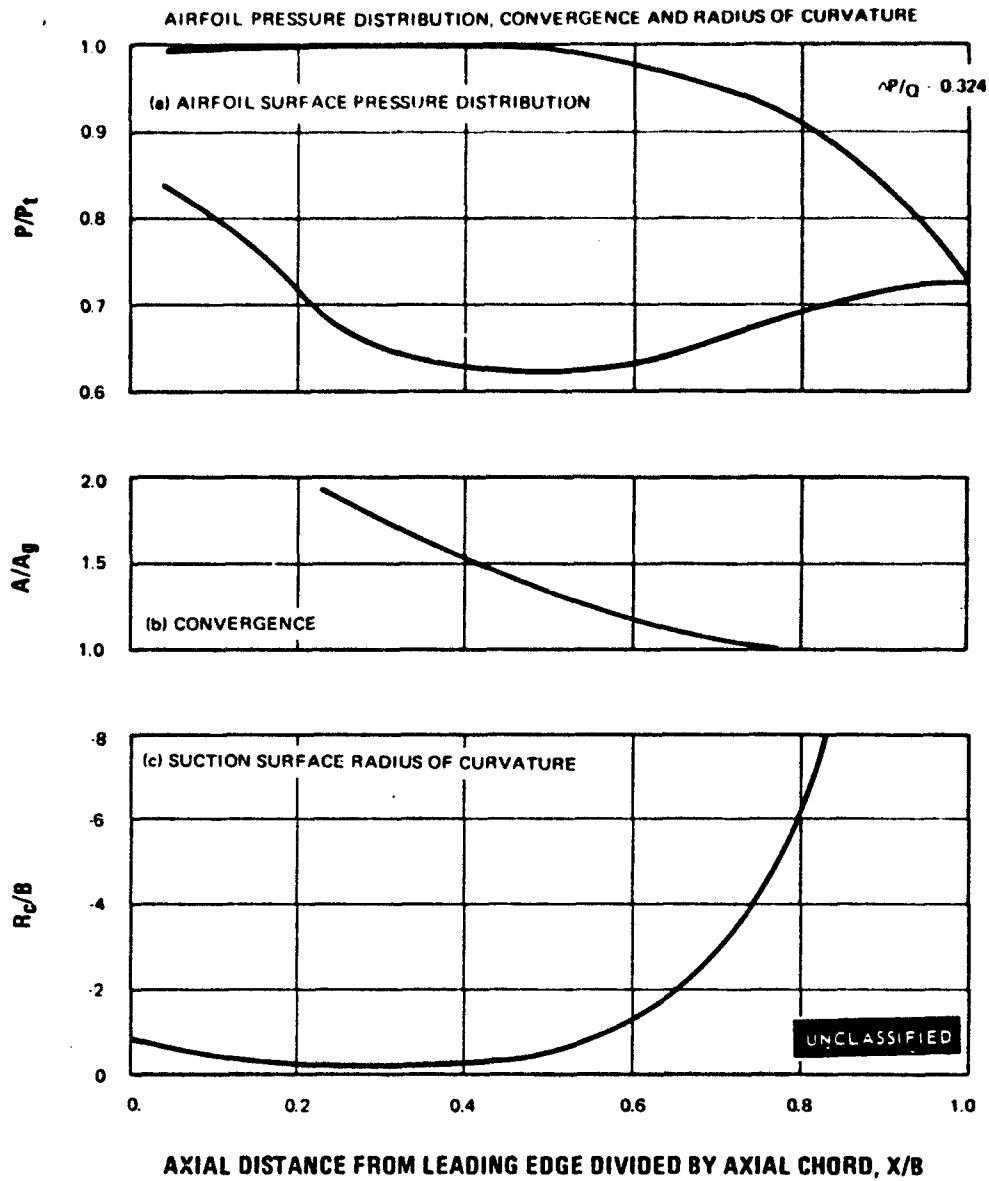


Figure 92

UNCLASSIFIED

UNCLASSIFIED

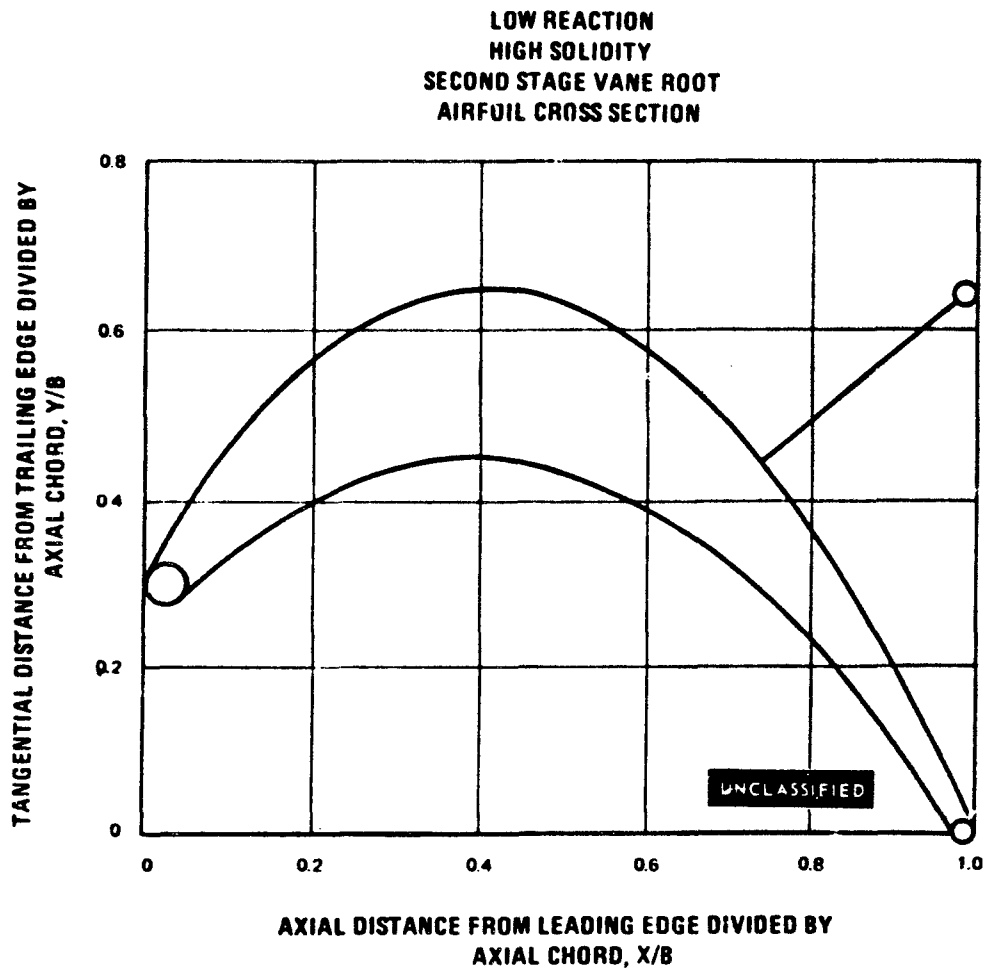


Figure 93

UNCLASSIFIED

UNCLASSIFIED

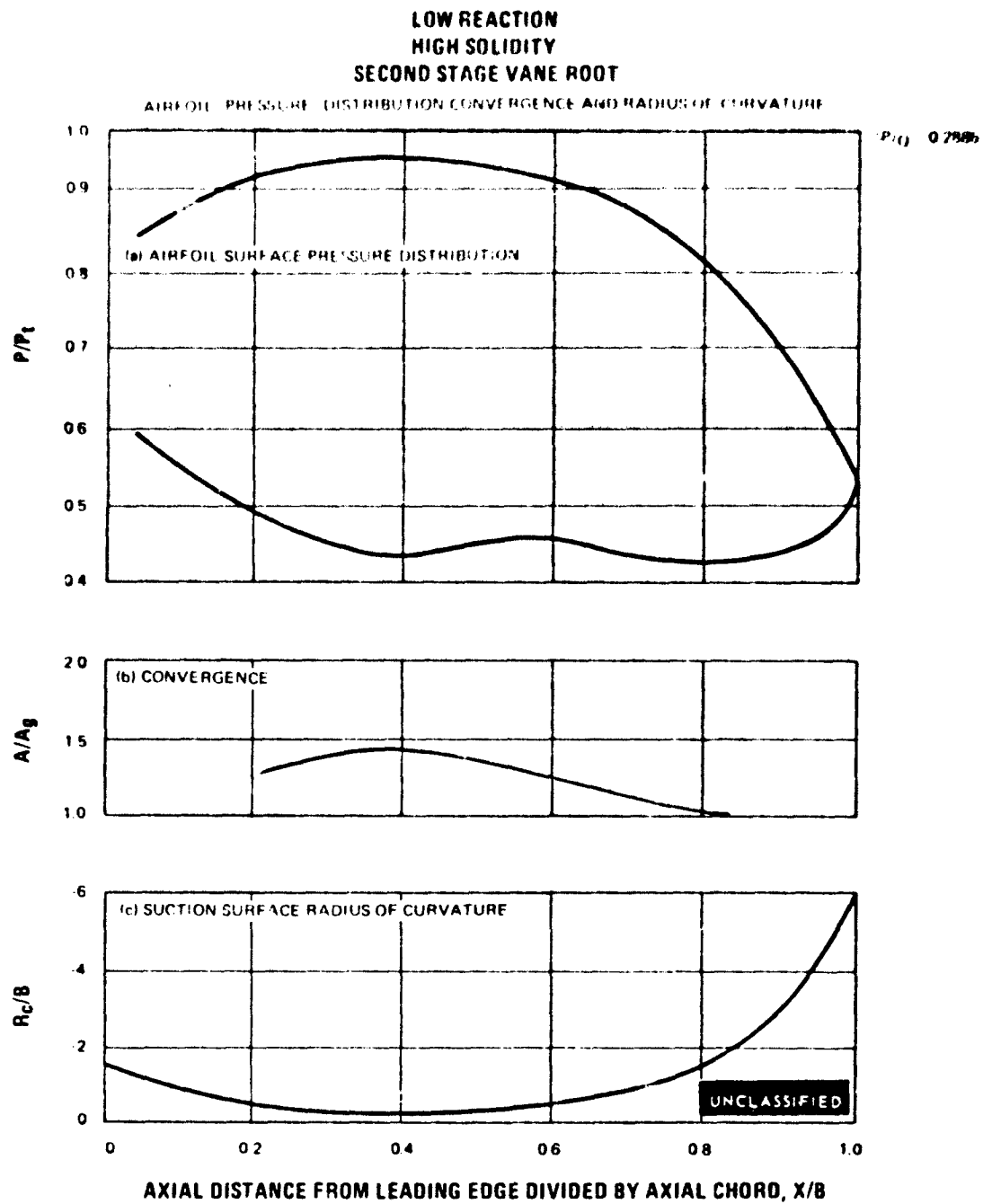


Figure 94

UNCLASSIFIED

UNCLASSIFIED

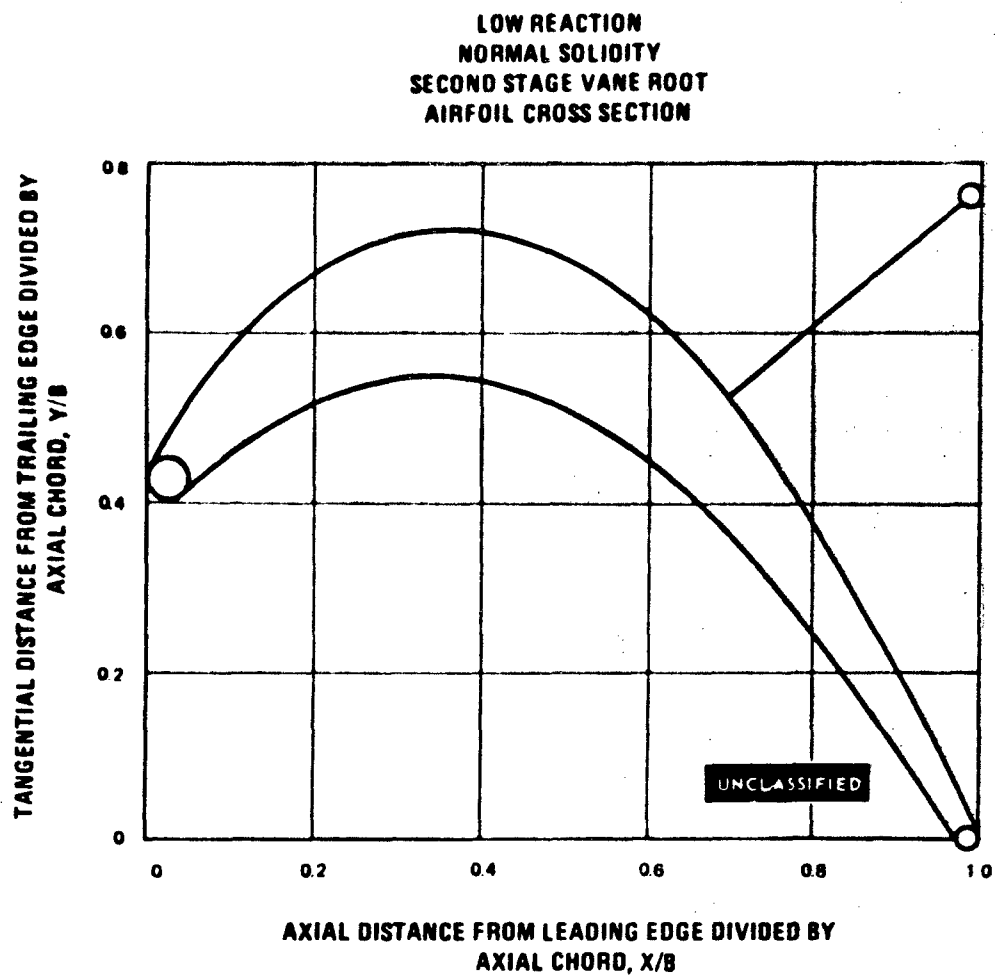


Figure 95

UNCLASSIFIED

UNCLASSIFIED

LO/ REACTION
NORMAL SOLIDITY
SECOND STAGE VANE ROOT

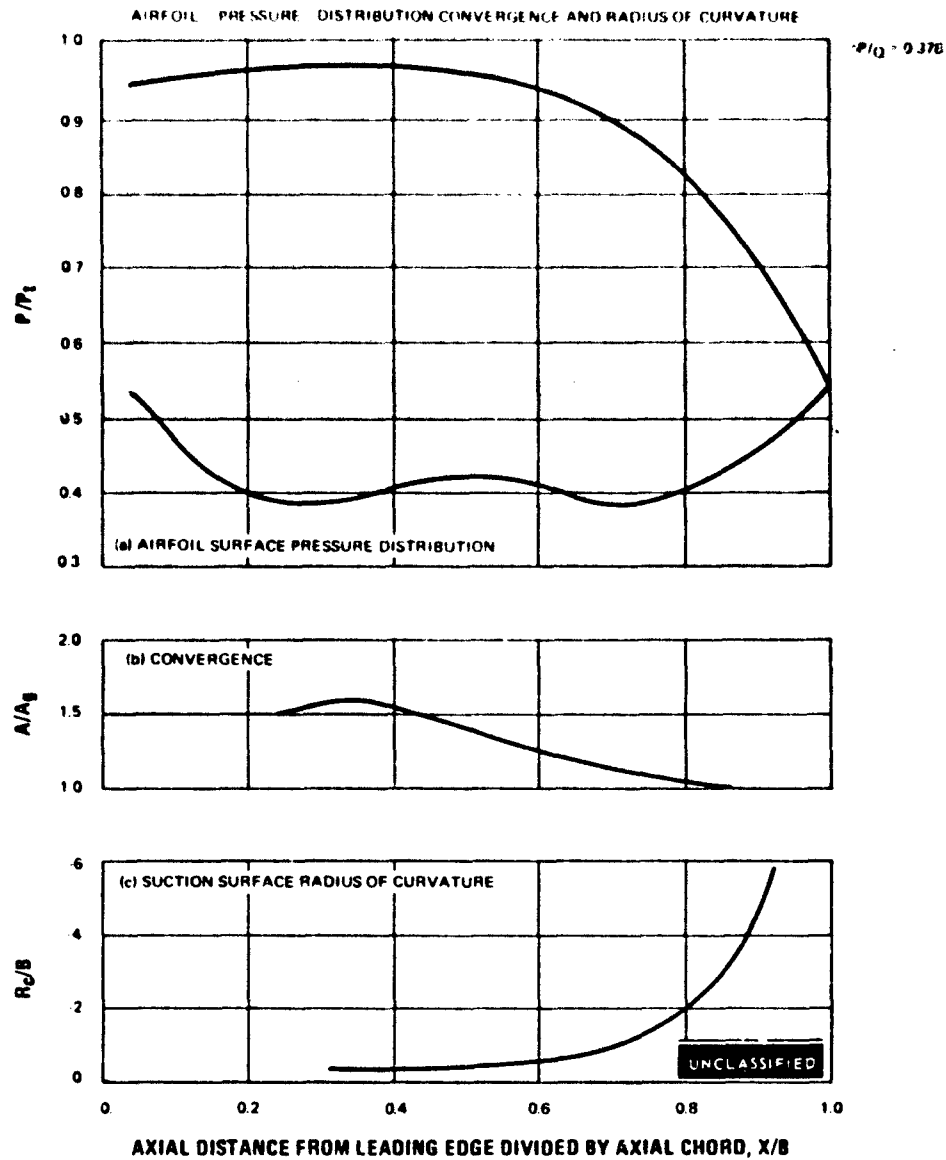


Figure 96

UNCLASSIFIED

UNCLASSIFIED

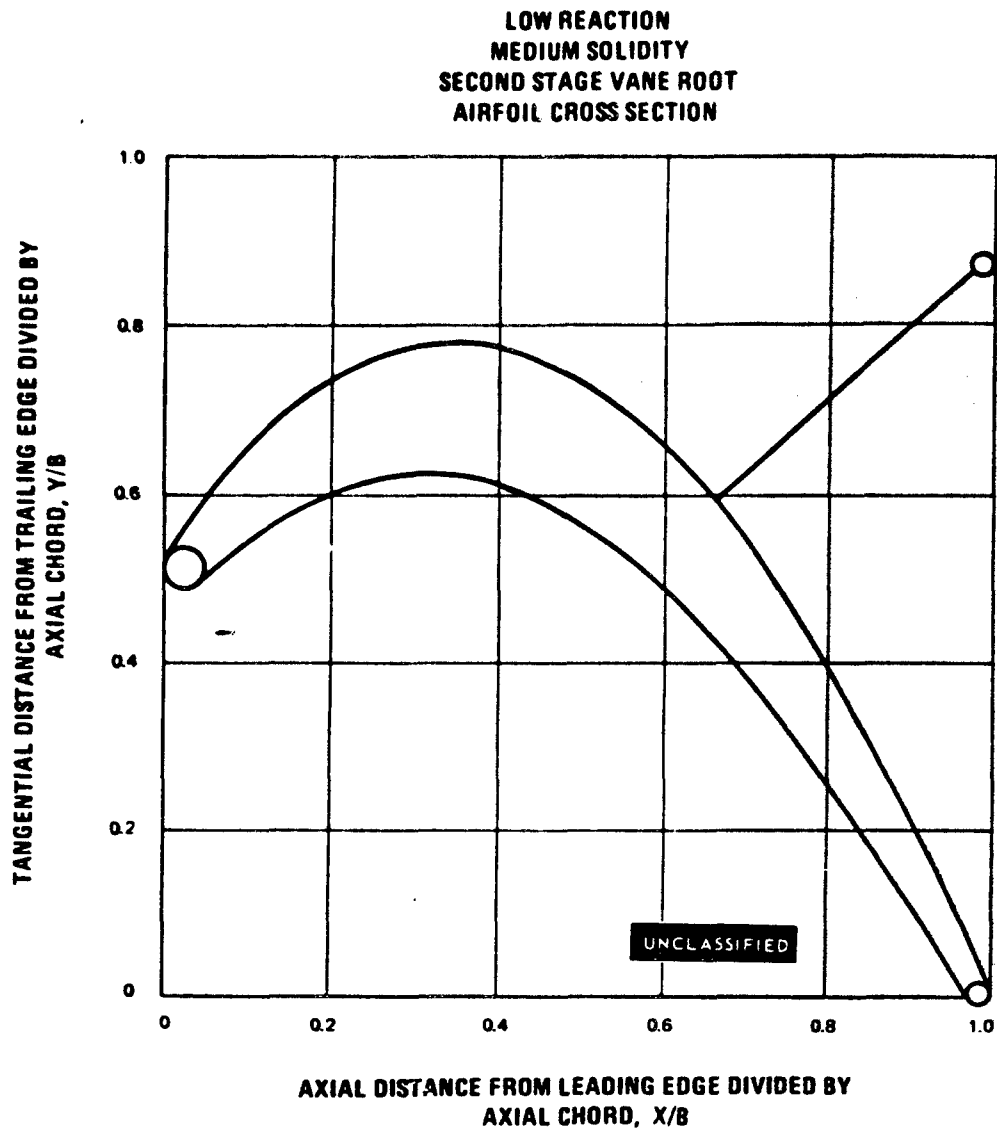


Figure 97

UNCLASSIFIED

UNCLASSIFIED

LOW REACTION
MEDIUM SOLIDITY
SECOND STAGE VANE ROOT

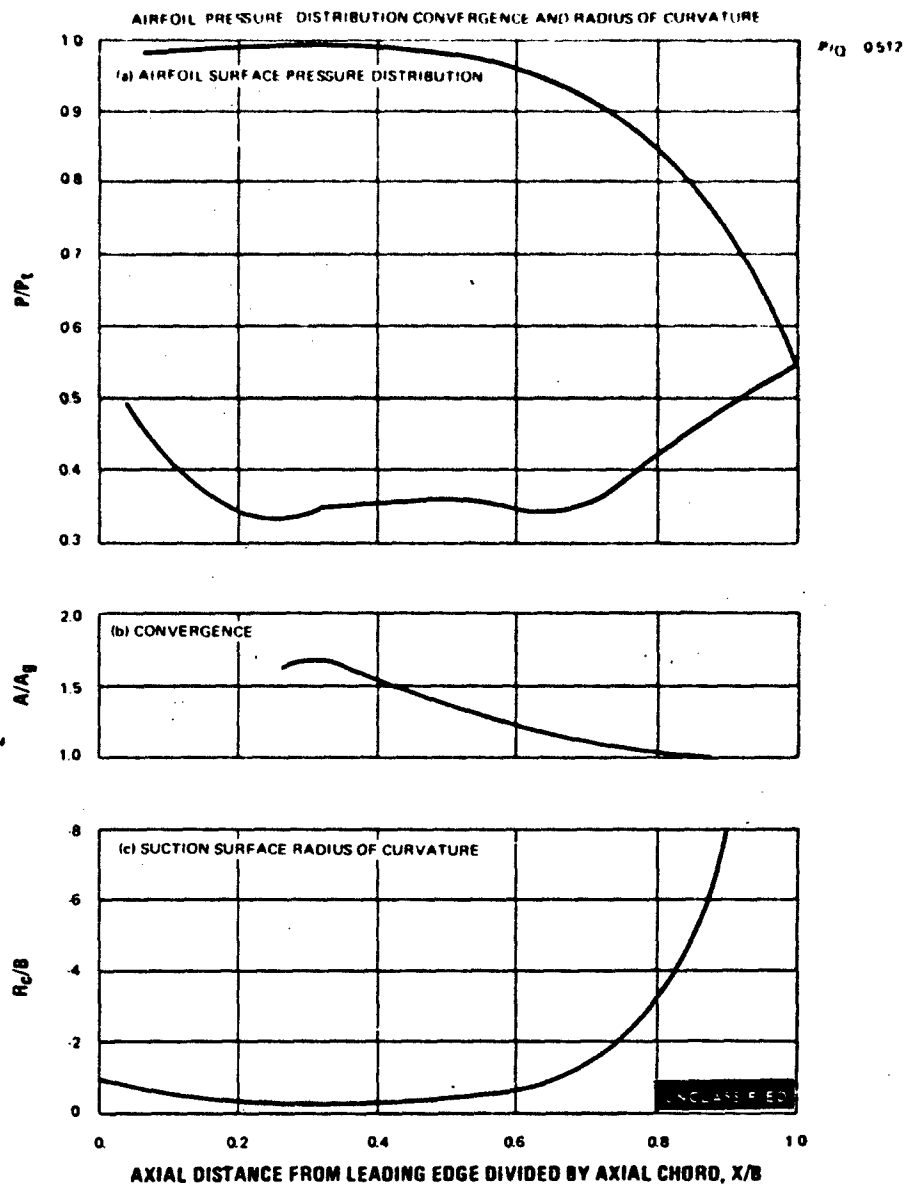


Figure 98

UNCLASSIFIED

UNCLASSIFIED

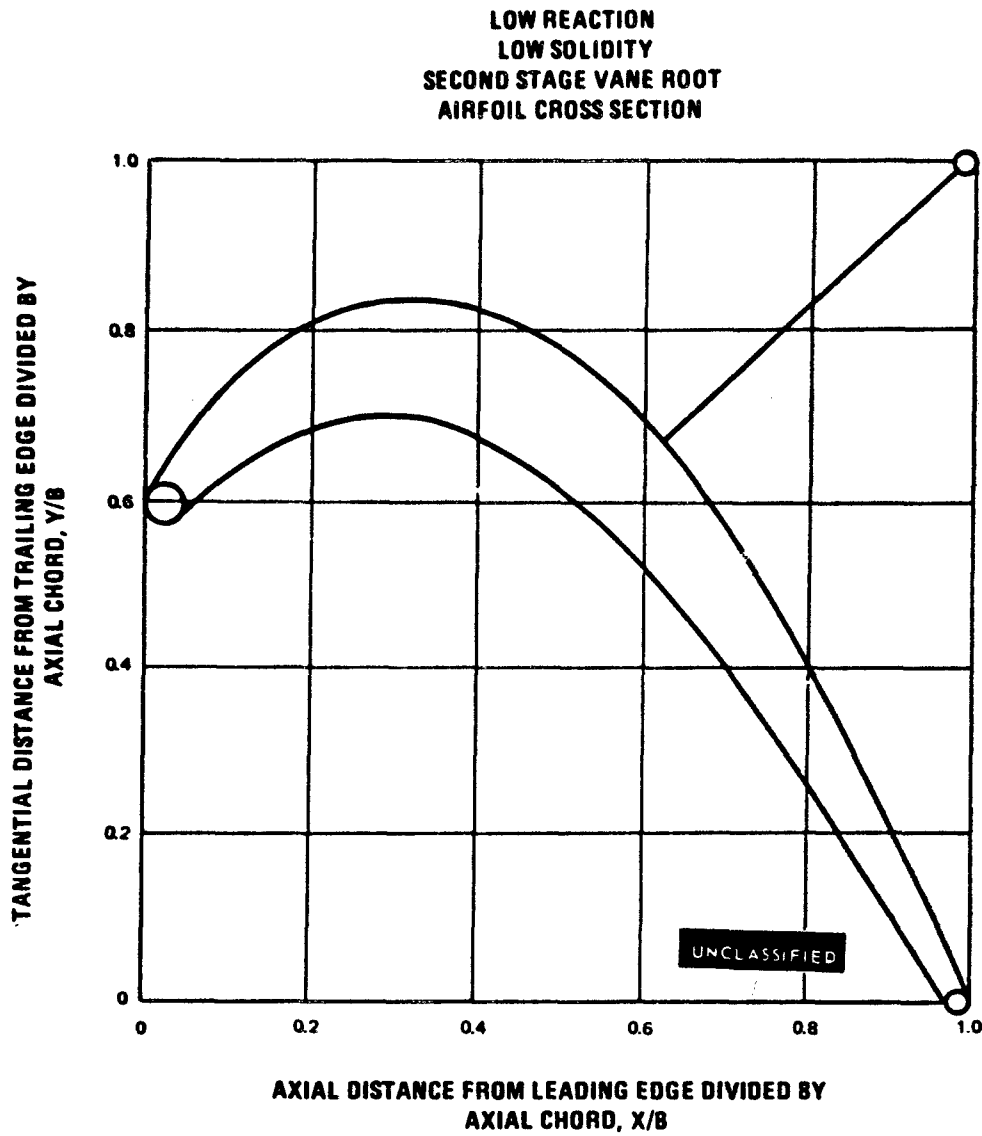


Figure 99

UNCLASSIFIED

UNCLASSIFIED

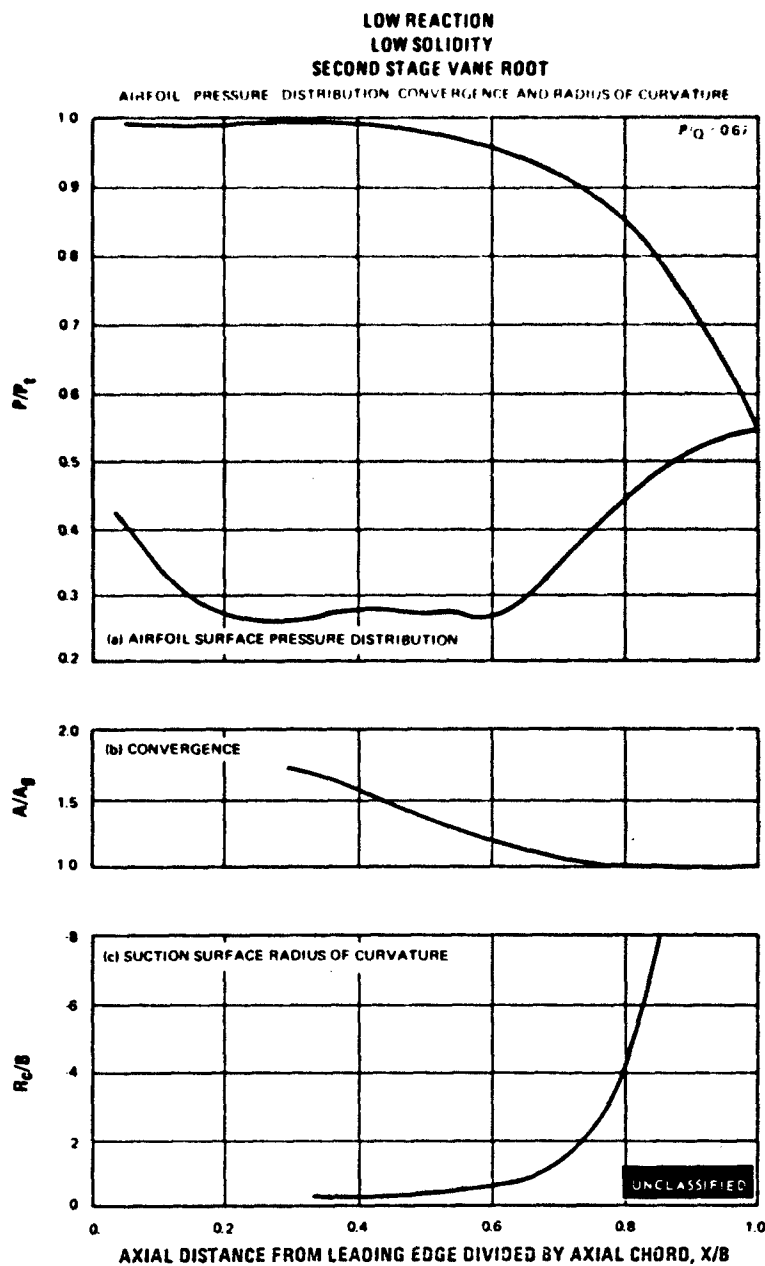


Figure 100

UNCLASSIFIED

UNCLASSIFIED

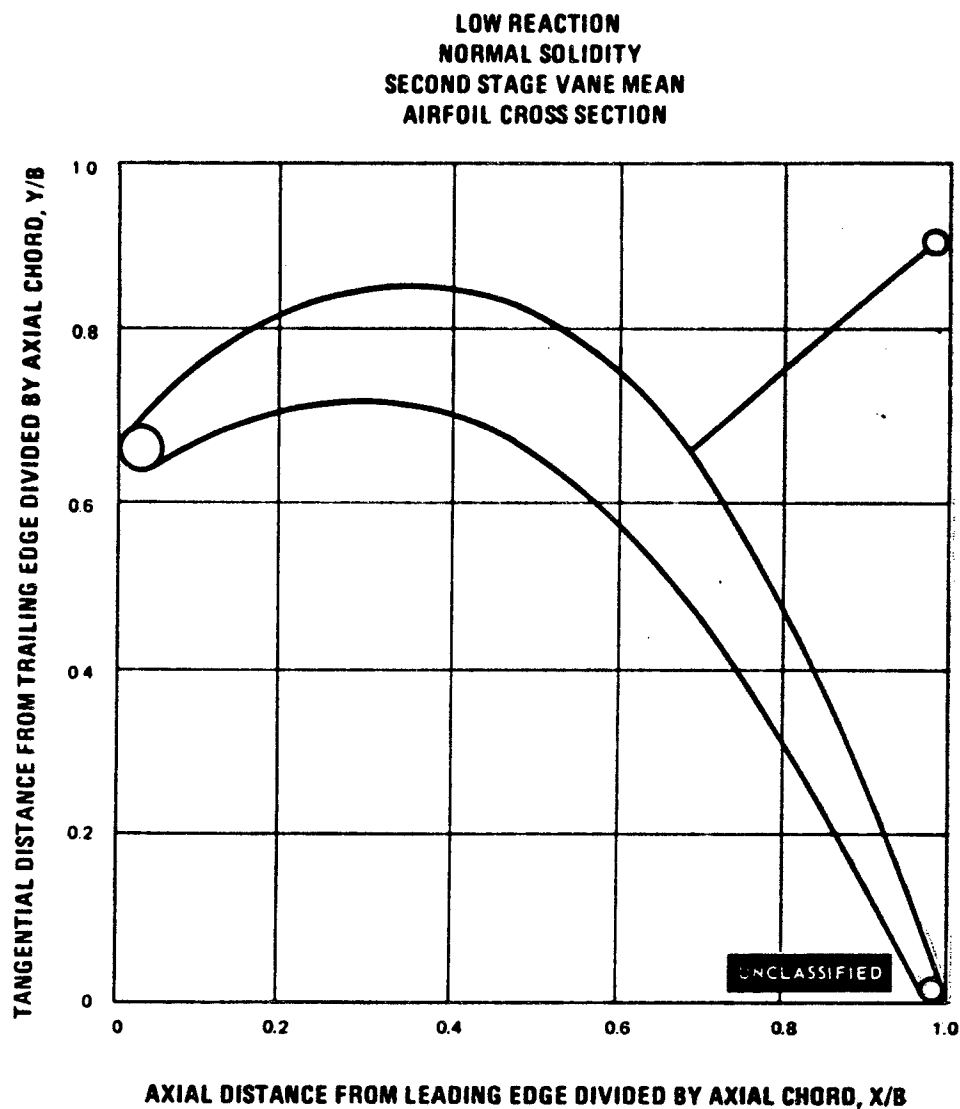


Figure 101

UNCLASSIFIED

UNCLASSIFIED

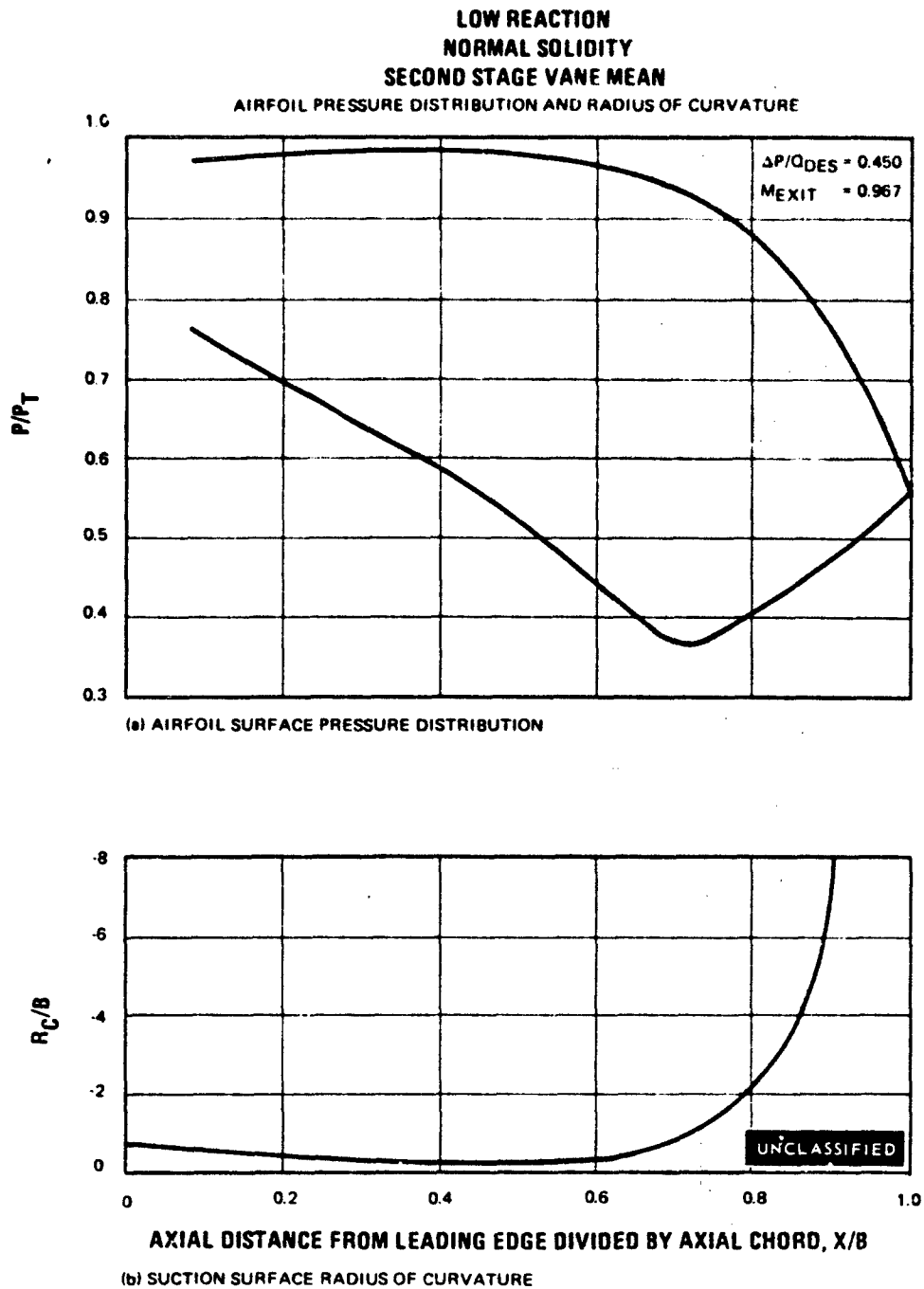


Figure 102

UNCLASSIFIED

UNCLASSIFIED

LOW REACTION
MEDIUM SOLIDITY
SECOND STAGE VANE MEAN
AIRFOIL CROSS SECTION

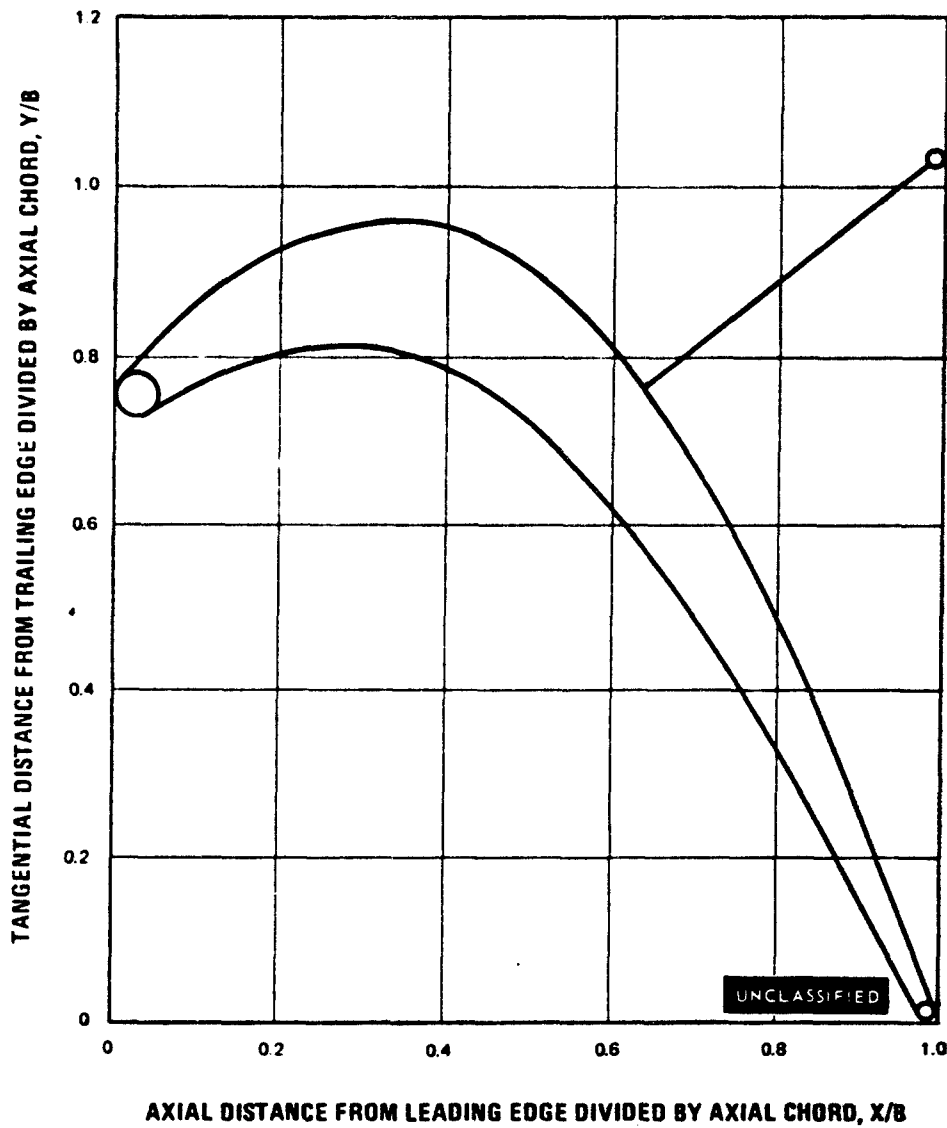


Figure 103

UNCLASSIFIED

UNCLASSIFIED

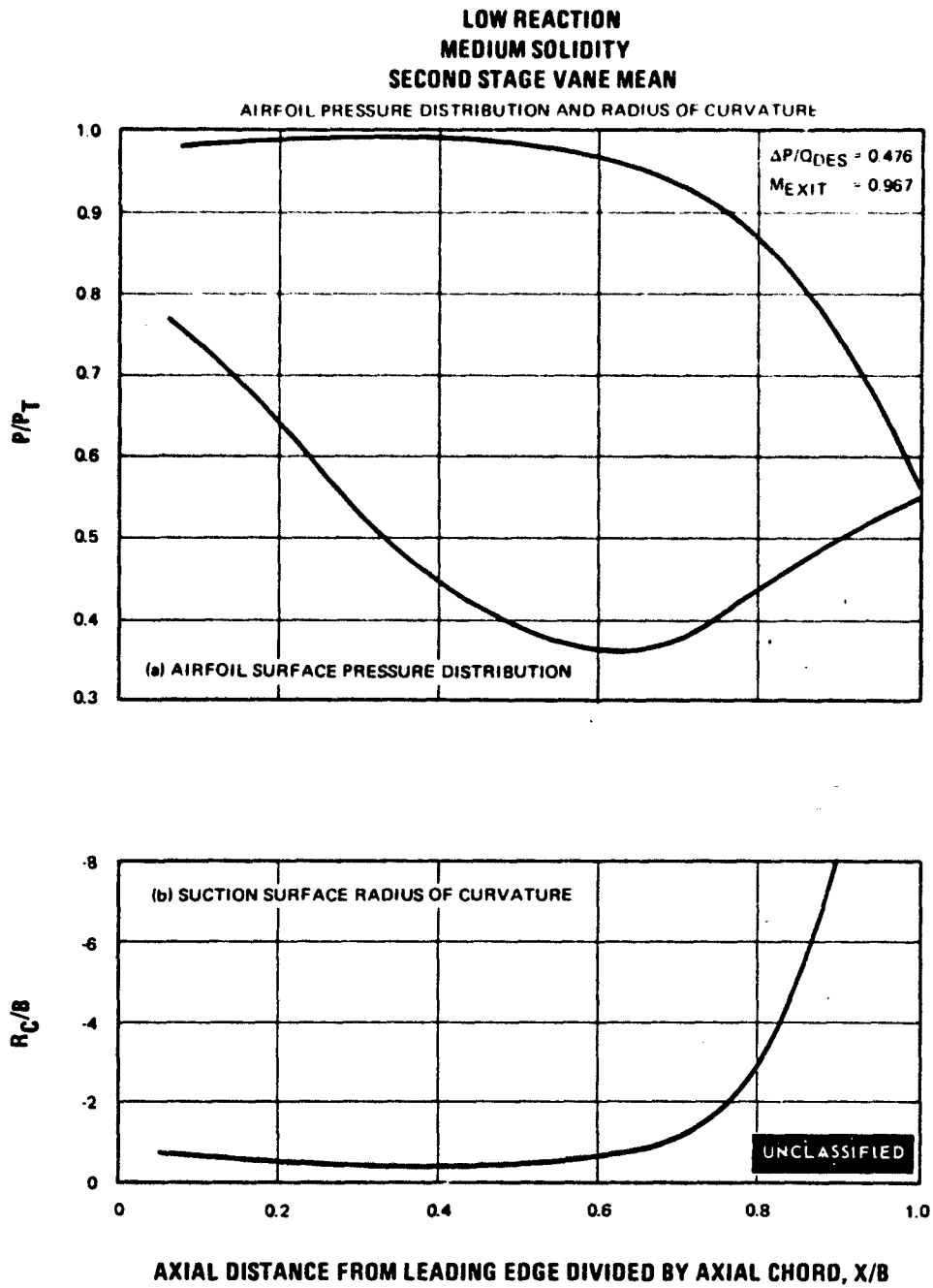


Figure 104

UNCLASSIFIED

UNCLASSIFIED

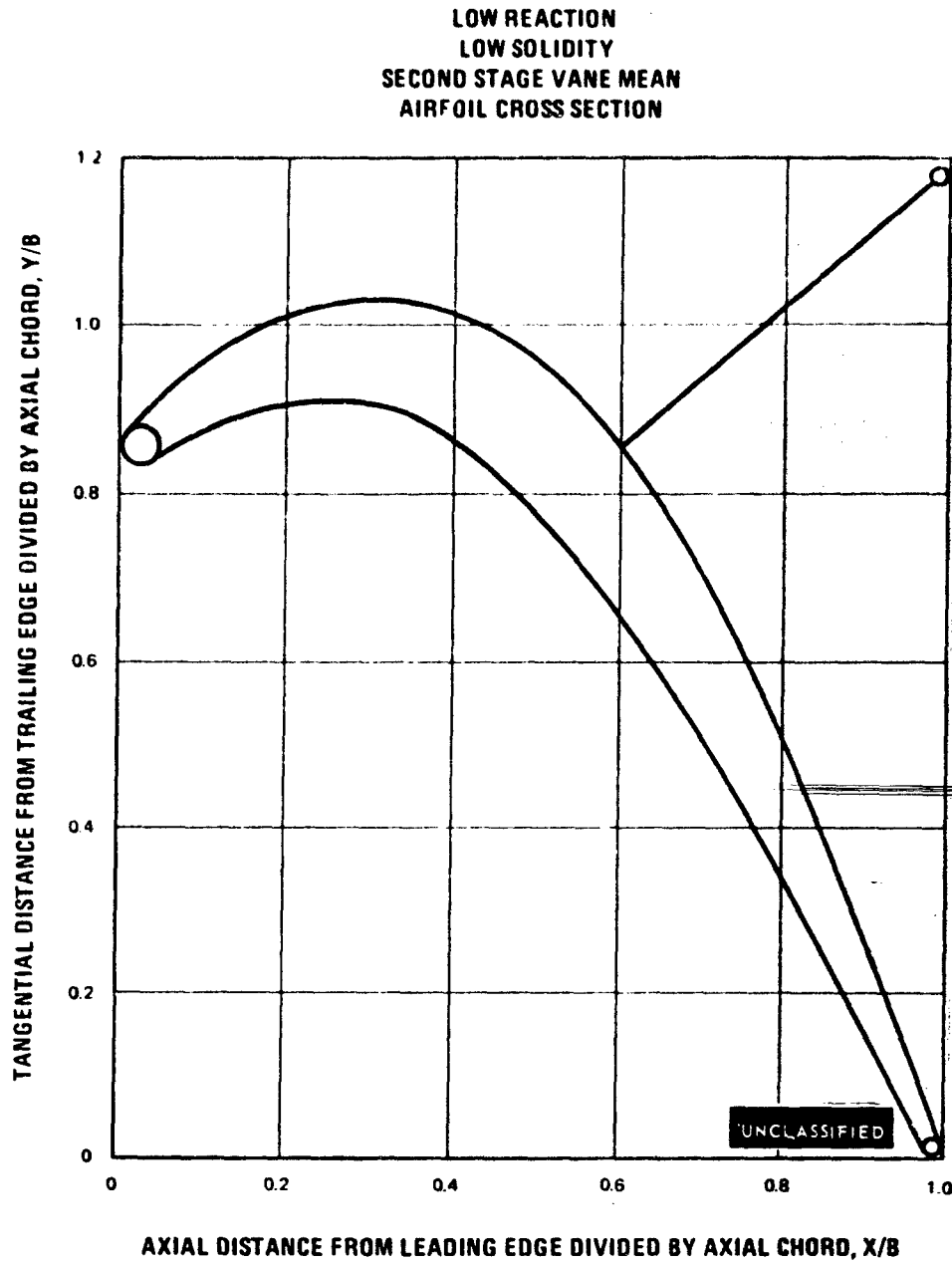


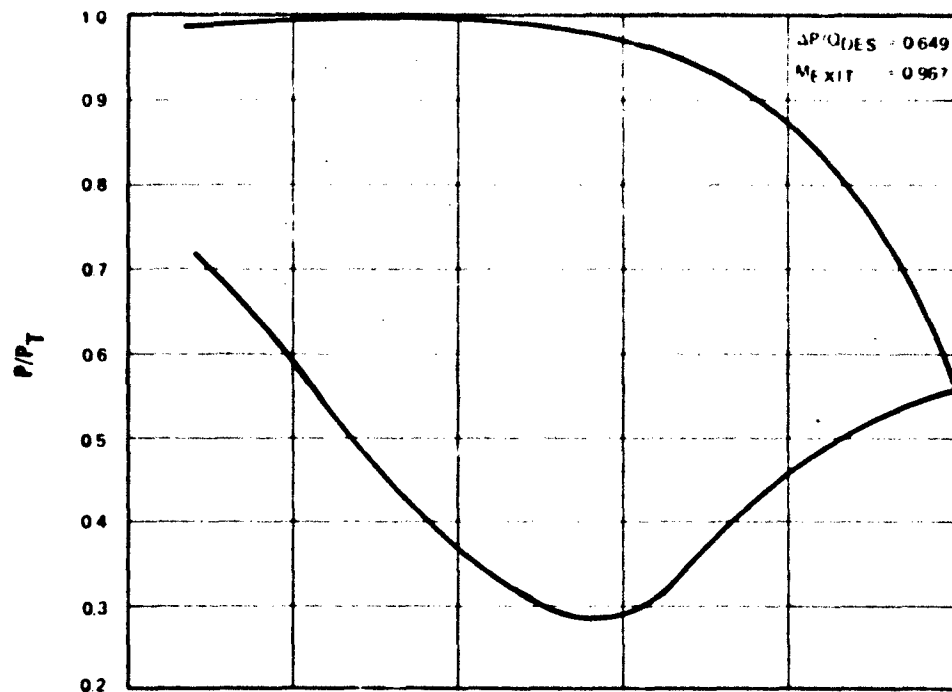
Figure 105

UNCLASSIFIED

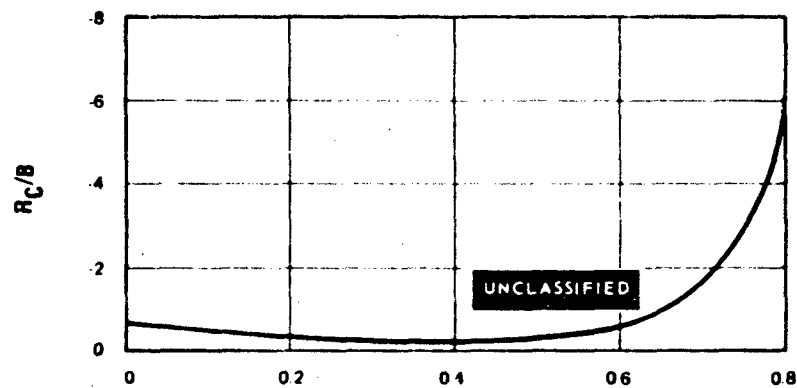
UNCLASSIFIED

LOW REACTION
LOW SOLIDITY
SECOND STAGE VANE MEAN

AIRFOIL PRESSURE DISTRIBUTION AND RADIUS OF CURVATURE



(a) AIRFOIL SURFACE PRESSURE DISTRIBUTION



AXIAL DISTANCE FROM LEADING EDGE DIVIDED BY AXIAL CHORD, X/B
(b) SUCTION SURFACE RADIUS OF CURVATURE

Figure 106

UNCLASSIFIED

UNCLASSIFIED

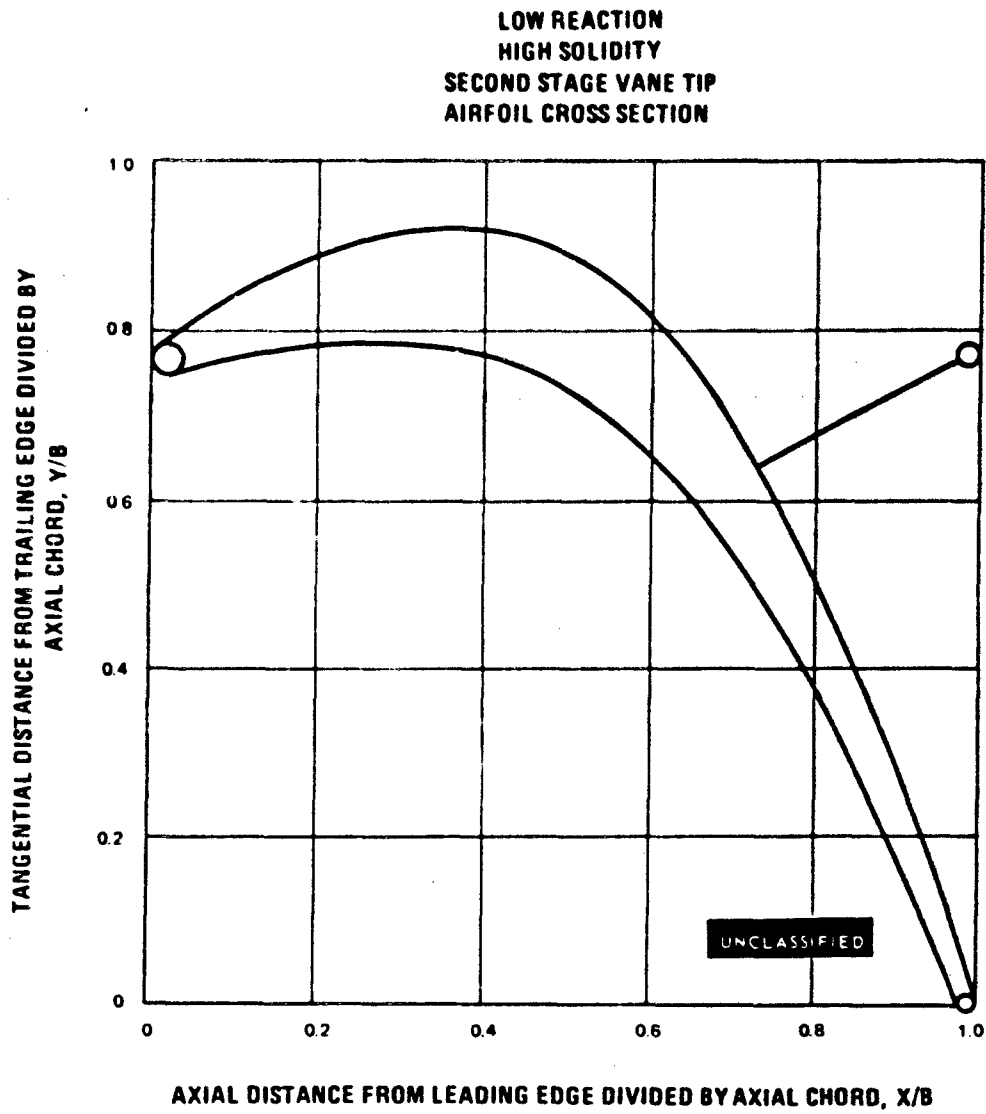


Figure 107

UNCLASSIFIED

UNCLASSIFIED

LOW REACTION
HIGH SOLIDITY
SECOND STAGE VANE TIP

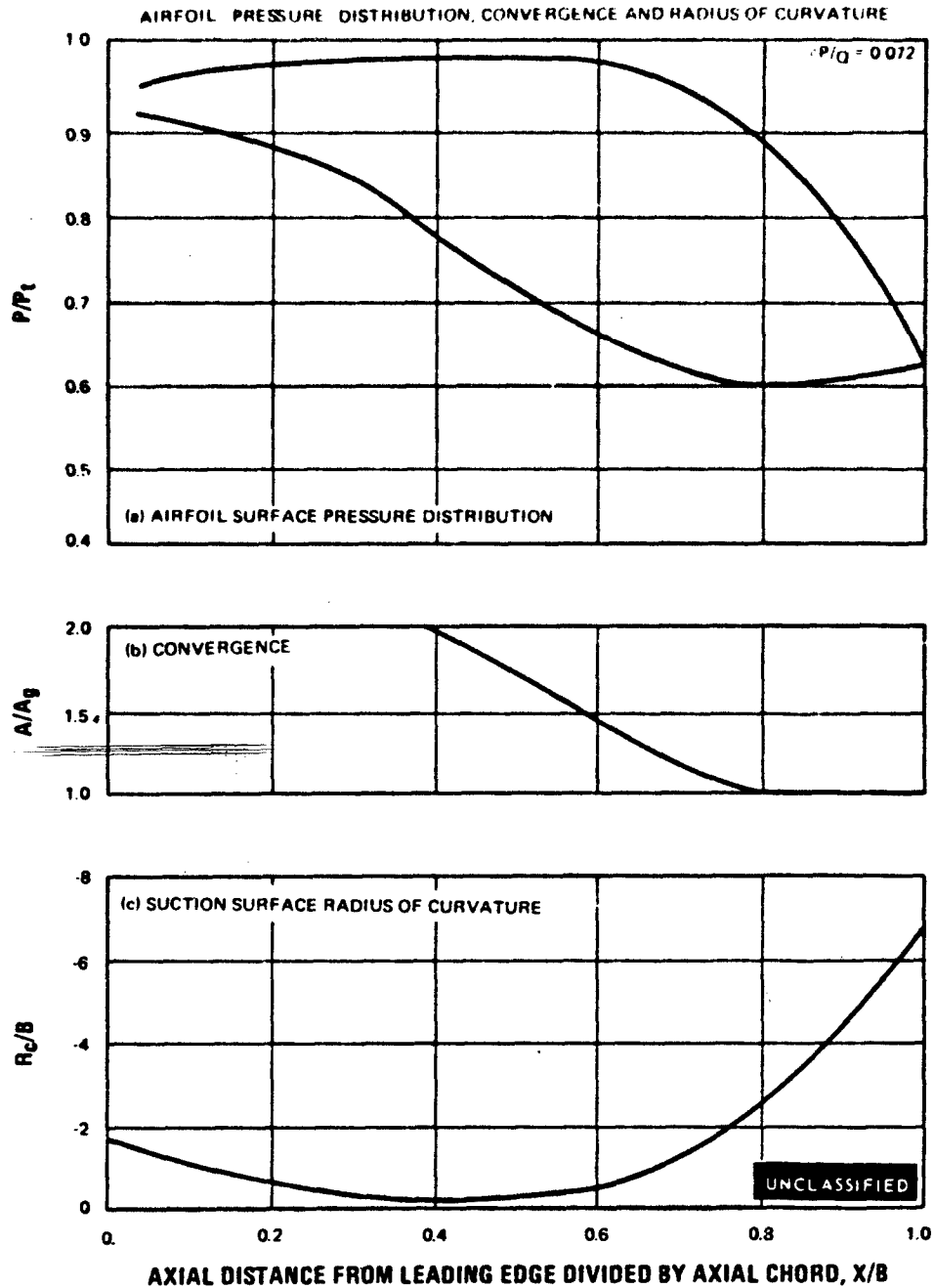


Figure 108

UNCLASSIFIED

UNCLASSIFIED

LOW REACTION
NORMAL SOLIDITY
SECOND STAGE VANE TIP
AIRFOIL CROSS SECTION

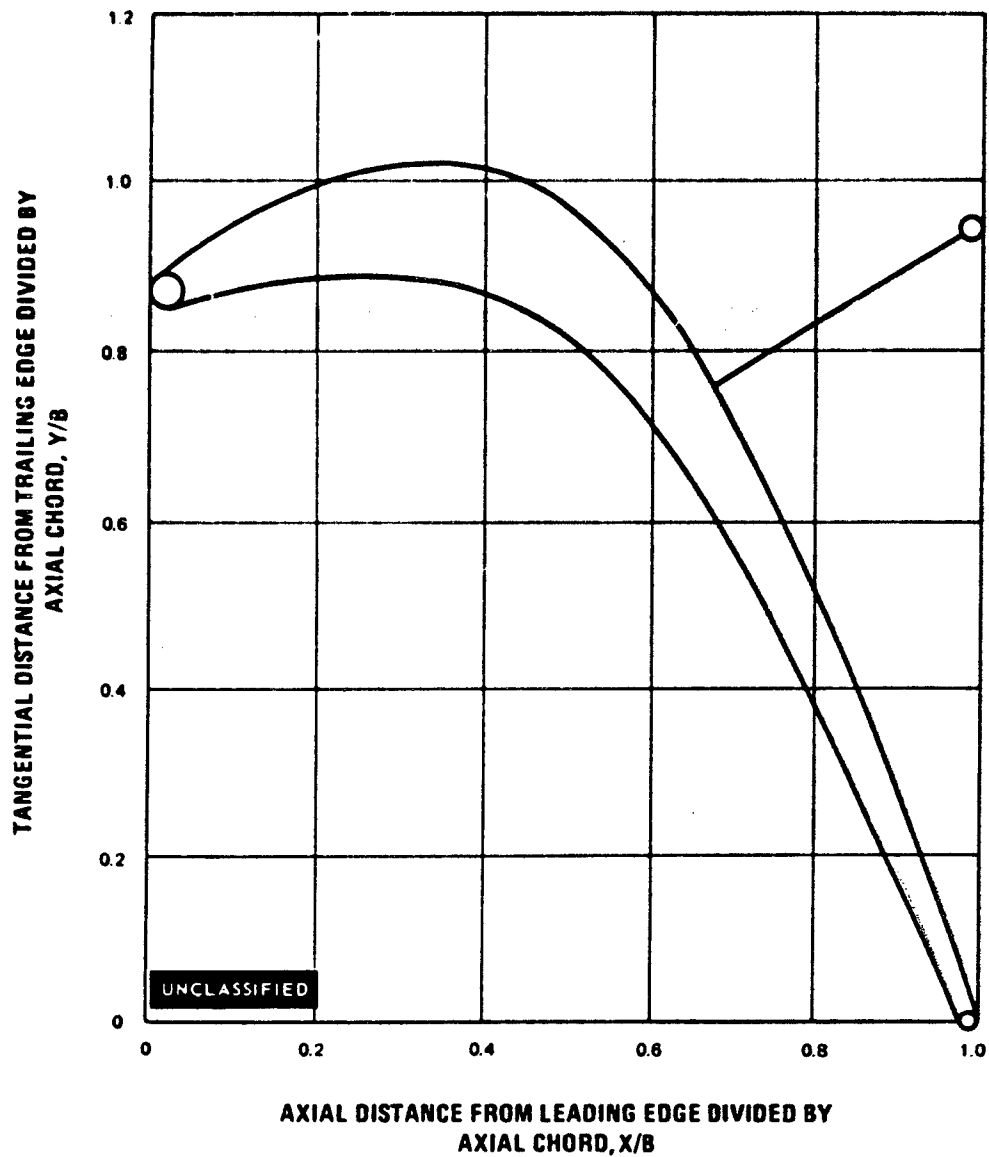


Figure 109

UNCLASSIFIED

UNCLASSIFIED

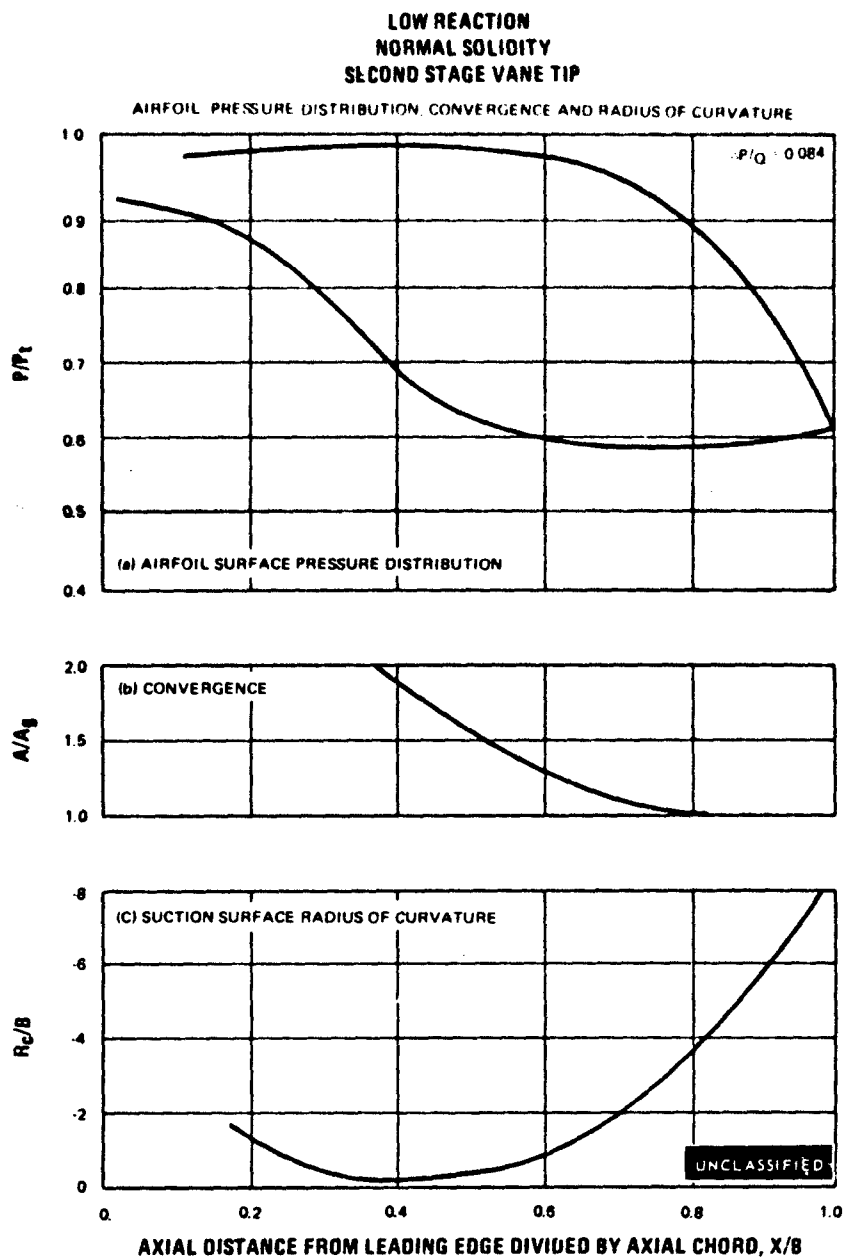


Figure 110

UNCLASSIFIED

UNCLASSIFIED

LOW REACTION
MEDIUM SOLIDITY
SECOND STAGE VANE TIP
AIRFOIL CROSS SECTION

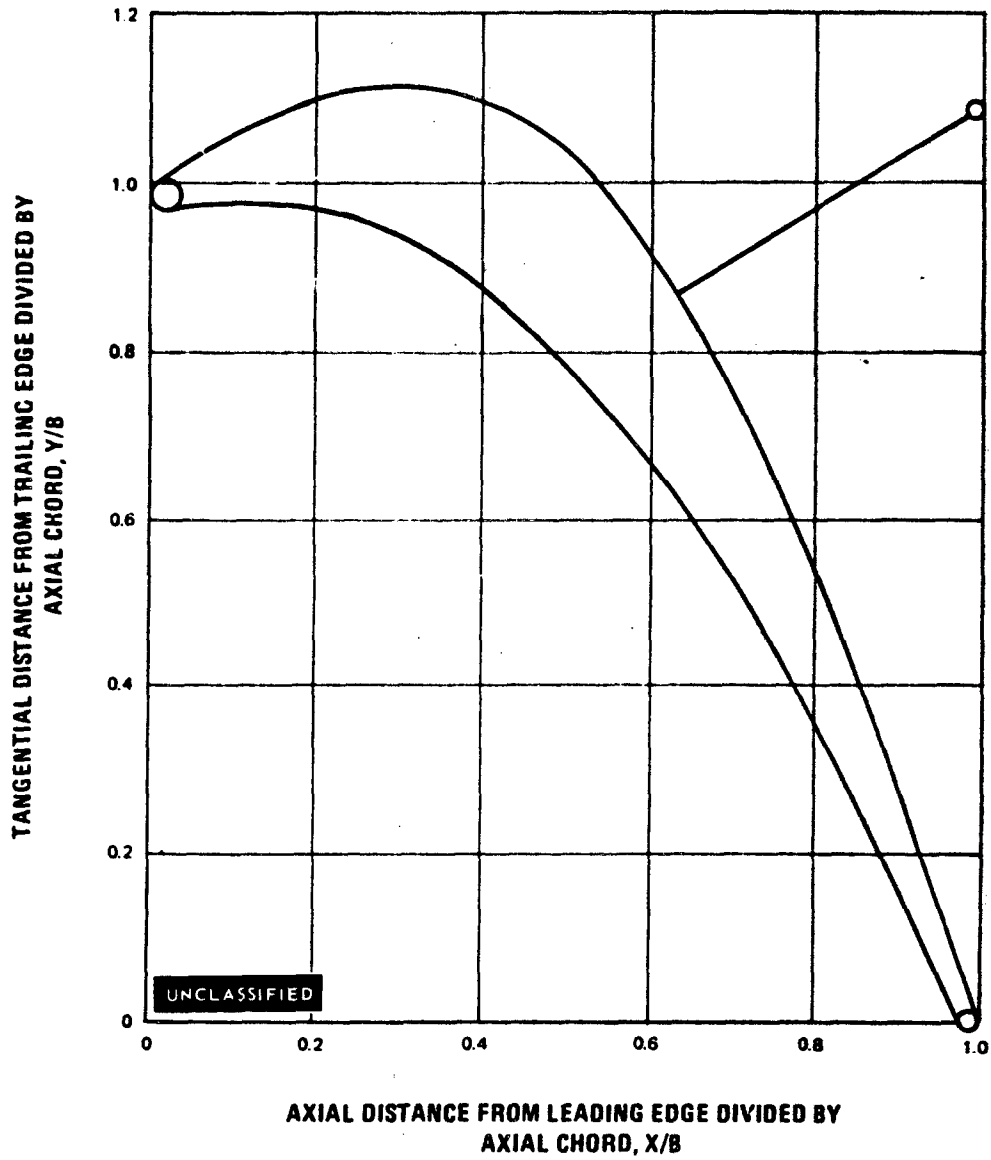


Figure 111

UNCLASSIFIED

UNCLASSIFIED

LOW REACTION
MEDIUM SOLIDITY
SECOND STAGE VANE TIP

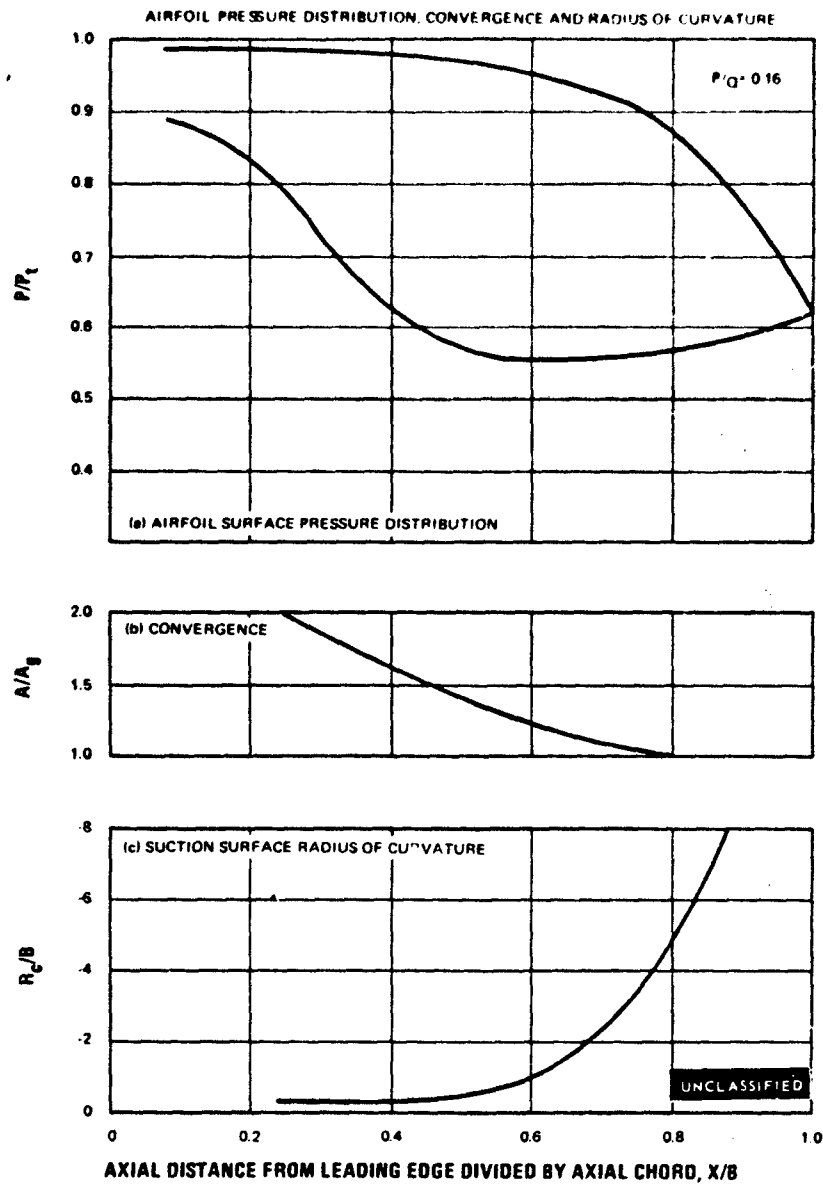


Figure 112

UNCLASSIFIED

UNCLASSIFIED

LOW REACTION
LOW SOLIDITY
SECOND STAGE VANE TIP
AIRFOIL CROSS SECTION

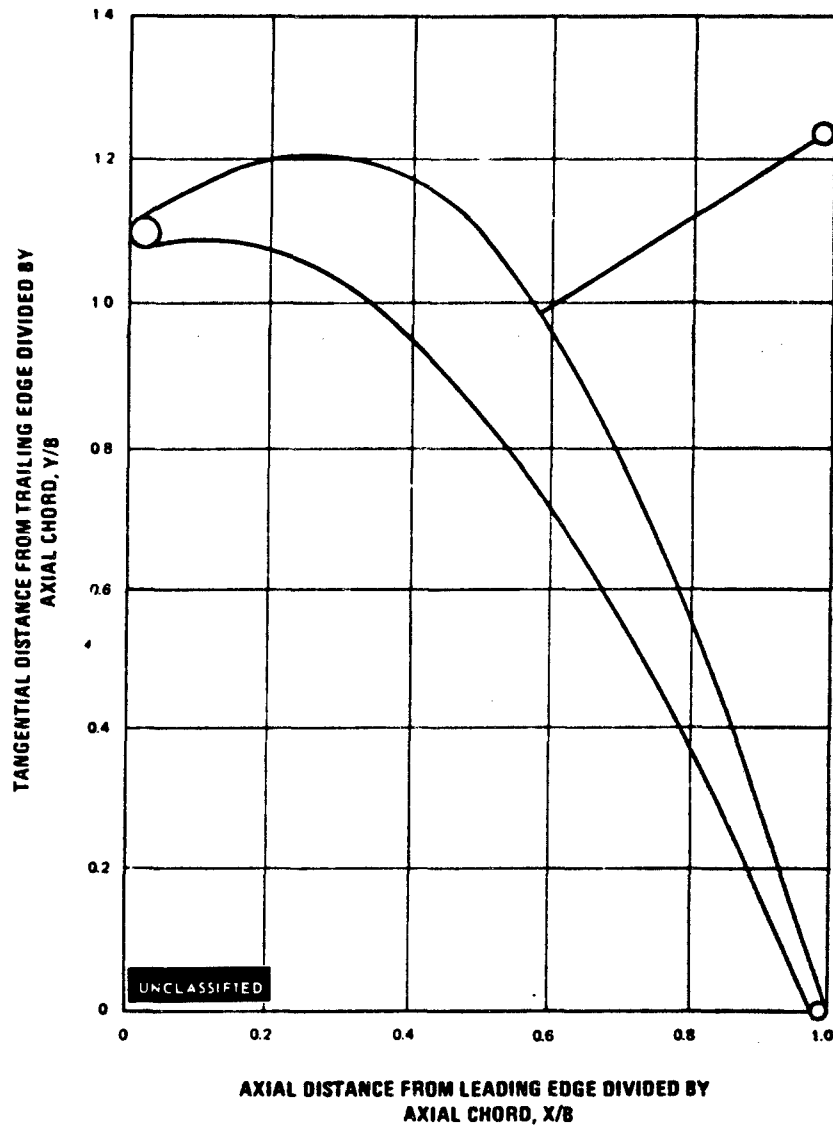


Figure 113

UNCLASSIFIED

UNCLASSIFIED

LOW REACTION
LOW SOLIDITY
SECOND STAGE VANE TIP

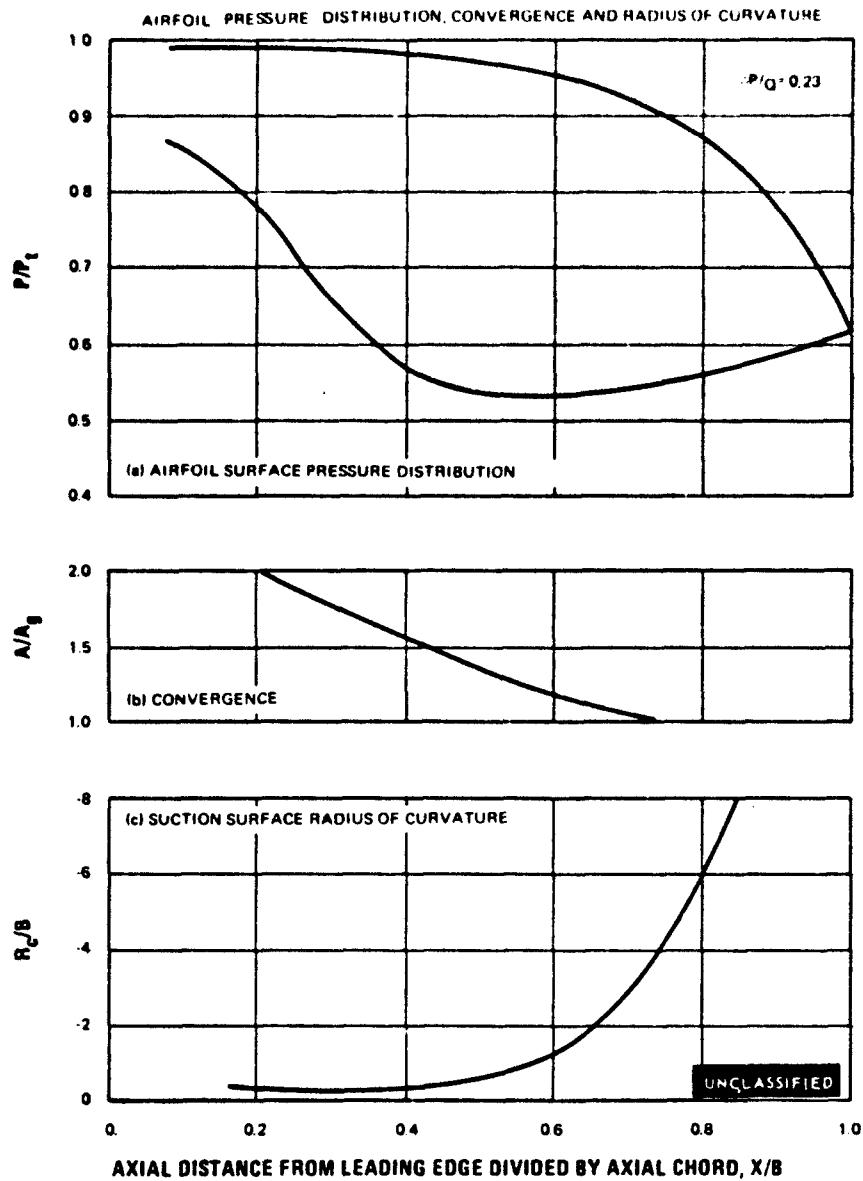


Figure 114

UNCLASSIFIED

UNCLASSIFIED

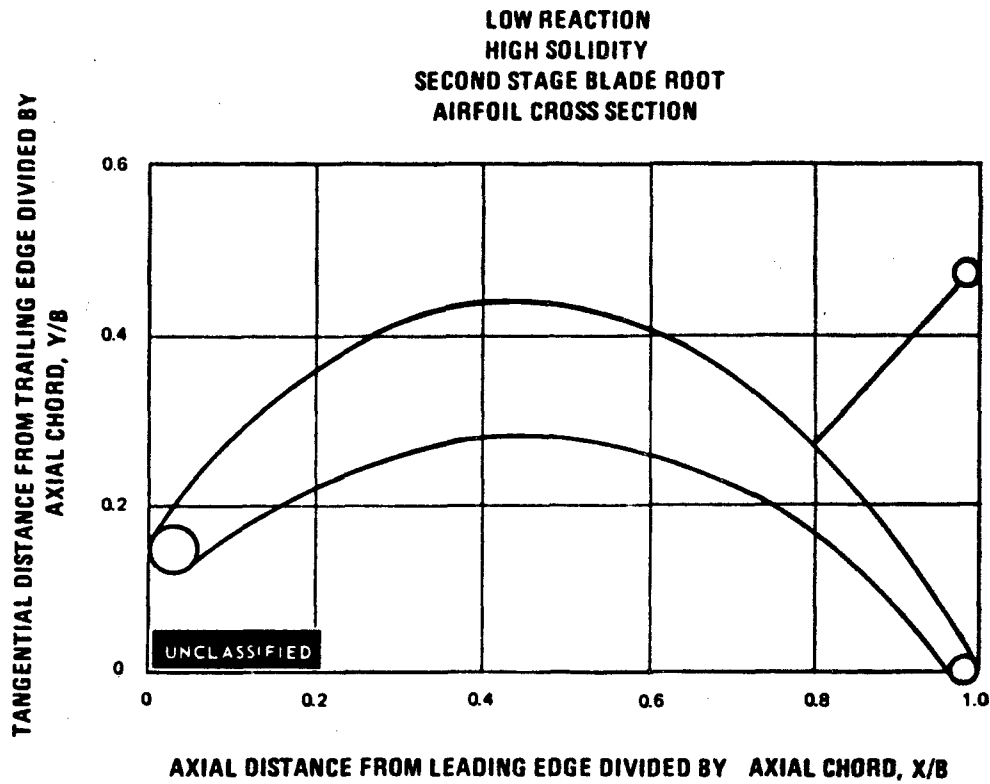


Figure 115

UNCLASSIFIED

UNCLASSIFIED

LOW REACTION
HIGH SOLIDITY
SECOND STAGE BLADE ROOT

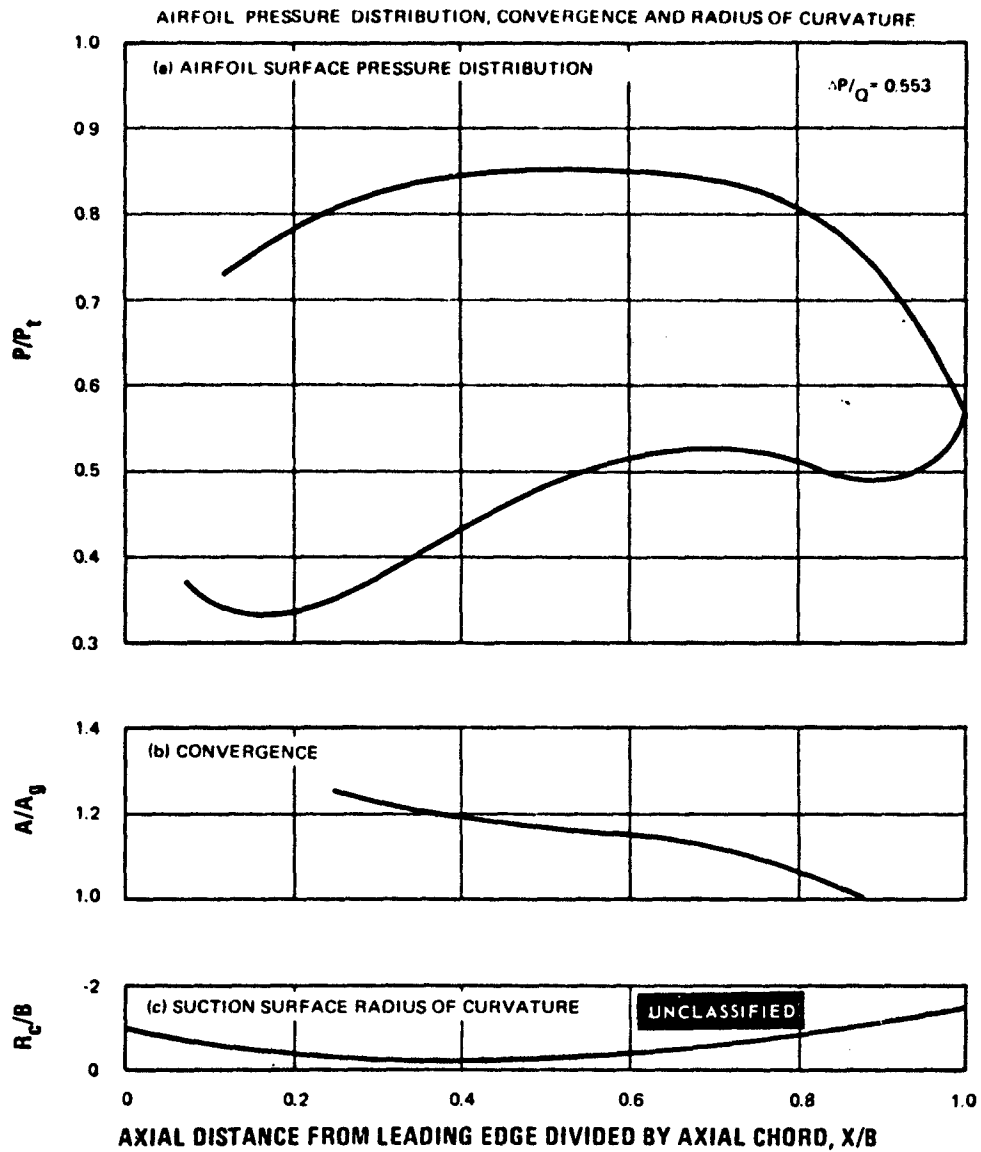


Figure 116

UNCLASSIFIED

UNCLASSIFIED

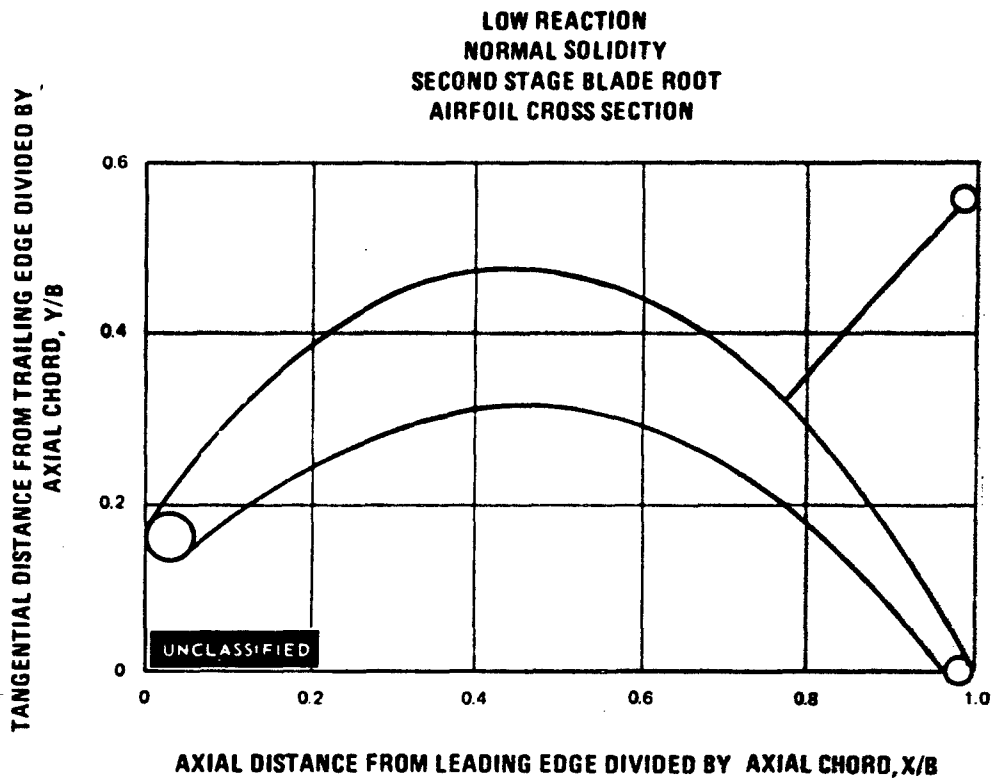


Figure 117

UNCLASSIFIED

UNCLASSIFIED

LOW REACTION
NORMAL SOLIDITY
SECOND STAGE BLADE ROOT

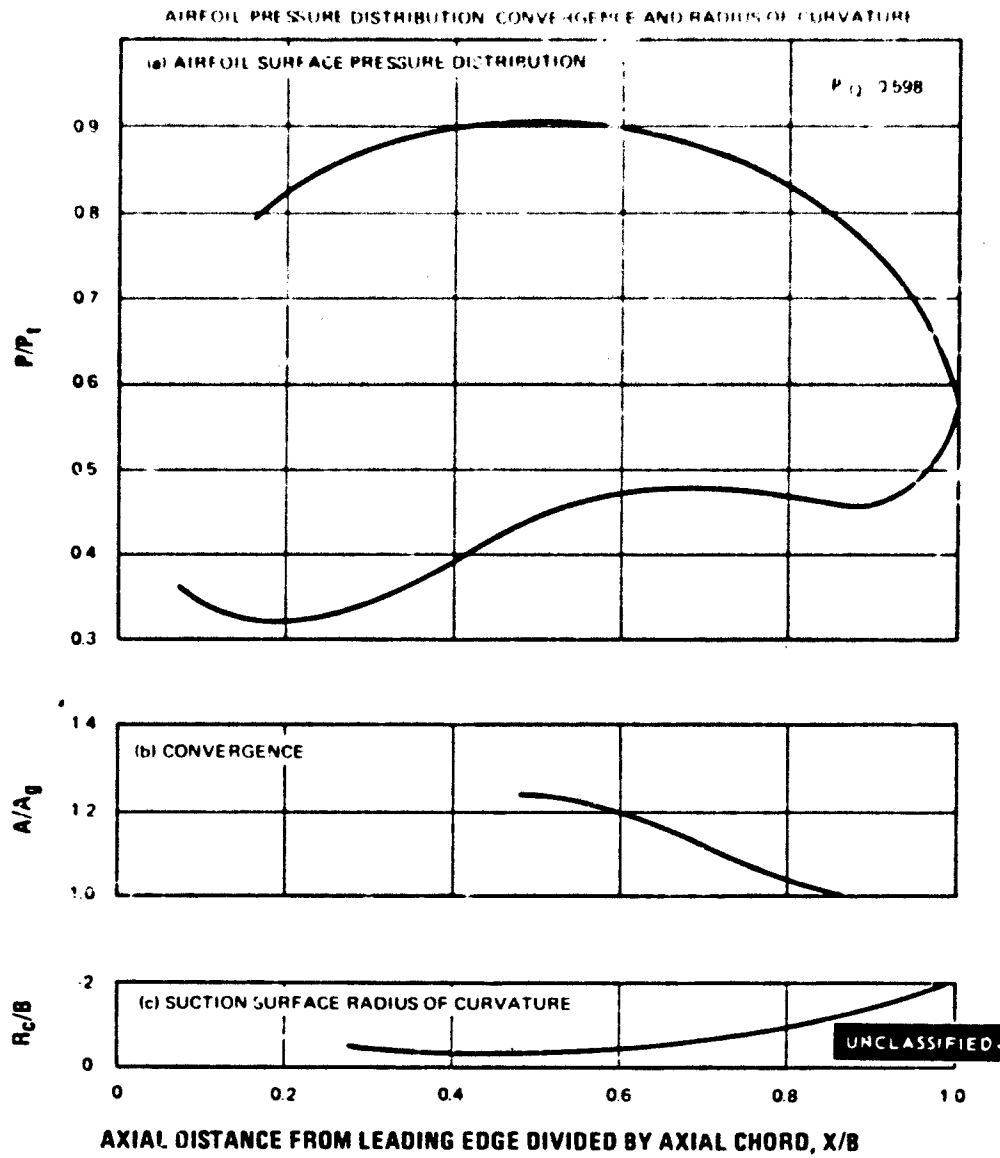


Figure 118

UNCLASSIFIED

UNCLASSIFIED

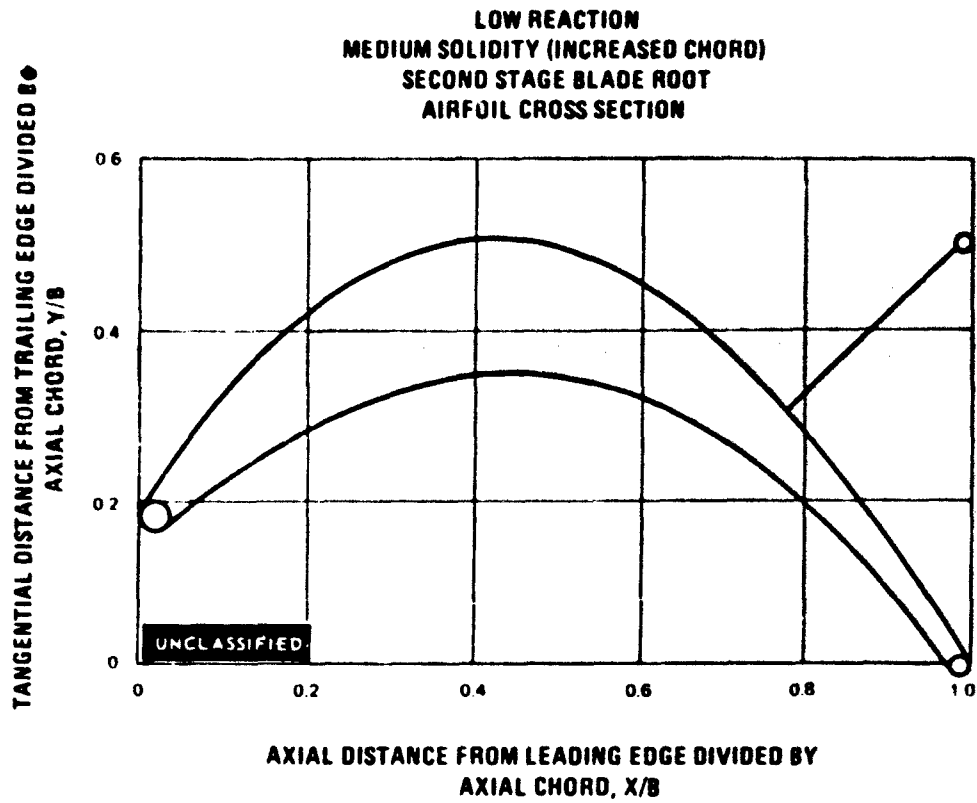


Figure 119

UNCLASSIFIED

UNCLASSIFIED

LOW REACTION
MEDIUM SOLIDITY (INCREASED CHORD)
SECOND STAGE BLADE ROOT

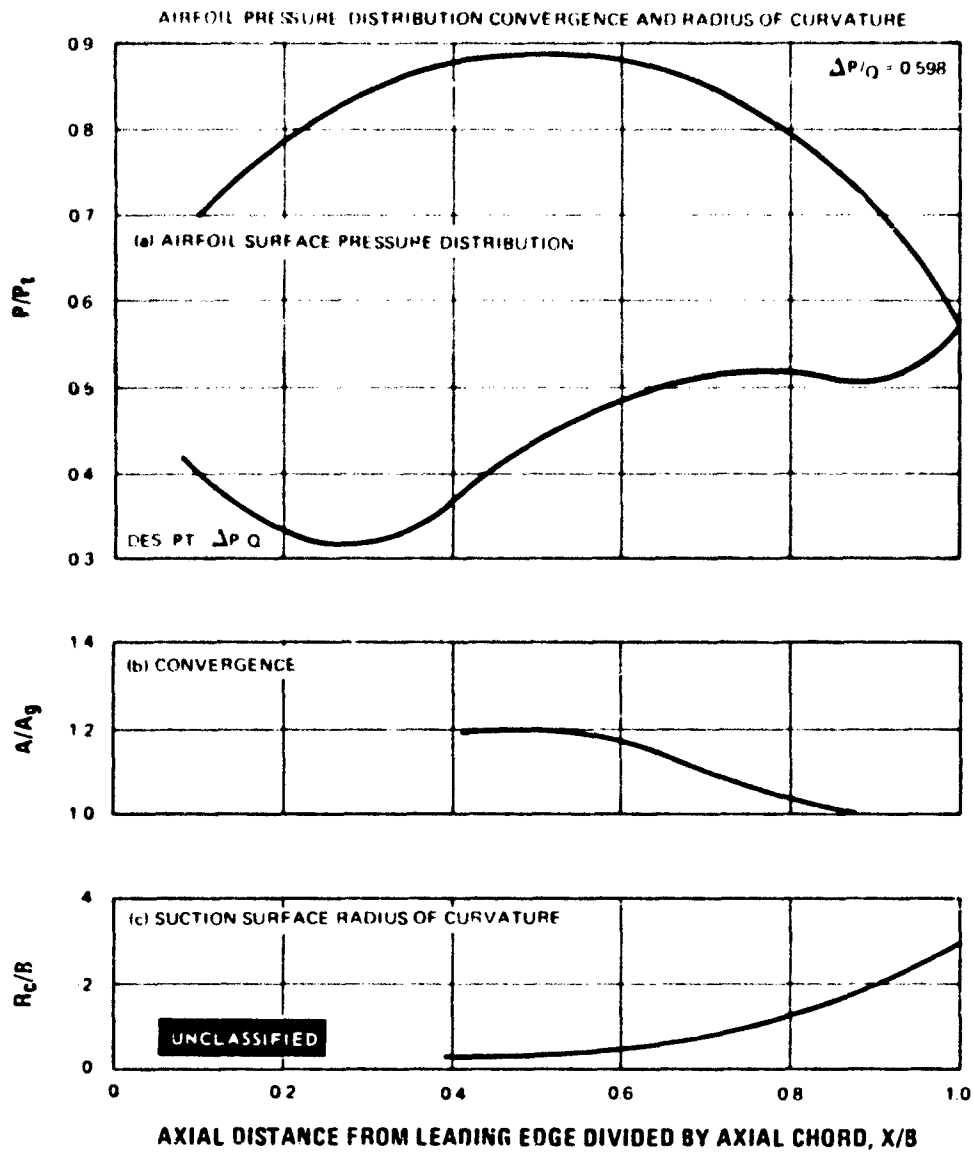


Figure 120

UNCLASSIFIED

UNCLASSIFIED

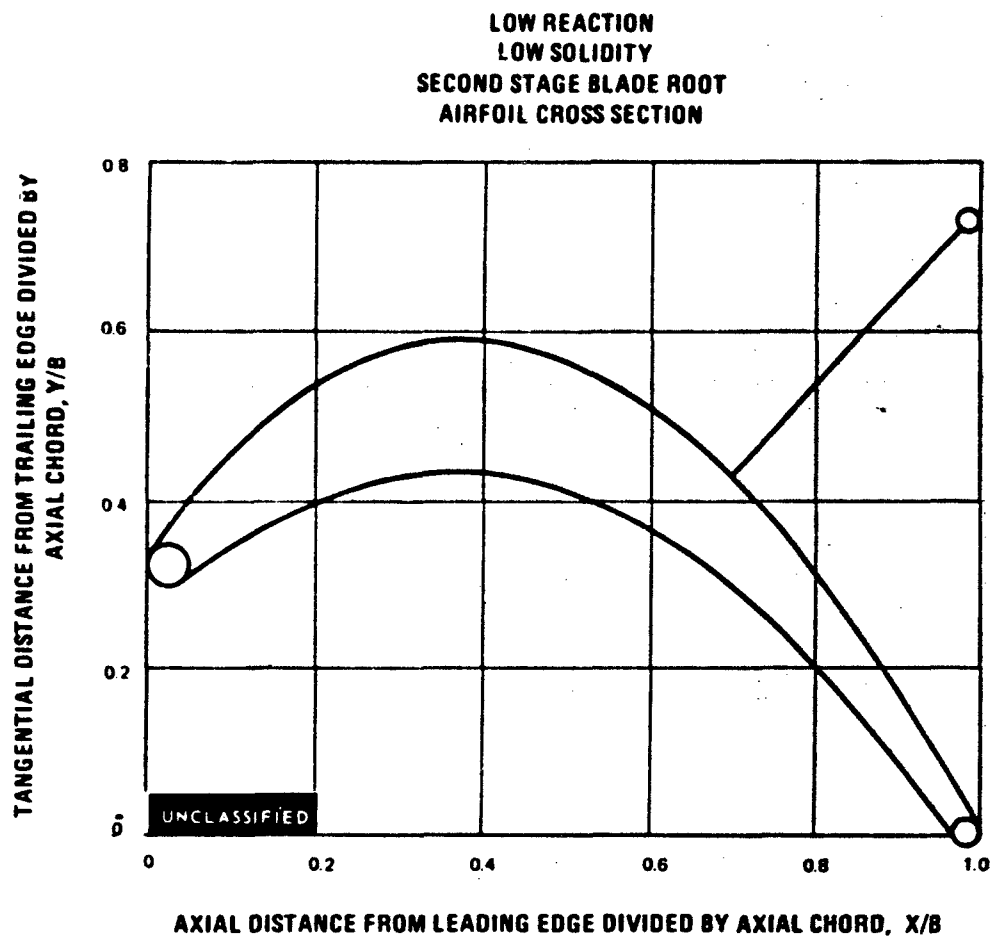


Figure 121

UNCLASSIFIED

UNCLASSIFIED

LOW REACTION
LOW SOLIDITY
SECOND STAGE BLADE ROOT

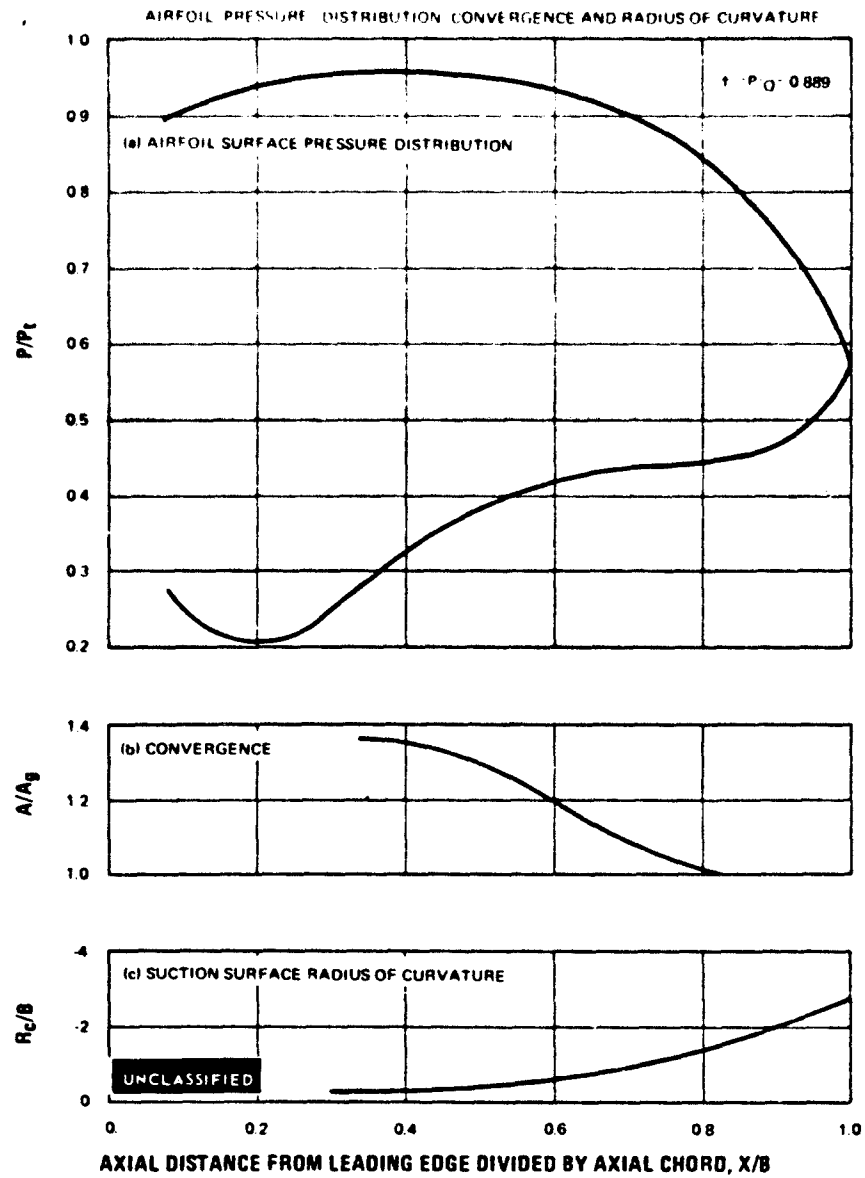


Figure 122

UNCLASSIFIED

UNCLASSIFIED

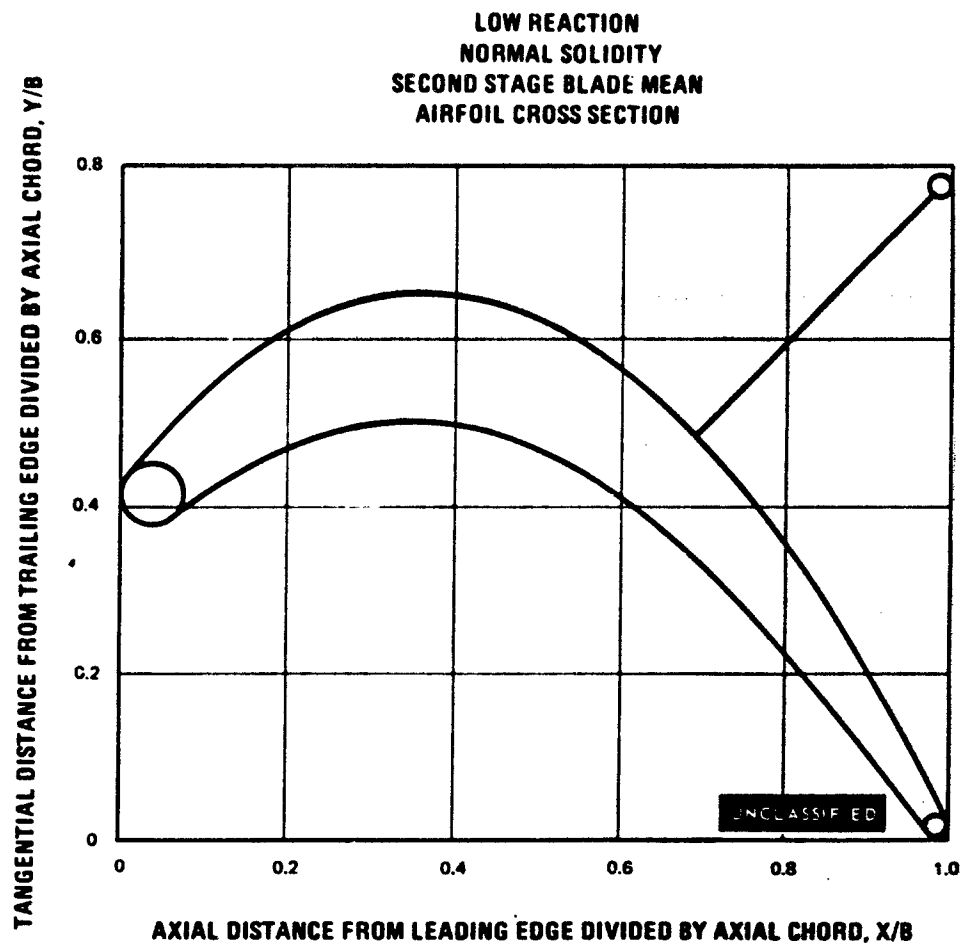


Figure 123

UNCLASSIFIED

UNCLASSIFIED

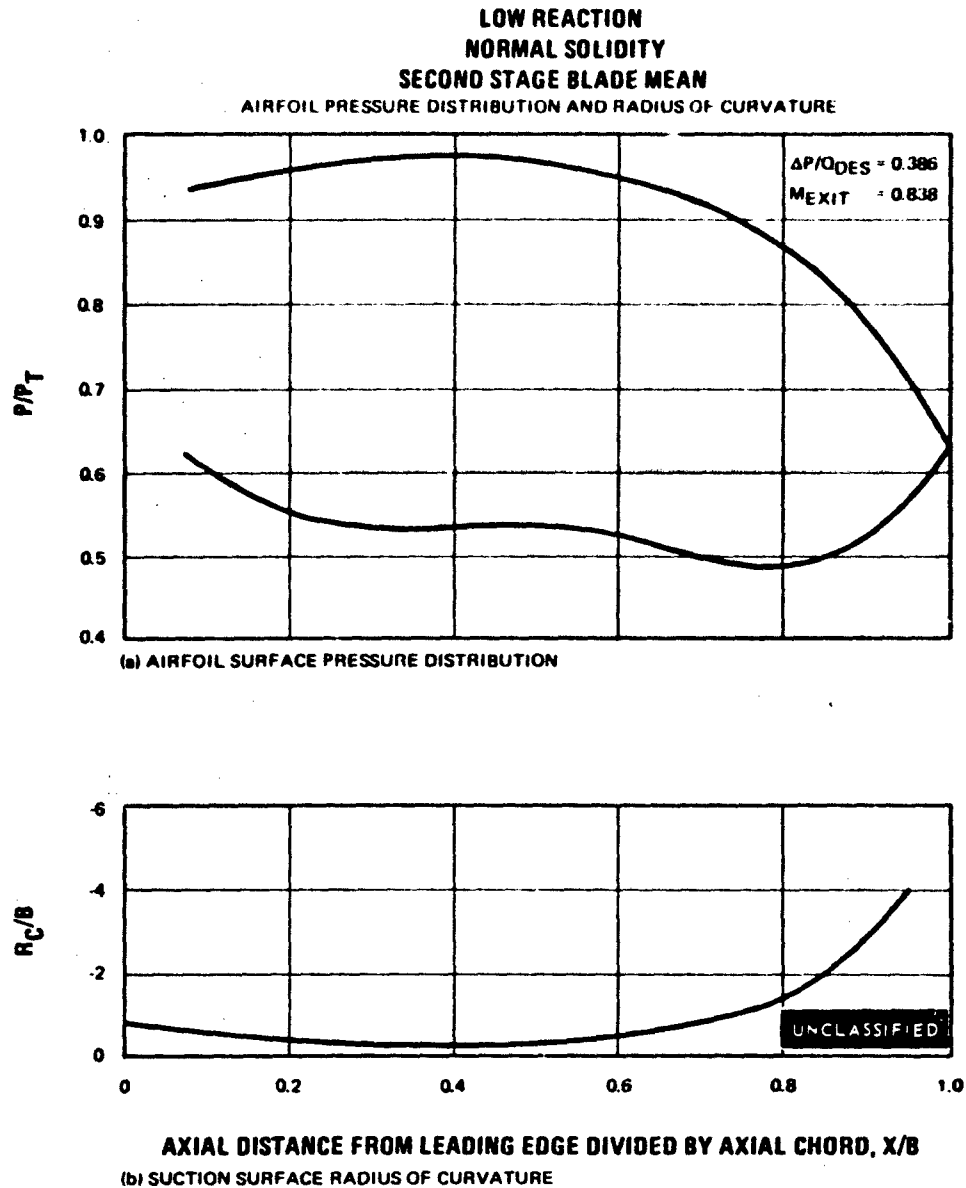


Figure 124

UNCLASSIFIED

UNCLASSIFIED

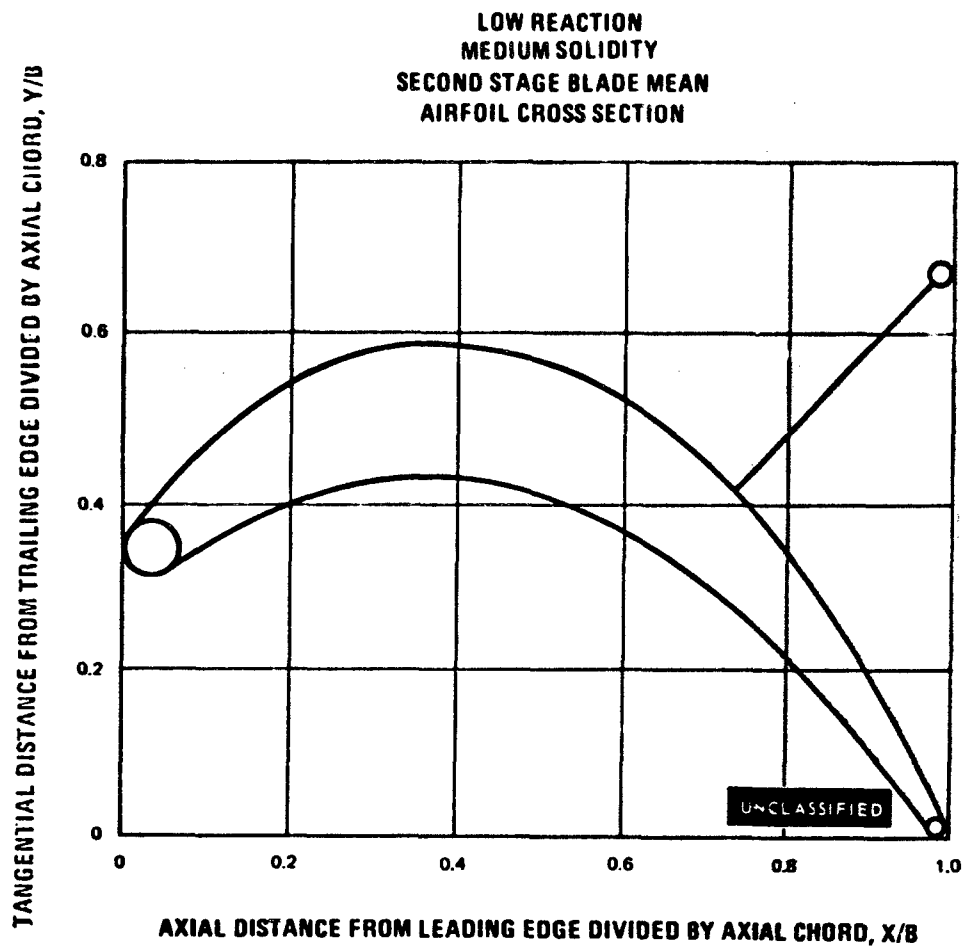


Figure 125

UNCLASSIFIED

UNCLASSIFIED

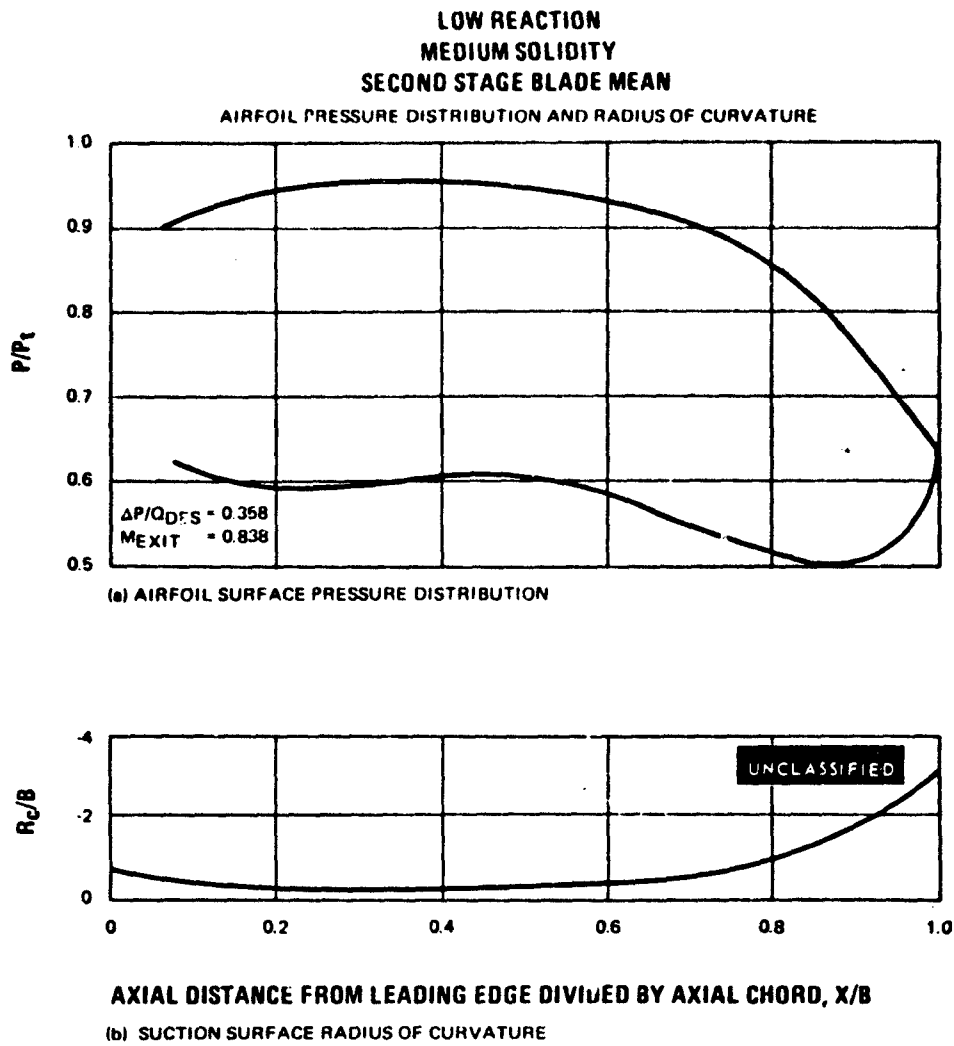


Figure 126

UNCLASSIFIED

UNCLASSIFIED

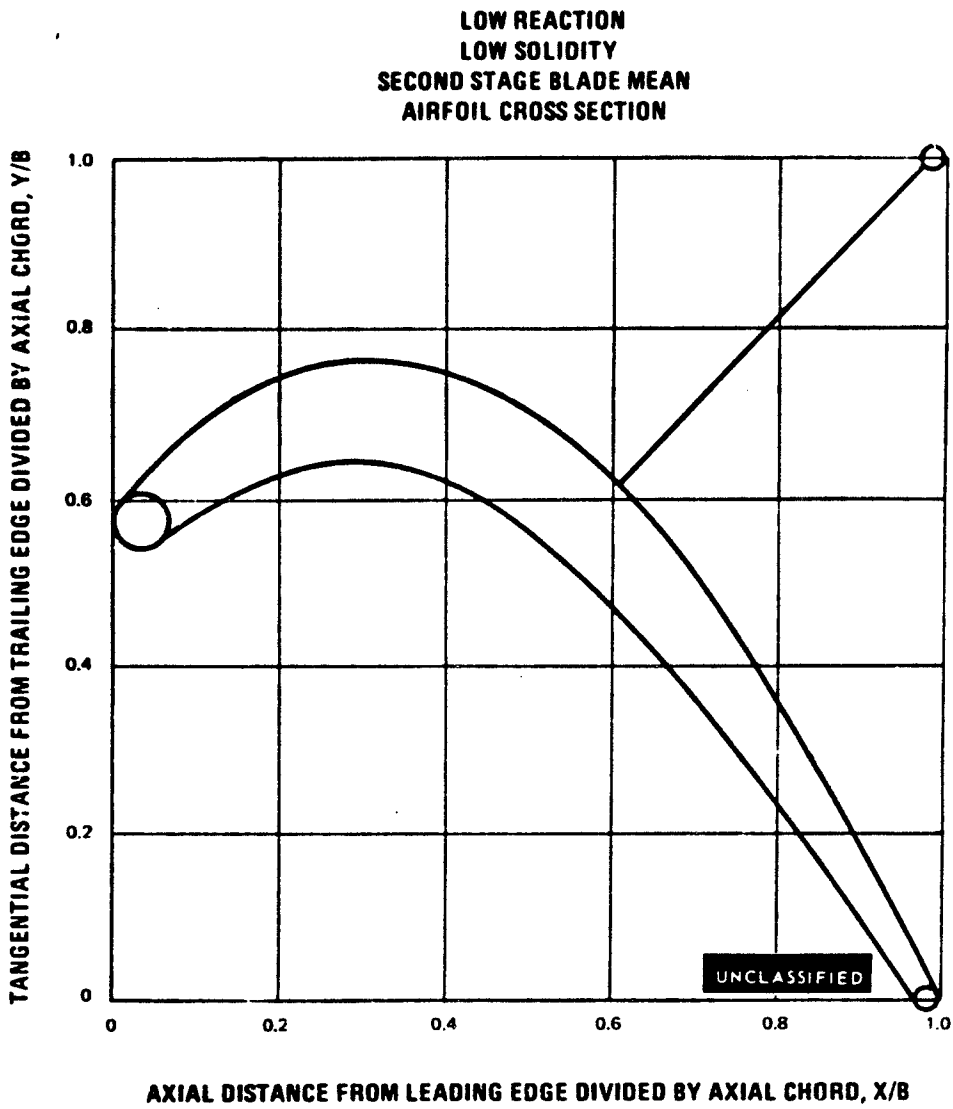


Figure 127

UNCLASSIFIED

UNCLASSIFIED

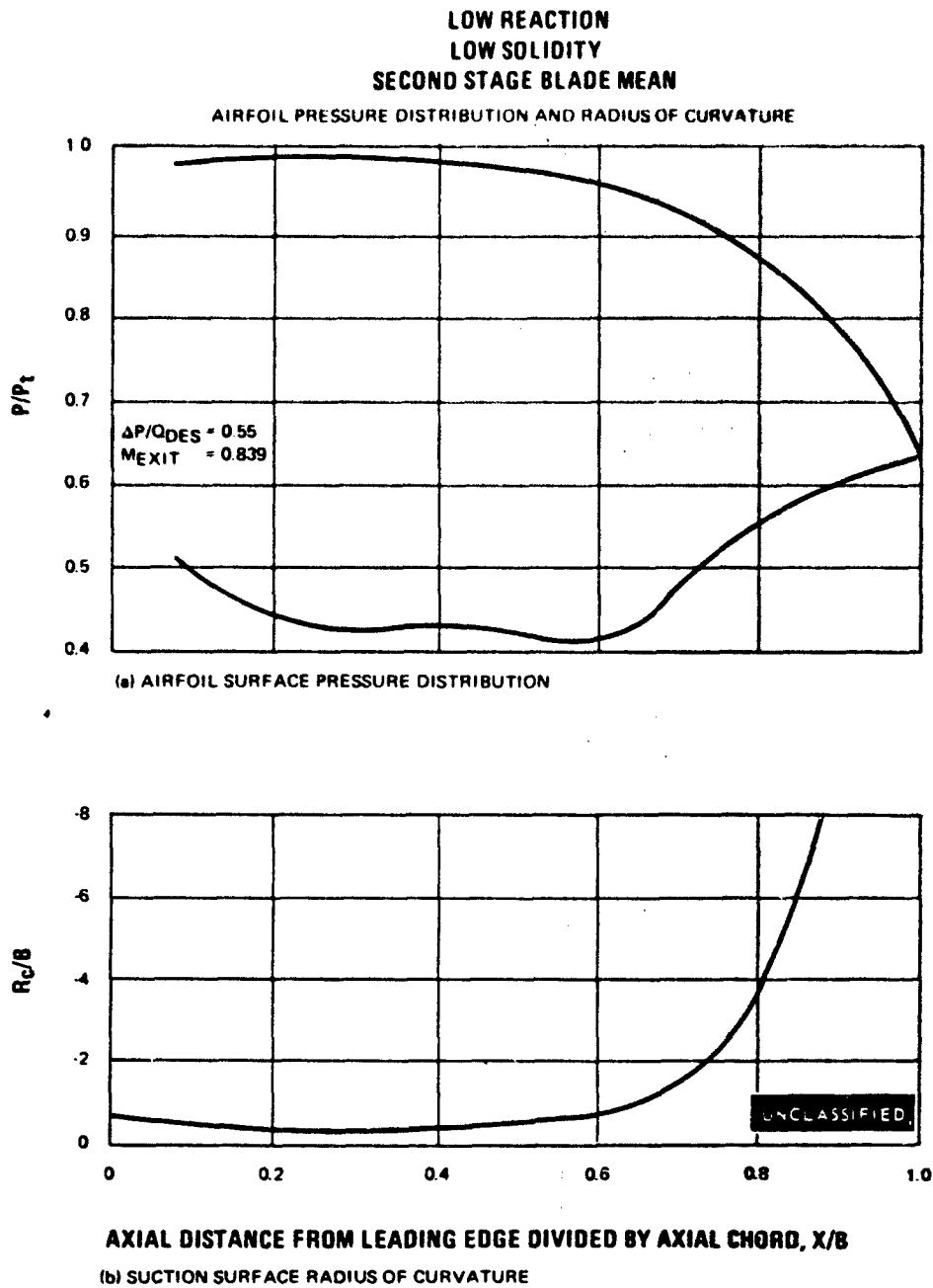


Figure 128

UNCLASSIFIED

UNCLASSIFIED

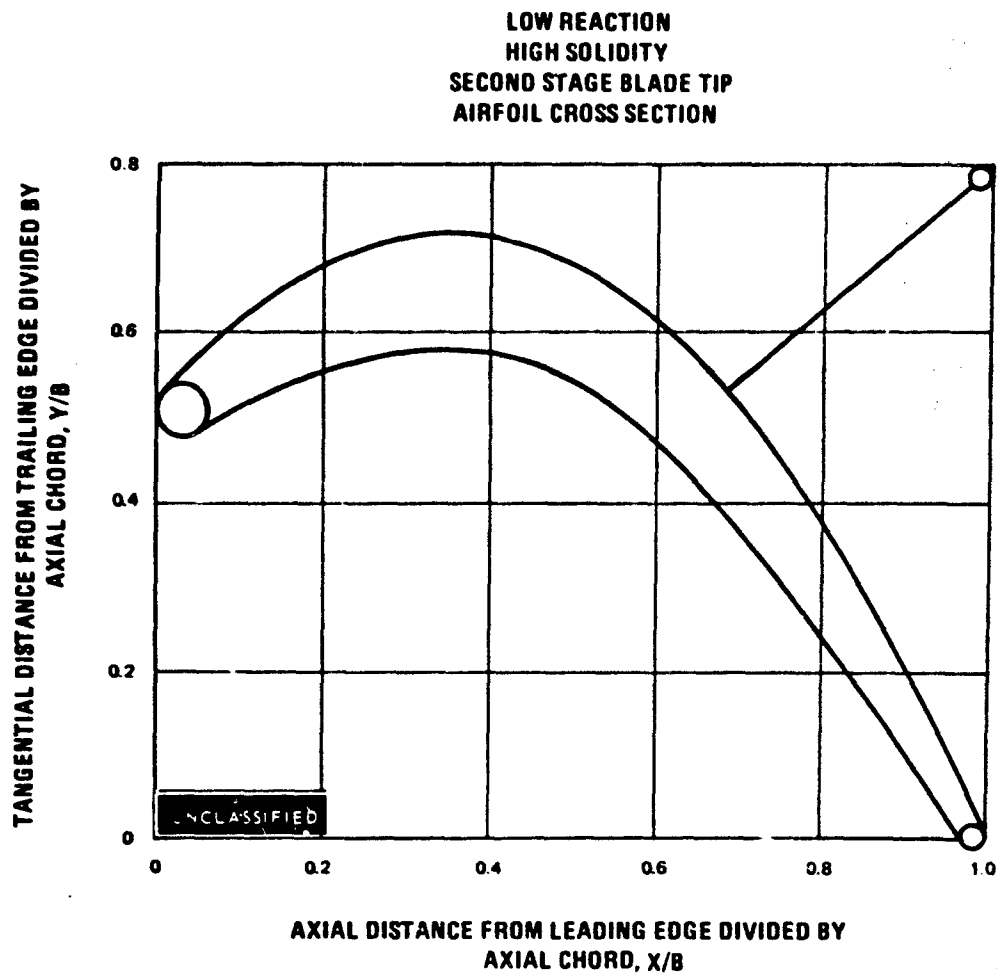


Figure 129

UNCLASSIFIED

UNCLASSIFIED

LOW REACTION
HIGH SOLIDITY
SECOND STAGE BLADE TIP

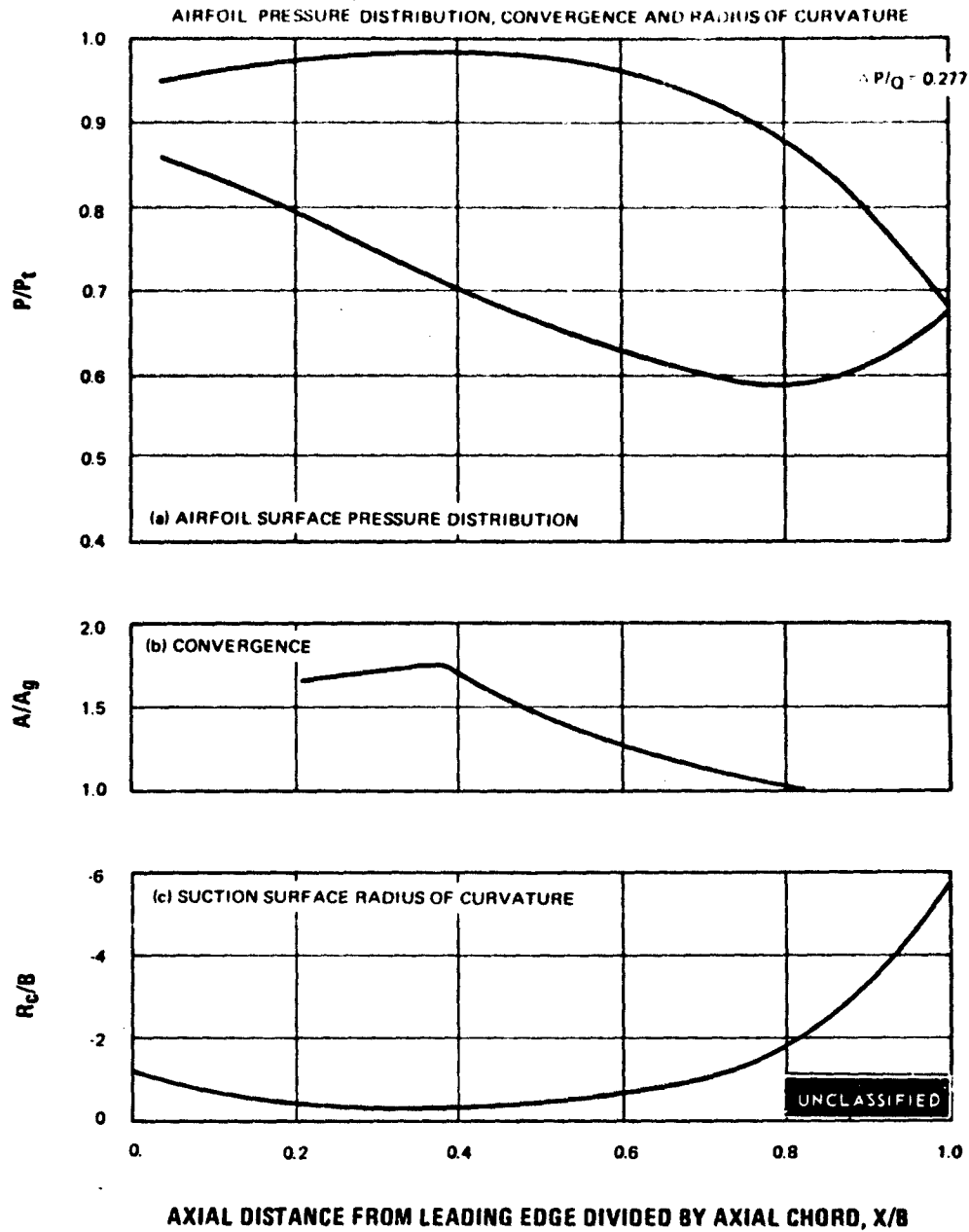


Figure 130

UNCLASSIFIED

UNCLASSIFIED

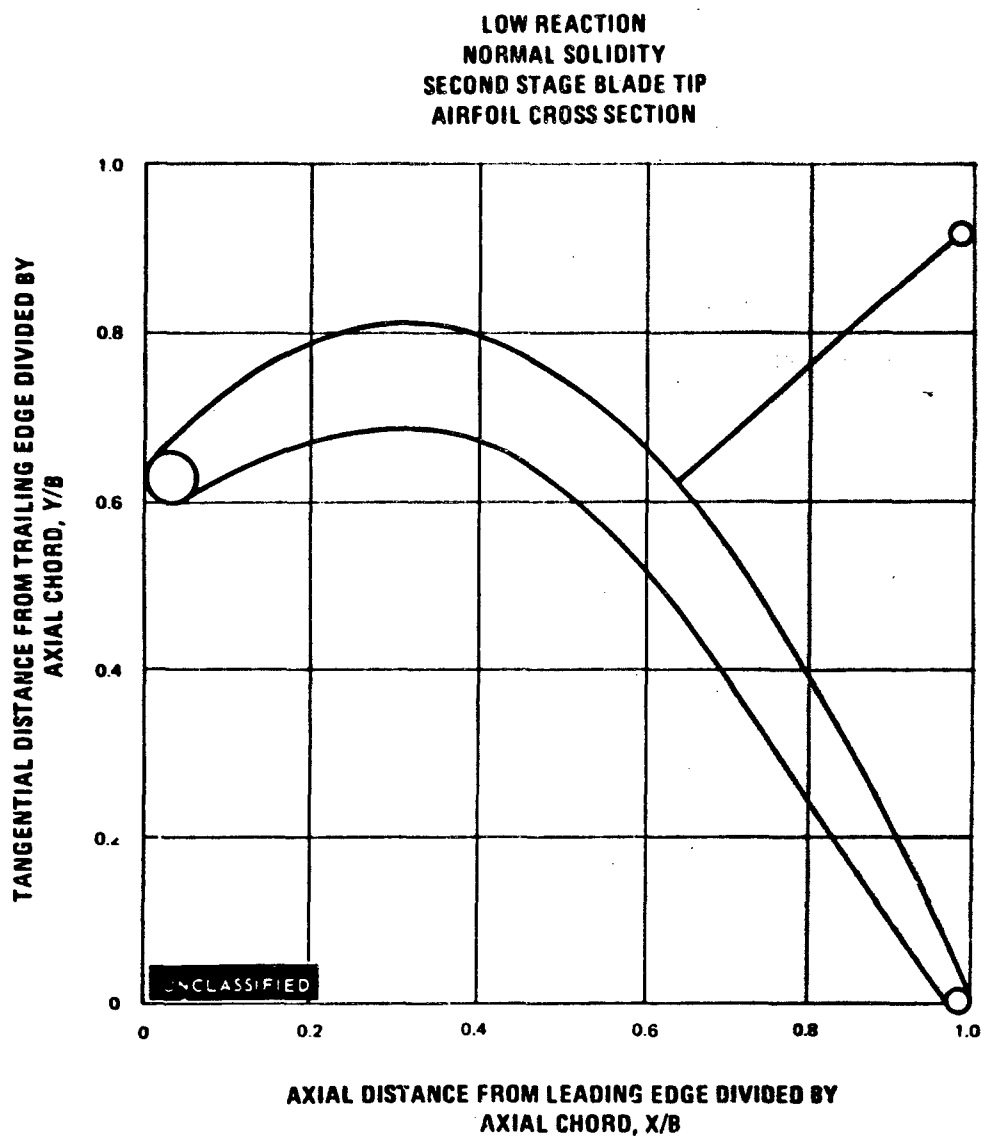


Figure 131

UNCLASSIFIED

UNCLASSIFIED

LOW REACTION
NORMAL SOLIDITY
SECOND STAGE BLADE TIP

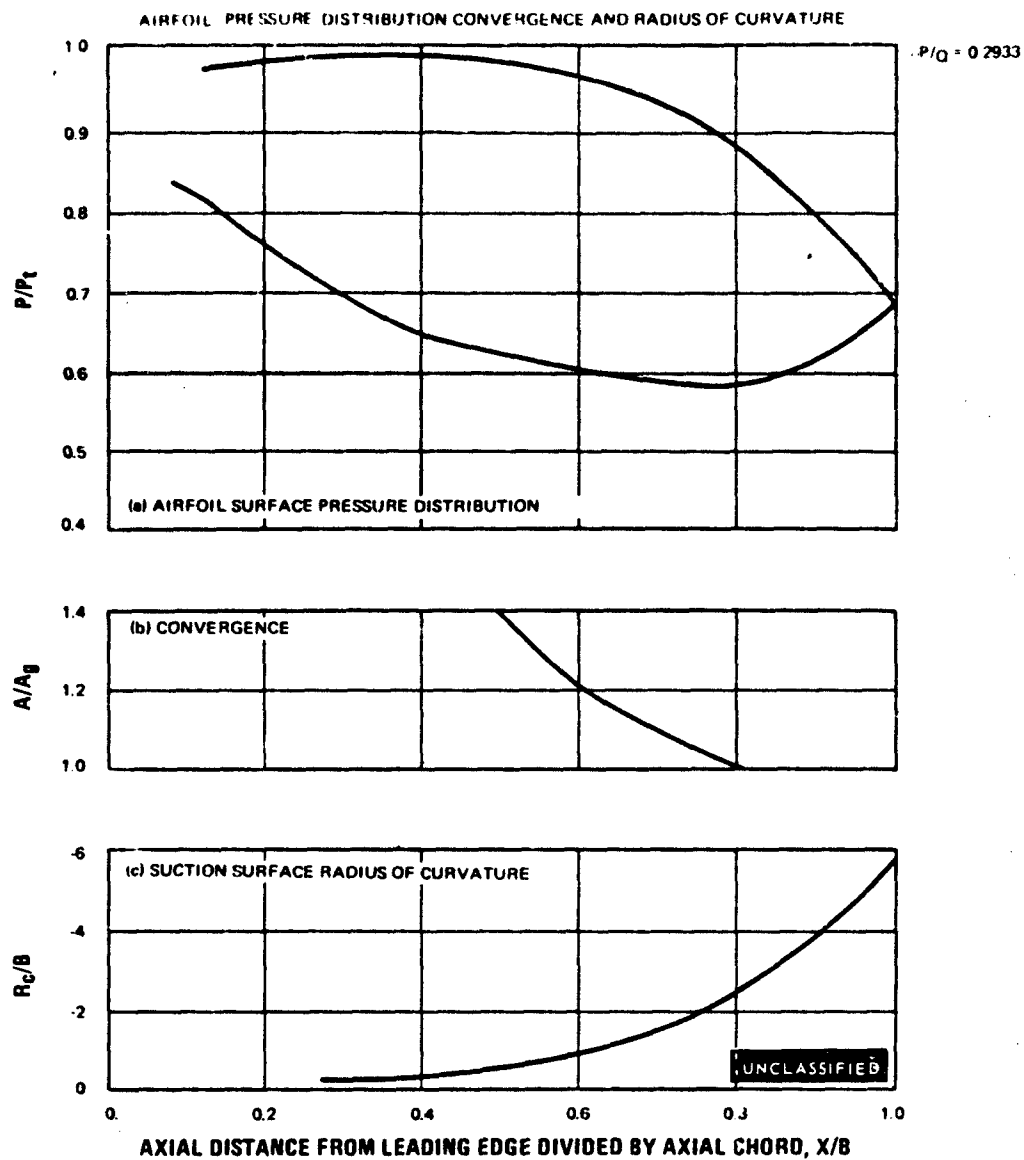


Figure 132

UNCLASSIFIED

UNCLASSIFIED

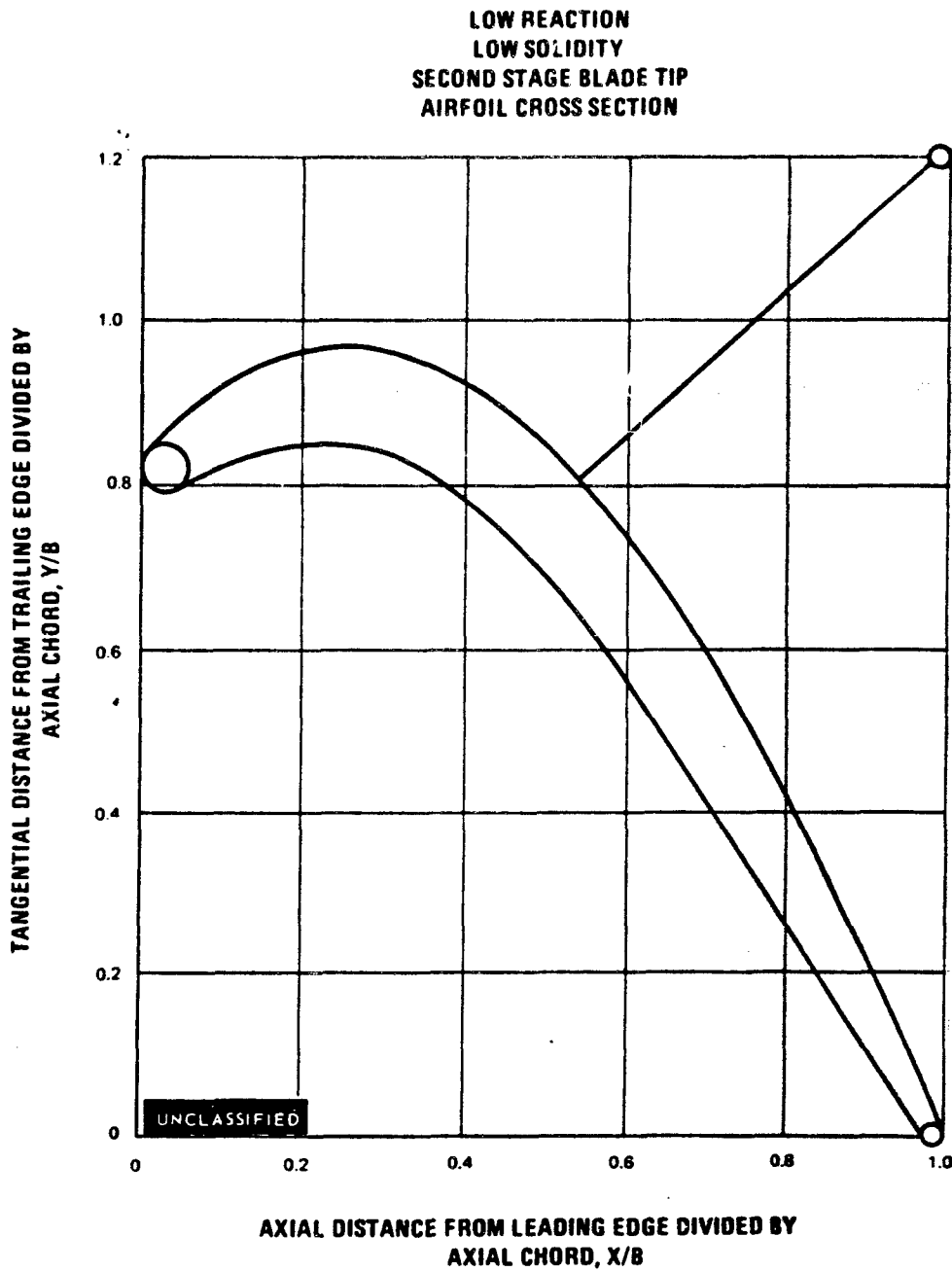


Figure 133

PAGE NO. 170

UNCLASSIFIED

UNCLASSIFIED

LOW REACTION
LOW SOLIDITY
SECOND STAGE BLADE TIP

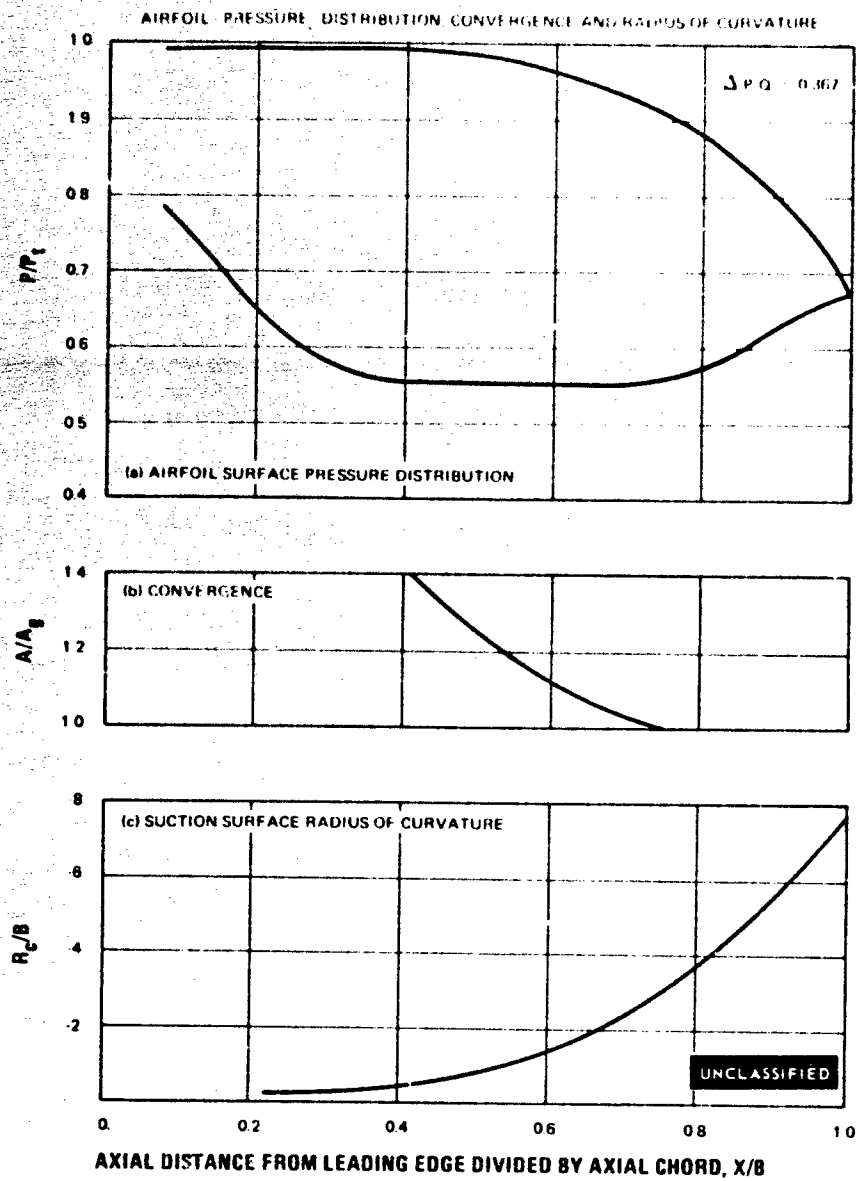


Figure 134

UNCLASSIFIED

UNCLASSIFIED

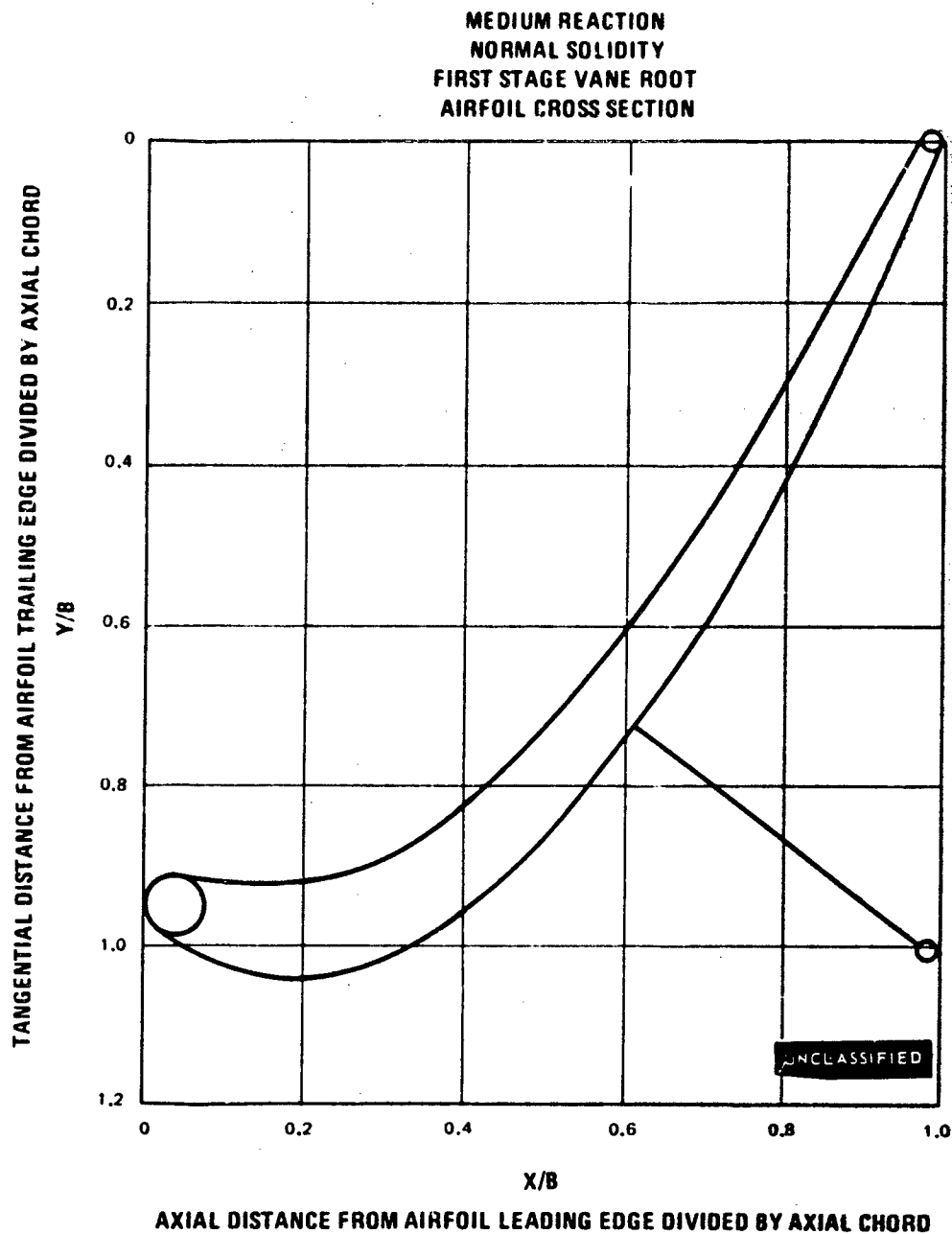


Figure 135

UNCLASSIFIED

UNCLASSIFIED

MEDIUM REACTION
NORMAL SOLIDITY
FIRST STAGE VANE ROOT

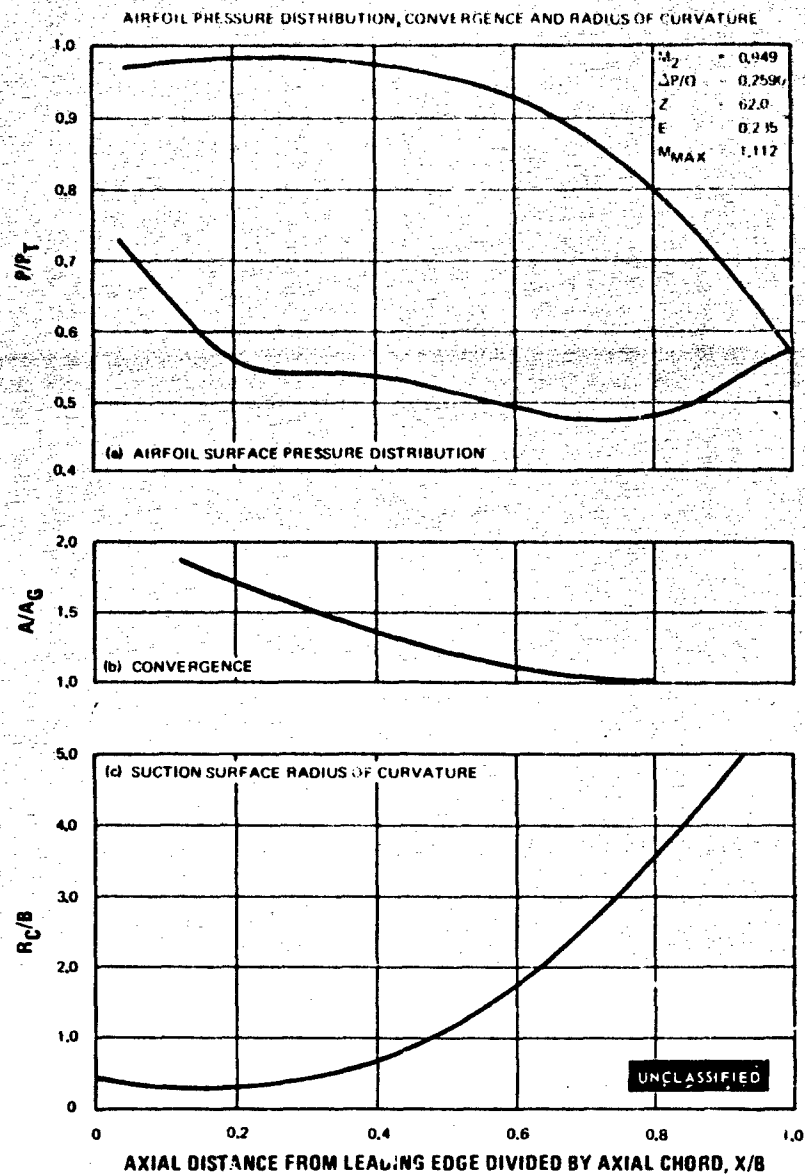


Figure 136

UNCLASSIFIED

UNCLASSIFIED

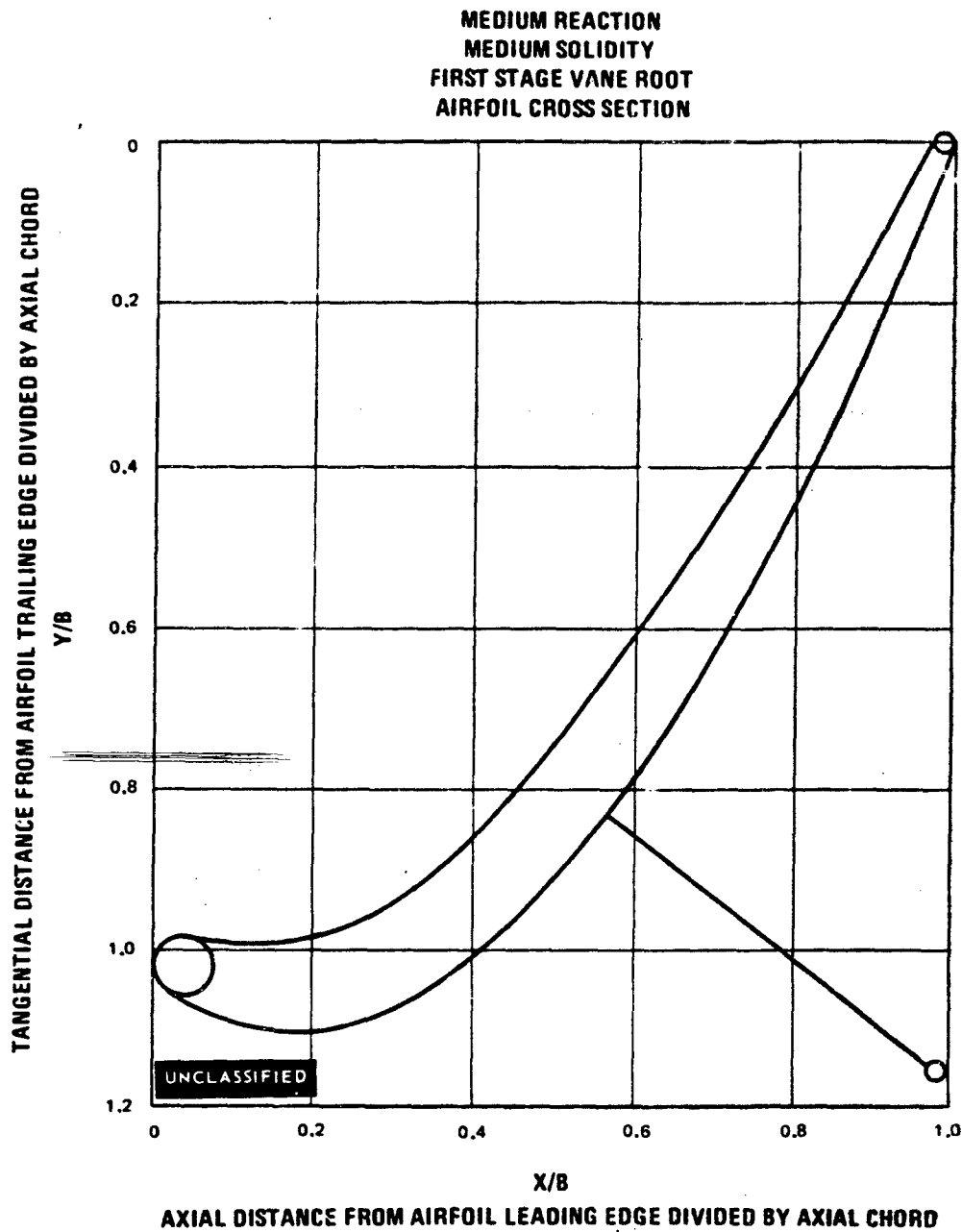


Figure 137

UNCLASSIFIED

UNCLASSIFIED

MEDIUM REACTION
MEDIUM SOLIDITY
FIRST STAGE VANE ROOT

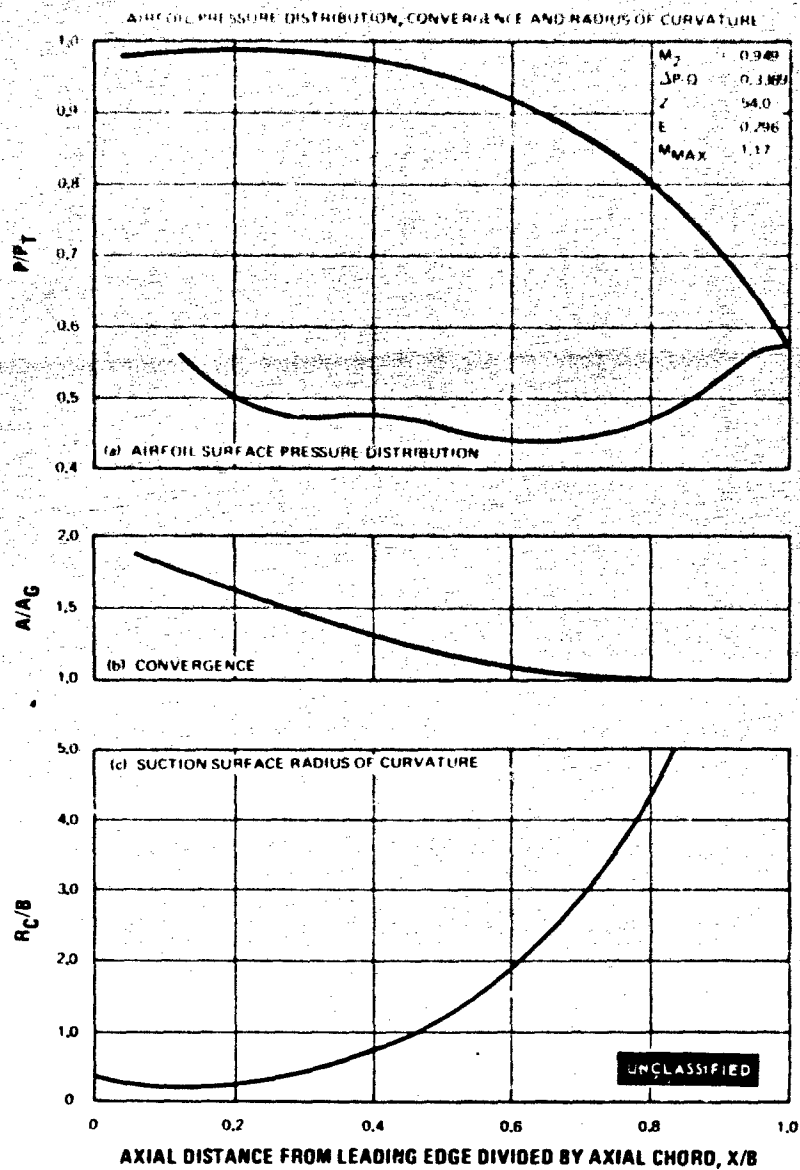


Figure 138

UNCLASSIFIED

UNCLASSIFIED

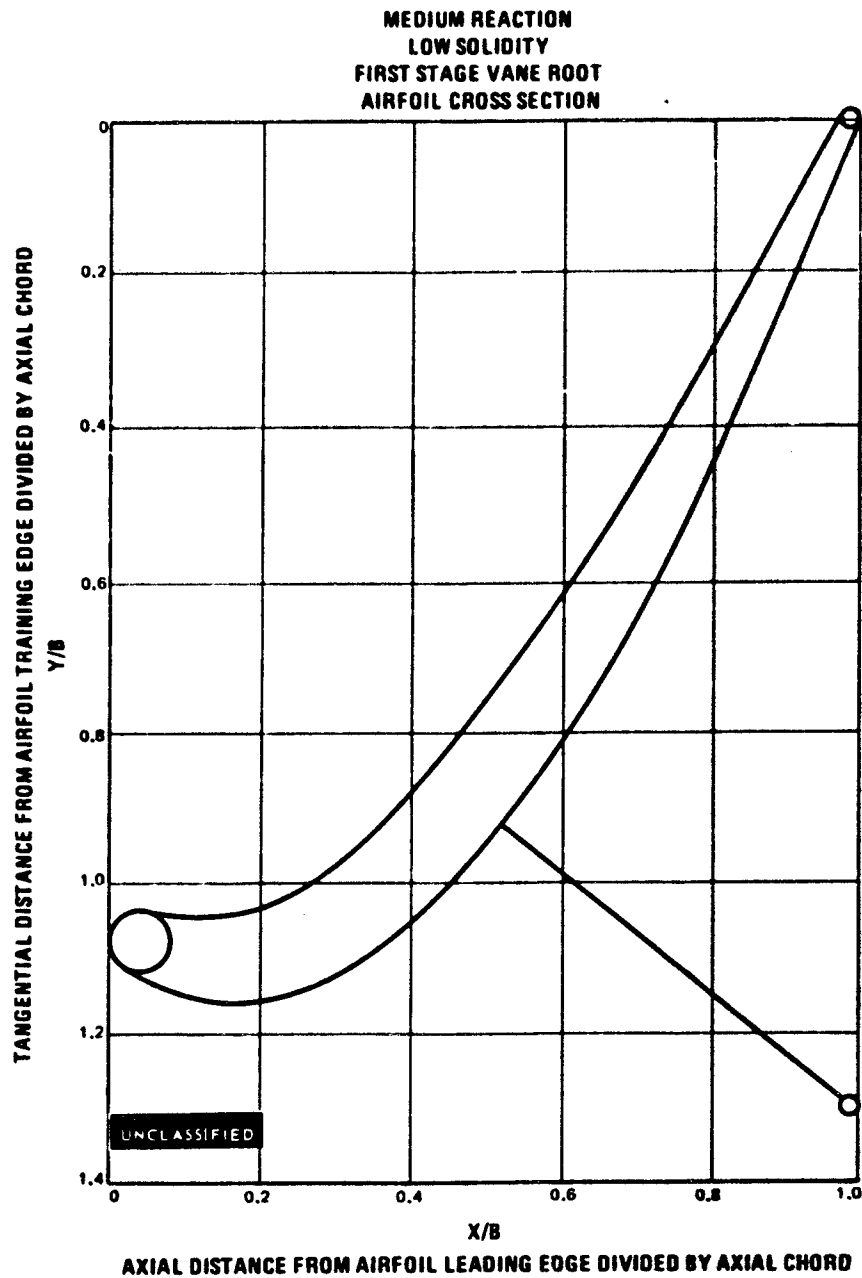


Figure 139

UNCLASSIFIED

UNCLASSIFIED

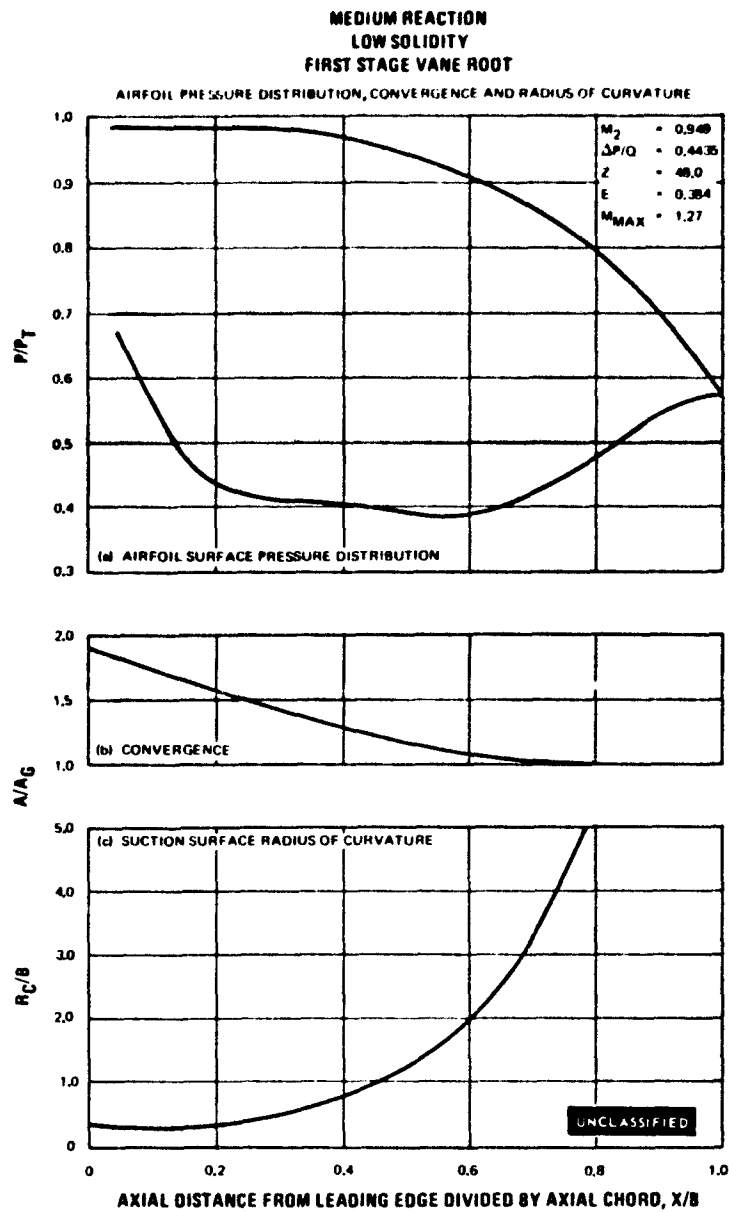


Figure 140

UNCLASSIFIED

UNCLASSIFIED

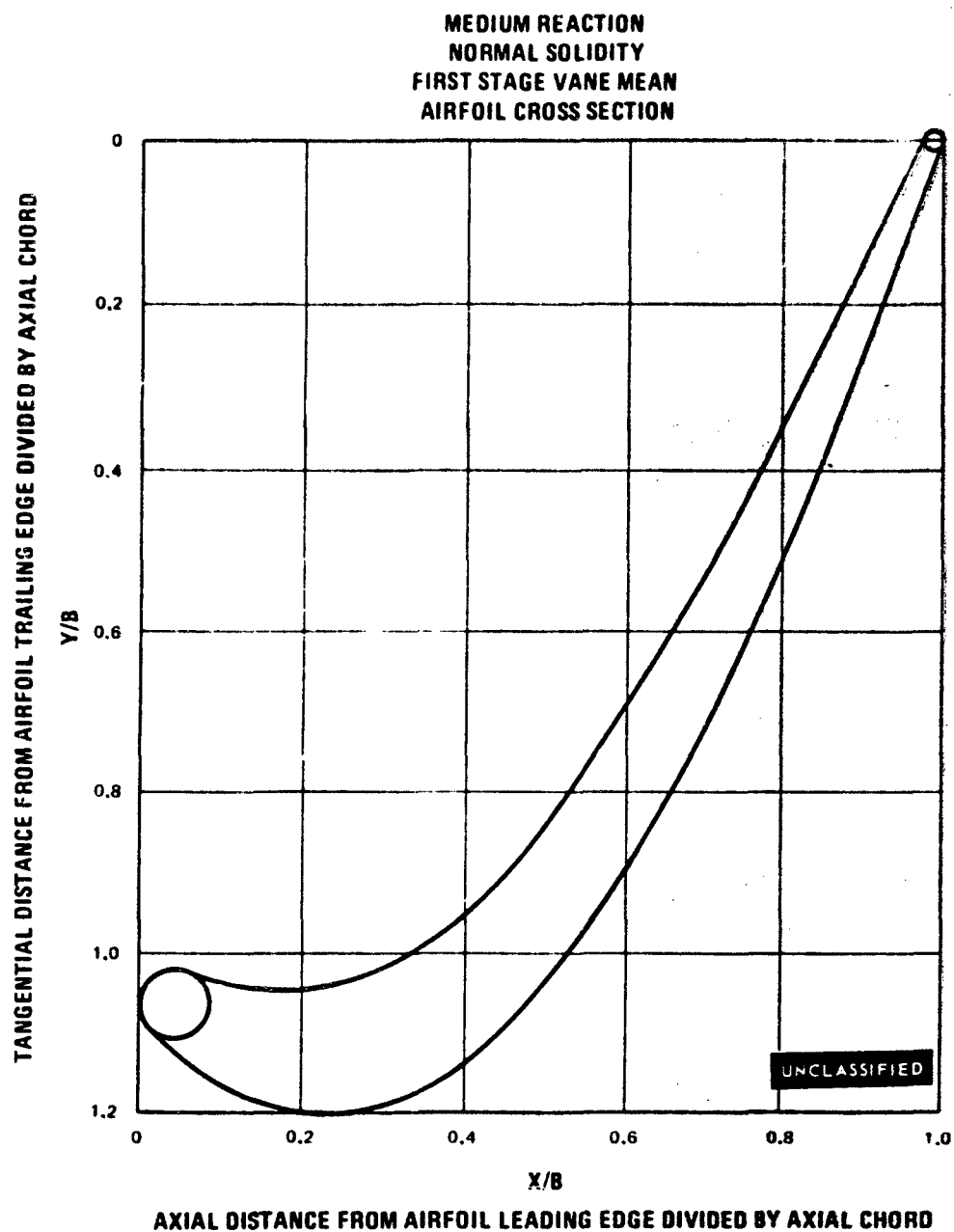


Figure 141

UNCLASSIFIED

UNCLASSIFIED

MEDIUM REACTION
NORMAL SOLIDITY
FIRST STAGE VANE MEAN

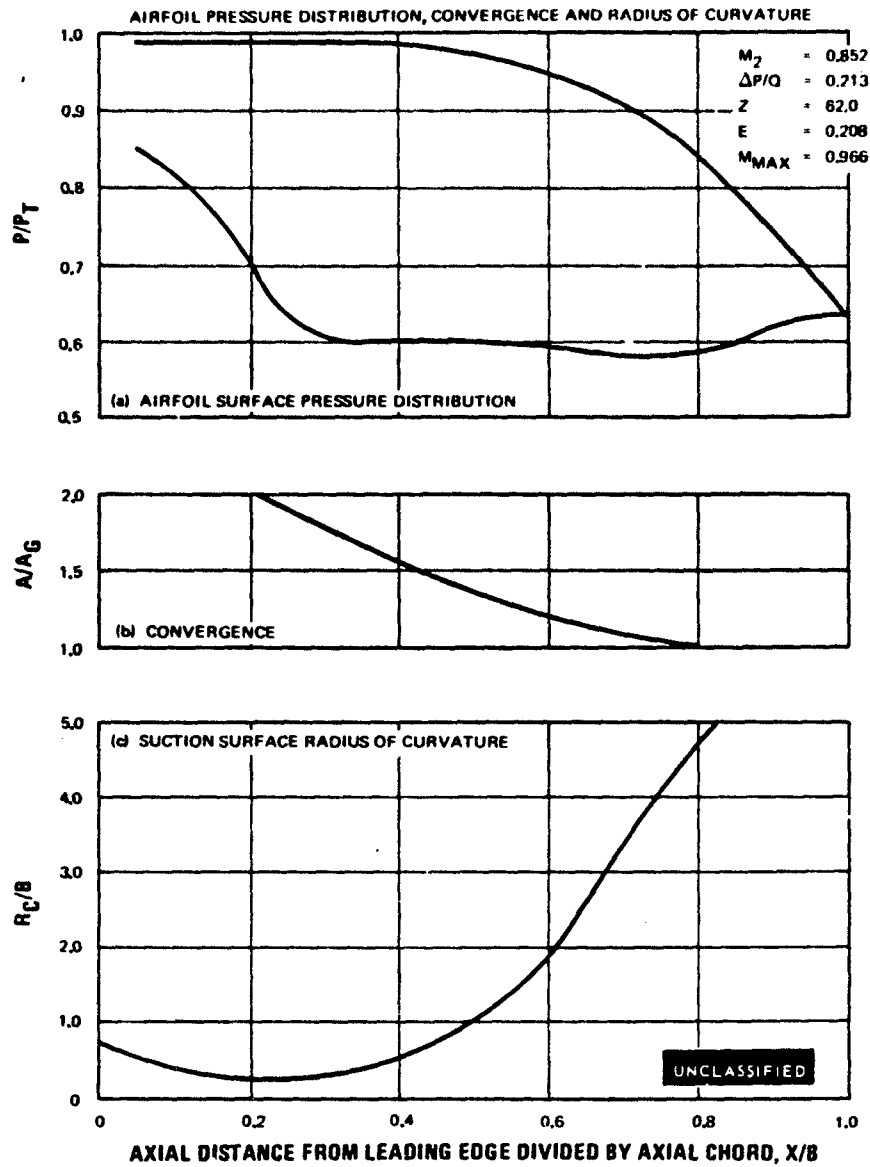


Figure 142

UNCLASSIFIED

UNCLASSIFIED

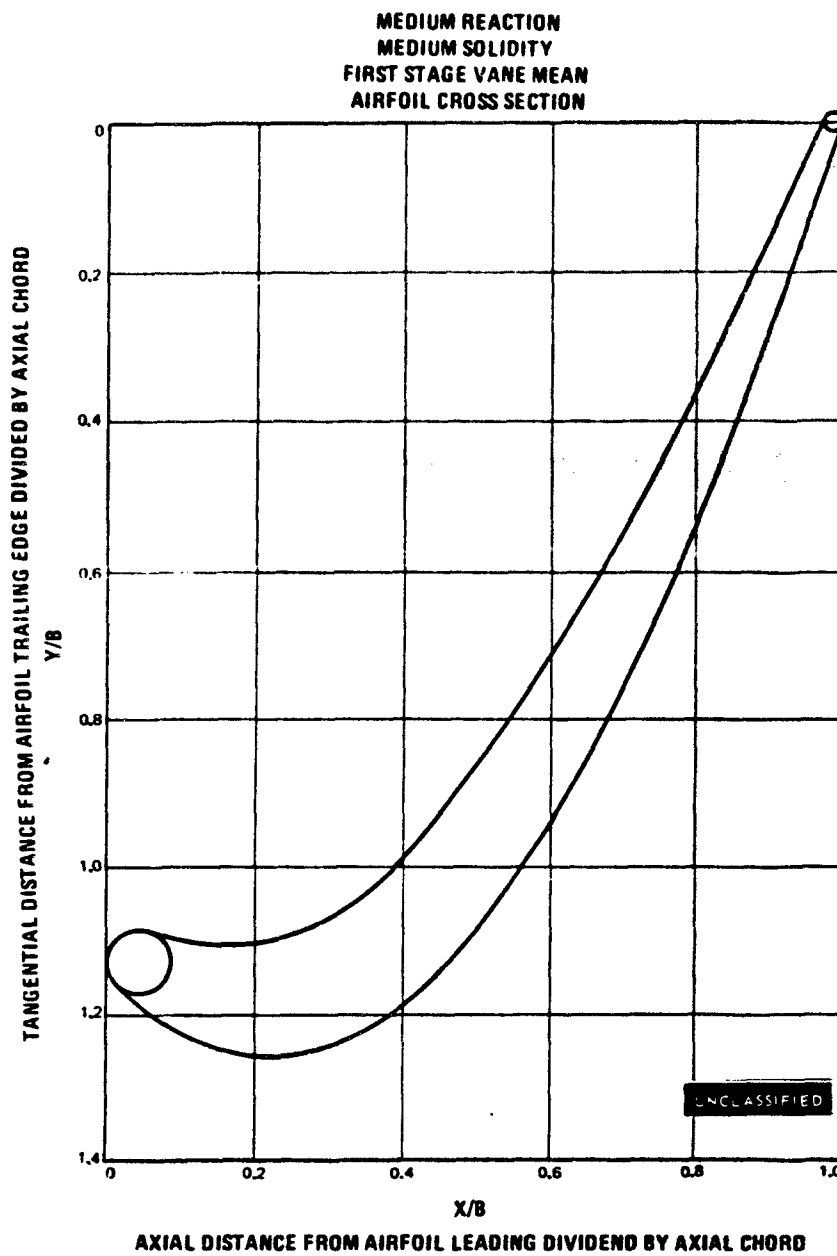


Figure 143

UNCLASSIFIED

UNCLASSIFIED

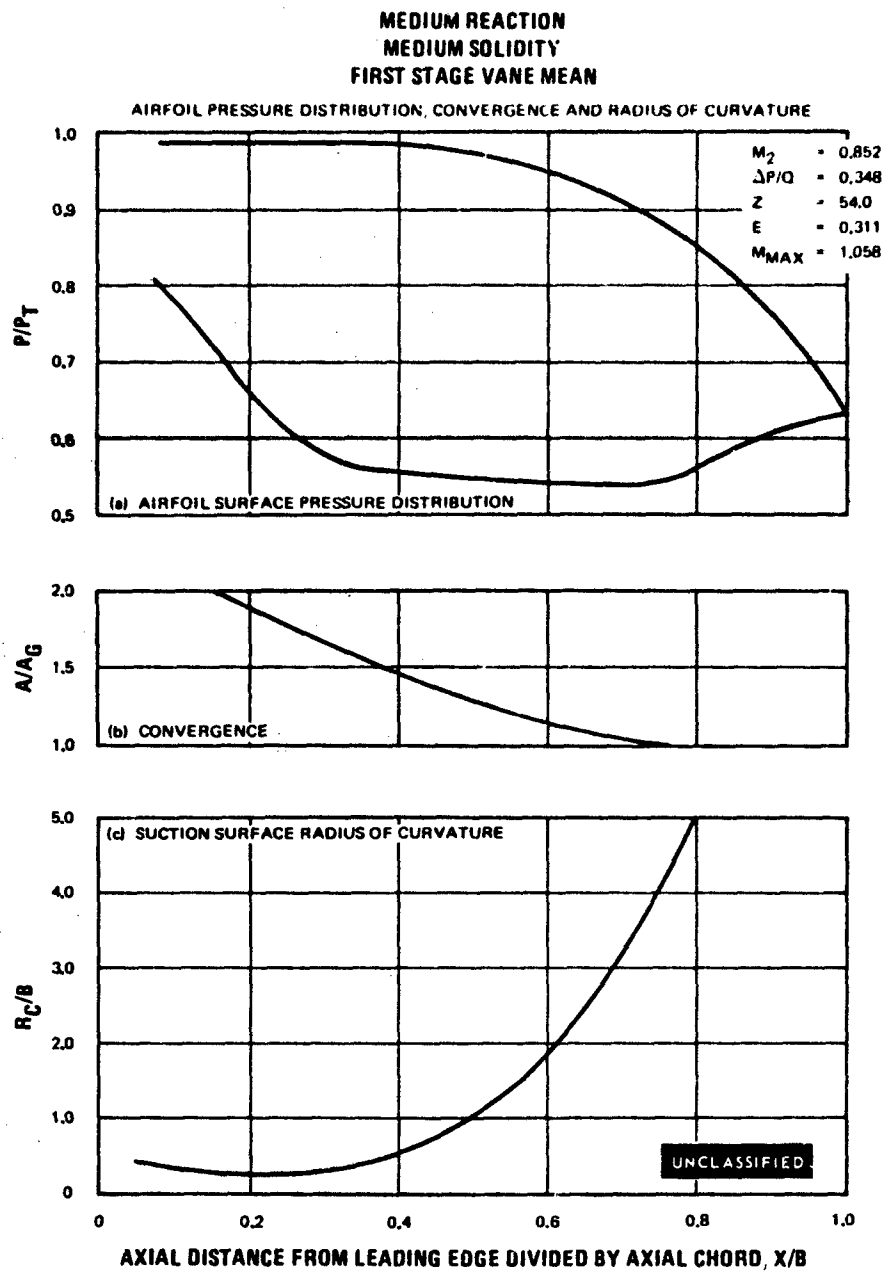


Figure 144

UNCLASSIFIED

UNCLASSIFIED

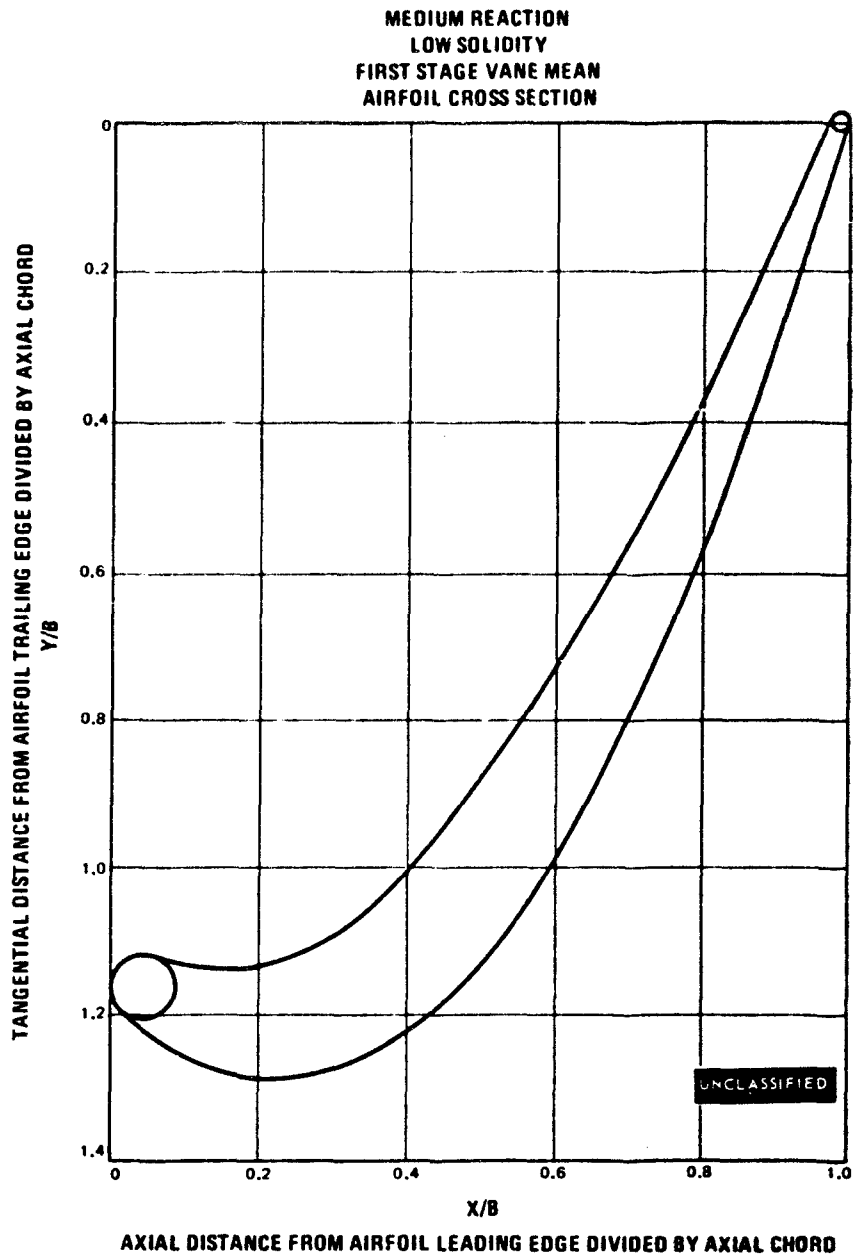


Figure 145

UNCLASSIFIED

UNCLASSIFIED

MEDIUM REACTION
LOW SOLIDITY
FIRST STAGE VANE MEAN

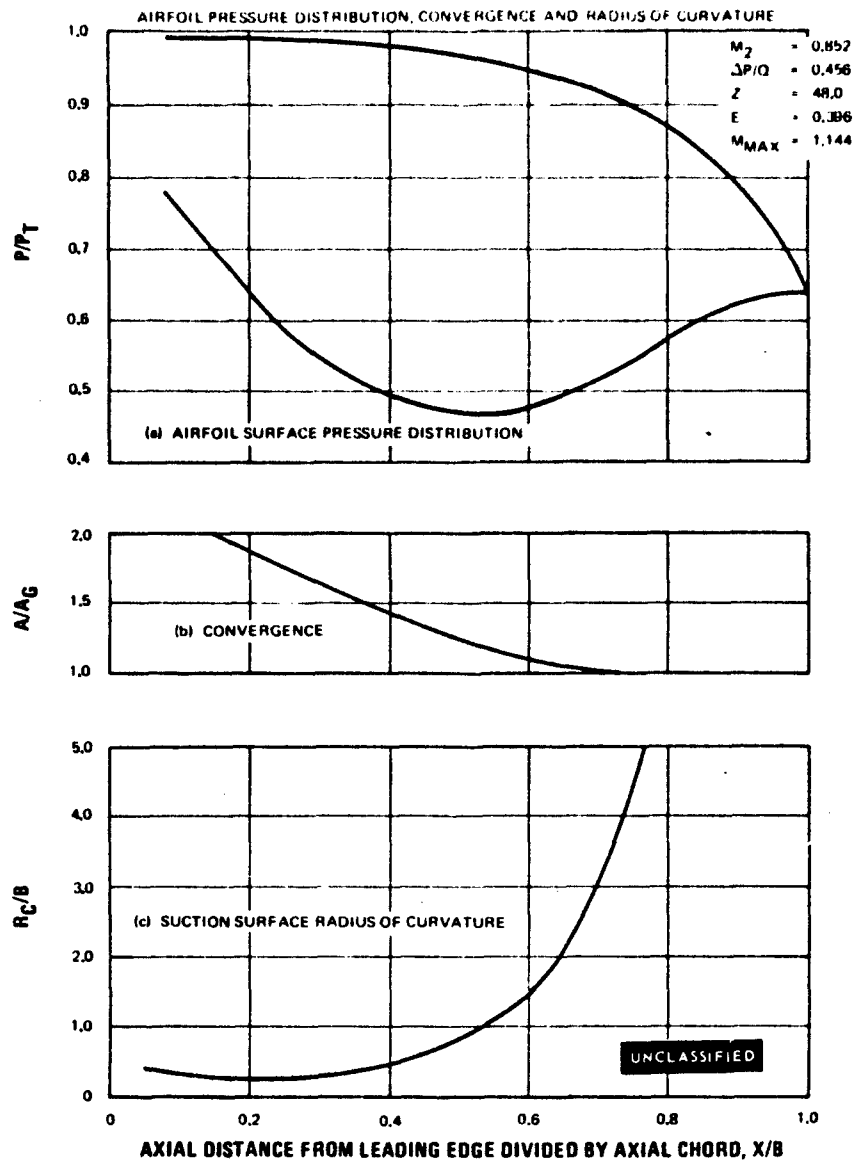


Figure 146

UNCLASSIFIED

UNCLASSIFIED

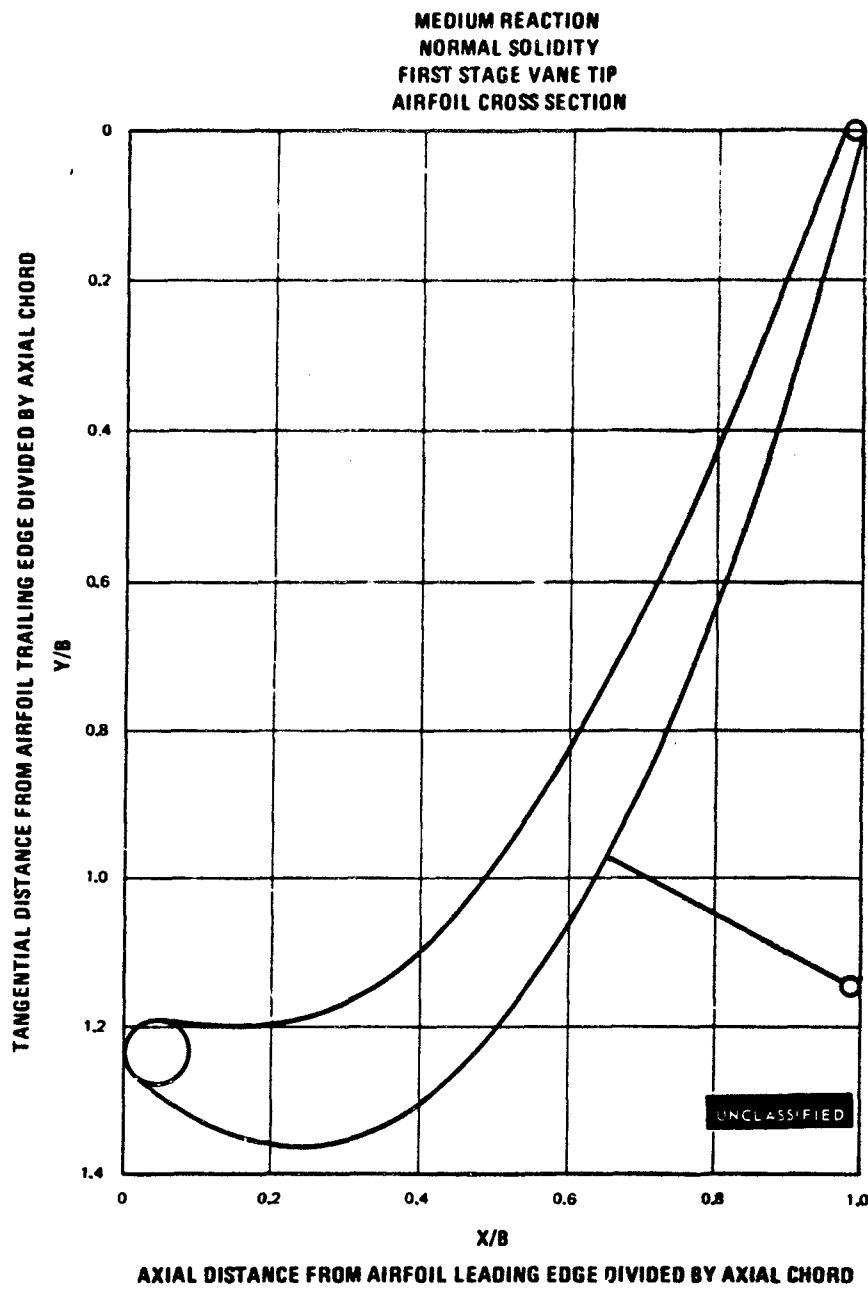


Figure 147

UNCLASSIFIED

UNCLASSIFIED

MEDIUM REACTION
NORMAL SOLIDITY
FIRST STAGE VANE TIP

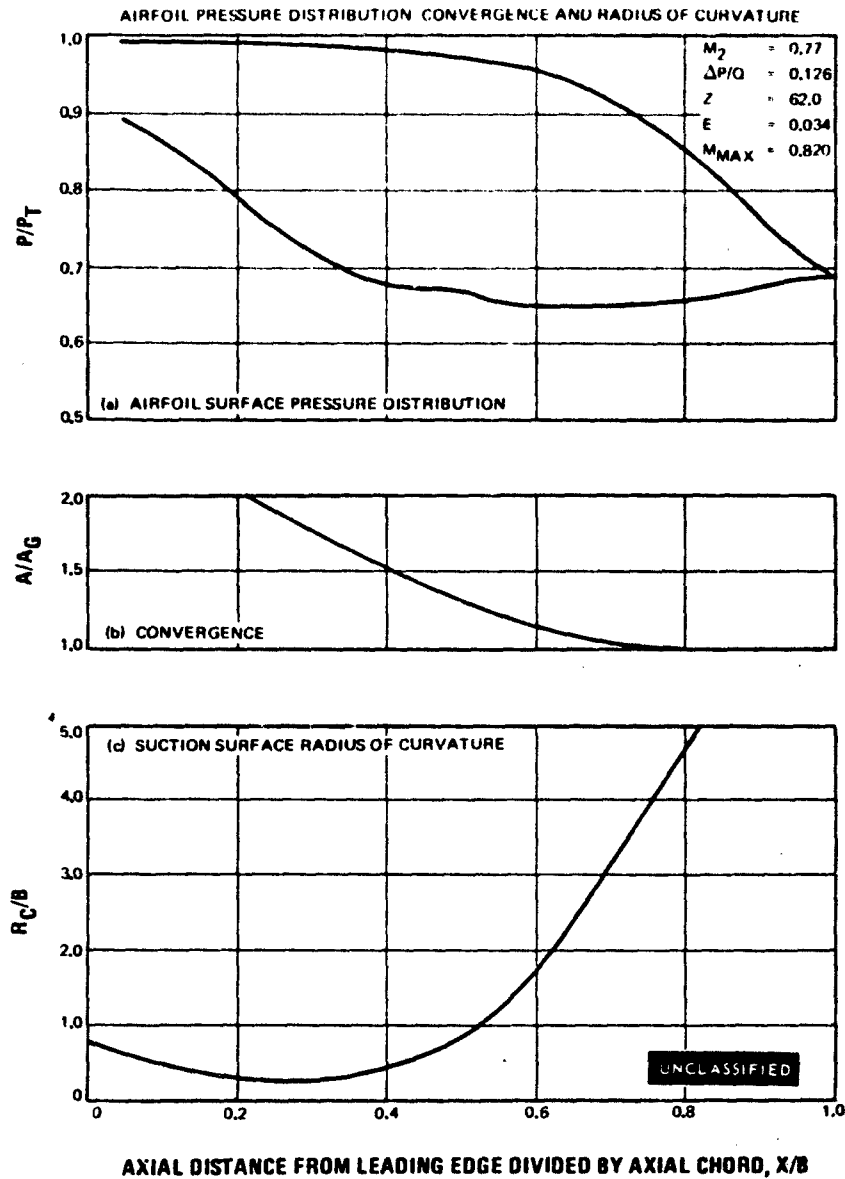


Figure 148

UNCLASSIFIED

UNCLASSIFIED

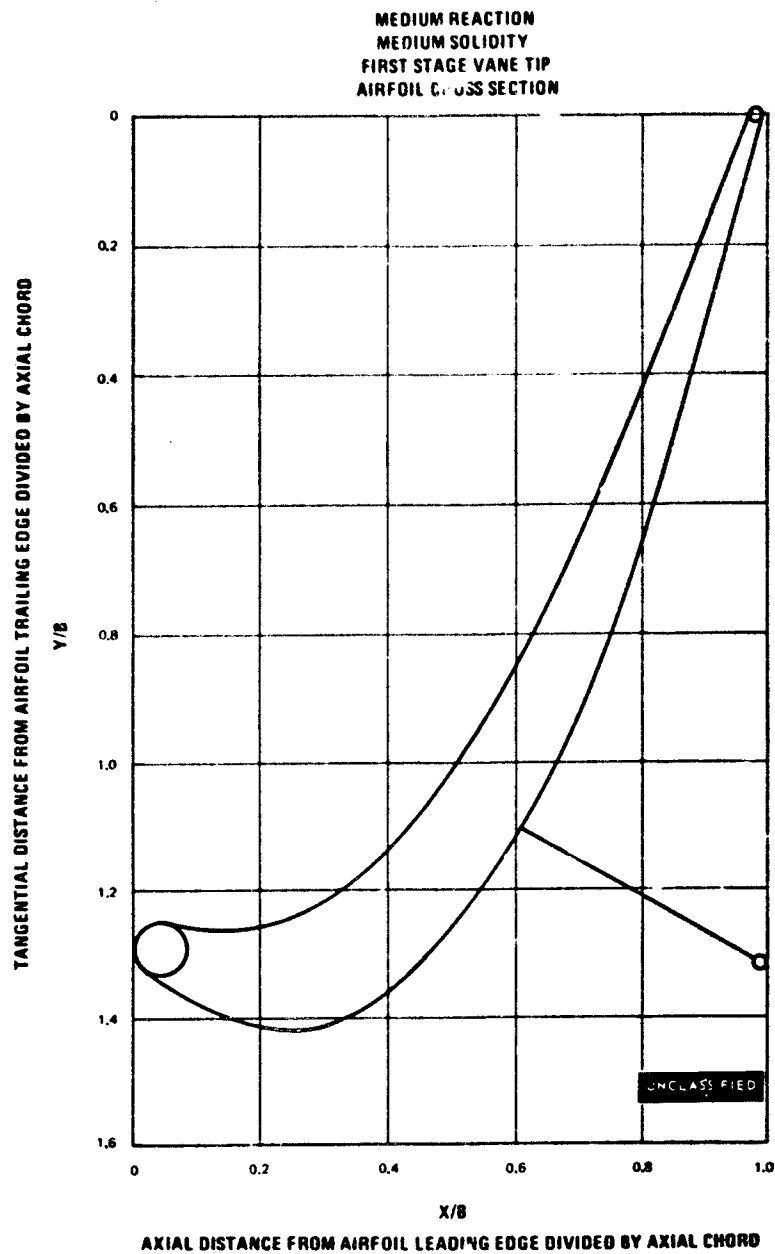


Figure 149

UNCLASSIFIED

UNCLASSIFIED

MEDIUM REACTION
MEDIUM SOLIDITY
FIRST STAGE VANE TIP

AIRFOIL PRESSURE DISTRIBUTION CONVERGENCE AND RADIUS OF CURVATURE

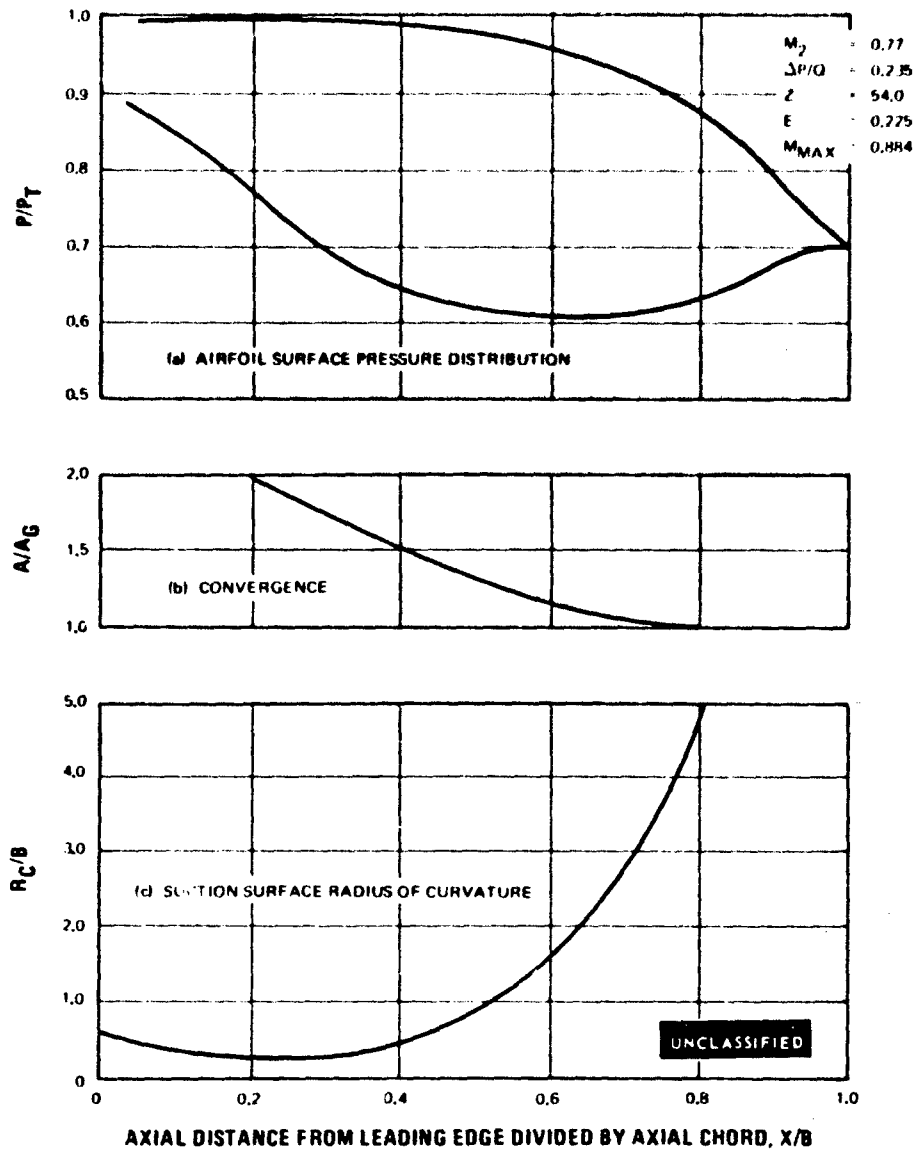


Figure 150

UNCLASSIFIED

UNCLASSIFIED

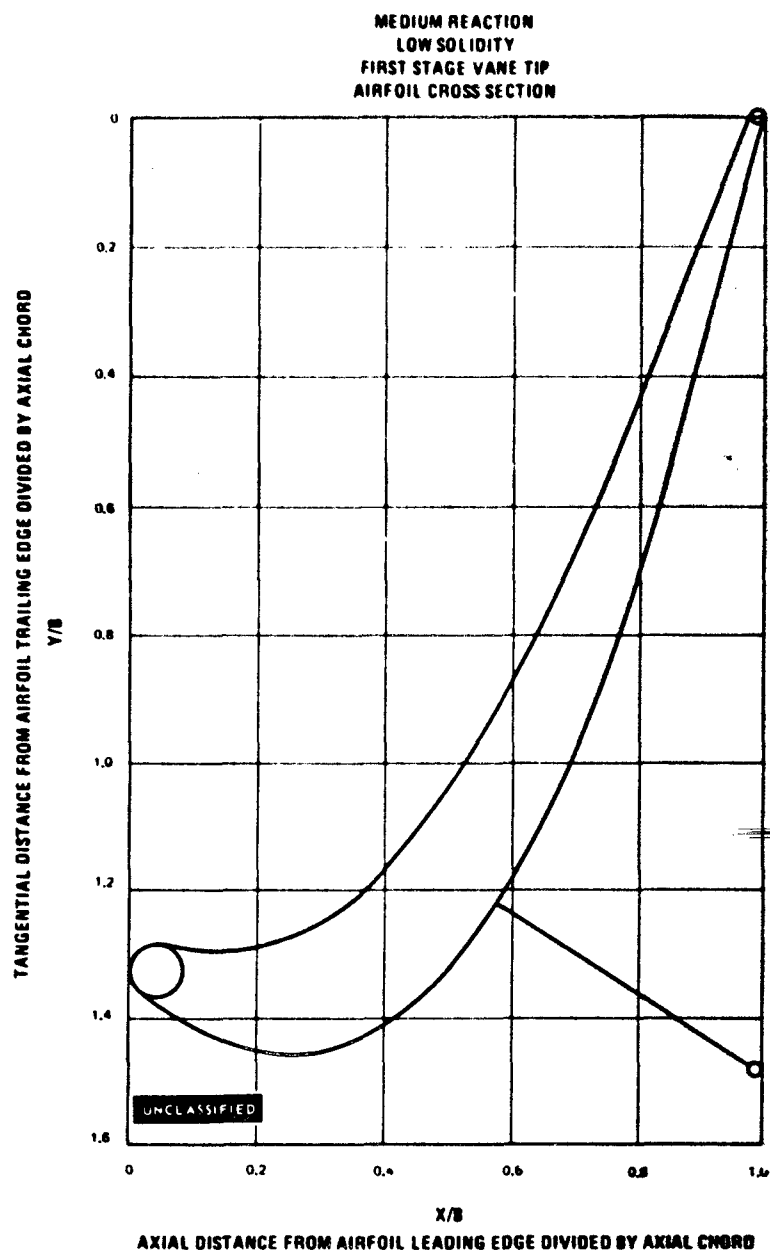


Figure 151

UNCLASSIFIED

UNCLASSIFIED

MEDIUM REACTION
LOW SOLIDITY
FIRST STAGE VANE TIP

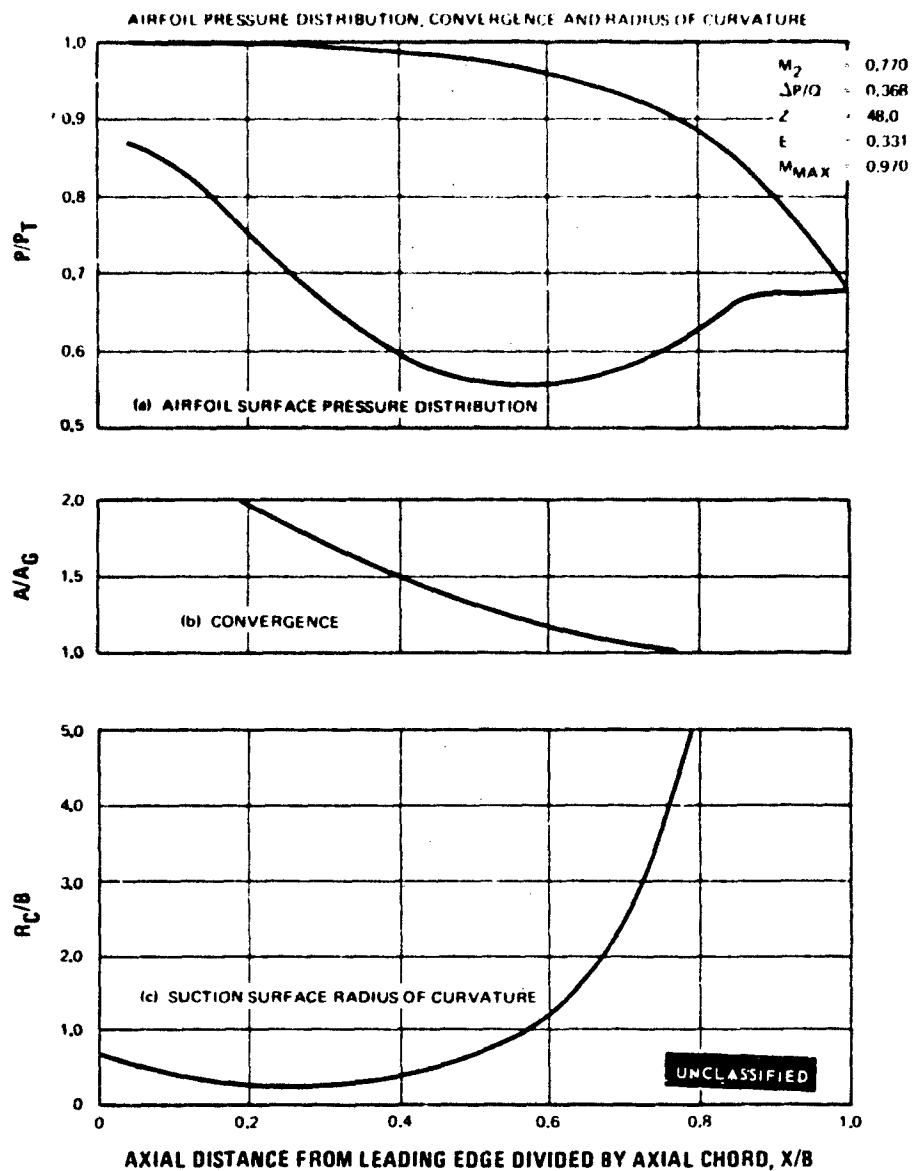


Figure 152

UNCLASSIFIED

UNCLASSIFIED

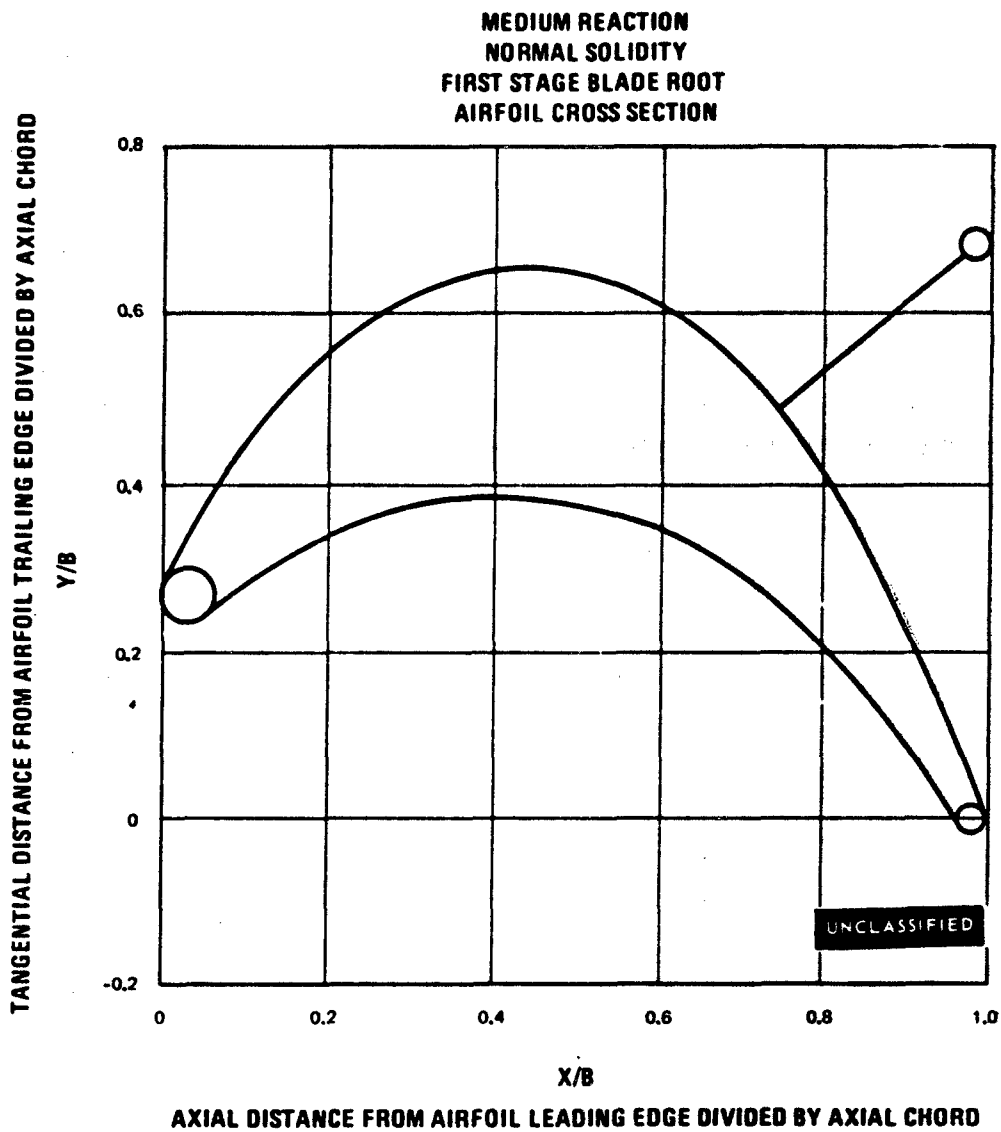


Figure 153

UNCLASSIFIED

UNCLASSIFIED

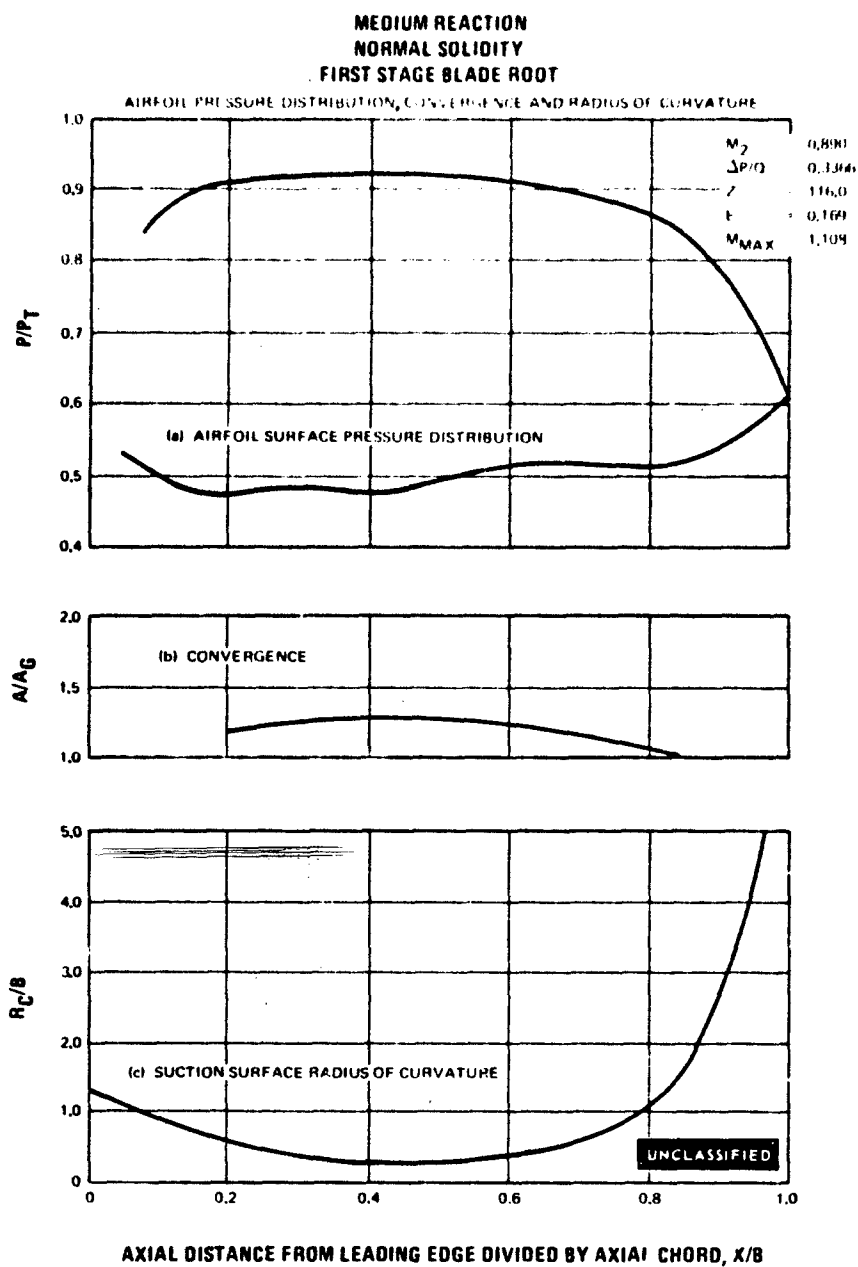


Figure 154

UNCLASSIFIED

UNCLASSIFIED

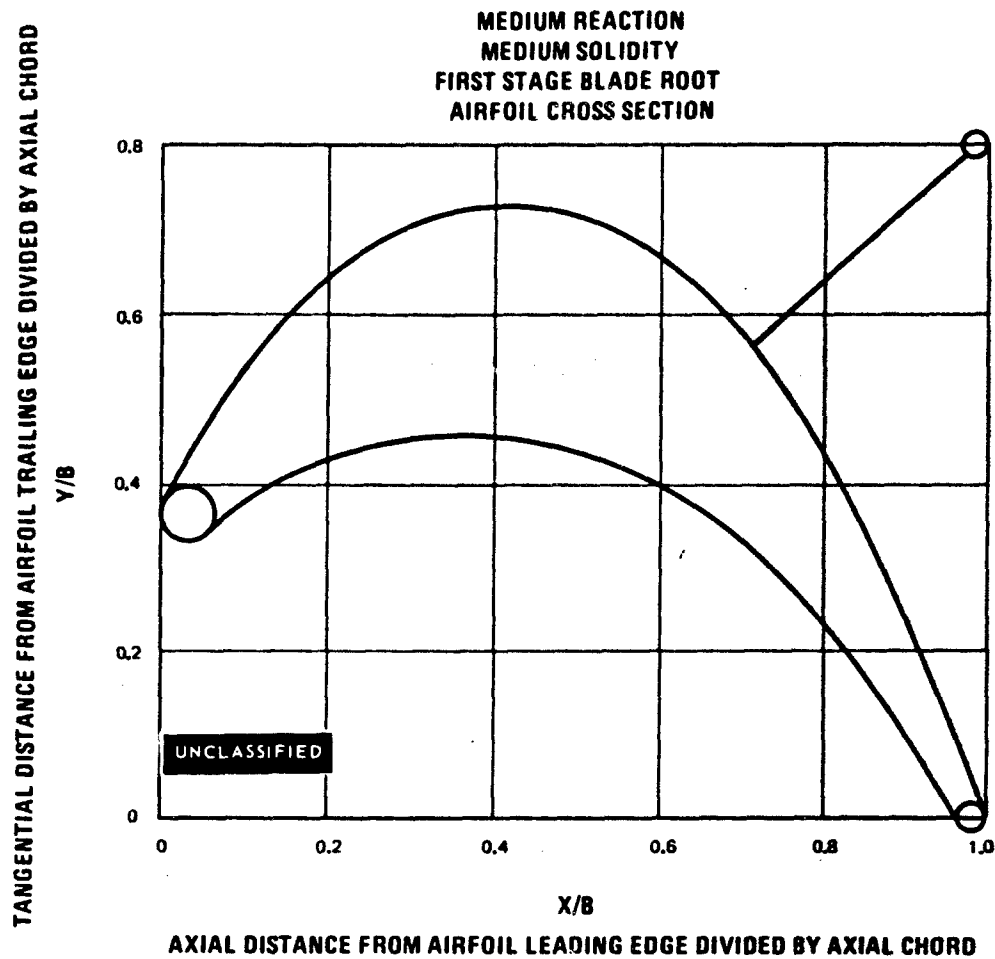


Figure 155

UNCLASSIFIED

UNCLASSIFIED

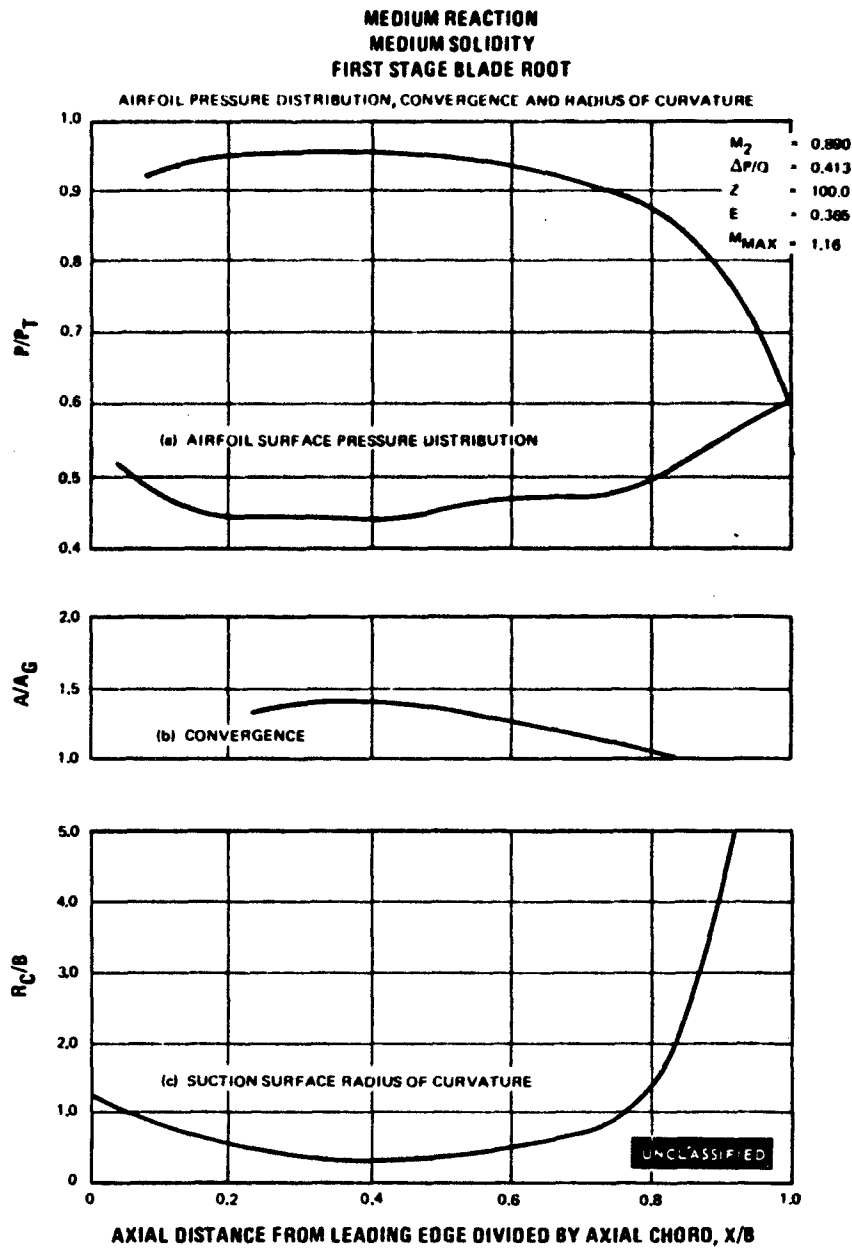


Figure 155

UNCLASSIFIED

UNCLASSIFIED

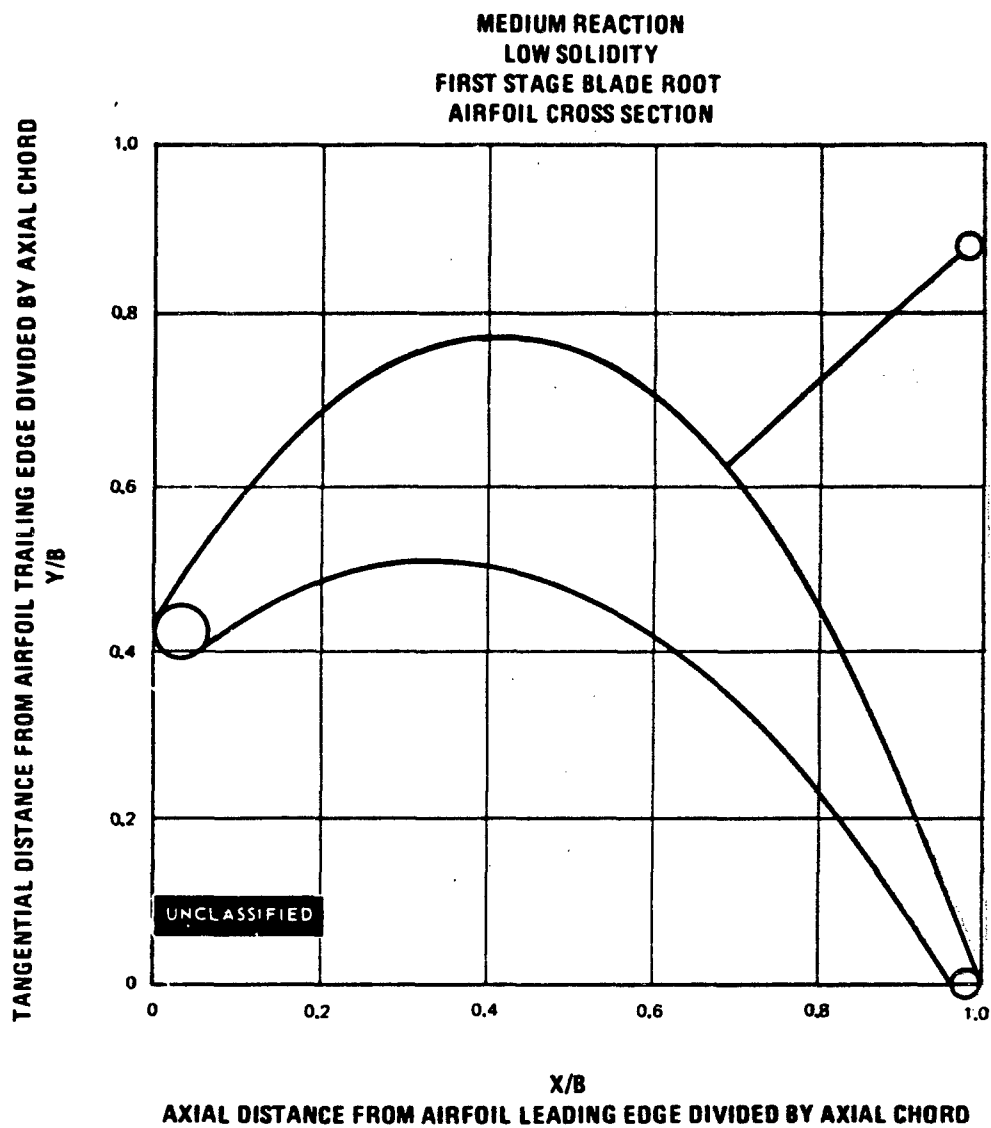


Figure 157

UNCLASSIFIED

UNCLASSIFIED

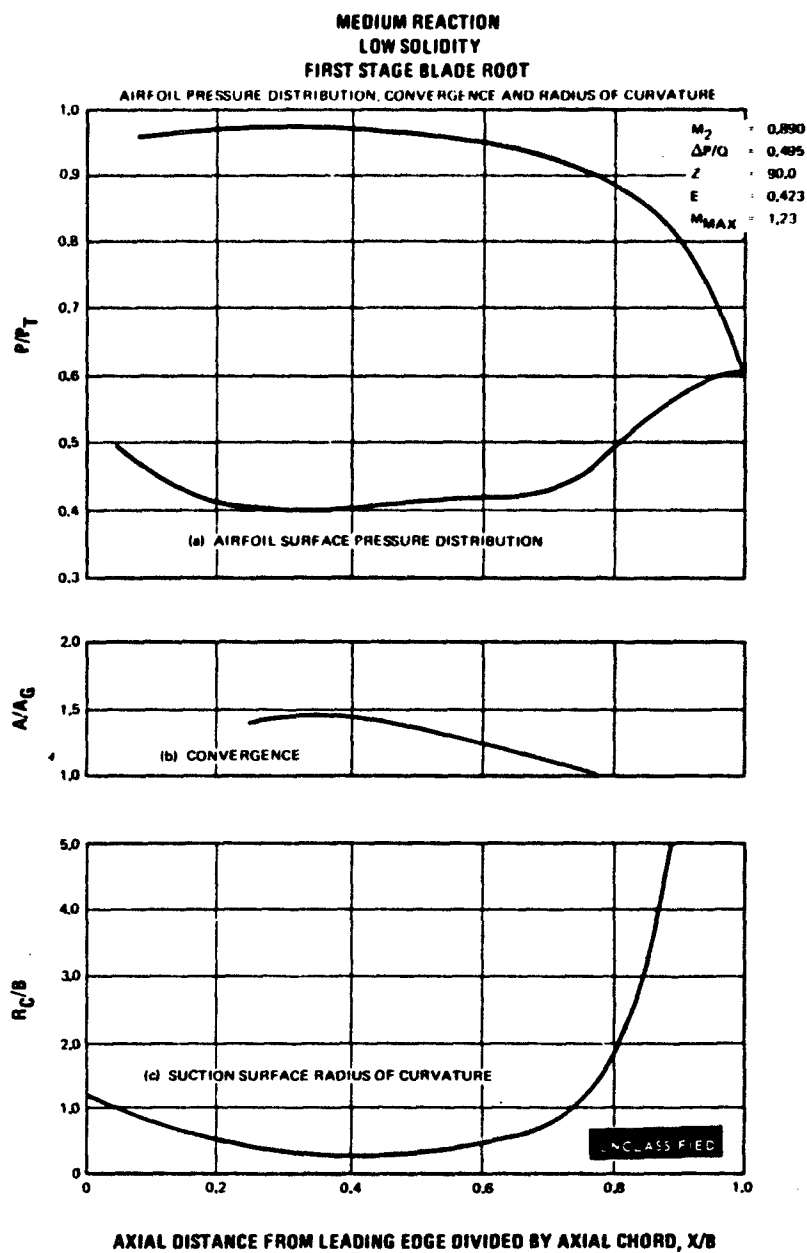


Figure 158

UNCLASSIFIED

UNCLASSIFIED

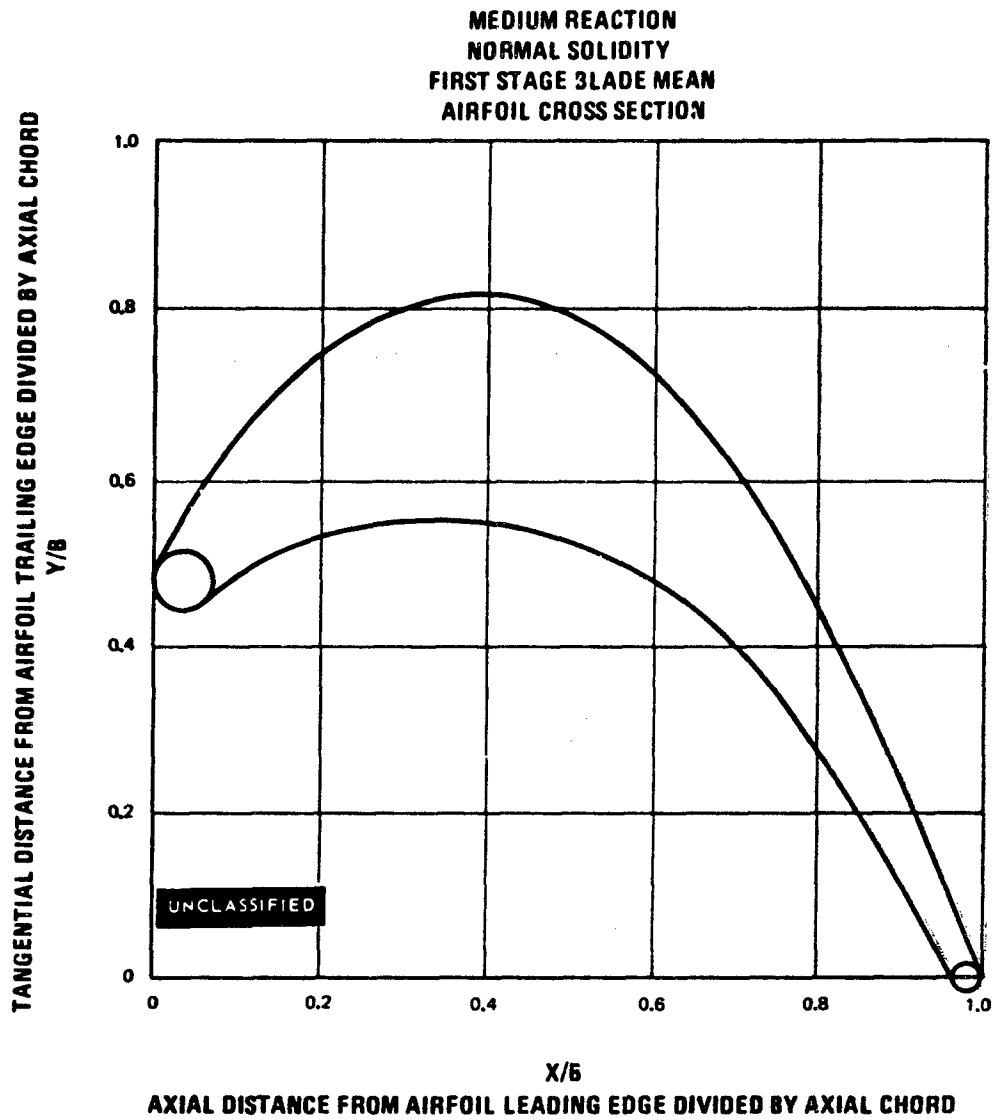


Figure 159

UNCLASSIFIED

UNCLASSIFIED

MEDIUM REACTION
NORMAL SOLIDITY
FIRST STAGE BLADE MEAN

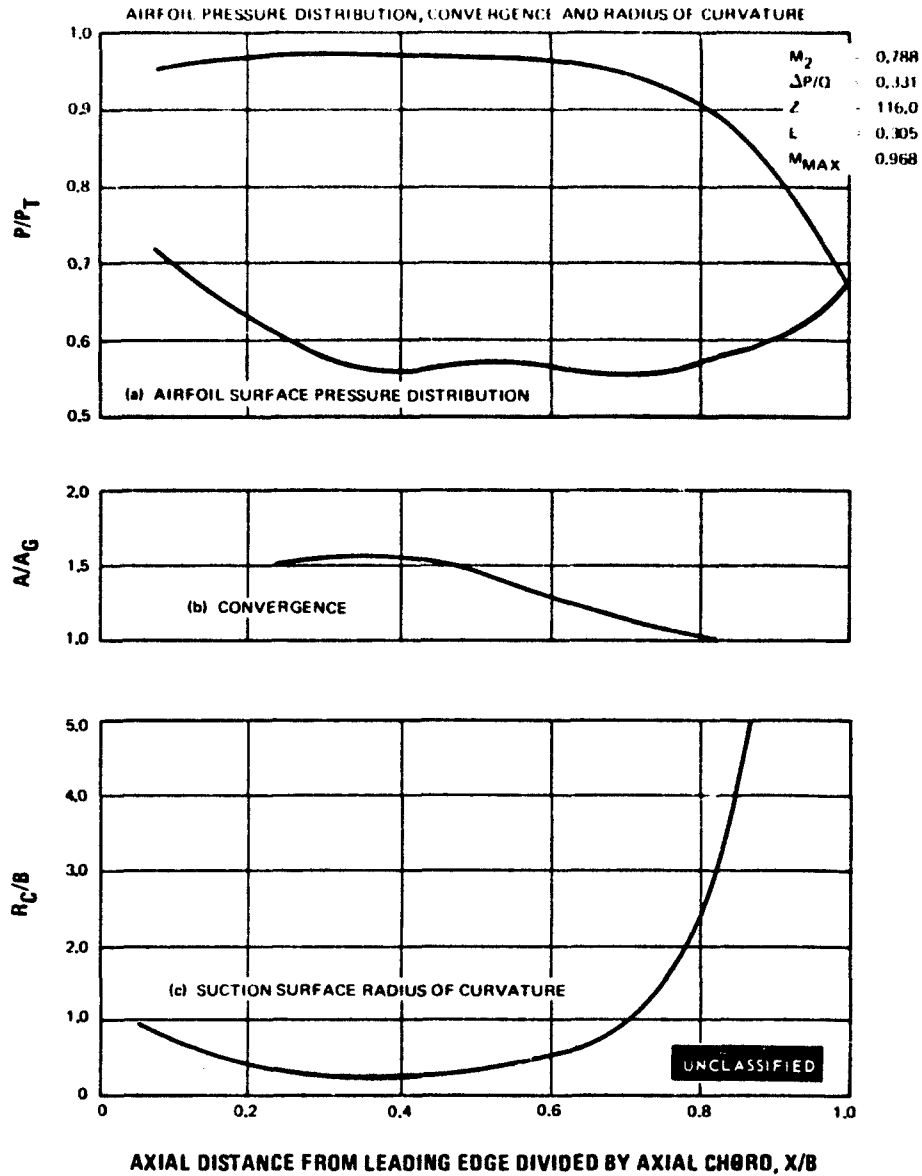


Figure 160

UNCLASSIFIED

UNCLASSIFIED

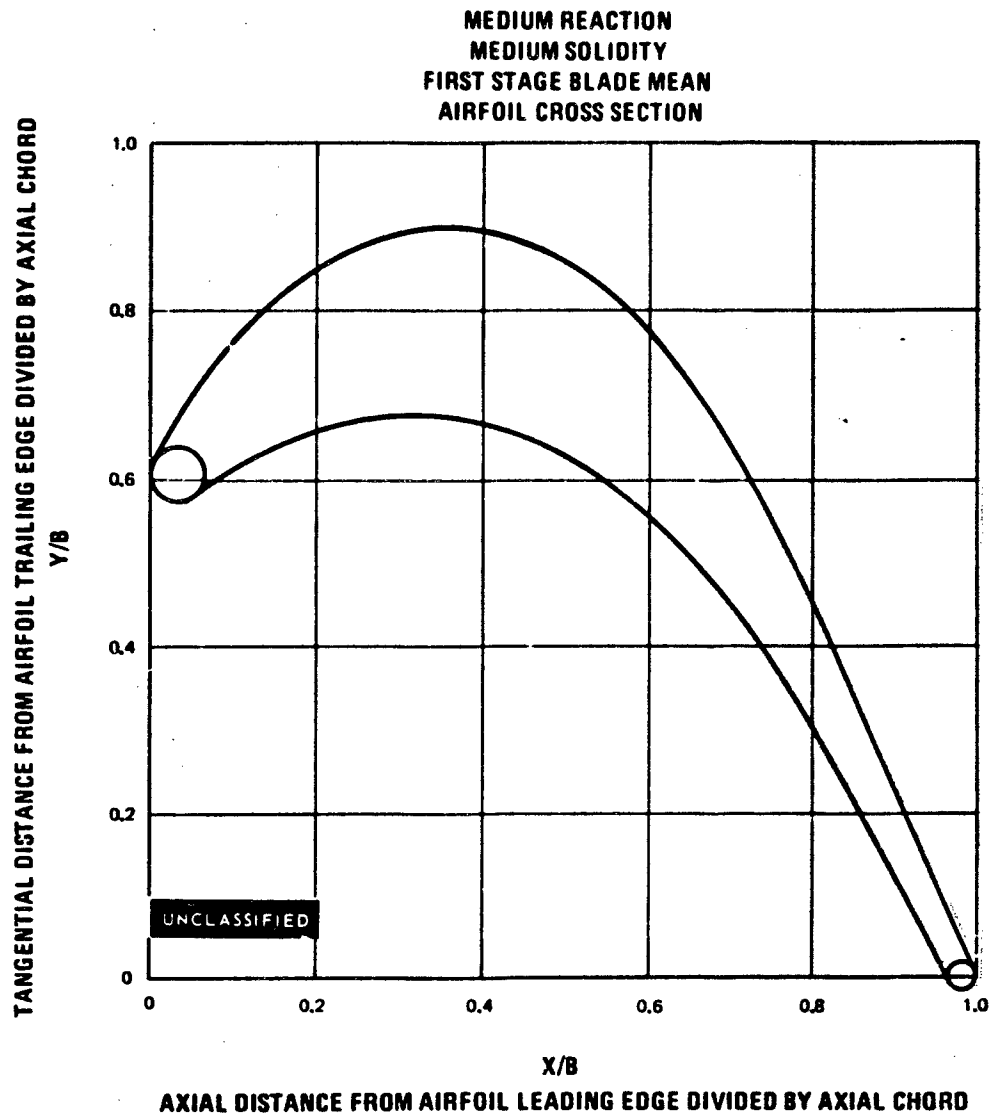


Figure 161

UNCLASSIFIED

UNCLASSIFIED

MEDIUM REACTION
MEDIUM SOLIDITY
FIRST STAGE BLADE MEAN

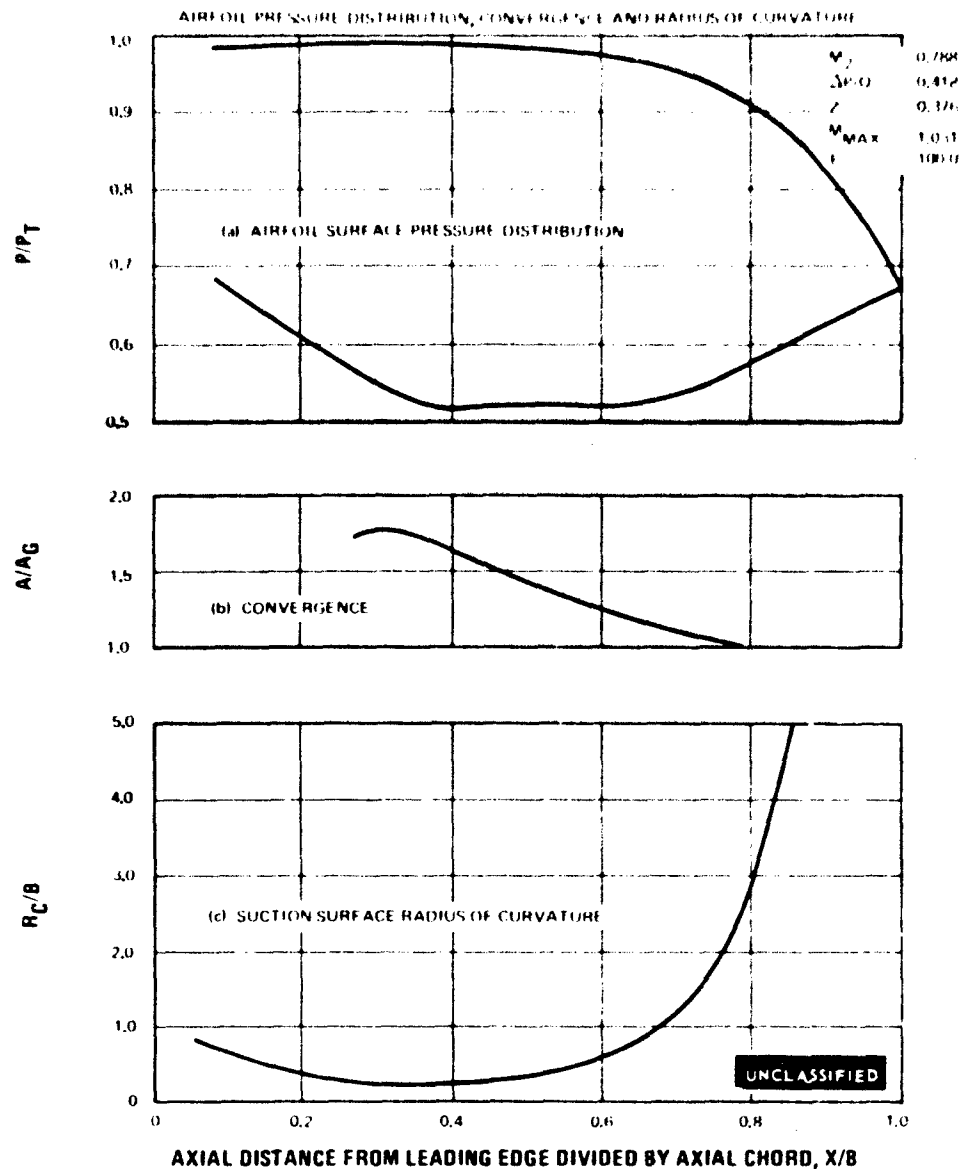


Figure 162

UNCLASSIFIED

UNCLASSIFIED

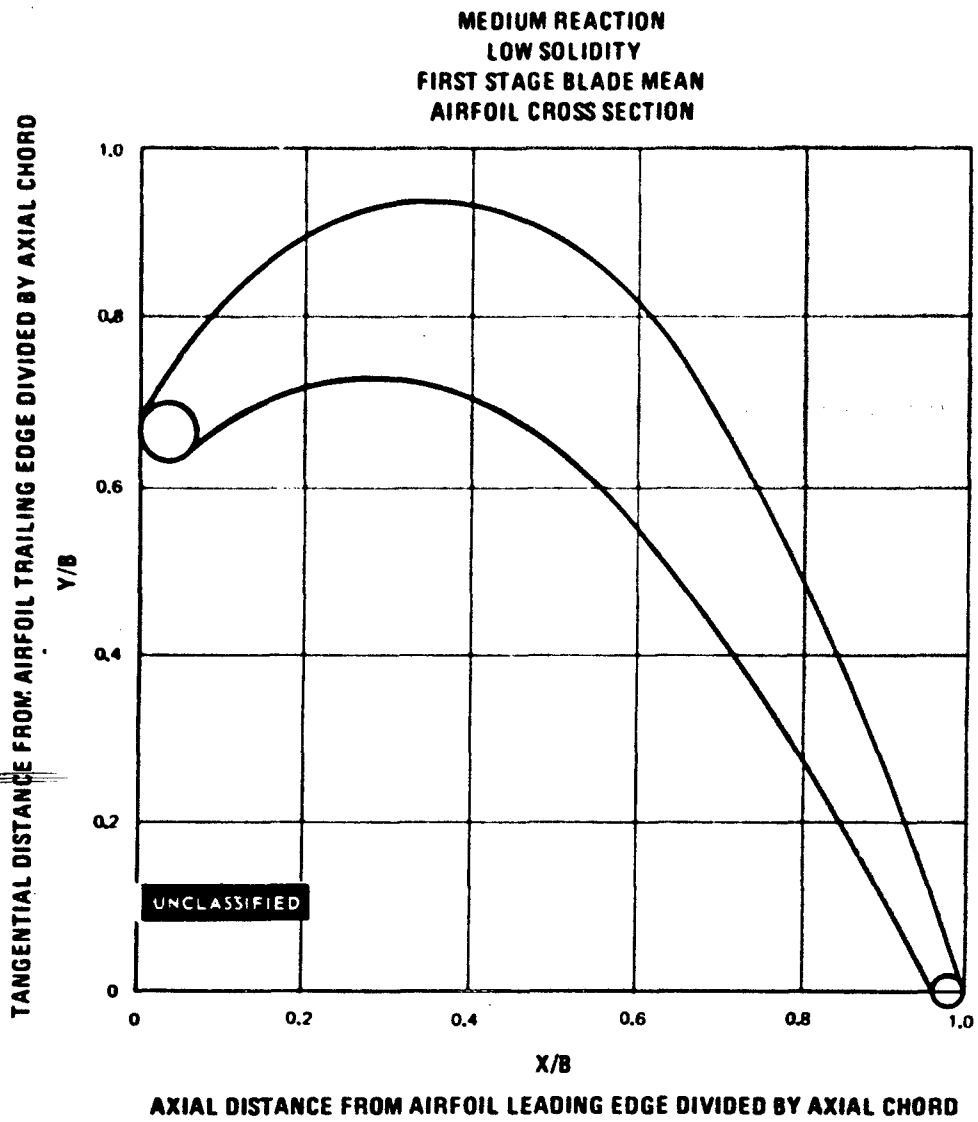


Figure 163

UNCLASSIFIED

UNCLASSIFIED

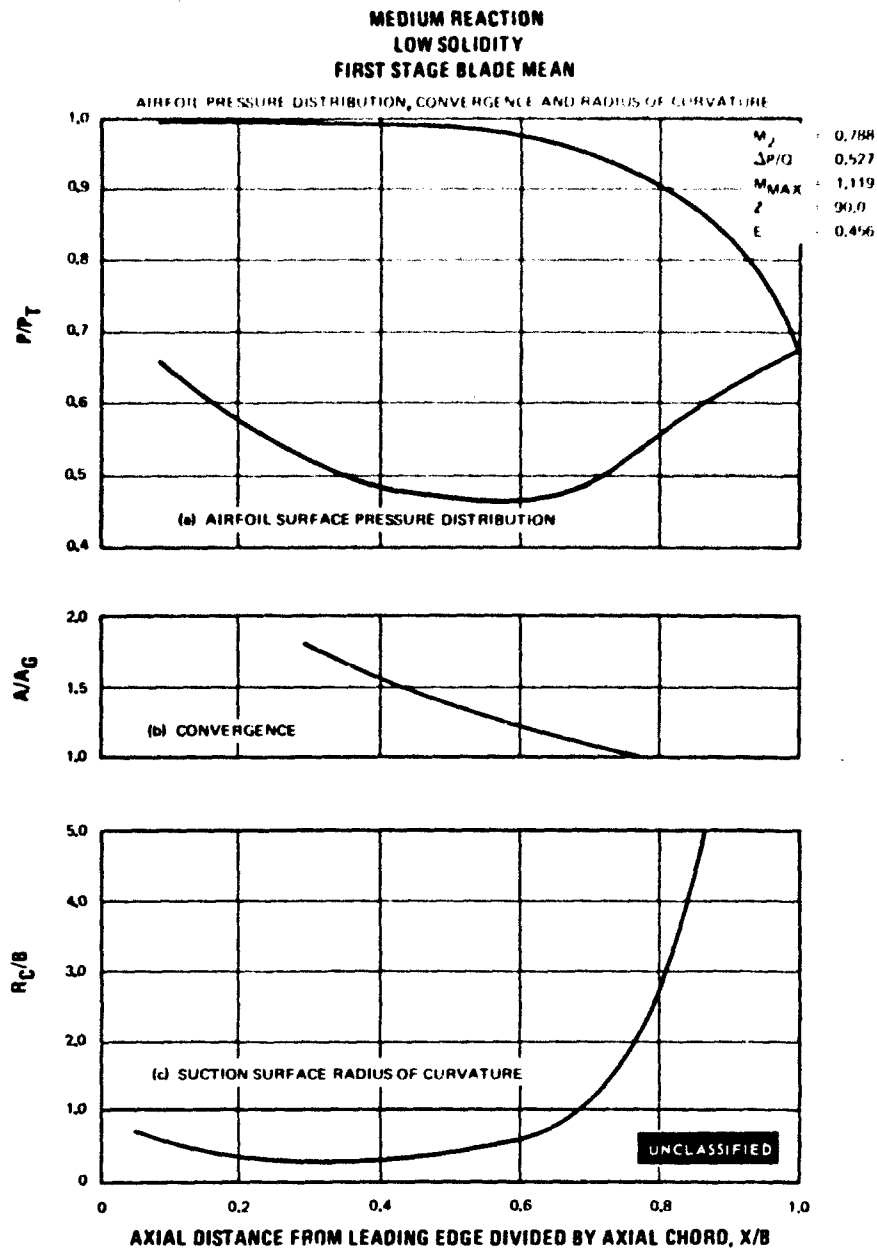


Figure 164

UNCLASSIFIED

UNCLASSIFIED

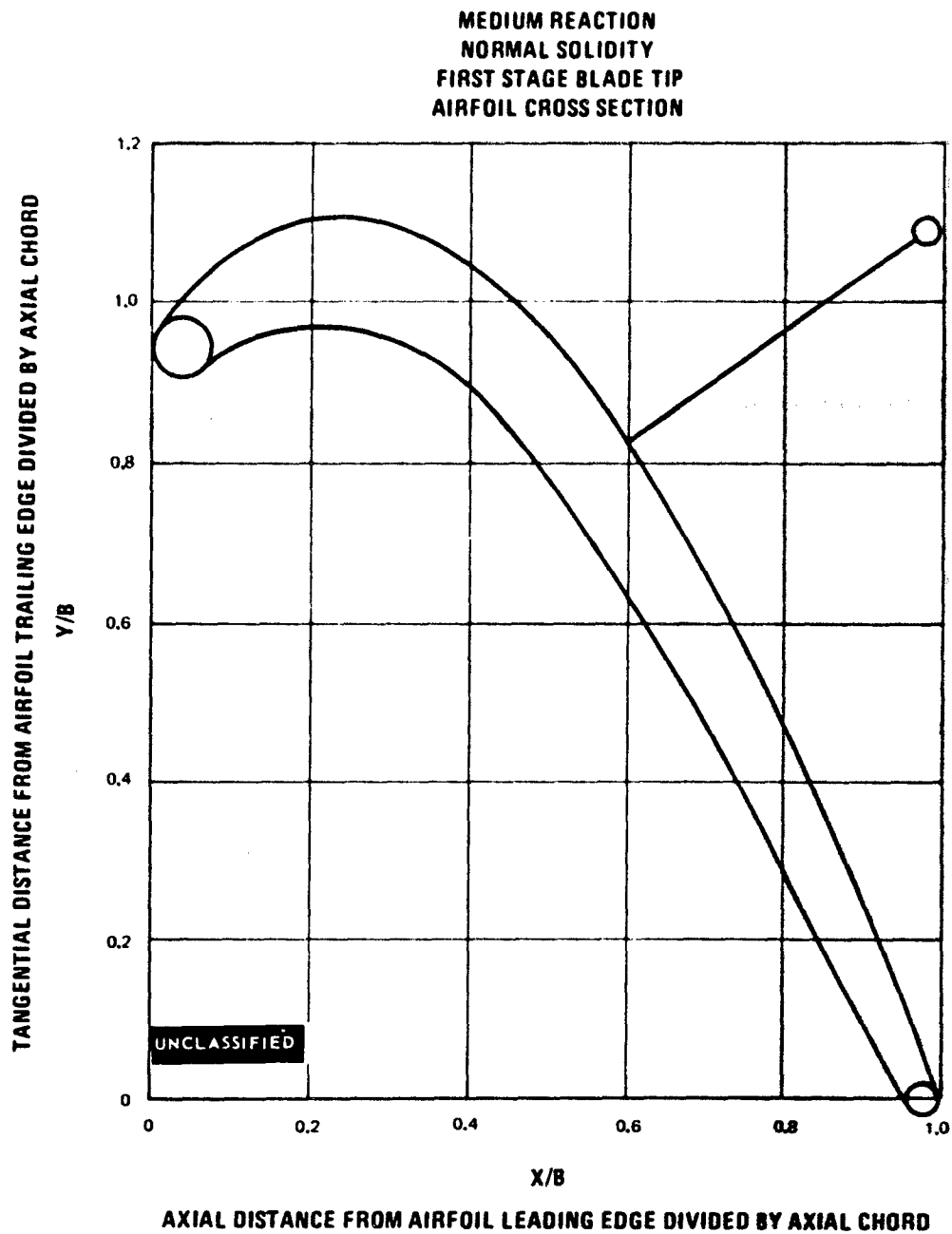


Figure 165

UNCLASSIFIED

UNCLASSIFIED

MEDIUM REACTION
NORMAL SOLIDITY
FIRST STAGE BLADE TIP

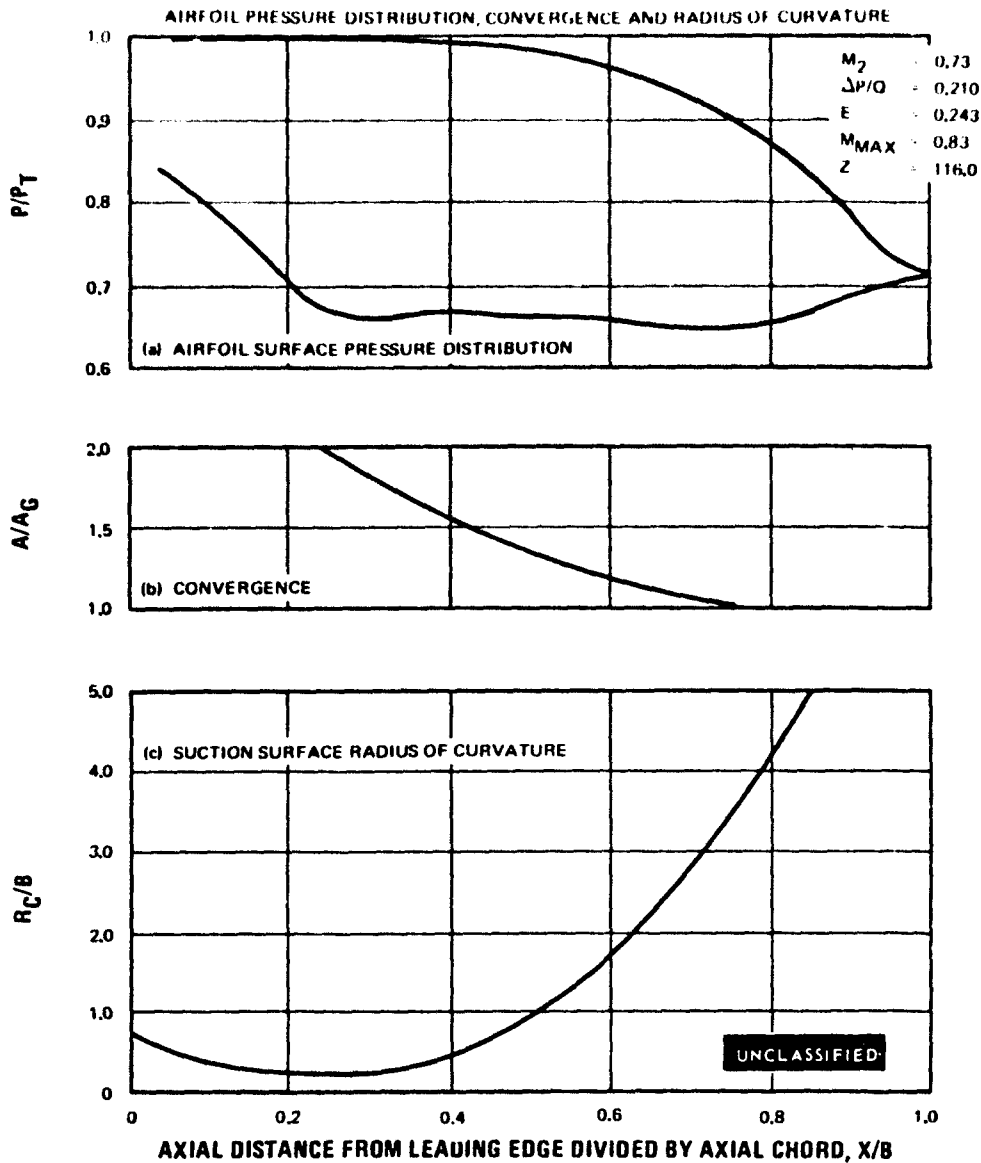


Figure 166

UNCLASSIFIED

UNCLASSIFIED

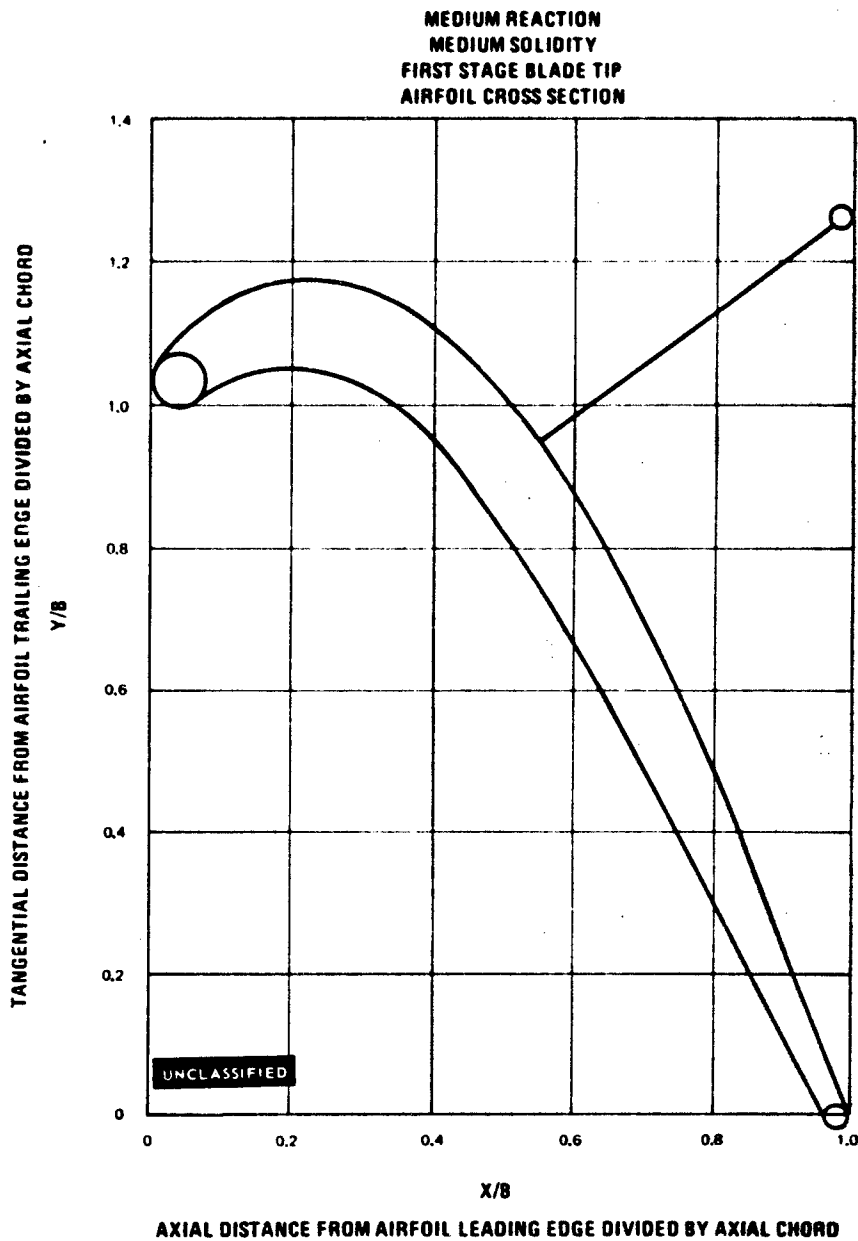


Figure 167

UNCLASSIFIED

UNCLASSIFIED

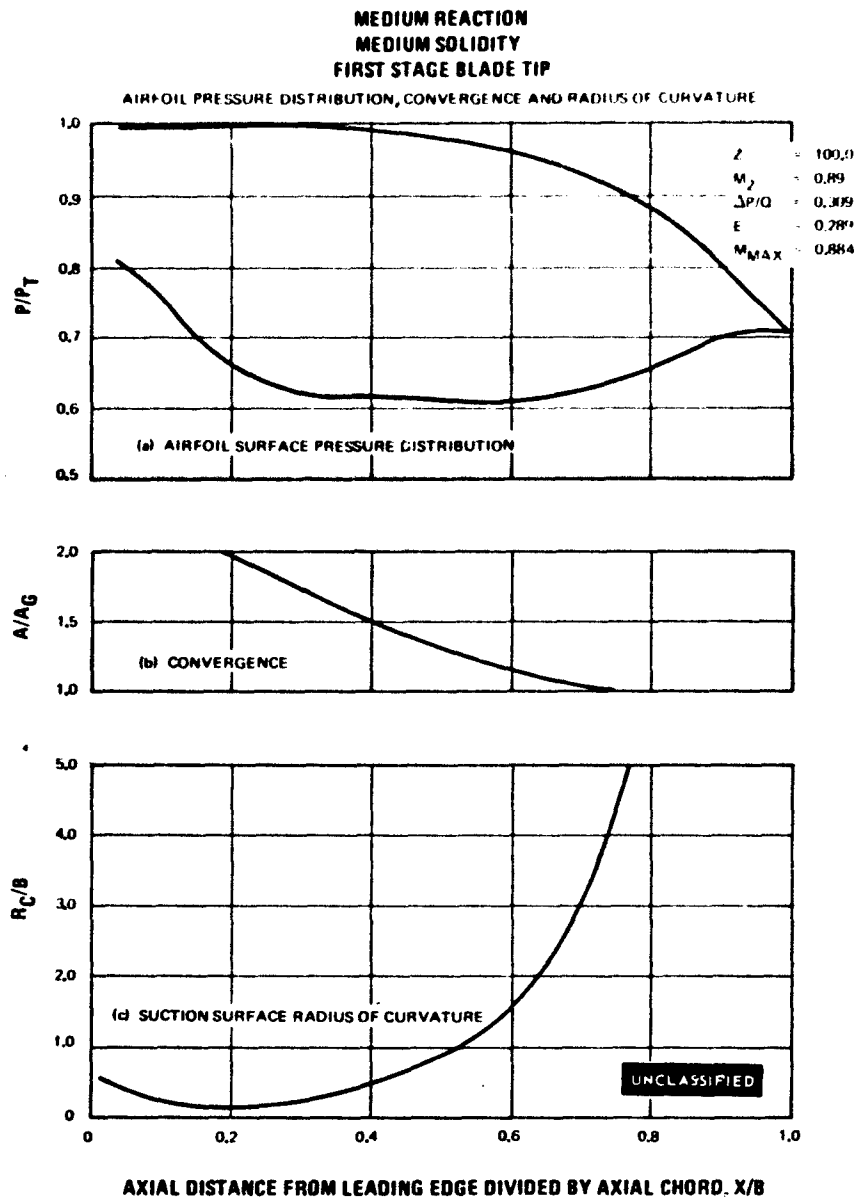


Figure 168

UNCLASSIFIED

UNCLASSIFIED

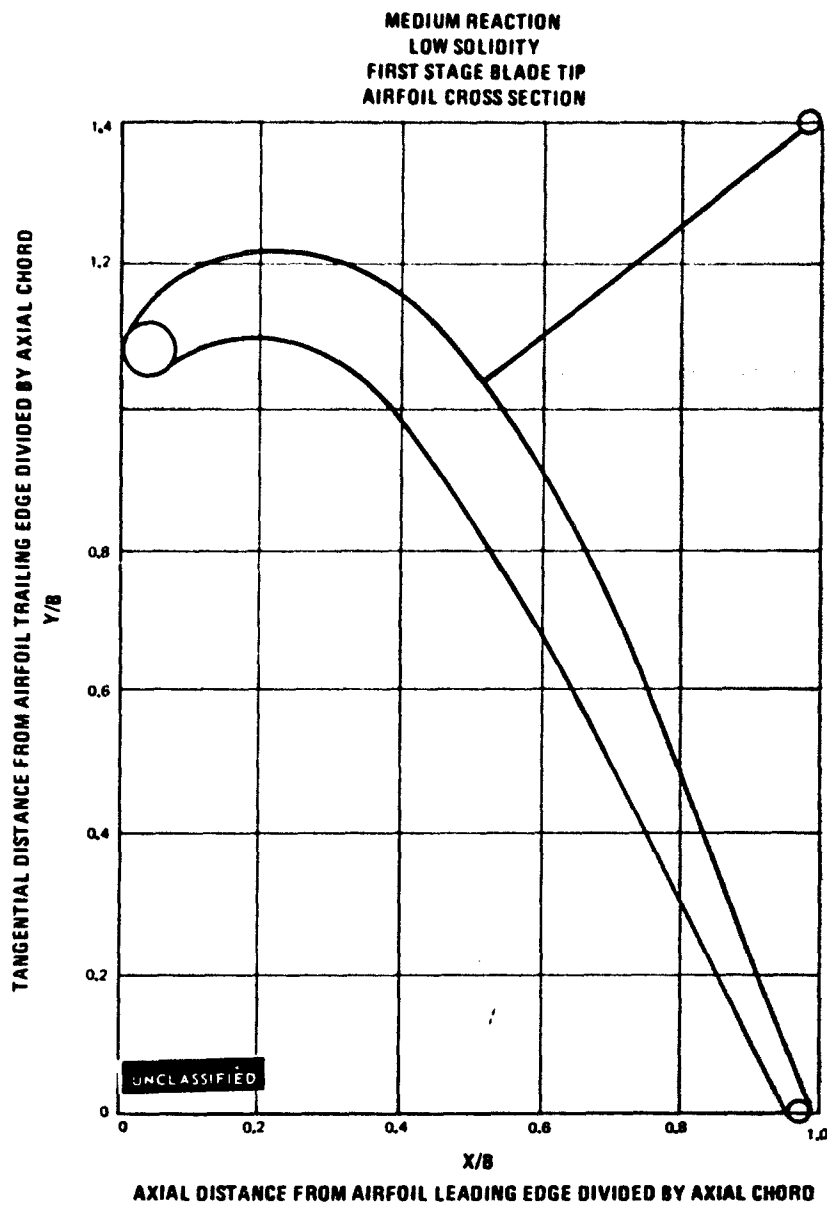


Figure 169

UNCLASSIFIED

UNCLASSIFIED

MEDIUM REACTION
LOW SOLIDITY
FIRST STAGE BLADE TIP

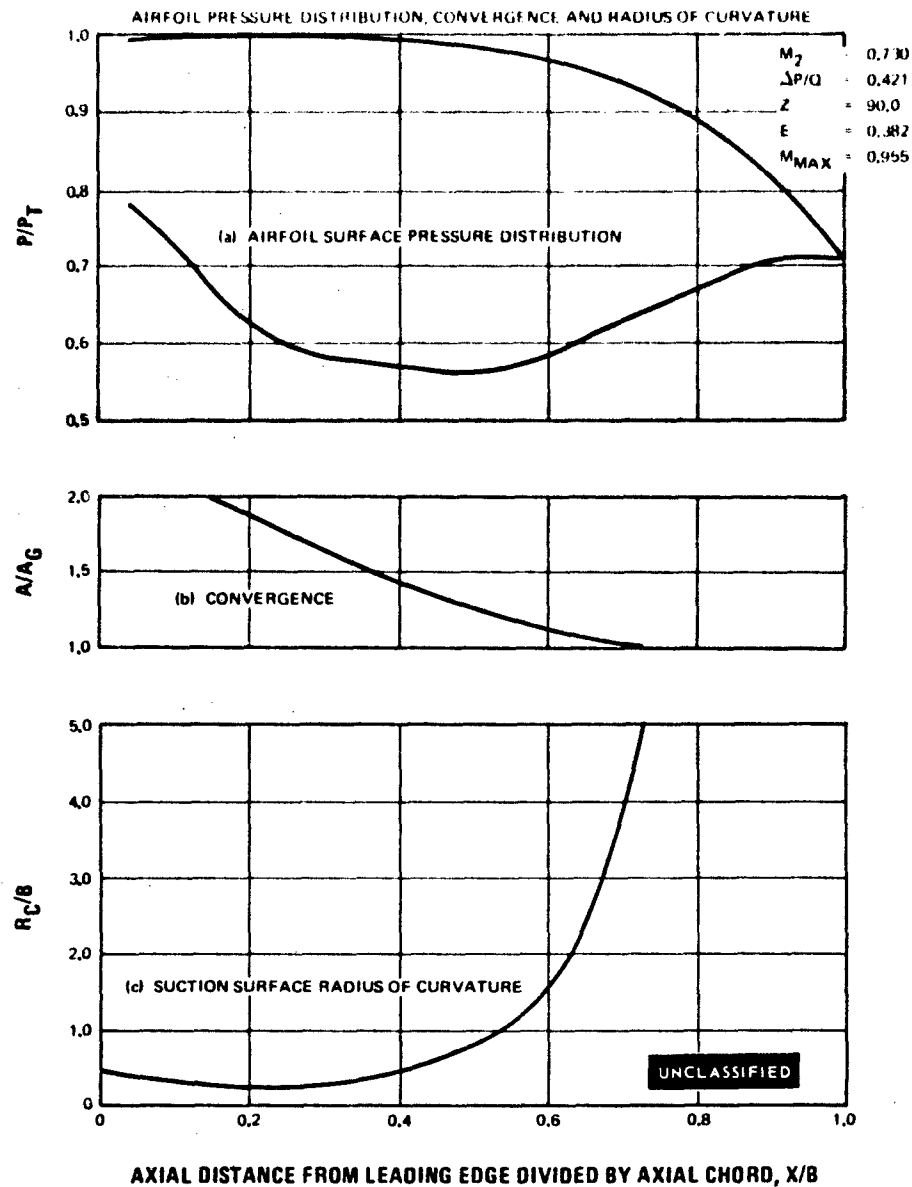


Figure 170

UNCLASSIFIED

UNCLASSIFIED

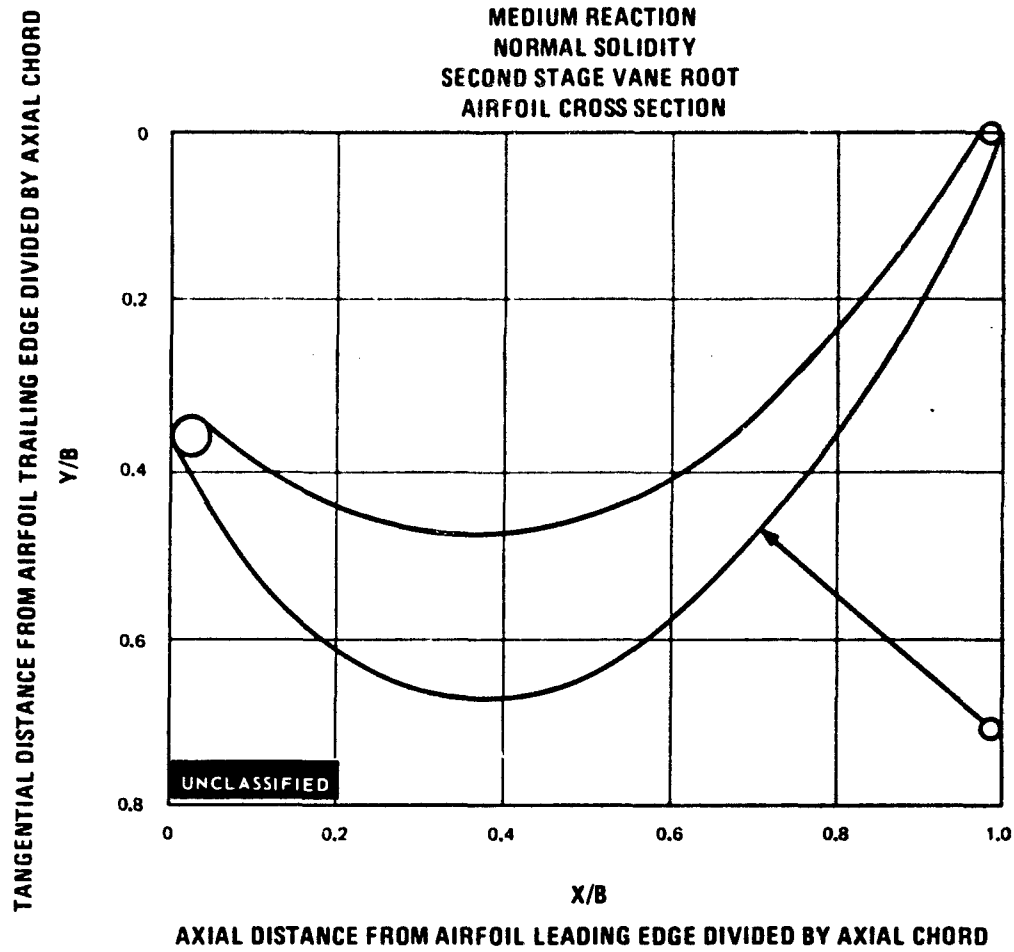


Figure 171

UNCLASSIFIED

UNCLASSIFIED

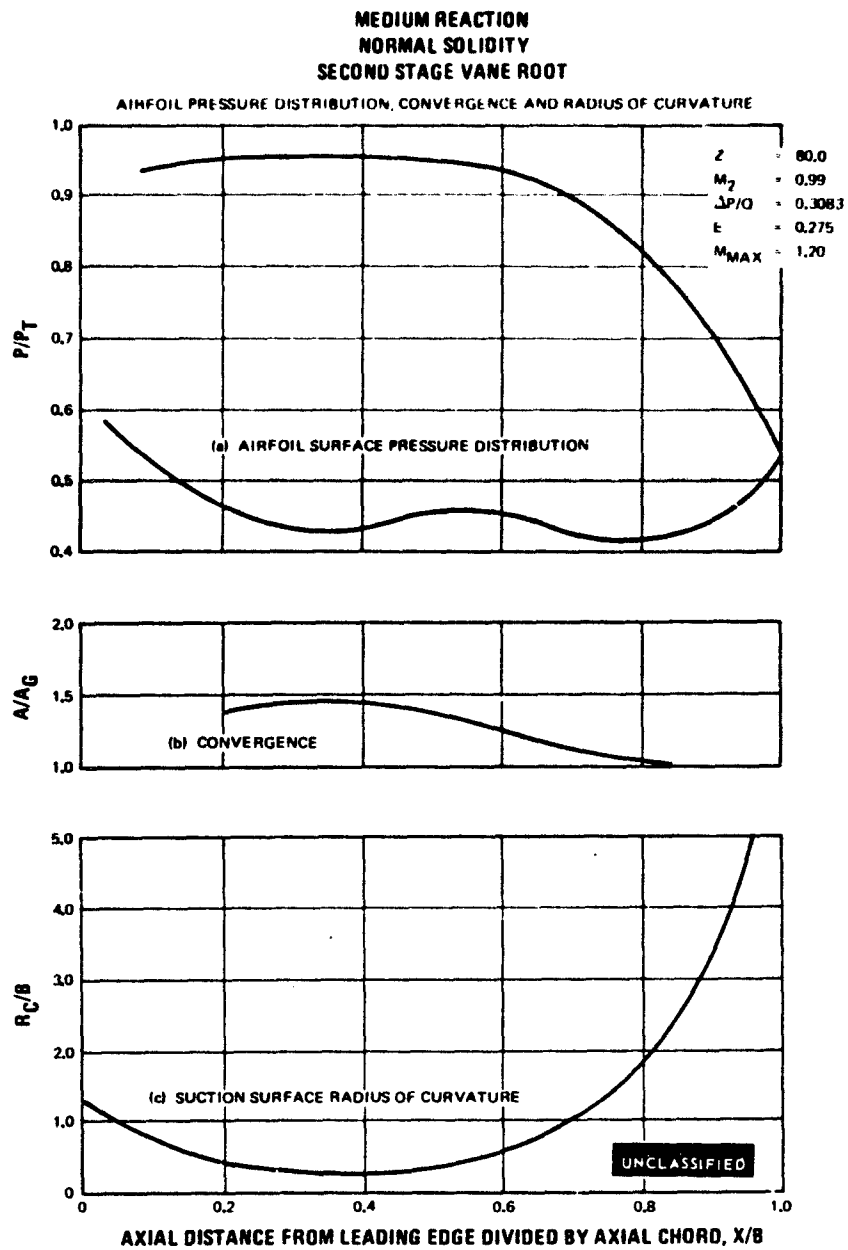


Figure 172

UNCLASSIFIED

UNCLASSIFIED

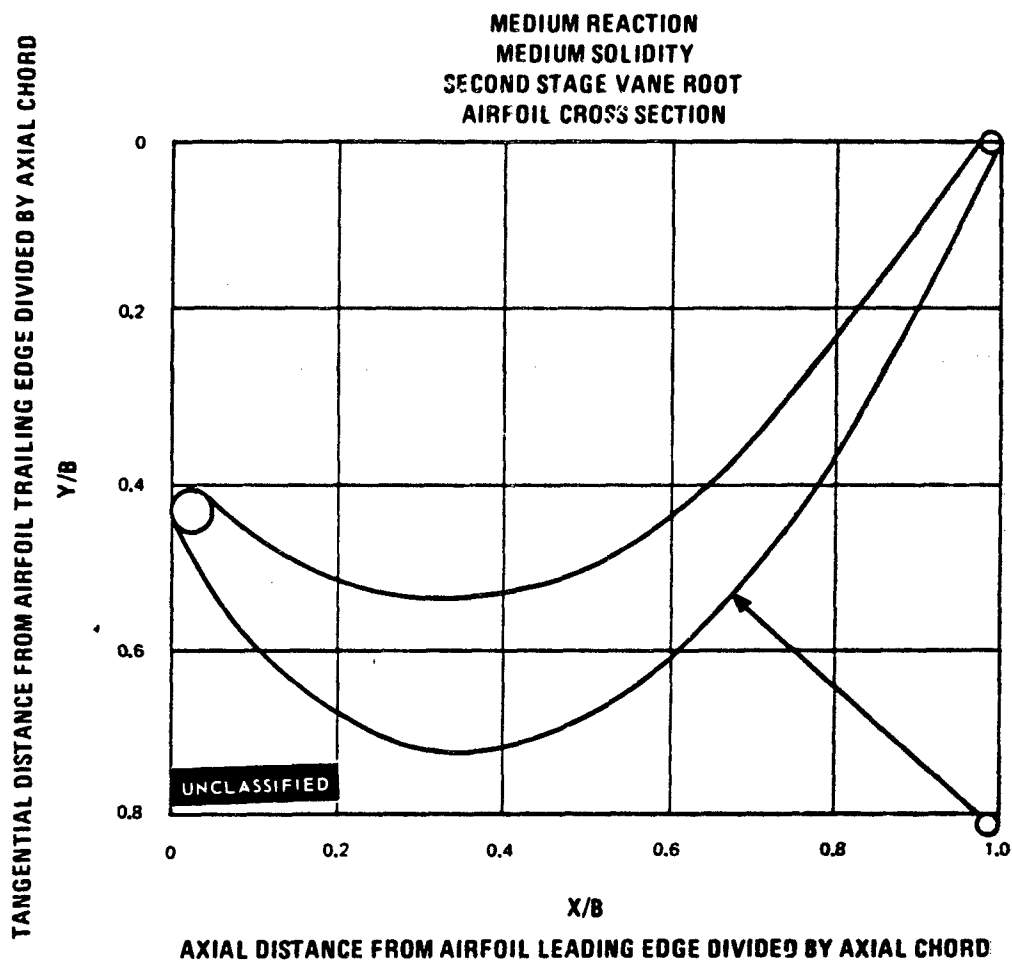


Figure 173

UNCLASSIFIED

UNCLASSIFIED

MEDIUM REACTION
MEDIUM SOLIDITY
SECOND STAGE VANE HOOT

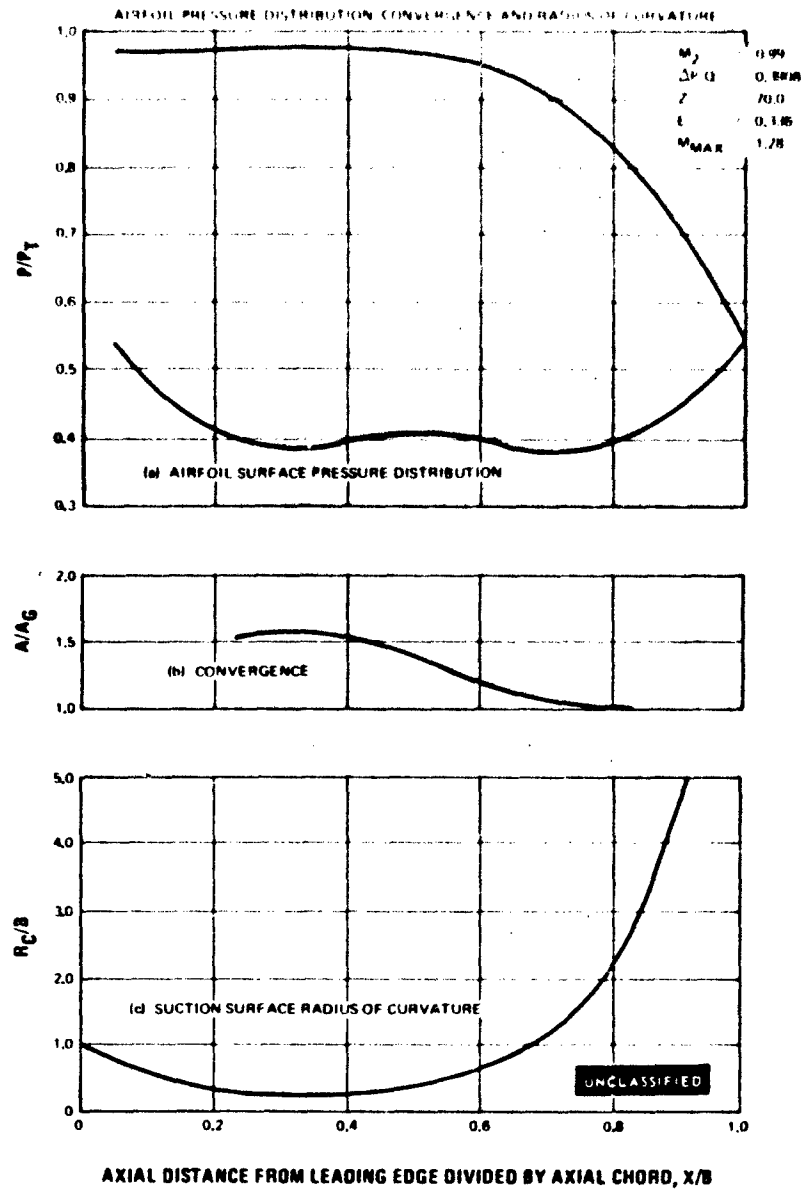


Figure 174

UNCLASSIFIED

UNCLASSIFIED

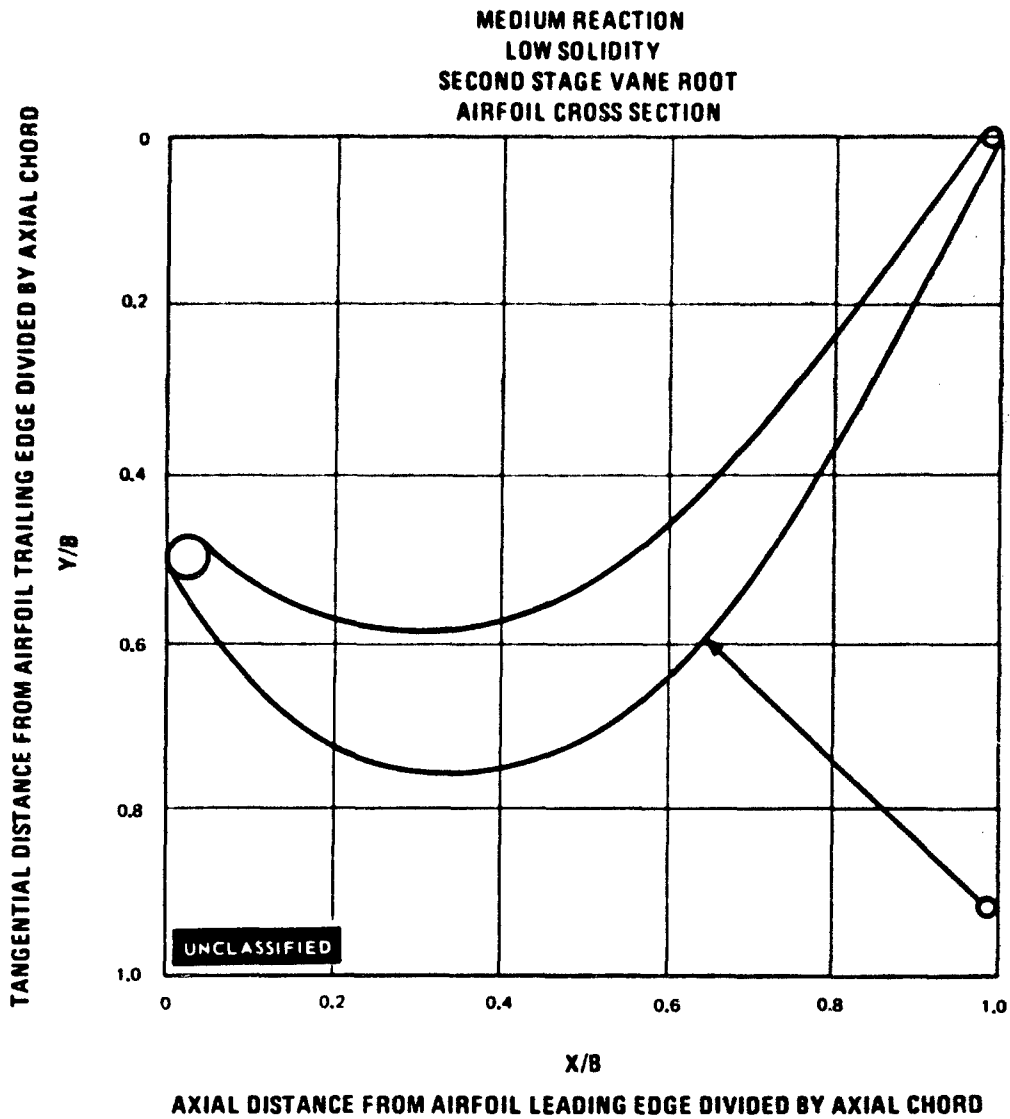


Figure 175

UNCLASSIFIED

UNCLASSIFIED

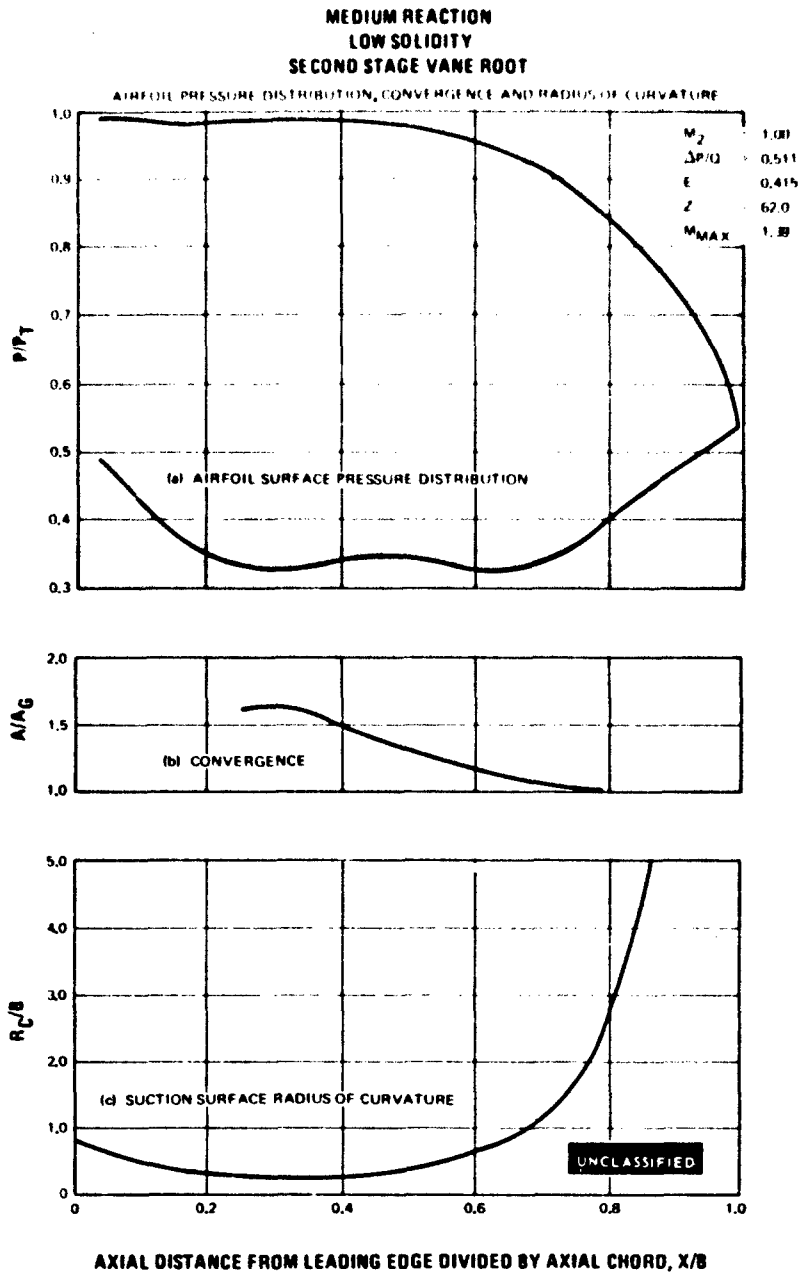


Figure 176

UNCLASSIFIED

UNCLASSIFIED

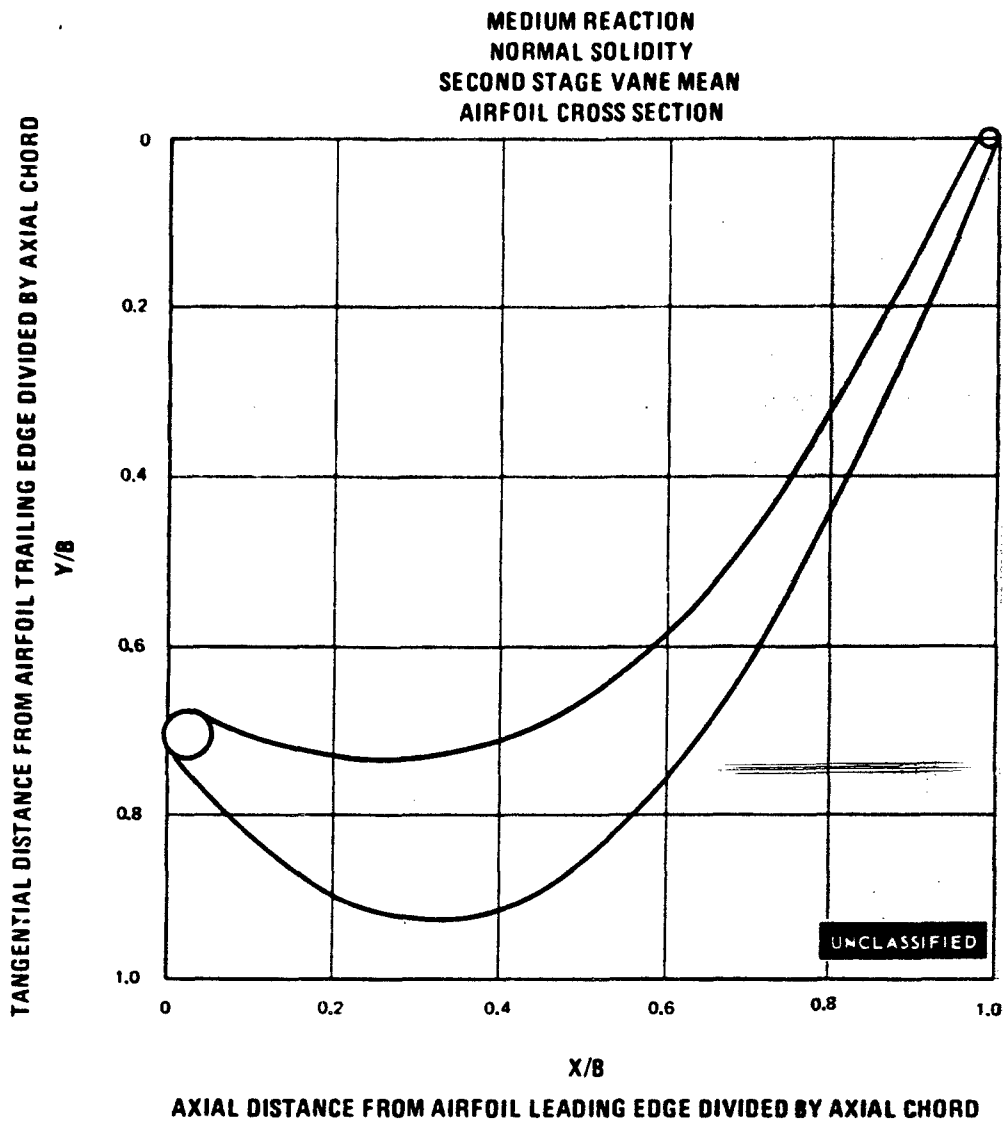


Figure 177

UNCLASSIFIED

UNCLASSIFIED

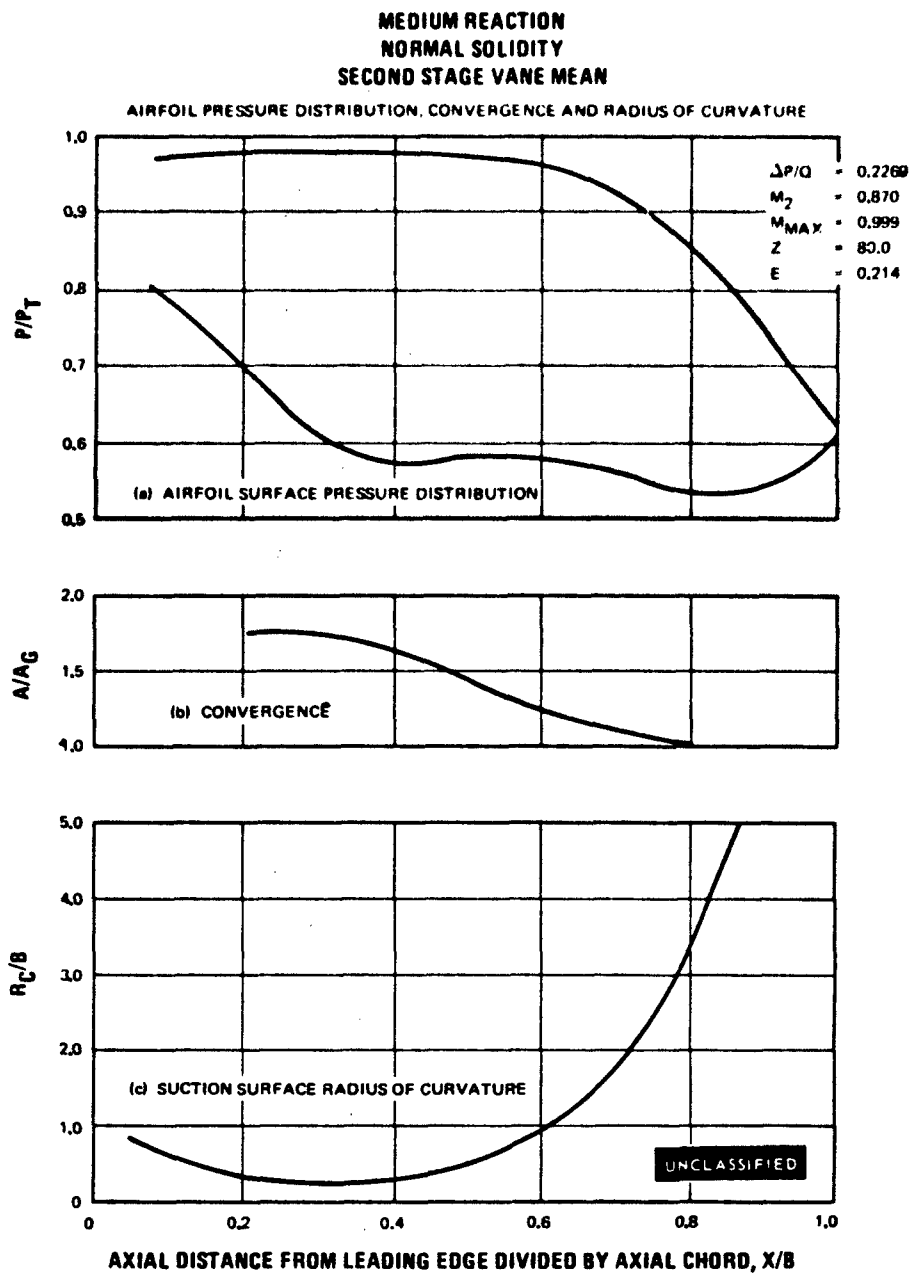


Figure 178

UNCLASSIFIED

UNCLASSIFIED

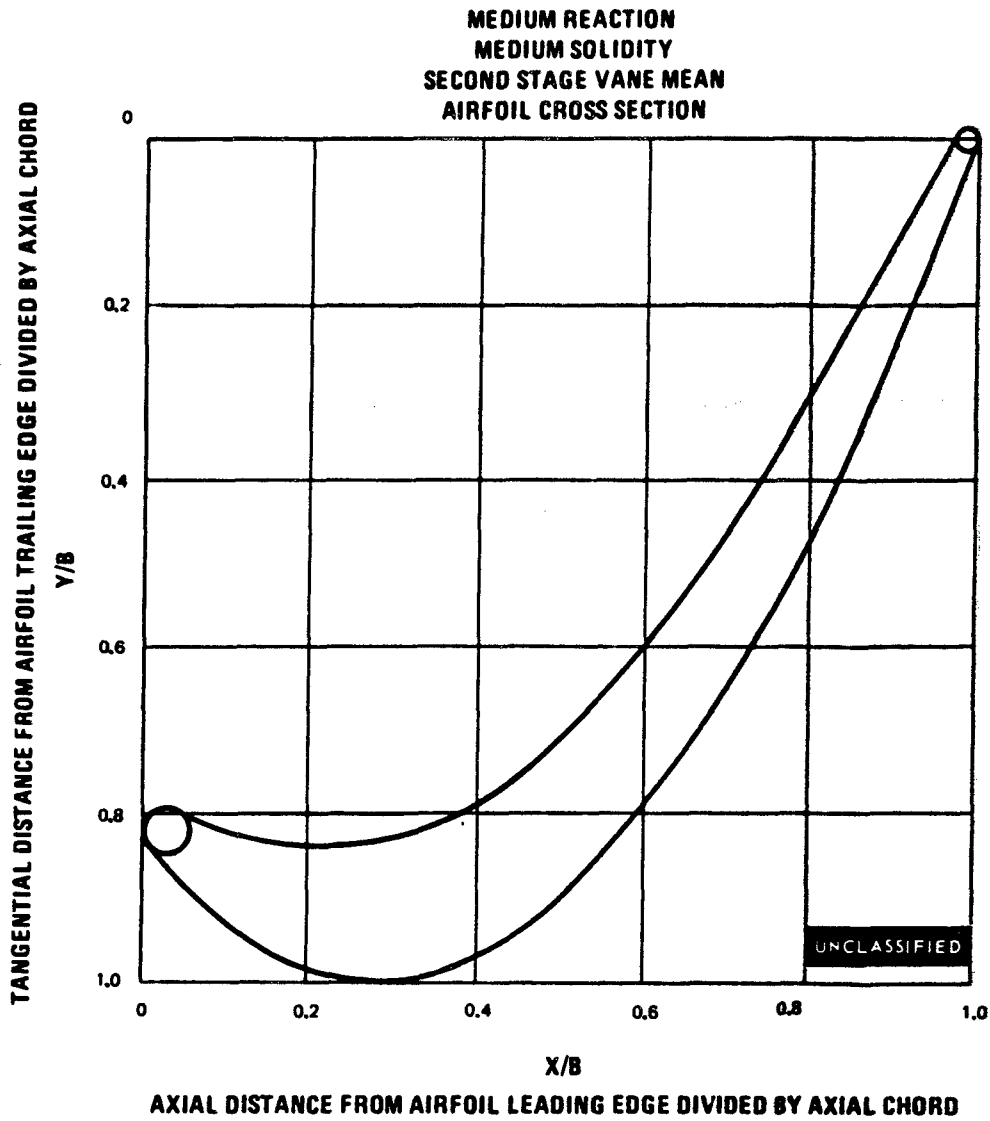


Figure 179

UNCLASSIFIED

UNCLASSIFIED

MEDIUM REACTION
MEDIUM SOLIDITY
SECOND STAGE VANE MEAN

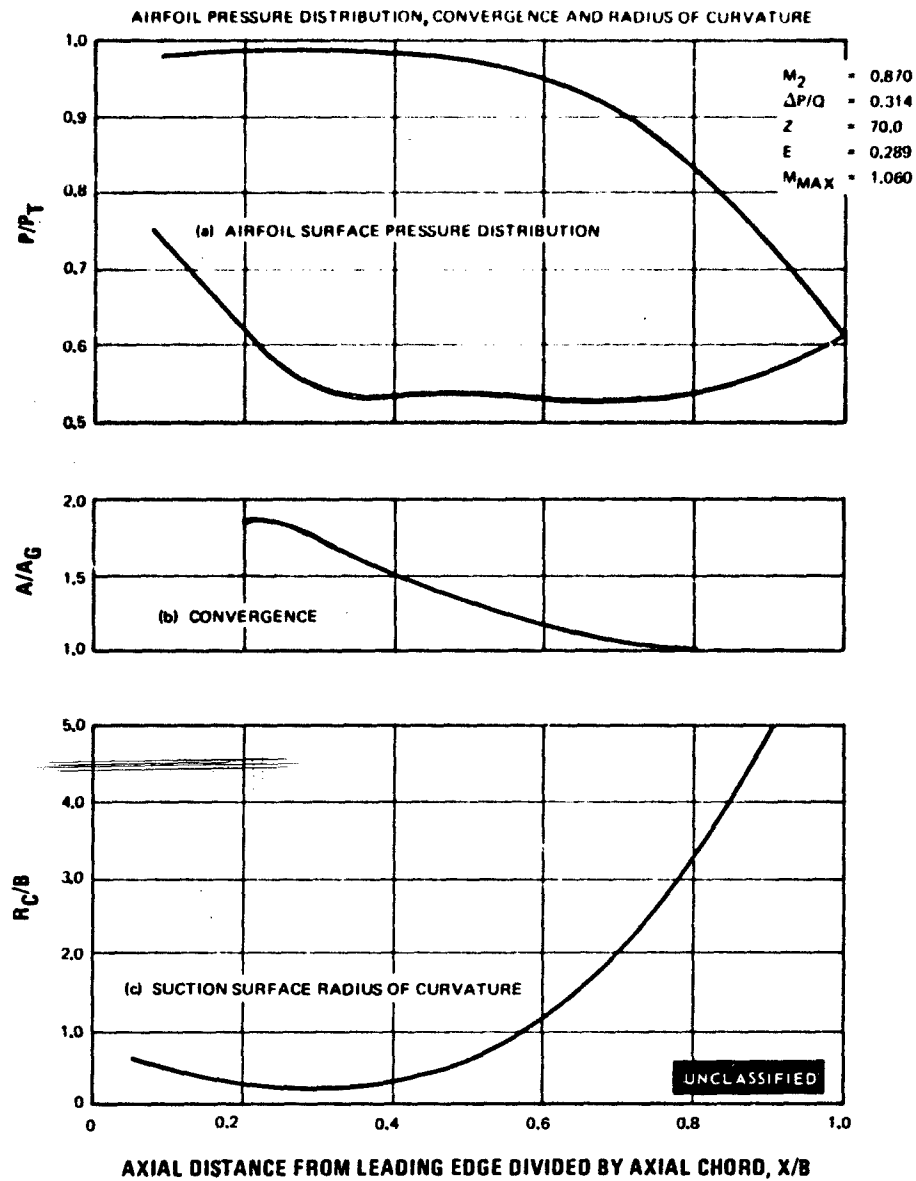


Figure 180

UNCLASSIFIED

UNCLASSIFIED

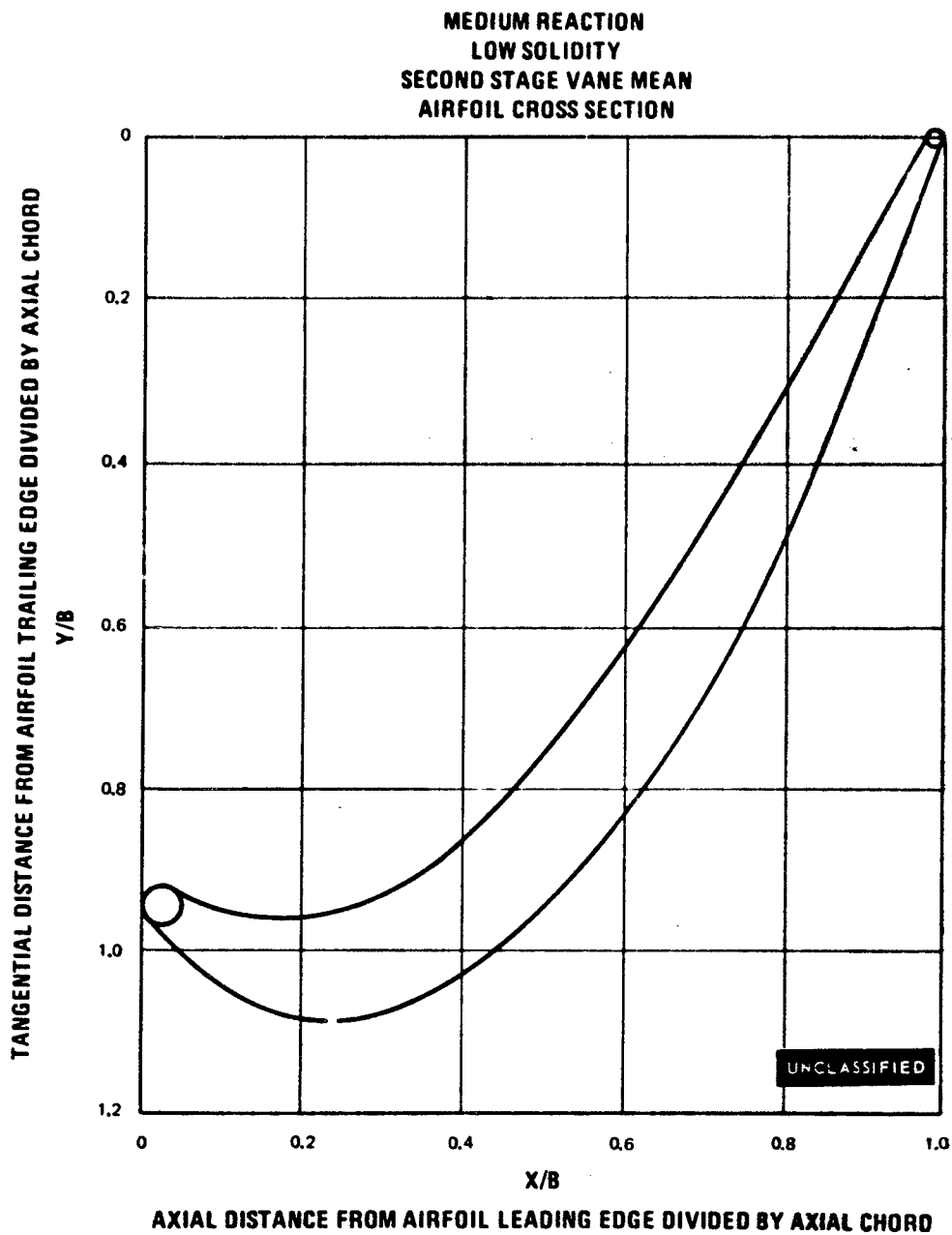


Figure 181

UNCLASSIFIED

UNCLASSIFIED

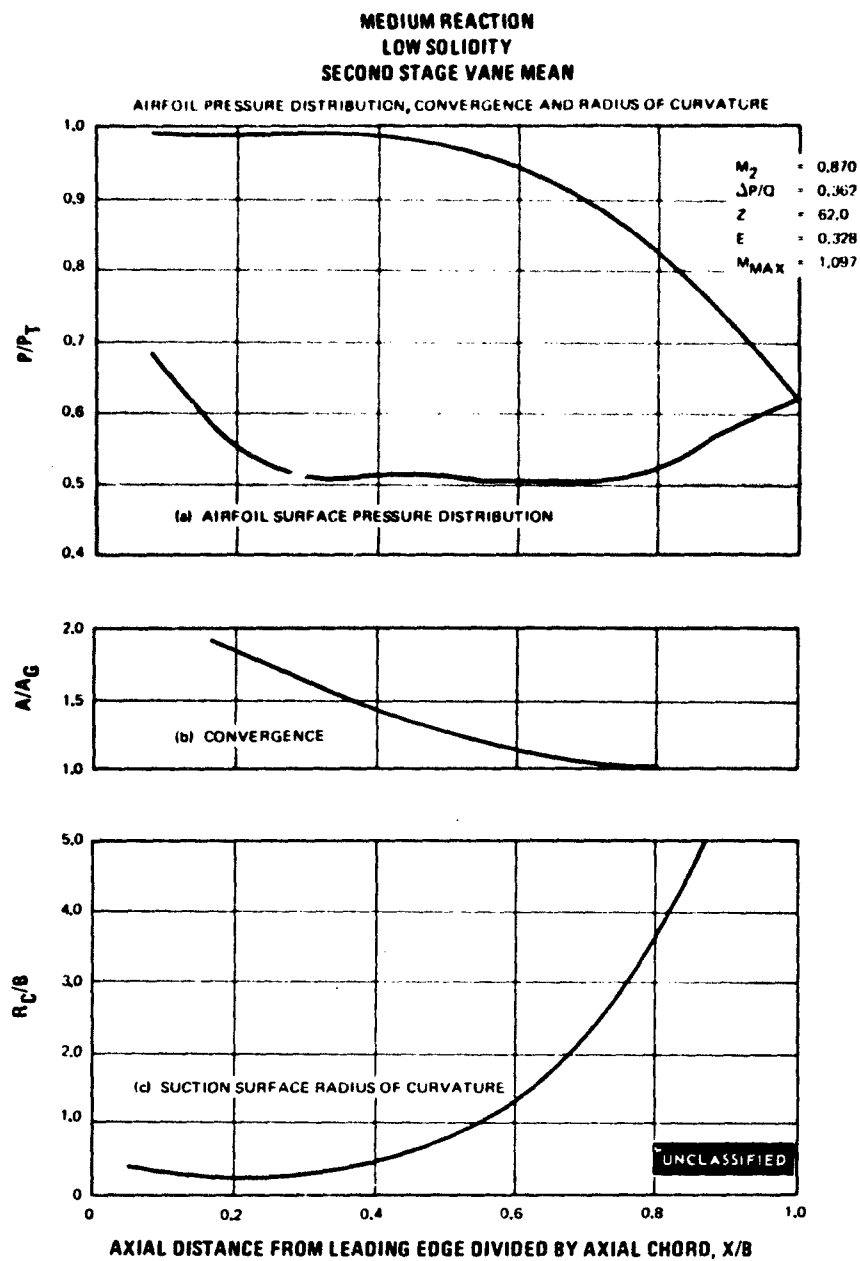


Figure 182

UNCLASSIFIED

UNCLASSIFIED

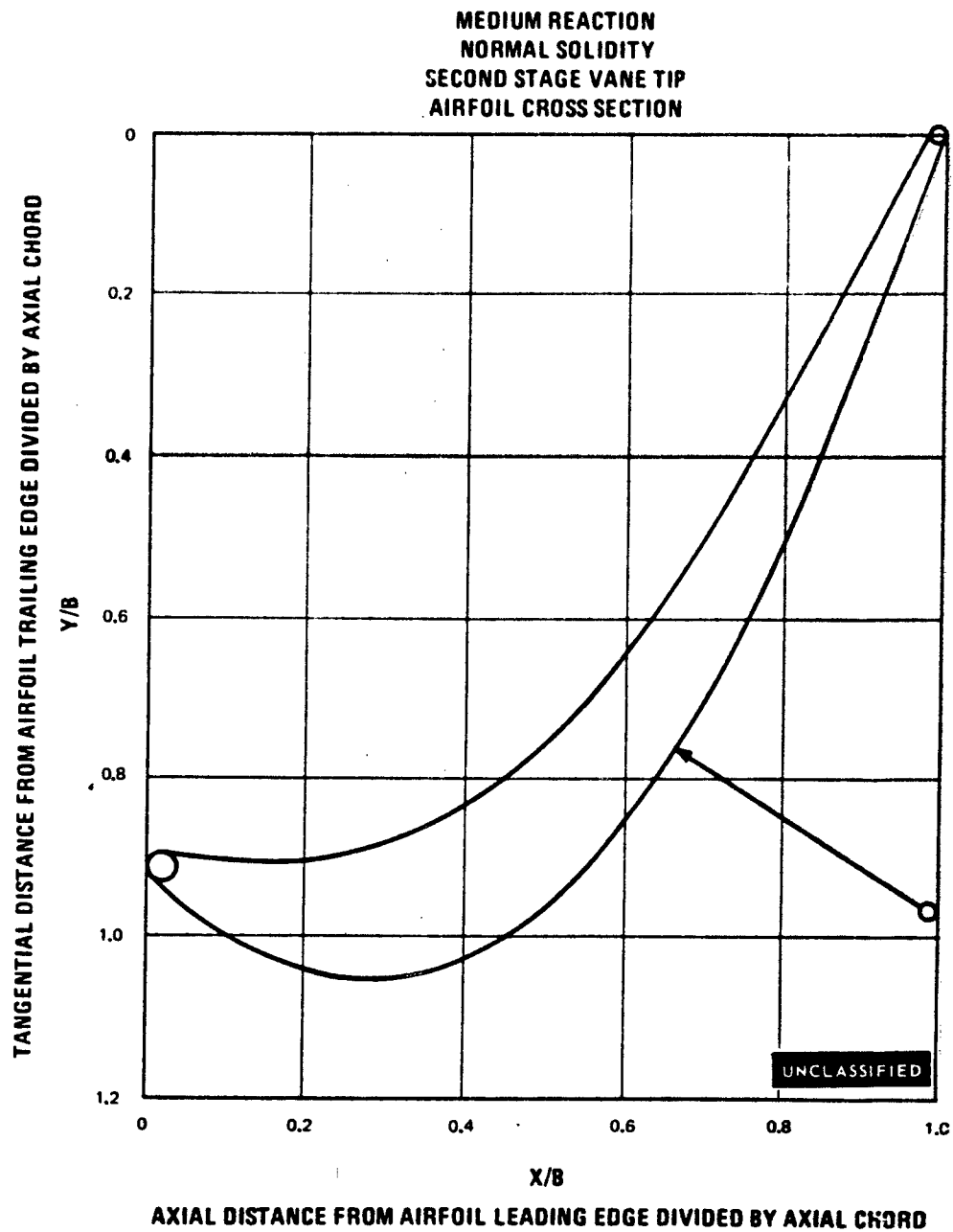


Figure 183

UNCLASSIFIED

UNCLASSIFIED

MEDIUM REACTION
NORMAL SOLIDITY
SECOND STAGE VANE TIP

AIRFOIL PRESSURE DISTRIBUTION, CONVERGENCE AND RADIUS OF CURVATURE

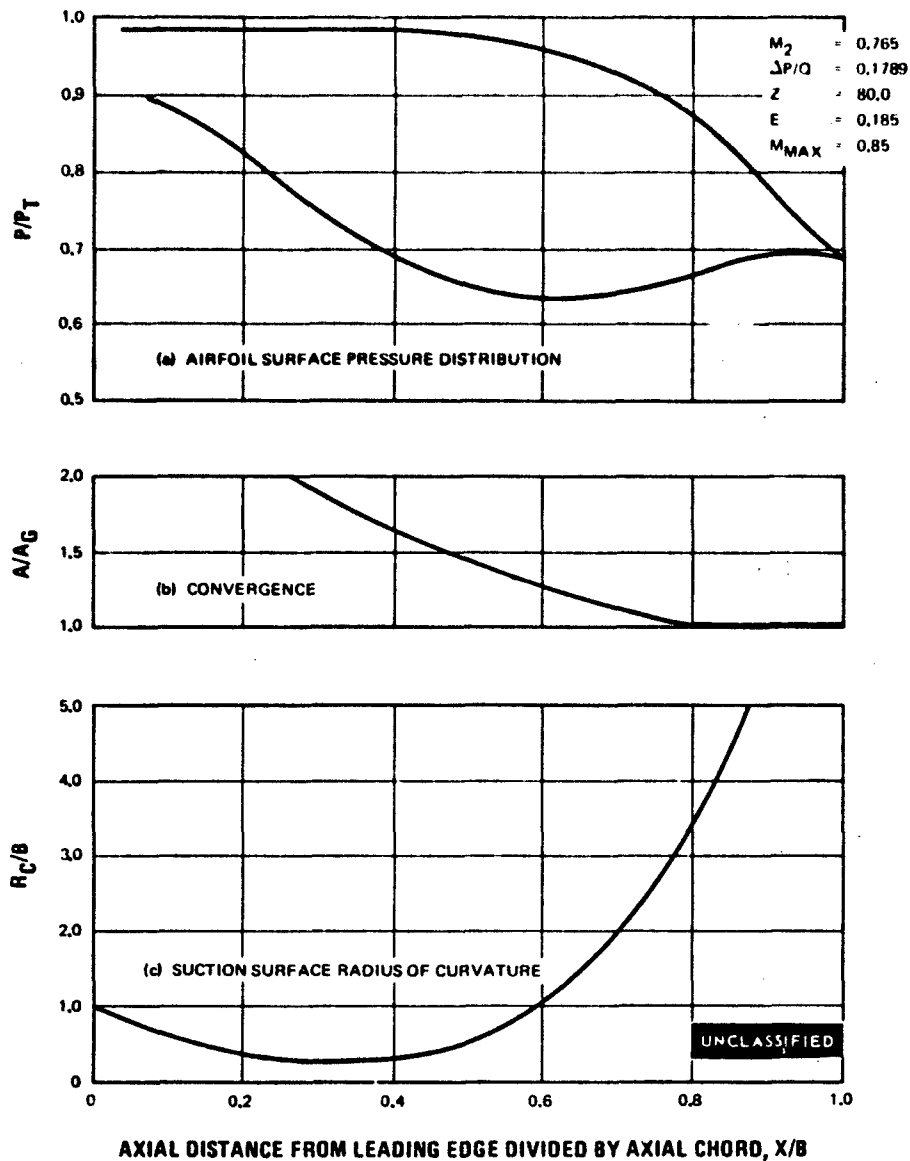


Figure 184

UNCLASSIFIED

UNCLASSIFIED

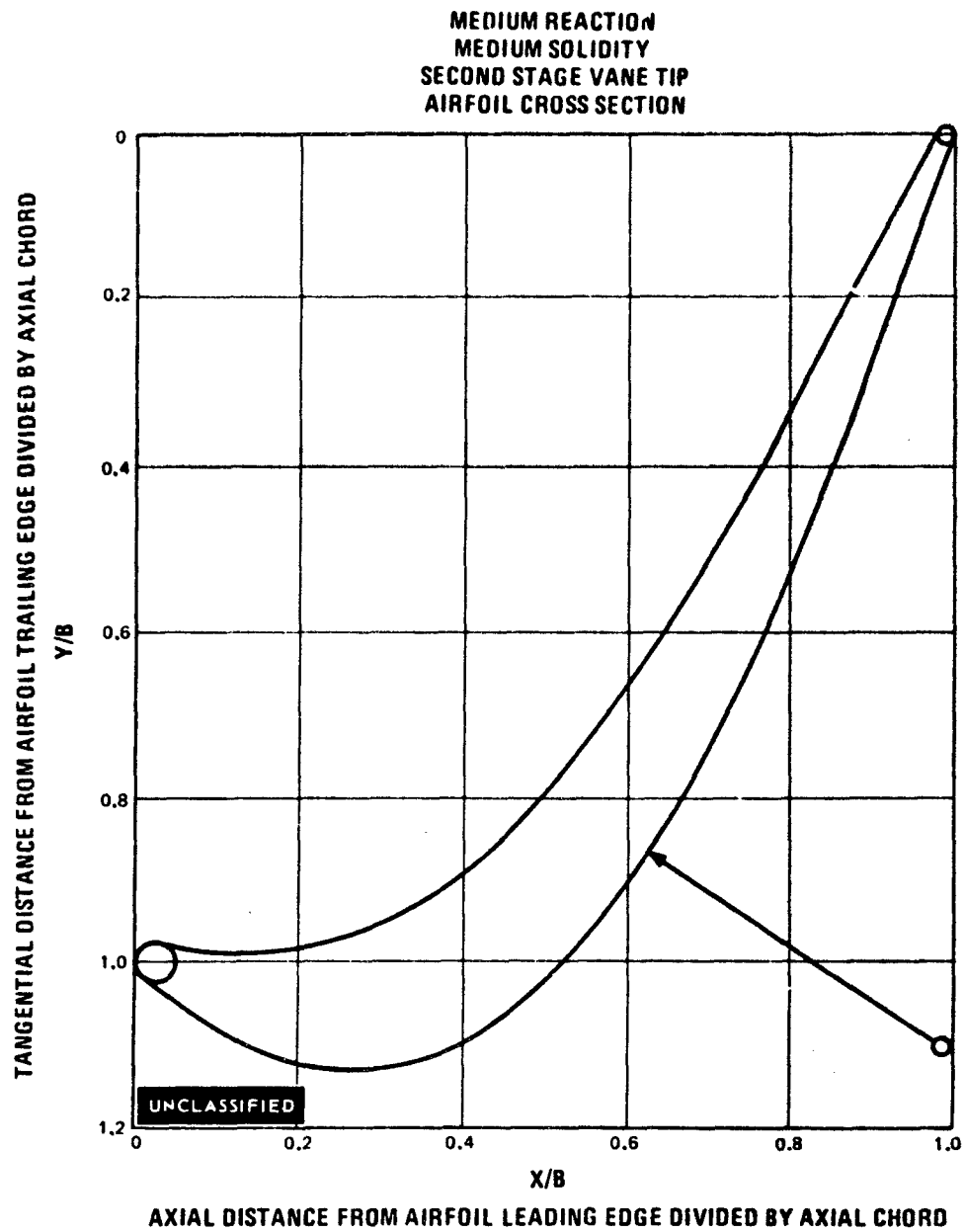


Figure 185

UNCLASSIFIED

UNCLASSIFIED

MEDIUM REACTION
MEDIUM SOLIDITY
SECOND STAGE VANE TIP

AIRFOIL PRESSURE DISTRIBUTION, CONVERGENCE AND RADIUS OF CURVATURE

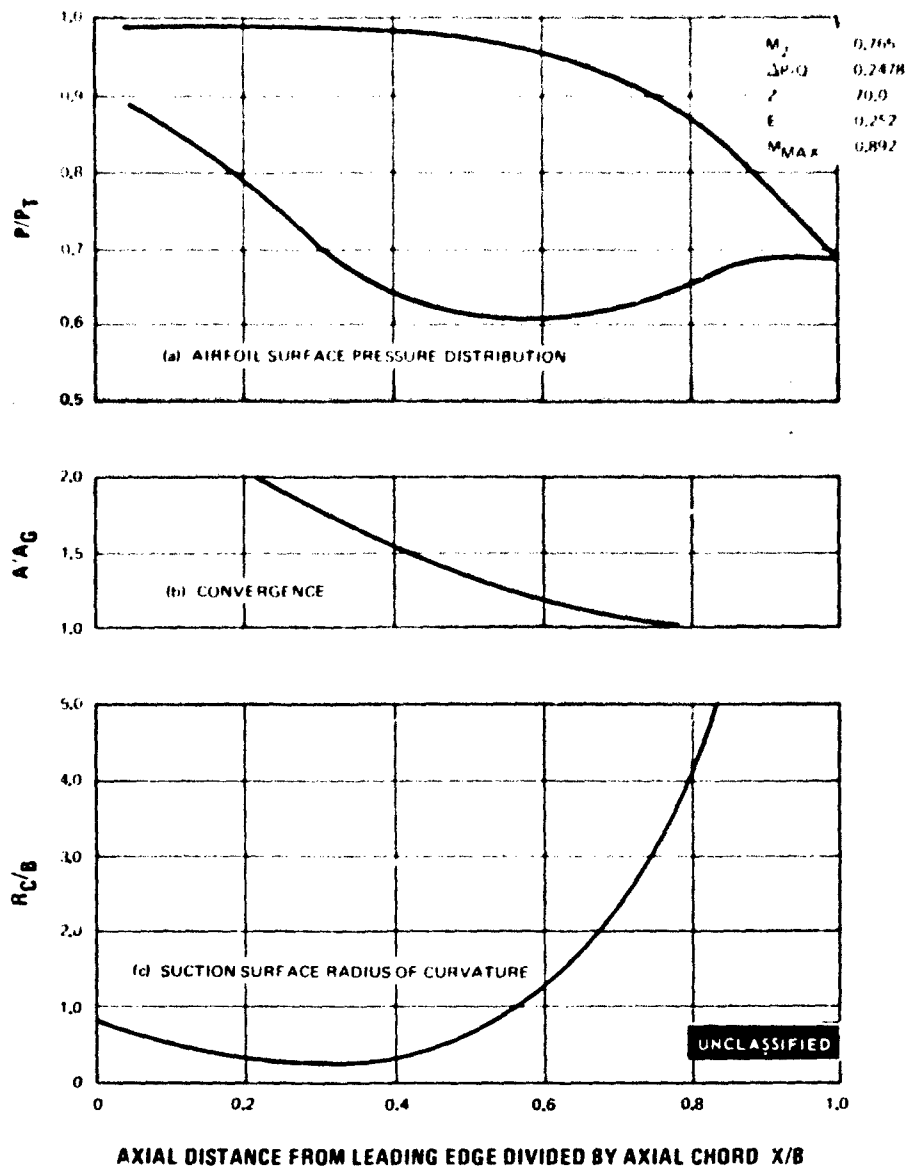


Figure 186

UNCLASSIFIED

UNCLASSIFIED

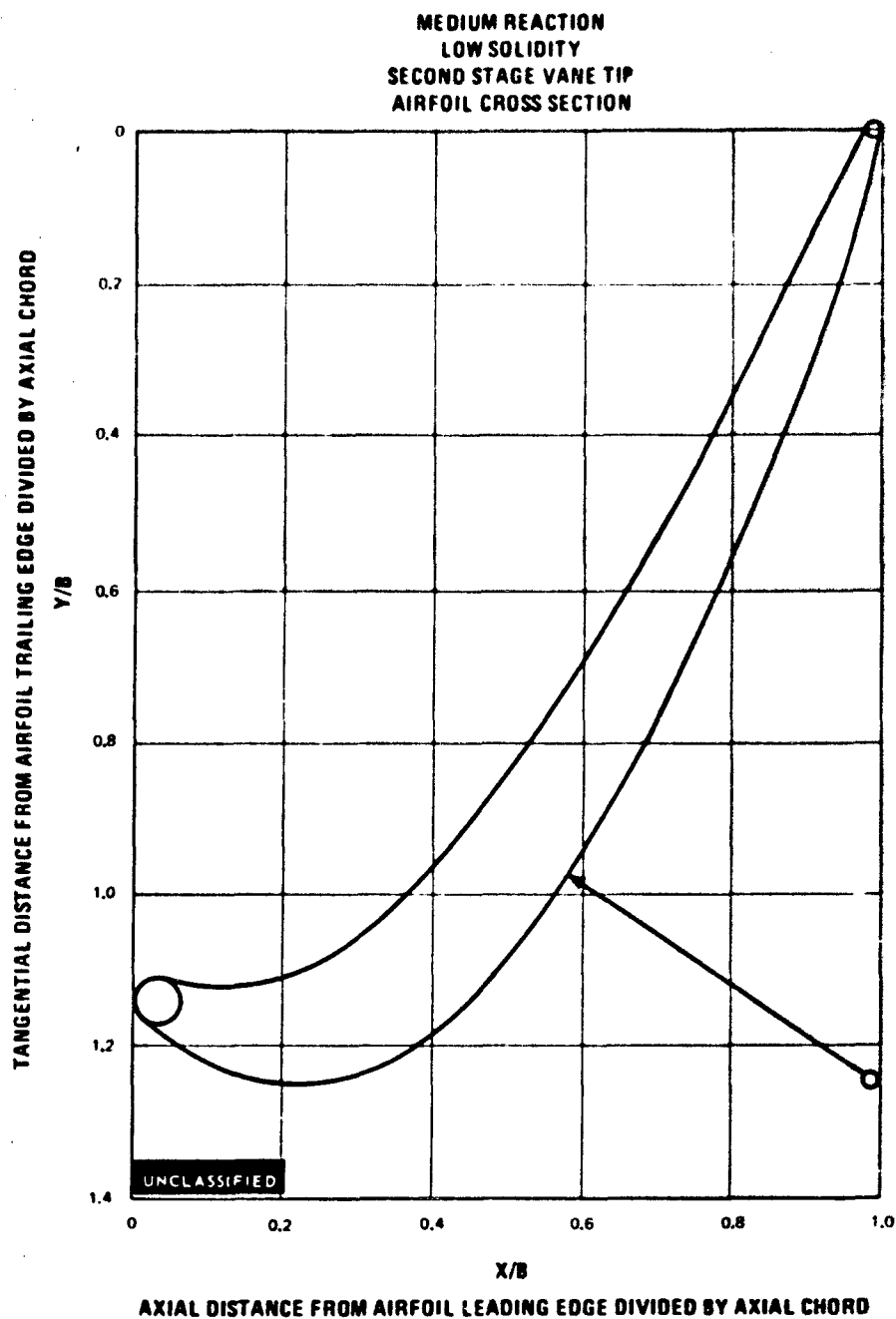


Figure 187

UNCLASSIFIED

UNCLASSIFIED

MEDIUM REACTION
LOW SOLIDITY
SECOND STAGE VANE TIP

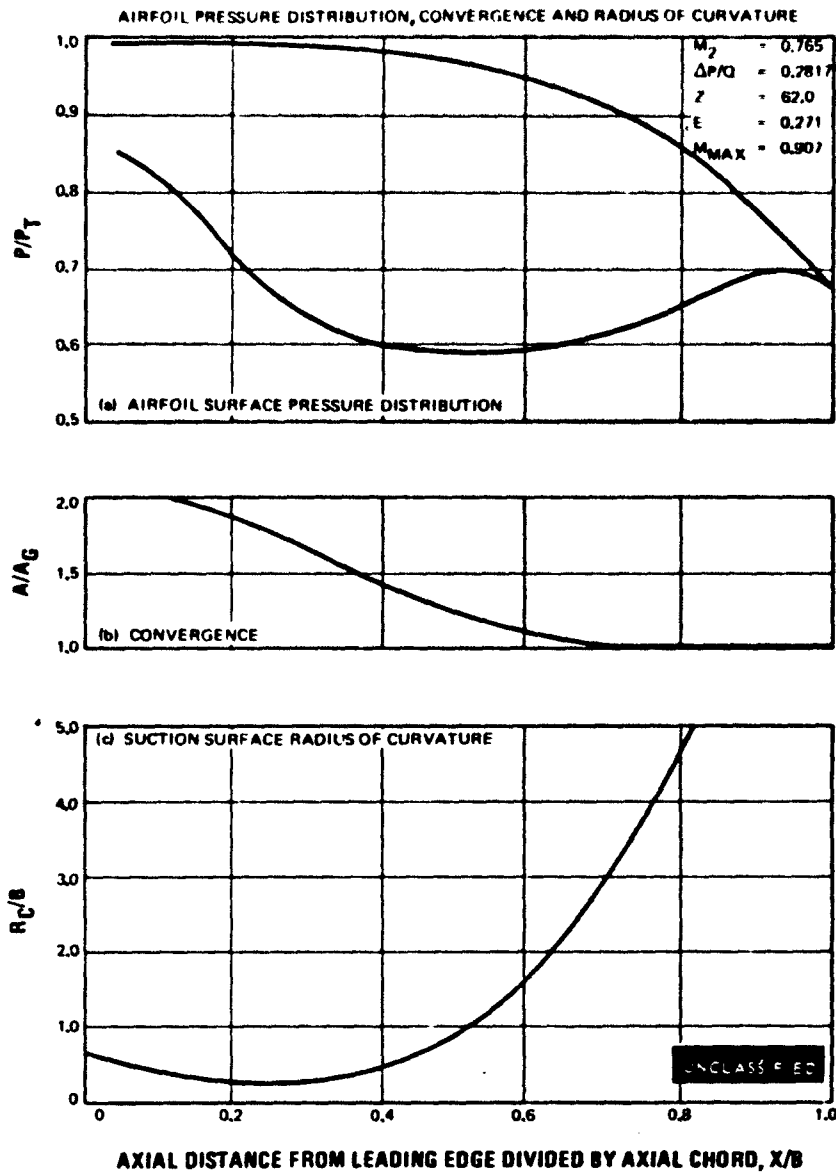


Figure 188

UNCLASSIFIED

UNCLASSIFIED

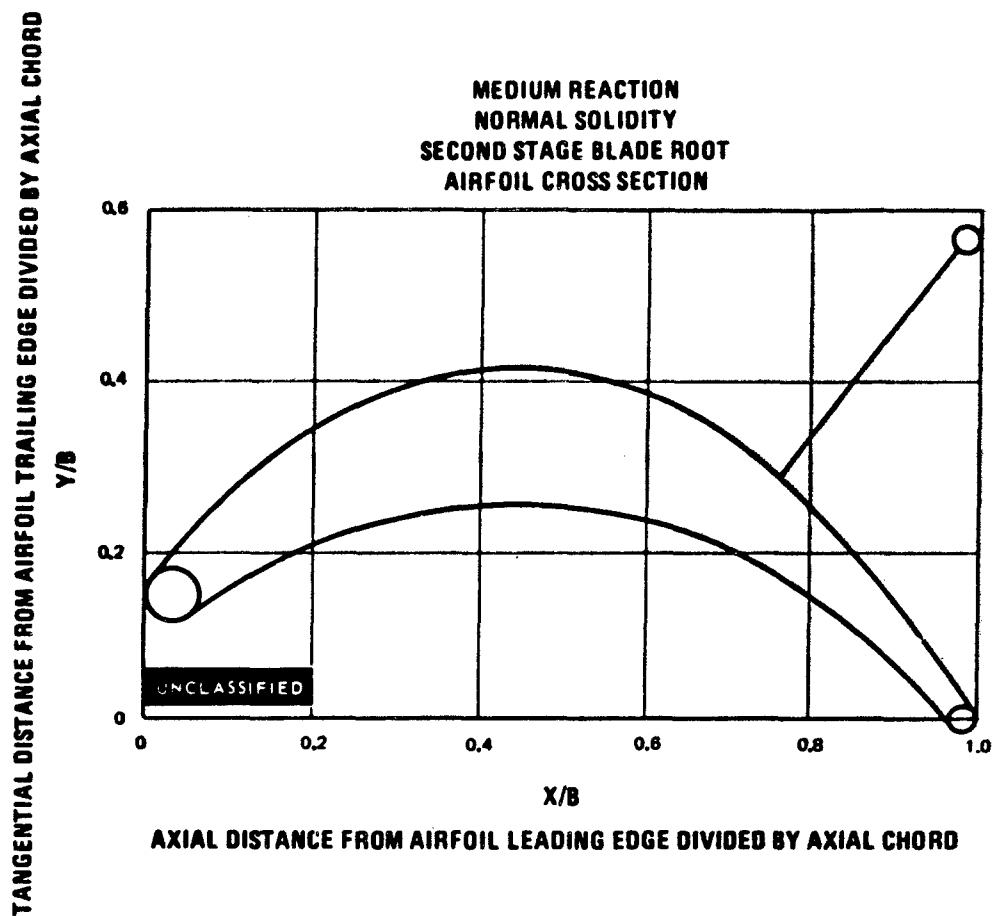


Figure 189

UNCLASSIFIED

UNCLASSIFIED

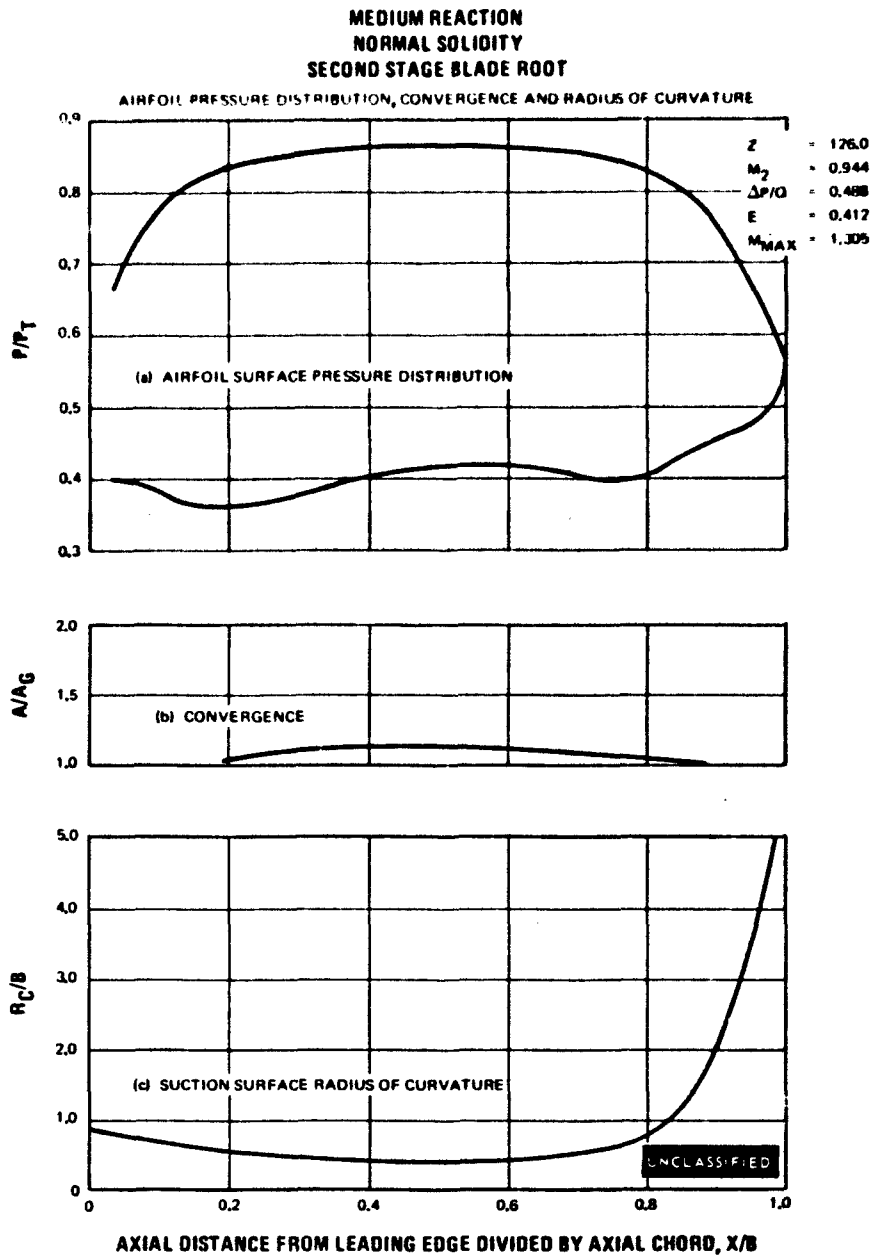


Figure 190

UNCLASSIFIED

UNCLASSIFIED

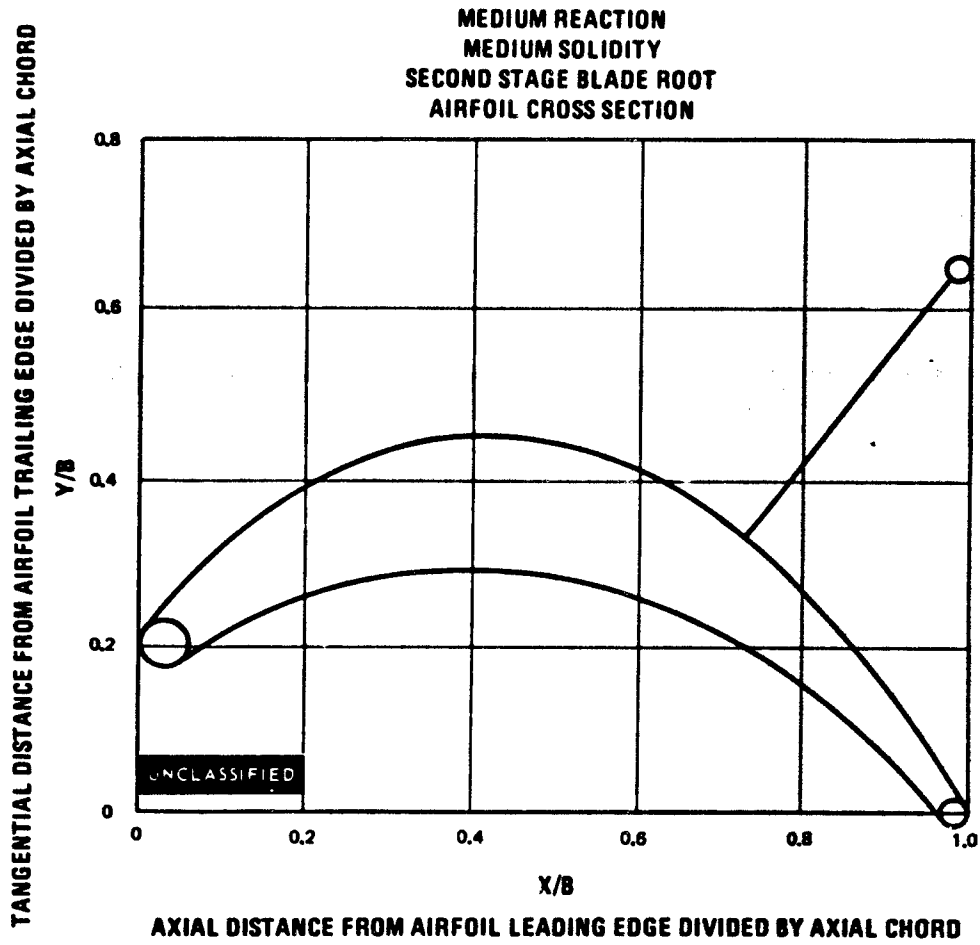


Figure 191

UNCLASSIFIED

UNCLASSIFIED

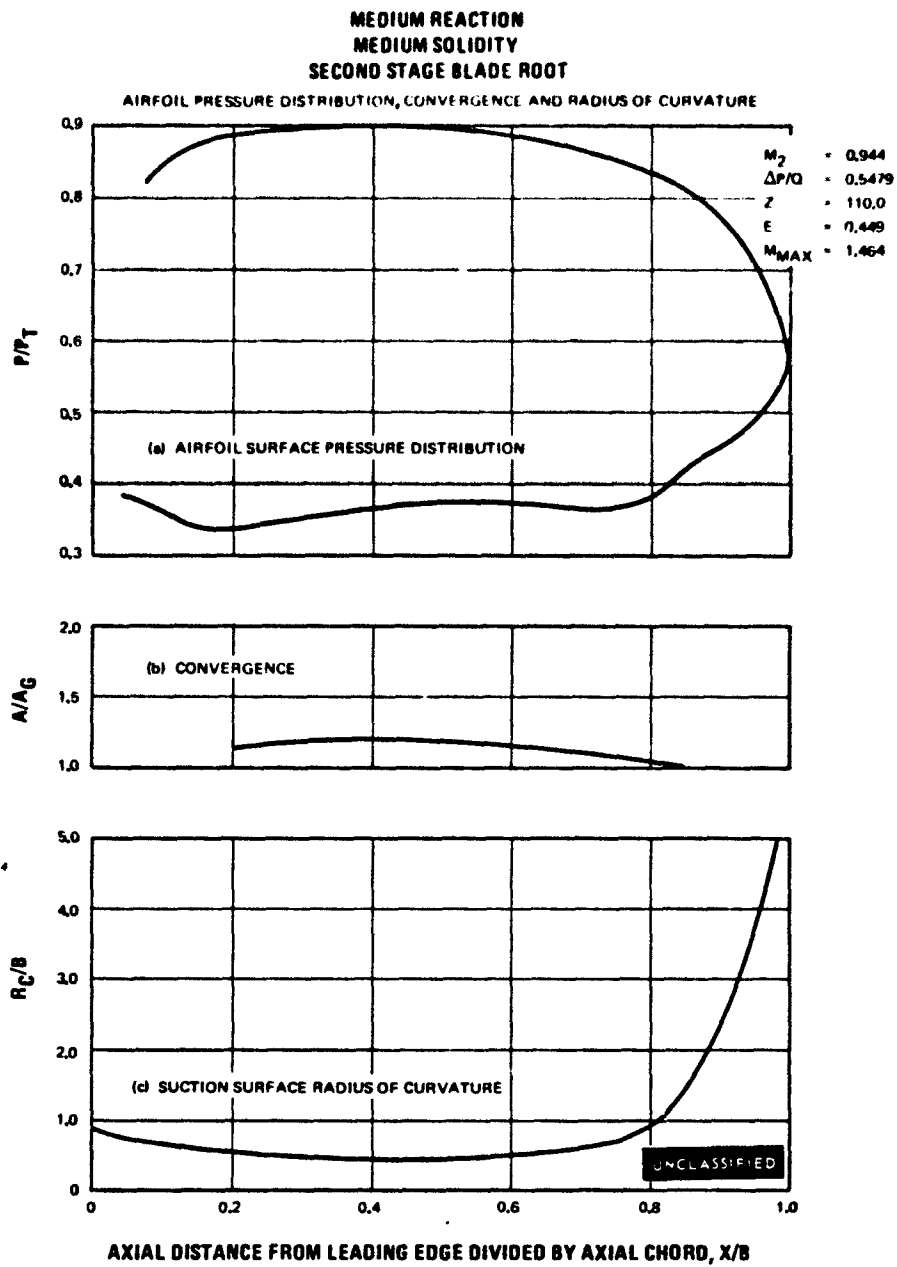


Figure 192

UNCLASSIFIED

UNCLASSIFIED

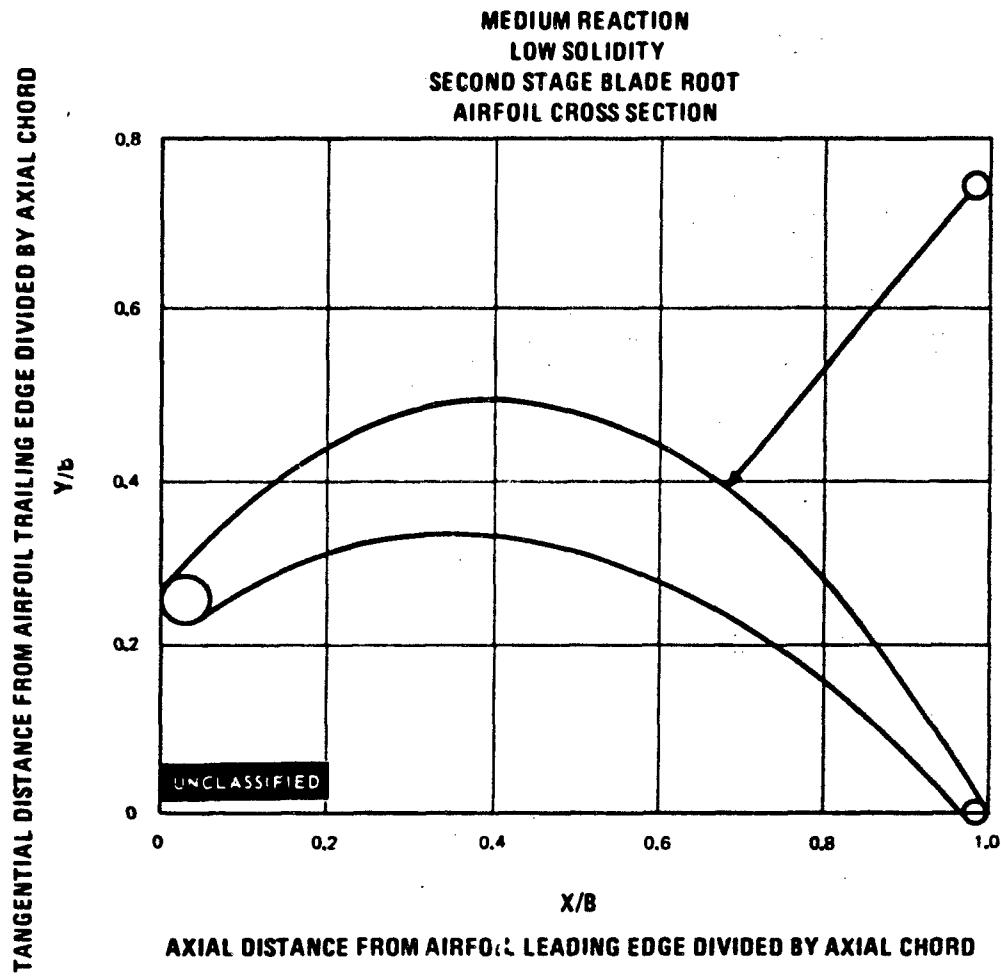


Figure 193

UNCLASSIFIED

UNCLASSIFIED

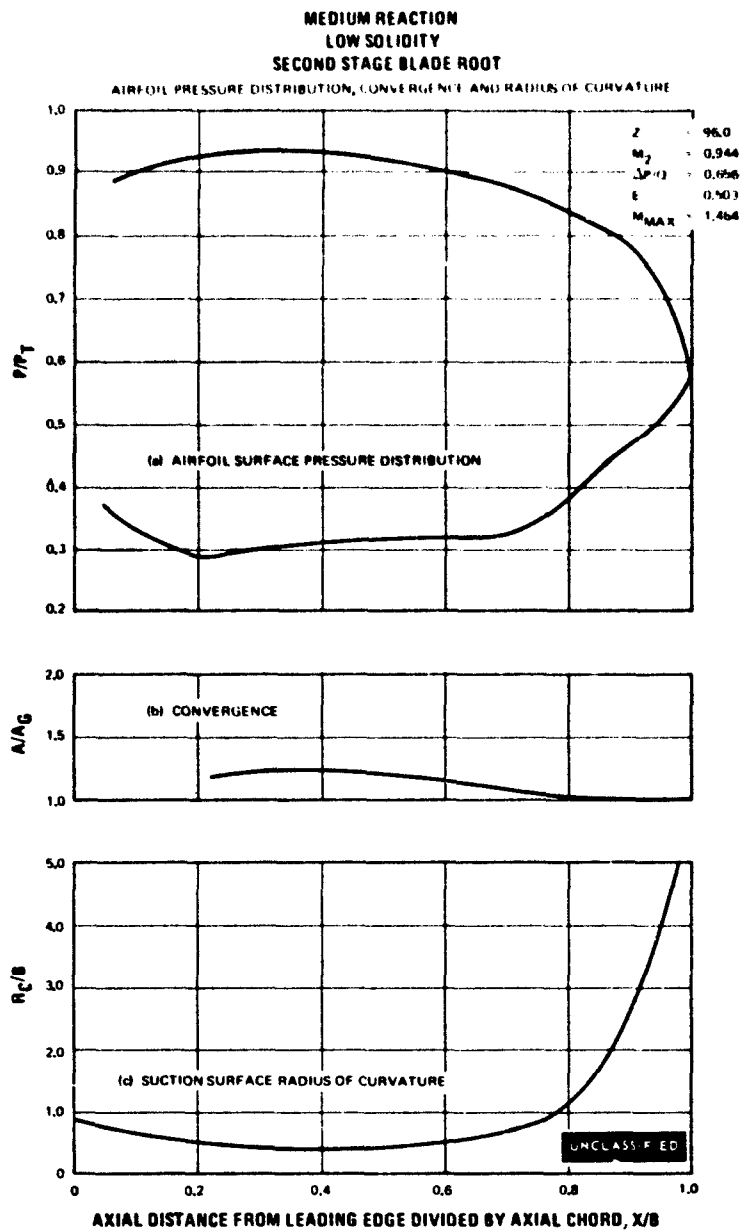


Figure 194

UNCLASSIFIED

UNCLASSIFIED

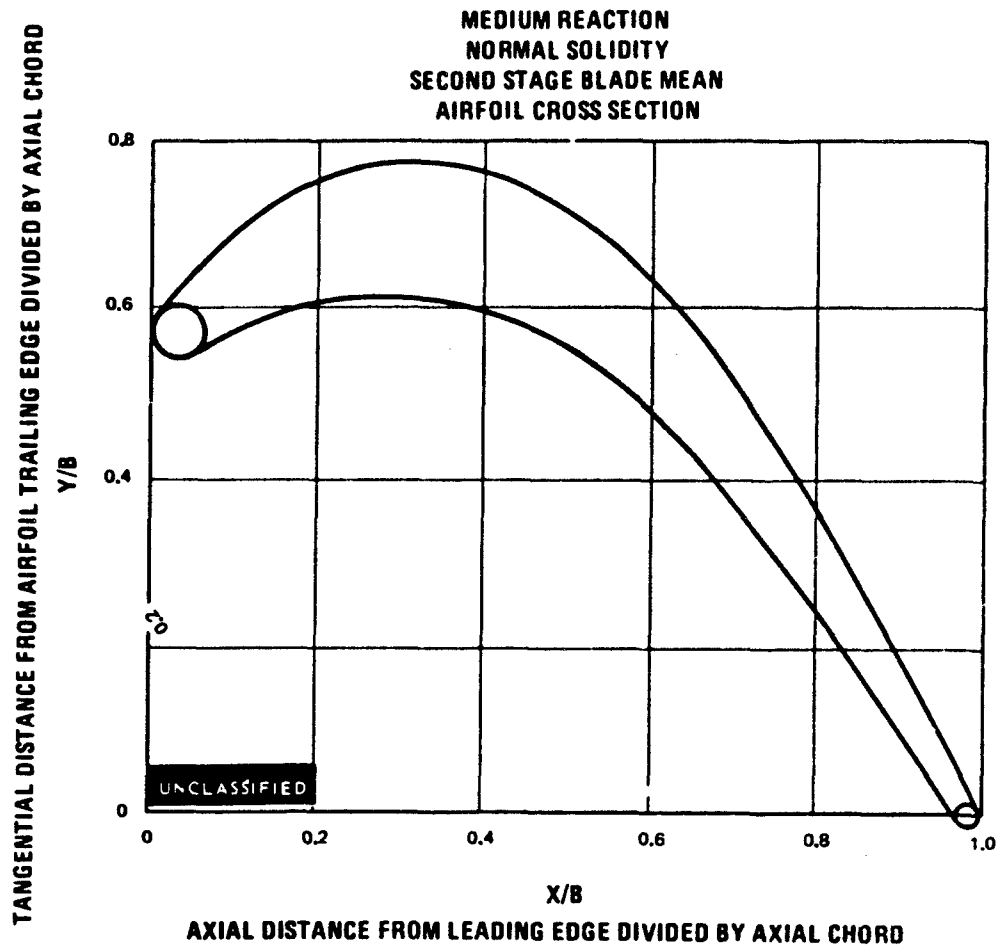


Figure 195

UNCLASSIFIED

UNCLASSIFIED

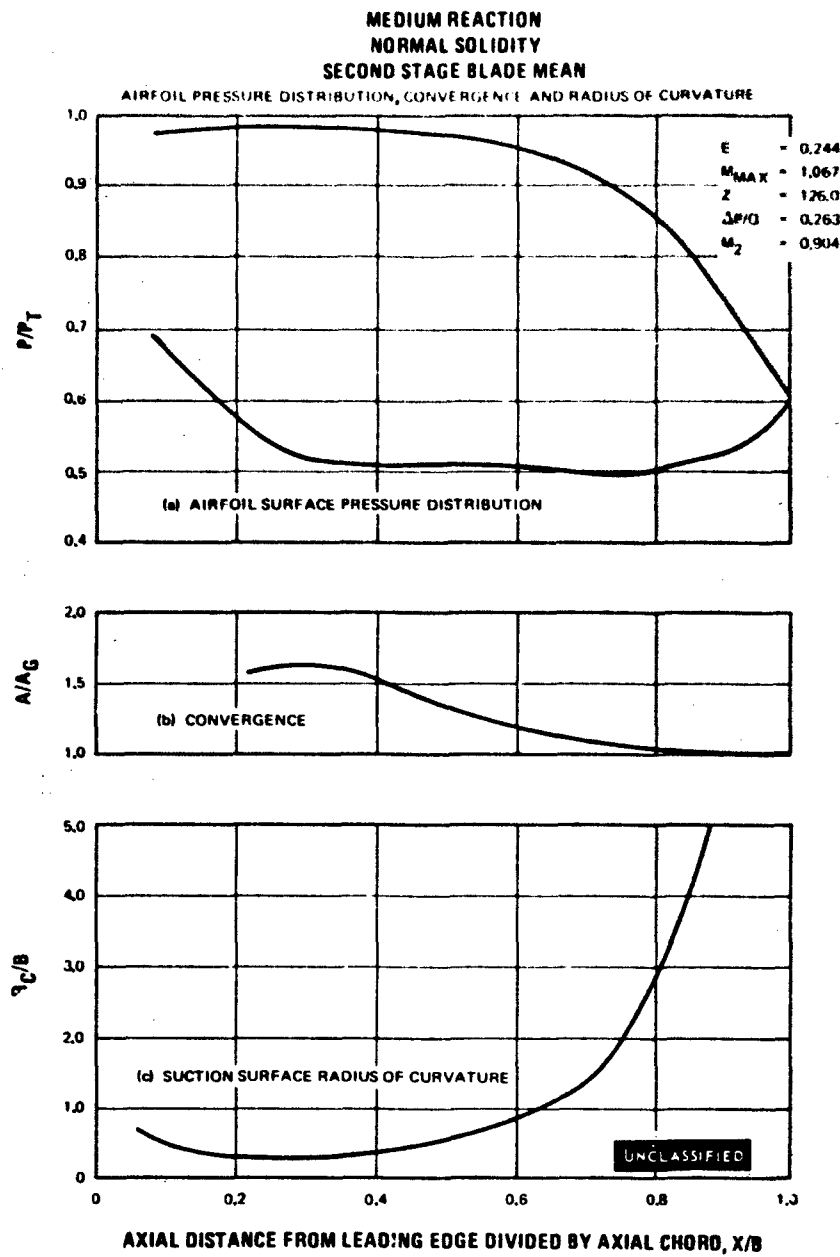


Figure 196

UNCLASSIFIED

UNCLASSIFIED

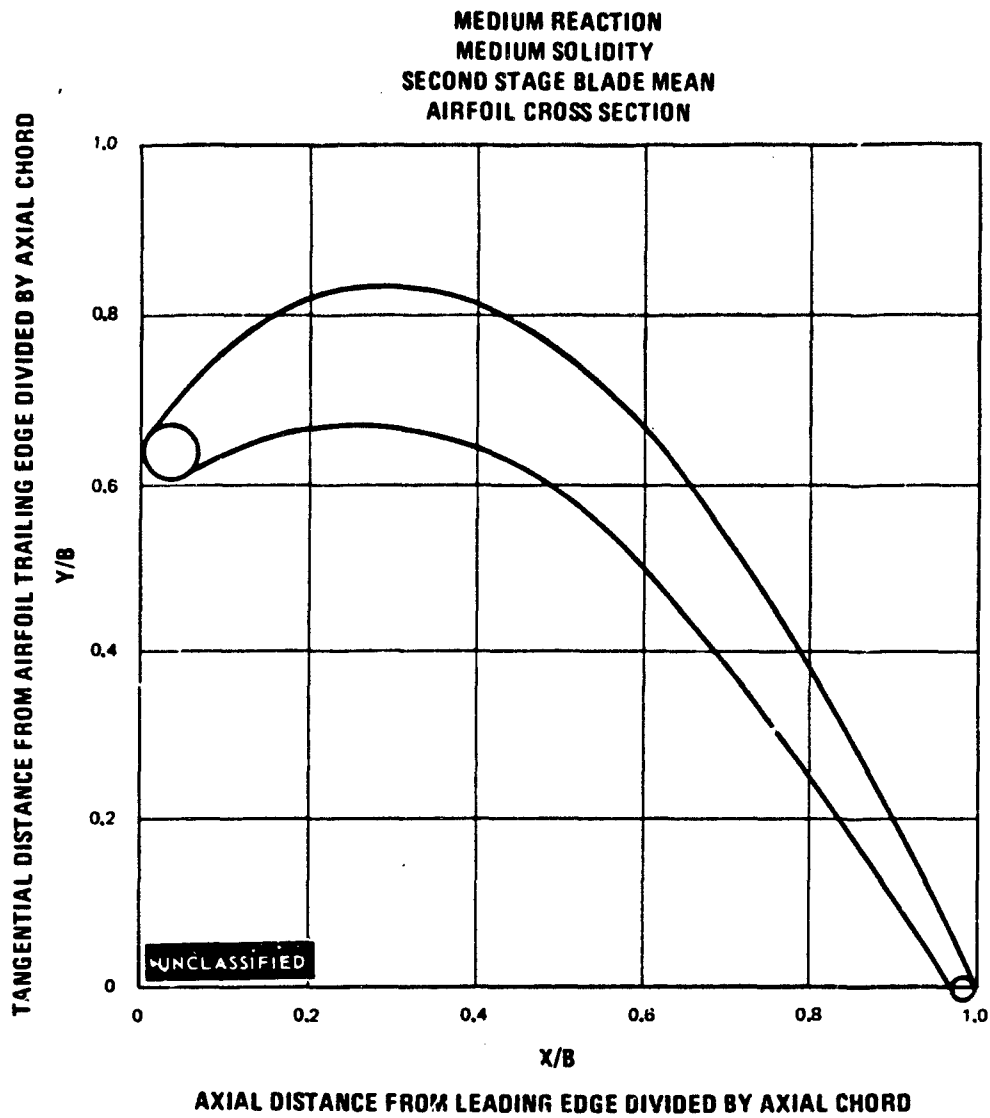


Figure 197

UNCLASSIFIED

UNCLASSIFIED

MEDIUM REACTION
MEDIUM SOLIDITY
SECOND STAGE BLADE MEAN

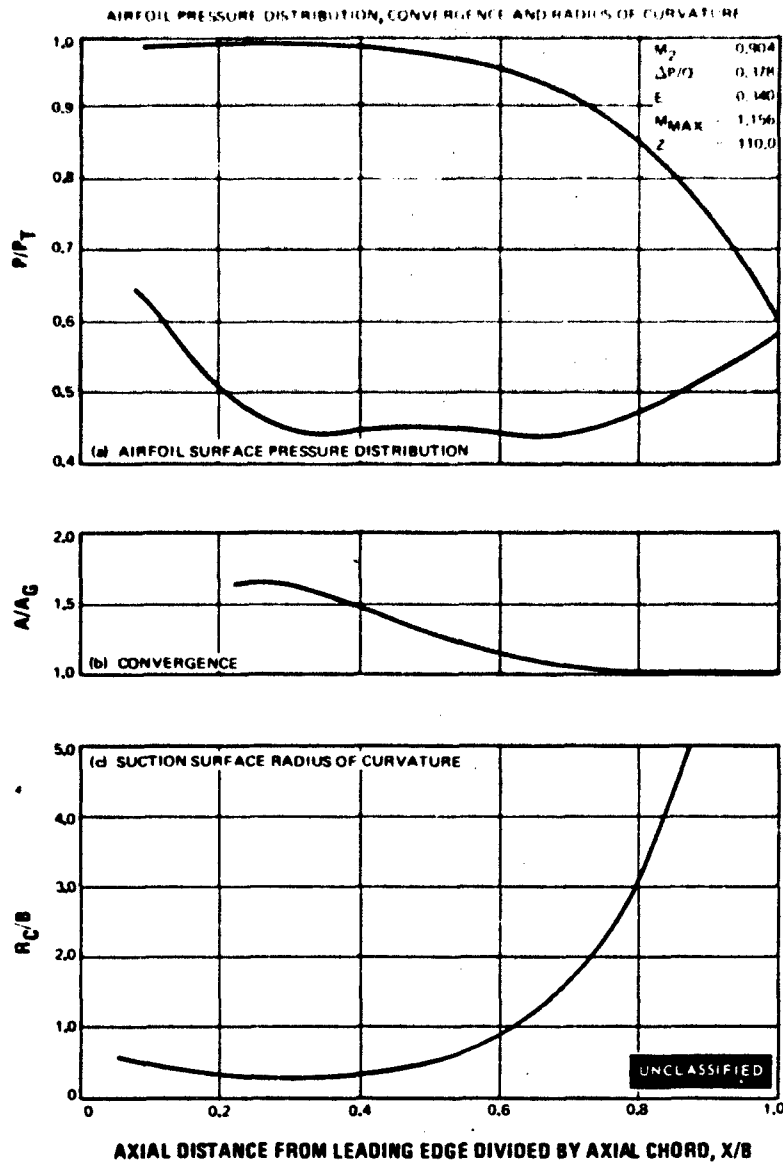


Figure 198

UNCLASSIFIED

UNCLASSIFIED

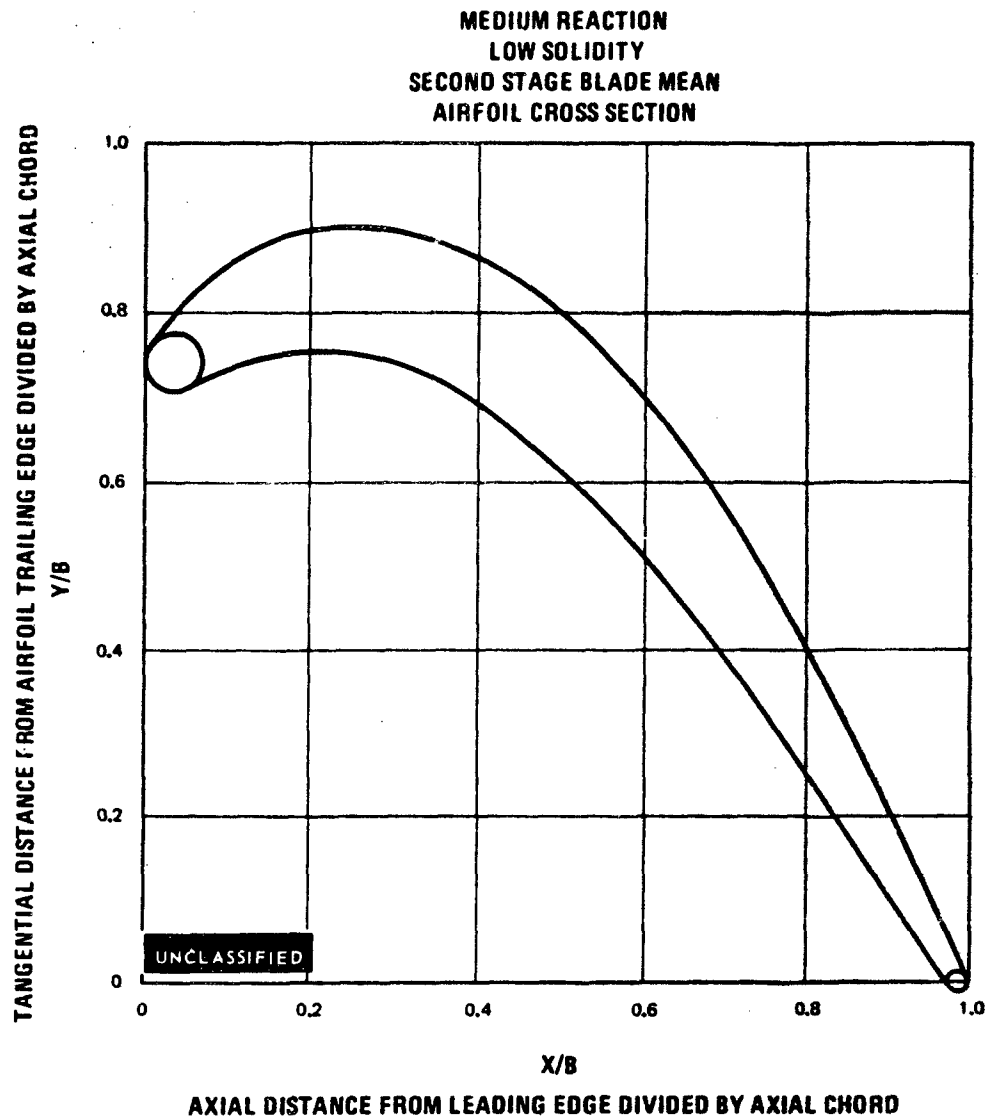


Figure 199

UNCLASSIFIED

UNCLASSIFIED

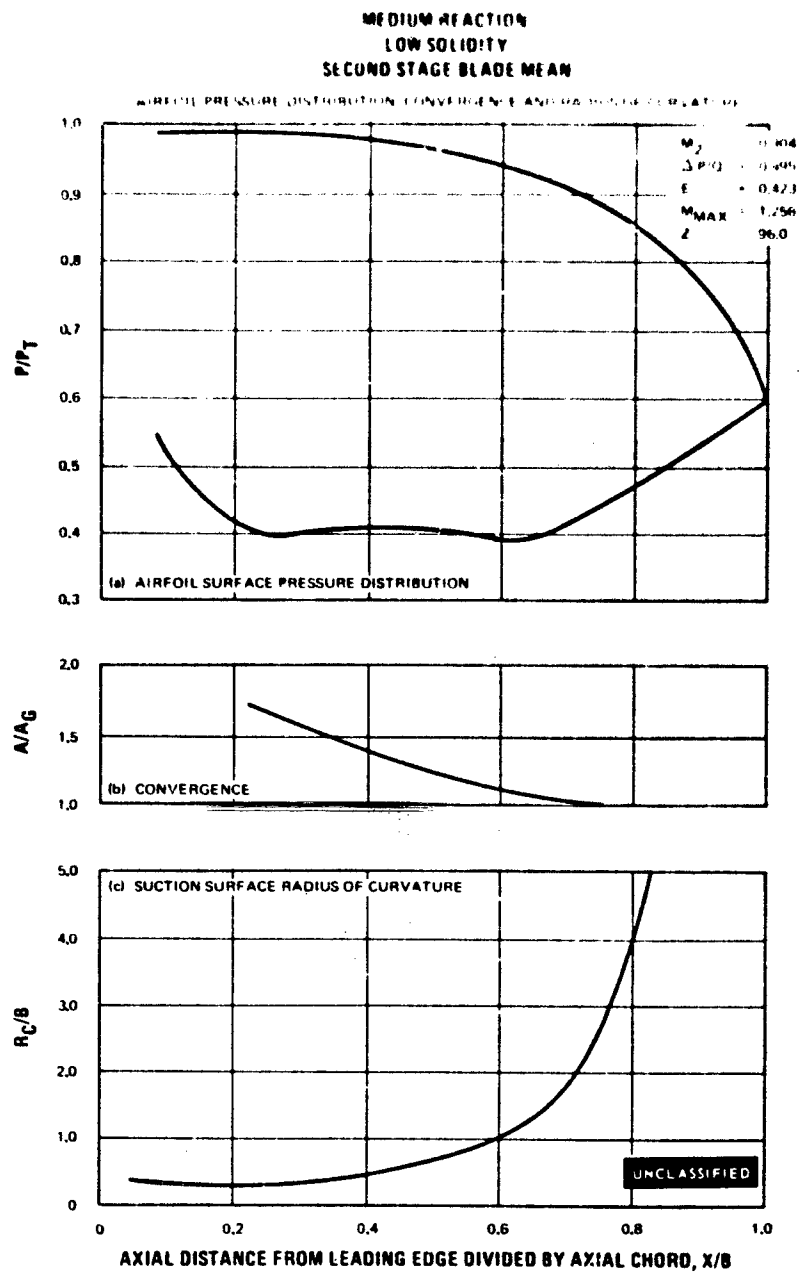


Figure 200

UNCLASSIFIED

UNCLASSIFIED

MEDIUM REACTION
NORMAL SOLIDITY
SECOND STAGE BLADE TIP
AIRFOIL CROSS SECTION

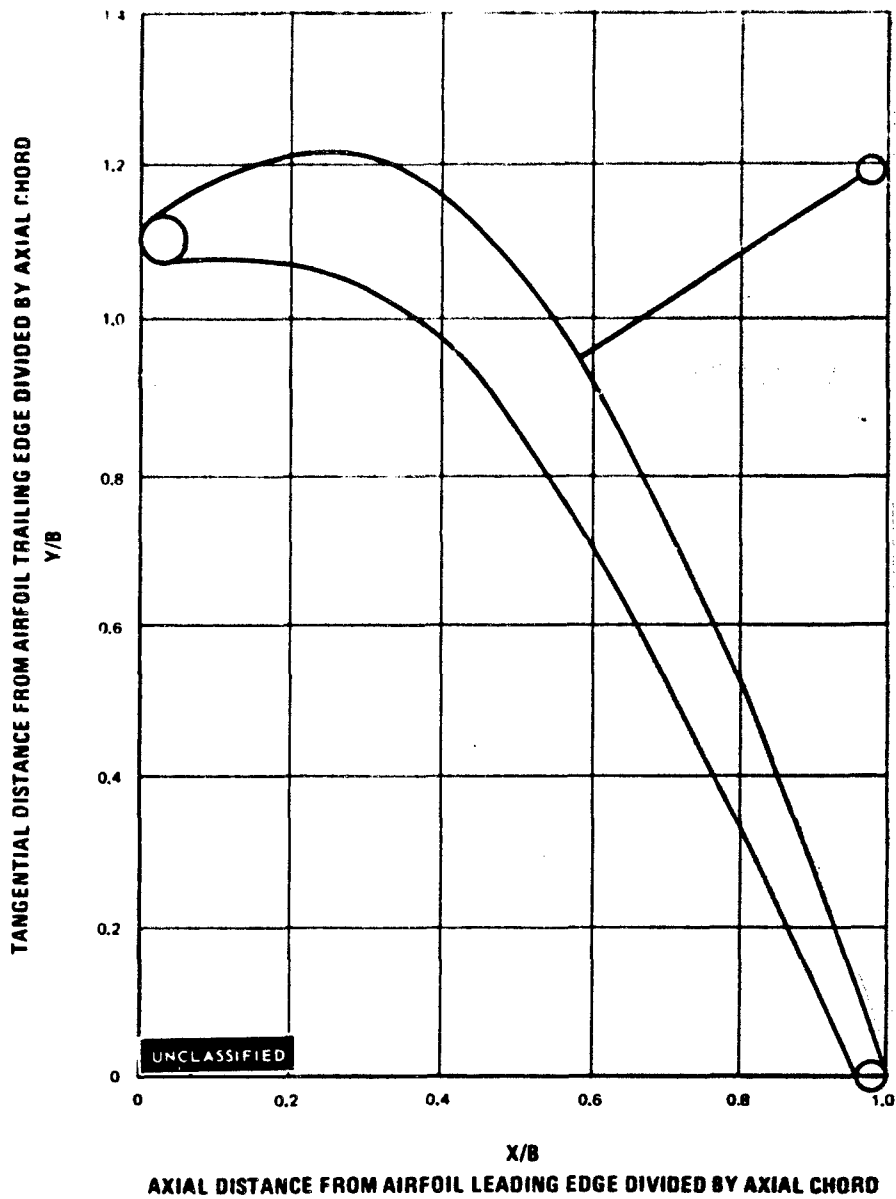


Figure 201

UNCLASSIFIED

UNCLASSIFIED

MEDIUM REACTION
NORMAL SOLIDITY
SECOND STAGE BLADE TIP

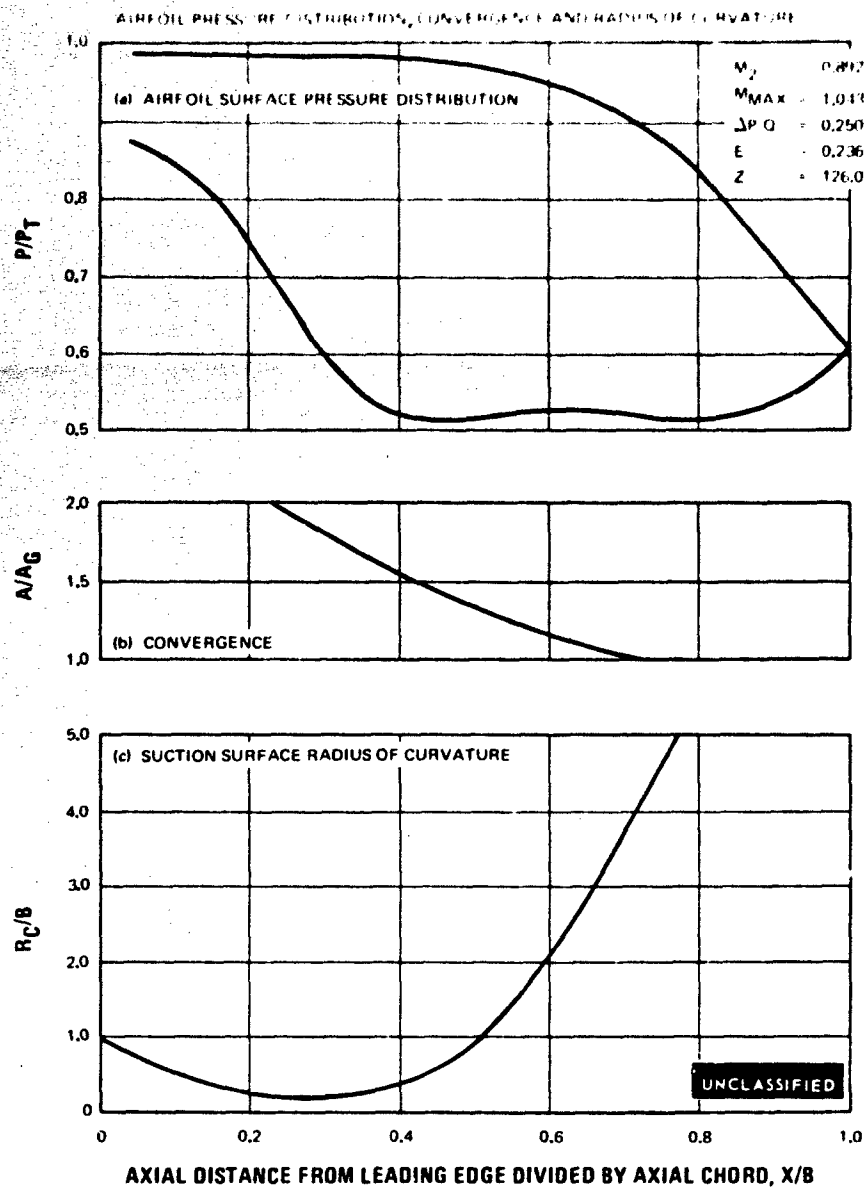


Figure 202

UNCLASSIFIED

UNCLASSIFIED

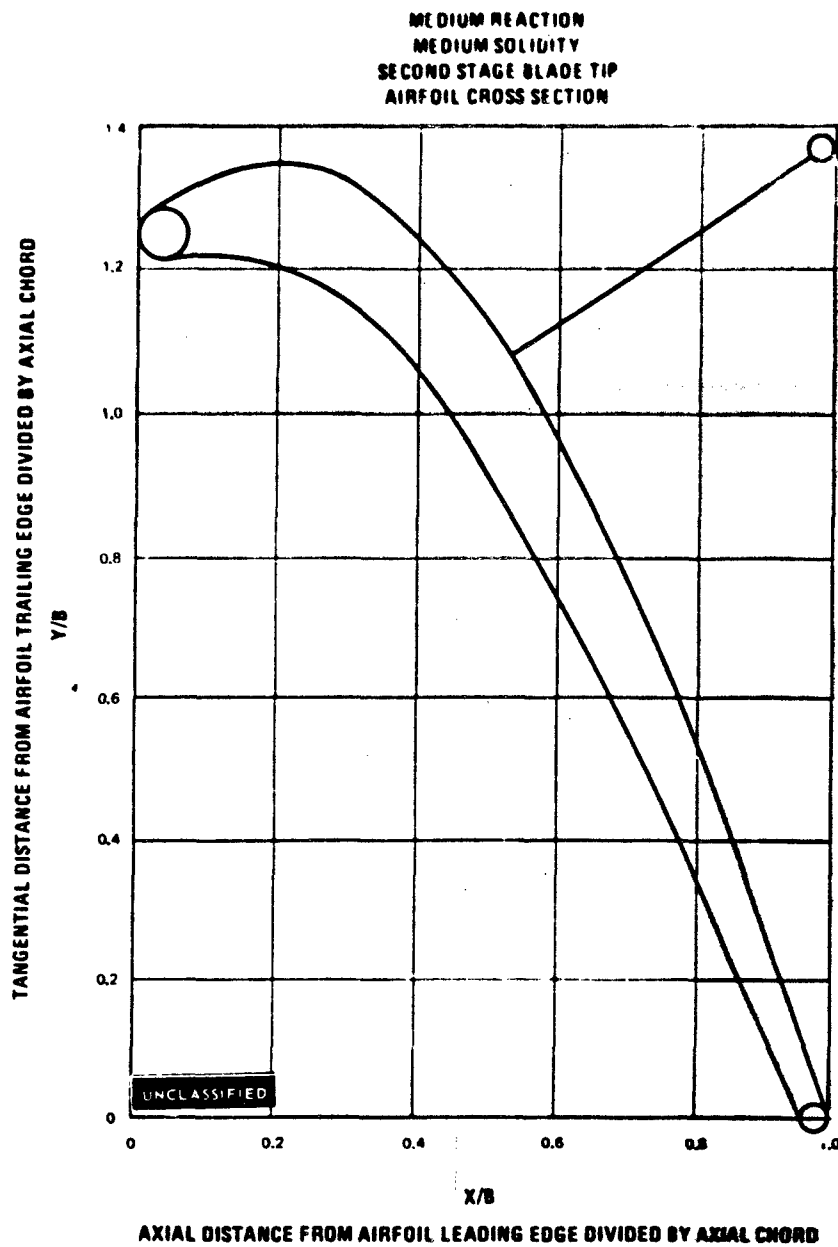


Figure 203

UNCLASSIFIED

UNCLASSIFIED

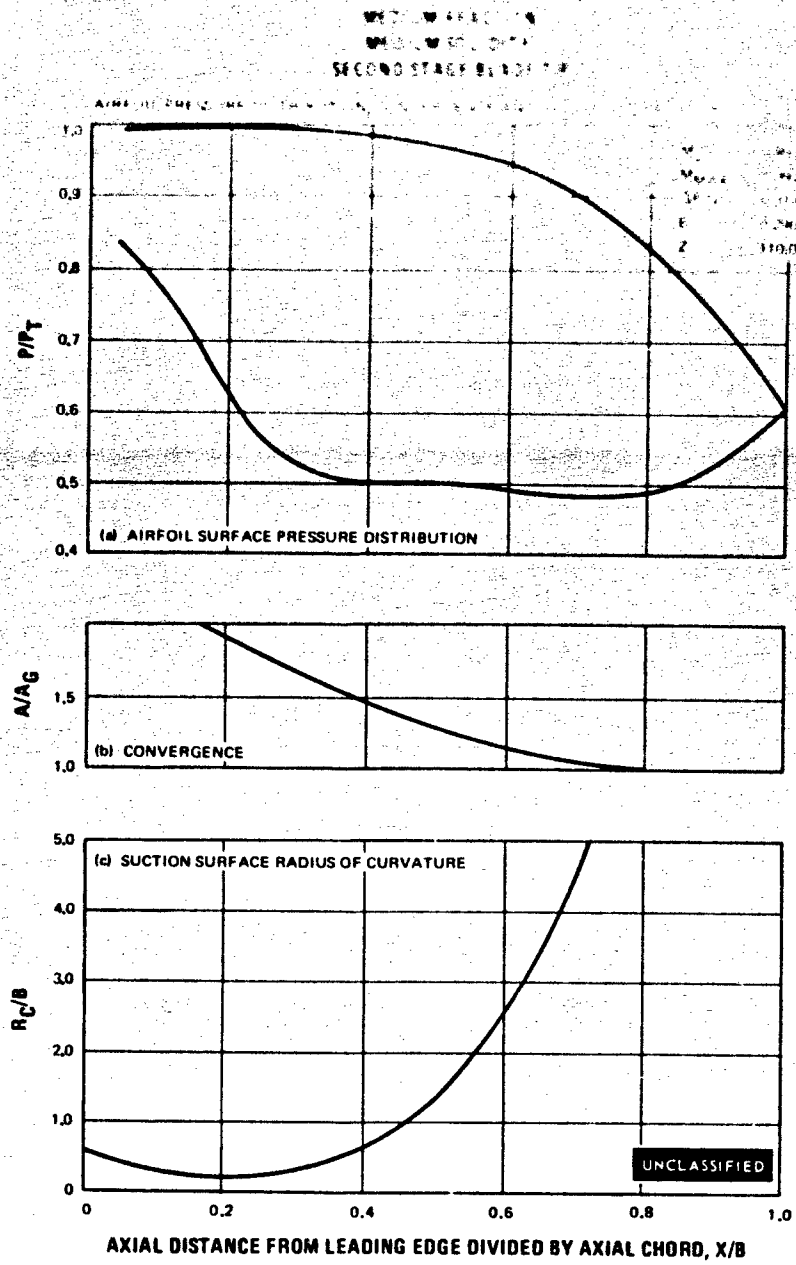


Figure 204

UNCLASSIFIED

UNCLASSIFIED

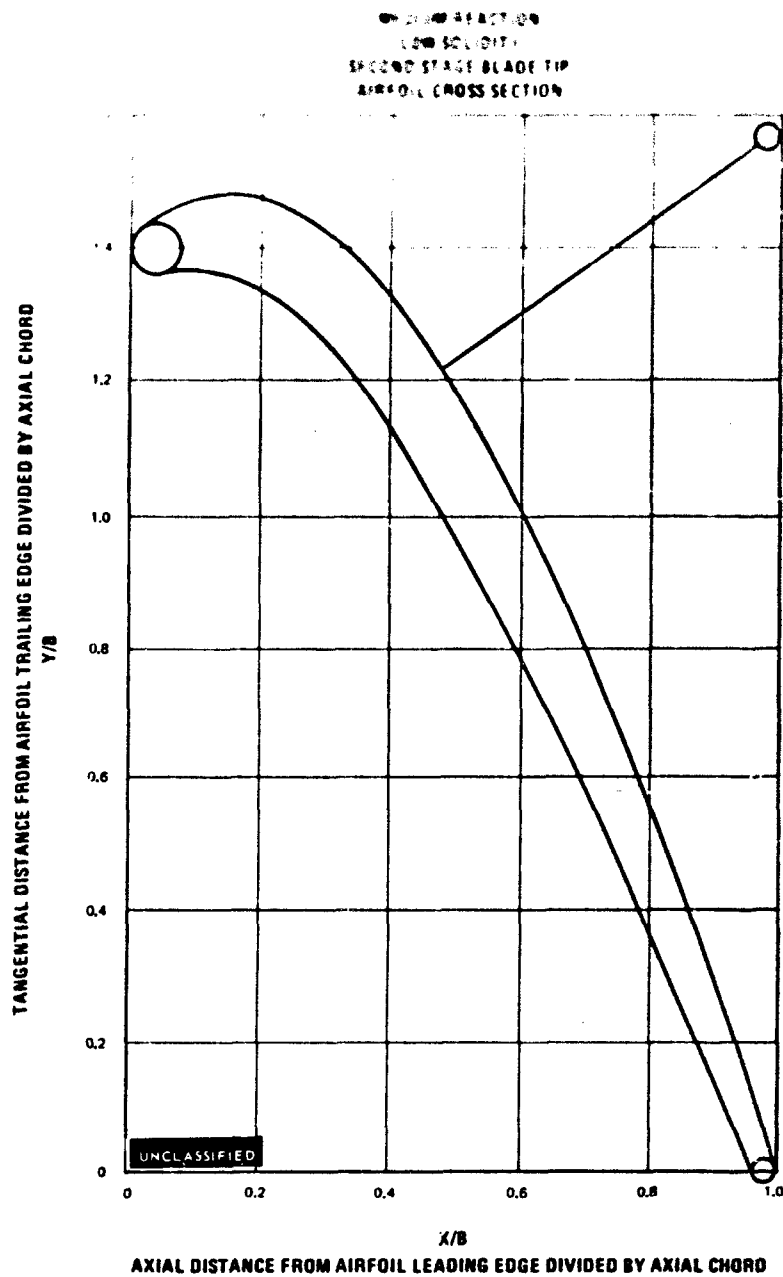


Figure 205

UNCLASSIFIED

UNCLASSIFIED

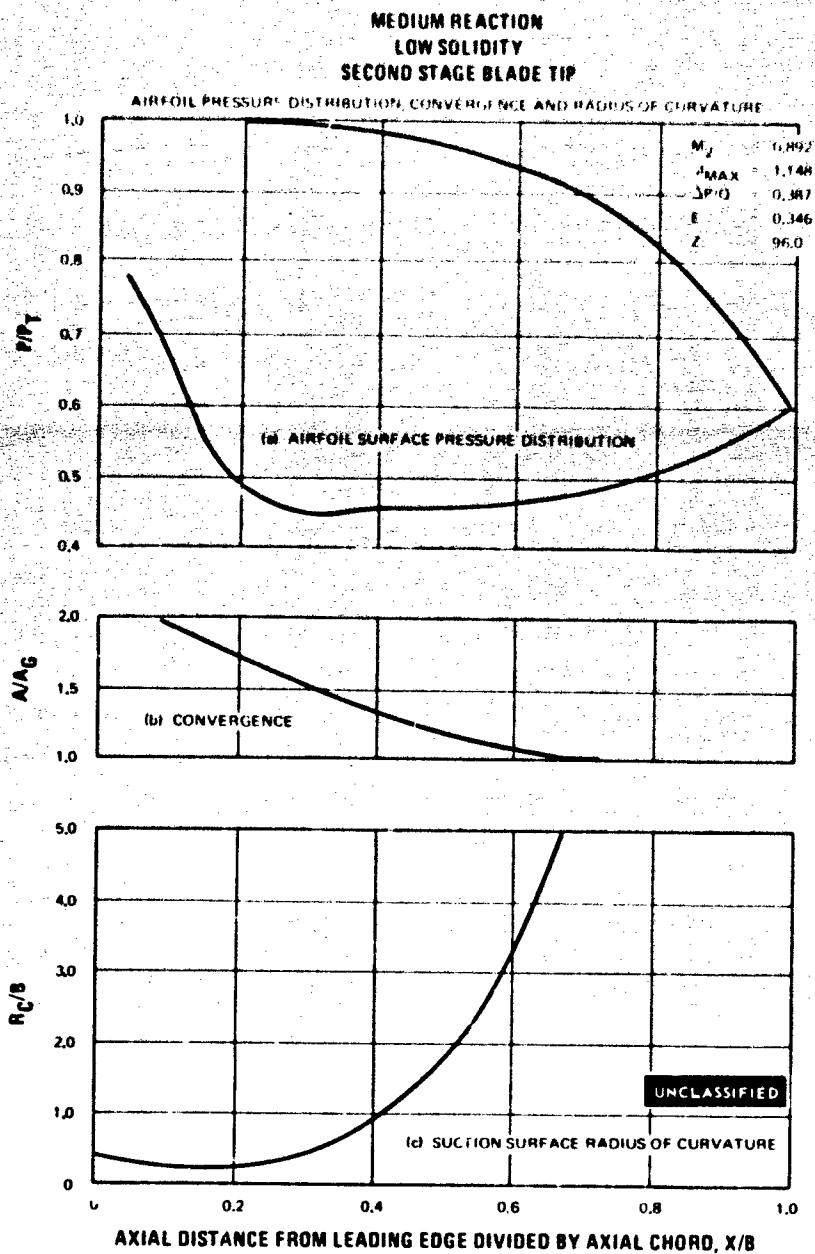


Figure 206

(The reverse of this page is blank)

UNCLASSIFIED

UNCLASSIFIED

APPENDIX II
FINAL AIRFOIL SECTIONS

PAGE NO 245

UNCLASSIFIED

UNCLASSIFIED

MEDIUM REACTION
LOW SOLIDITY
FIRST STAGE VANE ROOT
AIRFOIL CROSS SECTION

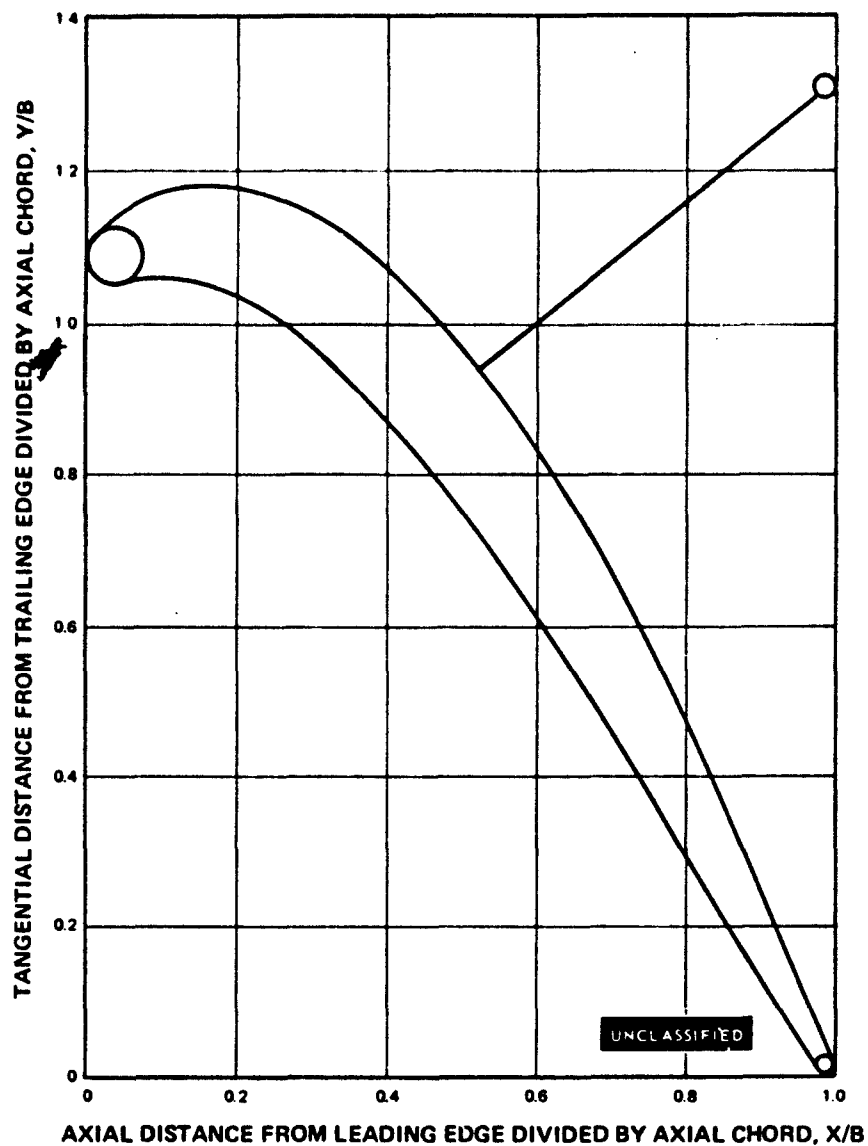


Figure 207

UNCLASSIFIED

UNCLASSIFIED

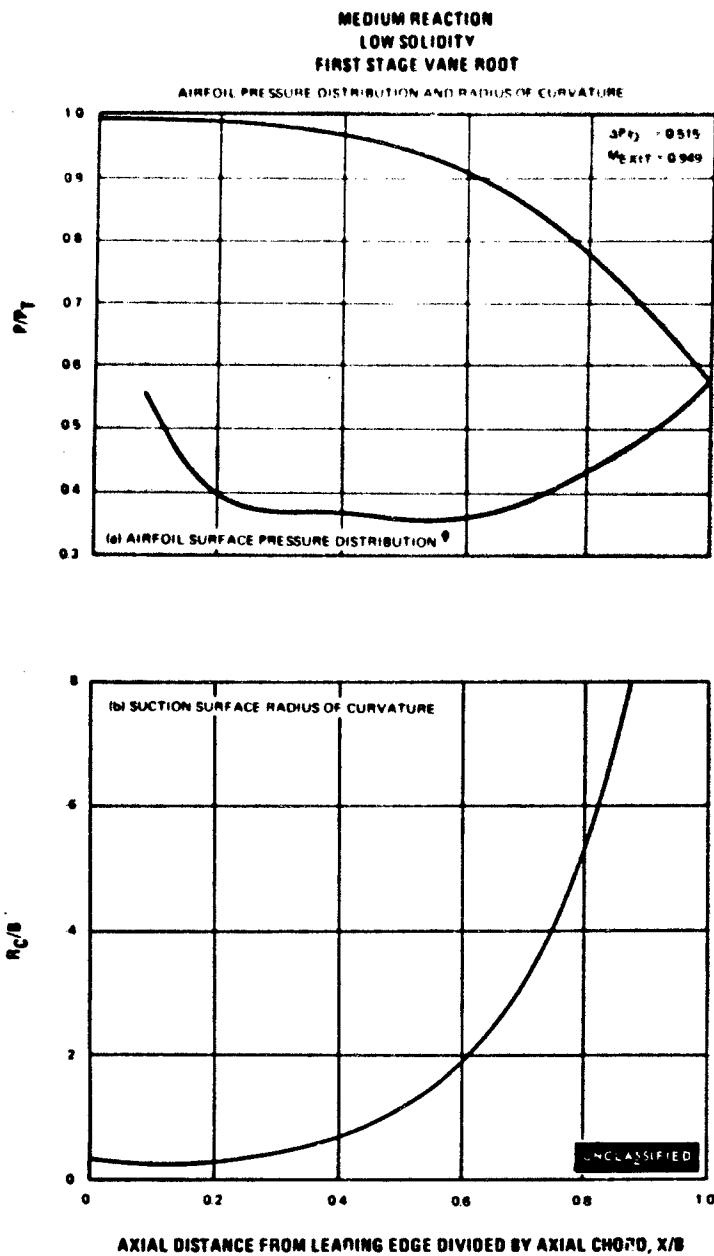


Figure 208

UNCLASSIFIED

UNCLASSIFIED

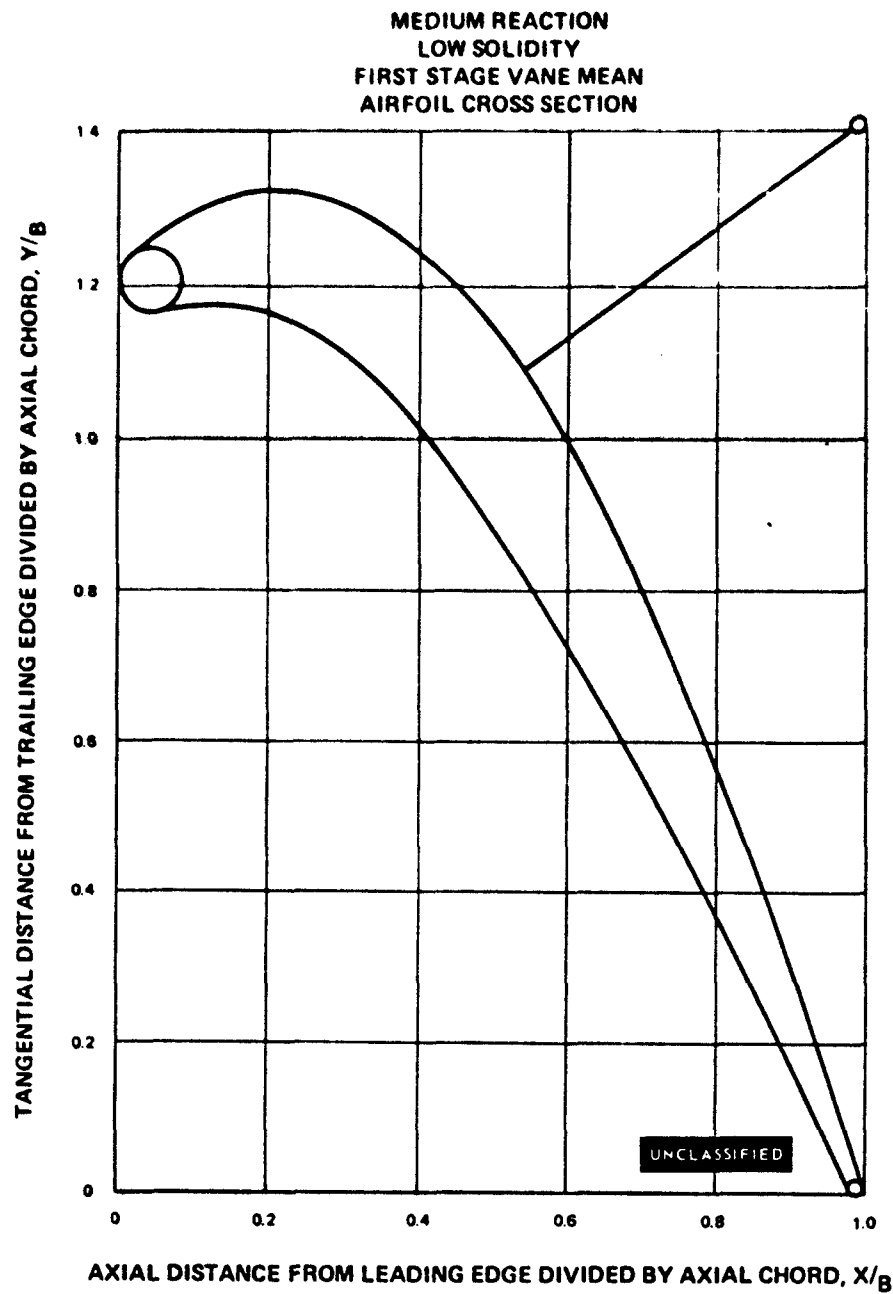


Figure 209

UNCLASSIFIED

UNCLASSIFIED

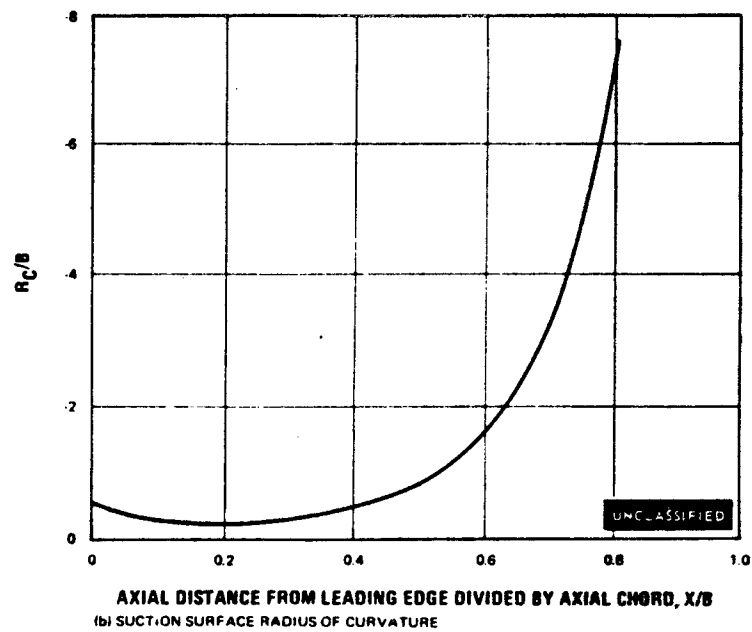
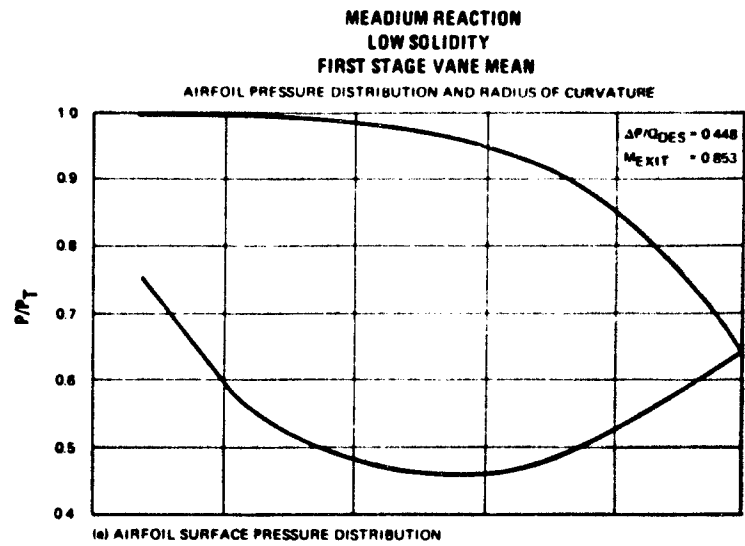


Figure 210

UNCLASSIFIED

UNCLASSIFIED

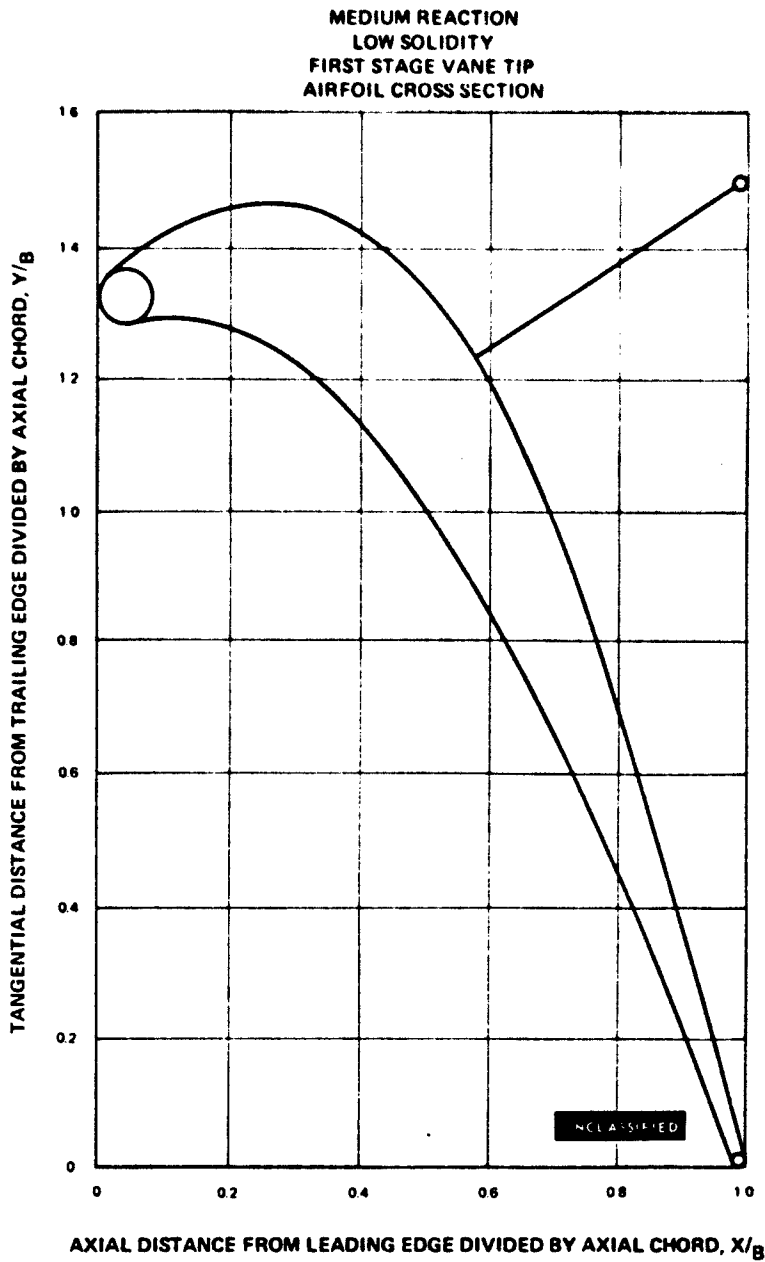


Figure 211

UNCLASSIFIED

UNCLASSIFIED

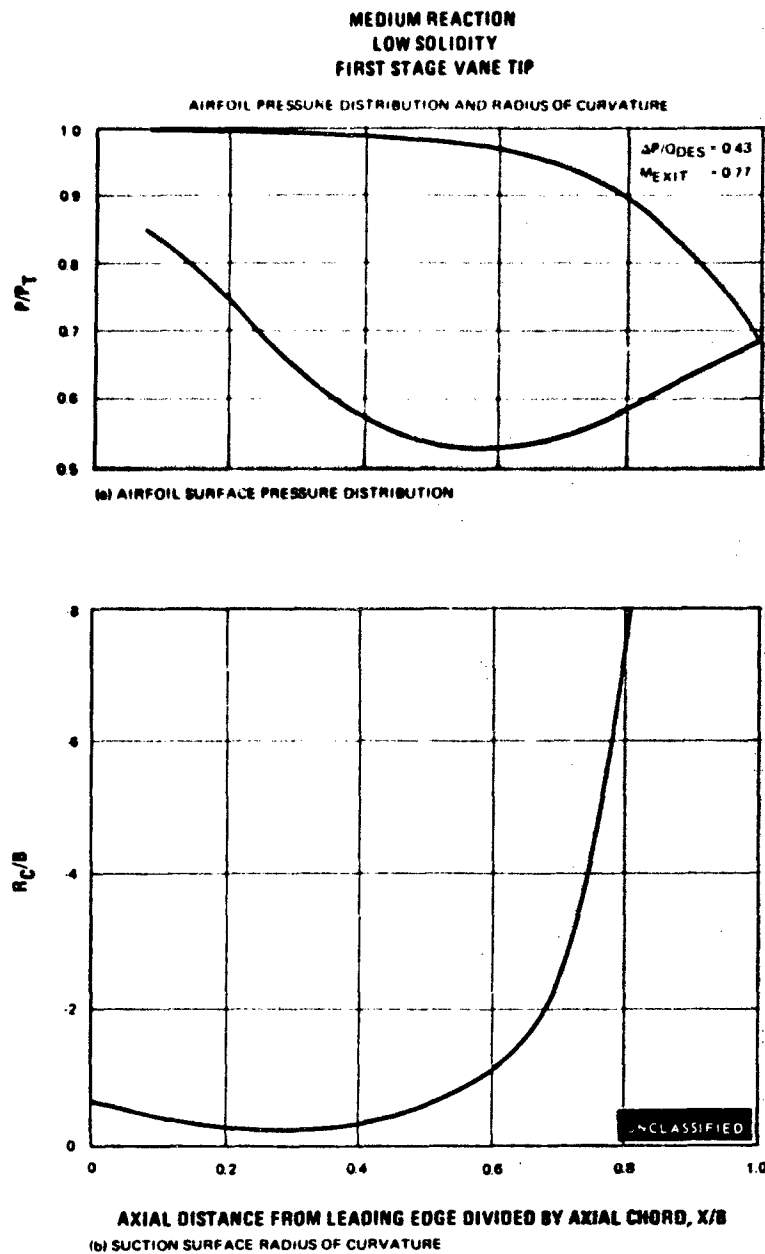


Figure 212

UNCLASSIFIED

UNCLASSIFIED

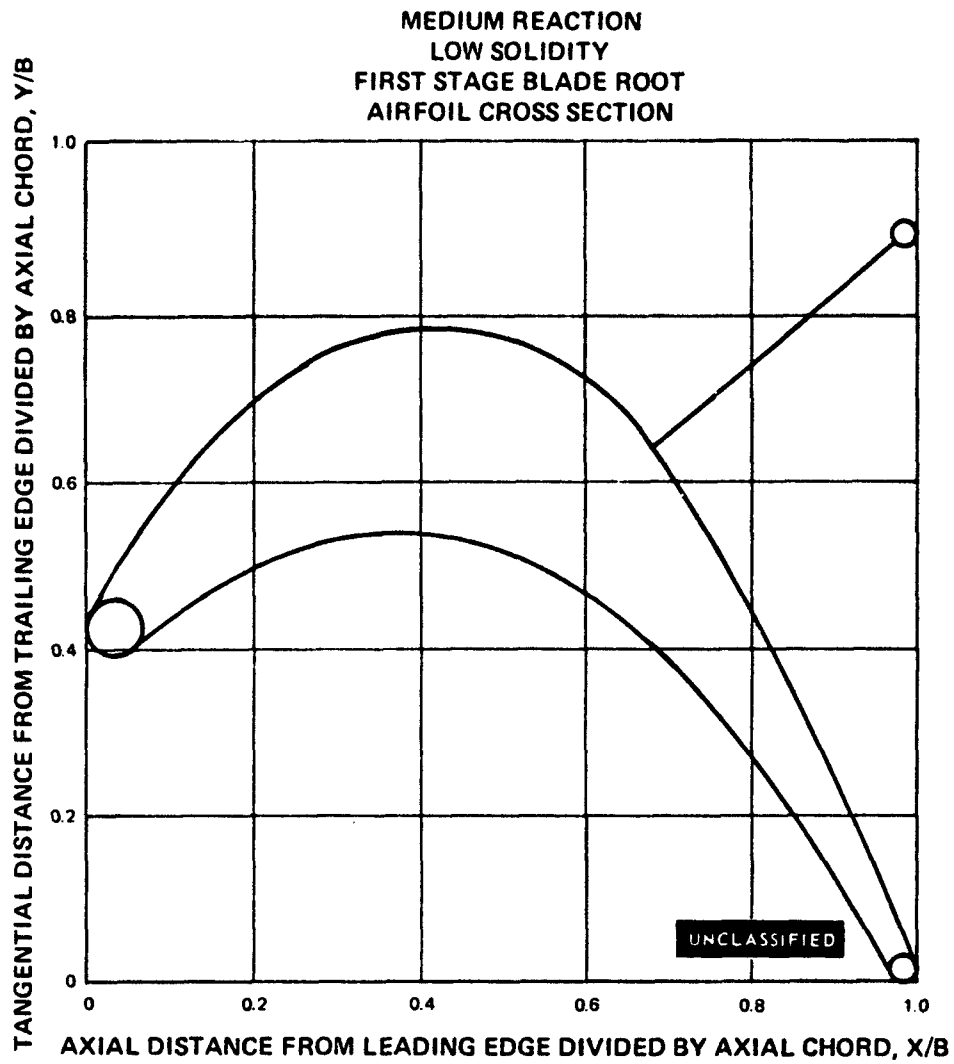


Figure 213

UNCLASSIFIED

UNCLASSIFIED

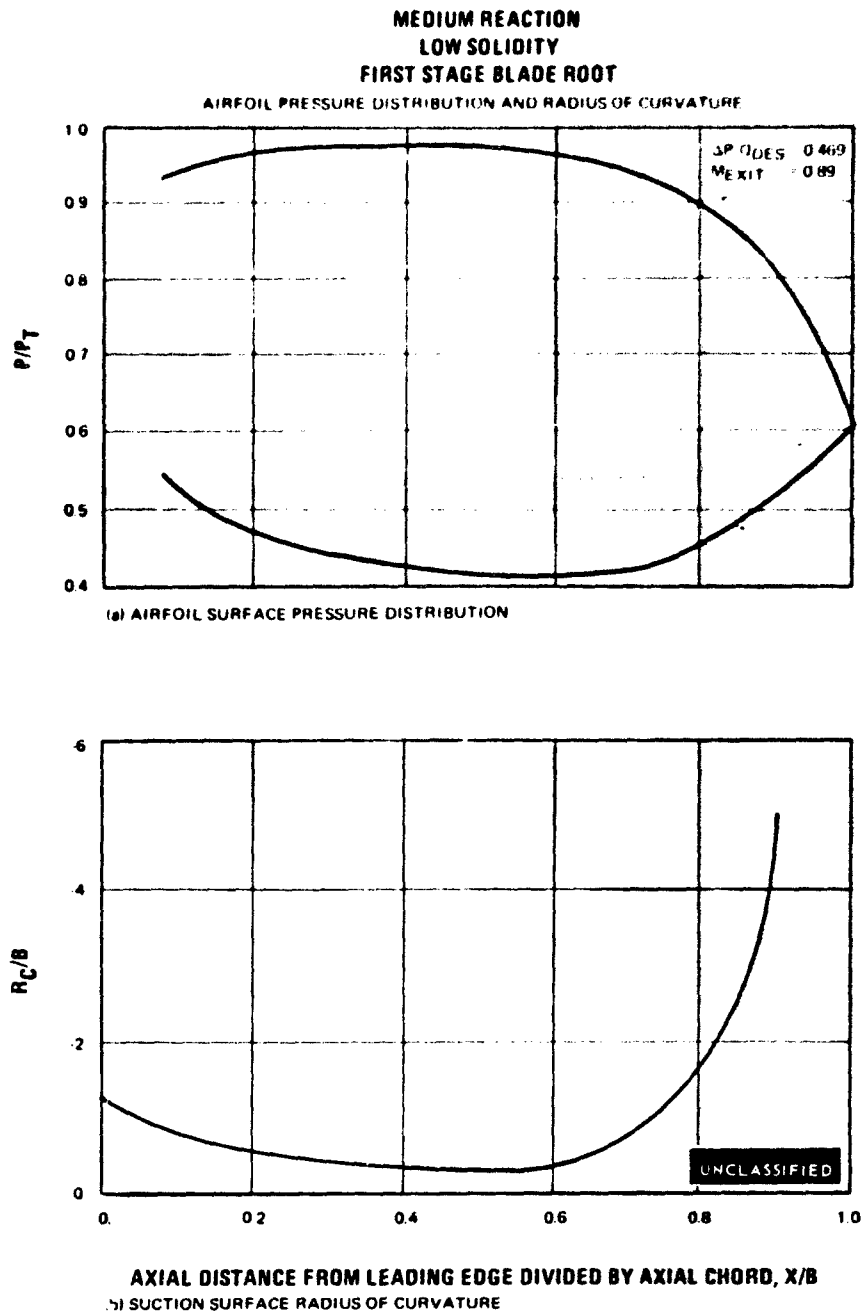


Figure 214

UNCLASSIFIED

UNCLASSIFIED

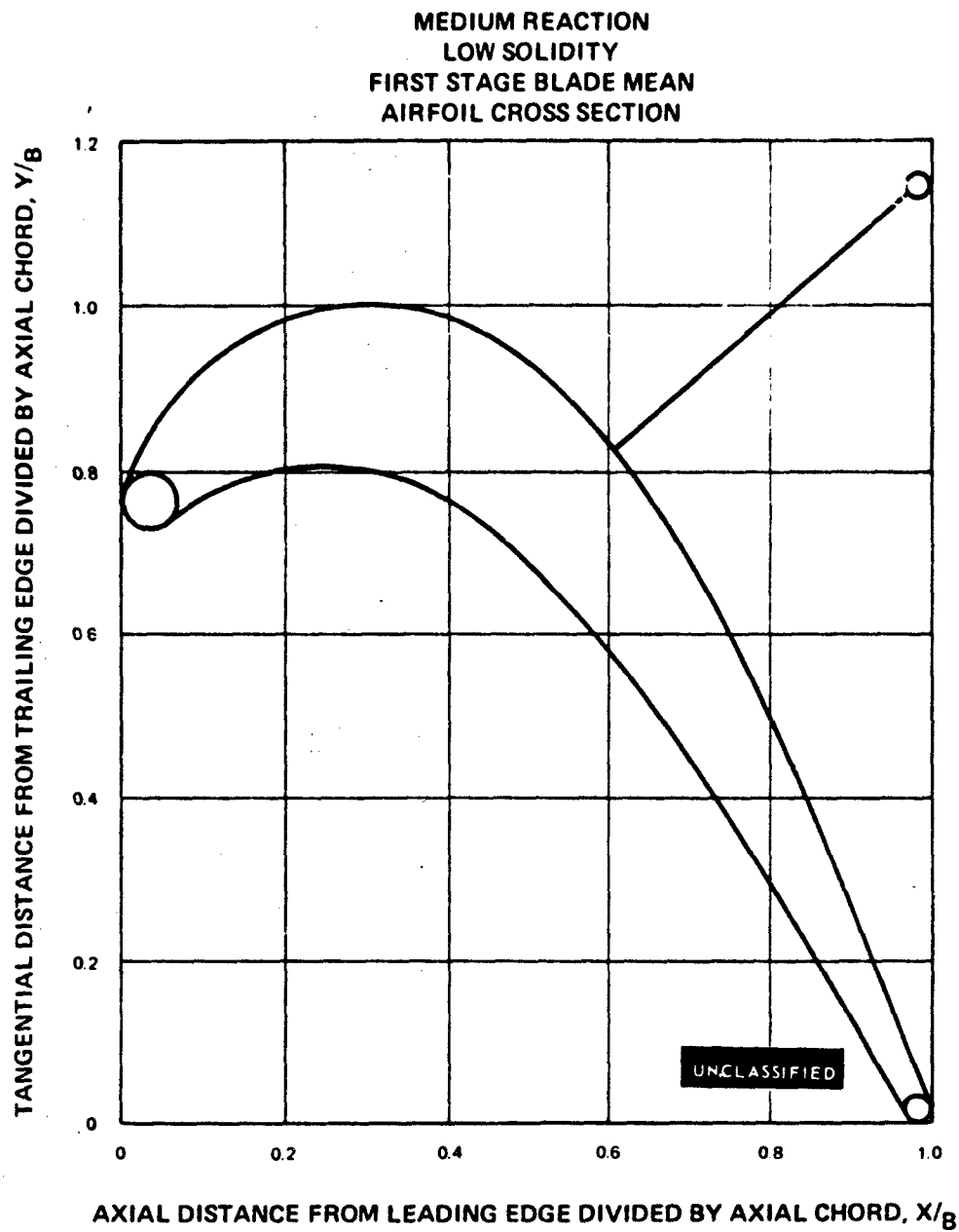


Figure 215

UNCLASSIFIED

UNCLASSIFIED

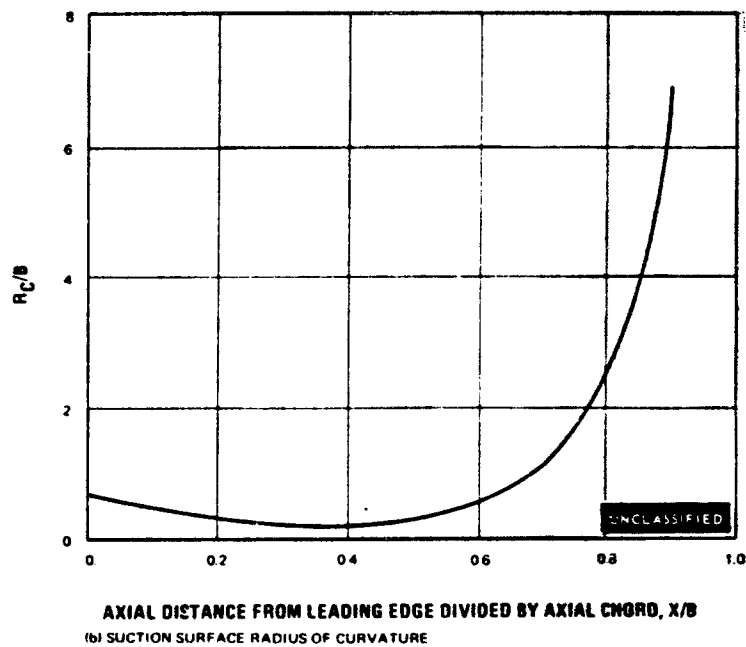
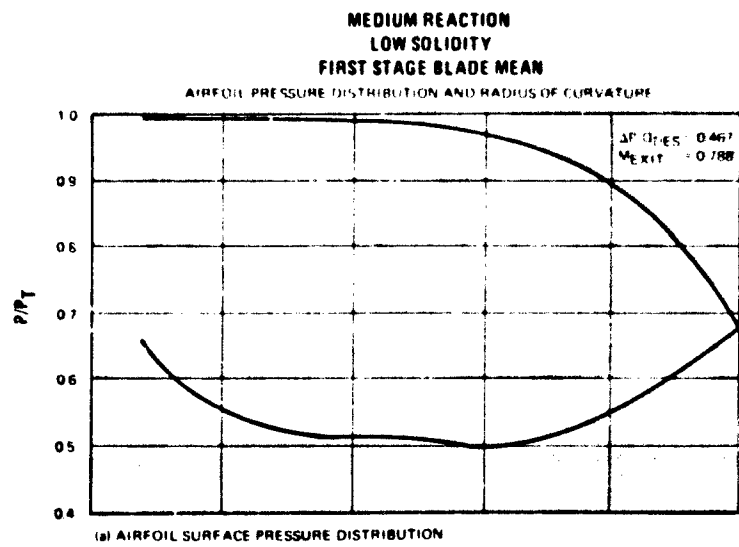


Figure 216

UNCLASSIFIED

UNCLASSIFIED

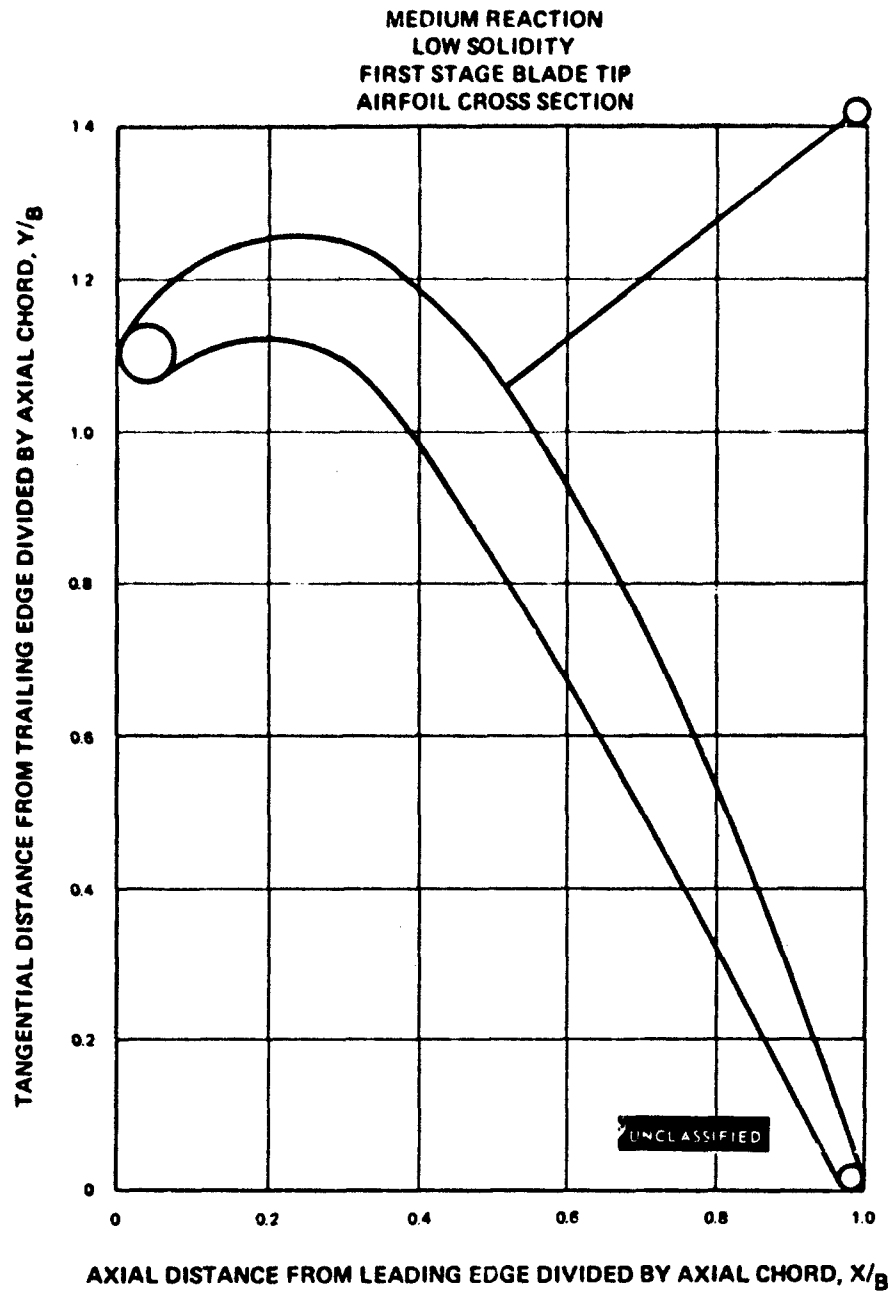


Figure 217

UNCLASSIFIED

UNCLASSIFIED

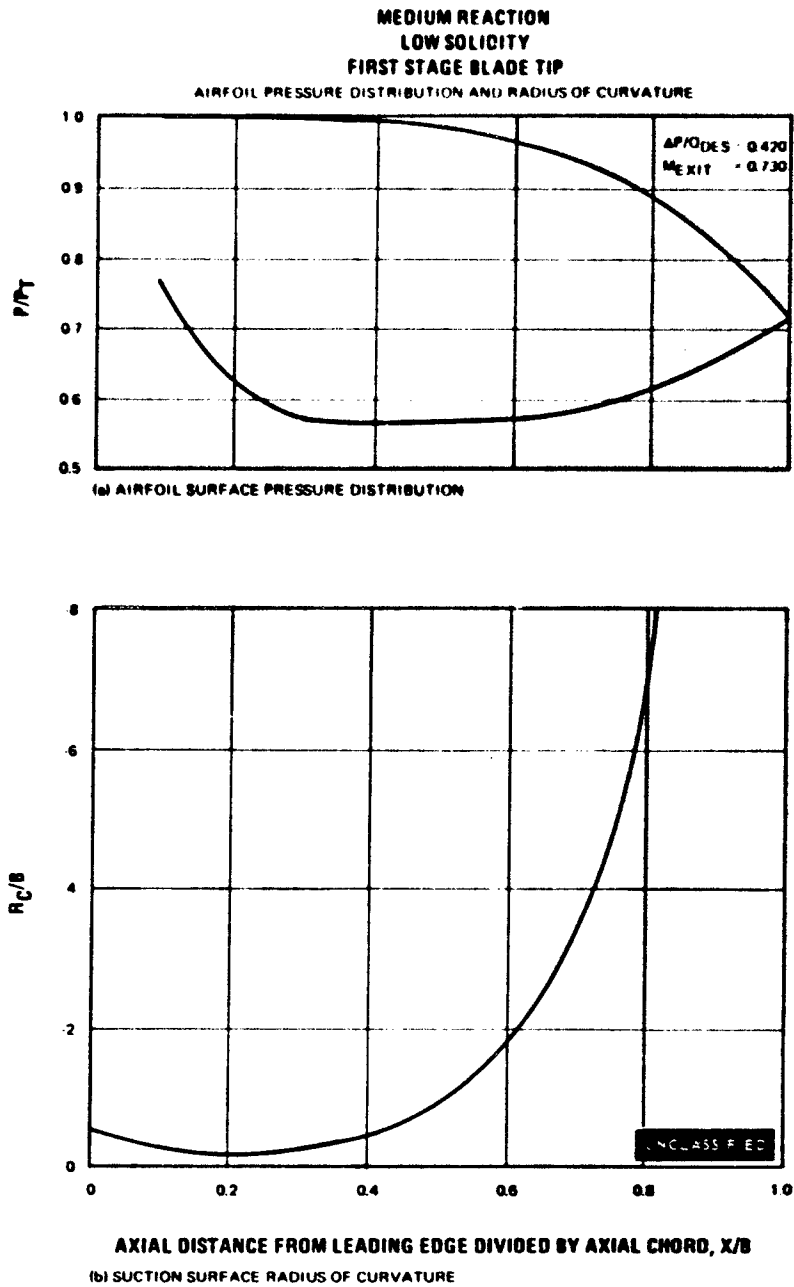


Figure 218

UNCLASSIFIED

UNCLASSIFIED

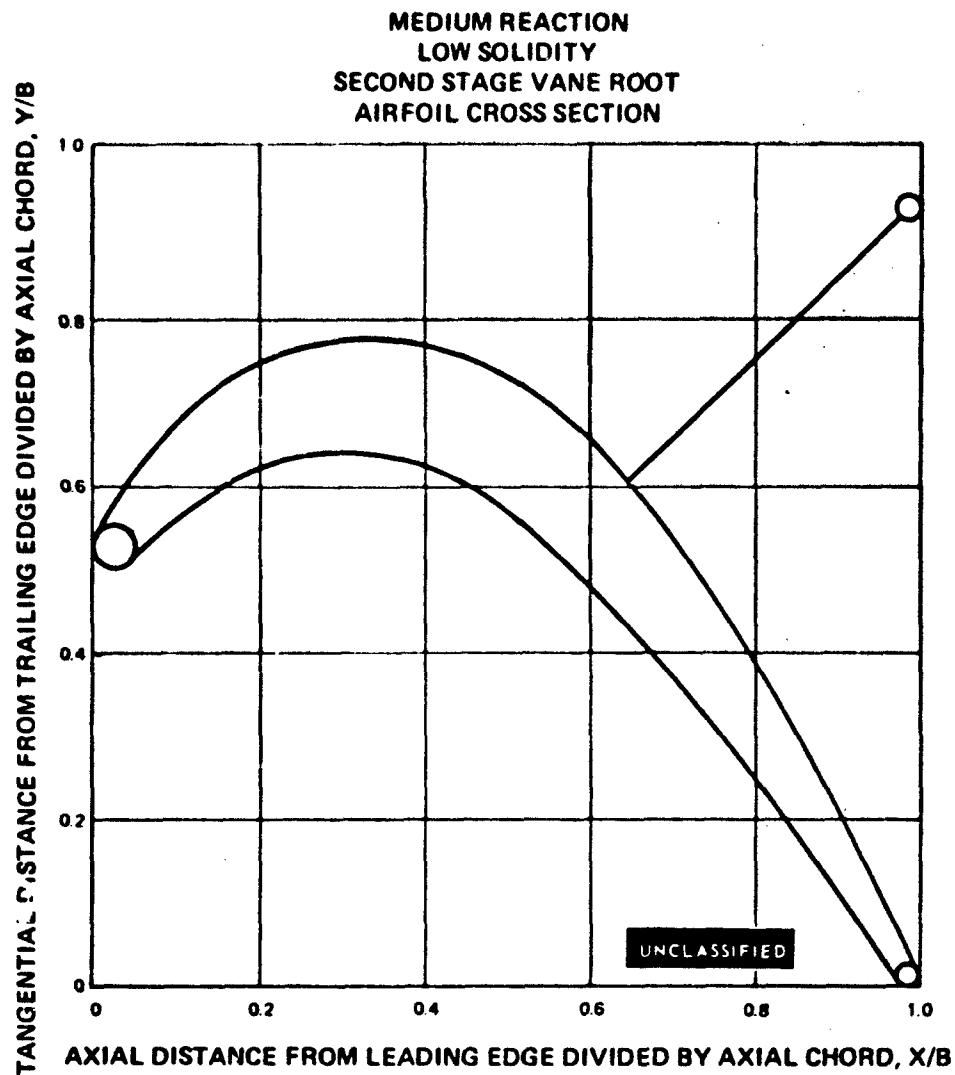


Figure 219

UNCLASSIFIED

UNCLASSIFIED

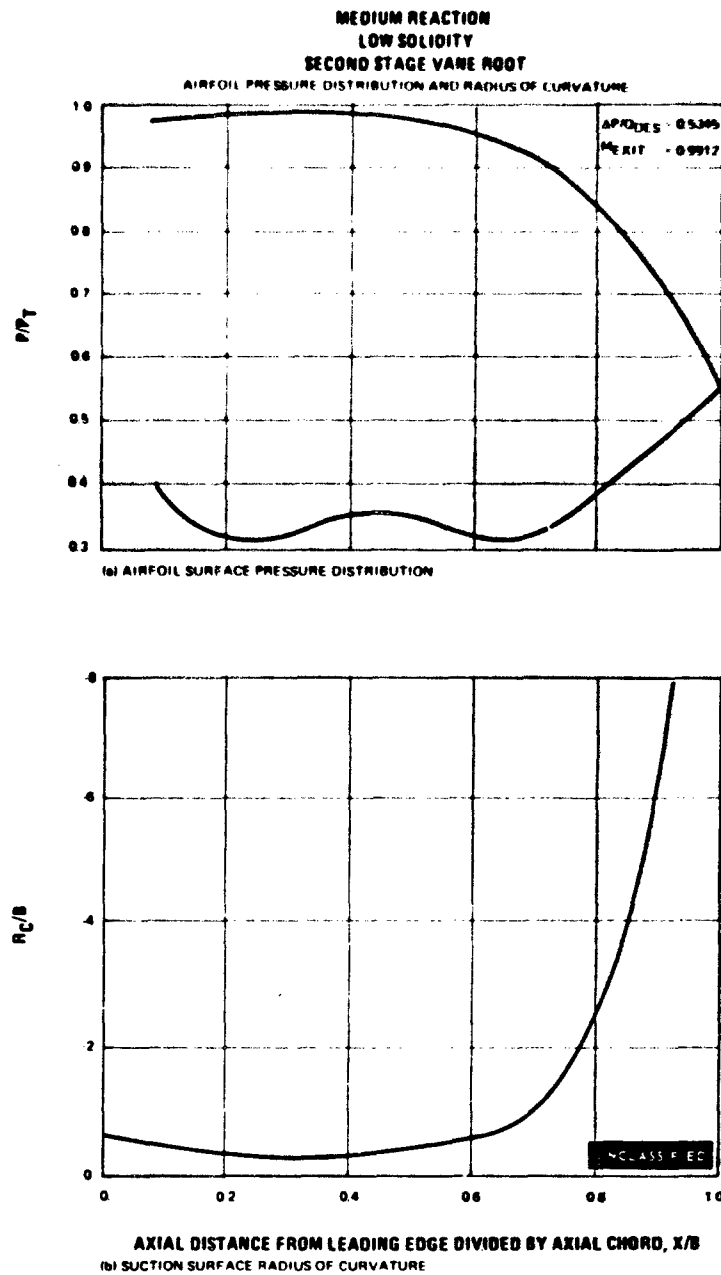


Figure 220

UNCLASSIFIED

UNCLASSIFIED

MEDIUM REACTION
LOW SOLIDITY
SECOND STAGE VANE MEAN
AIRFOIL CROSS SECTION

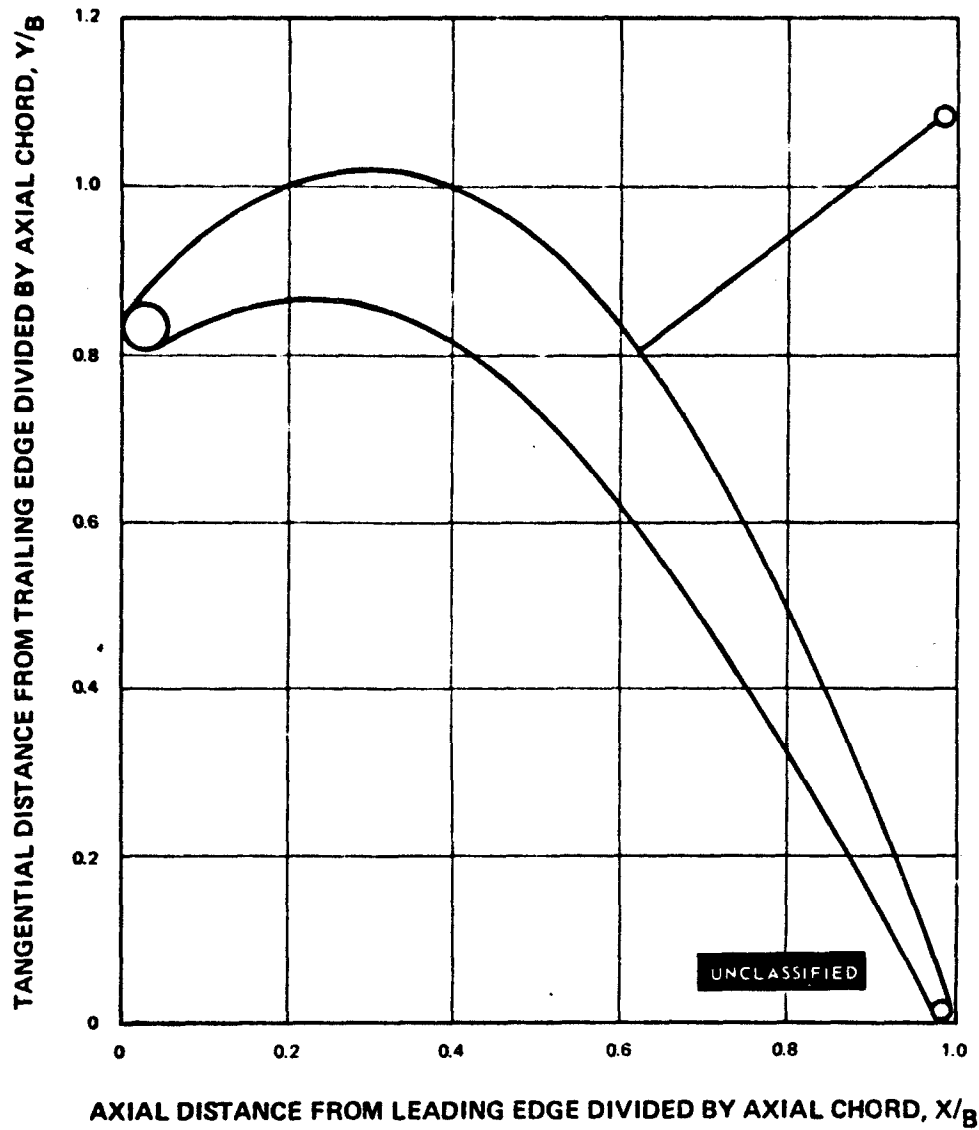


Figure 221

UNCLASSIFIED

UNCLASSIFIED

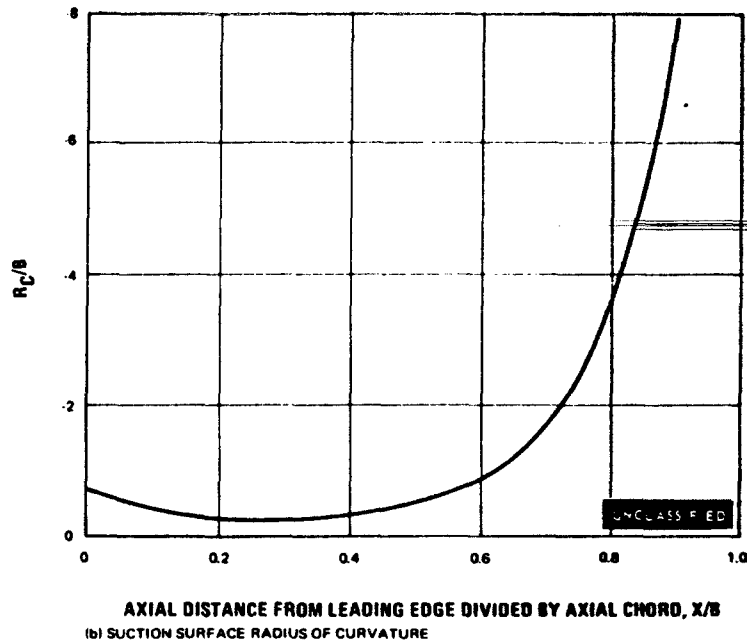
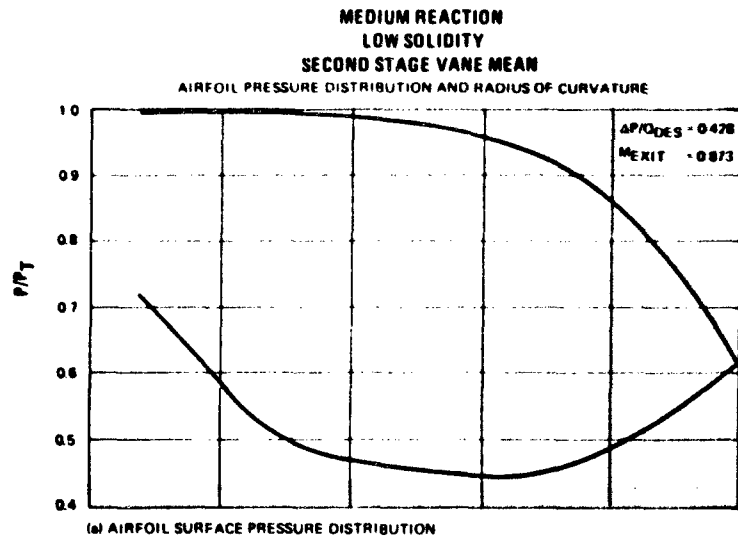


Figure 222

UNCLASSIFIED

UNCLASSIFIED

MEDIUM REACTION
LOW SOLIDITY
SECOND STAGE VANE TIP
AIRFOIL CROSS SECTION

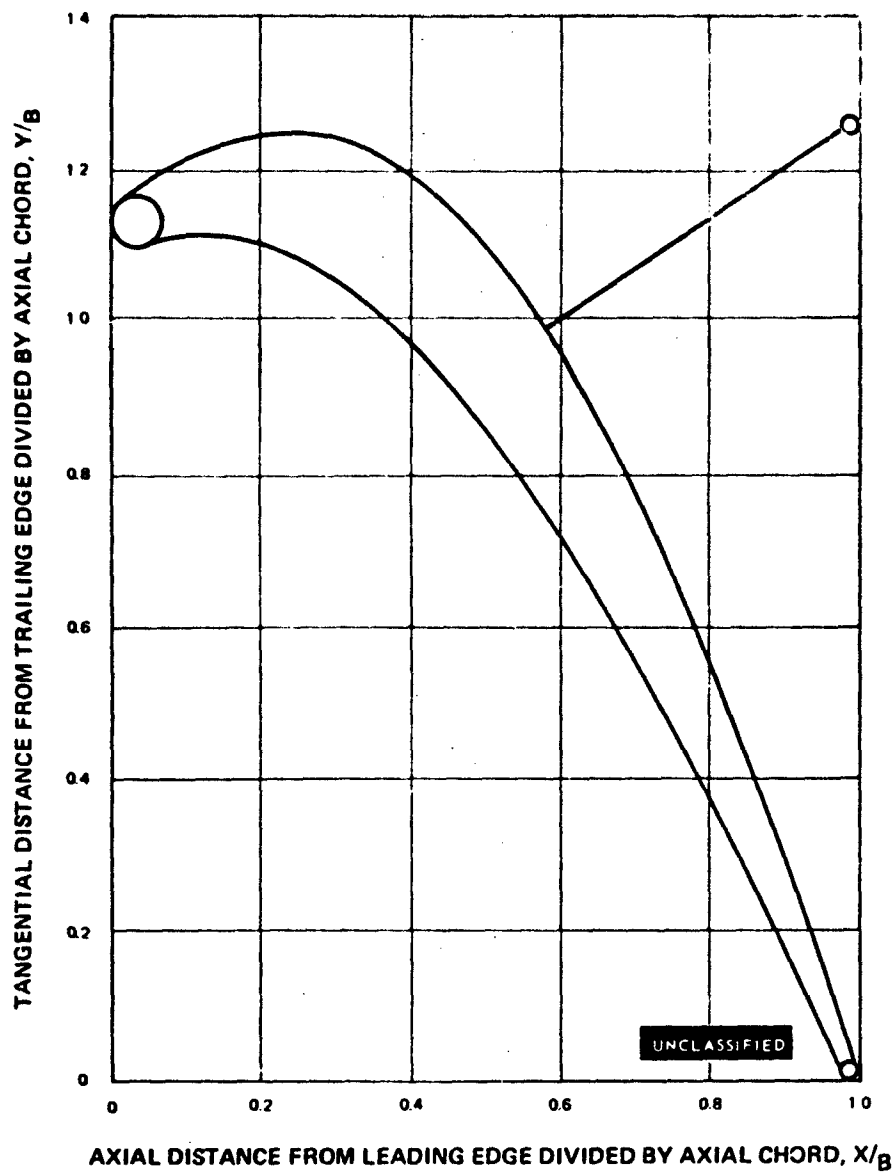


Figure 223

UNCLASSIFIED

UNCLASSIFIED

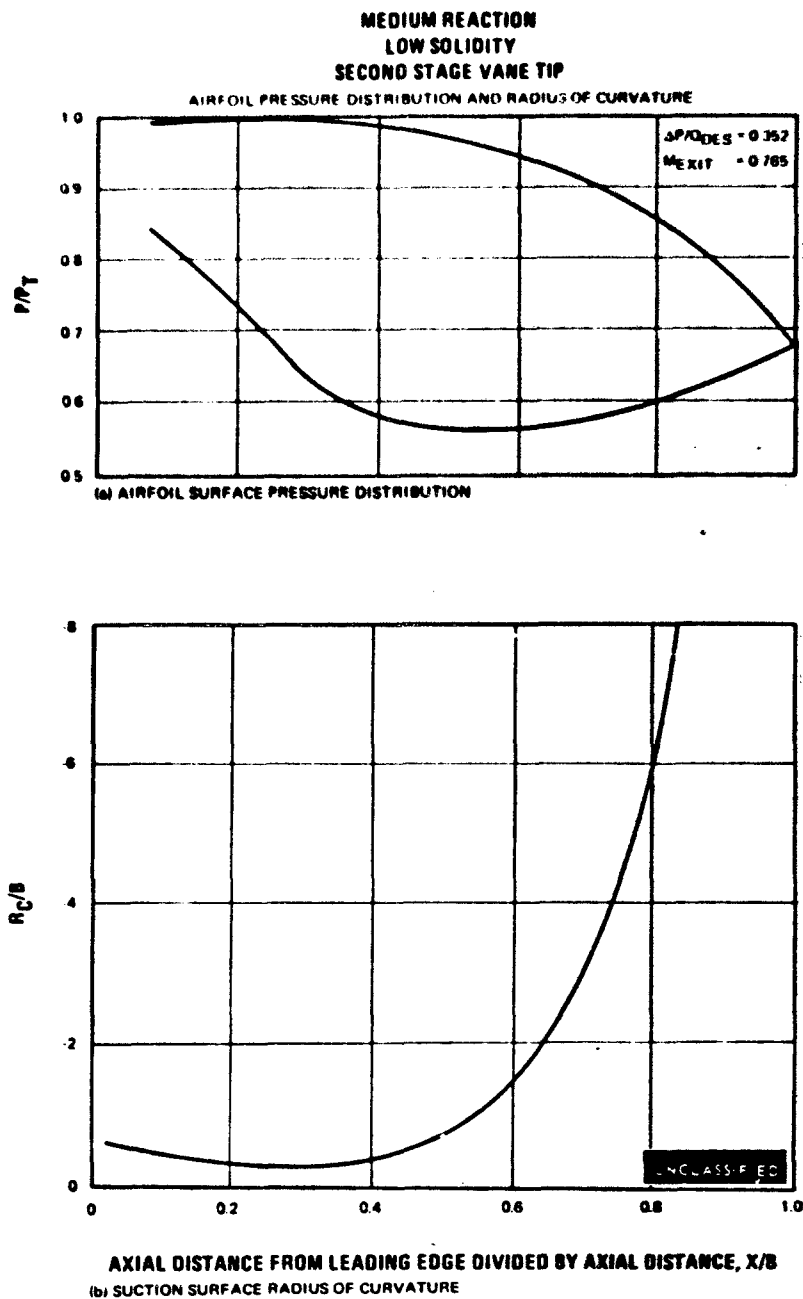


Figure 224

UNCLASSIFIED

UNCLASSIFIED

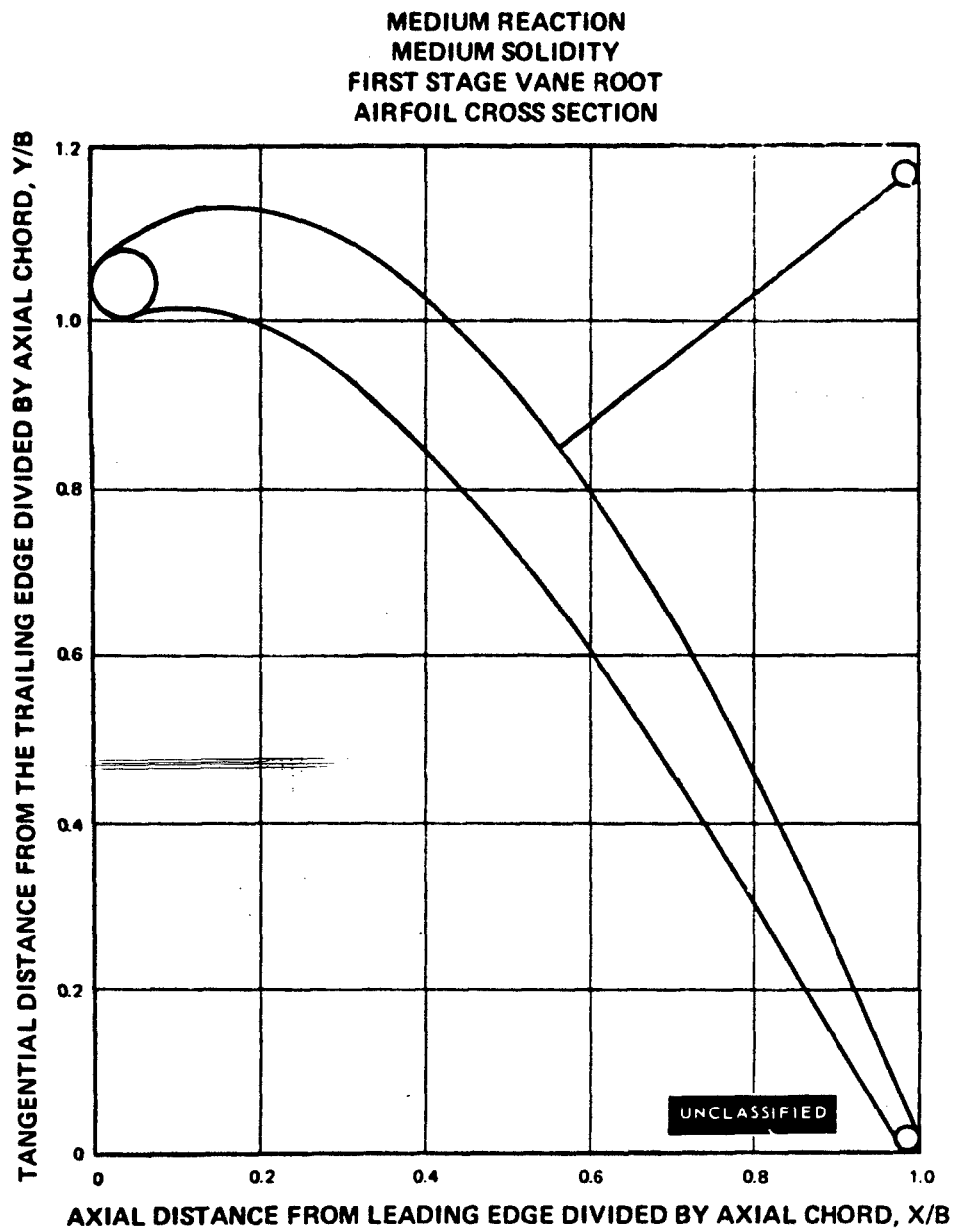


Figure 225

UNCLASSIFIED

UNCLASSIFIED

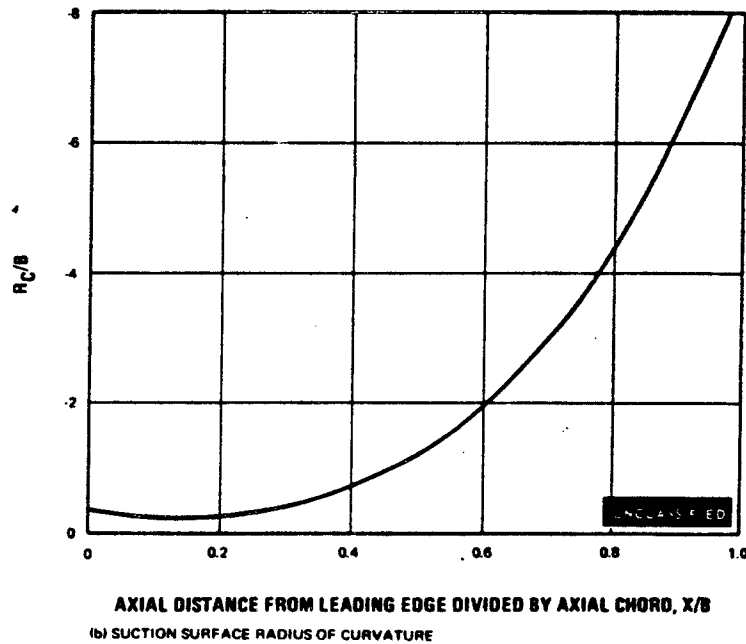
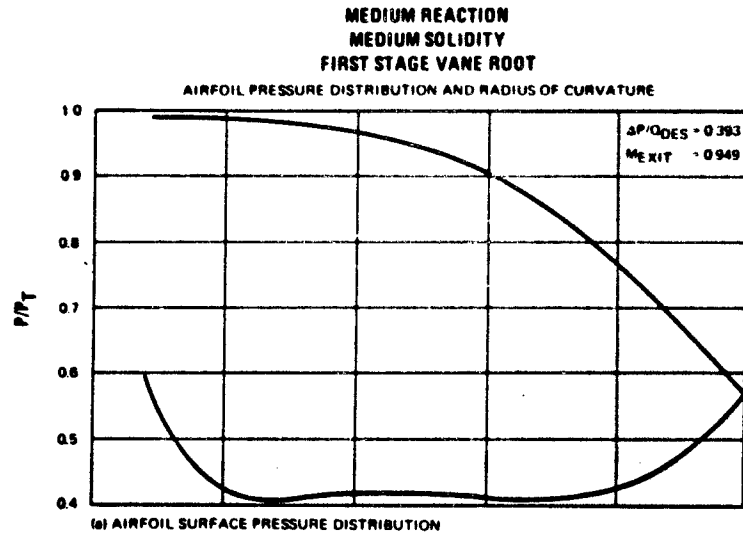


Figure 226

UNCLASSIFIED

UNCLASSIFIED

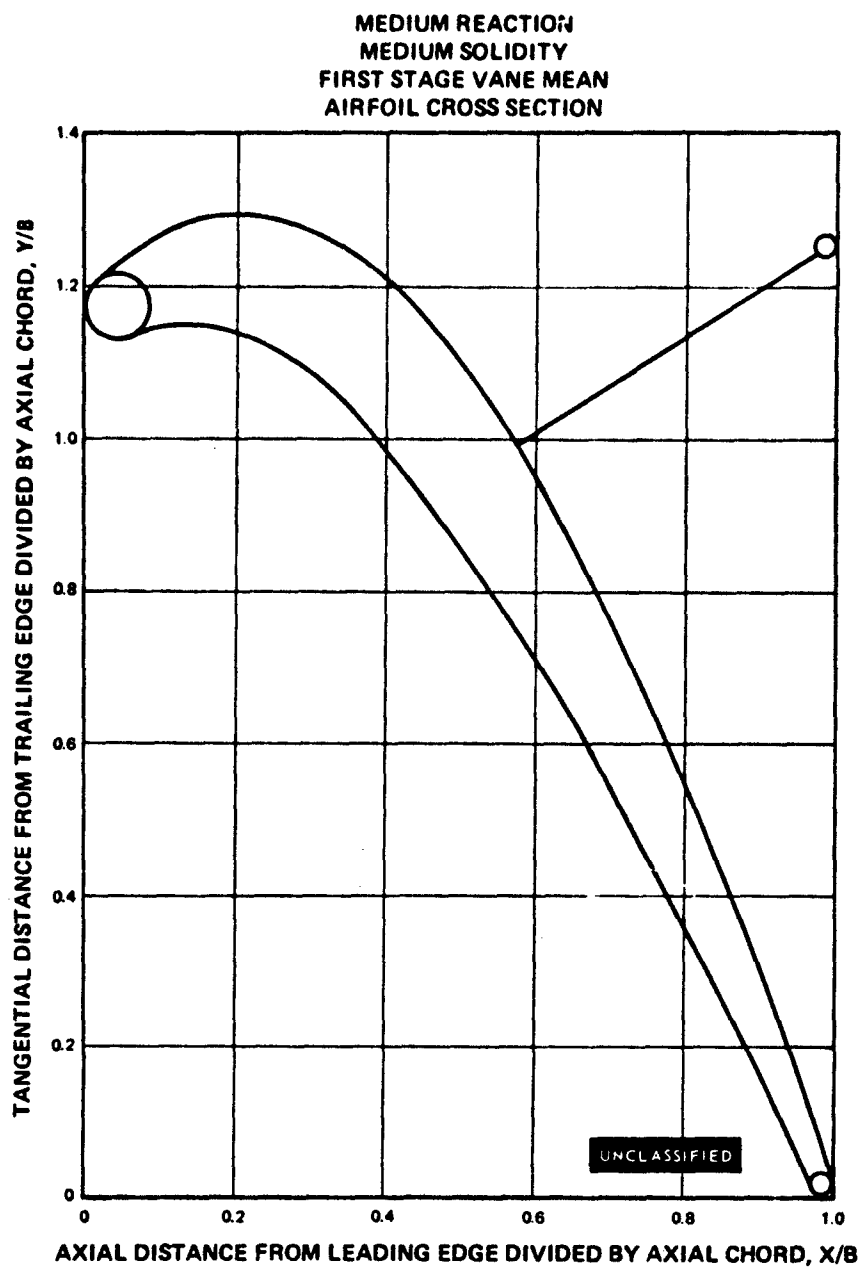


Figure 227

UNCLASSIFIED

UNCLASSIFIED

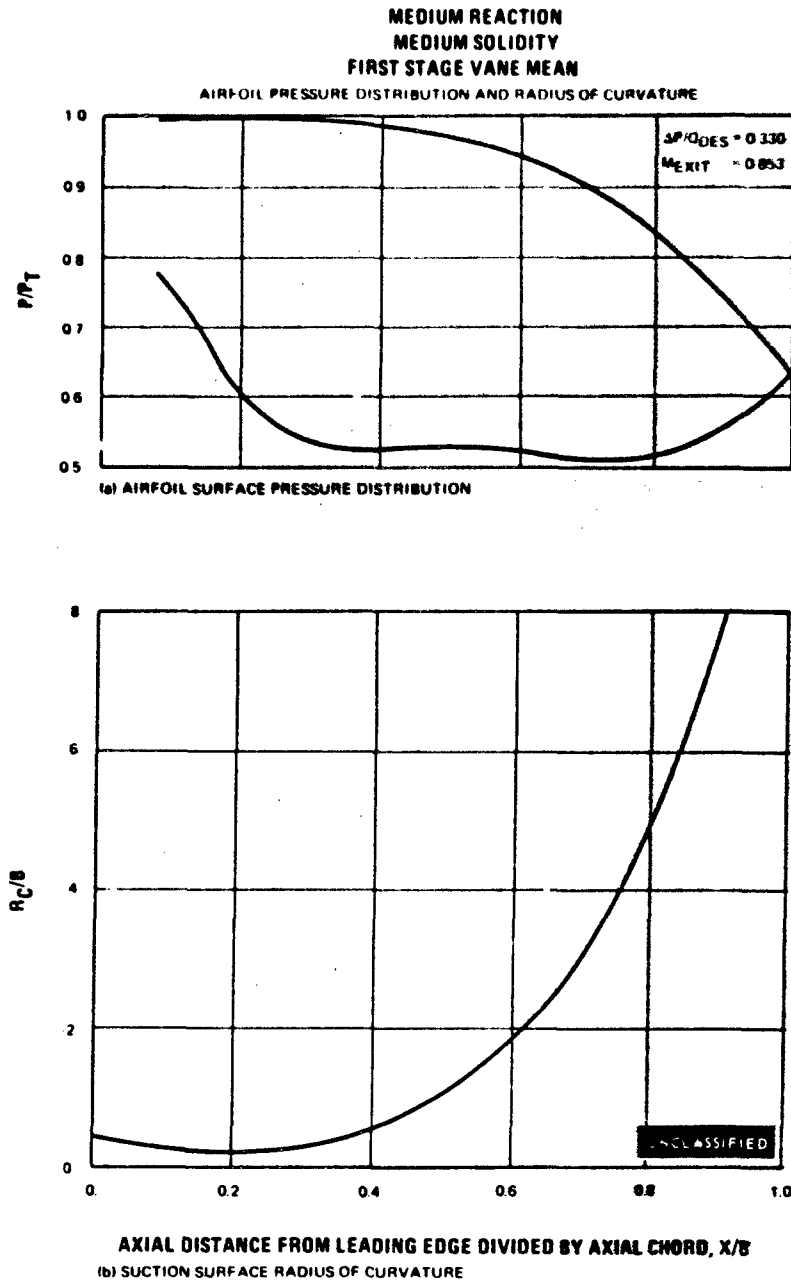


Figure 228

UNCLASSIFIED

UNCLASSIFIED

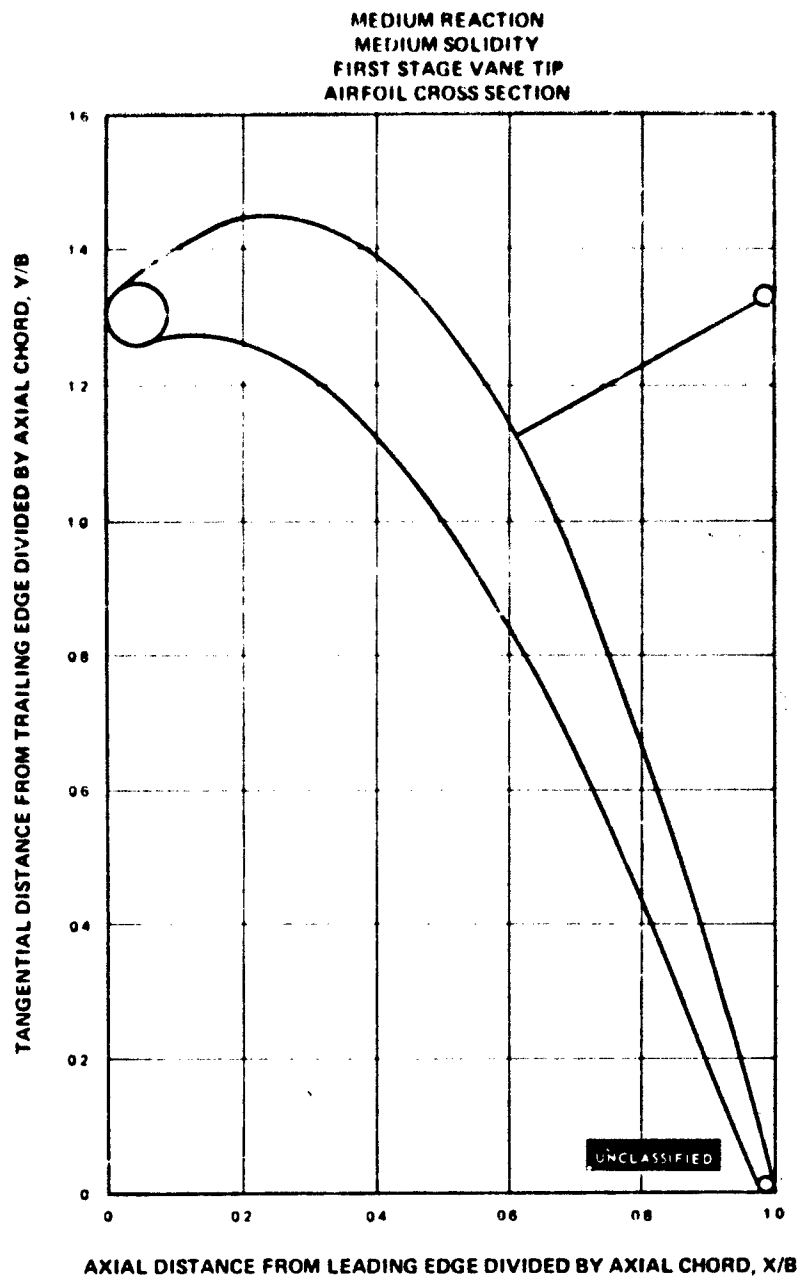


Figure 229

UNCLASSIFIED

UNCLASSIFIED

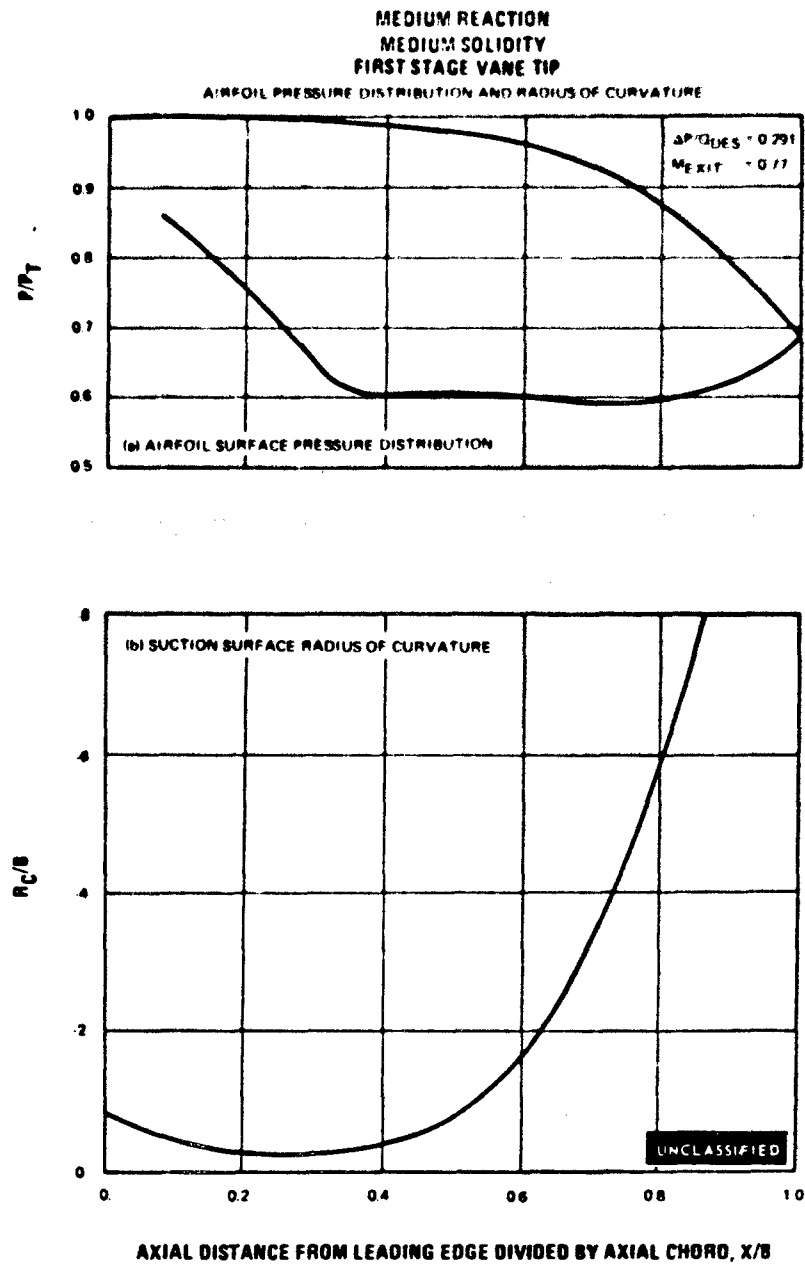


Figure 230

UNCLASSIFIED

UNCLASSIFIED

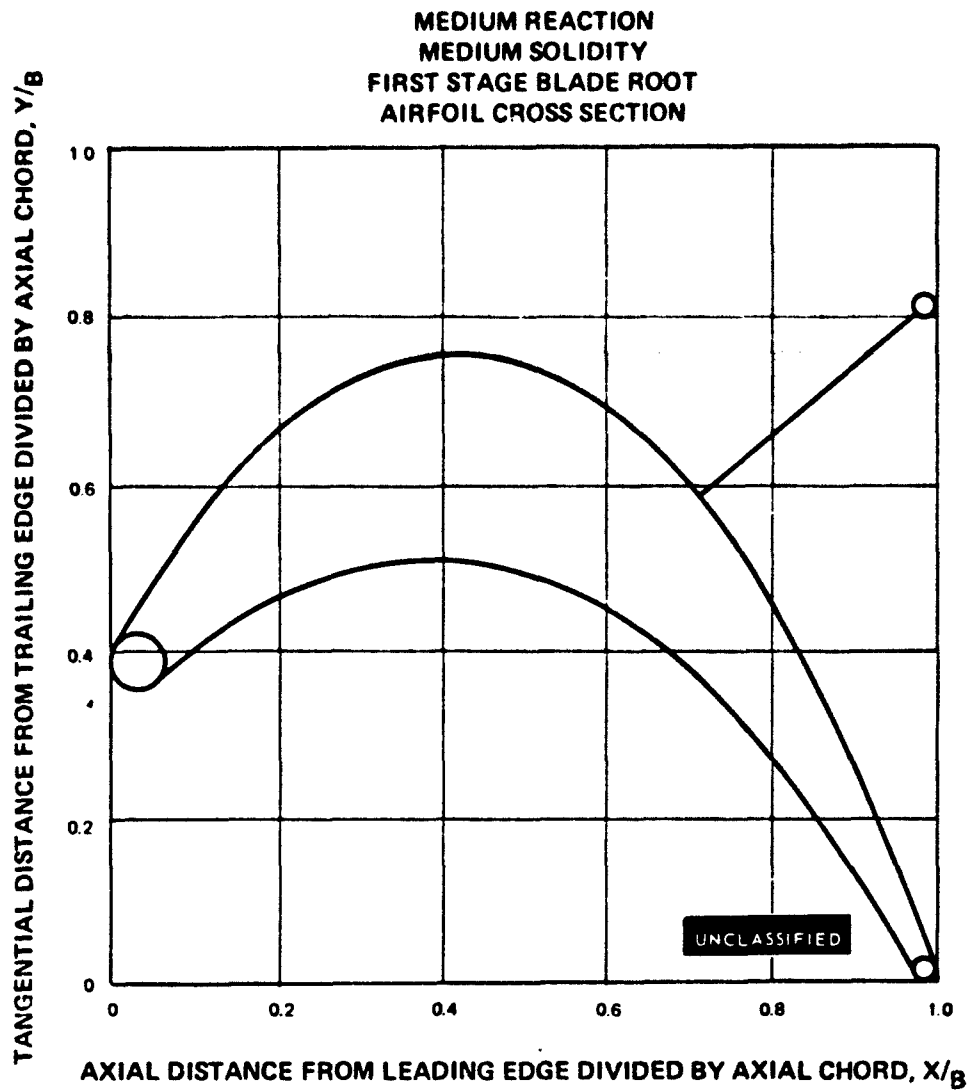


Figure 231

UNCLASSIFIED

UNCLASSIFIED

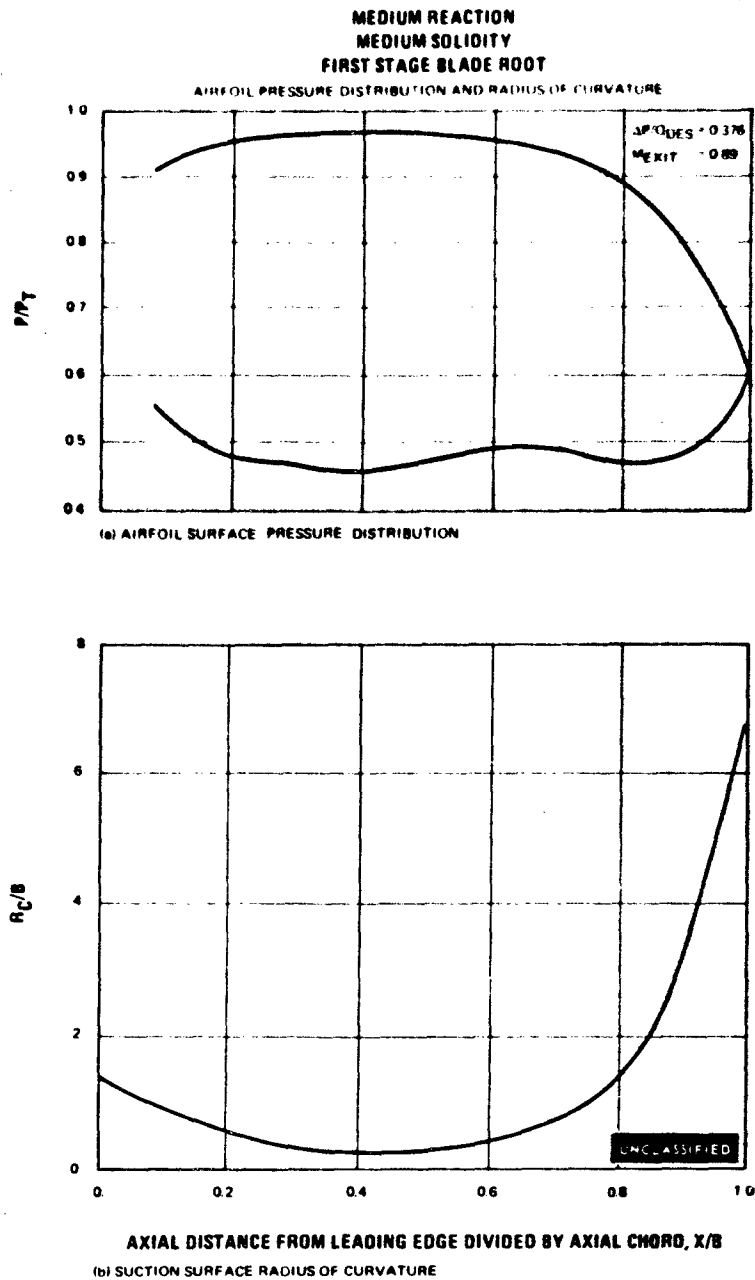


Figure 232

UNCLASSIFIED

UNCLASSIFIED

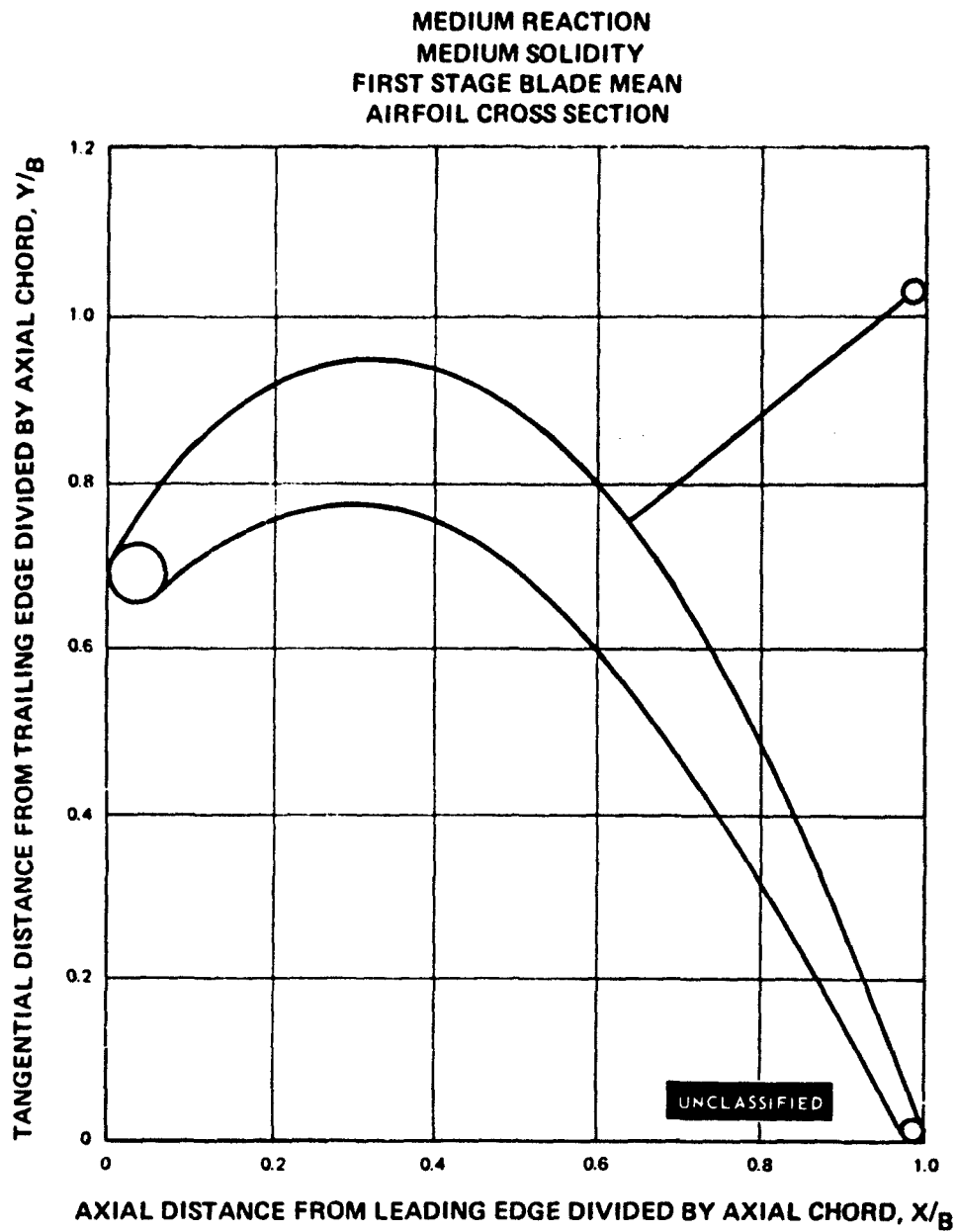


Figure 233

UNCLASSIFIED

UNCLASSIFIED

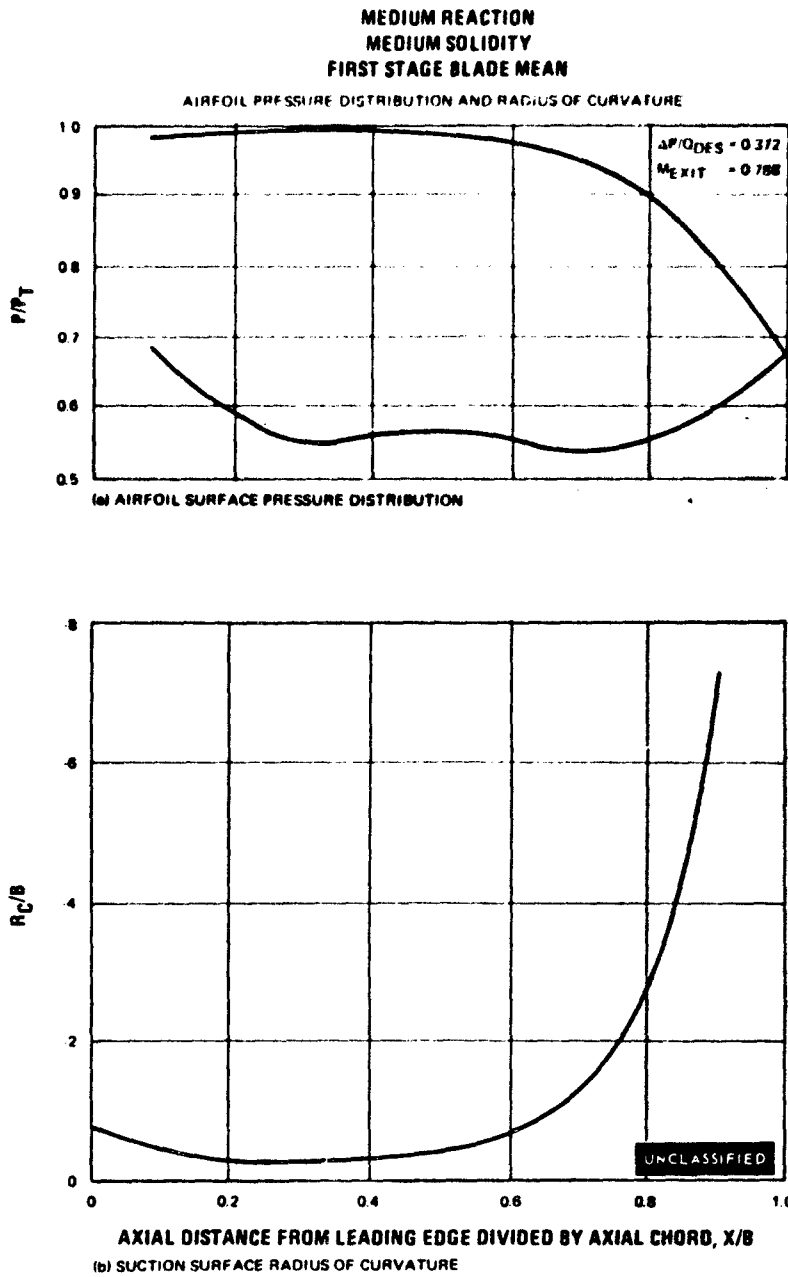


Figure 234

UNCLASSIFIED

UNCLASSIFIED

MEDIUM REACTION
MEDIUM SOLIDITY
FIRST STAGE BLADE TIP
AIRFOIL CROSS SECTION

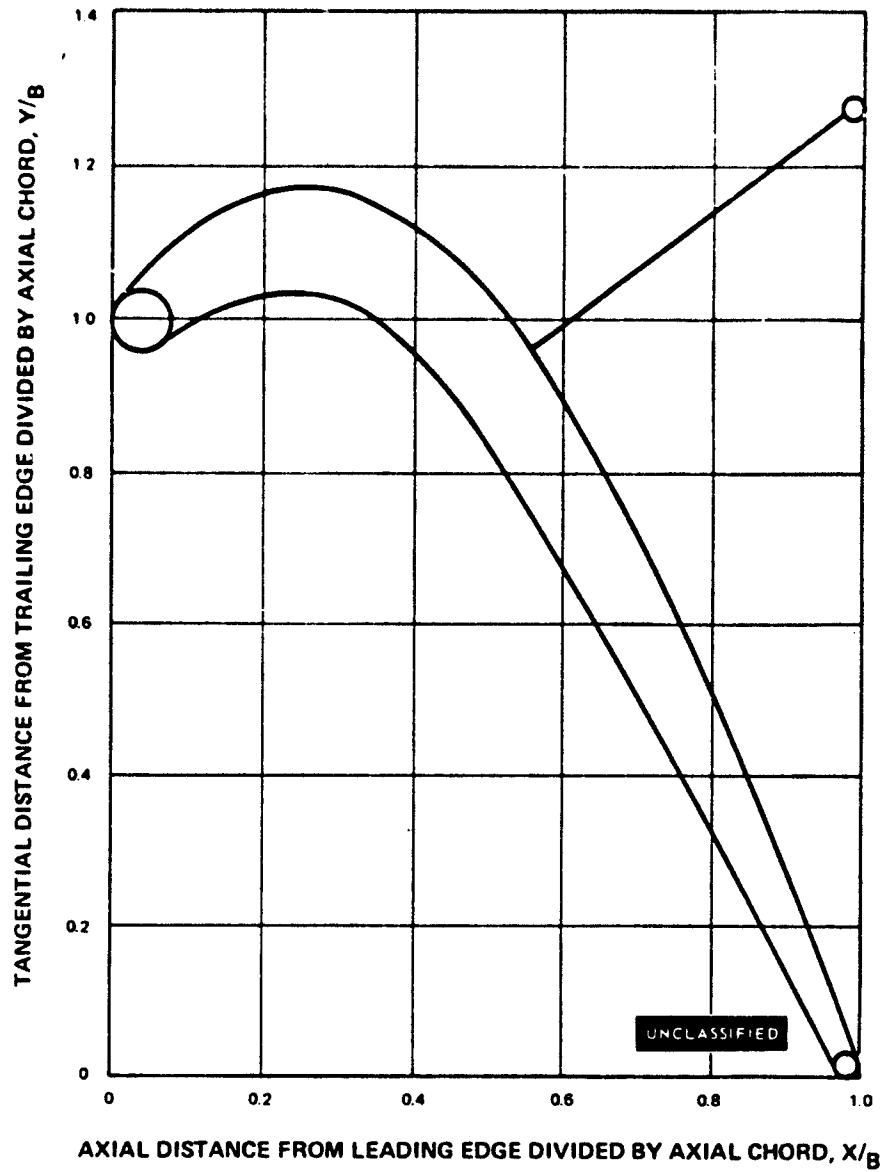


Figure 235

UNCLASSIFIED

UNCLASSIFIED

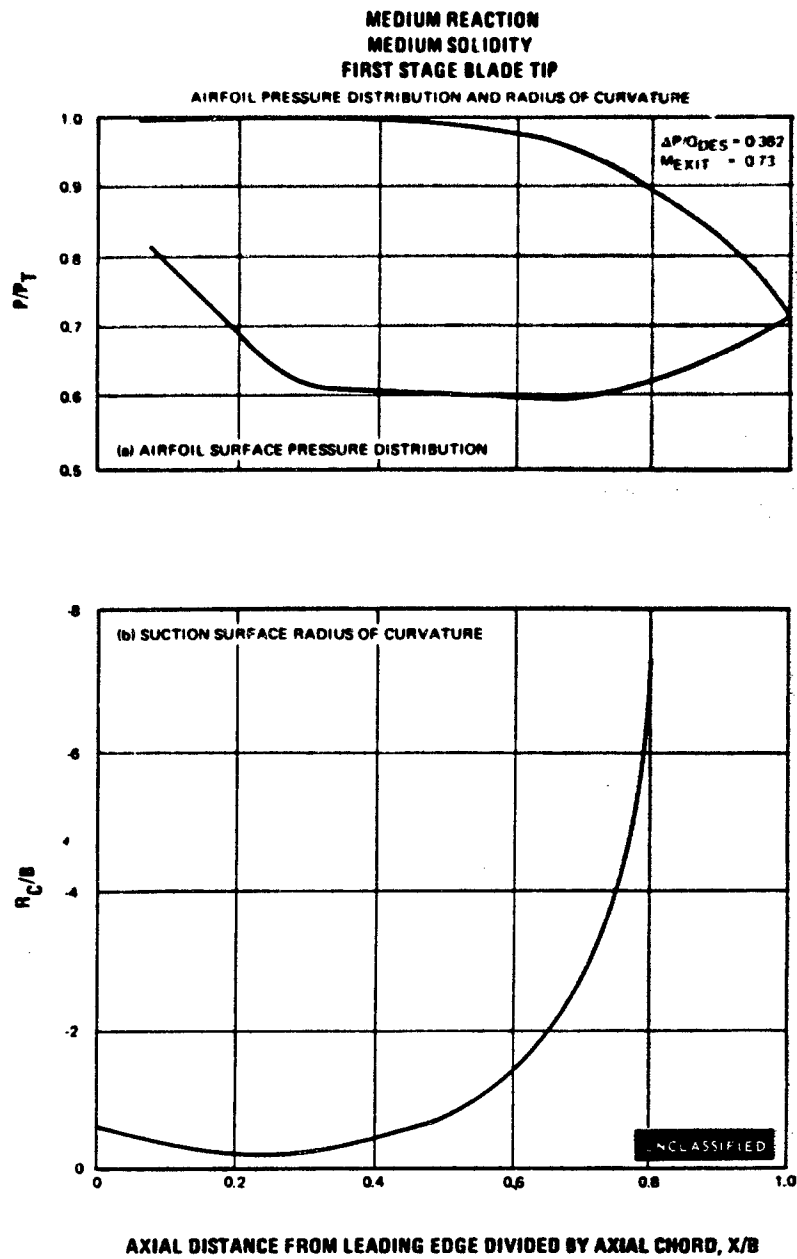


Figure 236

UNCLASSIFIED

UNCLASSIFIED

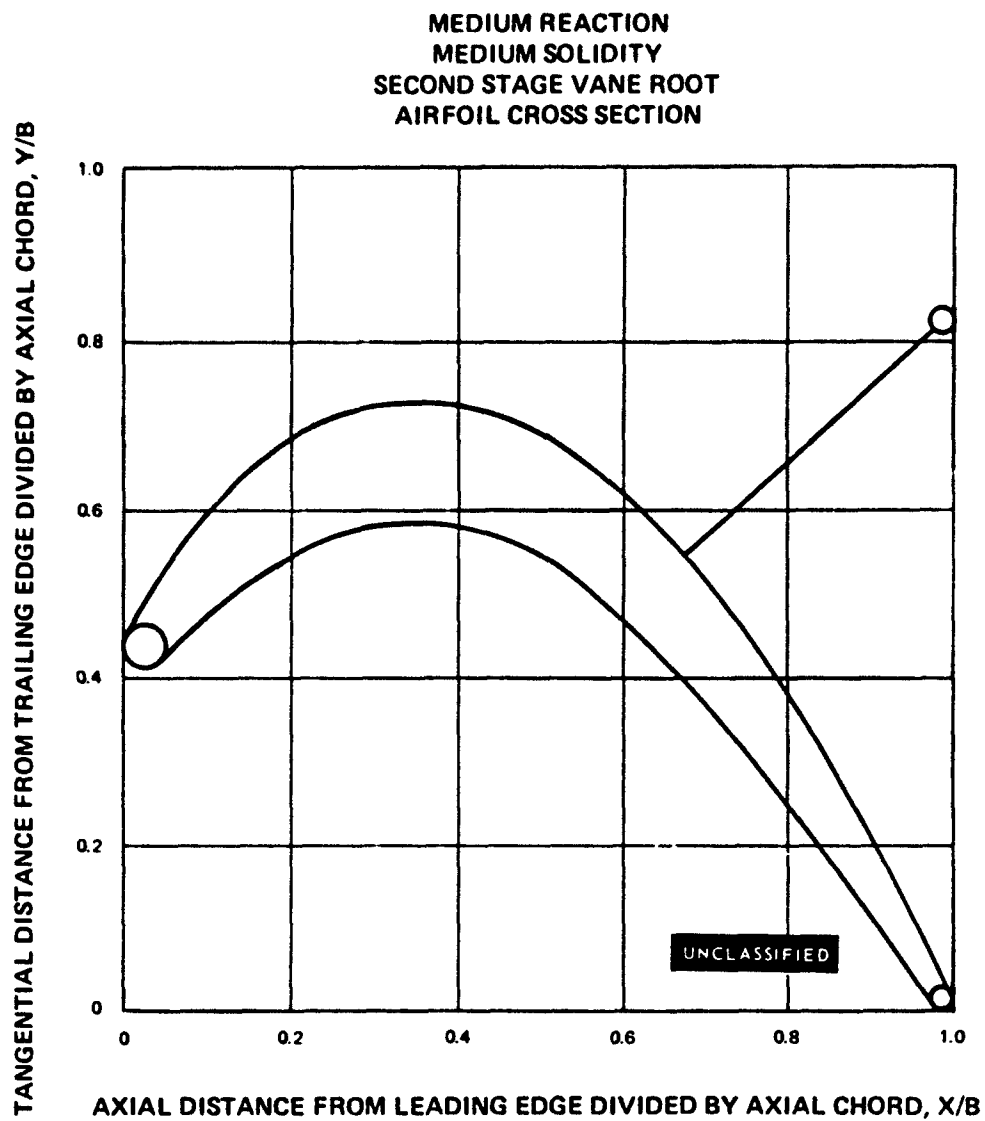


Figure 237

UNCLASSIFIED

UNCLASSIFIED

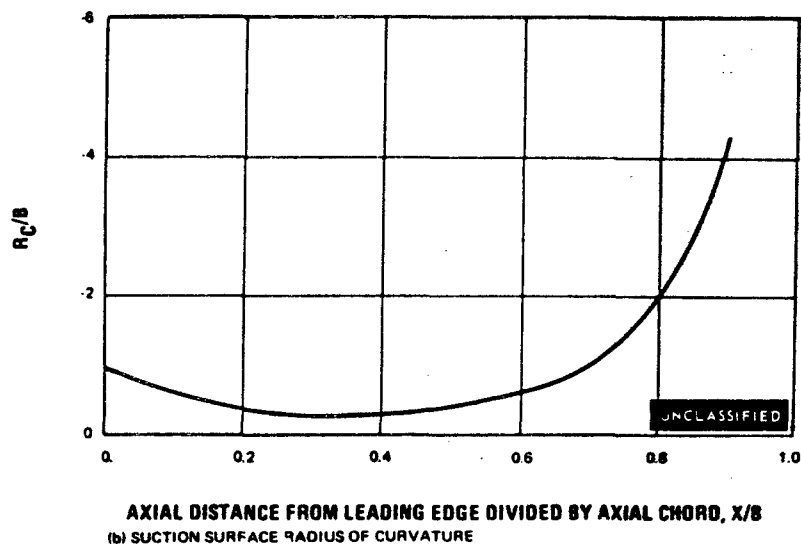
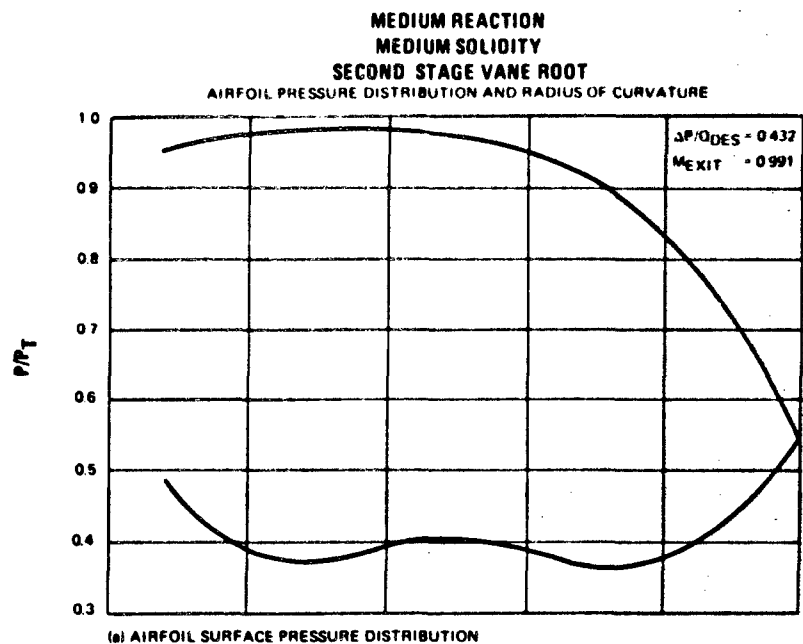


Figure 238

PAGE NO. 277

UNCLASSIFIED

UNCLASSIFIED

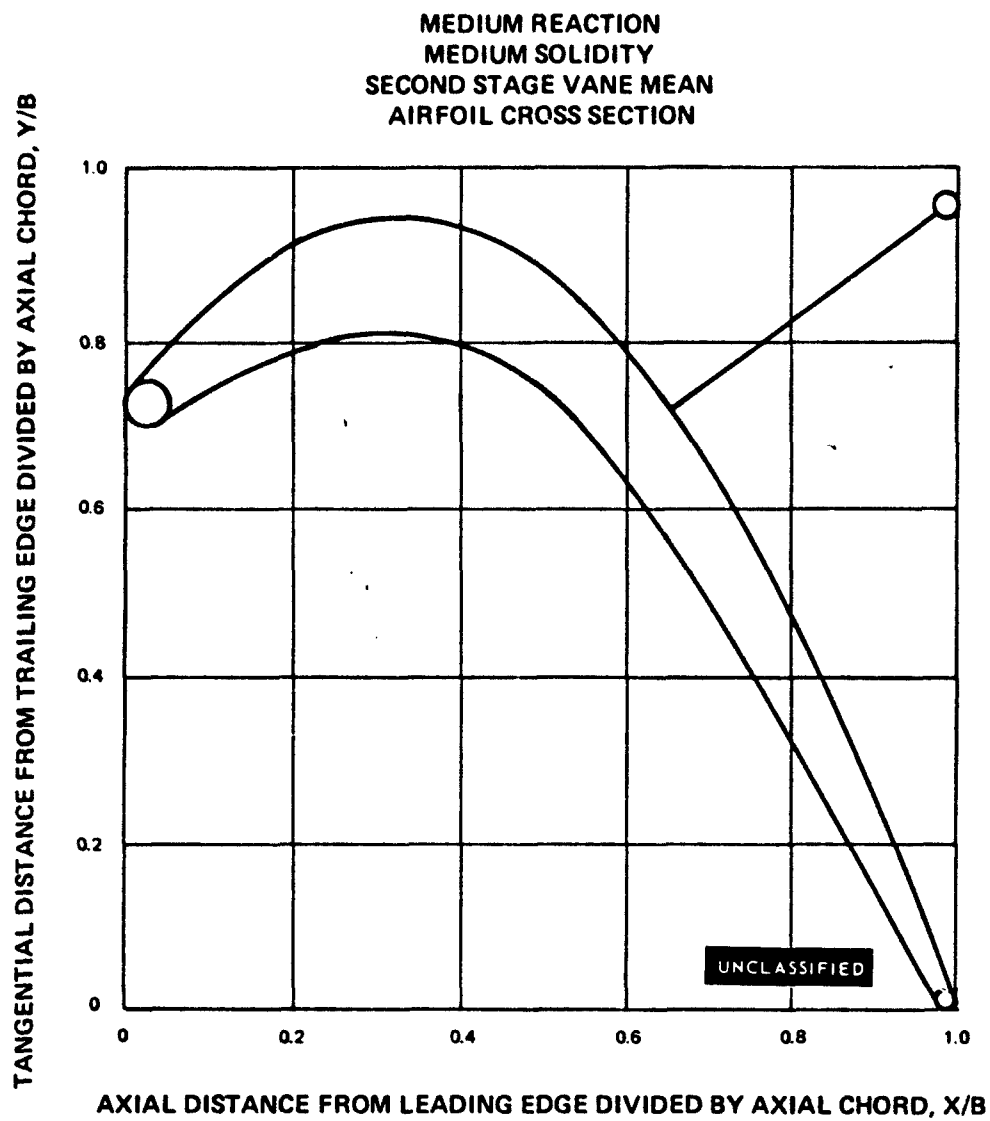


Figure 239

UNCLASSIFIED

UNCLASSIFIED

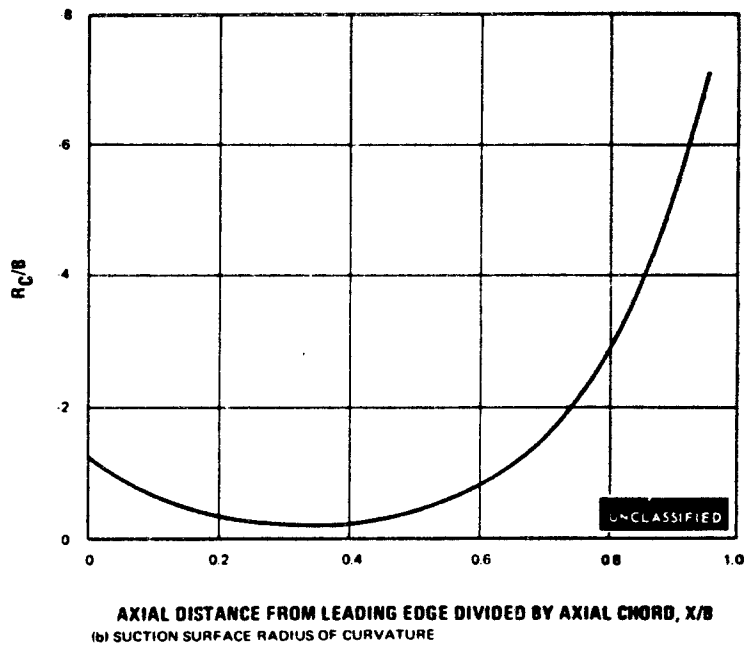
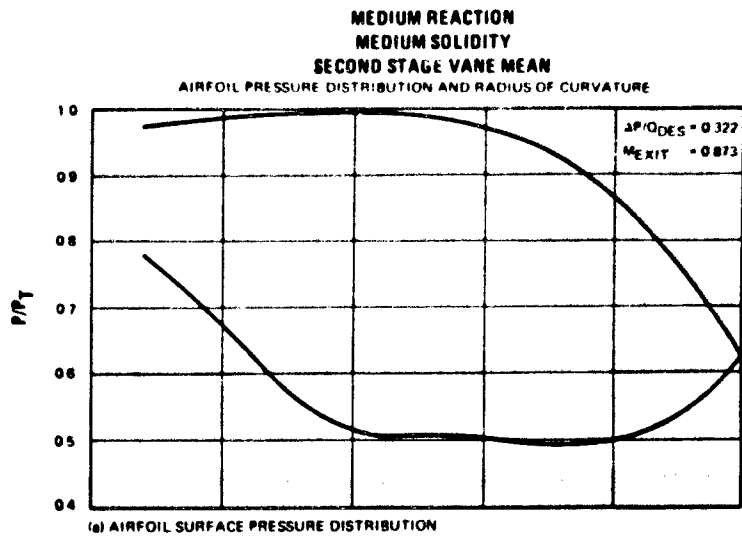


Figure 240

UNCLASSIFIED

UNCLASSIFIED

MEDIUM REACTION
MEDIUM SOLIDITY
SECOND STAGE VANE TIP
AIR FOIL CROSS SECTION

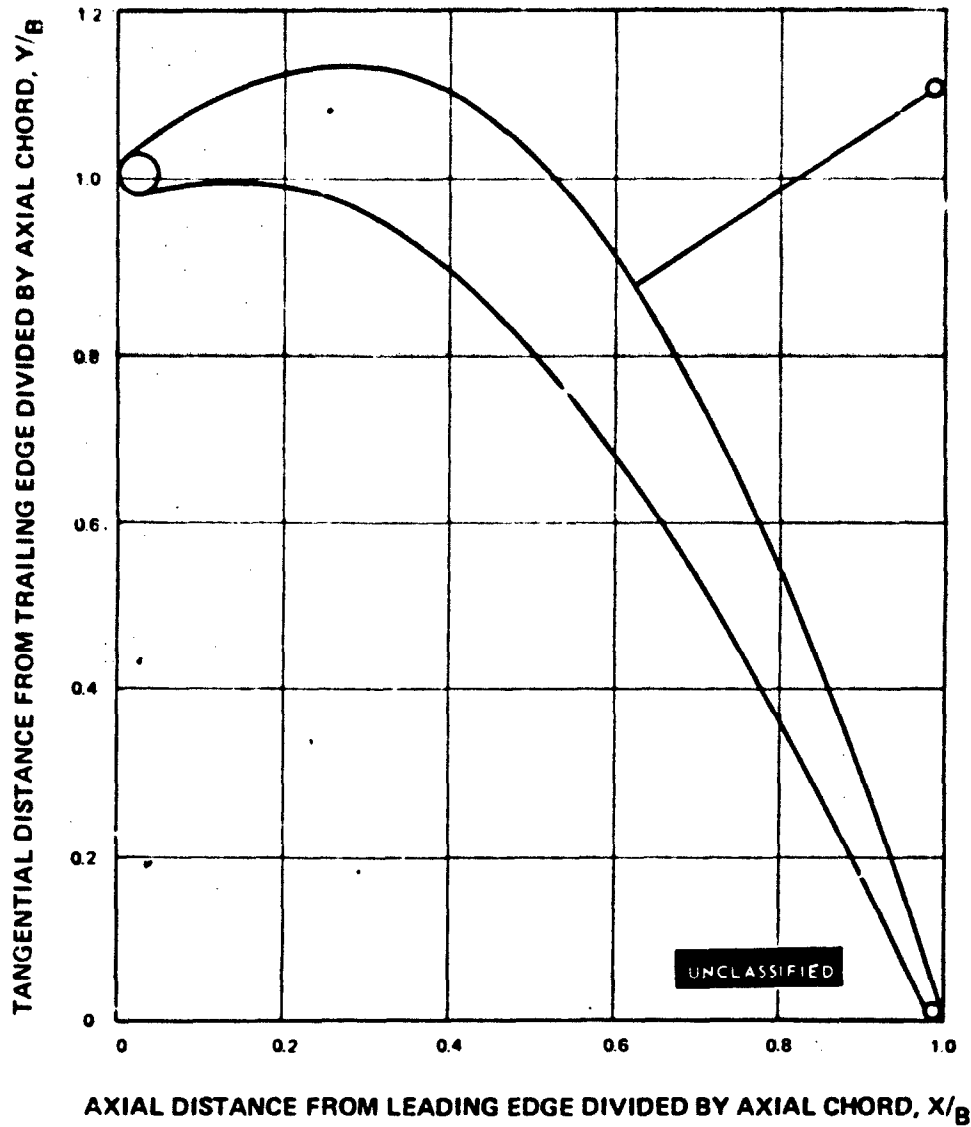


Figure 241

UNCLASSIFIED

UNCLASSIFIED

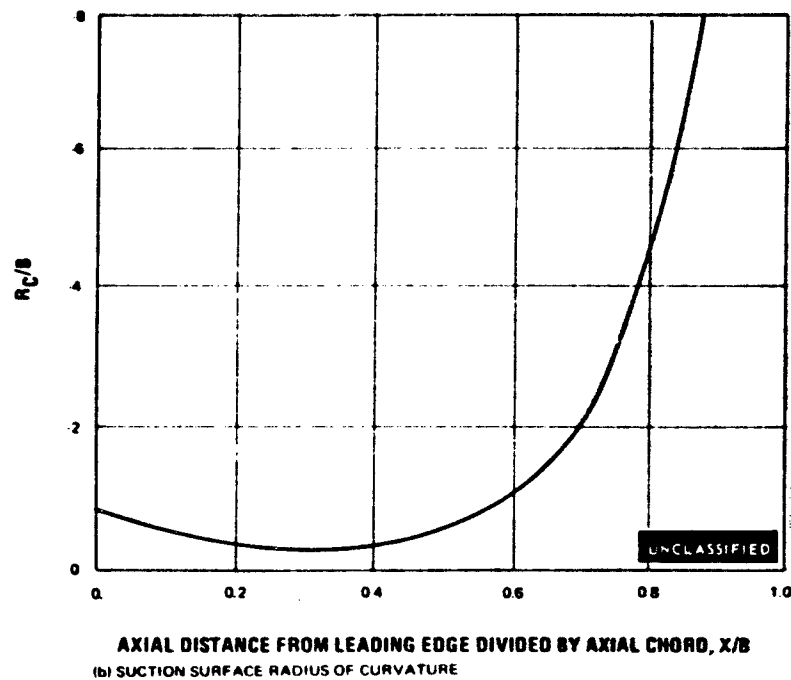
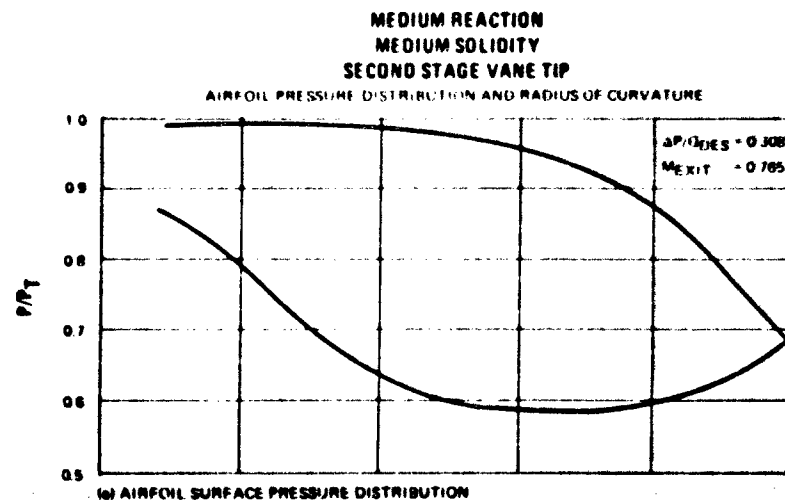


Figure 242

UNCLASSIFIED

UNCLASSIFIED

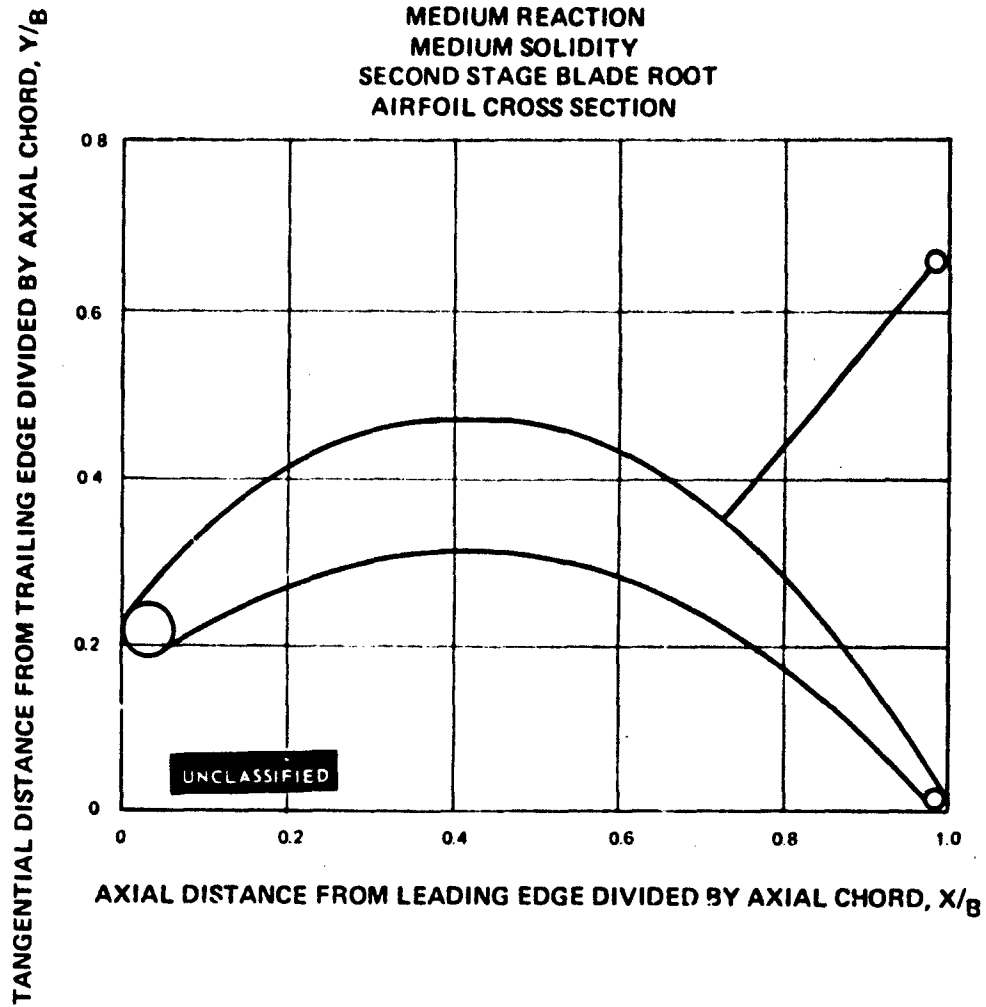


Figure 243

UNCLASSIFIED

UNCLASSIFIED

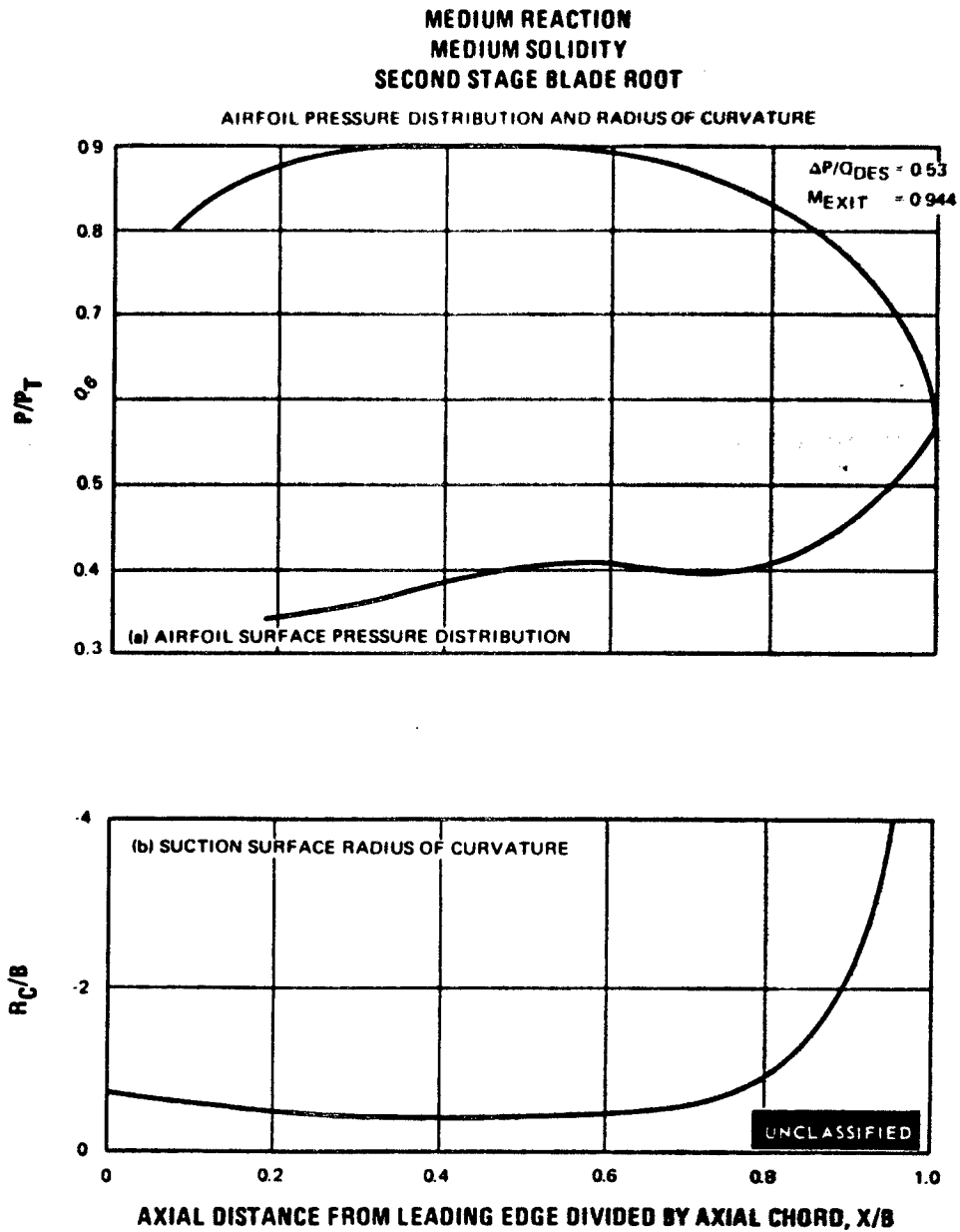


Figure 244

UNCLASSIFIED

UNCLASSIFIED

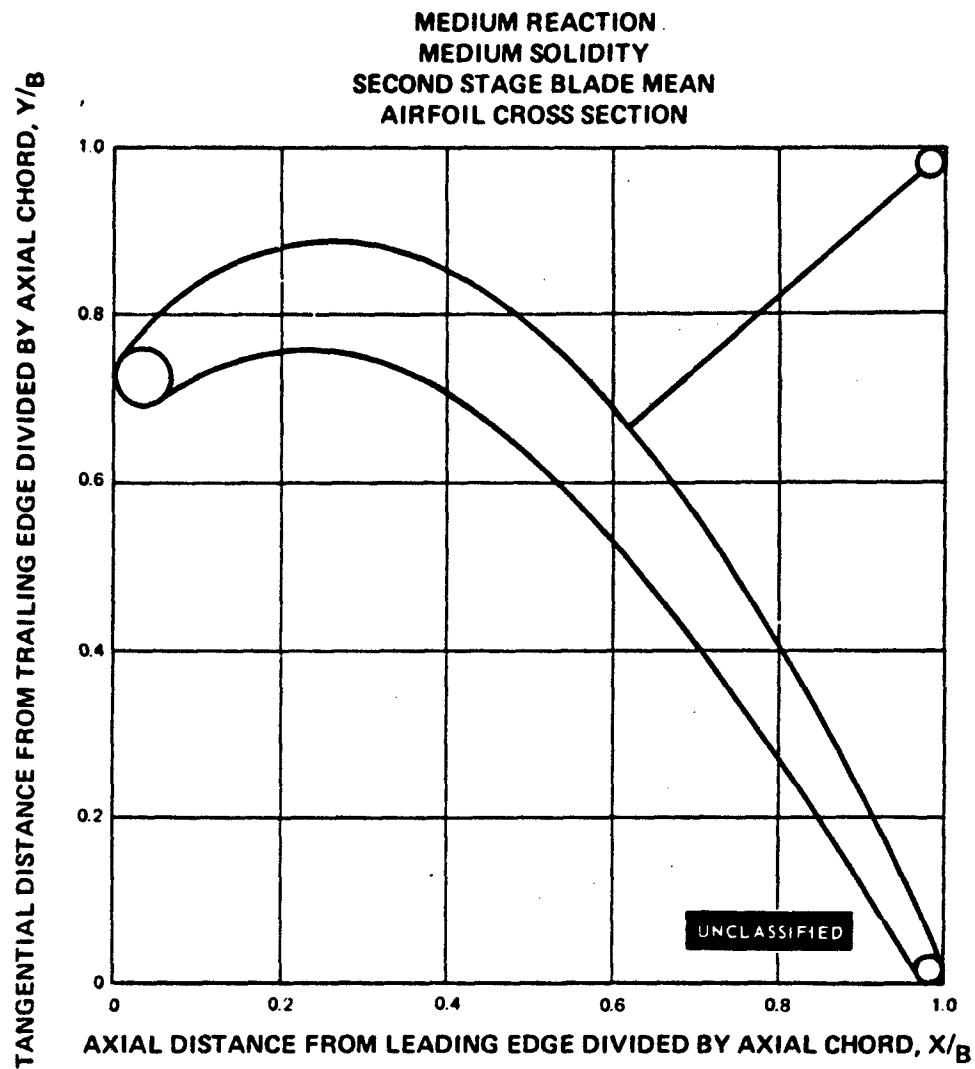


Figure 245

UNCLASSIFIED

UNCLASSIFIED

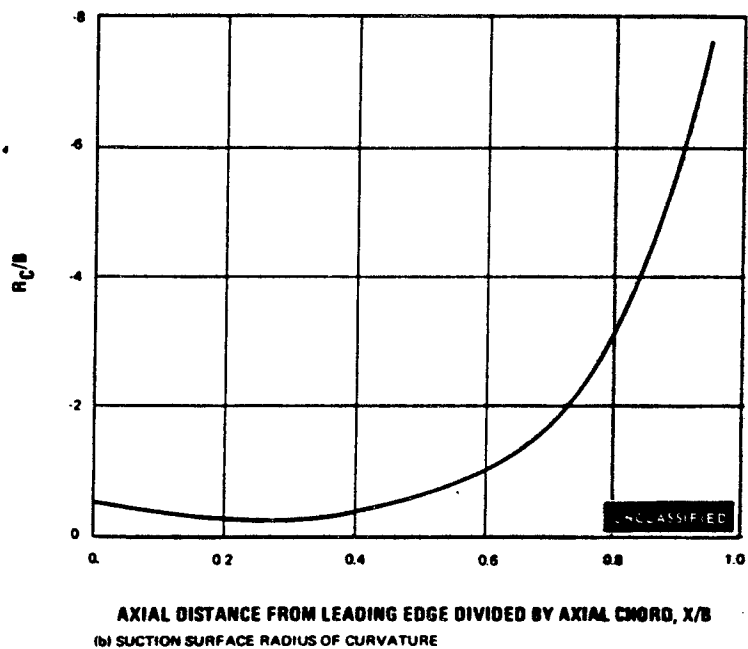
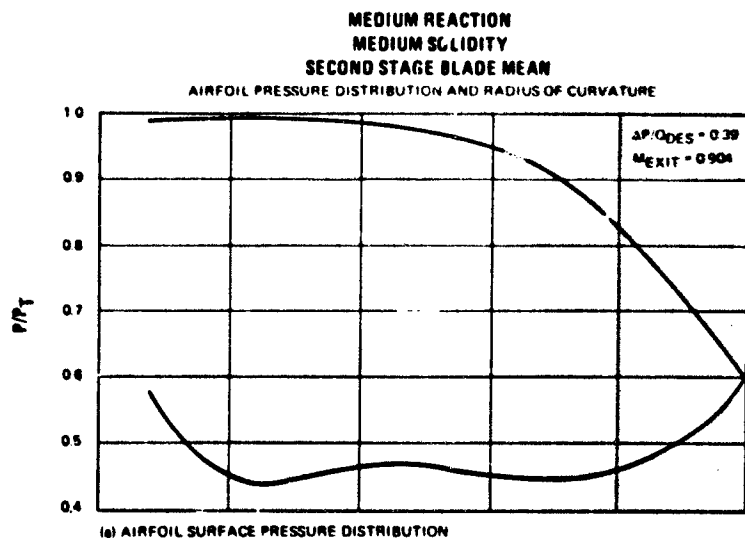


Figure 246

UNCLASSIFIED

UNCLASSIFIED

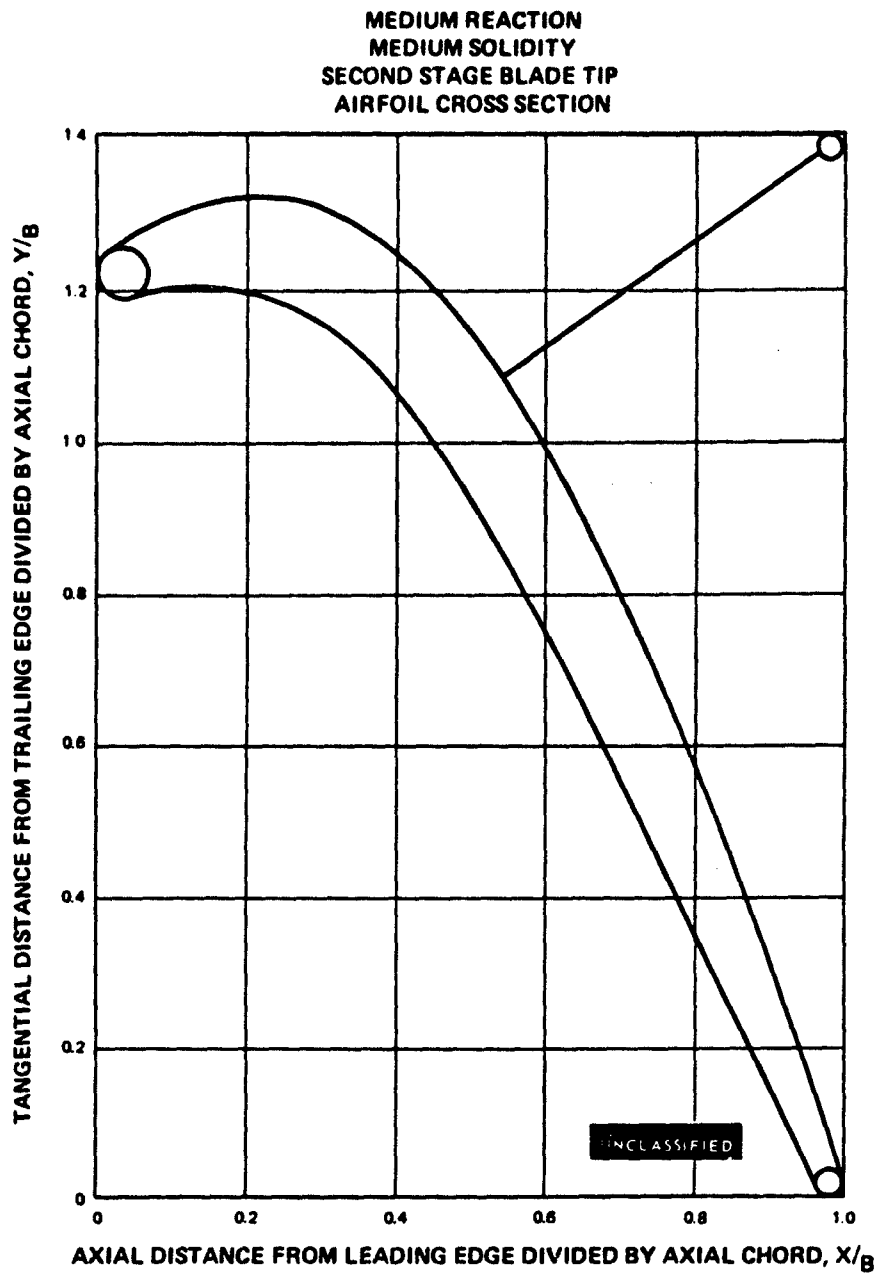


Figure 247

UNCLASSIFIED

UNCLASSIFIED

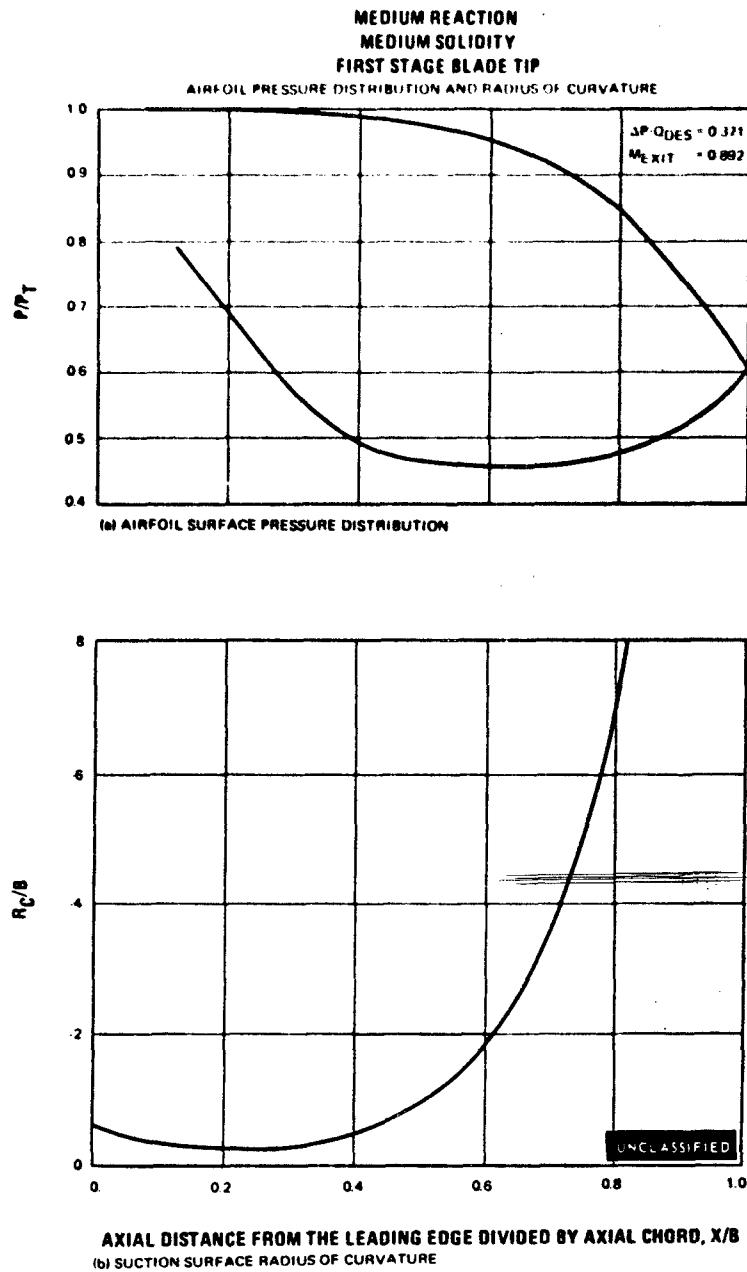


Figure 248

UNCLASSIFIED

UNCLASSIFIED

MEDIUM REACTION
NORMAL SOLIDITY
FINAL FIRST STAGE VANE ROOT

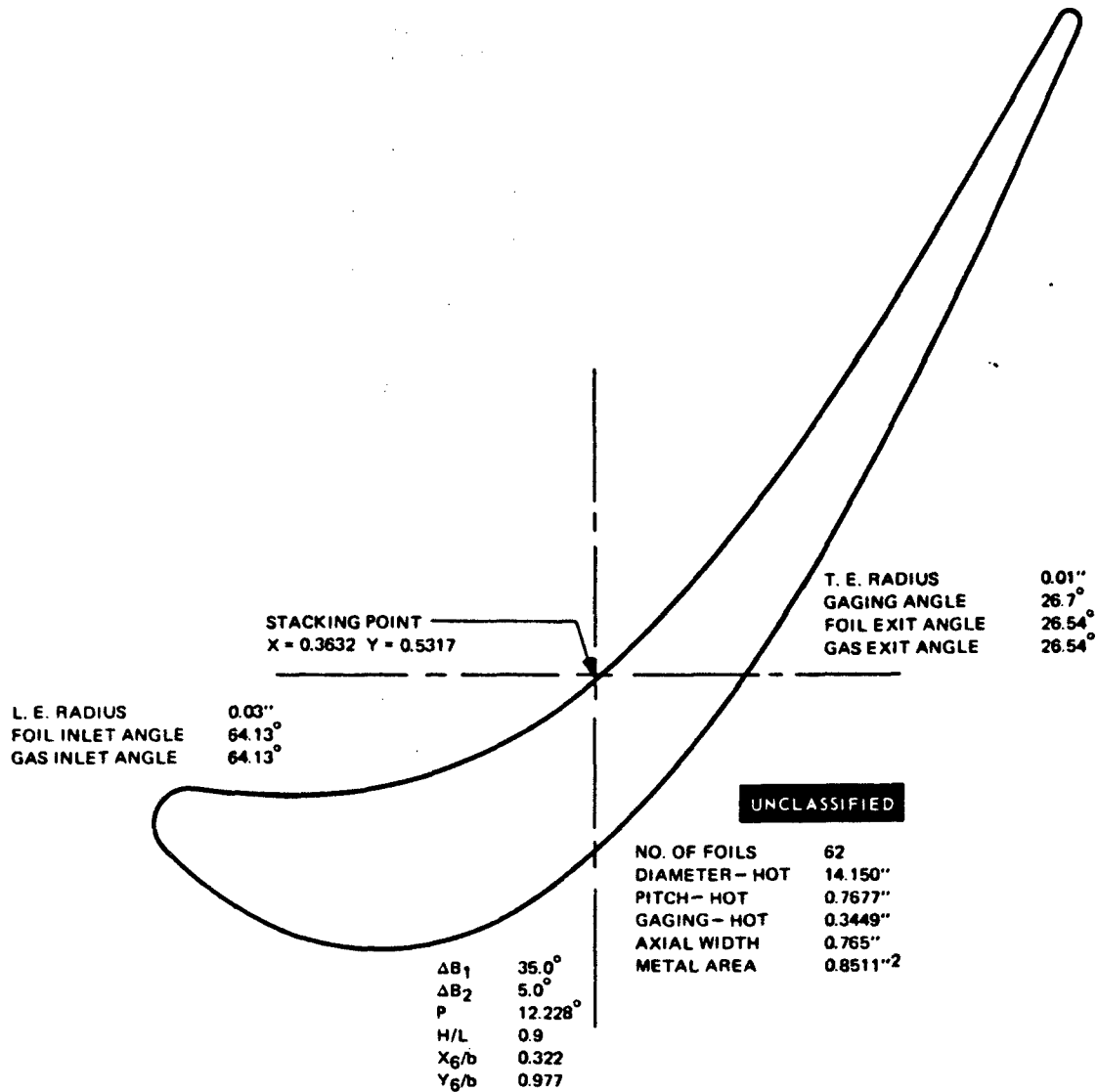


Figure 249

UNCLASSIFIED

UNCLASSIFIED

MEDIUM REACTION
FIRST STAGE VANE ROOT
NORMAL SOLIDITY

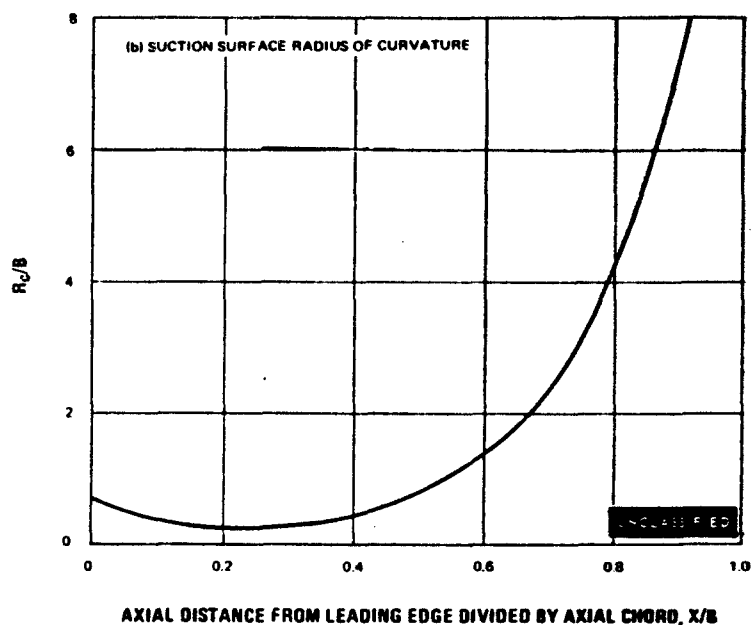
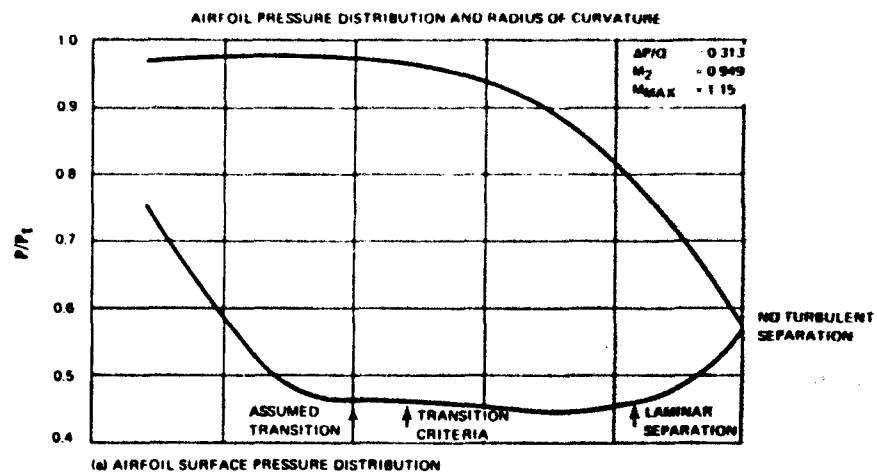


Figure 250

UNCLASSIFIED

UNCLASSIFIED

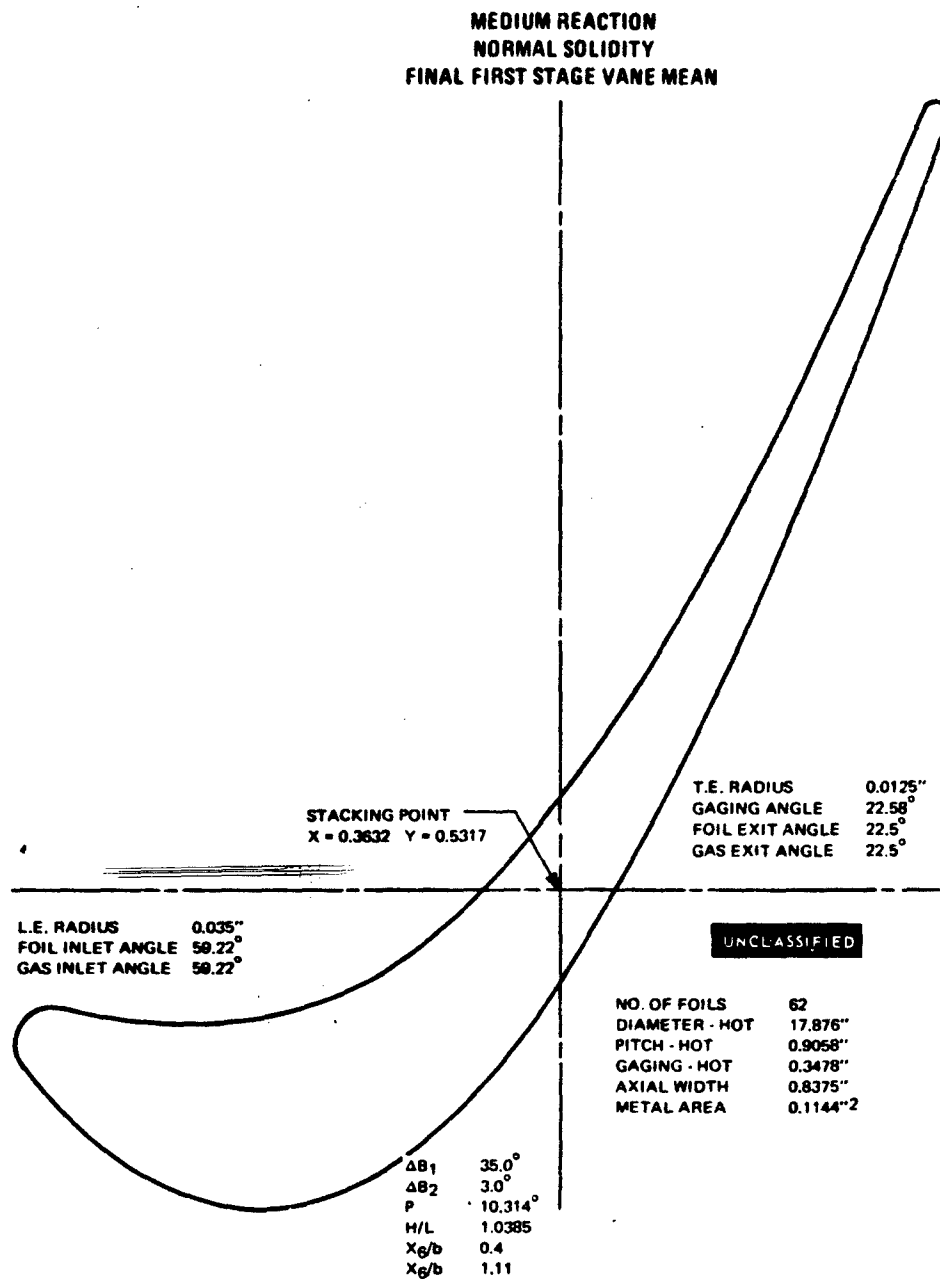


Figure 251

UNCLASSIFIED

UNCLASSIFIED

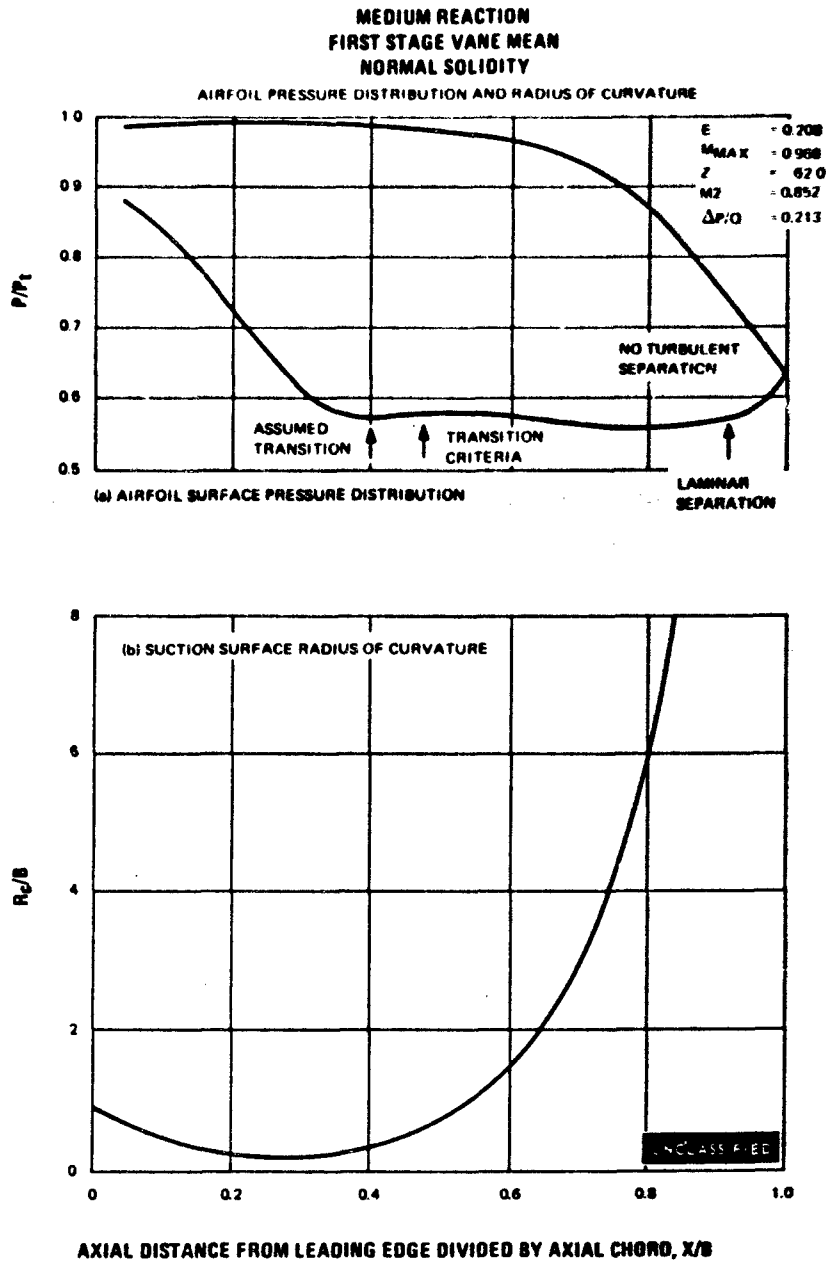


Figure 252

UNCLASSIFIED

UNCLASSIFIED

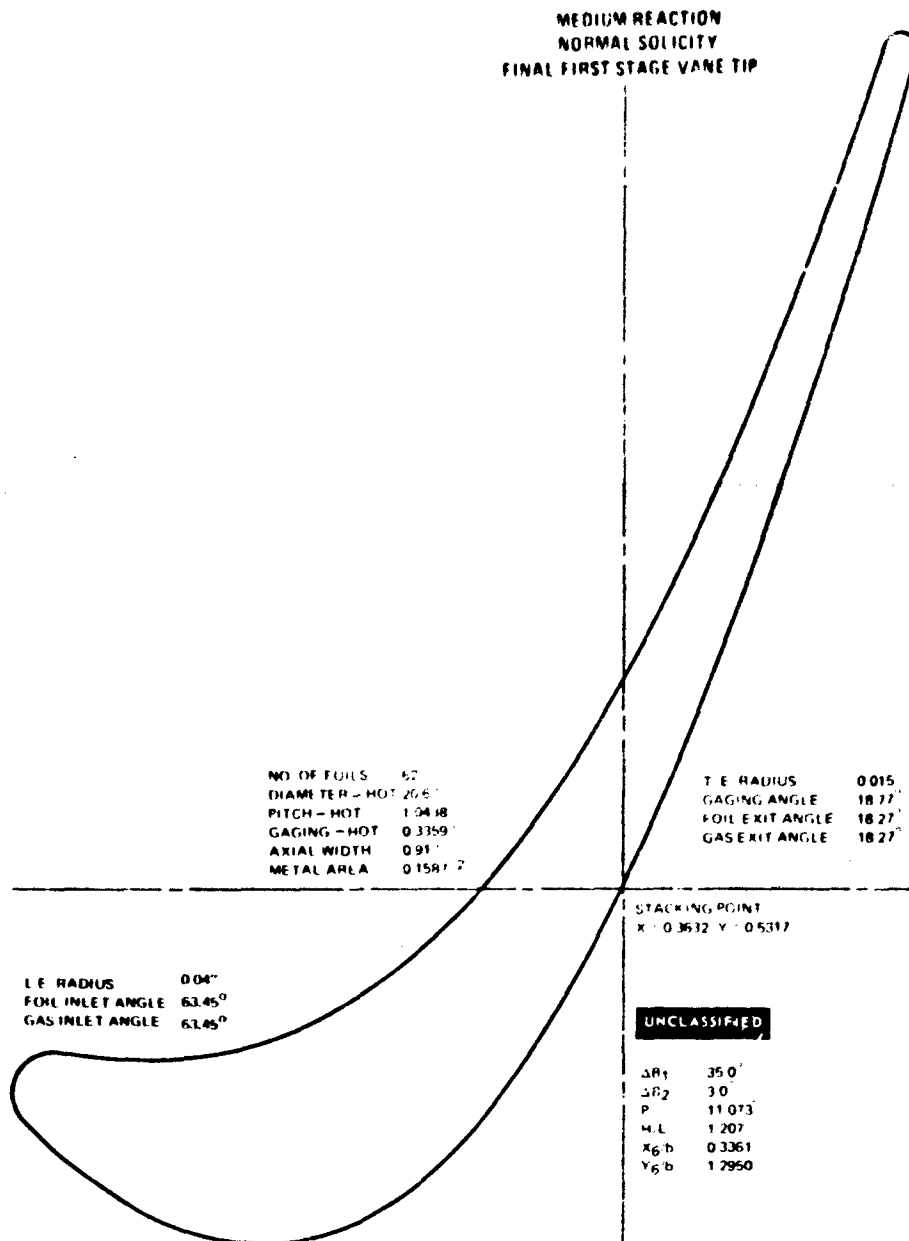


Figure 253

UNCLASSIFIED

UNCLASSIFIED

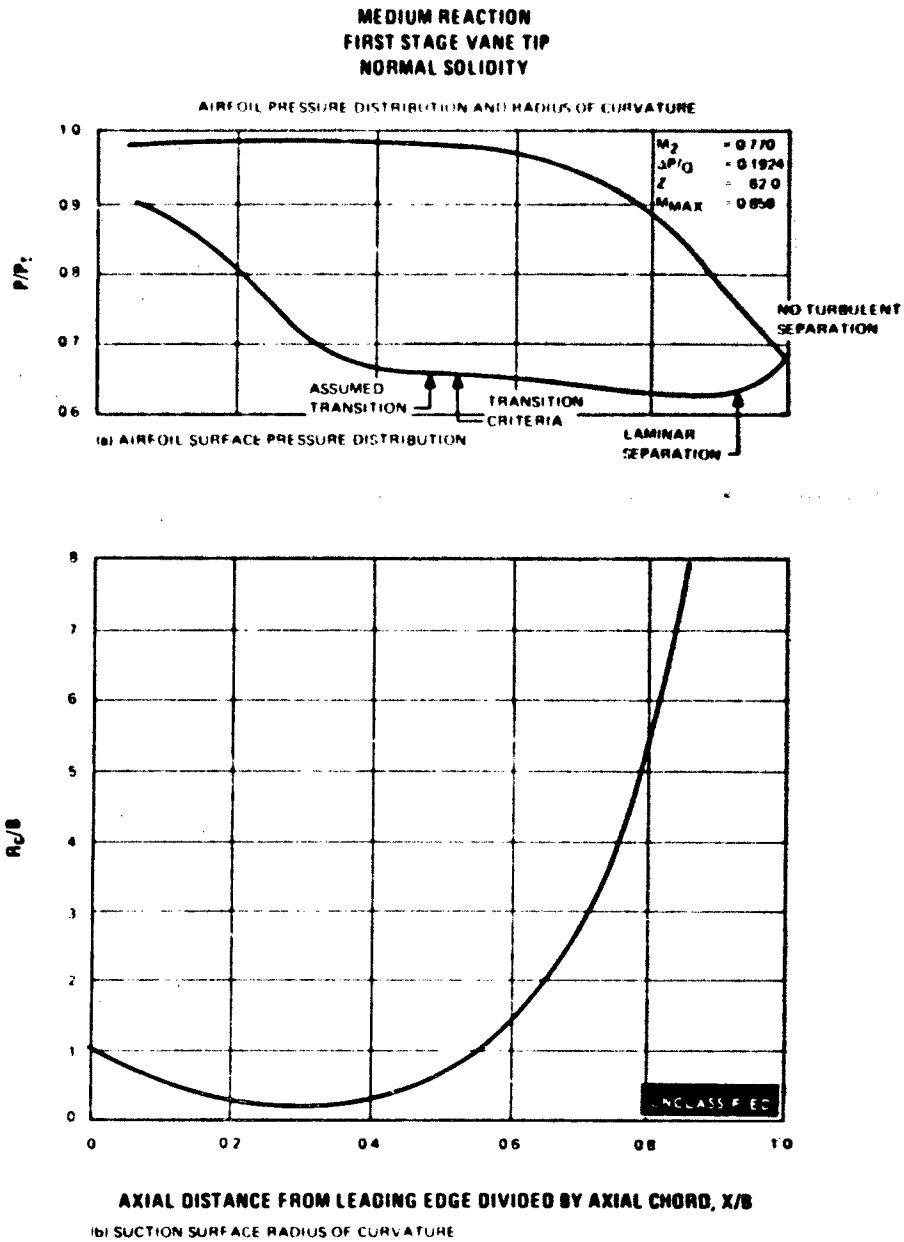


Figure 254

UNCLASSIFIED

UNCLASSIFIED

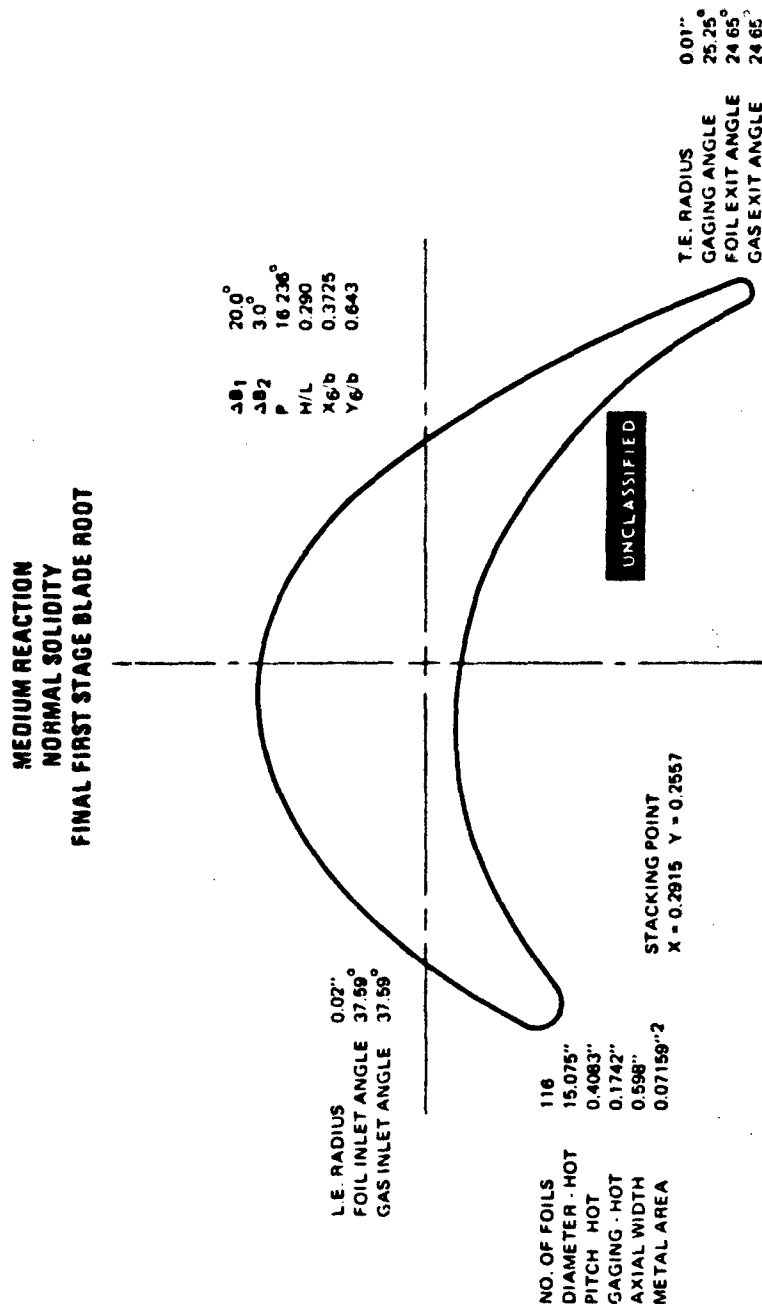


Figure 255

UNCLASSIFIED

UNCLASSIFIED

MEDIUM REACTION
FIRST STAGE BLADE ROOT
NORMAL SOLIDITY

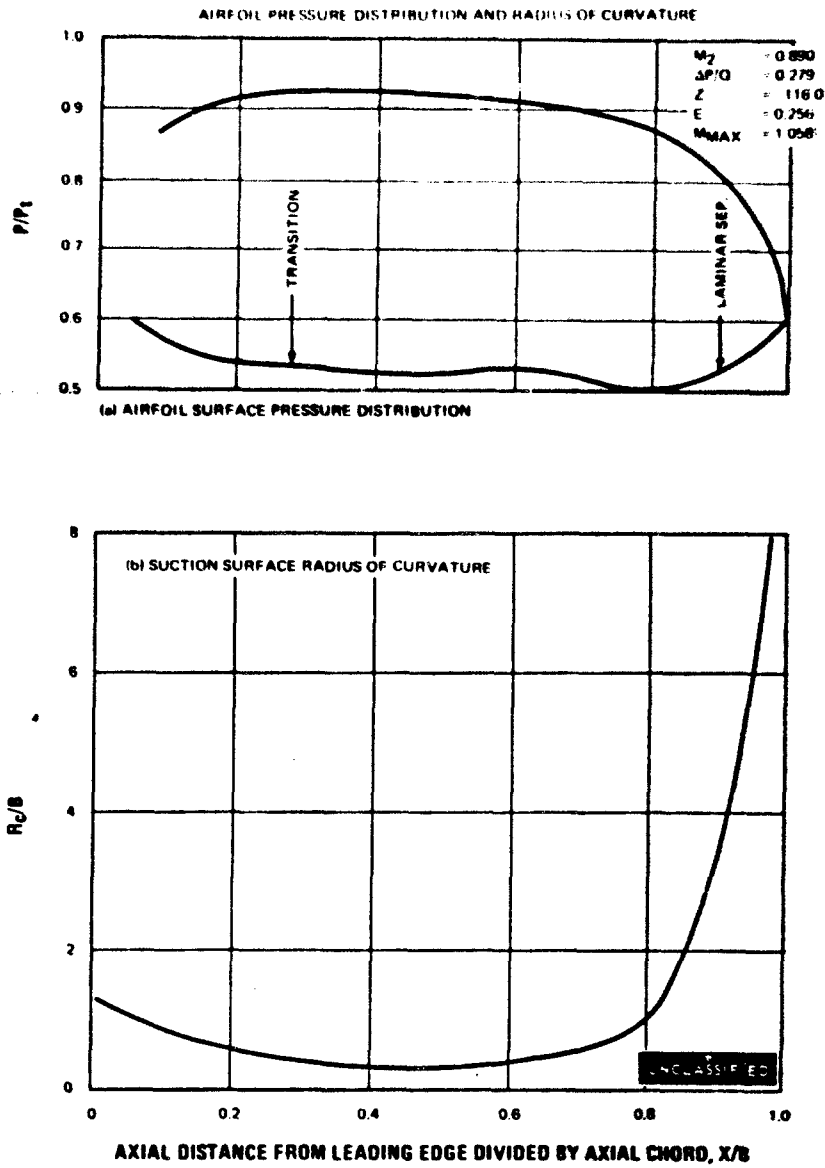


Figure 256

UNCLASSIFIED

UNCLASSIFIED

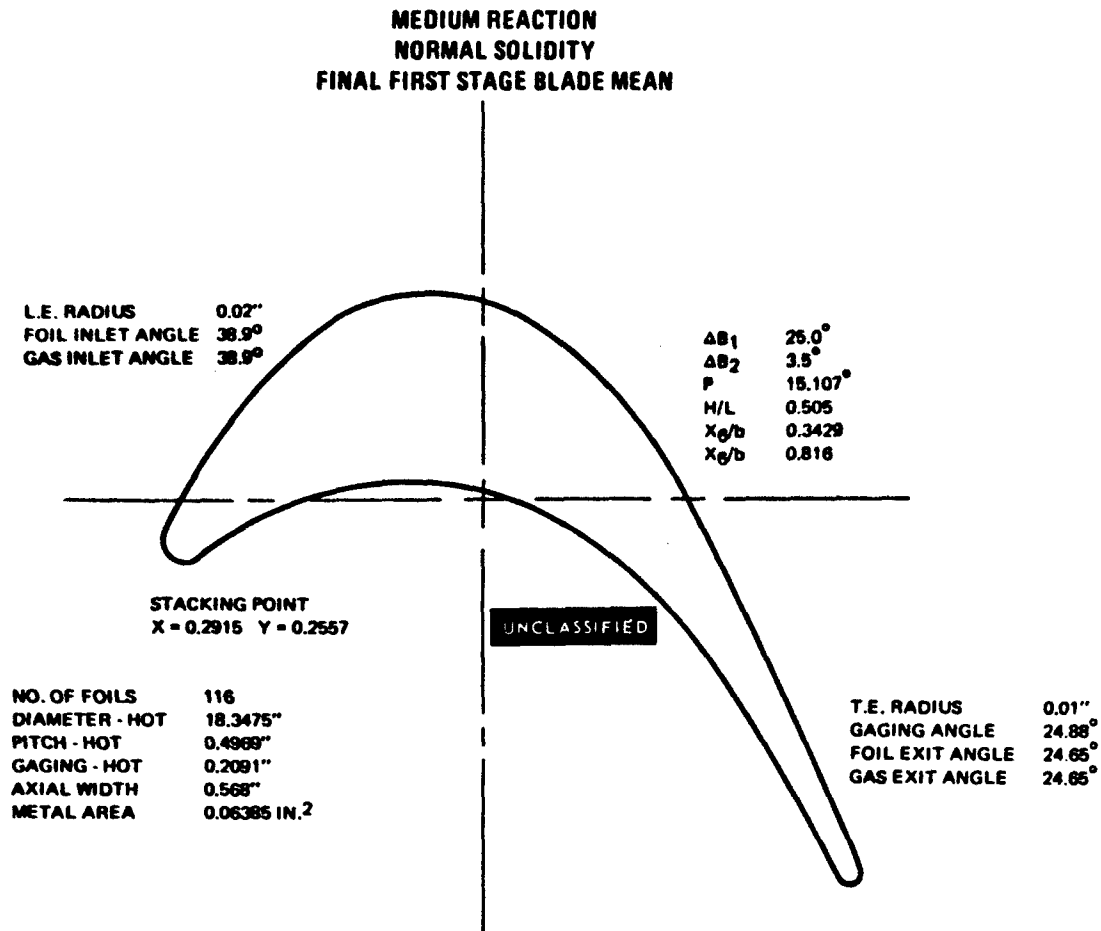


Figure 257

UNCLASSIFIED

UNCLASSIFIED

MEDIUM REACTION
FIRST STAGE BLADE MEAN
NORMAL SOLIDITY

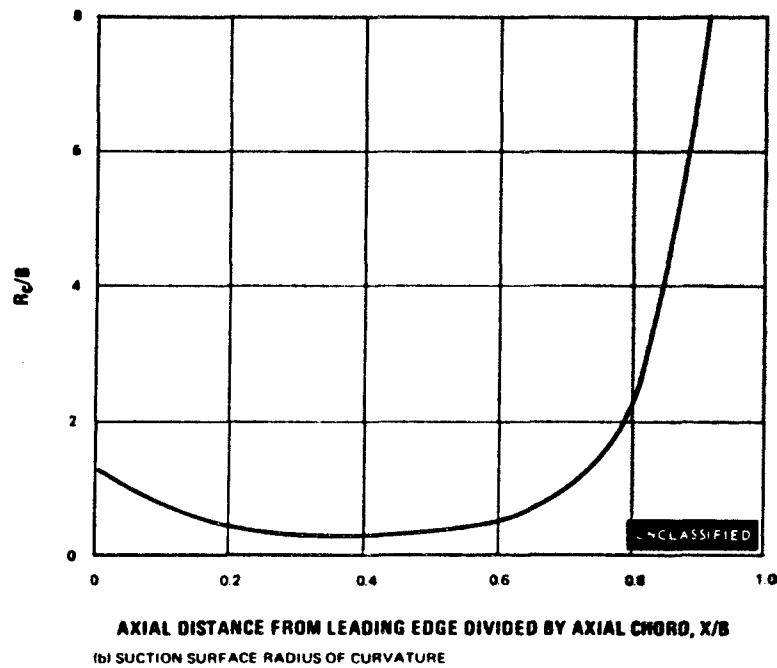
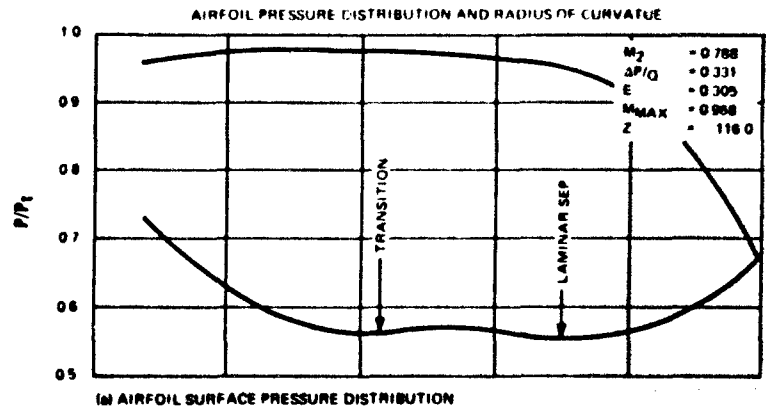


Figure 258

UNCLASSIFIED

UNCLASSIFIED

MEDIUM REACTION
NORMAL SOLIDITY
FINAL FIRST STAGE BLADE TIP

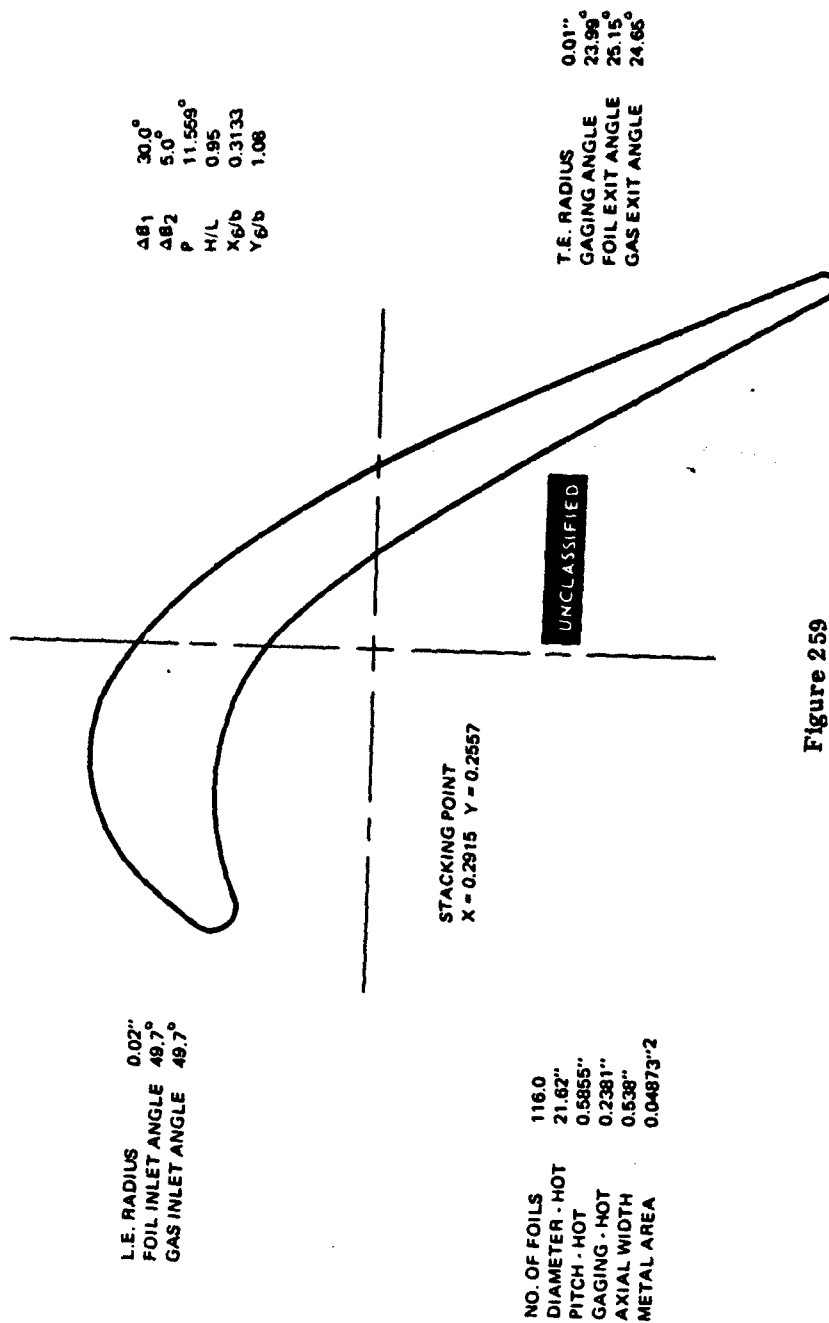


Figure 259

UNCLASSIFIED

UNCLASSIFIED

MEDIUM REACTION
FIRST STAGE BLADE TIP
NORMAL SOLIDITY

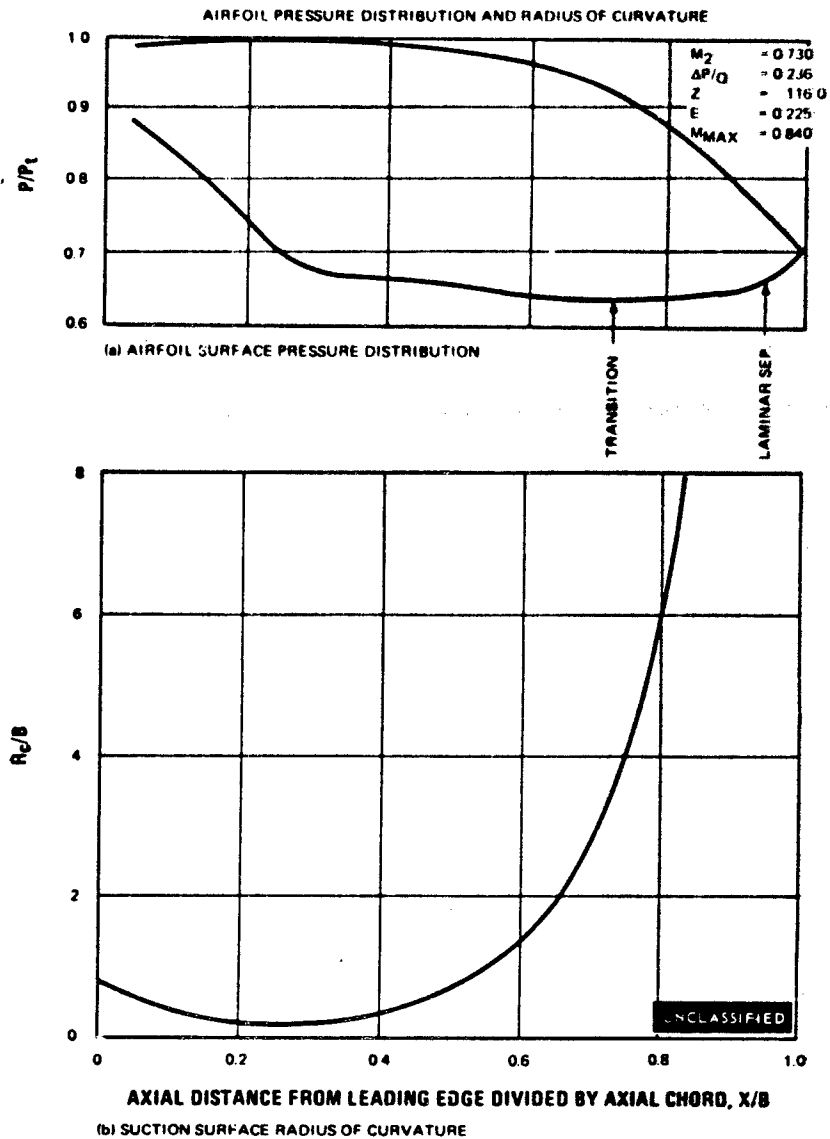


Figure 260

UNCLASSIFIED

UNCLASSIFIED

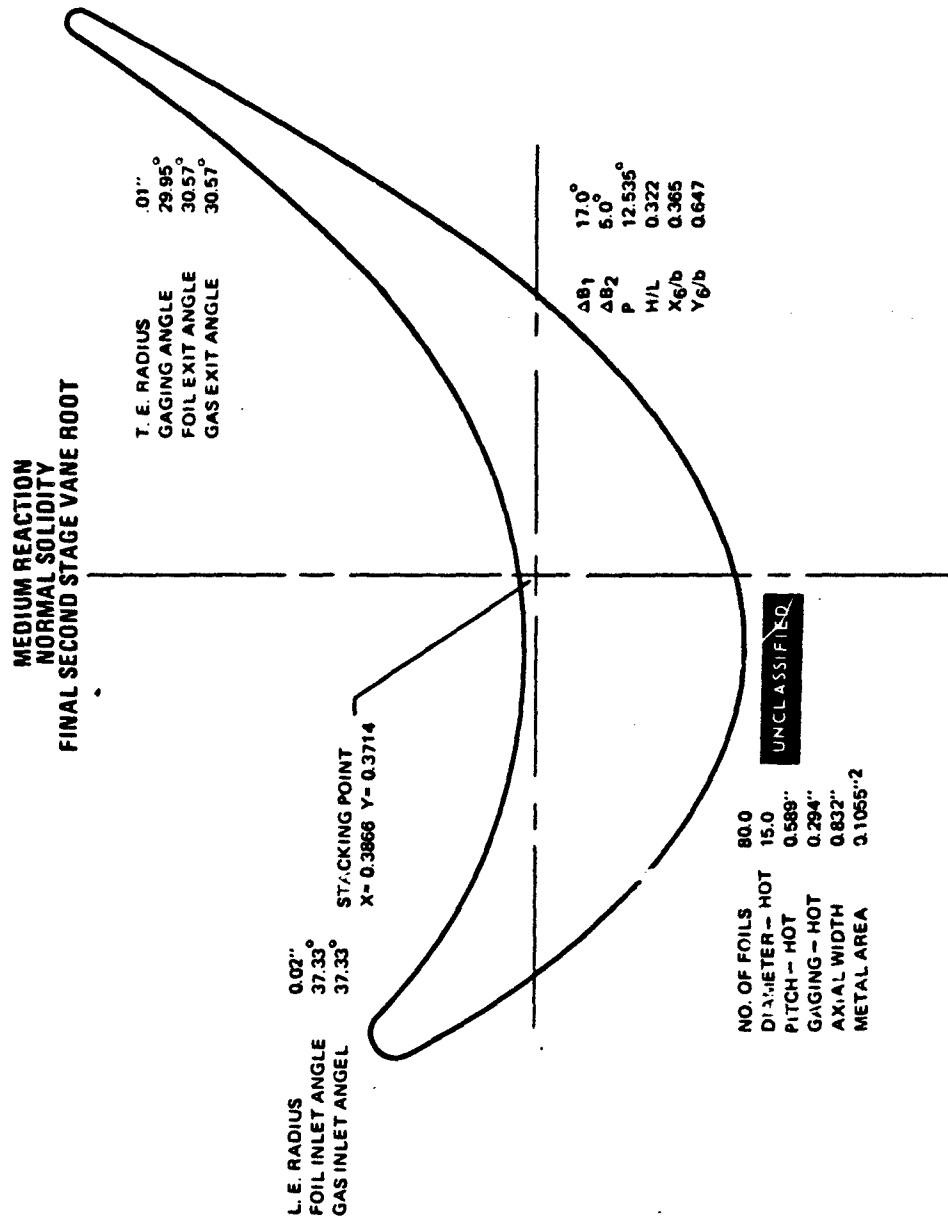


Figure 261

UNCLASSIFIED

UNCLASSIFIED

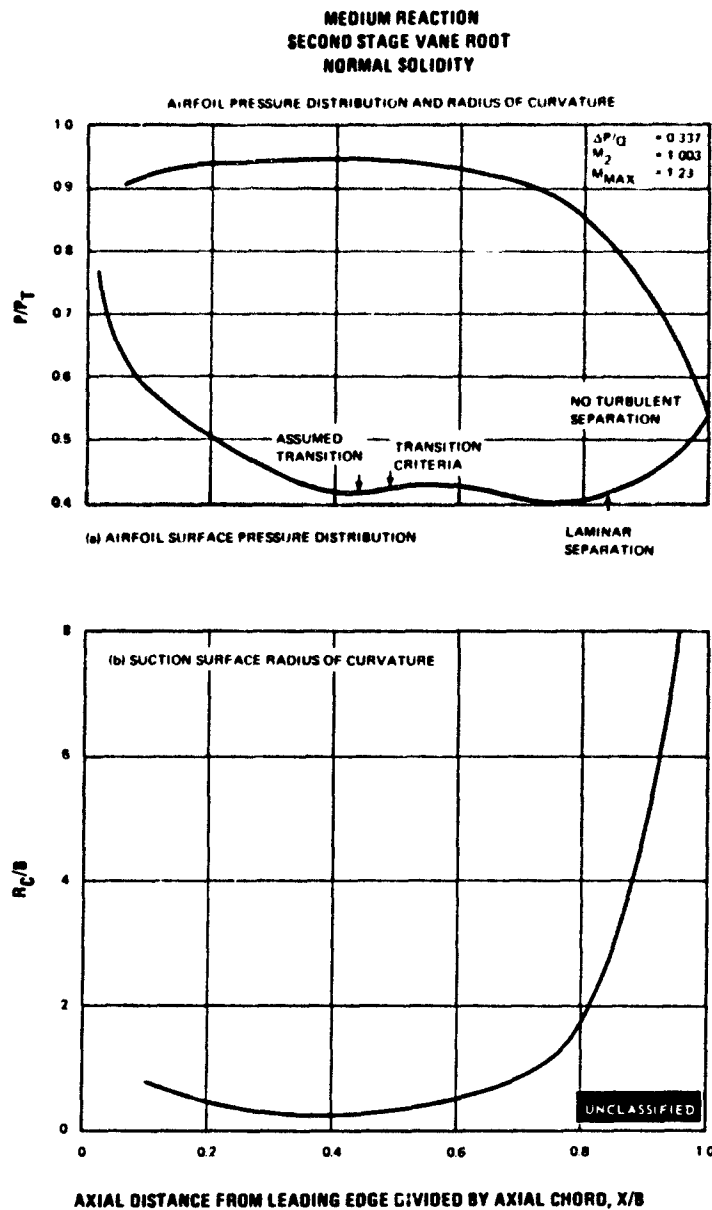


Figure 262

UNCLASSIFIED

UNCLASSIFIED

MEDIUM REACTION
NORMAL SOLIDITY
FINAL SECOND STAGE VANE MEAN

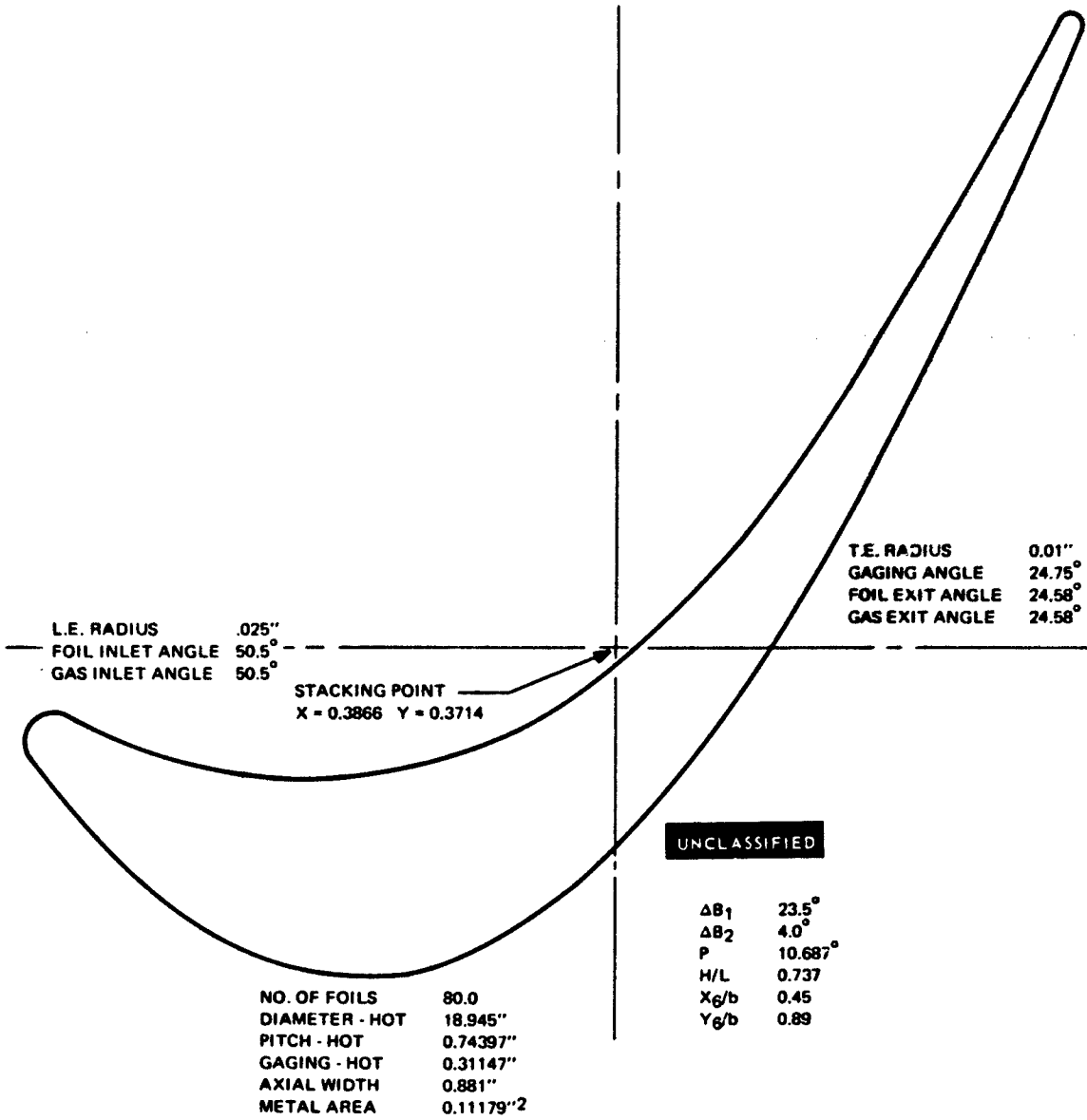


Figure 263

UNCLASSIFIED

UNCLASSIFIED

MEDIUM REACTION
SECOND STAGE VANE MEAN
NORMAL SOLIDITY

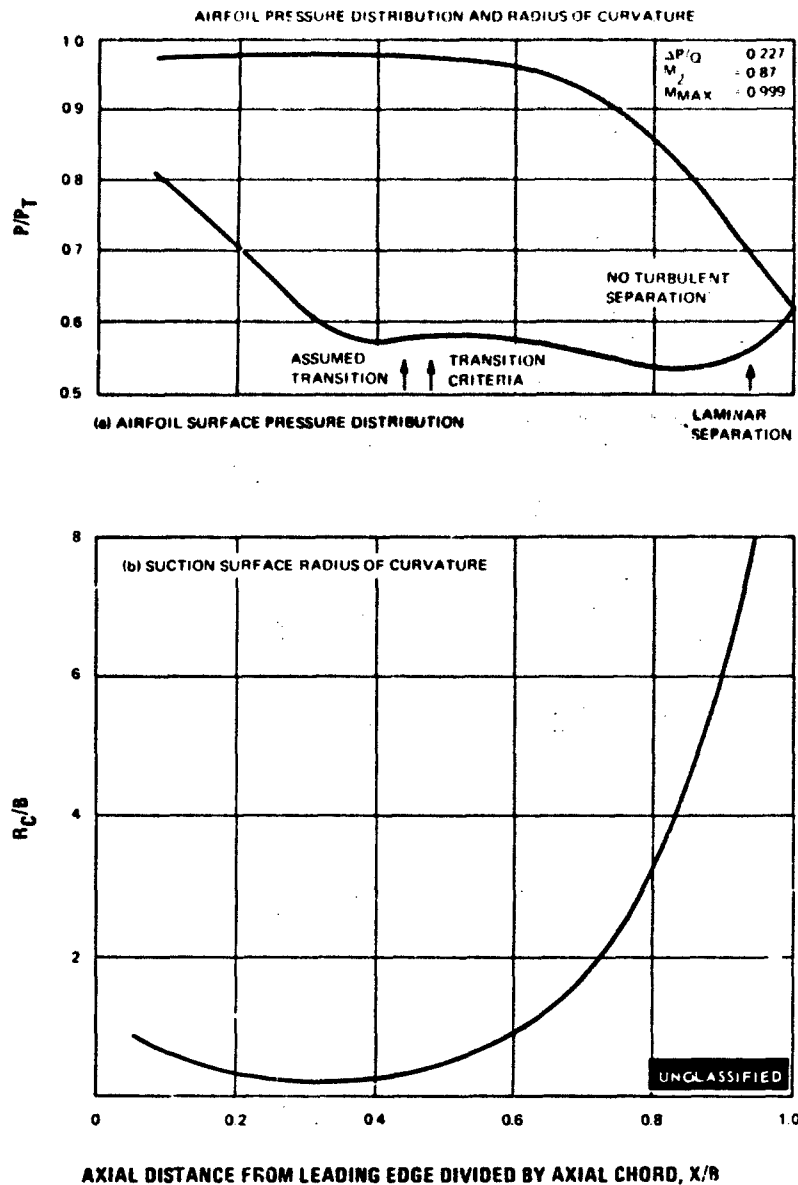


Figure 264

UNCLASSIFIED

UNCLASSIFIED

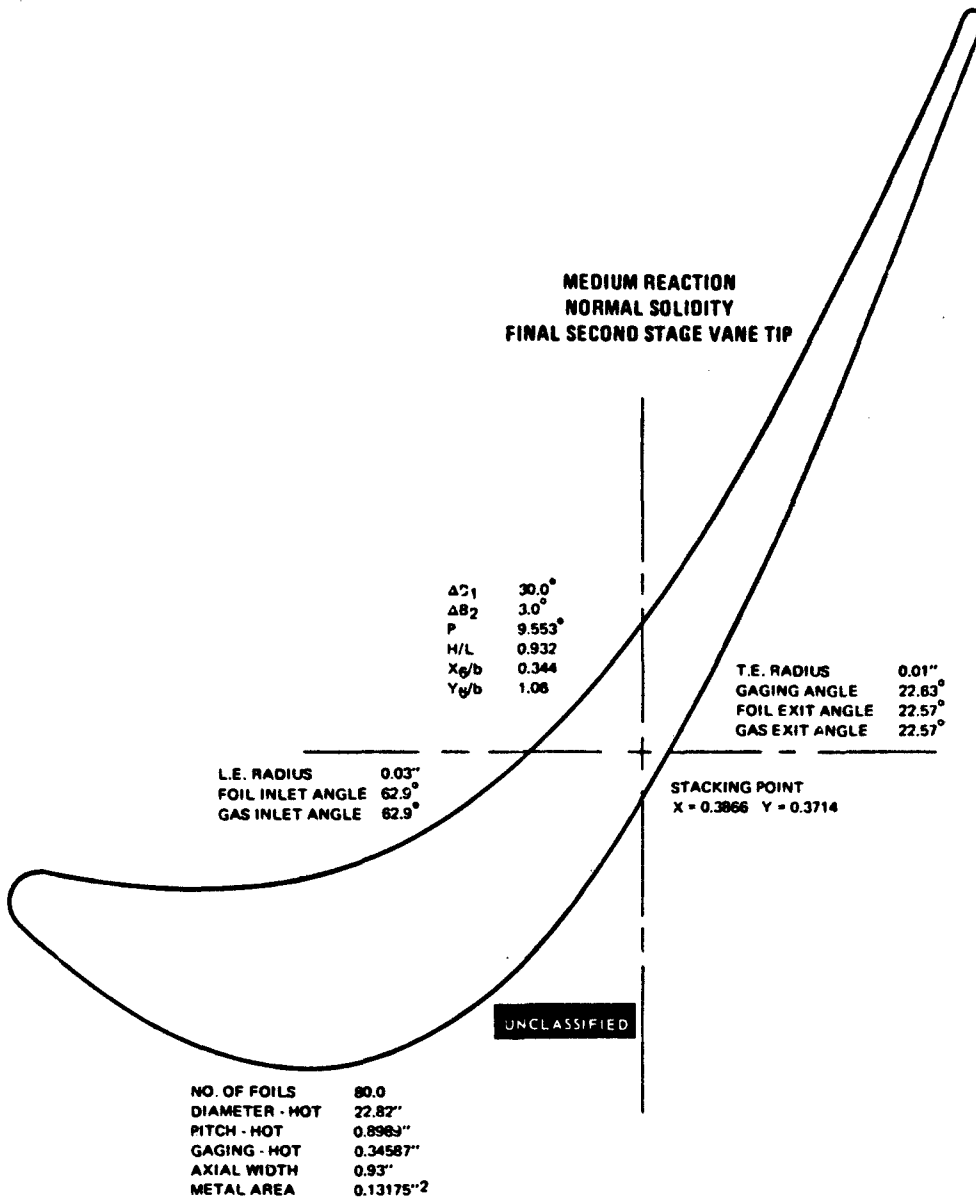


Figure 265

UNCLASSIFIED

UNCLASSIFIED

MEDIUM REACTION
SECOND STAGE VANE TIP
NORMAL SOLIDITY

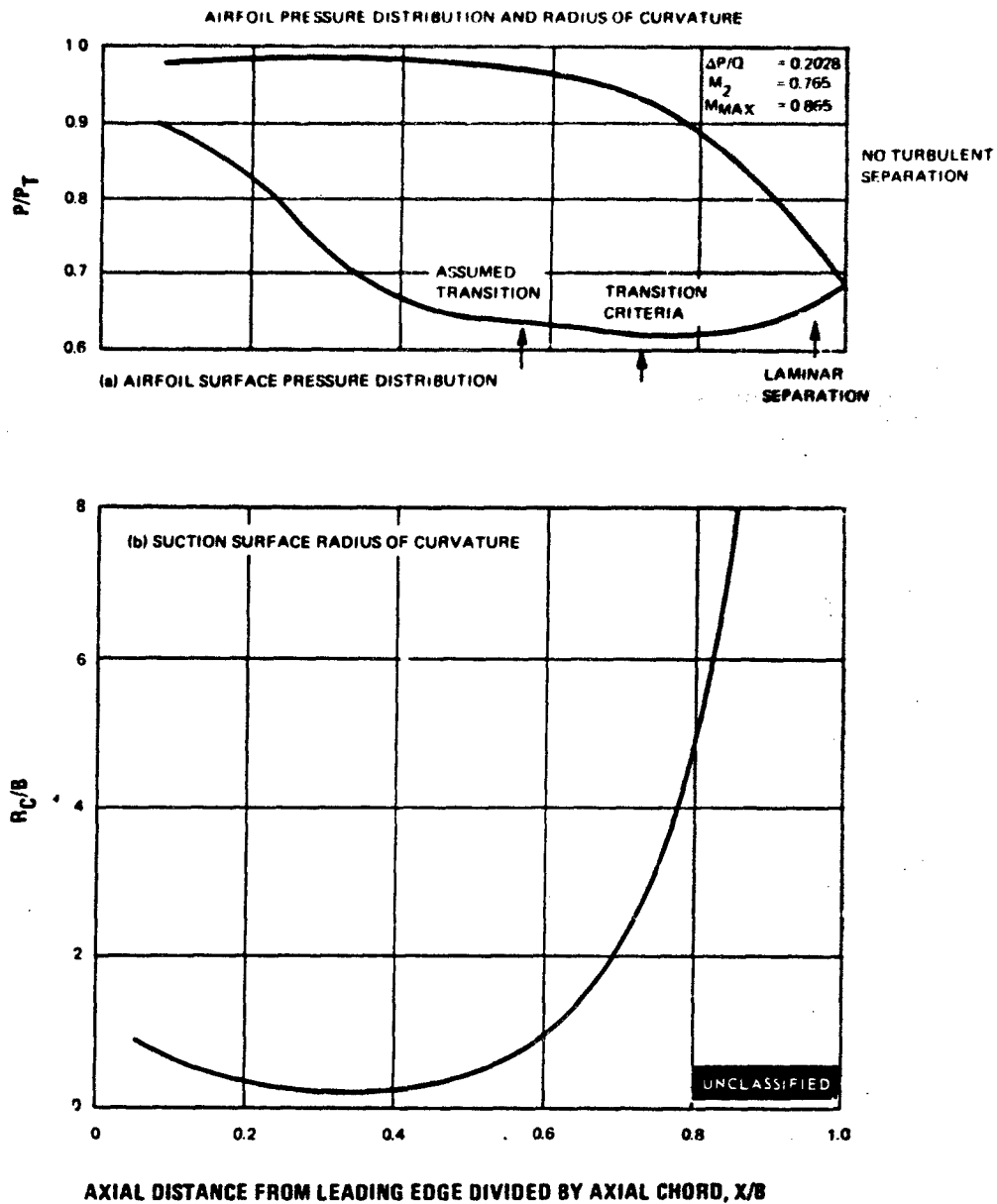


Figure 266

UNCLASSIFIED

UNCLASSIFIED

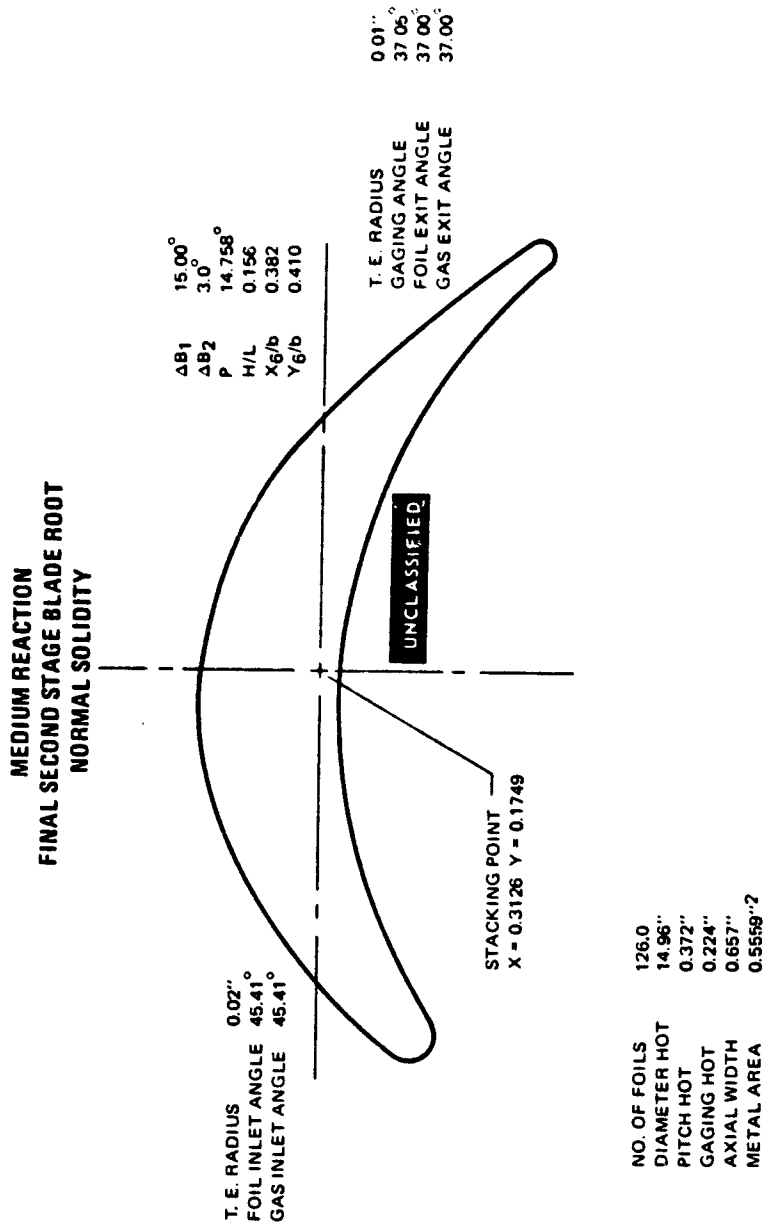


Figure 267

UNCLASSIFIED

UNCLASSIFIED

MEDIUM REACTION
SECOND STAGE BLADE ROOT
NORMAL SOLIDITY

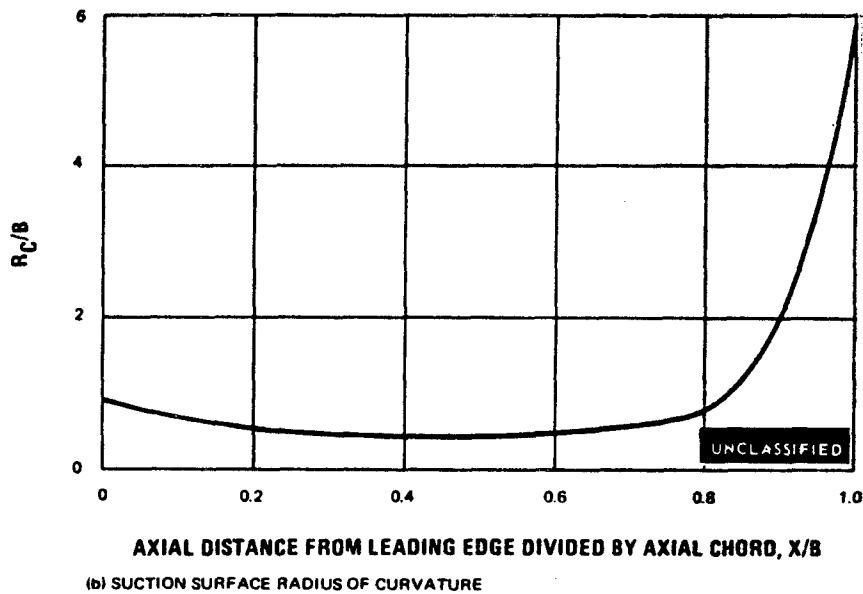
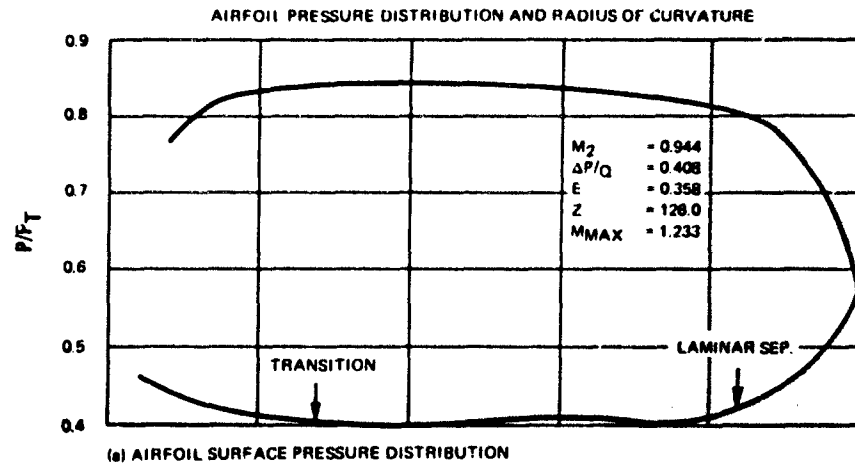


Figure 268

UNCLASSIFIED

UNCLASSIFIED

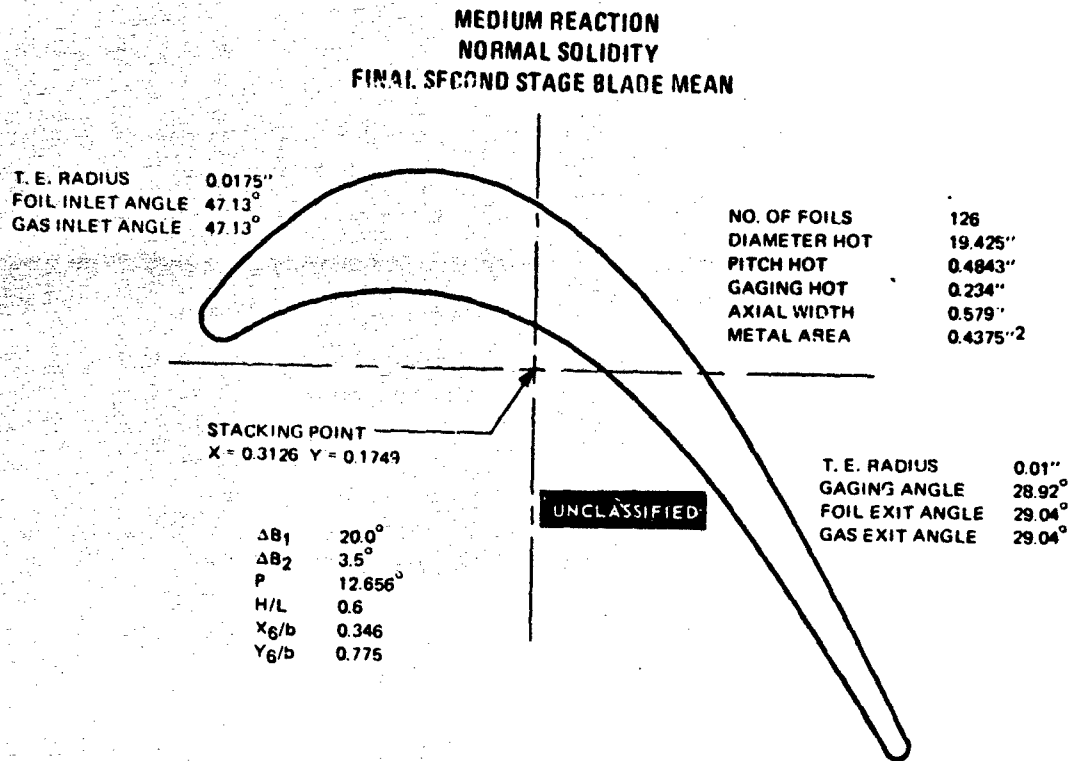


Figure 269

UNCLASSIFIED

UNCLASSIFIED

MEDIUM REACTION
SECOND STAGE BLADE MEAN
NORMAL SOLIDITY

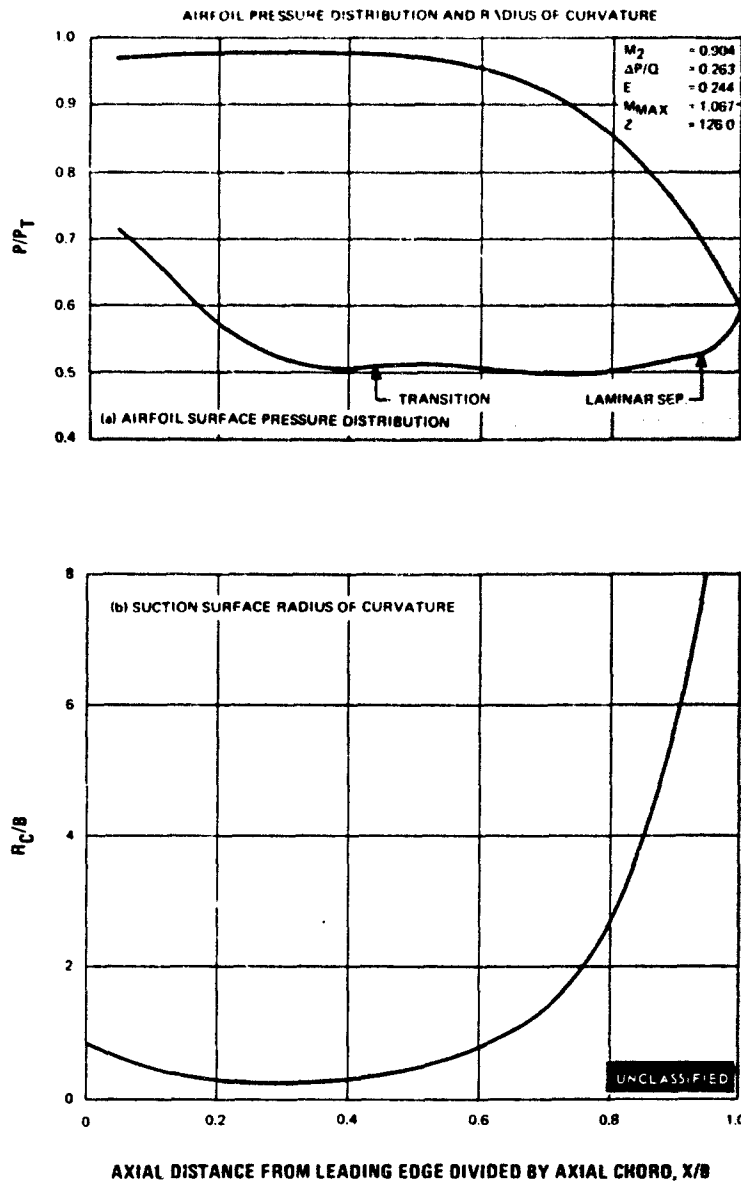
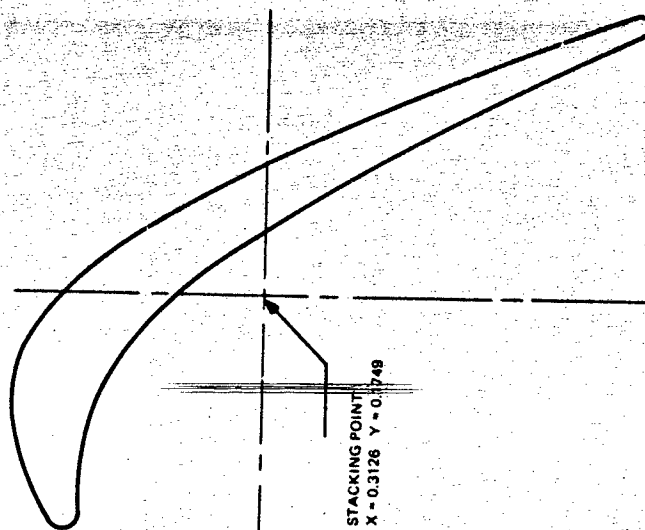


Figure 270

UNCLASSIFIED

UNCLASSIFIED

~ MEDIUM REACTION
NORMAL SOLIDITY
FINAL SECOND STAGE BLADE TIP



NO. OF FOILS 126
DIAMETER - HOT 2.930"
PITCH - HOT 0.5967"
GAGING - HOT 0.224"
AXIAL WIDTH 0.5"
METAL AREA 0.4241"²

UNCLASSIFIED

T.E. RADIUS 0.01"
GAGING ANGLE 22.08°
FOIL EXIT ANGLE 22.3°
GAS EXIT ANGLE 22.3°

L.E. RADIUS 0.015"
FOIL INLET ANGLE 71.3°
GAS INLET ANGLE 71.3°

ΔB1 25.00°
ΔB2 4.00°
P 11.65°
H/L 1.16
Xg/b 0.3068
Yg/b 1.2

Figure 271

UNCLASSIFIED

UNCLASSIFIED

MEDIUM REACTION
SECOND STAGE BLADE TIP
NORMAL SOLIDITY

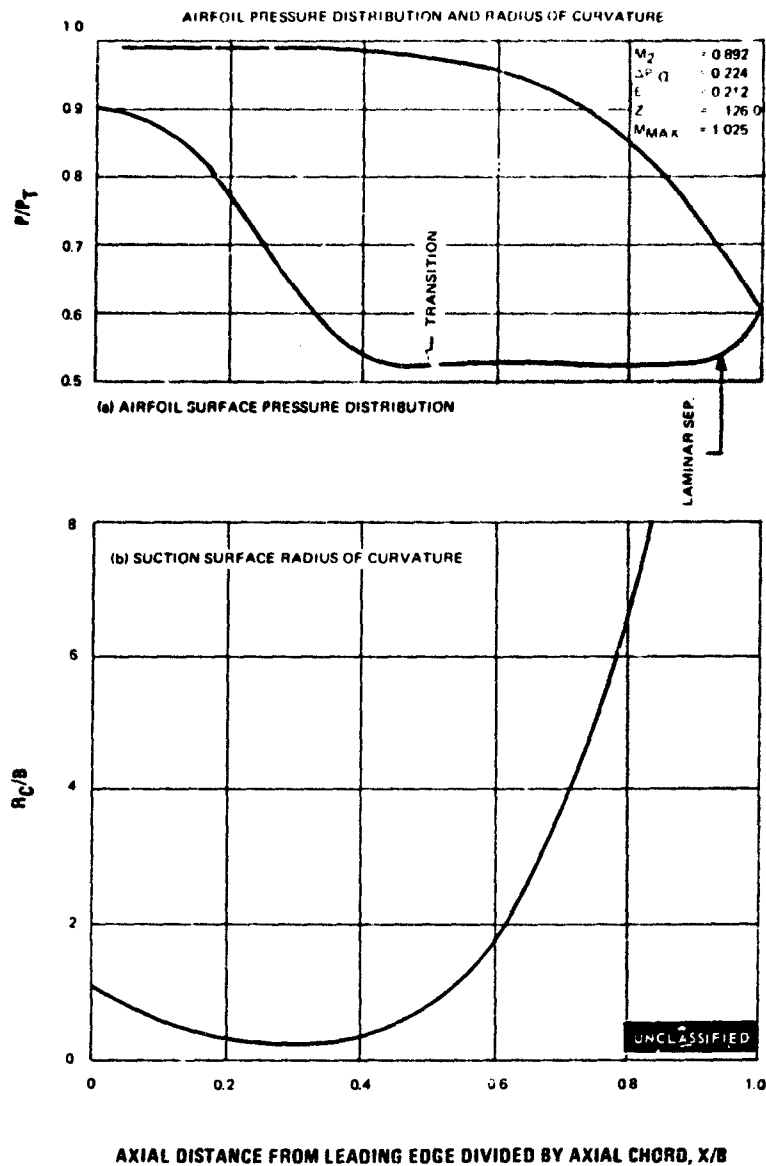


Figure 272

(The reverse of this page is blank)

PAGE NO. 311

UNCLASSIFIED

UNCLASSIFIED

REFERENCES

DIRECTLY APPLICABLE REFERENCES

- (1) Carter, A. D. S., "Three-Dimensional-Flow Theories for Axial Compressors and Turbines," reprinted in ASME Transactions, pp 255-268, April 1949.
- (2) Deich, M. E., A. E. Zaryankin, G. A. Frippov, and M. F. Zatselin, "Method of Increasing the Efficiency of Turbine With Short Blades," Translation No. 2816, SIA Translation Center, 29 April 1960.
- (3) Dorman, E. E., H. Welna, and R. W. Lindlauf, "The Application of Controlled Vortex Aerodynamics to Advanced Axial Flow Turbines," ASME Paper No. 68-GT-4, March 1968.
- (4) Gersten, K., "Corner Interference Effects," AGARD Report No. 299, 1959.
- (5) Grose, R. M., "Theoretical and Experimental Investigation of Various Types of Vortex Generators," UARL Report No. R-15362-5, 16 March 1954.
- (6) Hansen, A. G., and H. Z. Herzig, "Cross Flows in Laminar Incompressible Boundary Layers," NACA Technical Note 3651, February 1956.
- (7) Herzig, H. Z., A. G. Hansen, and G. R. Costello, "A Visualization Study of Secondary Flows in Cascades," NACA Report No. 1163, 1954.
- (8) Horlock, J. H., J. F. Louis, P. M. E. Percival, and B. Lakshminarayanna, "Wall Stall in Compressor Cascades," Journal ASME of Basic Engineering, September 1966.
- (9) Iachmann, G. V., Boundary Layer and Flow Control, Vol I and II, Pergamon Press, 1961.
- (10) Martin, M. E., "A Note on the Control of Secondary Flow by Using Cascades of Twisted Blades," Aeronautical Research Council, CP No. 425, March 1958.
- (11) Oickle, C., "Secondary Flow Investigations in the UAC Research Department Cascade Tunnel," UAC Report No. M-13010-1, 12 April 1948.

UNCLASSIFIED

- (12) "Single Stage Experimental Evaluation of Slotted Rotor and Stator Blading," Pratt & Whitney Aircraft Company Report, PWA FR-1669 October 1966.
- (13) Powers, W. E., "Application of Vortex Generators for Boundary Layer Control Through a Shock," UARL Rept. R-95477-6, July 11, 1952.
- (14) Roche, Lt. R. F., Lt. L. R. Thomas Jr., "The Effects of Slotted Blade Tips on the Secondary Flow in a Compressor Cascade," MIT Thesis, May 1959.
- (15) Rohlik, H. F., M. G. Kofskey, H. W. Allen, and H. Z. Herzig, "Secondary Flows and Boundary Layer Accumulations in Turbine Nozzles," NACA Rept. 1168, 1954.
- (16) Schlichting, H., Boundary Layer Theory, McGraw-Hill, 1960.
- (17) Schlichting, H., "Three-Dimensional Boundary Layer Flow," Gen. Assembly of Int. Assoc. of Hydraul. Res., 1961.
- (18) Schlichting, H., "Some Developments in Boundary Layer Research in the Past Thirty Years," Journal of the Royal Aeronautical Society, February 1960.
- (19) Schlichting, H., and Das, A., "Recent Research on Cascade Flow Problems," ASME Jour. Basic Engineering, March 1966.
- (20) Senoo, Y., "The Boundary Layer on the End Wall of a Turbine Nozzle Cascade," MIT Report No. 35, November 1956.
- (21) Staniforth, R., "Some Tests on Cascades of Compressor Blades Fitted with Vortex Generators," Aeronautical Research Council, C. P. No. 487, January 1958.
- (22) Taylor, E. S., R. Stevenson, R. C. Dean, Jr., "The Control of Secondary Flow in the Wall Boundary Layers of Axial Turbomachines," MIT Report No. 27-4, December 1954.
- (23) Taylor, W., "The Investigation of Flow Separation Inhibitors in the UAC Research Department Cascade Tunnel," UAC Rept. M-13010-2, February 25, 1949.

UNCLASSIFIED

UNCLASSIFIED

BIBLIOGRAPHY

1. SECONDARY FLOW IN TURBOMACHINERY

Allen, Hubert W. & Milton G. Rofskey, "Visualization Study of Secondary Flows in Turbine Rotor Tip Region". NACA TN 3519 Sept. 1955.

Arnold, K. O., "Untersuchungen Über Die Austriebserhöhung eines Klappenflügels Durch Schlitzabsaugung", Zeitschrift Für Flug-Wissenschaften, Feb. 1967.

Bartocci, J. E., "Cascade Test of the Blading of a High-Deflection, Single-Stage, Axial-Flow Impulse Turbine & Comparison of Results with Actual Performance Data," U.S.N. Post Grad. School, May 1966.

Brown, Alan C., H. Franz Nawrocki, and Peter N. Paley; "Subsonic Diffusers Designed Integrally with Vortex Generators", J. Aircraft May-June, 1968.

Camek, J., and O. Bunata, "Losses in Stage of Axial Turbine at Speeds of Approaching in the Vicinity of the Speed of Sound," FTD-TT 65-1846/1+2+4, February 1966.

Culick, F. E. C., "The Compressible Turbulent Boundary Layer with Surface Mass Transfer," M. I. T. Tr 454, August 1960.

Davison, E. H., D. A. Petrash, and H. J. Schum, "Investigation of Turbines Suitable for Use in a Turbojet Engine with High Compressor Pressure Ratio and Low Compressor Tip Speed," NACA Rm E56H14a, 29 October 1956.

Ehrich, F. F., and R. W. Detra, "Transport of the Boundary Layer in Secondary Flow," Journal of Aerospace Science, February 1954.

Gomi, Marusuke, "On the Deviation of Outlet Flow Angles Caused by Secondary Flow in Turbine Cascades" (1st Report) Bulletin of JSME.

Hanley, W. T., "A Correlation of End Wall Losses in Plane Compressor Cascades", ASME 68-GT-15.

Hansen, A. G., G. R. Costello, and H. Z. Herzig, "Effect of Geometry on Secondary Flows in Blade Rows," NACA Rm E52H26, 16 October 1952.

Hawthorne, W. R., "Secondary Circulation in Fluid Flow," Proc. of Roy. Soc. A206, 1951.

UNCLASSIFIED

UNCLASSIFIED

Herzig, H. A., and A. G. Hansen, "Visualization Studies of Secondary Flows With Application to Turbomachines," ASME Paper No. 53-A56, 1953.

Horlock, J. H., J. F. Norbury, and J. C. Cooke, "Three-Dimensional Boundary Layers A Report on Euromech 2," J. Fluid Mech. (1967) Vol. 27, 1967.

Horlock, J. H., "Some Actuator-Disc Theories for the Flow of Air Through an Axial Turbo-Machine," Aeronautical Research Council, Rm No. 3030, December 1952.

Johnston, I. E., G. E. Sansome, "Tests on an Experimental Three-Stage Turbine Fitted with Low Reaction Bladings of Unconventional Form," Aeronautical Research Council, Rm No. 3220, January 1958.

Johnston, J. P., "On the Three-Dimensional Turbulent Boundary Layer Generated by Secondary Flow," Journal of Basic Engineering, March 1960.

Kline, S. J., W. C. Reynolds, F. A. Schraub, and P. W. Runstadler, "The Structure of Turbulent Boundary Layers," J. Fluid Mech. (1967) Vol. 30, Part 4, 1967.

Kofsky, M. G., and W. Allen, "Investigation of a 0.6 Hub-Tip Radius-Ratio Transonic Turbine Designed for Secondary Flow Study," NACA Rm E58B27, 20 May 1958.

Kofsky, Milton G., & Hubert W. Allen, "Smoke Study of Nozzle Secondary Flows in a Low-Speed Turbine", NASA TN 3260.

Kriebel, A. R., B. S. Seidel, and R. G. Schwind, "Stall Propagation in a Cascade of Airfoils," NASA TR R-61, 1960.

Lakshminarayana, B., J. H. Horlock, "Review: Secondary Flows and Losses in Cascades and Axial-Flow Turbo-Machines," Int. Jour. Mech. Sci., Vol. 5, 1963.

Lakshminarayana, B., and J. H. Horlock, "Methods of Predicting the Effect of Shear Flows on the Outlet Angle in Axial Compressor Cascades," ASME 65WA/FE-2, 1963.

Lakshminarayana, B., and J. H. Horlock, "Effect on Shear Flows on the Outlet Angle in Axial Compressor Cascades - Methods of Prediction and Correlation with Experiments," Journal of Basic Engineering, March 1967.

UNCLASSIFIED

UNCLASSIFIED

Loos, H. G., "Compressibility Effects on Secondary Flows," Journal Aeronautical Sciences, January 1956.

Loos, H. G. "Analysis of Secondary Flow in the Stator of an Axial Turbomachine," C. I. T. Technical Report No. 3, AD20614, September 1953.

Loos, H. G. & J. Zwaaneveld, "Secondary Flow in Cascades", Jour. Aero Sciences, Sept. 1952.

Mendahl, L., "The End Losses of Turbine Blades," Brown Bover Review, November 1941.

Miser, J. W., and L. S. Warner, "Effect of High Rotor Pressure Surface Diffusion on Performance of a Transonic Turbine," NACA RM E55H29a, 2 November 1955.

Miser, J. W., W. L. Stewart, and W. J. Whitney, "Analysis of Turbomachine Viscous Losses Affected by Changes in Blade Geometry," NACA RM E56F21, 2 October 1956.

NASA-Allison; "Single-Stage Experimental Evaluation of Boundary Layer Blowing Technique for High Lift Stator Blades," NASA CR-54564, Feb. 1968, Allison EDR-5636.

Rohlik, H. E. and M. G. Kofskey, "Secondary Flow Phenomena in Stator and Rotor Blade Rows and Their Effect on Turbine Performance," ASME 63 AHG-T-72, 1963.

Rohlik, H. E., W. T. Wintucky, and H. W. Scibbe, "Investigation of a 0.6 Hub-Tip Radius-Ratio Transonic Turbine Designed for Secondary Flow Study," NACA RM E56J16, 9 January 1957.

Rohlik, H. E., W. T. Wintucky, and T. P. Moffitt, "Investigation of a 0.6 Hub-Tip Radius-Ratio Transonic Turbine Designed for Secondary Flow Study," NACA RM E57G08, 17 September 1957.

Rubin, S. G., "Incompressible Flow Along a Corner Part I. Boundary Layer Solutions and Formulation of Corner Layer Problem," Polytech Institute, AD 621 987, May 1965.

Senoo, Y., "Three-Dimensional Laminar Boundary Layer in Curved Channels with Acceleration", MIT Report No. 37, November 1956.

UNCLASSIFIED

UNCLASSIFIED

Sinnette, John Jr. & George R. Costello, "Possible Application of Blade Boundary-Layer Control to Improvement of Design & Off-design Performance of Axial-Flow Turbomachines", NACA TN 2371, May 1951.

Smith, L. H., Jr., "Secondary Flow in Axial-Flow Turbomachinery", Transactions ASME, October 1955.

Steinheuer, J., "Three-Dimensional Boundary Layers on Rotating Bodies and In Corners," AGARD No. 97, 1965.

Stewart, W. L., "Analysis of Two-Dimensional Compressible-Flow Loss Characteristics Downstream of Turbomachine Blade Rows in Terms of Basic Boundary Layer Characteristics," NACA TN 3515, July 1955.

Stewart, W. L., W. J. Whitney, and R. Y. Wong, "A Study of Boundary Layer Characteristics of Turbomachine Blade Rows and Their Relation to Over-All Blade Loss," Journal Basic Engineering, ASME, September 1960.

Stewart, W. L., W. J. Whitney, and R. Y. Wong, "Use of Mean-Section Boundary Layer Parameters in Predicting Three-Dimensional Turbine Stator Losses," NACA RM E55L12a, 23 March 1956.

Stewart, W. L., W. J. Whitney, and J. W. Miser, "Use of Effective Momentum Thickness in Describing Turbine Rotor-Blade Losses," NACA RM E56B29, 14 May 1956.

Taylor, H. D., "United Aircraft Research Department Summary Report on Vortex Generators," Report R-05280-9, March 1950.

Truckenbrodt, E., "A Method of Quadrature for Calculation of the Laminar and Turbulent Boundary Layer in Case of Plane and Rotationally Symmetrical Flow," NACA TM 1379, 1952.

Whitney, R. L., J. A. Heller, and C. H. Hauser, "Investigation of Distribution of Losses in a Conservatively Designed Turbine", NACA RM E53A16, 16 March 1953.

Whitney, W. J., D. E. Monroe, and R. Y. Wong, "Investigation of Transonic Turbine Designed for Zero Diffusion of Suction-Surface Velocity", NACA RM E54F23, 24 August 1954.

Whitney, W. J., W. L. Stewart, and R. Y. Wong, "Effect of Reduced Stator Blade Trailing Edge Thickness on Overall Performance of a Transonic Turbine", NACA RM E55H17, 1 November 1955.

UNCLASSIFIED

UNCLASSIFIED

Whitney, W. J., W. L. Stewart, and J. W. Miser, "Experimental Investigation of Turbine Stator-Blade-Outlet Boundary-Layer Characteristics and a Comparison with Theoretical Results", NACA RM E55K24, 16 March 1956.

Wong, R. Y., D. E. Monroe, and W. T. Wintucky, "Investigation of Effect of Increased Diffusion of Rotor-Blade Suction Surface Velocity in Performance of Transonic Turbine", NACA RM E54F03, 24 August 1954.

Wong, R. Y., "Removal of Secondary Flow Accumulations in a Two Dimensional Turbine Nozzle Passage by Boundary Layer Bleed", RM E55E11, 30 June 1955.

Wu Chung-Hua, "A General Theory of Three Dimensional Flow in Subsonic and Supersonic Turbomachines of Axial, Radial, and Mixed-Flow Types", NACA TN 2604, January 1952.

2. LOSSES IN TURBOMACHINERY - GENERAL

Ainley, D. G. and G. C. R. Mathieson, "A Method of Performance Estimation for Axial-Flow Turbines," Gt. Br. ARC. R&M, No. 2974, NGTE Report R.111, 11 December 1951, issue 1957.

Ainley, D. G. and G. C. R. Mathieson, "An Examination of the Flow and Pressure Losses in Blade Rows of Axial Flow Turbine," London, HMSO, 1955, p 33, et (R&M 2891, R.86, March 1951).

Ainley, D. G., "Performance of Axial-Flow Turbines," Proc. Instn. Mechanical Engineers, 1948, vol. 159, No. 41, pp 230-244.

Albring, W., "Flow Stall at the Straight Cascades and Vanes of Axial Turbines (Das Abreißen Der Stromung Bei Geraden Flugelgittern und Auf Den Schaufeln Axialer Stromungsmaschinen)". (Dresden, Technische Universitat, Institut fur angewandte Stromungslehre, Dresden, East Germany). Periodica Polytechnica, Engineering Series, vol 8, No. 2, 1964, p 111-132, 23 refs. In German.

Balje, O. E. "Axial Cascade Technology & Application to Flow Path Designs. Part I - Axial Cascade Technology", ASME 68-GT-5
Part II - "Application of Data to Flow Path Designs"
ASME 68-67-6

Balje, O. E. & R. L. Binsley, "Axial Turbine Performance Evaluation. Part A - Loss Geometry Relationships"
ASME 68-GT-13
"Part B - Optimization with & without Constraints"
ASME 68-GT-14

UNCLASSIFIED

UNCLASSIFIED

Bammert, K., and K. Fiedler, "Flow in Axial-Flow Turbines (Die Stromung in Axialen Turbomaschinen)". Ingenieur-Archiv, vol 33, No. 5, 1964, p 322-329. In German.

Bammert, K., "Die Stromung Durch Vielstufige Axialturbinen Mit Geraden Schaufeln. (Flow Through Multistage Axial Turbines With Straight Blades.)" N62-14342, Deutsche Forschungsanstalt fur Luftfahrt, Institut fur Strohltriebwerke, Braunschweig (Germany), 18 February 1961, 39 p., 6 refs., (DFL Bericht Nr. 135).

Bammert, K., "Calculation of Flow in Multi-stage Axial Turbines With Arbitrary View" (in German), Forsch. Geb. Ing.-Wes., 26, 6, 179-184, 1960.

Bammert, K., "Computation of Flow of Multistage Axial Turbo Engines With Arbitrary Cascading System (in German), Dtsch. Versuchsanstalt Luftfahrt, Ber. 137, 6 pp, 1960.

Barlit, V. V., "On the Character of a Flow Through a Radial-Axial Hydroturbine" (in Russian) Izv. Vyssh. Uchebn. Zavedenii: Energetika No. 12, 124-132, 1959; Ref Zh. Mekh, No. 2 1961, Rev 2B 402.

Baumgartner, F., and R. Armsler, "Presentation of a Blade-Design Method for Axial-Flow Turbines, Including Design and Test Results of a Typical Axial-Flow Stage." ASME Trans ser A 82:19-26 Ja 1960.

"Performance Evaluation of Reduced-Chord Rotor Blading as Applied to J73 Two-Stage Turbine," NACA Research Memo. Part 1 - Berkey, W. E., J. J. Rebeske, Jr., and R. E. Forrette, "Overall Performance With Standard Rotor Blading at Inlet Conditions of 35 inches of Mercury Absolute and 700°R," RM E52G31, 11 July 1957, 21 p. Part 2 - Schum, H. J., J. J. Rebeske, Jr., and R. E. Forrette, "Overall Performance at Inlet Conditions of 35 inches of Mercury Absolute and 700°R," RM E53B2, 11 July 1957, 21 p.

Beavers, Gordon S., "A Parameter Theory for the Compressible Flow Through Variable-Area Turbo-Machines," January 1963, 114 p. Report No. ARC-CP-755, Unclassified Report.

Birmann, R., "The Elastic-Fluid Centripetal Turbine for High Specific Outputs," Trans. ASME 76, 2, 173-185, February 1954.

PAGE NO 320

UNCLASSIFIED

UNCLASSIFIED

Bolte, Walter, "Calculation and Optimization of the Efficiency of Axial Flow Machines (Zur Berechnung Und Optimierung Des Wirkungsgrades Axialer Stromungsmaschinen)." (Verein Deutscher Ingenieure, Essen, Germany). VDI-Forschungsheft No. 501, 1964, 48 p, 90 refs. In German.

Boxenhorn, Burton, Yvonne Brill, Henry Hidalgo, and Sheldon Dolinger, report on the 1952 annual ASME meeting in New York City, United Aircraft Corporation, Research Division, East Hartford, The div., 1952, 12 p, charts. UAC Report No. M-15280-34, 11 December 1952.

Buhning, P. G., "On the Behavior of Axial-Flow Machines of Extremely High Specific Speed" (in German), VDI-Forschungsheft 24, 468, 44 pp., 1958.

Calbere, T., "Calculation of Vane Profiles and the Flow About the Vanes of Fluid-Flow Turbines (Über Die Berechnung Der Schaufelprofile Und Der Stromung Um Die Schaufeln Von Stromungsmaschinen)." Vol 33, No. 4, 1964, p 215-230, Ingenieur-Archiv. In German.

Camek, J., and O. Bunata, "Losses in Stage of Axial Turbine at Speeds of Approaching in the Vicinity of the Speed of Sound," Foreign Technology Division Wright-Patterson AFB, Ohio. 18 February 1966, 24 p, Report No. 11d-TT-65-1846, TT 66-60816.

Case, Leonard F., "Experimental Investigation of Devices for Reducing Flow in Compressor Stators & Rotors", UAC R-0132-1. Aug. 18, 1959.

Cavicchi, Richard H. "Analysis of Limitations Imposed on One-Spool Turboprop-Engine Designs by Compressors and Turbines at Flight Mach Numbers of 0, 0.6, and 0.8," NACA Research memo, Washington, The Comm., 1956, 66 p, (RM E56105, 6 December 1956).

Comolet, R., "Contribution A l'etude de Rendement d'une Turbomachine Axial A Fluide Incompressible," France Ministere de l'Air- Publications Scientifiques et Techniques - Notes Techniques 372, 1960, 54 p.

Csanady, G. T., "Theory of Turbomachines," New York, McGraw-Hill Book Co., Inc., 1964, viii + 378 pp.

Cuming, H. G., "The Secondary Flow in Curved Pipes," Aero; Res. Counc. Lond. Rep. Mem. No. 2880, 17 pp., February 1952, published 1955.

UNCLASSIFIED

UNCLASSIFIED

Davis, H., H. Kottas, and A. M. G. Moody, "Influence of Reynolds Number on Performance of Turbomachinery," Am. Soc Mech; Engrs., Trans v 73 n 5 July 1951, p 499-503.

Dearing, H. F., Jr. and R. V. Hayes, Thesis, "Design and Test of a Small Single Stage Turbine," Cambridge, Massachusetts, The Lib 1952.

Deich, M. E., "Basic Turbine Gasdynamics," West Concord, Massachusetts. Morris D. Friedman Translation, 1953, p 412-420.

Deich, M. E., "Tekhnicheskaya Gasodynamika, D324t, Moscow, Gas Engineering. Izdatel, 1953. 544 p. (In Russian) Title translated - Technical Gasdynamics, library also has translation of pp 412-420.

Detra, R. W., "The Secondary Flow in Curved Pipes," Mitt. Inst. Aerodyn., ETH. Zurich No. 20, 50 pp., 1953.

Dolapchiev, B., "Generalized Procedure for the Stability Analysis of Arranged Vortex Streets" (in Bulgarian, with German summary), Godishnik, Univ. Sofia, Fac. Sci. Livre 1, 46, 369-376, 1950.

Eckert and Korbacher, "The Flow Through Axial Turbine Stages of Large Radial Blade Length," Nat. Advis. Comm. for Aero. Tech. Memo., No. 1118, April 1947, pp 1-26, (Transl. from Dtsch. Luft., Report No. 1750).

Ehrich, F., "Circumferential Inlet Distortions in Axial Flow Turbomachinery," Journal of Aeronautical Sciences v 24 n 6 June 1957, p 413-7.

Egbert, Gerald W., "Estimation of Compressible Boundary-Layer Growth Over Insulated Surfaces with Pressure Gradient", NACA TN-4002.

English, R. E. and R. H. Cavicchi, "Comparison of Measured Efficiencies of Nine Turbine Designs with Efficiencies Predicted by Two Empirical Methods," NACA, Research Memorandum. Washington, The Comm., 1951, 23 p, charts, tables. (RM No. E51F13, 20 August 1951).

English, R. E., D. H. Silvern, and E. H. Davison, "Investigation of Turbines Suitable for Use in a Turbojet Engine With High Compressor Pressure Ratio and Low Compressor Tip Speed," Washington, The Comm., 1952, charts, tables, V. 1 "Turbine Design Requirements for Several Engine Operating Conditions," RM No. E52A16, 4 March 1952.

UNCLASSIFIED

UNCLASSIFIED

Ershov, V. N., "The Unidentical Nature of the Solutions of the Problem on the Form of the Flow in an Axial Turbomachine" (in Russian), *Izv, Vyssh, Uchebn, Zavendenii: Aviats, Tekh*, No. 2, 80-87, 1960; *Ref Zh, Mekh*, No. 6, 1961, Rev 6B242.

Evans, D. G., "Design and Experimental Investigation of a Three-Stage Multiple-Reentry Turbine," NASA Memo, Memo, 1-16-59E. 32 p. January 1959, (Title Unclassified).

Fleming, W. A., L. E. Wallner, and J. T. Wintler, "Effect of Compressor-Outlet Bleedoff on Turbojet-Engine Performance," U.S. NACA, Research Memorandum No. E50E17, 7 August 1950, 27 pp., Illus. 1 Reference.

Forrette, R. E., "Experimental Investigation of Stage Performance of J71 Three Stage Turbine," Washington, The Comm., 1954, NACA Research Memo, (RM E54109, 20 December 1954).

Forster, V. T., "Turbine-Blading Development Using A Transducer Variable Density Cascade Wind Tunnel",
Proc. Instn Mech Engrs., 1964-1965.

Gazarin, A., "Graphical Treatment of Compressible and Incompressible Flow Through the Stages of Turbomachines," (in German), Thesis, ETH, Zurich, Prom. No. 2059, 89 pp., 20 figs., 1951.

Gorelov, D. N., "Three-Dimensional Subsonic Nonstationary Flow Through a Cascade of Blades of an Axial Turbomachine," (in Russian), *Izv. Akad. Nauk SSSR, Mekh. i Mashinostr.* No. 6, 36-44 November/December 1963.

Gostelow, J. P., "Potential Flow Through Cascades - A Comparison Between Exact and Approximate Solutions", Ministry of Aviation.
UR-65-00499 1965.

Gratler, L. B.; R. H. Smith, "Boundary Layer Control for Wide Angle Diffusers", Univ. of Washington, Aeronautical Lab., Seattle, Report No. 300, Nov. 1948.

Gravalos, F. G., "Laminar Theory of Flow Through Turbo-Machine," Rensselaer Polytechnic Inst---Eng & Science Series, Bulletin No. 62 January 1950, 44 p.

UNCLASSIFIED

UNCLASSIFIED

Green, J. E., "The Prediction of Turbulent Boundary Layer Development in Compressible Flow",
Jour. Fluid Mech. (1968) Vol. 31 Part VI.

Gruber, J., "On the Observation of Streamlines in Radial Flow Impellers,"
Acta Techn. Hung. Budapest 7, 1-2, 29-41, 1953.

Hall, W. S. and R. Thwaites, "On the Calculation of Cascade Flows",
Ministry of Aviation, CP No. 806.

Harlow, British Hydromechanics Research Association, V63-2005-4,
"A Bibliograph on Axial- and Mixed-Flow Machines With Particular
Reference to Pumps", November 1962, 28 p, 133 refs (BIB-9).

Hauser, Cavour H., and William J. Nusbaum, "Experimental Investigation of
Effect of High Aspect Ratio Rotor Blades on Performance of Conservatively
Designed Turbine," NACA Research Memo, Washington, The Comm., 1954,
(RM E54C18, May 28, 1954).

Hauser, Cavour H., and William J. Nusbaum, "Experimental Investigation
of a High Subsonic Mach Number Turbine Having Low Rotor Suction-Surface
Diffusion," NACA Research Memo, Washington, The Comm., 1956,
(RM E56G25, October 10, 1956).

Heaton, T. R., R. E. Forrette, and D. E. Holeski, "Investigation of a
High Temperature Single Stage Turbine Suitable for Aircooling and Turbine
Stator Adjustment". Part 1, "Design of Vortex Turbine and Performance
With Stator at Design Setting, Washington, The Comm, 1954, RM E54C15,
25 May 1954, 42 p.

Herzig, H. Z., "Visualization Studies of Secondary Flows With Applications
to Turbomachines," ASME Ann. Meet., New York, December 1953,
Pap. 53, A-56, 18 pp.

Holmquist, C.O., W.D. Rannie, "Approximate Method of Calculating Three-
Dimensional Compressible Flow in Axial Turbomachines," Aeronautical
Sciences v 23 n, 6 June 1956, p 543-56, 582.

Hong, Yong S. and F. G. Groh, "Axial Turbine Loss Analysis and Efficiency
Prediction Method," Boeing Co., Seattle, Washington Turbine Division, 11 March
1966, 118p, Rept. No. D4-3220.

UNCLASSIFIED

UNCLASSIFIED

Horlock, J. H., "Some Experiments on the Secondary Flow in Pipe Bends," Proc. Roy. Soc. Lond. (A) 234, 1198, 335-346, February 1956.

Horlock, J. H., "Some Aerodynamic Problems of Axial Flow Turbomachines," Microfilm A179, Thesis, Cambridge University, Cambridge, England, The University, 1955. 221p. (January 1955).

Horlock, J. H. & G. J. Fahmi, "A Theoretical Investigation of the Effect of Aspect Ratio on Axial Flow Compressor Performance", Ministry of Technology CP No. 943, May 1, 1966.

Howard, R. E. Jr., "The Performance of High Power Output Axial Flow Turbines Utilizing Flows in the Transonic Regime, " Appendix V, Naval Postgraduate School, Monterey, California, 1963, 163p.

Howell, W. T., "Approximate Three-Dimensional Flow Theory for Axial Turbo-Machines," Aeronautical Quarterly v 14 pt 2 May 1963, p 125-42.

Huntley, S. C., J. N. Sivo, and C. L. Walker, "Effect of Circumferential Total-Pressure Gradients Typical of Single-Inlet Duct Installation on Performance of an Axial-Flow Turbojet Engine," NACA Res. Memo. Washington, The Comm., 1955, (RM E54K26a, June 3, 1955).

Hurley, D. G., "A Theoretical Investigation of an Airfoil Equipped with a Split Flap", Jour. of Australian Math Soc. Vol. 2, Oct. 1961.

Iku, T., "Flow in Axial Blade," Bull. JSME 3, 9, 29-35, February 1960.

Ipatenko, A. Ya & A. M. Antonov, "Visualization of Transition Phenomena in the Boundary Layer on the Blades of Turbine Cascade" (Russian Periodical), Ivua, Aviatsionnaya Tekhnika, No. 3, 1965.

Katsanis, T., "Use of Arbitrary Quasi-Orthogonals for Calculating Flow Distribution in the Meridional Plane of a Turbomachine," NASA TN D-2546, 46 pp., December 1964.

Kavanagh, Paterk & George K. Serovy, "Through-Flow Solution for Axial-Flow Turbomachine Blade Rows", NASA CR-363 Jan. 1966.

Kaye, J., and K. R. Wadleigh, "New Method of Calculation of Reheat Factors for Turbines and Compressors," ASME, Trans (J Applied Mechanics) v 18n 4, December 1951, p 387-92.

UNCLASSIFIED

UNCLASSIFIED

Kearton, W. J. . "Effects of Inertia on Flow of Stream Through Nozzles and Blading of Axial-Flow Turbines," Instn. Mech. Engrs. Proc. (A) 166, 4, 429-435, 1952.

Kofskey, M. G. . "Performance Evaluation of a Two-Stage Turbine Designed for a Ratio of Blade Speed to Jet Speed 0.146," (Title Unclassified) 35p. , (January 1960). NASA Tech Memo.

Kromauer, R. E. . "Secondary Flow in Fluid Dynamics," Proc. First U. S. Nat. Congr. Appl. Mech. , June 1951; J. W. Edwards, Ann Arbor, Michigan, 747-756, 1952.

Lamb, C. W. . "A Method of Predicting The Performance of Axial Flow Turbines Using a Digital Computer to Develop Performance Maps," Master's Thesis, Naval Postgraduate School, Monterey, California, 1962, 168p.

Laskin, A. S. . "Investigation on the Influence of the R Number and the Surface Roughness on the Efficiency of Rows of Turbine Working Blades," (in Russian,) Nauchno-Tekhn. Inform. Byul. Leningrad Politekh. In-ta No. 3, 51-59, 1958; Ref. Zh. Mekh. No. 6, 1959, Rev. 6175.

Lewis, R. I. . "Annular Cascade Wind Tunnel," (Cambridge University, Engineering Laboratory, Cambridge, England). The Engineer, vol. 215, February 22, 1963, p. 341-344.

Linhardt, H. D. , and D. H. Silvern, "Analysis of Partial Admission Axial Impulse Turbines," ARS J v 31 n 3, March 1961, p 297-308.

Liu, K. -I. , and Hsueh, M. -I. , "Comments on the Aerodynamic Design of Radially Long Blades of Turbomachines With Conical Stream Surfaces," (in Chinese), Chinese J. Mech. Engng. 11, 4, 93-97, 1963.

Liu, C. Y. & V. A. Sandborn, "Laminar Velocity Profiles in Adverse Pressure Gradients", Engineering Notes, Colorado State University Jan-Feb. 1968.

Lukowsky, Georg, "Contribution to the Theory of Frictionless Axial-Symmetrical, Three-Dimensional Flow Through Axial Turbines (Beitrag Zur Theorie der Reibungsfreien, Axialsymmetrischen Raumlichen Stromung in Axial-Turbiren). Forschung Im Ingenieurwesen, Vol. 31, No. 1, 1965, p. 1-10, 7 Refs. (In German).

Lukowsky, G. . "Contribution to the Theory of Frictionless, Axial-Symmetrical, Three-Dimensional Flow Through Axial Turbines" (in German), Ingen. -Arch. 33, 5, 322-329, 1964.

UNCLASSIFIED

UNCLASSIFIED

Lysen, J. C., and G. K. Serovy, "Estimation of Velocity Distribution at Inlet of Axial-Flow Turbomachine," ASME-Paper 63, WA-162 for Meeting November 17-22, 1963, 12 p.

Lysen, J. C. & G. R. Serovy, "The Boundary Layer in a Pressure Gradient", Iowa State University Bulletin, Eng. Report No. 43, May 6, 1964.

Lyubchenko, I. S. "Toward the Design of a Turbine with Variable Parameters at the Inlet", U. S. AF Foreign Tech. Div. FTD-MT-63-274, May 21, 1964.

Makarov, A. F., "A Three-Dimensional Flow of a Liquid in the Interblade Ducts of a Radial-Axial Turbine" (in Russian), Trudy Leningrad Politekhn. Inst. No. 248, 14-24, 1965; Reference Zh, Mekh. No. 1, 1966, Rev. 1 B 321.

Mann, L. B. Jr., A. H. Bell, and G. W. Thebert, "Determination of Turbine Stage Performance for an Automotive Power Plant," ASME, Preprint, March 18-21, 1957. 10p.

Marble, F. E., "Three-Dimensional Flow in Turbomachines," (California Institute of Technology, Department of Mechanical Engineering, Pasadena, California), In: Aerodynamics of Turbines and Compressors. (High Speed Aerodynamics and Jet Propulsion, Volume 10), Edited by W. R. Hawthorne, Princeton, Princeton University Press, 1964, p. 83-166. 23 Refs.

McDonald, H., "The Departure from Equilibrium of Turbulent Boundary Layers", The Aeronautical Quarterly, Vol. XIX February 1968.

Mellor, G. L. "Reconsideration of the Annulus Flow Problem in Axial Turbomachinery," ASME Preprint, November 26-December 1, 1961, 7 p., Winter Annual Meeting, N. Y. C., ASME Paper No. 61-WA-186.

Meyer, R. E., "The Mean Flow in Kaplan Turbines," Trans. ASME 74, 7, 1283-1289, October 1952.

Miser, J. W., W. L. Stewart, and D. E. Monroe, "Effect of High Rotor Pressure Surface Diffusion on Performance of a Transonic Turbine," NACA Res. Memo. Washington, The Comm., 1955, 35p., idct (RM E55H29a, November 3, 1955).

Miser, J. W., and W. L. Stewart, "Investigation of Two-Stage Air-Cooled Turbine Suitable for Flight at Mach Number of 2.5; Part 1 - Velocity-diagram Study," NACA Res. Memo. RM E56H14, October 22, 1956, Washington, The Comm, 1956.

UNCLASSIFIED

UNCLASSIFIED

"PART VIII - Data & Performance for Slotted Stator 3", NASA CR-54551, PWA FR-2288, Oct. 13, 1967.

Railly, J. W., "Flow of Incompressible Fluid Through Axial Turbomachine With Any Number of Rows, "Aeronautical Quarterly v 3, pt 2, September 1951, p 133-44.

Rehbach, J., "Investigation of Clearance Losses of Turbine Stators With Rotating Clearance Wall," (in German), Dtsch. Forschungsanstalt Luftfahrt, Ber. 90, 74 pp., 1959.

Ribaut, M., "Three Dimensional Calculation of Flow in Turbomachines with the Aid of Singularities", ASME 68-GT-20.

Richter, W., "Calculation of Pressure Distribution on Plane Blades With Strongly Arched Thick Profiles in the Case of Incompressible Flow," (in German), Ing.-Arch. 29, 5, 351-372, September 1960.

Robbins, W. H. and H. W. Plohr, "Recent Advances in the Aerodynamic Design of Axial Turbomachinery," IAS, preprint, IAS Preprint No. 762, October 21-22, 1957 16p+.

Rochen, H. D., "Determination of Transient Characteristics of an Axial Flow Turbojet Engine," U. S. Naval Air Material Center, Aeronautical Engineering Laboratory, Philadelphia, Pennsylvania, The Laboratory, 1953, 10p+, c, AEL 1252, July 1952 to April 1953, dated June 1, 1953.

Rogo, Casimir, "Experimental Aspect Ratio and Tip Clearance Investigation on Small Turbines", SAE Paper 680448, May 1968.

Rogo, C. & Talbey, A., "Experimental Investigation of Low Aspects Ratio and Tip Clearance on Turbine Performance and Aerodynamic Design", Continental Aviation & Engineering Corporation. Continental Report No. 1043.

Rose, Jr., Charles C. and Darold I. Guttormson, "Installation and Test of a Rectilinear Cascade," Naval Postgraduate School, Monterey, California. AD 481-351, 1964.

Schlichting, H., and E. Truckenbrodt, "Flow in Axial Direction About a Rotating Disk," (in German), ZAMM 32, 4/5, 97-111, April/May 1952.

Schnittger, J. R., "Vortex Flow in Axial Turbo Machines," Trans. Roy. Inst. Technol. Stockholm No. 74, 62 pp., 1954.

UNCLASSIFIED

Plohr, Henry W., Donald E. Holeski, & Robert E. Forrette "Design and Experimental Investigation of a Single-Stage Turbine with a Downstream Stator", NASA RM E56K10, Jan. 25, 1957.

Pochobradsky, B., "Effect of Centrifugal Force in Axial-Flow Turbines, ", Engineering, March 21, 1947, Vol. 163, pp 205-207.

Polasek, J., "Computation of Flow Through Cascades of Thin Airfoils With High Camber (in Czech), Aplikace Matematiky 3, 5, 346-347, 1958.

Poulos, E. N., and E. R. Furman, "Turbine Design and Testing," Thompson Ramo Wooldridge, Inc., Tapco Group, 44p. (ER-3896, SNAP II Power Conversion System Topical Rpt. No. 4, AECU-4686, January 18, 1960).

Preston, J. H., "A Simple Approach to the Theory of Secondary Flows", The Aeronautical Quarterly Vol. V, Sept. 1954.

Proskuryakov, G. V., "Problem of Determination Delivery Coefficients and Angles of Outflow From Bladed Devices of Axial Gas Turbines," Air Force Systems Command. Wright-Patterson AFB, Ohio, Foreign Technology Div. N65-28724. 5 May 1965, 14 p REFs, Transl, into English from Teploenerg, (Moscow) No. 9, 1964, P 16-19 (FTD-TT-65-430/1+2: AD-615533).

Puzyrewski, Romvald, "Vortex Line Convection in Curved Conduits as a Basis for Computations of Losses at the Walls", USAF Foreign Tech. Div. FTD-TT-65-1501, Aug. 18, 1966.

"Single Stage Experimental Evaluation of Slotted Rotor & Stator Blading"
"Part I - Analysis & Design", NASA CR-54544, PWA FR-1713, July 27, 1966.

"Part III - Data & Performance for Slotted Rotor 1", NASA CR-54546, PWA FR - 2110, Feb. 21, 1967.

"Part IV - Data & Performance for Slotted Rotor 2", NASA CR-54547, PWA FR-2111, Feb. 24, 1967.

"Part V - Data & Performance for Slotted Rotor 3 - Slotted Stator 2", NASA CR-54548, PWA FR-2285.

"Part VI - Data & Performance for Slotted Stator 1 & Flow Generation Rotor", NASA CR-54549, PWA FR-2286, July 21, 1967.

"Part VII- Data & Performance for Slotted Stator 2", NASA CR-54550, PWA FR-2287, Sept. 28, 1967.

UNCLASSIFIED

UNCLASSIFIED

Miser, J. W., W. L. Stewart, and R. Y. Wong, "Effect of a Reduction in Stator Solidity on Performance of a Transonic Turbine," NACA Res. Memo Washington, The Comm., 1956, (RM E55L09a, March 23, 1956).

Moffitt, T. P., "Design and Experimental Investigation of a Single-Stage Turbine With a Rotor Entering Relative Mach Number of 2, (u) NACA Res. Memo (RM E58F20a, September 15, 1958).

Moffitt, T. P., and F. W. Klag, Jr., "Experimental Investigation of the Partial-Admission Performance Characteristics of a Single-Stage Mach 2 Supersonic Turbine (Title U)," NASA Tech Memo. TM x-80 (September, 1959).

Mori, Y., "On Wakes Behind a Single Aerofoil and Cascade," Y. JSME 2, 7, 463-469, August 1959.

Murata, S., "Research on the Axisymmetric Flow Through an Axial-Flow Turbo-Machine: Part 1., On the Flow Through a Free Vortex-Type Impeller," Bull. JSME 6, 24, 730-735, November 1963.

Nickel, K., "Supplement to J. Dorr: Exact Solution of the Integral Equation for an Airfoil Cascade," (in German), Ing.-Arch. 20, 1, 6-7, 1952.

Nilsson, J. E. V., "On Ideal Flow Through Axial Turbomachine Cascades," Stockholm Kungl Tekniska Hogskola (Roy Inst. Technology) --Thesis n 164, Stockholm 1962, 95p.

Nusbaum, W. J., and Cavour H. Hauser, "Experimental Investigation of a High Subsonic Mach Number Turbine Having High Rotor Blade Suction-Surface Diffusion," NACA Res. Memo. Washington, The Comm., 1956., (RM E56118, November 20, 1956).

Ohlsson, Gunnar, "Partial Admission, Low Aspect Ratios, and Supersonic Speeds in Small Turbines," Thesis, MIT., Dept. of Mech. Eng. Cambridge, Massachusetts, The Dept., 1956. n.p. (Jan. 1956).

Perl, W., and M. Tucker, "General Representation for Axial-Flow Fans and Turbines," NACA, Report n 814, 1945 (released 1948) 5 p. 10c.

Petrash, D. A., H. J. Schum, E. H. Davison, "Component Performance Investigation of J71 Experimental Turbine," Part 10 - "Effect of First-Stator Adjustment; Internal Flow Conditions of J71-97 Turbine With 132-Percent-Design Stator Area," NACA Res. Memo. RM E57E29, 16 January 1958, 19p.

UNCLASSIFIED

UNCLASSIFIED

Schwaar, P., "Some Remarks on the Aerothermodynamic Calculation of Blades in Axial Turbomachines," (in French), Bull. Tech. Suisse Rom. 78, 19, 254-251, September 1952.

Schwartz, Frank L., "Gas Turbine and Free Piston Engine Lectures," June 13-June 17, 1955. Ann Arbor, Michigan, The Department of Mechanical and Industrial Engineering, 1955. n.p. (June 13-17, 1955). Strong, Robert E., "Axial Flow Gas Turbines," 49 p.

Seashore, Ferris L., and Lester O. Corrington, "Component Performance of J71-A-2(600-D1) Turbojet Engine at Several Reynolds Number Indices," NACA Res. Memo, Washington, The Comm. 1956. 38 p (RM E56B14, 28 December 1956).

Serovy, G. K. and J. C. Lysen, "Prediction of Axial-Flow Turbomachine Performance by Blade-Element Methods," ASME - Paper 61-WA-134 for meeting November 26 - December 1, 1961, 6 p.

Serovy, G. K. and E. W. Anderson, "Method for Predicting Off-Design Performance of Axial-Flow Compressor Blade Rows," NASA TN D-110, 37 pp., August 1959.

Shepherd, D. G., "Principles of Turbomachinery," MacMillan Company, 1956, 463p. TM 21 5548p.

Shoichi, Fujii, "A Theoretical Investigation of the Compressible Flow Through the Axial Turbo-Machines. First Report: Non-Swirling Fluids in Ducts," National Aerospace Laboratory, Tokyo (Japan), N66-31883, 1965, 31 p, refs In Japanese: English summary.

Sledel, Barry S., "Asymmetric Inlet Flow in Axial Turbomachines," (Massachusetts Institute of Technology, Gas Turbine Laboratory, Cambridge, Massachusetts). (American Society of Mechanical Engineers, Winter Annual Meeting, New York, N.Y., November 25-30, 1962, Paper 62 - WA-45.) ASME, Transactions, Series A - Journal of Engineering for Press, vol. 86, January 1964, p. 18-28.

Silvern, David H. and William R. Slivka, "Experimental Investigation of an 0.8 Hub-Tip Radius Ratio, Nontwisted Rotor Blade Turbine," NACA Res. Memo. Washington, The Comm, 1951, 18 p. diagra., charts. (RM no. E51G14, December 12, 1951).

Sinclair, R. I., "A Preliminary Investigation Into the Performance of Miniature Impulse Turbines," English Electric Co., Ltd. 32 p+, (LC.t.036, AD 117793, November 16, 1956).

UNCLASSIFIED

UNCLASSIFIED

Smith, D. J. L. & J. F. Barnes, "Calculation of Fluid Motion in Axial Flow Turbomachines", ASME 68-GT-12, 1967.

Smith, Jr., H., "Secondary Flow in Axial-Flow Turbomachinery," Am. Soc. Mech. Engrs. - Paper n 54 - A - 158 for meeting Nov. 28-Dec. 3, 1954, 24 p.

Smith, Jr., L. H. and H. Yen, "Sweep and Dihedral Effects in Axial-Flow Turbomachinery," Trans. ASME 85 D (J. Basic Engng.) 3, 401-416, September 1963.

Smith, Jr., L. H., "Radial - Equilibrium Equation of Turbomachinery," ASME - Paper 65-WA/GTP-1 for meeting November 7-11 1965, 12 p.

Sokolov, K. K., "Flow of Gas in the Channel of an Axial Friction Turbine," in its Theory, Design, Calculation, and Testing of Internal Combustion Engines. 31 July 1964, p 1-8, refs (See N64-31756 23-27). Air Force Systems Command. Wright-Patterson AFB Ohio, Foreign Tech. Div.

Sorensen, H. A., "Gas Turbines," New York, Ronald Press Company, 1951. TM 21 S713g.

Soundranayagam, S., "Approximate Estimation of the Passage Vorticity in the Secondary Flow Behind a Cascade," J. Roy. Aero. Soc. 64, 598, 635-638 (Tech. Notes), October 1960.

Stanitz, J. D., and G. O. Ellis, "Flow Surfaces in Rotating Axial-Flow Passages," NACA TN 2834, 31 pp, November 1952.

Stanitz, J. D., and G. O. Ellis, "Two-Dimensional Flow on General Surfaces of Revolution in Turbomachines," NACA TN 2654, 44 pp, March 1952.

Stanitz, J. D., W. M. Osborn, and J. Mizisin, "An Experimental Investigation of Secondary Flow in an Accelerating Rectangular Elbow with 90° of Turning," NACA TN 3015, 60 pp., October 1953.

Stechkin, B. S., M. G. Dubinskii, K. K. Sokolov, Tsao Syao-Tszyan, "O radial nom ravnovesii potoka," Akademiya Nauk SSSR, Izvestiya, Otdelenie Tekhnicheskikh Nauk, Energetika i Avtomatika, n 4, July-Aug. 1961, p 11-15.

Steinberger, M., "Development of the First German Postwar M.A.N. RB 153 Jet Engine (Die Entwicklung Des Ersten Deutschen Nachkriegs - Strahltriebwerks M.A.N. RB 153)," (MAN-Turbomotoren GmbH, Munich, West Germany). Luftfahrttechnik Raumfahrttechnik, vol. II, December 1965, p. 319-324. (in German).

UNCLASSIFIED

UNCLASSIFIED

Stewart, W. L. , "A Study of Axial-Flow Turbine Efficiency Characteristics in Terms of Velocity Diagram Parameters," National Aeronautics and Space Administration, Lewis Research Center, Cleveland, Ohio. N.Y., Am. Soc. Mech. Eng. (1961). 10 p, 7 refs. Presented at the ASME Winter Annual Meeting, N. Y. C. , November 26-December 1, 1961.

Stewart, W. L. , "Analytical Investigation of Single-Stage-Turbine Efficiency Characteristics in Terms of Work and Speed Requirements," NACA Res. Memo, Washington, The Comm. 1956. , 45 p (RM E56G31, October 15, 1956).

Stewart, W. L. , W. J. Whitney, and R. Y. Wong, "Use of Mean-Section Boundary-Layer Parameters in Predicting Three-Dimensional Turbine Stator Losses," NACA Res. Memo. Washington, The Comm. 1956. , 21p (RM E55L12a, March 23, 1956).

Stewart, W. L. , R. Y. Wong, and D. G. Evans, "Design and Experimental Investigation of Transonic Turbine with Slight Negative Reaction Across Rotor Hub," NACA Res. Memo. Washington, The Comm. , 1954. , (RM E53L29a, March 12, 1954).

Stewart, W. L. , "A Study of Axial-Flow Turbine Efficiency Characteristics in Terms of Velocity Diagram Parameters," ASME Preprint, November 26-December 1, 1961. 9 p. Winter Annual Meeting, N. Y. C. ASME Paper No. 61-WA-37.

Stewart, W. L. , "Analytical Investigation of Single-Stage-Turbine Efficiency Characteristics in Terms of Work and Speed Requirements," NACA Res. Memo, Washington, The Comm. 1956. 45 p. (RM E56G31, October 15, 1956).

Stewart, W. L. , "Analytical Investigation of Multistage-Turbine Efficiency Characteristics in Terms of Work and Speed Requirements," 18 p. (RM E57K22b, February 18, 1958).

Stodola, A. , "Stream and Gas Turbines, with a Supplement on the Prospects of the Thermal Prime Mover," New York, McGraw-Hill Book Company, Inc. , 1927. TM 20 S869S, Volumes I and II - translated by Louis C. Loewenstein from the sixth German edition.

Strscheletzky, M. , "Gap Losses in Axial Flow Machinery, Especially in Kaplan Turbines," (in German), Forsch Geb. Ing. -Wes. 21, 4, 101-106, 1955.

Thwaites, B. , "The Production of Lift Independently of Incidence - The Thwaites Flap, Parts I and II," Aero. Res. Counc. Lond. Rep. Mem. 2611, 20 pp, November 1947, published 1952.

UNCLASSIFIED

UNCLASSIFIED

Traupel, W., "Vortex Systems in Airfoil Cascades and Turbines," (in German), ZAMP 4, 4, 298-311, 1953.

Traupel, W., "Thermal Turbomachines: Vol. 2," (Thermische Turbomaschinen: Zweiter band, Regelung und Teillastverhalten, Festigkeit, Temperaturprobleme, Schaufelschwingungen, Dynamische Probleme des Laufers), Berlin, Springer-Verlag, 1960, vii + 420 pp. DM 61-50.

Torda, T. P., H. H. Hilton, and F. C. Hall, "Analysis of Viscous Laminar Incompressible Flow Through Axial-Flow Turbomachines With Infinitesimal Blade Spacing," J. Appl. Mech. 20, 3, 401-406 September 1953.

Vallander, S. V., "On The Application of the Method of Singularities to the Calculation of Fluid Flow in Radial-Axial Turbines," Soviet Phys.-Doklady 3, 6, 1113-1116, June 1959. (Translation of Dokladi Akad. Nauk SSSR (N.S.) 123, 3, 413-416, November 1959 by Amer. Inst. Phys., Inc., New York, N. Y.)

Van Ie, N., "Optimum Stage For Axial Flow Turbines," J. Aero. Sci. 22, 7, 503-504, July 1955.

Vazsonyi, A., "On the Aerodynamic Design of Axial-Flow Compressors and Turbines," J. Appl. Mech., March 1948, vol 15, pp 53-64.

Walker, L. A. and E. Markland, "Heat Transfer to Turbine Blading in Presence of Secondary Flow," Int J Heat & Mass Transfer v 8, n 5, May 1965 p 729-48.

Watson, E. J., "The Asymptotic Theory of Boundary-Layer Flow With Suction," Aero. Res. Coun. Lond. Rep. Mem. 2619, 45 pp., Sept. 1947, published 1952.

Weske, J. R., "An Investigation of the Aerodynamic Characteristics of A Rotating Axial-Flow Blade Grid," U.S., N.A.C.A., Technical Note No. 1128, February, 1947, 43 pp., illus. 5 references.

Weske, J. R., "Fluid Dynamic Aspects of Axial-Flow Compressors and Turbines," J. Aero. Sci., November 1947, vol. 14, pp. 651-656.

Weske, J. R., "Three-Dimensional Flow in Axial Flow Turbomachines," Institute for Fluid Dynamics and Applied Mathematics, Univ. Of Maryland, College Park. Final Report - 26 August 1960, 6 p. Contract AF49 638 385, AFOSR 211.

Whyte, R. R., "The Influence of the Gas-Turbine Axial-Flow Aero-Engine on Blade Manufacturing Methods," Instn. Mech. Engrs., Prept., 14 pp., 1956.

UNCLASSIFIED

UNCLASSIFIED

Wintucky, William T., & W. L. Stewart, "Analysis of Efficiency Characteristics of a Single-Stage Turbine with Downstream Stators in Terms of Work & Speed Requirements", NASA RM ES6119, Jan. 23, 1957.

Wintucky, W. T., and W. L. Stewart, "Analysis of Two-Stage Counterrotating Turbine Efficiencies in Terms of Work and Speed Requirements," NACA Res. Memo. (RM E57105, March 18, 1958).

Wong, R. Y., and D. E. Monroe, "Effect of Stator and Rotor Aspect Ratio on Transonic-Turbine Performance," NASA-Memo n 2-11-59E, February 1959, 27 p.

Wu, Chung-Hua and L. Wolfenstein, "Application of Radial-Equilibrium Condition to Axial-Flow Compressor and Turbine Design," Nat Advisory Committee Aeronautics - Report n 955, 1950, 30 p.

Wu, Chung-Hua and L. Wolfenstein, "Application of Radial-Equilibrium Condition to Axial-Flow Compressor and Turbine Design," Nat. Adv. Comm. Aero. Rep. 955, 30 pp., 1950.

Wu, Chung-Hua, "Matrix and Relaxation Solutions that Determine Subsonic through Flow in an Axial Flow Gas Turbine," NACA TN 2750, 65 pp., July 1952.

Wu, Chung-Nua, "Survey of Available Information on Internal Flow Losses Through Axial Turbomachines", NACA RM E-50412, Jan. 26, 1951.

Yeh, H., and J. J. Eisenhuth, "Unsteady Wake Interaction in Turbomachinery and its Effect on Cavitation," ASME - Paper n 58-A-114 for meeting November 30-December 5, 1958, 8 p.

Ye Zaryankin, A., and M. F. Zatsepin, "On the Influence of Losses in the Runner on the Efficiency of a Radial-Axial Turbine," Foreign Tech. Div., Air Force Systems Command, Wright-Patterson Air Force Base, Ohio. 4 February 1963, 11 p incl. illus. 2 refs. (Trans. no. FTD-TT-62-1801 from Izvestiya Vrshevikh Uchebnykh Zavedeniy, Energetika, No. 4, pp. 79-84, 1962).

Zysina-Molozhen, L. M., "Approximate Method for Calculating Losses in Cascade Profiles of Turbomachines," (in Russian), Teploenergetika 2, 9, 43-48, 1955.

UNCLASSIFIED

Unclassified

Security Classification

UNCLASSIFIED

DOCUMENT CONTROL - R & D		
(Security classification of title, body of abstract and indexing annotations entered when the overall report is classified)		
1. ORIGINATING ACTIVITY (Corporate author) Pratt & Whitney Aircraft Division United Aircraft Corporation East Hartford, Conn. 06108		2a. REPORT SECURITY CLASSIFICATION [REDACTED]
3. REPORT TITLE (U) Investigation of a highly loaded two-stage fan-drive turbine. Volume I. Phase I. Preliminary Design Evaluation		2b. GROUP 4
4. DESCRIPTIVE NOTES (Type of report and inclusive dates) Technical Report (Jan. 1, 1968 - June 28, 1968)		
5. AUTHOR(S) (First name, middle initial, last name) Welna, Henry; Dahlberg, Donald E.; Heiser, William H.		
6. REPORT DATE December 1969	7a. TOTAL NO. OF PAGES 358	7b. NO. OF REFS 23
8a. CONTRACT OR GRANT NO. F33615-68-C-1208	8b. ORIGINATOR'S REPORT NUMBER(S) PWA 3456	
a. PROJECT NO. 3066	9b. OTHER REPORT NO(S) (Any other numbers that may be assigned this report)	
c. Task No. 306606	AFAPL-TR-69-92, Volume I	
10. DISTRIBUTION STATEMENT		
11. SUPPLEMENTARY NOTES		12. SPONSORING MILITARY ACTIVITY Air Force Aero Propulsion Laboratory Wright-Patterson AFB, Ohio 45433
13. ABSTRACT <p>(U) A three-year program was initiated to provide a direct attack on the problem of attaining high efficiency in highly loaded turbine stages. The goals of this program are to develop turbine aerodynamic techniques and design procedures for efficient, high work, low pressure turbines by means of analytical studies and cascade testing, and to demonstrate the effectiveness of the techniques and procedures by designing and testing a two stage turbine that meets or exceeds the contract stage work and efficiency goals. The first phase effort described in this report was directed toward defining a turbine design with the highest inherent resistance to boundary layer separation and to select boundary layer control techniques that are best suited for extending the loading limits of the basic turbine design.</p> <p>Distribution of this abstract is unlimited.</p>		

DD FORM 1473 REPLACES DD FORM 1473, 1 JAN 64, WHICH IS OBSOLETE FOR ARMY USE.

Unclassified
Security Classification

UNCLASSIFIED

Unclassified

Security Classification

10	KEY WORDS	LINK A		LINK B		LINK C	
		ROLE	WT	ROLE	WT	ROLE	WT
	Turbine Aerodynamic Design Boundary Layer Control Survey						

Unclassified

Security Classification